Liang Yun
Alan Bliault
Johnny Doo

WIG Craft and Ekranoplan

Ground Effect Craft Technology

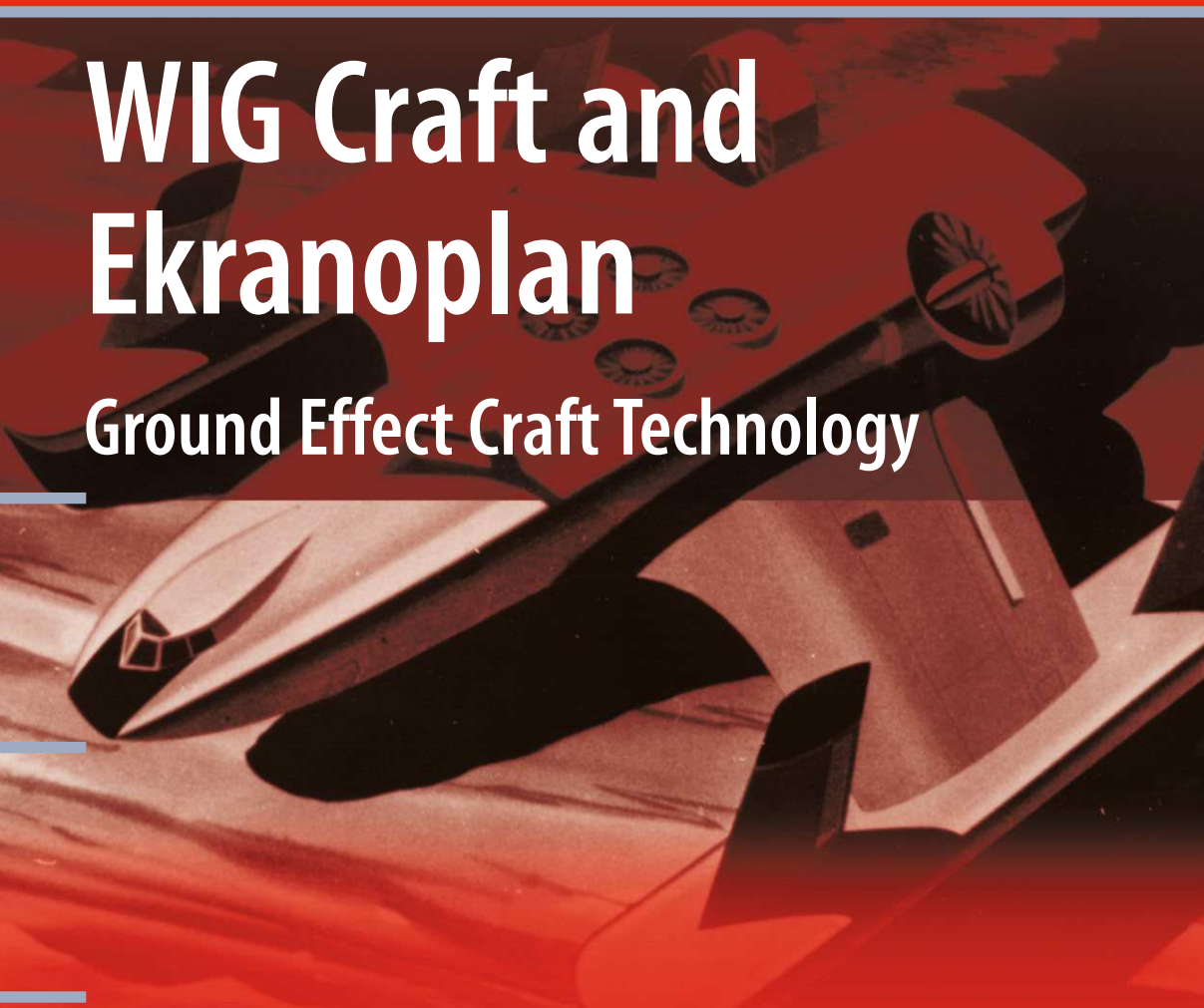

Springer

WIG Craft and Ekranoplan

Liang Yun · Alan Bliault · Johnny Doo

WIG Craft and Ekranoplan

Ground Effect Craft Technology

Springer

Liang Yun
Marine Design and Research Institute
of China (MARIC)
1688 Xizhang Nan Road
200011 Shanghai
People's Republic of China
liangyunb@yahoo.com

Alan Bliault
A/S Norske Shell
4098 Tananger
Norway
alan.bliault@shell.com

Johnny Doo
Teledyne Continental Motors
2039 Broad Street
P.O. Box 90
Mobile, AL 36601
USA
dsn99@aol.com

ISBN 978-1-4419-0041-8 e-ISBN 978-1-4419-0042-5
DOI 10.1007/978-1-4419-0042-5
Springer New York Dordrecht Heidelberg London

Library of Congress Control Number: 2009937415

Preface

In the last half-century, high-speed water transportation has developed rapidly. Novel high-performance marine vehicles, such as the air cushion vehicle (ACV), surface effect ship (SES), high-speed monohull craft (MHC), catamaran (CAT), hydrofoil craft (HYC), wave-piercing craft (WPC) and small water area twin hull craft (SWATH) have all developed as concepts, achieving varying degrees of commercial and military success.

Prototype ACV and SES have achieved speeds of 100 knots in flat calm conditions; however, the normal cruising speed for commercial operations has remained around 35–50 knots. This is partly due to increased drag in an average coastal seaway where such craft operate services and partly due to limitations of the propulsion systems for such craft. Water jets and water propellers face limitations due to cavitation at high speed, for example. SWATH are designed for reduced motions in a seaway, but the hull form is not a low drag form suitable for high-speed operation.

So that seems to lead to a problem – maintain water contact and either water propulsion systems run out of power or craft motions and speed loss are a problem in higher seastates. The only way to higher speed would appear to be to disconnect completely from the water surface.

You, the reader, might respond with a question about racing hydroplanes, which manage speeds of above 200 kph. Yes, true, but the power-to-weight ratio is extremely high on such racing machines and not economic if translated into a useful commercial vessel.

Disconnection of the craft from the water is indeed a logical step, but it has its consequences. The craft must be propelled by air and it will have to be supported by air as well. A low flying aircraft? In some ways – yes – but with a difference. When an airplane flies very close to the ground a much higher pressure builds up under the wings – ground effect. Some early hovercraft were configured to capture air as they moved forward – captured air bubble craft.

Combine ground effect with a geometry specifically designed to enhance the effect and you have a craft that might be able to achieve much higher cruising speed. Flying above waves, its motions might also be much reduced. This idea gave birth to the wing-in-ground effect (WIG) craft.

The original type of WIG can be traced from at the beginning of last century. Actually, in 1903, the Wright Brothers flew their first airplane over relatively long

distances in the surface effect zone. Engineer Kaario of Finland started tests of craft lifted by ground effect in the middle of 1930s. However, due to limitations in the efficiency of structural materials and available engine power, the WIG was not developed further until the beginning of the 1960s.

These were ideas that excited Alexeev in Russia in the 1960s and 1970s after his institute had developed several series of hydrofoil designs. Alexeev and his team of Russian pioneers in this new vehicle technology were interested in very high speeds, and their programme was developed directly from hydrofoil research. The craft were christened "Ekranoplan". Parallel efforts on prototype craft and theoretical analysis gradually built experience and understanding through the 1970s and 1980s leading to the first military service craft based in the Caspian Sea. This was a truly outstanding technological achievement delivered through visionary support from the Russian Navy.

In Germany, also in the 1970s, research and prototype craft aimed at using ground effect was also carried out. Rather than the large military budget available in Russia, the German programmes were funded privately and later with low level support from government. This work led to ground effect craft suitable for high-speed coastal patrol, though in limited sea conditions.

At the beginning of 1970s, Russian engineers Bartini and R.Y. Alexeev invented power-assisted lift arrangements for WIG craft by mounting jet engines in front of the main wing to feed engine exhaust air into the air channel under the wing to create the so-called power-augmented ram wing-in-ground effect craft (PARWIG). This augmented lift improved the take-off and landing performance by reducing take-off speed and distance.

The full story of Alexeev's craft is outlined in Chapter 2 together with other developments from around the world. The technical achievements were highly significant, and it is a pity that the economic situation in Russia through the 1990s was such that the programme had to be stopped. It may be some time before we see machines to equal the KM and Spasatel.

In recent years, researchers in China and Russia have mixed air cushion technology into the WIG to create the dynamic air cushion craft (DACC) and dynamic air cushion wing-in-ground effect craft (DACWIG) to produce craft with amphibious capability and much higher transport efficiency at medium cruise speeds in the range 150–250 kph.

Since a WIG has several operational modes (floating hull, cushion and planing, and air-borne modes), the craft design is rather more complex than aircraft or other marine craft. A WIG normally just transits through all the modes except flying in ground effect, but unfortunately the drag forces and motions are the greatest at speeds below take-off, so effective design for the conditions met during the take-off and landing runs is essential to a successful WIG design. The challenges are not over though – quasi-static and dynamic stability of a WIG when flying is strongly influenced by both the flying height and the craft pitch angle.

Research into these areas is at an early stage and much more knowledge in the different areas is needed. In this book, we give an outline of the knowledge as it

exists right now. This provides a starting point, though readers are encouraged to seek out further sources for themselves!

Some accidents have occurred on full-scale WIG craft, so that there is some uncertainty as to the safety of WIG for potential operators at present. This is being addressed by a technical committee of the International Maritime Organisation (IMO) who have published a safety code in the form of guidelines for WIG in 2003.

The technology is indeed still somewhat experimental and needs a build-up of operational experience, even if it is at relatively small scale, in order to develop confidence for the commercial industry to gain enthusiasm for this new form of transportation. The IMO guidelines should help a lot in this respect, but practical operations, perhaps following the example of the many SR.N6 hovercraft trials operations and expedition journeys in the 1960s and 1970s, will be needed to prove their capability and value to society.

On an international basis, the WIG craft is now recognised basically as a high-speed marine vehicle and will be certified as such, rather than being certified by aerospace authorities. This has significant cost and operational advantages that should assist in the craft's commercialisation.

WIG are based upon a combination of aircraft and marine technology while being different from either. WIG operate both on water and in air as well as on the edge of both media. A WIG is neither an airplane nor watercraft as such. It is rather different either from airplane industry (sophisticated lightweight structures, high power intensity, automated, heavy certification requirements, expensive construction etc.) or from watercraft (experience based design, relatively heavy structure, robust, low cost, etc.). The WIG borrows from both technologies to achieve a high speed and lightweight, yet low-cost marine vehicle.

Our book begins with a general review of ground effect technology and a historical review to give a background to the main body of the text covering the theory, as well as a design approach for WIG. This is the first major text on this subject outside Russia, so we hope to reach a worldwide audience and encourage interest in this technology in between the marine and aerospace worlds!

There are this Preface, 13 chapters and Backmatter in the book. We introduce WIG craft concepts and background development in Chapters 1 and 2. From Chapters 3, 4, 5, 6, 7, 8 and 9, the book describes trim and longitudinal force balance, static hovering performance, aerodynamic characteristics, stability, drag and powering performance, seakeeping quality and manoeuvrability, and model experimental investigations. The materials and structures, power plant selection, and lift and propulsion system selection are introduced in Chapters 10, 11 and 12. In these chapters, the issues related to WIG design are considered as a derivation from aircraft or marine design rather than giving a detailed treatise. In Chapter 13, a general approach to WIG concept specification and design is described.

The Postscript discusses prospects for the future and a series of technical issues concerned with the development of WIG that face researchers and engineers in this area at present. There is so much to work on at present. The WIG principle can be applied to a wide envelope of operational speed and environmental conditions,

leading to craft as different as gliders and jet airliners in the aircraft world. In addition, if long distance transportation is to become reality, WIG will need a new form of "traffic lane" agreed at international level and documented on charts. Significant opportunities await us!

A comprehensive listing of references is included at the end of the book, classified by chapter. These should be useful to the reader to provide more detailed information and support for the analysis and design.

The authors aim with this book to provide a useful reference for engineers, technicians, teachers and university students (both undergraduate and postgraduate), involved in the marine engineering world who are interested in WIG research, design, construction and operation.

Since the WIG is a novel technology and still in its initial development, the presentation of some of the theory should be considered as statement of current state of (limited) art, so readers should take care to check for themselves the validity of the theories presented here. The authors will be pleased to have comments and feedback from readers.

Shanghai, PR China — L. Yun
Tananger, Norway — A. Bliault
Mobile, Alabama — J. Doo
May 2009

Acknowledgements

The authors would like to express their sincere thanks to the leadership and colleagues of the Marine Design and Research Institute of China (MARIC) and HPMV Design Subcommittee of CSNAME, including Prof. Xing Wen Hua, Prof. Liang Qi Kang (Managing Director, MARIC), Mr. Wang Gao Zhong (Deputy Managing Director of MARIC and also Former Chief Designer of WIG type SWAN), Prof. Peng, Gui-Hua (Director of HPMV Division, MARIC), Prof. Xie, You-Non (Deputy Chief Designer of "SWAN"), Mr. Wu Cheng Jie, (Principal Designer of SWAN), Mr. Hu, An-Ding (Chief Designer of WIG "750", MARIC) and Mr. Li, Ka-Xi (Chief Designer of WIG "XTW", CSSRC), for their help and using their papers and research during the writing of this book.

We also wish to thank the following for material contributions and for permission to use illustrations and photos: Johnny Doo (SSAC), Edwin van Opstal (SE Technology), Boeing Aircraft Company, Flightship Ground Effect Pty Ltd, Fischer Flugmechanik/AFD Airfoil Development and Bob Windt (Universal Hovercraft).

Finally we wish to thank our peer review group who provided most valuable feedback on the content and presentation of the book.

Contents

Chapter 1
Wings in Ground Effect

Introduction

This book aims to introduce you, our readers, to a new type of marine craft. At present there are still very few of these machines, though as long ago as the 1970s, a secret military craft of this type twice as large as a Boeing 747 airliner was already on trials in the Caspian Sea for the Russian Navy.

The subject is the wing-in-ground effect craft or WIG for short. The authors, together with a significant number of engineers and scientists around the world working on WIG craft small and large, feel that the technology has an important future as part of the marine transport spectrum. Since the technology and indeed the craft that have been built so far are not well known, this book first introduces the craft themselves, and the researchers who have developed them. Following this, we outline the various theoretical aspects and introduce the basic steps for design.

This is not meant to be a design handbook for WIG specialists, since to do this effectively we would have to concentrate on one particular WIG subtype. Rather, we aim to provide an interesting introduction to the craft and their theory for the wider audience of marine and aeronautical engineers who are interested in broadening their knowledge of an aspect of the aero-marine interface.

WIG designers working on new designs right now have computing power and software available to them that did not exist in the 1960s and 1970s when WIG were first being designed. Most WIG craft introduced in this book have been developed from analytical theory, model testing and building of prototypes. In the last two decades, finite element programmes for structural design and fluid analysis have moved from the mainframe to the personal computer. It is now possible to model relatively complex airfoil configurations using tools such as "Autowing" (see References and Resources) to determine aerodynamic forces and coefficients and so reduce the physical modelling required. In this book, our aim is to provide a basic understanding of the phenomena of ground effect, so we stay with analytical descriptions and leave the reader to investigate further with the modern tools available. While as technology evolves some of the analytical theory goes out of date for modern design, it should nevertheless assist in understanding the rationale for the earlier designs.

L. Yun et al., *WIG Craft and Ekranoplan*, DOI 10.1007/978-1-4419-0042-5_1,

This book also introduces a number of acronyms and terms related to WIG technology. At present, engineers in different parts of the world have their own favourite terms, and there is often not common agreement. In this book, selection of terms has been made by the authors based on ease of understanding so far as possible.

WIG theory and technology is at a very early stage and covers a wide range of possible craft configurations. WIG craft size and speed envelope ranges from single-passenger prototypes operating at 50 kph to large military craft at 500 kph. The technical challenge is similar to that for the aeronautical engineer investigating light aircraft as well as jet airliners. In addition, a WIG interfaces with the water surface during take-off and landing at speeds higher than most marine craft. To date, most of the theory has been developed by experiment, and by comparison to ACVs and seaplanes.

Each of the craft concepts has its exponents! This book is not dedicated to any one concept; rather, we wish to introduce sufficient information to allow the interested engineer to investigate any of the concepts further. The concepts and theories presented here should be carefully considered in this light.

To start, let us consider why a marine craft such as the WIG might be useful at all.

Marine Transport and WIG Development

High-speed marine transportation has been important in society's development over the last century and a half, as industrialisation has spread, and wind power was supplanted by steam and internal combustion engines. Initially, it helped manufacturing industries to expand on a national and an international basis. More recently, during the last half-century fast-passenger transportation around and between many coastal cities has also become important for both work and pleasure travel.

The development of tourism as a leisure activity has further spurred growth in marine transportation and become the dominant market for many ferry operators. The search for new vehicle types with higher speed and greater transport efficiency has continued throughout the 20th century to enable more attractive and profitable services. This has encouraged development of high-speed planing monohulls, hydrofoils, hovercraft, surface effect ships and fast catamarans. As the market has developed, all of these concepts have been used as passenger and vehicle ferries.

The central theme in fast marine vehicle concepts is to find a way to reduce the hydrodynamic resistance acting on the main body of the craft. Hydrodynamic resistance increases dramatically at high speed, so to reduce it the body of the ship must be lifted clear of the water surface. Hydrofoil craft use small lifting surfaces just under the water surface, while hovercraft and surface effect ships (SES) use pressurised air cushions to achieve this.

Wing-in-ground effect craft (WIG) create a load-carrying air cushion under their wings while flying just a small distance above the surface and offer another step

upwards in service speed, to well above 100 knots for passengers and vehicles, freight and military missions.

Why not simply build seaplanes and flying boats to perform such duties? The main reason is payload capacity, and cost. WIG craft have potential for payload capacities closer to fast marine craft, and if the construction techniques are based on marine practice, then cost should be much lower than aircraft. Both payload and cost are targets – if a WIG is designed to operate at 300 knots, then clearly it will require use of much more aerospace technology and costs will rise equivalently. This is why the most interesting target is a little lower down the speed scale, in the range from 60 to 200 knots.

The WIG (Fig. 1.1) is currently still at an early stage of development. Just now, there are a number of experimental prototypes of various sizes and a number of rather larger military craft that have been tested and operated in Russia. A historical review of WIG development is presented in Chapter 2 to orientate readers, following an outline of the background and basic concepts in this chapter.

Fig. 1.1 Orlyonok wing in ground effect craft

If we consider its place in the transport spectrum, the WIG concept offers significant potential for fast paramilitary coastal patrol applications, a niche in the passenger ferry market, and a rather larger possible market in intercontinental freight. At present, the potential of these craft is limited by technical knowledge and a lack of commercial operating experience. This book aims to widen the circle of this specialist knowledge, so that new generations of WIG craft may be developed, primarily for commercial operations.

Alternative Technologies

Let us first consider three of the alternative fast marine craft types that have been developed, the hydrofoil, SES and ACV, before moving on to consider the WIG craft basics and the challenges that the concept presents us.

The Hydrofoil

A hydrofoil operates above the water surface by having foils suspended beneath the hull that act like an aircraft's wings in the water (Fig. 1.2). However, the hydrofoil itself still operates in the water, which causes high water-friction and profile drag. Cavitation on the hydrofoil upper surface during high-speed operation is the most challenging problem for hydrofoils as it limits the carrying capacity and ultimate speed of such craft. A Russian, R.Y. Alexeyev, invented the hydrofoil craft and developed its theoretical fundamentals. So far about 800 hydrofoils have been built. The fully submerged hydrofoil craft "Jetfoil" developed by Boeing in the United States represents the most advanced development of hydrofoils to date. It has excellent seakeeping qualities, but the cavitation barrier still limits its service speed to approximately 50 knots.

Fig. 1.2 Supramar hydrofoil

The SES

The side hulls of SES (Fig. 1.3) are lifted out of the water by their air cushion, and this reduces wave-making; however, the two side hulls still have significant water-friction and wave-making drag. In addition, sea waves passing between the two hulls cause wave pumping inside the cushion that in turn induces vertical motions to the craft. This is less of a problem for larger craft. SES can be designed up to much larger sizes than hydrofoils, as high as thousands of tons payload, in the speed range up to around 100 knots. Above 60 knots, propeller or water jet cavitation significantly reduces propulsion system efficiency and consequently also reduces transport efficiency.

In recent years, there has been enthusiasm with shipbuilders to build slender high-speed ships as passenger ferries based upon the design idea to maintain Froude number (Fr) at between 0.6 and 1.0 so as to optimise wave-making effects. This leads to craft with improved economy and seakeeping qualities, for service speeds in the range between 30 and 50 knots. A similar design approach can be applied

Fig. 1.3 Surface effect ship, Bell Halter 110

for both catamarans and SES. Since these conventional craft are supported by both hydrostatic and hydrodynamic lift and employ water propulsion, there are no difficulties to scale up to a larger size.

High-speed catamaran vessels suitable for carrying trucks and cars as well as large numbers of passengers are in operation in many parts of the world. However, these large 2,000–3,000 t vessels are again limited to a practical service speed at about 50 knots. This is because Froude number is proportional to length, L, while displacement and required propulsion power are proportional to L^3. Faster craft following this principle would have to be much larger so as to stay in the optimum Froude number region for minimum resistance and powering.

The Hovercraft

The hovercraft (air cushion vehicle, or ACV), see Fig. 1.4, pumps air into a cushion cavity with fans in a similar way to the SES. The difference is that an ACV has flexible skirts right around the cushion periphery. During operation, the craft is almost isolated from the water surface by its skirt and has no underwater appendages, so it can operate over both land and water. Such craft can theoretically reach much higher speeds than SES or hydrofoils; however, the skirt system does cause various additional drag components through its interaction with the water surface. When operating in waves, the wide frontal area of hovercraft skirts and dynamic vertical motions due to the soft spring of the skirt cause significant added resistance, so that from 60 knots in calm water, service speeds may drop to between 30 and 40 knots in waves. Responsive skirts and other technical developments have improved hovercraft performance in recent years; nevertheless, their most important attribute remains their amphibious qualities rather than high speed in an open seaway.

Fig. 1.4 Hovercraft, BHC AP1-88

Ground Effect for Higher Service Speed

An ideal marine transport would combine much higher speed, in the range of 150 knots or greater, with high transport efficiency, and so high capacity for passengers and freight. To achieve this, a greater disconnection between the water surface and the hull and lifting surfaces of the craft is required. Such a vehicle may be developed from the ground effect experienced by an aircraft wing when it flies close to the ground, for example during landing. In the case that surface clearance is less than twice the airfoil chord length, lift force is greatly increased compared to operation in free air. The air at higher pressure on the wing underside begins to act like an air cushion. The lift force can be further enhanced by altering the wing geometry and by blowing air into the "cushion" space. This is the basic premise behind a wing-in-ground effect vehicle or WIG for short.

Let us step back for a moment and consider a marine vehicle with a combination of static and dynamic lifting forces [1]. Figures 1.5 and 1.6 show a craft supported by three types of forces, i.e. static lift from buoyancy of a single hull or catamaran twin hull *X*, dynamic lift from a planing hull or hydrofoil *Y* and alternatively static lift from an air cushion *Z*. The example craft weighs 75 t, with a length of 25 m, width of 10 m and speed of 45 knots. The range of combinations of supporting force may be plotted, so as to compare the total installed power for the variations of the distribution of lifting forces. The numbers in brackets give the percentages of *X*, *Y* and *Z* respectively. Figure 1.7 shows the lift–drag ratio of an SES model versus Froude number (Fn) with different cushion lift to craft weight ratio, where *w* represents the model weight, P_c the air cushion pressure and S_c the air cushion area [2].

Plots such as these may be used to estimate the combination of various supporting forces on the craft, and from that estimate drag in calm water, so as to select an optimal design. However, while calm water performance can be high, the hull, hydrofoil or skirt around the air cushion still interacts with the water surface when operating in waves, causing high drag forces that limit realistic service speeds, and also caused significant motions to the craft.

The alternative is to develop a new type of craft that rides sufficiently high above the water surface to remove significant interaction at all service speeds. Such a craft

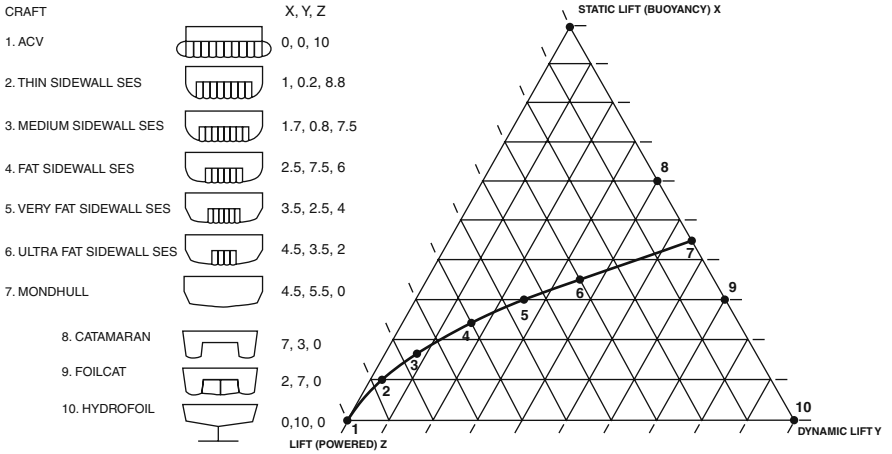

Fig. 1.5 Powering comparison for air cushion craft

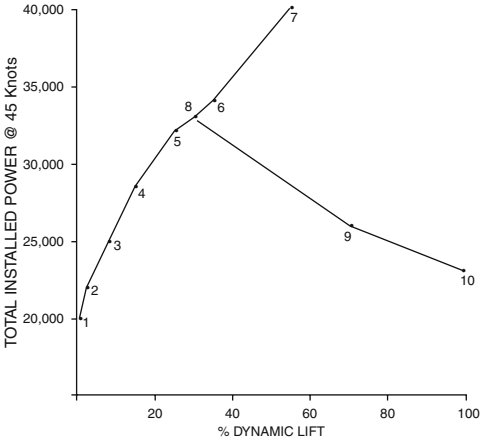

Fig. 1.6 Powering comparison for dynamically supported craft

might have a cruise speed in the range of 100 knots up to possibly as high as 400 knots.

Some WIG Technical Terms

It may be helpful at this point to give some definitions relating to WIG technology for reader guidance, as the following. At the end of the book, there is a glossary of terms to give more complete reference.

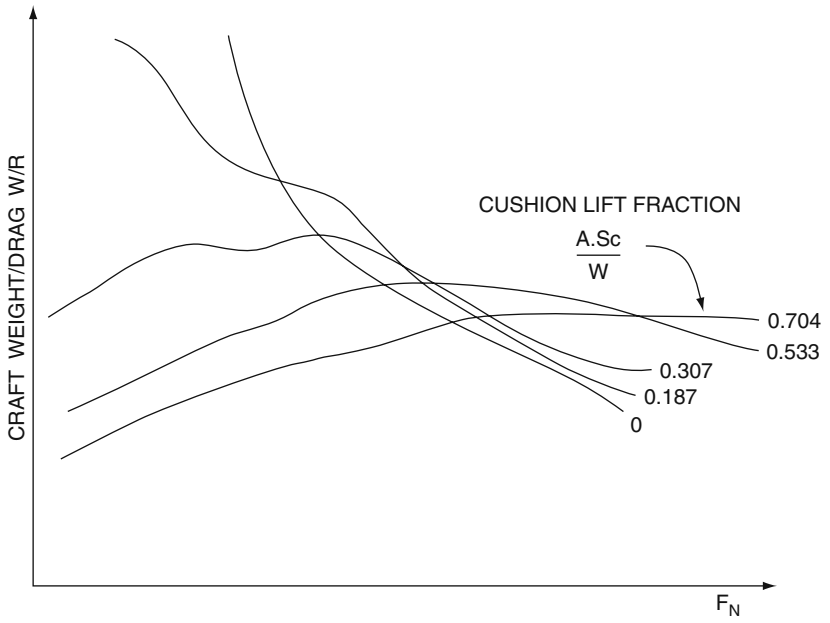

Fig. 1.7 Lift–drag ratio versus Fn with different cushion lift to craft weight ratio of an SES

Ground Effect

Ground effect is the enhanced lift force acting on a wing that is travelling close to the ground or water surface, commonly less than one wing chord height. The enhanced lift is generated by the greater pressure increase on the undersurface of the wing due to higher deceleration of the air trapped between the ground and wing surfaces. This can be enhanced by lowering the wing flaps, installing fences below the wing tips and adjusting the wing plan geometry.

Dynamic Air Cushion

Dynamic air cushion is a high-pressure region originating between the airfoil and a water surface or some other surface as the airfoil moves within the zone of enhanced aerodynamic effect. A dynamic air cushion can be created in two different ways:

- The craft hull geometry can be shaped so that air enters an opening and is retained except for air released through a small gap under the craft except at the bow. This is the captured air bubble concept of the 1960s mostly called the ground effect machine.

- Air is blown under a wing at a much higher speed than the craft's forward speed, to enhance lift. This may be enhanced by lowered wing flaps and wing tip fences and adjusted wing geometry. This is the basis for the Russian Ekranoplan programme.

Static Air Cushion

Static air cushion means a high-pressure region originating from air jets, propellers or fans that are directed between an airfoil or other base plane of the craft and water surface when the craft stays still or moves slowly over surface and is sufficient to support the craft's total weight. An ACV or SES has seals right around the periphery for containing the air cushion under the base plane of the craft. A WIG with bow thrusters designed to create a static air cushion will normally close the main-wing flap at zero or low speed to assist retaining the static air cushion. This is the basis for the DACC in Russia and the DACWIG in China and Russia.

Basic Principles of Ground Effect

All aircraft pilots experience the same phenomenon during landing, where additional lift is gained just before the undercarriage reaches the ground. This ground effect leads to the aircraft gliding above the runway until sufficient speed is lost for the cushion to decay. This effect is caused by the following physical phenomena.

- Owing to flow blockage between the wing underside and the ground, the pressure on the lower surface of the wing increases, so as to increase the lift [3]. A comparison of a wing section operating in ground effect with the same section operating in free air is shown in Fig. 1.8.
- In addition, for a wing operating close to the ground or water surface, the down-wash velocity caused by wing tip vortices will be reduced. The decrease may be visualised by considering a mirror image of the same wing profile at a position symmetric to the ground, Fig. 1.8b. This effect also reduces the induced resistance caused by the wing tip vortex-induced velocity.

Figure 1.9 illustrates these phenomena. The upper figure shows the wing tip vortex without ground effect, while the lower figure shows that with ground effect. The decrease of down-wash velocity due to the ground effect leads to an increase in lift and decrease of resistance, as well as an increase of effective aspect ratio for the wing. These are the two most important characteristics of wings in ground effect.

Figure 1.10 shows the lift–drag ratio versus the aspect ratio of a wing, and height of the wing tip or endplate above the sea or land, as a ratio of the mean chord, i.e.

$$L/D = (AR,h/c) \tag{1.1}$$

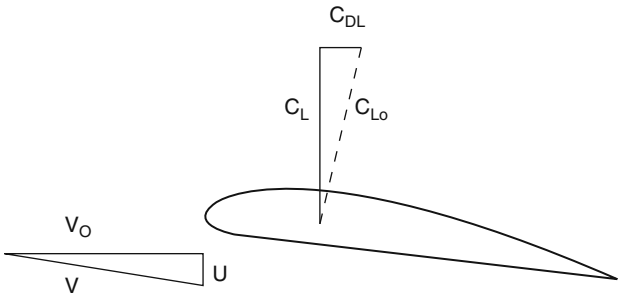

(a) WING OUT OF GROUND EFFECT

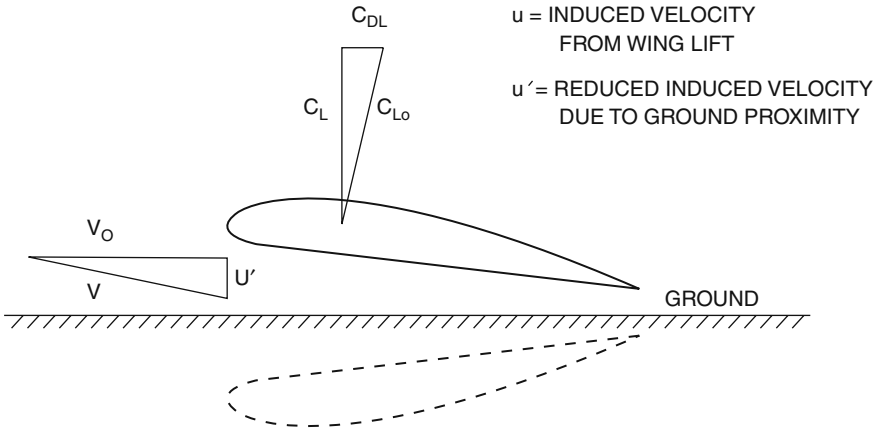

(b) WING IN GROUND EFFECT

Fig. 1.8 Comparison of a wing section operating in ground effect with section operating in free air

where

L	Lift,
D	Drag,
h	Flying height,
c	Chord length of wing,
AR	Aspect ratio of wing.

The figure shows that L/D increases in direct proportion with AR and in inverse ratio with h/c.

Figure 1.11 shows the operational altitude of various high-speed craft. The WIG actually fills the gap between surface-supported craft and free flying aircraft. It has potential for higher transport capacity than an aeroplane, while operating at much higher speed than normal marine vehicles.

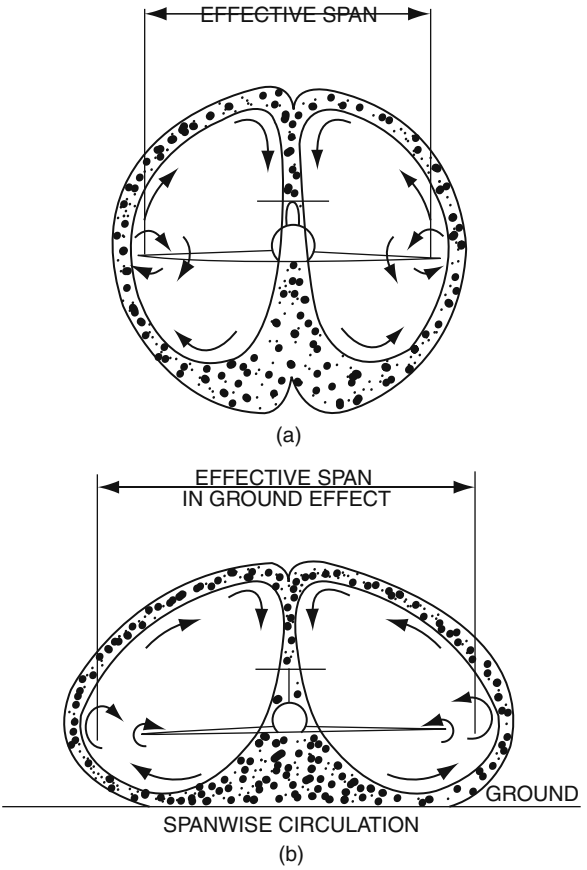

Fig. 1.9 Ground effect reduces down-wash and lift-induced drag

To accelerate from standstill to its normal service speed over water, a WIG starts in displacement mode at low speed. It then transits through planing mode to flying mode. During transition, the craft operates as a hydroplane. A very high hydrodynamic pressure will act on the lower hull and may also cause a large drag during take-off (so-called hump drag). The hump drag of a seaplane is often several times the drag during flight at cruising speed. A WIG generally has a lower hump drag than a seaplane, although this may still be the parameter-controlling power system sizing, rather than cruising power.

A WIG should therefore have well-dimensioned planing surfaces and high power for the take-off transition. In a similar way to the design of a seaplane, design of a WIG for the acceleration phase is the key to success. Engineers involved with WIG research have therefore focused on seeking methods to improve take-off performance and to reduce total installed power.

There are many different design approaches that can be used to improve the take-off and flying performance of WIG, resulting in a wide range of possible design

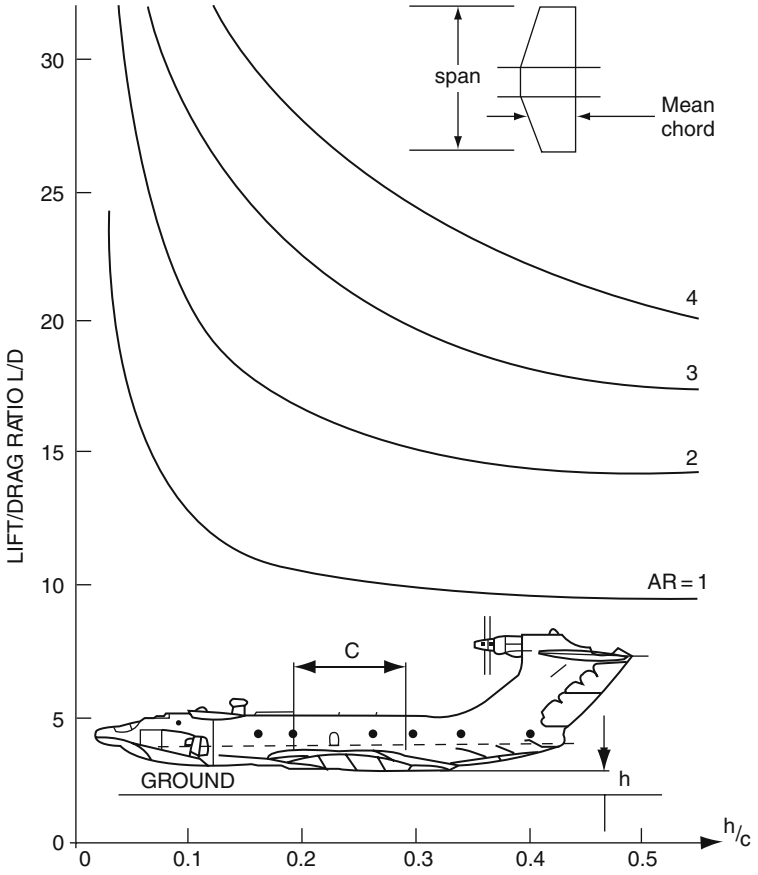

Fig. 1.10 Lift–drag ratio versus relative flying height of WIG craft with different aspect ratio

configurations. The lift supporting a WIG in its various operation modes includes four forces – buoyancy, hydrodynamic lift, static air cushion lift and aerodynamic lift. We therefore add an aerodynamic lift component to the supporting triangle of Figs. 1.5 and 1.6. WIG craft can be considered an extension to the triangle of Figs. 1.5 and 1.6, the combinations of buoyancy, hydrodynamic lift and air cushion lift providing options to optimise the drag forces during take-off and landing [4]. While from the powering point of view hydrofoils might seem a useful way to reduce take-off drag and powering, in fact this option has safety problems due to the possibility that the hydrofoils could pull the WIG down to a pitchover if entering the water (waves with a negative angle of attack). They have been tried (see X-114 in Chapter 2), but abandoned after the tests. The key options for WIG are therefore geometry options for the hull (catamaran with or without air cushion, open or skirted blown cushions under the main wings and stepped hull forms to minimise planing drag).

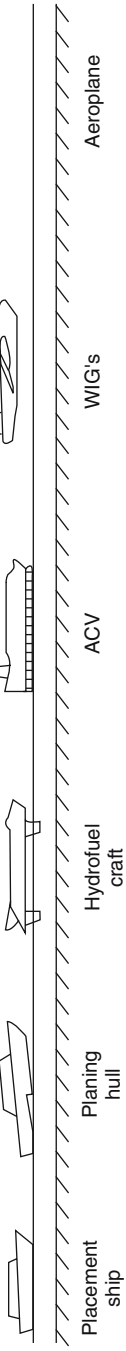

Fig. 1.11 Running attitude of various high-speed craft

Returning to the aerodynamic form for a WIG, the traditional geometry of a monoplane aircraft is to have the main supporting wing forward, usually with some backward sweep and dihedral, and a rather smaller rudder and tailplane right at the stern to control turning and pitch attitude. In contrast, a hydrofoil generally has a bow and stern foil of similar dimensions that both lift the craft hull from the water. Alexeyev's hydrofoil designs developed the surface skimming hydrofoil to a fine art and gave him his original idea for development of a WIG or Ekranoplan.

The tandem wing arrangement is a popular geometry for smaller WIG craft even today, as it is relatively stable operating in the strong ground effect zone. At higher speeds and greater flying height, the more traditional aircraft arrangement has been found more effective. Due to the high lift coefficient in ground effect, the main lifting wing can be of much lower aspect ratio than a free flying aircraft. To reliably control craft attitude and flying height within a small tolerance, it has been found necessary to use very large tail fin and rudder dimensions, and large tailplane surfaces mounted at the top of the rudder so as to avoid the turbulence from the main lifting surface.

The design challenge for a WIG at its cruising speed is one of aerodynamic stability and control within very fine limits due to its proximity to the water surface. This is an operational environment not experienced in any other marine craft. An aircraft transits through this region when landing, but is not normally kept in steady flight in this mode. WIG inherent stability is a compromise between the need for aerodynamic manoeuvrability and righting moments when the hull or wing endplates impact the water surface. Optimisation is a difficult task for the designer, and on large WIG craft can only be approached by use of automated flying controls to balance the alternative need for very large aerodynamic control surfaces.

The transitory phases of operation from rest through boating, planing or hovering through hump speed and accelerating through take-off into ground effect flight all require optimisation by the WIG designer so as to minimise installed power. As WIG size or design cruising speed is increased, the optimum wing loading increases, and so more powerful lift enhancements are required to assist take-off – the WIG equivalent of an airliner's wing flaps that are lowered for take-off and landing.

In this book, we focus our attention on the larger WIG that have been developed in Russia and China and so devote a significant part of our presentation to power-assisted lift, including air cushion systems. Design for smaller craft tends to focus on lifting wing geometry, including the use of anhedral and trapezoidal plan forms to create a craft with easy handling characteristics for manual control. There are as many views on the optimum in this respect as there are designers. Nevertheless, there are general rules to follow, and these are outlined to the best of the authors' ability in this book.

The basic components from which a WIG is constructed are as follows:

- A hull or fuselage, with lower planing surfaces and buoyancy
- A main lifting wing that has a low aspect ratio and high camber form or alternatively two tandem lifting wings in the case of some small craft designs

Item	Orlyonok (1980)	KM (1966–1980)	Boeing 747–400ER (2006)	Airbus A380 (2006)
Length (m)	58.0	92.4	70.6	73.0
Fuselage width	10.0	8.0	6.3	7.1
Wingspan	31.5	37.8	64.4	79.8
Tail height	16.0	21.8	19.4	24.1
Maximum weight (t)	140.0	544.0	413.0	590.0
Maximum payload	20.0	130 approx.	112.7	150.0
Cruising speed knots	200.0	270.0	485.0	511.0
Installed power	2 × 10 t thrusters 1 × 15,000 HP propulsion	2 off VD-7 M 8 off VD-7 at bow	4 × PW4062 282 kN	4 × Trent 900, 340 kN

- A large area tail fin for longitudinal directional stability
- A large area high-mounted horizontal stabiliser
- Endplates to the main wing that also have planing surfaces and buoyancy
- Optional extension winglets with dihedral outboard of the endplates, for improved roll stability
- Propulsion engines and propellers or turbofans mounted above the main wing or on the tail fin and/or
- Lift and propulsion engines and ducted propellers or turbofans mounted forward of the main wing

These components have been varied a great deal as the successive generations of WIG have developed through the 1970s to the present in search of minimised hump drag and take-off power, and later for improving WIG control and stability at high speed. The basic design techniques are derived from a combination of ACV technology and seaplane design, extended up to airframe sizes significantly larger than the largest commercial jet aircraft of today.

The Russian Orlyonok described in Chapter 2 represents the upper bound of WIG craft size built for operational service to date. Below this, WIG have been built at sizes down to single man craft that are similar in size to microlight aircraft. The main development locations for the technology have been in Russia, China, Japan and Germany. Recently, small passenger WIG have also been built by organisations in Australia, Singapore and the United States. Elsewhere in the world, there has been interest in the theory, but no development of WIG construction.

A comparison of dimensions and weights of the Orlyonok PARWIG with the Boeing 747 and Airbus A380 is shown in table above.

Types of WIG

The challenge of designing a configuration of main hull, lifting wing(s) and stabilising surfaces to give minimum drag in all the modes from floating, possibly hovering

on cushion, through planing, to flying in ground effect has led to a wide range of concepts from different designers. They do nevertheless tend to conform to a number of generic configurations or types. Several of them are known by acronyms.

The general name covering all such vehicles is WIG. Other names used are the Ekranoplan (this is a Russian name that means a lifting surface close to a ground plane), flaircraft, wingship, hoverwing, wing-in-surface-effect ships or WISES, power-augmented wing-in-ground effect craft or PARWIG, dynamic air cushion craft or DACC, dynamic air cushion wing-in-ground effect craft or DACWIG, and the ground effect machine or GEM.

In this book, we will refer to all these craft collectively as WIG or ground effect craft. All of these names relate to variations of the basic lifting method of placing a wing close to the ground or water surface, and the method used to augment lift for improving the take-off through hump speed. The variations may be summarised as follows:

WIG or Ekranoplan	Generic name, also applied to craft without special lift enhancement features
DACC or GEM	Craft operating very close to the ground in the strong surface effect region
PARWIG	Craft operating at a larger flying height in the surface effect region and that use air from bow-mounted propulsors to create enhanced lift under the wings at low speed
DACWIG	Craft operating at a larger flying height in the surface effect region and that use air from bow-mounted propulsors, and wing endplates to create an air cushion under the wings at low speed rather than just enhanced lift

Variations in the hull form, whether monohull or catamaran, give further alternates to the basic types above. WIG performance has improved as the understanding of how to provide effective power-assisted lift or air cushion support at below hump speed has improved over time. A summary of this historical background is given in Chapter 2.

The four main alternative WIG designs are introduced briefly below to illustrate the design variations in these craft.

Classic WIG

The WIG is configured as a deep chord lifting wing with side plates or side buoys, without lift enhancement by fans or propellers, and is most suited to lower cruise speeds and lower load density. The key attribute for selection of this WIG type is its simplicity. Capital and maintenance costs will be lower for this craft type than other WIG craft. Smaller passenger WIG craft for commercial or utility tasks fit well with this configuration. The most efficient configurations developed to date are those using the reverse delta wing.

Fig. 1.12 Lippisch X-113

Many small craft and newer small passenger WIG are designed for relatively low take-off speeds and cruise speed. In this case, the main lifting wing can be designed with a low-pressure loading, and by incorporating a combination of anhedral, tapered chord and forward sweep, such a craft is relatively stable in flight. The propulsion system can be pylon mounted above the hull or on the tail. Outer winglets with dihedral can provide additional stability and so control in higher ground effect or free flight. An example of classic WIG, following a configuration developed by Alexander Lippisch in Germany in the 1960s and 1970s, is shown in Fig. 1.12.

Alexeyev's SM prototype series in the same time period showed that highly loaded lifting wings aimed at high cruising speeds close to 200 kph are less successful, unless supplemented by jet lift.

It is interesting that WIG configurations follow a similar pattern to aircraft, with lightly loaded wings for smaller slower (100–150 kph) craft, and propeller or ducted fan propulsion, and a graduation to jet or turbofan propulsion, and much higher wing loading for faster (200–450 kph) larger craft. With the additional options for including air cushions for slow-speed support, WIG configuration selection has many opportunities for the designer.

PARWIG

A pair of ducted air propellers or turbofans is mounted in front of the leading edge of the main wing to provide pressured air to create a dynamic air cushion. This ram air improves take-off performance and seakeeping below take-off speed by creating a high lift force at low speed that in turn leads to reduced hump drag and take-off speed, as well as reducing the slamming of the hull in waves. Take-off performance, hull strength, stability and seakeeping quality are all improved by this design approach, see [5].

In Fig. 1.13 curve 1 represents the lift–drag ratio of a WIG without forward-mounted ducted air propeller in calm water and curve 3 represents that with air injection, while curves 2 and 4 represent the craft without and with air injection in

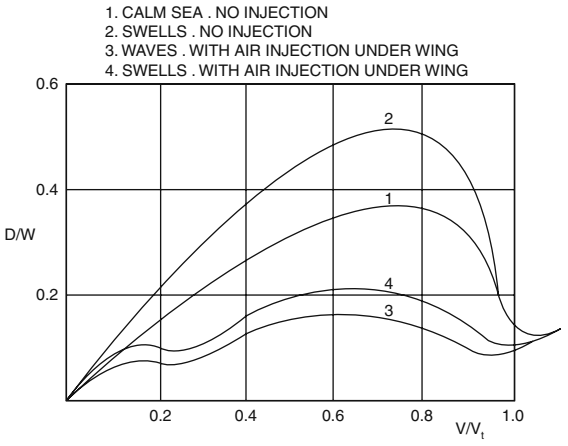

Fig. 1.13 Drag of WIG on calm water and waves with and without air injection

beam seas. It can be seen that hump drag is reduced significantly due to air injection under the main lifting wing by forward-mounted air propellers [6].

Similar results [7] are shown in Fig. 1.14 where the WIG and seaplane are compared. In the figure, curve 1 shows a seaplane and curve 2 the WIG with air injection (PARWIG), where L is the aerodynamic lift and W is the craft weight. One can see that the PARWIG aerodynamic lift during take-off is significantly higher than the seaplane.

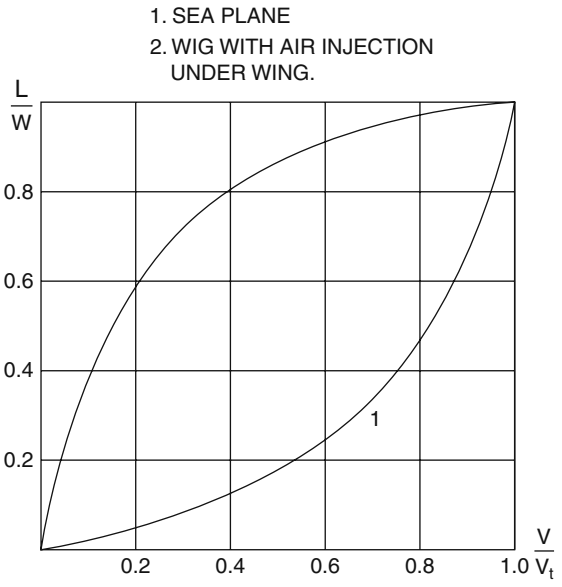

Fig. 1.14 Relative lift of seaplane and WIG with air injection

Air injection from forward-mounted air propellers or jets is very effective to improve the take-off performance, seakeeping qualities and "landing" characteristics, and so has been an important design improvement to the basic WIG concept. This technique has been used by the Russian Ekranoplan design team since the early 1970s.

Basic data for Ekranoplan built in Russia are listed in Table 2.1. The key PARWIG attribute is its potential for operation at very high service speeds and potentially also long range.

The different operation modes [8] can be seen in Fig. 1.15. The angle of the forward-ducted air propeller may be rotated downward before hump speed and take-off as well as when landing, to increase static lift. It is rotated to horizontal after take-off in order to increase the effective thrust and thrust recovery coefficient for maximum transport efficiency at cruise speed.

A typical first-generation Russian PARWIG is the so-called Caspian Sea Monster, see Fig. 2.7 a prototype designated "KM" in Russia. This experimental craft had a maximum take-off weight of 544 t. Examples of second-generation PARWIG craft in Russia are the "Orlyonok" and "Spasatel" with turbofans mounted in the fuselage nose and rotating exhaust ducts to direct the air jet under the main wing. Their leading particulars are listed in Table 2.1.

In order to improve the aerodynamics and stability of WIG craft, endplates are mounted at the tips of the main wing to increase its effective aspect ratio as shown in Fig. 1.16. Endplate design development together with secondary-extended winglets was a particular feature of second-generation Russian Ekranoplans, see [9–12].

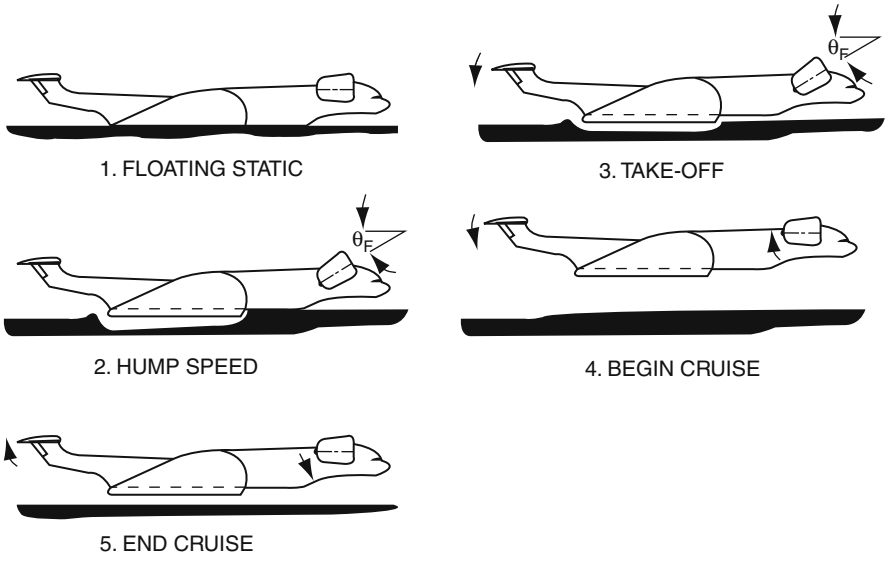

Fig. 1.15 Running attitude of WIG at various operation modes

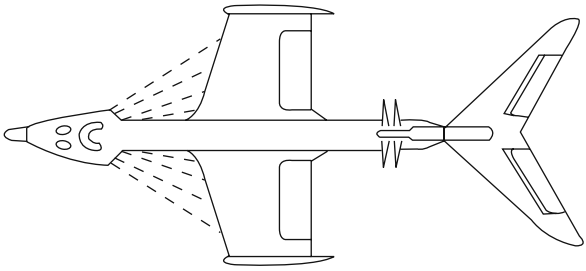

Ekranoplan 1

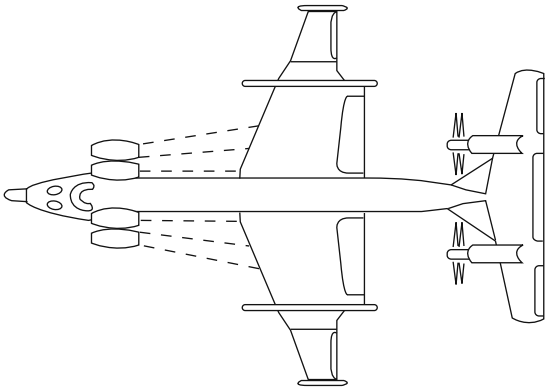

Ekranoplan 2

Fig. 1.16 Passenger WIG with composite wing (latest generation)

Although forward-mounted ducted thrusters were mounted on such craft to improve take-off, the lift force provided by the thrusters at zero forward speed was equal to only a part of the craft weight. The hump drag was reduced, but was still high. The craft still relied on the supporting part of its weight on the hull planing surfaces and moving through the displacement and planing modes of operation before taking off. On Orlyonok (Fig. 2.15), there are rotating bow-thruster nozzles, hydro-skis, and wheeled landing gear mounted on the craft. The landing gear is composed of two steerable bow wheels and nine main support wheels. With the aid of hydraulic actuators, the wheels can be retracted into the hull. The forward wheels are located behind the hydro-skis. The hydro-skis, landing gear and forward-mounted thrusters give the craft capability to drive up on a concrete apron, launch into water and operate over ice, snow and flat land or beach.

The two hydro-skis are located at bow and amidships, respectively. The ski is in a rectangular shape and linked to a hydraulic actuator for adjusting the vertical

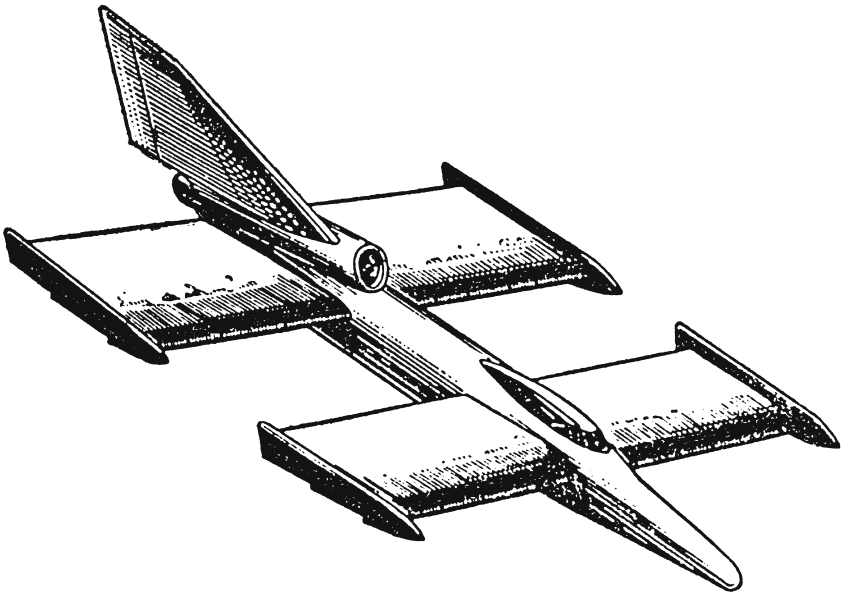

Fig. 1.17 WIG with tandem aerodynamic arrangement

position and angle of attack of the plate so as to improve the hydrodynamic properties of the craft during take-off. In addition, the hydraulic actuator can absorb wave slamming during take-off and touchdown, so as to protect the hull structure.

In order to maintain positive pitch stability, the initial design idea for Ekranoplans was similar to that used to ensure the longitudinal stability of the hydrofoils developed by Alexeyev, i.e. a tandem arrangement of main wings (Fig. 1.17). This gives very good longitudinal stability at low flying height along with improved craft hydrodynamics once at cruise speed, but it is difficult to arrange power augmentation under both wings.

The forward- and rear-wing configuration evolved gradually during WIG development to become the supporting and stability wings, respectively, and the rear wing evolved into a high tailplane configuration as on Orlyonok (Fig. 2.15). In order to keep good pitch stability, a large plane area is used. Sometimes it is as large as 50% of the main supporting wing area [7]. Some measures can be taken to decrease the tail wing area needed, such as using an S-profile main-wing camber line so as to improve the aerodynamic stability directly through the main-wing response to the changing angle of attack.

Most WIG craft have to be operated not only in the strong surface effect region but also higher in the ground effect region for short periods at least during turning and manoeuvring at high speeds. Both transverse and longitudinal stability therefore need control by surfaces similar to aircraft ailerons, tail stabiliser and rudder. Reliable manoeuvring control can only be assured by means of effective flaps and ailerons. Large high-speed craft need automated control systems similar in function

to an airliner's automatic pilot with more precise instrumentation to measure the craft in-flight parameters, as manual control would be extremely tiring for the pilot to maintain steady cruise altitude.

Due to lack of any height reserve for WIG flight, in contrast to an aircraft that has full freedom of movement in three dimensions, the requirements for reliability and response rate of automated control systems are very high [13]. The "Caspian Sea Monster" crashed over the Caspian Sea due to loss of control when at running at high speed. This was attributed to pilot error at the time, but the very complicated controls to maintain the craft in steady flight in its restricted flying height envelope made the Ekranoplan very difficult to fly at that time of limited automation. Pilots found the craft very difficult to handle, and so this might be one of reasons that led to the accident.

PARWIG Attributes

(a) The transport efficiency (power/[payload × range]) of a PARWIG is approximately twice that of an aircraft and 2–4.5 times that of ACV, SES and hydrofoils, see Chapter 13 [3]. This is due to flying in the surface effect zone (compared with aircraft in free air), the high aspect ratio of the main wing compared with DACC, and DACWIG, and the higher aspect ratio of the composite wing outboard of the main-wing endplate, see Tables 2.1 and 2.2.
(b) The cruising speed (or economic speed) of PARWIG is 3–5 times higher than ACV, SES, catamarans and hydrofoils and 10 times higher than displacement vessels, see Tables 2.2 and 3.1.
(c) Craft of this type generally have the ability to rise above the surface effect zone and fly in free air, so the manoeuvring space for the craft can be extended, and banking used to improve cornering manoeuvres. In addition, flying in the surface effect zone very close to the water/ground surface is a blind area for radar, so it is very suitable for military stealth applications.
(d) PARWIG size can in theory be significantly larger compared to large commercial aircraft where there are limitations due to airport and runway facilities available worldwide.

PARWIG Limitations

Due to its specific configuration some limitations restrict the operation and commercial opportunities as a passenger craft as follows.

Configuration: The PARWIG is difficult to operate alongside other craft and at jetties due to its protruding components such as main and tail wing. This also increases collision risk during slow-speed manoeuvring. In addition, the field of vision for pilots with the currently adopted arrangement of the cockpit is

limited, so that they are difficult to drive by eyesight. The pilot vision issue is simply solved with today's camera technology, while locating and designing terminals along the lines of a Hoverport or Seaplane terminal can provide a suitable operating environment.

Seaworthiness: There are three operation modes, i.e. hull borne, flying and transition mode between these two. The seakeeping quality of hull-borne operation and during take-off and launching is poor due to the high hydrodynamic impact loads acting on the hull. In addition, the motion in these phases is a little unsteady, due to the low righting forces from the buoyancy floats. Clearly, services should be designed to allow WIG to take off into cruising mode as quickly as possible. Shallow water "runway" areas close to the terminal are to be preferred. Once in flight, these craft operate smoothly in open water conditions.

Manoeuvrability: During hull-borne operation, the PARWIG can operate at speeds of 15–20 knots with no limitation of manoeuvrability, similar to a conventional monohull, while in flying mode the PARWIG will be operated at speeds of 300–400 km/h at a flight height of 3–10 m. The turning radius of PARWIG in such conditions is very large; moreover, the take-off distance of such craft is also long. It can manoeuvre neither as a ship on the water surface nor as an aircraft in free air. A WIG operating where other marine vehicles are present must take responsibility for manoeuvring around other traffic, due to its speed, while obeying normal marine collision avoidance rules.

Collision: The collision risk for PARWIG is higher than that of conventional fast marine craft, because of its extreme high speed so the navigation equipment on board needs to be able to respond consistent with vehicle speeds up to 500 kph. The limited height may cause some problems for collision avoidance radar in this respect to identify other small vessels.

Military Applications

The following statement may be found in Chapter 13 [2]:

> A principal operational requirement is the WIG craft's speed in relation to present logistical methods. The traditional image of amphibious vessels deploying landing craft to assault the beach in the face of prepared positions, can still be relevant. At the operational level of the military forces, the larger the geographical area the less easy it is to defend with fixed defences. It is possible to protect assets with speed of deployment, allowing the force to operate dispersed but to deploy concentrated. The speed over distance, or time taken to reach the theatre of operations, is the exact characteristic that a rapid reaction force must have.
>
> A characteristic that will have a significant impact on the WIG's future is the extent to which speed remains important, the WIG being faster than both the helicopter and the assault landing craft, and with greater range. To the operational analyst, a force including WIG

craft in its military planning will be able to reduce the time or increase the distance able to be reached.

One useful feature that has been mentioned is the ability of the WIG to carry and launch anti-ship missiles. The principal WIG that has such capabilities is the Russian Lun class. A number of advantages are apparent in that the height of the rocket trajectory is greatly reduced, and hence detection and response time is shorter.

The experience of using the Orlyonok WIG craft in the Russian Navy [14] has verified the following attributes:

- Speed similar to aircraft (5–10 times that of conventional marine craft);
- Possibility to take troops directly from and to the shore over long distances;
- Invulnerability from mines and torpedoes;
- High level of concealment from radar and satellite detection;
- Ability to maintain its operation in open sea conditions for a relatively long time, both in floating and at low-speed mode;
- Safe operation in the GEZ with inherent heave stability, ability to fly in weak GEZ and emergency landing.

The Russian WIG "Lun" carrying 6 "Mosquito" missiles with associated radio-electronic equipment carried out launch trials during the 1980s. The navy were concerned during these experiments about possible resonant vibration from the missile launch impulse forces that might reach magnitudes of 90 t per launch, and the effect on craft stability and structural integrity. Observations in [14] confirmed that motions of the craft in flight in reaction to rocket launch were about 0.5 m. They appeared to be safe for the craft operation and did not affect the craft performance, mainly because the WIG acted as a very powerful shock absorber.

The craft trials also showed advantages against any other existing missile-launching vehicles:

- Lun was able to be operated as an independent unit away from its base and temporarily stationed on any near-shore region;
- Low visibility for radar and other electronic devices;
- High payload capability compared to conventional vessels.

PARWIG should therefore be useful as the following:

- Naval Logistics and Landing craft, for example, the "Orlyonok", shown in Fig. 2.15 and Table 2.1;
- WIG missile craft, for example, the Lun as shown in Fig. 2.17. There are three twin missile launcher units on the craft, the right corner of the picture shows a missile launching from the craft. (The leading particulars are shown in Table 2.1.);
- Naval salvage craft, see also Fig. 2.18 and Table 2.1, showing the craft Spasatel which was rebuilt from the "Lun";
- Naval patrol or minelayer craft.

Civil Applications

The PARWIG should be suitable for civil use as a passenger/cargo ferry on medium to long over water routes in competition with aircraft. Craft in the size range 3,000 t displacement, 250–400 kph cruising speed, accommodating perhaps 3,000 passengers together with high value freight, operating in the medium surface effect zone with high aerodynamic efficiency ($K > 20$), will give excellent seaworthiness and comfort. On routes across the Pacific for example, a significant improvement in air traffic density could result.

Dynamic Air Cushion Craft (DACC)

This type of craft, Fig. 1.18, has one or two small aspect ratio lifting wings in tandem formation and a large cushion length/beam ratio. In addition, the craft has deepened sidewalls or buoys at both sides of the main wings, and flaps at the main wing trailing edge, creating a configuration similar to a ram air cushion supported platform, with the added ability to take off into surface effect flight.

Forward-mounted ducted air propellers blow pressured air into the cushion to enable the craft to statically hover both on ground and over water. They are designed to give the craft a high static lift–thrust ratio and thrust recovery coefficient. On the wing's upper surface, the under-pressured airflow from air accelerated by the propellers creates additional lift from the Coanda Effect once the craft is moving forward.

The static lift–thrust ratio (L/T_{so}) is as high as 6, where L is the lift and T_{so} is the bow-thruster static thrust, and creates a daylight clearance under the base plane of the craft similar to an amphibious ACV. DACC take off at low speed on calm water surfaces and are also amphibious, being able to operate on rough ground such as swampy areas, ice/snow and beaches. When operating at high speed over open water, the main-wing flap may be opened to give more effective high-speed

Fig. 1.18 Russian DACC type "Volga-2"

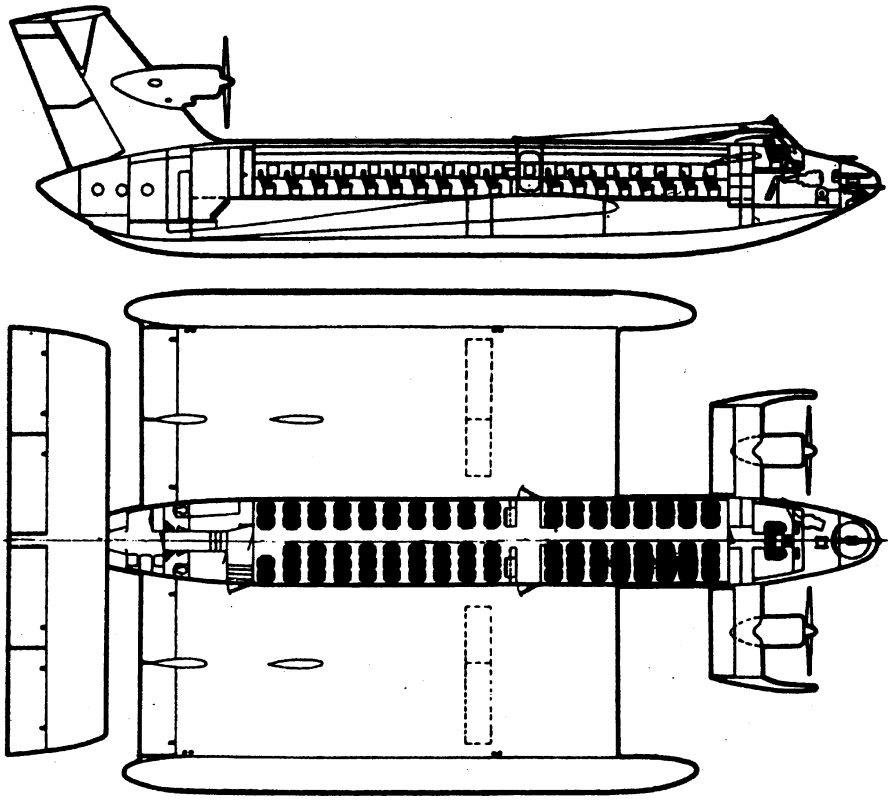

Fig. 1.19 Russian WIG type "Rocket-2"

aerodynamics; however, the lift–drag ratio of such craft is lower than that of the PARWIG (Ekranoplan) due to its smaller aspect ratio.

Figure 1.18 shows the Russian 8 seat DACC Type "Volga-2", and Fig. 1.19 shows a 90-seat craft of similar design. The leading particulars of such craft are listed in Table 2.2. The "Volga-2" has been in batch production for passenger transportation with seven passengers and one crew on each craft and is in service operating on a number of Russian inland waterways.

Two rotary engines, type BA3-413 drive ducted four-bladed air propellers located at the bow to provide pressurised air into the air channel during static hovering and before take-off, and thrust only at cruising speed.

Longitudinal stability in the various operation modes is controlled statically by the CG and the main-wing profile and dynamically by pilot control of guide vanes aft of the bow propeller, main-wing flaps and aft horizontal stabiliser. Course stability is maintained by differential thrust of the two propellers at low speed, and by the tail fin-mounted rudder at high speed.

There are inflatable structures (air bags) mounted under the main hull and side buoys to form flexible cushion seals. These absorb the impacting hydrodynamic load to improve passenger comfort and also protect the hull hard structure during operation on uneven ground, ice surfaces, sand beach and on water. The air pressure of the air bag can be adjusted to adapt to the surface that the Volga-2 travels over, rather like an ACV bag skirt. All of the hull structure, wings, rudders, stabilisers, side buoys, ducts, etc. are made of aluminium alloy.

Handling of the craft is simple, similar to driving an ACV, and needs no aviation training for the pilot. Tests have validated that the craft has almost the same hydrodynamic properties (lift–drag ratio) as an ACV, at the same displacement of both craft but for DACC at double the speed of an ACV.

Craft performance trials carried out in both summer and winter conditions have demonstrated the following:

- The craft is inherently stable in flight, resulting in simple handling;
- The craft also has low environmental impact, i.e. low wave-making in rivers, satisfactory external noise level, no harm to plants over which craft passing through, etc.;
- The craft has low hydrodynamic impact loads, favourable to passenger comfort, and hull structure design;
- Low craft capital cost, operating cost and reliability make it attractive for both passenger and small cargo transport.

DACC Characteristics

The leading particulars of some operational and paper design DACC passenger craft are listed in Table 1.1 as follows, see Chapter 13 [1]:

DACC Applications

The DACC can be useful as a pleasure or small passenger craft for rivers and coastal areas due to its easy handling and maintenance. It is unsuitable for open sea operation due to its small flying height. Larger DACC may be designed with capabilities approaching that of the DACWIG, while operating at lower service speed, which will be discussed in the following. Leading particulars of further craft are listed in Table 2.2.

Dynamic Air Cushion Wing-in-Ground Effect Craft (DACWIG)

This is a hybrid type of craft developed from the DACC and PARWIG, see [15]. The craft may be operated over water surfaces and ground in the strong ground

Table 1.1 Leading particulars of some Russian DACC and DACWIG proposed for operation on Gorky–Kasan route along the Volga River

Type	Volga-2 (Fig. 1.18)	Rocket-2	Rocket-2.2 (Fig. 1.19)	Meteor-2	Kometa-2 DACWIG	Virheli-2 DACWIG
Passengers	8	50	90	120	150	250
Classification in Russian Register	<L>	<O>	<O>	<O>	<M>	<M>
AUW (t)	2.5	16	31	32	42	105
Length (m)	11.4	16	31	32	42	54
Width (m)	7.5	14.9	19.5	20	25	28
Draft (m)	0.2	0.35	0.5	0.45	0.5	0.7
Type of engine	BAZ-413	TVD-10 Type M601	TVD-117A	TVD Type AP-24	TVLD Type D-36	TVLD Type D-36
Number, power (kw)	2, 103	2, 662	3, 1840	2, 1840	2, 6.5 t thrust	4, 6.5 t thrust
Speed (km/h)	120	150	180	170	185	280
Range (km)	500	500	800	800	930	1,000
Seaworthiness (m)	0.5	1.3	1.2	1.5	Seastate 4	Seastate 5
Crew (in operation)	1	3	3	4	4	6
Crew (total on board)	2	6	6	8	8	12

Fig. 1.20 Chinese passenger DACWIG type "SWAN"

effect region, where $h/c = 0.1$–0.15 (c is the main-wing chord). The aerodynamic arrangement of the craft has similarities to the DACC; however, some measures have been taken to provide stability when operating above the strong ground effect region. The craft is unable to operate completely above the ground effect, so no complicated automatic control system and/or other equipment on the craft to assure its stability during flying is required. A craft typical of this type is the Chinese WIG "Swan" (Fig. 1.20)

The DACWIG combines the advantages of the PARWIG high-speed and good seakeeping qualities after take-off, and the DACC amphibious capabilities, easier handling and less-expensive construction. The DACWIG has sufficient flying height to enable operation in coastal or open ocean areas, depending on the craft size.

DACWIG Attributes

The DACWIG is a development of PARWIG but with a fully developed dynamic air cushion under the main wing at zero speed to support the craft for manoeuvring and take-off. This leads to attributes as follows:

Intermediate high-speed and transport capabilities: The speed of DACWIG is double that of hydrofoils and ACV/SES with same lift–drag ratio. The design cruising speed can be as high as 150 knots based on current design experience.

Economy: Table 1.2 lists the leading particulars and transportation efficiency as well as the fuel consumption of various high-speed vehicles, where

$$K_n = WV_s/(102N) = \eta W/D = \eta_t \eta_p W/D = \eta_t \eta_p K$$

where

W	Craft weight	(kg);
V_s	Craft speed	(m/s);

N	Power output	(kw);
η	Propulsion efficiency;	
η_t	Transmission efficiency;	
η_p	Thruster efficiency	(including hull coefficient);
D	Drag of craft;	
K	Lift–drag ratio.	

From the formula, it can be seen that the non-dimensional coefficient K_n represents only the hydrodynamic characteristics of the craft, without relating to the construction technology, the specification of the main engine, equipment, etc.

From Table 1.2, it can be seen that DACWIG can operate at Froude number close to that of other high-speed craft or be designed for speeds 2–3 times higher, at improved transport efficiency. Due to the reduction in power needed to be dedicated to air cushion feed at the cruising speed, the fuel consumption of the craft at cruising speed is also lower and close to the other high-speed vessels with lower speed. Fuel consumption over calm water and with no wind (kg/person-km) has been estimated for these different craft types based on general references and test results, as follows:

SES	($V = 60$–80 km/h)	0.03–0.05
ACV	($V = 70$–90 km/h)	0.035–0.05
DACC and DACWIG	($V = 120$–160 km/h)	0.035–0.065
Small low-speed aircraft	($V = 100$–500 km/h)	0.04–0.07
Conventional planing monohull	($V = 60$–80 km/h)	0.07–0.13

Operational characteristics: The DACWIG is able to operate efficiently both at medium speed when cushion borne and flying at higher speeds in the ground effect zone. The craft can therefore be operated in an open seaway as well as on rivers or estuaries. Its slow-speed air cushion even allows the consideration of semi-amphibious operation in wetland areas. Since the craft has a strong air cushion, it has a higher lift–drag ratio at very low flight height. The craft also can be hovered statically over ground, so it is amphibious, and has low-speed manoeuvrability similar to an air cushion vehicle without a flexible skirt. Moreover, wave-making caused by the craft is small due to its low cushion pressure, which may lessen influence on the operation of nearby small marine craft.

Inherent stability in strong ground effect region: From Fig. 1.10, it can be seen that the lift–drag ratio (or lift–thrust ratio) will increase significantly with decrease of non-dimensional flying height into the strong ground effect region ($\bar{h} = h/c < 0.1$, where h is the flying height and c is the chord of main wing). The craft has inherent longitudinal and transverse stability and does not need an active control system for running trim.

Table 1.2 Leading particulars and performance parameters of fast-transportation vehicles

Craft type	DACWIG	DACC	Small aircraft	Light aircraft	Helicopter	Hydrofoil	ACV	SES
Model	Swan	Volga-2	Y-11	AH-28	AS332C	Jetfoil	7113	SEMO-SES
Country	China	Russia	China	Russia	France	USA	China	South Korea
Production status	Design	Batch production	Batch	Batch	Batch	Batch	Design	Batch
Total weight (kg)	6,500	2,500	3,500	5,800	8,350	11,500	26,000	167,000
Payload (kg)	1,400	900	940	2,000	2,734	2,900	4,000	40,000
Seats	20	9	7	15–19		290	47	350
Machinery	HS-6A Aviation piston engine	VA-413	HS-6A Aviation piston engine	Turbo propeller	Turbomeca Makila	Allison 501-K20A Gas Turbines	Deutz diesel	2 × MTU16V-396TE74 2 × GM12V-92TA
Cost, US$/seat, ($000)	20–25	Not available	100	100–200	>200	62	17	17
Total power (kw)	3 × 210	2 × 103	2 × 210	1,385	2 × 1,327	5,456	1,150	4,998
Speed (km/h)	130–150	120	170	350	280–296	78	83	83–92
Fn	4.0	4.2	n/a	n/a	n/a	1.3	1.67	1.3
Transport efficiency (K_n)	3.6–3.8	4.0	3.9	3.16	2.4	4.2	5.13	7.0

Safe and reliable handling: The craft can be operated safely due to its strong ground effect and inherent stability. Operating in this ground effect zone, handling is similar to an ACV [15].

Good seakeeping: The craft will have low hump drag both on calm water and in a seaway due to its strong dynamic air cushion. It possesses good take-off and touchdown ability, and small slamming loads on the hull in rough seas. For instance, a DACWIG with 90 seats, 32 t overall weight and a flight height of 1.8–2.7 m can be operated safely in seas with a significant wave height of 2.5–3.5 m, as the cushion will be effective enough to ensure contouring over the largest waves in such a seaway. In addition, since the cruising speed of the craft is very high, say about 80–120 knots, and the encounter wave frequency is higher than the natural frequency of the craft pitching and heaving, the craft will be running in supercritical mode. As a result, the speed loss of the craft due to both wind and waves will be smaller than ACV/SES and other high-speed vessels. The craft can be operated in platforming mode for most of the time, with minimised vertical motion and accelerations.

Medium cost construction and maintenance: The cost of DACWIG will be lower than aircraft and PARWIG, and only a little higher than ACV (Table 1.2). The DACWIG can be designed following seaplane practice and without special equipment (hydrofoil for hydrofoil, flexible skirt for ACV/SES, landing gear and pressurised fuselage for aircraft, automatic control systems for PARWIG and hydrofoil, etc.).

DACWIG Applications

The DACWIG operates on or very close to the water surface and will be able to comply with the navigation rules, equipment, safety code, instruments and observation for navigation complied with by conventional high-speed vessels, such as SES, ACV, CAT, hydrofoil, WPC and SWATH.

The DACWIG is suitable as a fast sea and river civil transport, at speeds 2–5 times the current service speed for fast ferries (30–50 knots). Relative to the PARWIG, it is a slow craft and has lower aerodynamic efficiency due to the low aspect ratio, lower flying height, etc., but this is compensated by the air cushion effect, to bring the overall transport efficiency up to an attractive level. In short, the DACWIG as well as DACC are most suitable for commercial application as ultra high-speed passenger craft either in inland waterways or on coastal routes.

The DACWIG has similarities to a DACC due to the low aspect ratio of the main lifting wing that contains the air cushion, and pressured air-jet cushion feed supplied by the forward thrusters. From the point of view of operational flight height, it is similar to the PARWIG, while being unable to operate beyond the ground effect zone. It can be thought of as a hybrid derived from both DACC and PARWIG (Fig. 2.34).

Chapter 2
WIG Craft Development

Introduction

Our aim in this chapter is to introduce the reader to the WIG development programmes carried out in a number of countries in the last half of the twentieth century and up to date, so as to give a historical perspective on the origins of the technology.

Prior to this, ground effect was already being used for flying machines. In 1903, the Wright Brothers flew relatively long distances in the surface effect zone with their biplane. They were aware of the higher lift forces when gliding close to the ground, but were aiming to fly higher into the air.

Later, in the mid-1930s, Kaario of Finland started to build and test craft operating in strong ground effect, see [1]. Kaario's concept was for a high-speed boat that could glide over ice as well as water. However, due to greater interest in the aeronautical industry for development of passenger aircraft, floatplanes and seaplanes, the captured air bubble craft built by Kaario was not developed further. It was 30 years later, at the beginning of the 1960s, that Alexeyev began his development of Ekranoplans in Russia. The Russian R&D was the world's first major WIG programme, targeted at a new military capability, so we will begin by reviewing it together with the steps leading up to it.

Russian Ekranoplan Development

Two major research and development initiatives were undertaken in Russia to increase ship speeds in the twentieth century. The first initiative in the 1940s and 1950s was aimed at breaking through the so-called wave-making barrier and so decrease wave-making resistance at high speed. The second initiative was to lift a marine craft completely from the water surface to glide just above it.

All displacement-type marine craft cause a pressure wave pattern as they move through the water. This wave-making exhibits itself as a water surface deformation and also as a resistance to motion that increases in proportion with the square of forward speed. High-speed craft with inclined, flat lower surfaces rise out of the displacement mode into "planing" mode once the dynamic pressure of the water on

L. Yun et al., *WIG Craft and Ekranoplan*, DOI 10.1007/978-1-4419-0042-5_2,

the inclined underside becomes high enough to balance the craft weight. The power needed to enable a boat to accelerate to planing mode is very high and was only achievable until recently by small craft such as racing powerboats and military fast patrol boats.

In the 1950s, marine engineers in Russia and Switzerland adopted an alternative way to lift the hull of a boat clear of the water, by attaching lifting foils under the hull to produce hydrodynamic lift in a similar way to the wings of an aeroplane. In water, 800 times denser than air, the foils can be relatively small. This idea was developed in Russia by a naval architect, R.Y. Alexeyev.

The hydrofoil craft, as defined by Alexeyev, had shallow submerged hydrofoils located under the water surface, however still in the region where the pressure field around the foil is strongly affected by the water surface itself. The hydrofoil lift reduces rapidly as the draft of the hydrofoil decreases and the hydrofoils approach the water surface. In Russia, this is called the Alexeyev effect after its discoverer. Alexeyev was the first to use this effect together with a tandem configuration of hydrofoils to provide longitudinal stability, avoiding the problems that occurred on very early hydrofoil prototypes. This success led to the building of significant numbers of both river and seagoing hydrofoil passenger ferries in the Former Soviet Union in the period from 1949.

A whole series of different hydrofoils were developed and built in series production, including the river craft "Volga", "Raketa", "Meteor", "Sputnik", "Chaika", "Byelorus"; and seagoing hydrofoils "Kometa" and "Vikhr". The passenger capacity of these craft was from about 30 up to 300 seats. They had service speeds up to 100 km/h. More than one thousand such craft have been constructed in the Former Soviet Union and operate in domestic rivers, lakes and seas. A significant number have also been exported to over 30 other countries for service on rivers such as the Danube and Rhine and in the Mediterranean and Aegean seas.

Hydrofoils can operate at speeds up to 130 kph; however, at this speed another barrier is met – the so-called cavitation barrier – which limits the further increase of speed due to the cavitation phenomenon that occurs on the hydrofoil's upper surface. This effect reduces the lift force and increases drag of the foil. The effect is similar to propeller cavitation. When the pressure on the foil's upper surface drops below water vapour pressure, a bubble of vapour is formed and the lifting force reaches a limit. As forward speed increases, the cavity will grow and limit the lifting force, unless the foil geometry is specifically designed to operate in this mode. Such foils have a sharp leading edge form and are less efficient at speeds below the cavitation region [1]. Hydrofoil craft designed for very high speeds therefore require much higher power density and are less economical for commercial service.

The new idea proposed by Alexeyev at the end of the 1950s was to put aircraft wings onto a high-speed boat and lift the hull out of the water to glide just above it supported by aerodynamic lift. Such a concept would also require aerodynamic propulsion. It was the logical extension of his shallow submerged hydrofoils providing hydrodynamic lift to clear the hull from the water surface.

A most important contributor to stable flight is lift force variation with the distance from the foil to the water surface (screen or "ekran" in Russian), which allows

a WIG craft to fly at a steady clearance height, the most important design challenge for WIG craft [2]. The shallow submerged hydrofoil and aerofoil close above the water surface can be considered as a mirror image of each other. In the case of a surface piercing hydrofoil (Fig. 2.1), the lift force of the foil decreases with the decrease of the foil draft. In the case of an airfoil (Fig. 2.2), the lift force increases with the decrease of flying height of the wing.

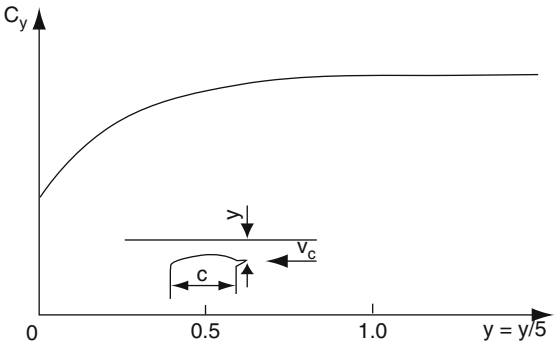

Fig. 2.1 Lift coefficient versus relative immersed depth for hydrofoil craft

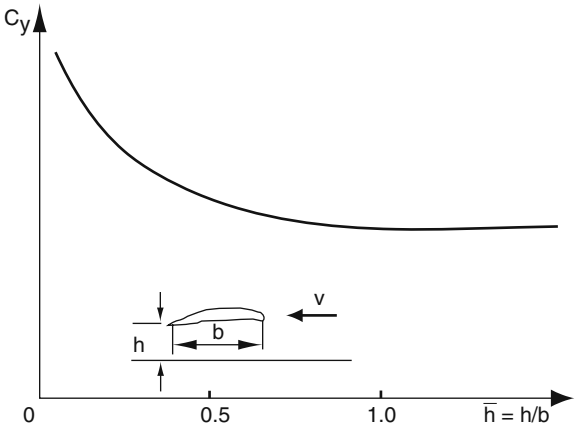

Fig. 2.2 Lift coefficient versus relative flying for WIG

Alexeyev together with the team at his design institute designed and constructed the first WIG test craft, SM-1, in 1960 (in Russia, this designation stood for self-propelled model number 1), with twin wings in a tandem arrangement and weighing 2.8 t (Fig. 2.3). The design was derived from his shallow submerged hydrofoil craft [3]. SM-1 had a 20-m long cigar-shaped fuselage and tandem lifting wings at amid-ships and at the stern. Side plates in the form of wing tip floats were installed on the main wing and tail wing to reduce the tip vortices so as to increase the lift/drag ratio of the craft. Power was provided by a jet engine mounted above the fuselage aft of the forward wing. SM-1 had a crew of three and was tested over calm water

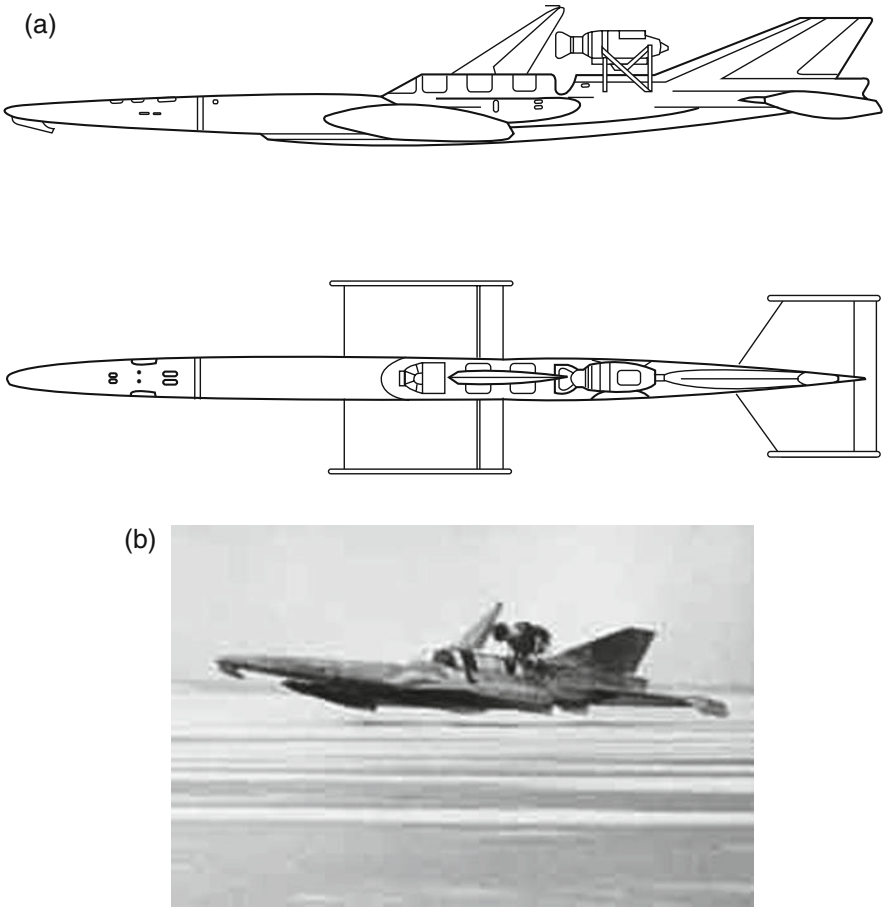

Fig. 2.3 SM-1 (**a** diagram, **b** pic)

at speeds of 200 km/h. It first flew on 22 July 1961. The trials of this craft showed up the problems of the low mounted rear wing to provide steady stabilisation. The rear wing of SM-1 operated directly in the rather unsteady slipstream of the forward wing, so causing the craft to be unsteady in pitch.

SM-1 proved the basic principles; however, it also demonstrated several problems with the configuration, as well as the pitch instability. It had a very hard ride due to high reaction forces/accelerations to wave surface undulations and a very high take-off speed from the water surface (about 150 km/h). It also had rather low pitch stability. SM-1 crashed in January 1962 from engine failure when in a climb manoeuvre. All the crew survived the crash without injury.

Modification of the tandem airfoil arrangement could not solve the "hard" ride problem as all the lifting surfaces of such a wing system operate in strong ground effect and interfere with each other. Alexeyev developed a new aerodynamic arrangement to overcome the problems of SM-1. In the new arrangement one main

wing supported the craft in the ground effect region and another horizontal tail stabiliser wing was mounted at the top of a vertical fin outside ground effect to maintain positive longitudinal stability. A first step was also taken by Alexeyev to decrease take-off speed by mounting a jet engine in the bow to deliver pressurised air through a diffuser system under the main wing giving added static lift to the craft.

These design developments were built into a second test craft, the 5 t SM-2 completed in March 1962 (Fig. 2.4a, b). This craft was similar in size to SM-1 and was demonstrated to the President of the USSR Nikita Khrushchev, gaining his support for the Ekranoplan development programme.

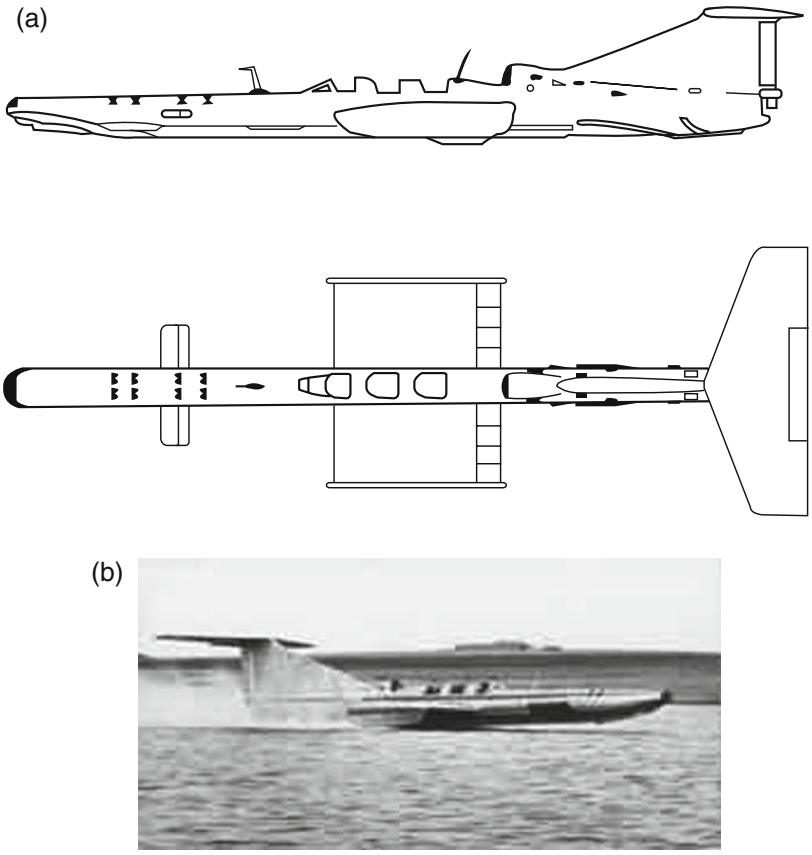

Fig. 2.4 SM-2 (**a** diagram, **b** pic)

The original SM-2 was damaged in a hangar fire and was subsequently modified and given the designation SM-2P after installation of a high mounted rectangular tail wing. The tail wing size of SM-2P was increased compared to tandem winged SM-2, and the RU-19-300 jet engine producing about 1 t of thrust was enclosed in a nacelle at the base of the vertical tail fin. A second RU-19-300 was mounted in the nose and provided jet air augmentation to the main-wing lift from a bank of

Table 2.1 The initial series of Ekranoplan prototypes

	SM-1	SM-2P	SM-3	SM-4	SM2-P7
Build year	1961	1962	1962	1963	1964
Length (m)	20.0	20.0	14.5	20.0	19.4
Main wing span (m)	4.50	5.25	3.80	7.50	9.4
Tail wing span (m)	3.70	6.70	4.10	7.30	8.5
Tail height (m)	3.15	3.40	2.80	3.60	3.5
Hull breadth (m)	1.0	0.9	0.9	0.9	0.9
Hull height (m)	1.4	1.5	1.3	1.96	1.6
Draught (m)	0.3	0.4	0.3	0.5	0.4
Aspect ratio, main	1.26	1.73	0.48	2.0	1.73
Tail	1.35	2.00	2.00	2.0	2.0
Pilot and passengers	1	1	1	1	1
AUW (t)	2.83	3.20	3.40	4.80	6.3
Thrust (t)	1.0	1.8	1.0	3.0	2.0
Engine	1 off	1 off		1 off	
stern	TS-12L	RU-19-300		KR7-300	
Engine		1 off	1 off	1 off	1 off
bow		RU-19-300	RU-19-300	RU-19-300	KR7-300
Take-off speed (kph)	170	160	140	140	140
Maximum speed (kph)	270	270	180	230	270
Cruise speed (kph)	250	250	160	200	250
Flying height (m)	0.5–1	0.5–2	0.5–2	0.5–2.5	0.5–2.5
Maximum seastate (m)	0.5	0.5	0.5	0.7	1.0

nozzles halfway between the nose and the wing. This craft showed that the revised configuration was stable in flight (see Table 2.1 above for characteristics of the early series of craft including SM-2P).

Later in 1962, SM-3 was designed and built (Fig. 2.5a, b). This developed the configuration of SM-2 further, with a much longer, low aspect ratio main lifting wing and smaller tail wing. The crew of three had enclosed cockpits. The main jet engine intake was moved right forward to the nose of the fuselage, and the exhausts from the single RU-19-300 jet blown underneath the leading edge of the main wing. SM-3 began to explore the potential for higher lifting capacity craft. Unfortunately, the low aspect ratio wing did not appear to offer the ideal solution, particularly at higher speeds. Above about 1.5 m flying height the yaw stability of the craft was insufficient for steady flight. Clearly the low aspect main wing was only suitable for small ground clearance concepts.

SM-3 was succeeded in 1963 by the SM-4 (Fig. 2.6a, b), based on the SM-2 configuration, but using a larger KR7-300 jet in the bow driving the lift enhancing system. This jet had a thrust of 2 t, compared to the RU-19-300s 1 t. The maximum take-off weight of this craft was 4.8 t compared with SM-2 at 3.2 t.

SM-4 performance was so encouraging that the design bureau began plans to build a very large WIG, the KM late in 1963 (Fig. 2.7). Prior to building the KM itself, a 1:4 "model" was built. This was the test craft SM-5 (Fig. 2.8). SM-5 had a similar configuration to SM-4, powered by two KR7-300 jet engines and a take-off

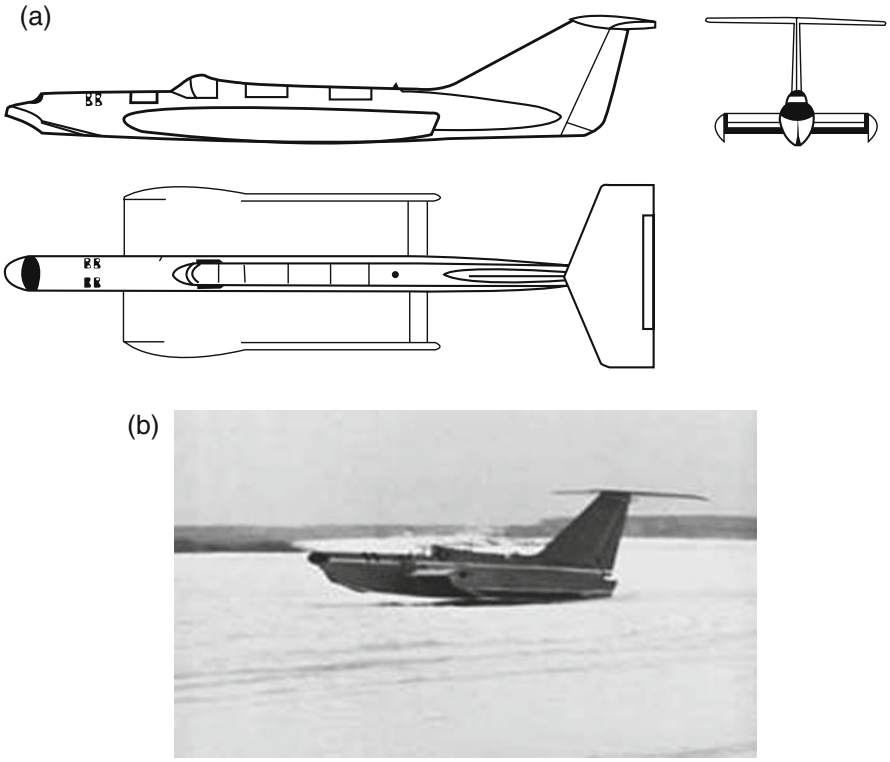

Fig. 2.5 SM-3 (**a** diagram, **b** pic)

weight increased to 7.3 t. The blower nozzles at the bow were moved higher so that at high speed the efflux would not destabilise the aerodynamics of the main wing.

Tests with SM-5 were short lived as the craft crashed in 1964, unfortunately killing the pilot. Flying against a strong wind during a trial run, the craft started to gain height. The pilot increased power instead of reducing, further gaining height and losing stability, after which the craft ditched.

Also in 1964, a further new test craft was built with revised bow jet blowers closer to the main wing and higher aspect ratio tail wing, the 6.3 t SM-2P7 (Fig. 2.9), with a single bow-mounted KR7-300 for power. This craft was able to cruise at 250 km/h with a wing efficiency K of 10–11. Take-off speed was approximately 140 km/h after a 600-to 800-m run.

This work completed the research targeted at developing the very large cargo and personnel carrier KM, so that further research craft could look at configurations suitable for smaller logistics craft. The SM-6 was the first of these, a smaller scale version of the Orlyonok production design. SM-6 (Fig. 2.10) was designed and built in 1972, following completion of KM, so that experience with the much larger craft could be included.

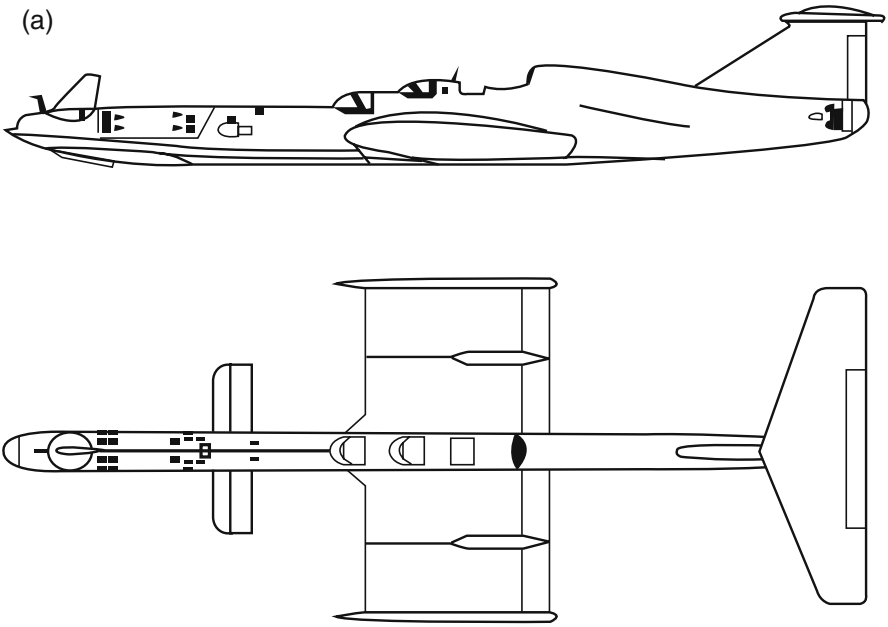

Fig. 2.6 SM-4 (**a** diagram, **b** pic)

Extending the fuselage to 31 m and the main wingspan out to 14.8 m, SM-6 used a turbo-propeller gas turbine AI-20 K at the top of the tail fin for main propulsion and a revised bow blower system also powered by two RD-9A jets for lift augmentation. This craft operated at 26.5 t at speeds up to 350 km/h and had an endurance of 700 km.

In parallel with this work, a further quarter-scale prototype of the KM was built in 1967 with similar specifications to SM-5 but with a high dihedral tail wing, and bow engine intake modified to reduce spray ingestion. This craft had the designation

Fig. 2.7 KM

Fig. 2.8 SM-5

Fig. 2.9 SM-2P7

SM-8 (Fig. 2.11). Test prototypes designated SM-9 and SM-10 were also built, but are related to the Volga-2 programme, see Table 2.2 .

Fig. 2.10 SM-6

Fig. 2.11 SM-8

KM or "Caspian Sea Monster"

Normally, a medium-size craft weighing 50–100 t would be designed and constructed following the successful self-propulsion tests of a craft such as the SM-5 and SM-2P7. Alexeyev believed that the aerodynamic and hydrodynamic characteristics were predictable enough that a step directly to a production craft was possible. He was able to convince the Russian Navy of this approach and gain their support for funding the 500-t KM immediately. In Russian KM stands for "Naval Ship Prototype", not "Caspian Sea Monster" [4]. The craft was 92.3 m overall length, 37.6 m maximum width, 22 m maximum height and weighed 544 t, almost twice that of the Boeing 747 jet airliner models available at that time, then the largest aircraft in the world.

The KM accommodated 900 marines and flew at a maximum speed of 300 knots (470 kph) at an optimal flying height of between 4 and 14 m. Eight VD-7-NM turbojet engines with 13 t thrust each were mounted at the bow for starting and

Table 2.2 Development series for the KM Ekranoplan

	SM-5	SM-8	KM
Build year	1963	1967	1966
Length (m)	18.0	24.5	92.4
Main wing span (m)	9.5	9.5	37.8
Wing area (m^2)			662.5
Tail wing span (m)	9.5		
Tail height (m)	5.5	5.5	21.8
Hull breadth (m)	2.0		
Hull height (m)	2.5		
Hull draught (m)	0.6		
Aspect ratio, main	2.0	2.0	2.0
Tail	2.0	2.0	2.0
Pilot and passengers			3 + 900
AUW (t)	7.3	8.1	544
Thrust (t)	4.0	4.0	104 + 26
Engine stern	1 off KR7-300	1 off KR7-300	2 off VD-7 M
Engine bow	1 off KR7-300	1 off KR7-300	8 off VD-7
Take-off speed (kph)	140	140	140
Maximum speed (kph)	230	220	500
Cruise speed (kph)	200	200	430
Flying height (m)	1–3	1–3	4–14
Maximum seastate (m)	1.2	1.2	3.5
Range (km)	n/a	n/a	1,500

take-off, and two VD-7-KM turbojet engines with 13 t thrust each were mounted at the stern for cruising. More detailed specifications can be found in Table 2.1.

The design was completed at 1963–1964 incorporating the results from SM-5 and SM-2P7. Some corrections to the craft structural design were also made based on the tests of the smaller prototypes. The KM was constructed at the "Chikarov" Naval Construction Facility nearby to Gorky city and was completed in 1966 (Fig. 2.7).

The newly launched craft was towed to the WIG test base on the Caspian Sea coast through the Russian river system for its sea trials. The first flight was on 18 October 1966. It lasted just under an hour and tested flight at clearances up to 4 m. Take-off speed was not above 140 km/h, and the craft proved it could fly stably at a cruise speed of 450 km/h at a flying height of 3–4 m as well as over waves of 3 m height in later tests.

Take-off is achieved by running the eight bow-mounted jet engines with thrust nozzles turned down to blow under the main lifting wing at maximum power. Once lifted from the sea surface, the nozzles can be turned horizontal to provide more thrust to accelerate. Once at cruise speed they can be throttled back and the rear-mounted cruise engines used for propulsion.

When stopping, the reverse procedure is employed. First, power is reduced so that craft speed can be slowed to about 210 km/h and flying height reduced. The bow jets' nozzles are then rotated down to augment the lift force. The cruise engines

are shut down and the speed slowed so that the craft settles on its dynamic cushion. Subsequently the hull touches down at about 120 km/h and planes down to displacement mode at 30 km/h or so.

The KM did not have automatic flight controls, so all of these procedures and the rather active adjustment of flight controls to maintain steady flight at cruise were carried out manually by the flight crew.

The KM generated very heavy spray at low speeds (Fig. 2.12), and in addition the bow turbines were prone to bird strike. Intake shields were fitted to the bow turbines, and the cruising engines moved from the base of the tail fin to a pylon between the bow engines in 1979.

Fig. 2.12 KM at low-speed generating spray

During one trial, in order to demonstrate good ditching stability, Alexeyev ordered the engines deliberately stopped and let the craft ditch without control intervention. The craft was able to land horizontally and safely. It gave the pilots on board at the time much improved confidence, flying at such high speed close to the surface. The craft also had excellent manoeuvrability such that it could complete a 360° turn by banking as far as the inner wing tip touching the water surface.

Mr. Alexeyev was a very experienced airplane pilot himself, so he generally explained the flying features of the WIG craft to pilots from the Russian Air Force himself. In particular, it was his experience that

> As an airplane pilot, one often realizes that the airplane would be safer if it would be less interactively flown. However, on a WIG, it is to the contrary. If a WIG rises above the ground effect region, the pilot should take measures to decrease the flying height, such as to throttle down the engine speed or decrease thrust so as to decrease the speed of craft below the normal cruising speed of 250 km/h temporarily. When the craft is to be brought to a stop from cruising speed, the pilot must first throttle back the stern engines, while changing the bow engines from cruising mode to blowing air mode and establish the air cushion under the wings. At the same time the main wing flap has to be dropped down. The craft will then touch down smoothly and safely.

If the procedures for adjusting bow thrusters to establish cushion lift augmentation when slowing down are not followed, a WIG may decelerate very quickly on touching the water and damage can occur, as happened on earlier test craft, and "KM" itself in 1980 [4]. In December of that year, the pilot attempted to change to cruise mode before having lifted off. The craft crashed into the sea and sank. The crew were safe, but recovery attempts for the craft were unsuccessful, the structure having broken up as it crashed and sank in the Caspian Sea.

Over its 14-year operational career, the KM wore a number of different tail numbers as it progressed through different test phases. This rather confused the western military observers, who thought that there may be up to ten KM craft!

UT-1

The SM series of test craft and the KM were very expensive craft to operate and so it was decided to build a low-cost pilot training Ekranoplan, the UT-1 (Fig. 2.13). This was a small craft with a single aircraft piston engine driving a propeller mounted above the central fuselage or hull. UT-1 was used as the test bed for the hydro-ski or shock absorber ski. This was a hinged plate mounted under the centre of the hull at the place where a step would be introduced on a single step hydroplane. The ski could be adjusted in angle and was used to improve take-off performance (reducing power and take-off run distance). Its success led to development of the much larger skis used on Orlyonok, Lun and Spasatel.

Fig. 2.13 UT-1

Orlyonok and Lun

Successful trials and operation of KM showed longitudinal and transverse stability in flight to be adequate, and its manoeuvrability and course stability satisfactory to the requirements of the Soviet Navy. Alexeyev and his colleagues therefore began design of a smaller military WIG, the heavy-duty landing craft "Orlyonok". Their initial task was to complete a small-scale prototype, as described above, the SM-6, at 0.5 linear scale to the production design.

Leading particulars of Orlyonok are as shown in Table 2.3 and below. The craft profile as well as some cross sections of the craft are shown in Fig. 2.14 and the general arrangement in Fig. 2.15.

Maximum length, width and height (m)	58, 31.5, 16
Maximum take-off weight (t)	140
Payload (t)	250 marines or 20 t military equipment, which could enter or exit from bow ramp
Lift engines	Two HK-8 gas turbine turbofan engines located at the bow with maximum thrust of 98KN, the nozzles of which can be rotated down to provide a positive cushion pressure under the main wings in take-off and used for additional thrust when rotated horizontal at cruising speed
Propulsion engines	One HK-12 gas turbine turbo-propeller engine rated at 11,030 kW located at the top of the tail fin driving contra-rotating propellers
Performance	The craft can operate at maximum speed of 350 km/h, at flying height of 2 m with a maximum range of 1,000 km

Orlyonok was designed to come ashore onto a concrete apron at its main operating base, so was fitted with a wheeled undercarriage. There are two rotating bow wheels and nine main support wheels located under the main hull. The bow wheels can be retracted with aid of hydraulic systems into the main hull and behind a large hydro-ski installed close to the hull centre. The rotating bow thruster nozzles (1), landing gear (2), hydro-ski (3), together assures efficient launch and landing operation and take-off performance. From Figs. 2.14 and 2.15, one can see the contra-rotating propellers mounted at the top of the tail fin for cruising and flaps on the main wings for improving stability.

The aspect ratio of Orlyonok's main wing is also extended from 2.0 (KM configuration) to 3.07 so as to improve the high-speed aerodynamic properties of the wings. This craft layout was called airplane style in the Former Soviet Union and achieved the following characteristics:

- Main-wing aerodynamic efficiency, $K = 15.0$, in operation close to the ground or water surface and 9.0 for the higher clearance strong ground effect zone
- Stability and self restoring characteristics to perturbations are acceptable over a wide range of operating pitching angle and flying height, including the ability to fly above the ground effect zone
- Manoeuvrability of the craft in the longitudinal and lateral planes that met the requirements specified by the Soviet Navy staff
- Range when flying at cruise speed in ground effect is 1,000–1,500 km
- Craft of Orlyonok size can take off and touch down on the sea surface in 1.5-m waves

Table 2.3 Development series for the Orlyonok, Lun and Spasatel

Data	UT-1	SM-6	Orlyonok	Lun	Spasatel
Build year	1967	1972	1973–1980	1986	1996
Length (m)	9.7	31.0	58.1	73.8	73.8
Main wing span (m)	5.4	14.8	31.5	44.0	44.0
Tail wing span (m)		12.2			
Tail height (m)	2.0	7.9	15.9	19.2	19.2
Hull breadth (m)			4.0		
Hull height (m)					
Draught (m)	0.2	0.6	1.5	2.5	2.5
Aspect ratio, main	2.2	2.8	3.0	3.0	3.0
Tail			4.0	4.0	4.0
Pilot and passengers	1		9 + 250	9 + 19 + 150	9 + 19 + 650
AUW (t)	0.9	26.5	140	380	390
Payload			20	137	143
Thrust (t)	140 shp	4.2 + 3,750 shp	2 × 10.5 + 15	78 + 26	78 + 26
Engine stern	1 off M332	1 off AI-20 K	2 off NK8-4	2 off NK-87	2 off NK-87
Engine bow		2 off RD-9A	1 off NK-12MK	6 off NK-87	6 off NK-87
Performance					
Take-off speed (kph)					
Maximum speed (kph)	170	350	400	550	550
Cruise speed (kph)	140	300	375	450	450
Flying height (m)	0.1–0.5	0.5–1.5	0.5–5	1–5	1–5
Maximum seastate (m)	0.3	1.0	2.0	>3.0	>3.0
Range (km)		700	1,500	2,000	3,000

The relatively low aerodynamic efficiency of such craft by modern standards can be explained by

(a) Using a wing configuration similar to an airplane while using a low aspect ratio, AR = 2.0–3.0
(b) The large area needed for tailplane, fin and rudder for pitch and yaw stability

Orlyonok's Accident

The prototype Orlyonok was completed in 1974. Sea trials were carried out in some hurry, as the Navy wanted immediate delivery. Once the sea trials had started the deputy minister of shipbuilding together with all members of the approval committee went on board to observe the testing. The sea nearby the Caspian Sea Test Base was rough, with a relative large swell because of a heavy storm that had passed

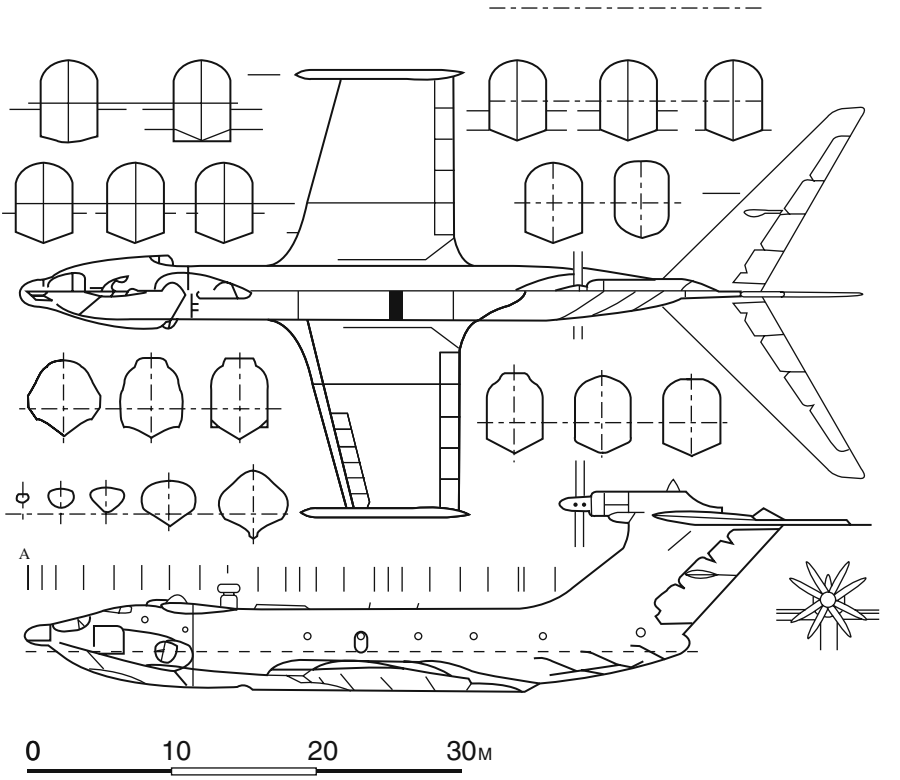

Fig. 2.14 Section profile of Russian WIG-type "Orlyonok"

through the area several days before. The length of swell was approximately equal to that of the craft.

After several runs, the craft made a strong impact with a wave at the stern part of craft, causing serious damage. Mr Alexeyev went aft to investigate the extent of the damage, opened the upper hatch and made an observation towards the stern part of the craft. He then returned to the cockpit and sat down in the pilot's seat to take personal control. The pilot himself was almost scared out of his wits. Mr. Alexeyev throttled up to the maximum output of the bow engines and drove the craft back to the base, a distance of almost 40 km from the test location.

The craft was seriously damaged over the whole of the stern area, including the fin and tailplane. The stern propulsion engine was also damaged. At the subsequent enquiry board meeting analysing the reasons for the incident, the members of committee, including the deputy minister of shipbuilding, concluded that the hull strength was unsatisfactory. Alexeyev, however, insisted that the main reason causing this accident was incorrect handling by the pilot.

The remainder of the committee did not agree, referring to another similar casualty that happened to one of the smaller test craft. The members of committee

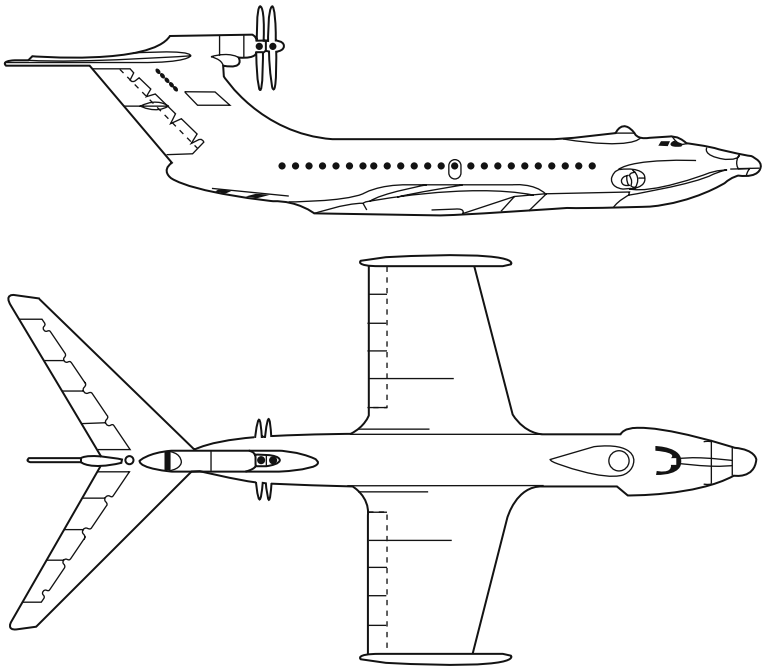

Fig. 2.15 General profile of "Orlyonok"

concluded that these accidents were attributed to Mr. Alexeyev's incorrect design approach. Alexeyev continued to insist that all of the accidents were caused by incorrect pilot handling. Subsequently he was dismissed as the chief designer of WIG and director of the WIG design bureau, and appointed as a head of the test laboratory instead. Mr. Alexeyev died 6 years later in 1980 at the age of 64.

Russian specialists on WIG and high-speed vessels have described to the principal author Prof. Yun that Mr. Alexeyev was indeed a gifted high-speed vessel research engineer and designer and was the founder of Russian hydrofoil craft and Ekranoplan development. He loved and was devoted to the research and design of high-speed vessels and was tenacious in his investigation of the secrets of high-speed marine transport science. He was a great research professional, professor and designer and also an experienced pilot, and a sportsman in high-speed sport on water and on snow. His death was a great loss to Russian WIG craft development (Fig. 2.16).

The enquiry determined that the steel material used for the rear hull and fin structure (steel, grade K482T1) had developed corrosion and fatigue cracking from early on in the trials. Orlyonok was subsequently repaired after redesign to utilise Al–Mg alloy in place of the steel material and several craft built as a series. Structural design of such craft could only be an art at that stage of development, and such engineering art requires operating experience, both positive and negative to move forward.

Fig. 2.16 Photo of Russian WIG pioneer Mr. R.Y. Alexeev

The Orlyonok craft constructed are as follows:

One static test airframe
Orlyonok 01 – S23, 1973, rebuilt and re-designated S-21, 1975–1977
Orlyonok 02 – S25 delivered 1980
Orlyonok 03 – S26 delivered 1983

Following extensive trials with the rebuilt Orlyonok 01, the Russian Navy accepted the craft into marine service on 3 November 1979 as part of the Caspian Sea Fleet based in Kaspiisk on the West Coast. There were plans in the early 1980s to order up to 100 Orlyonok craft, but in 1985 the funds were switched to building nuclear submarines. Operations with the fleet continued after the rebuilding of Orlyonok 01 in 1977 through until October 1993 after which the craft have been static (Fig. 2.17).

Fig. 2.17 Orlynok in formation

The Development of Lun

In parallel with the development programme for the military transport WIG "Orlyonok", the design bureau was also issued an order from the Russian central navy staff to design a naval-guided missile WIG, the "Lun". This craft was to be 400 t all up weight with a payload of up to 100 t.

The design was developed from the Orlyonok basic configuration using eight 13-t thrust NK-87 turbofan engines for bow lift augmentation and two similar turbofan engines at the stern for propulsion in cruising mode once in ground effect. Six ship-to-ship guided missile launchers were mounted on the hull's mid section at an angle of approximately 45° (Fig. 2.18). Leading particulars are listed in the Table 2.3. The craft was constructed between 1983 and 1986. Craft trials were carried out from 1987 to 1989. Lun has travelled about 50,000 km in service and taken off and landed on seas with wave heights of up to 3 m. Figure 2.19 shows a guided missile launch from Lun.

Fig. 2.18 Russian guided missile WIG "Lun"

Fig. 2.19 A guided missile launch from Lun

After the disintegration of the Soviet Union, owing to the lack of budget funding the Russian Navy was not able to continue developing WIG craft. Construction of a second "Lun" was interrupted. However, the accident of nuclear submarine "Comsomoloz" in 1989, with the loss of 42 crew members demonstrated that the Navy needed salvage craft with high-speed capabilities to reach remote accident scenes quickly. They concluded that a WIG would be the best vehicle for such aims. The Alexeyev design bureau was subsequently given an order to design the modifications from the "Lun" to a search and rescue Ekranoplan "Spasatel" for the second hull [5].

Design of this craft was completed in 1991. During its development, tests for salvage operations had been carried out on the existing WIG "Lun". The tests demonstrated that the performance prediction was correct, and the Ekranoplan could shorten the specified rescue operation significantly, compared to alternatives available. Plans for the rebuilding of "Lun" were prepared and the work started. To date the craft has not been completed and put into service.

Key Performance Data for Lun and Spasatel are as follows:

Speed and range:	
Cruising	400–500 kph
Searching	350 kph
Range	3,000 km
Endurance (day and night)	5
Seakeeping quality, SS:	
In flying mode	Unlimited
At take-off/landing	5
Hull borne	6
Accommodation (persons):	
Seats and beds for refugees	70 + 80
Free open area capacity	500
Flying crew and sailors	9 + 19

The aerodynamic configuration of Lun is similar to that of Orlyonok, while its seakeeping is improved because of its larger size. The craft can take off and land in wave heights of up to 3 m.

Figure 2.20 shows the general arrangement of the craft, where

(a) Longitudinal section
(b) Upper deck plan
(c) Plan of observation location on vertical wing
(d) Lower deck plan

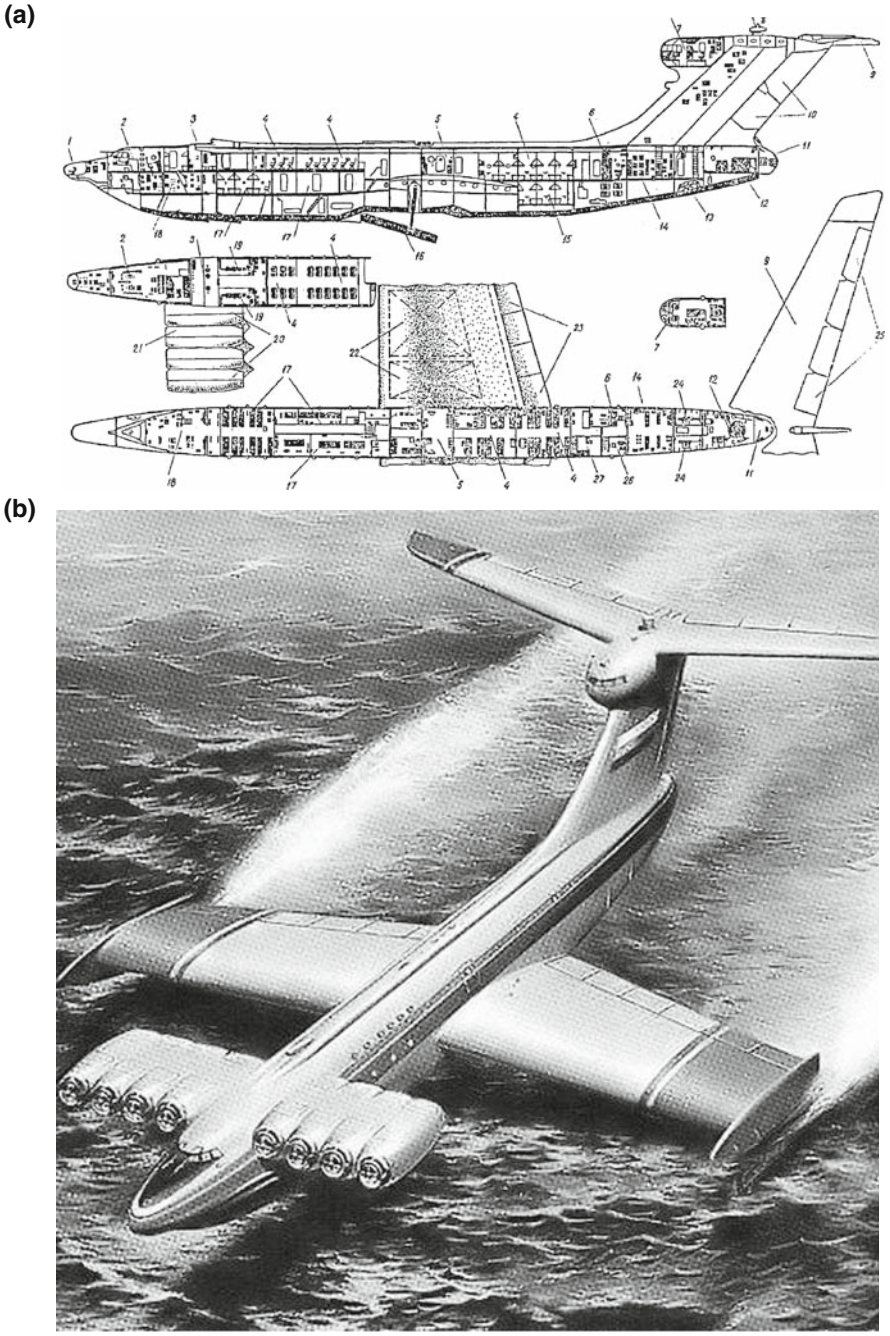

Fig. 2.20 (a) General arrangement of WIG "Spasatel" (b) Artists impression of "Spasatel"

Key to Fig. 2.20

1 Anti-collision surveillance radar
2 Navigation cabin
3 Cabin for engine systems
4 Cabin for refugees
5 Salvage equipment stowage
6 Hawser hold
7 Observation post
8 Radar
9 Elevators
10 Rudder
11 Stern door
12 Cargo hold
13 Container stowage
14 Electrical distribution compartment
15 crew cabin
16 Movable hydro-ski
17 Medicine post
18 main engine start machinery space
19 Auxiliary machinery space
20 NK 87 main engines
21 NK 87 main engines
22 fuel tank
23 Flaps
24 Electrical motor and main engine space
25 Upper rudder
26 Radio cabin
27 Kitchen

Second-Generation WIG

From the mid-1970s, R.Y. Alexeyev led an active research programme to improve the aerodynamic performance of WIG. Wing aerodynamic properties are strongly related to aspect ratio and the relative flying height of the wing above the ground when in ground effect (Fig. 2.21). Alexeyev initially planned to use a high aspect ratio of 5 and form the main configuration as a so-called flying wing (Fig. 2.22) for the second generation, doing away with the rear stabiliser; however, the stability problems with such an aerodynamic arrangement in ground effect were not able to be solved. Eventually he selected an alternative second-generation configuration that combined a main wing of low aspect ratio with additional high aspect ratio outer wings beyond the main wing endplates, and a small high mounted horizontal tailplane for improving trim stability (Fig. 2.23).

The design basis of this PARWIG aerodynamic arrangement is that the bow thruster or turbofan provides pressurised air to the main wing creating a dynamic air

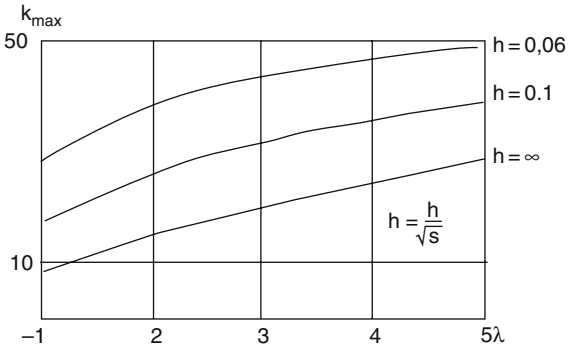

Fig. 2.21 Aerodynamic characteristics versus relative flying height and aspect ratio

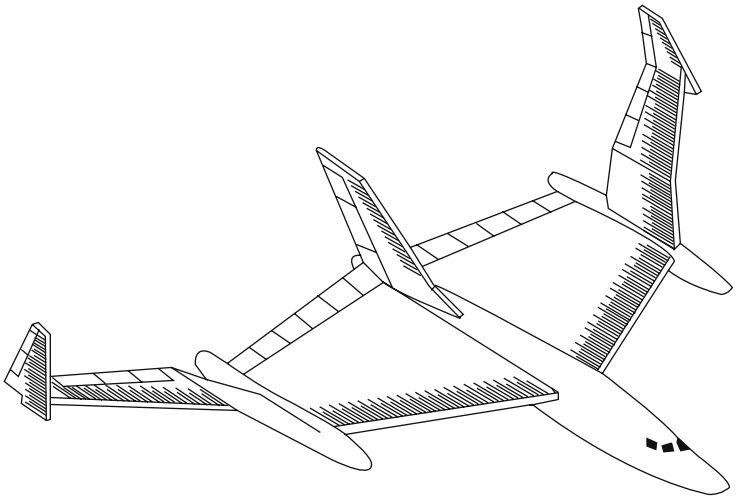

Fig. 2.22 Sketch for WIG with "Composite wing"

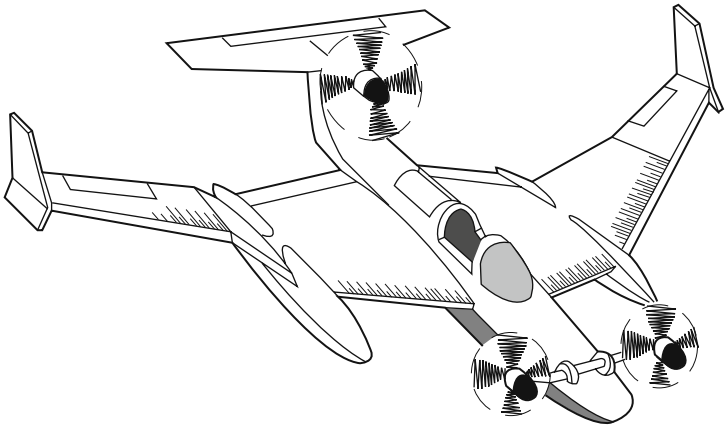

Fig. 2.23 Sketch for WIG with composite wing and small horizontal tail wing

cushion at very low speeds and added lift at trans hump speed to improve the take-off/landing performance. The high aspect ratio side wings provide improved aerodynamic performance at cruise speeds. The improved performance of this composite wing geometry is partly due to the higher aspect ratio of the outer wing, and in addition the outer wing taking advantage of vortex energy at the tips of the main wing.

Figure 2.24 shows an artists impression of the PARWIG configuration Ekranoplan 2 shown also in Fig. 1.17 illustrating the effect of bow-thruster positioning on the main wing.

Figure 2.25 shows the action of the main-wing tip vortex on the side wing (or composite wing). The tip vortex of the main wing induces a vertical upwards airflow V_i in addition to incoming flow velocity V_o. The resultant velocity impinging on the

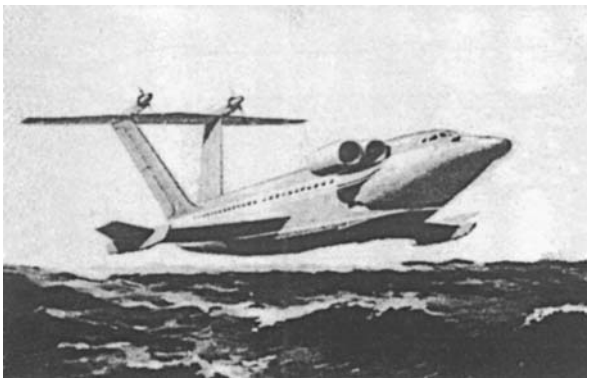

Fig. 2.24 Second-generation WIG

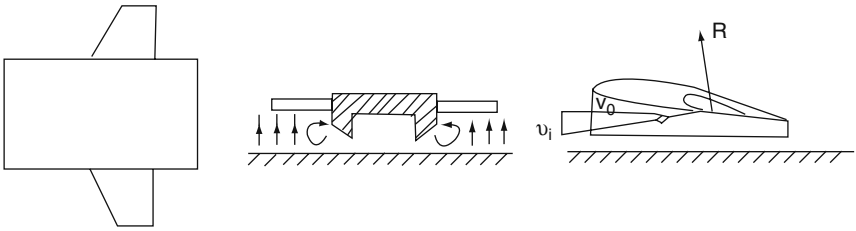

Fig. 2.25 Action of tip vortex of main wing on the side or composite wing

outer wing is increased and angled upwards. The effect is that the outer wing has an increased lift and *L*/*D* ratio, so that they can be smaller than if designed to operate in free air. Winglets are used on many modern jet airliners such as the Boeing 747, and Airbus A300 series to reduce tip vortex intensity and induced drag by interrupting the vortex.

D.N. Sinitsin, the successor of Alexeyev at the design bureau, further developed the second generation of WIG using the composite wing (CK-B) and also added a traditional aviation tailplane to improve stability [6]. Subsequently, his team designed a seagoing 250-seat passenger Ekranoplan with a planned cruise speed of 500 km/h, range 3,000 km, with take-off in 1.5 m significant height seas; and also a larger craft project with 450 seats, maximum speed of 500 km/h, range 6,000 km and take-off in up to 3 m wave height. The aerodynamic efficiency *K* of this craft was projected to be as high as 20.

Table 2.3 shows the potential leading particulars of some Russian second-generation Ekranoplan designs.

Russian WIG specialists concluded from their design studies on these craft that a number of problems concerning WIG aerodynamics needed to be solved before they could become commercially attractive:

(1) Improvements to the main-wing and side-wing aerodynamic characteristics, by selecting a more efficient wing profile for the main wing improve aerodynamic efficiency and craft stability. They projected that the maximum realisable *K*

value should be about 25, by decreasing as far as possible the area of tailplane and fin once the main wing had been optimised. This would improve the payload capacity.

(2) In order to improve craft transport efficiency, one needs to increase the aerodynamic efficiency at high cruising speed. However, a conflict exists between the requirements for the main wing at take-off, landing and cruising operations. The best way to solve these problems is to improve the effect of forward thrusters to increase lift on the main wing at lower speeds and use changing camber of the main wing at different speeds by a form of wing flap.

(3) In order to achieve satisfactory pitch, roll, heave and yaw stability, and at the same time decrease the fin and tailplane area, alternative section profiles to traditional wing sections need to be developed for main and side wings and the airfoils' arrangement optimised in relation to each other. In addition, an automatic control system is really needed for WIG cruise speeds in the 300–500 kph range to improve pitch and yaw control.

(4) A method for assuring course stability and manoeuvrability of the craft in transition operations at maximum lift power is needed. This might be procedural or by use of design attributes. In addition, automating the lift power control system with a programmed interlinked power and thrust direction control may improve craft stability and manoeuvrability during transition between modes.

(5) Development of improved flight dynamics to enable the WIG to fly above the surface effect zone for short periods. The design and operational requirements for craft flying hops and also cruising beyond the surface effect zone were developed from these investigations.

(6) Development of aero-hydrodynamic configuration to ensure safe emergency landing in a seaway from any point of the cruise path (safe ditching performance).

(7) Setting up an international safety code for WIG through the IMO so that maritime nations would have standards to refer to for WIG traffic (this has been done since the mid-1990s).

Second-generation WIG should also ideally be able to operate over water, land, snow or ice surfaces, giving them the ability to operate from unprepared bases, though this may be more important for military than commercial craft [7].

An artist impression of a large passenger and cargo carrying WIG based on these second-generation principles is shown in Fig. 2.26.

Design Studies for Large Commercial Ekranoplan in Russia

Since the first test WIG was constructed by Finnish engineer T. Kaario in 1935, about 70 Ekranoplans have been constructed worldwide, the majority in Russia. However, most of the craft are prototypes and craft built for military application. There are no commercially operated passenger ferries so far and no routes established for passenger transportation.

Fig. 2.26 Large passenger and cargo carrying WIG – FLHRO-PB

WIG designs based on military requirements do not need to be commercially efficient to be successful. Successful commercial WIG craft would need to combine low cost with high transport efficiency, demanding a different type of development programme. WIG terminal requirements will be more like a Hoverport than a ferry terminal, so the initial investment to allow entry into the passenger ferry market may be higher than new designs of fast ferry. All of these factors have restricted the development of Russian WIG. Dynamic air cushion craft are rather different, and fewer of the factors mentioned above resist its development.

Following the approach that larger craft are more efficient, and therefore reduce the unfavourable factors for developing WIG into commercial use, the Russian design houses have proposed to construct a very large seagoing passenger WIG of several thousand tons displacement, with 300 knots cruising speed and a thousand passenger seats in addition to freight capacity.

Such a craft could be operated in the strong surface effect zone, $\bar{h} = 0.05$–0.1, with high aerodynamic efficiency and inherent stability, so reducing the need for complex automatic control systems. Since the high tailplane would be beyond the surface effect zone and its aerodynamic performance would be less efficient, they suggested using a special S profile for the main wing section for improving stability, and reducing or even removing the tailplane. Such very large WIG would be operated on the open ocean. Economy would be satisfactory; however, new challenges would also be presented to research personnel.

It may be observed that the Russian Ekranoplan designs in recent years have generally been developments from the successful Orlyonok basic configuration, to include outer stability wings, etc. This craft configuration, with main-wing form optimised for cruising at 300 kph and faster, requires considerable jet-injected lift assistance for take-off. The performance characteristics are distinctly different below and above take-off and require careful operation of controls while taking off or landing.

Smaller craft have been evolving in Russia over recent years that include much more radical main wing geometries requiring less air cushion assist, and more statically stable while transiting operational modes. This work has paralleled the work in China and Australia during the 1990s.

Volga-2

In the middle of 1970s, Alexeyev realised that due to the complicated equipment, control systems and flying technique necessary for large WIG, it was very difficult to develop such craft as a cost-effective commercial transport at that time. He and his colleagues developed a much smaller and simpler vehicle they named the dynamic air cushion craft (DACC) as an intermediate type between the air cushion vehicle, hydrofoil craft and the Ekranoplan. These craft are designed to be operated in the strong surface effect zone (very close the ground or water surface), so as to obtain good hydrodynamic properties, similar to that of hydrofoils and ACV, but at higher Froude number, two or three times that of ACVs [8, 9].

Volga-2 was the first of this kind of craft designed by the R.Y. Alexeyev High-Speed Marine Craft Design Bureau. The craft could accommodate seven passengers and a pilot, with a maximum take-off weight of 2.7 t, driven by two rotary piston engines rated at 150 hp each as both lift and propulsion engines. The cruising speed of Volga-2 was about 120 km/h with a range of 300 km. The craft handling is simple, more like driving an ACV than flying an aircraft (Fig. 2.27). More detailed leading specifications can be found in Table 2.4 . The craft is characterised by the following:

Fig. 2.27 Dynamic air cushion craft (DACC) type "Volga-2"

(1) It has inherent stability without any automatic control systems as the craft is operated in the strong surface effect zone.
(2) Easy to manufacture, maintain and handle.
(3) Amphibious, and able to boat or cruise over the sea, and hover onto land at low speeds.
(4) Construction of the craft is designed as a boat rather than an aircraft, so is less complex and lower cost.
(5) The craft has a dynamic air cushion under the main wings in normal flight, so vertical slamming acceleration acting on the both main hull and main wing floats will be small. In addition, inflatable bag skirts are installed under the main hull and main wing floats, so its ride is softer to the passengers and gives less fatigue to the hull structure.

Table 2.4 Development series for the Volga and Strizh

	SM-9	SM-10	Volga-2	Strizh	E-Volga-2
Build year	1977	1985	1986	1991	1998–1999
Length (m)	11.14	11.43	11.6	11.4	15
Main wing span (m)	9.85	7.63	7.6	6.6	12.5
Wing area (m^2)					50
Tail wing span (m)					
Tail height (m)	2.57	3.32	3.7	3.6	4.7
Hull breadth (m)	2.0	2.0	2.0	2.0	
Hull height (m)					
Hull draught (m)	0.5	0.6	0.6	0.5	0.45
Aspect ratio, main	0.9	0.9	0.9	3.0	
Tail					
Crew + passengers	1+	1+	1+7	1+1	1+10
AUW (t)	1.75	2.2	2.7	1.63	3.3
Payload (t)	0.5	1.0	1.0	0.5	
Thrust (t)	300 bhp	300 bhp	300 bhp	320 bhp	300 bhp
Engine stern	n/a	n/a	n/a	n/a	
Engine bow	2 off ZMZ-4062-10	2 off ZMZ-4062-10	2 off ZMZ-4062-10	2 off VAS-4133	2 off 3M3-4062.10
Specific power (ps/kg)					11
Take-off speed (kph)	n/a	n/a	n/a	90	
Maximum speed (kph)	140	140	140	175	200
Cruise speed (kph)	120	120	120	150	150
Flying height (m)	0.2	0.2	0.2	0.2 skimming	0.2 skimming
Maximum seastate (m)	0.5	0.5	0.5	0.5 skimming	1.0 t/o and land
Range (km)	n/a	300	500	300	300

Recent Small Craft Designs

Ivolga

Reference [10] details work in Russia to develop a novel WIG named "E-Volga-2" from 1998 to 1999, which can operate over ground as well as water, and in or beyond the surface effect zone (GEZ). The Russian design team call such craft Ekranolet, rather than Ekranoplan, which in Russian suggests that the craft can be flown in free air.

Both the Russian WIG craft Orlyonok and Lun are able to fly in and beyond the GEZ, while Volga-2 can fly only in the strong surface effect zone. The E-Volga-2 combines these attributes in that it can operate on both ground and in or beyond the GEZ. The craft was designed by the "Kometa" Central Scientific Research Institute. Following 1999 the further development of the craft was named Ivolga

Ivolga has a traditional aviation control system including tailplane, fin and rudder, and wing ailerons. Pilots can choose the flying height according to the prevailing

conditions. The craft can be operated over waves with height of 1.0–1.5 m. It can traverse holes, ground, swamp and concrete landing aprons.

From Figs. 2.28 and 2.29, one can see the main craft characteristics. The central wing frontal surface is configured in a reverse V shape and with flaps at the rear part of the wing. The side buoys are slender and in catamaran form due to the deep chord of the main wing. They have both longitudinal and transverse steps for good hydrodynamic performance, particularly during take-off. The cabin is located on the centre of the wing arranged higher than the hull or fuselage and with a large window

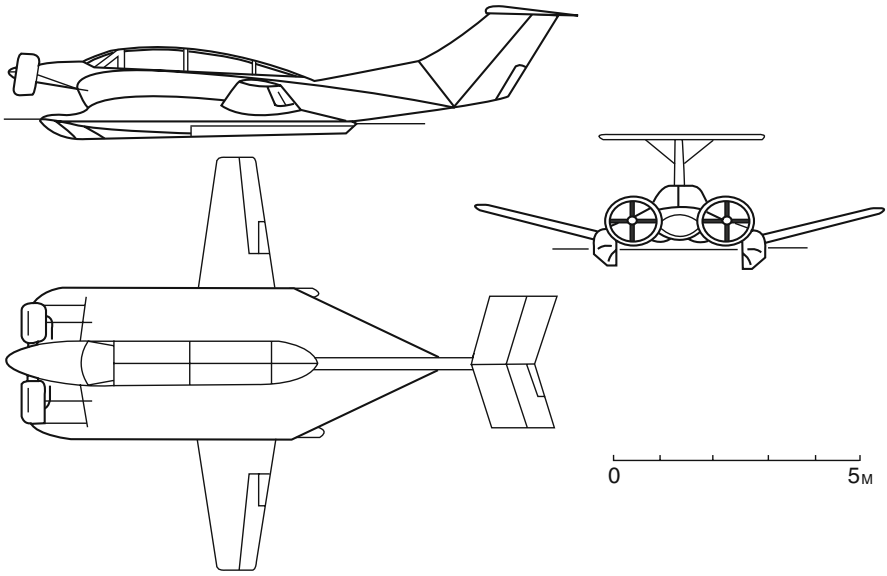

Fig. 2.28 Ivolga general arrangement

Fig. 2.29 Ivolga in flight

area, so that passengers in the cabin will have a good view. The craft also has high aspect ratio foldable composite wings with ailerons located outside the side buoys.

There are two engines located in front of the main wing, which drive a pair of 1.32 m diameter, four blade-ducted air propellers via transmission shafts and universal joints. The propeller shaft is inclined during operation on the ground and before take-off in order to feed the pressurised air into the air tunnels so as to give the craft amphibious ability, short take-off over water and good seakeeping performance. However, at cruising speed the propeller shaft axis is turned to horizontal so as to improve propulsion efficiency. The craft has a T-type tailplane with elevators and rudder. It is planned to be manufactured for both small commercial passenger operations and military applications. Technical data for this craft are as follows:

Maximum take-off weight	3,300 kg
Wing span	12.5 m
Wing area	50 m
Length overall	15 m
Wing load	65 kg/m
Specific power	11 kg/ps
Crew	1
Passenger	8–10
Engines	Two sets 3M3-4062.10
Power	2 × 150
Capacity of fuel tank	2 × 100 l
Maximum speed	200 kph
Cruising speed	120–150 kph
Flying height during skimming	0.1–0.2 m
Draught in hull borne	0.45 m
Seaworthiness	SS 3-4
Maximum size (length beam height)	15 12.5 4.7 m
Maximum size while composite wing retracted	15 4.6 4.7 m

From the figures one can see the ailerons and air bags at the wing tip plates, so the craft is able to operate both in free air (ailerons are needed for banking in free flight) and over ground (cushion with flexible skirts).

Tests of the prototype began in Moscow in September 1998. From January 1999, tests were carried out on Lake Baikal and on the Angara river with the craft based at Irkutsk supported by Verhne-Lenskiy river shipping company as a test for operation of these WIG craft in Eastern Siberia. The first flight in winter conditions in "hovering" mode was executed on Irkutsk reservoir, 16 February 1999. The first flight in a wing-in-ground effect mode in cruise configuration at speed 80–110 km/h occurred on 20 February 1999.

On 20 August 1999, the craft was demonstrated operating from the shore of Lake Baikal over water and wing-in-ground effect flight in cruise configuration. Up to December 1999, the flights were carried out in wing-in-ground effect mode flown by V. V. Kolganov. From December 1999 craft operation was mastered by D.G. Schebliakov, including on 10 December 1999 a flight in wing-in-ground effect mode

at heights up to 4-m manoeuvring around a designated course. On 15 December, flight and manoeuvring outside of wing-in-ground effect (more than l5 m) was demonstrated. On 10 February 2000, a flight was executed on lake Baikal and back during which the craft flew above snow, above water (Angara river stays unfrozen beyond 10–12 km from the source at Lake Baikal) and above ice on Baikal in wing-in-ground and aircraft modes. In 14 October 2000 at 3,700 kg weight, the EL-7 performed take-off, wing-in-ground effect flight at height up to 4 m and landing at height of waves more than 1 m, which corresponds to seastate 3.

The power capacity of the BMW S3-8 engines is sufficient for the continuation of wing-in-ground effect flight with failure of one engine. When in wing-in-ground effect, the EL 7 "Ivolga" has much greater aerodynamic efficiency ($K \geq 25$) in comparison with "airplane" modes ($K = 11$–12) at identical take-off weight and fuel capacity. The average fuel consumption when cruising with a variable flight profile including speed, track and height was 25–30 l of petrol Ai-95 on 100 km of a route at take-off weight of 3,700 kg and speed 150–180 km/h, and 75–90 l of petrol Ai-95 on 100 km route in a "airplane" mode.

Amphistar

Figure 2.30 shows the Russian second-generation WIG "Amphistar". Amphistar is a development from Volga-2 [8], which has been commercialised in Russia. A number of these craft are now in operation for passenger taxi services in Russia and in the Caribbean.

Fig. 2.30 Amphistar

Technical Data Summary for Russian WIG Craft

Additional performance data for a selection of Russian WIG and DACC are listed in Tables 2.5 and 2.6 for readers' interest:

Table 2.5 Summary data of Ekranoplans built in Russia

	SM-6	Orlyonok	KM	Spasatel	Volga-2
Type of craft	WIG	PARWIG	WIG	PARWIG	DACC
Mission	Small experimental model of Orlyonok	Transport	Experimental ship Caspian sea monster	Guided missile or/and rescue ship	Passenger boat
Displacement (maximum take-off, t)	26.42	140	544	Up to 400	2.7
Payload:	1.0	10–20	–	Up to 100	0.75
Transport modification (t)		15		45.0	0.75
Passenger modification		150 persons		450 persons	8 persons
Main dimensions, L B H (m)	31 14.8 7.85	58 31.5 16	92.3 37.6 22	73.8 44 19	11.6 7.6 3.7
Aerodynamic configuration (geometric supporting layout)	Aircraft-type layout with trapezium shape wing	As same as left	Aircraft-type layout with straight square wing	Aircraft type with swept formed wing	Aircraft-type layout with rectangular wing
Geometric characteristic of lift wing: *S* (m)	73.8	307.0	662.5	500	44.0
AR	2.81	3.07	2.0	3.0	1.0
Power plant:					
Starting, type and power	2 RD9 turbojet engine 2,040 kg thrust for each	2 NK-8-4 k fan-jet engine 10 t thrust each	8 VD-7-NM turbojet engine 11 t thrust each	8 NK-87 turbofan engine 13 t thrust each	2 rotary piston engine 150 hp each driving two propellers
Cruising: type and power	1 AI-20 turboprop engine 4,000 hp	1 NK-12 MK turboprop engine 15,000 hp	2 VD-7KM turbojet engine 11 t thrust each	8 NK-87 turbofan engines 13 t thrust	
Cruising speed, km/h (knots)	290 (157)	370–400 (200–215)	500 (270)	370–400 (200–215)	120
Range, km (n.mile)	800 (432)	1,300 (800) 2,200 (1,180)	2,000 (1,080)	4,000 (2,160)	300 (182)
Wave height *h* 3% (m)					
Take-off/landing	up to 1.0	1.5	5.0	2.5/3.5	0.5
Cruising mode	up to 1.5	no limit	no limit	no limit	0.3

Table 2.5 (continued)

	SM-6	Orlyonok	KM	Spasatel	Volga-2
Type of craft	WIG	PARWIG	WIG	PARWIG	DACC
Starting distance (km)					
On calm water	2.7	2.4–2.8	−6.0	2.4–2.8	1.0
In specification seastate	4.5	4–5		4–5	
Starting time (s)					
On calm water	50	80	130	80	70
In specification seastate	75	150	200	150	50
Touchdown to stop distance (km)					
On calm water	1.2	1.2	3.1	1.2	0.8
In specification seastate	1.8–2.7	1.7	4.5	1.7	1.0
Minimum turning radius at					
V_c,	50	50	100	50	15
R (m)	4,500	2,500	8,000	2,500	500
Rolling angle (degree)	3–5	15	10	15	0
Take-off speed (km/h)	210	220	280	220	80
Jump (permitted or not)	No	Yes	No	Yes	No
Jump attitude (m)		Up to 50		Up to 50	
Base	On unequipped relatively flat coast site or on pontoon platform	On pontoon platform or equipped site with ramp	Afloat or near special pier	Afloat or near special pier	On gently sloping coast with slope angle up to 3°

Some derivative passenger craft designs have been completed in Russia (see Table 2.5); however, high-speed passenger transport routes using WIG have still not been established there at the current time.

WIG Development in China

Chinese Research and development into WIG craft started in the late 1960s. Two types have been developed, the power-augmented wing-in-ground effect craft (PARWIG) and dynamic air cushion wing-in-ground effect craft (DACWIG). The PARWIG was developed by China Shipbuilding Scientific Research Centre (CSSRC), and China Academy of Science and Technology Development WIG Vehicle Development Centre (CASTD), while the DACWIG has been developed by the Marine Design and Research Institute of China (MARIC) in Shanghai.

Table 2.6 Leading particulars of some Russian DACC, Hydrofoils, ACV and catamarans

Craft type	Catamaran	Hydrofoil	Hydrofoil	ACV	SES	DACC	DACWIG	DACWIG	DACWIG
Model	Zalia	Raket	Lastochika	Irbis	Balguzin	Volga-2	Vilyou	Ardan	Vitim
Production condition	Batch production	Batch	Batch	Batch	Batch	Batch	Design	Design	design
Classification	P	P	O	P	M	P	O	O	O
Seats	60	58	70	28	130	8	80	50	50
Power (kW)	1,660	1,660	2,995	2,126	2,735	295	5,000	2,500	1,500
Speed (km/h)	42	60	85	45	50	100	300	270	240
Range (km)	500	500	700	450	600	500	1,500	1,000	500
Transport capability (Pass. km/h)	2,520	3,480	5,950	1,760	6,500	800	34,000	13,500	7,200
Transport efficiency (person. km/kW)	3.85	5.56	3	5	4.55	4.34	5	5.56	5

CSSRC PARWIG Craft

More than 40 small-scale models were built at CSSRC in the late 1960s to investigate the aerodynamic and hydrodynamic properties of WIG, as well as studying longitudinal, transverse and heaving stability. The models were tested out in the wind tunnel of MARIC in Shanghai and also in the towing tank of CSSRC in Wu-Xi.

Successful testing with the small-scale models (both self-propulsion and non-self-propulsion models), together with theoretical investigations led to a series of manned test craft and passenger craft that has been completed since the end of the 1970s [11, 12].

The full-size craft are characterised as follows: The craft can be launched and landed, without outside aid, from a suitable slipway or landing pad. The boarding and disembarkation of passengers, loading and unloading of cargo, and the inspection and maintenance are all carried out on land without the need of special facilities.

The craft are skidded into the water and complete take-off and landing over water. They can fly into the weak surface effect region and can clear obstacles such as small boats. They can stop safely on water when sudden danger or accident occurs. The leading particulars of CSSRC's PARWIG craft are listed in Table 2.7 (Figs. 2.31 and 2.32).

Fig. 2.31 CSSRC's PARWIG type "Sea skimmer 1"

CASTD PARWIG

This craft is designed following floatplane style and was developed by CASTD from 1995, to be used for passenger and goods transportation, tourism, anti-smuggling, patrol and rescue missions. The prototype was designed and constructed between 1995 and 1999. Leading particulars of the craft designated the TY-1 are as follows (Fig. 2.33):

Table 2.7 The leading particulars of CSSRC's PARWIG craft

Type	XTW-1	XTW-IS	XTW-II	XTW-III	XTW-IV	XTW-V	SDJ
Principal	12.60	14.40	18.50	17.90	21.70	29	13.7
dimensions,	8.20	9.80	12.72	12.05	14.50	23.8	11.8
L B H (m)	3.35	3.90	5.14	5.30	5.0	8.5	3.8
Maximum AUW (kg)	950	1,700	3,600	4,000	6,000	25,000	1,900
Crew and passenger	3	5	15	12	20	75	5
Cruising speed V_c (km/h)	100–130	130–150	150–180	144	150	300	130
Flying height at V_c (m)	0.6–1.0	0.5–1.0	1.0–1.5	0.5–2.0	0.0–2.0	1.0–2.0	0–20.0
Seastate for take-off and touch down	6–7 wind force in Tia Lake	SS-3	SS-2	SS-2	SS-2	SS-3	SS-2
Seastate for flying	6–7 wind force in Tia Lake	SS-3	SS-3	SS-3	SS-3	SS-4	SS-3
Maximum range (km)	400	200	900	>400	500	500	250
Engine type	Rotax-447	0–235	IO-540 K	IO-540K185	PT6A-15AG	WS-11	IO-350
Maximum power (ps)	2 × 80	200	2 × 600	2 × 600	2 × 750 kW		2 × 300
Remark	Complete	Complete	Complete	Complete	Complete	Design	Complete

Length overall	16 m
Width overall	11 m
Total height	4.9 m
Take-off weight	4,800 kg
Accommodation	15 persons or 1,125 kg
Engines	Two Lycoming IO-540-K1B5
Propeller	Two variable pitch propellers ducted made of aluminium alloy
Total power	447 kW
Fuel consumption	140 kg/h
Maximum speed	200 km/h
Cruising speed	165 km/h
Flying height	0.6–1.2 m
Seaworthiness	SS 3
Range	400 km

Fig. 2.32 Chinese test PARWIG type "XTW-II"

Fig. 2.33 CASTD TY-1 flying

DACWIG Craft Developed by MARIC

Since the middle of 1960s, MARIC has worked on development of ACV and SES and completed more than 15 different craft designs for civil applications. Due to the disadvantages of speed loss and low seakeeping qualities of ACV, MARIC searched for faster water transport possessing high speed, improved seakeeping and amphibious capabilities for take-off and landing. Model tests of CSSRC PARWIG craft at MARIC facilities encouraged the thought of trying to merge the advantages of ACV and WIG to create a more efficient vehicle. This led to the idea for DACWIG craft. The target was for civil application as a ferry.

Development of the DACWIG was started from the end of the 1970s [13–15]. A series of model tests with more than 30 wind-tunnel models were carried out in MARIC's wind tunnel with emphasis on the investigation of overall configuration, main-wing air-tunnel dimensions and the relationship between the jet-stream sources (bow thrusters) and air tunnel.

The overall configuration remained a simple low aspect ratio rectangular main lifting wing, no anhedral or taper, and side buoys shaped to efficiently contain a dynamic air cushion aimed at being able to hover statically.

The wind-tunnel models were succeeded by free flying radio-controlled model tests at the beginning of the 1980s and a manned test craft (type 750) that was completed in the middle of the decade, Fig. 2.34.

Fig. 2.34 MARIC's test DACWIG type "750"

The leading particulars of the type 750 are as follows:

Take-off weight (AUW)	745 kg
Payload	172 kg
Length overall	8.47 m
Span	4.8 m
Height	2.43 m
Cruising speed	132 km/h
Maximum flying height	0.5 m
Range	130 km
Maximum deceleration, emergency stop	1.54 g

Take-off performance: The craft can take off in 0.5–0.7 m wave height with 4–5 Beaufort wind scale and gusts to Beaufort 6 over the lake. Acceleration to take-off is about 30 s, equivalent to 160 m at 45 km/h.

Seakeeping quality: The 750 has flown in 0.5- to 0.7-m seas in Jin-Sa lake. The limited space has meant that there is no sheltered spot to take-off and fly into higher seas. It can be turned at flying speed and running at different wind and wave direction with 0.3° of average pitch angle, 0.52° of average roll angle.

Amphibious ability: The craft can take off from ground and run onto water and vice-versa and also fly over uneven as well as unprepared ground.

Manoeuvrability: The craft can be turned at low speed and rotate itself while hovering almost static and can fly in a zigzag course. The circling time at high speed was about 2.5 min, with 600-m turning radius.

Hull material: The craft is built entirely in GRP.

The trials of the 750 were completed at the end of the 1980s. Since then, MARIC started to develop a passenger DACWIG called the SWAN in the 1990s [16]. The features of "SWAN" (Fig. 2.35) are as follows:

- Operation in strong surface effect zone, with safe and easy handling and maintenance.
- Credible and reasonable construction cost.
- The craft is able to land on its air cushion and traverse slopes of 5° gradient and manoeuvre both on ground and water. It operates from a slipway rather than moored to a pier.
- The craft is able to operate hull borne, air cushion borne (0–80 km/h) and flying at speeds of 80–130 km/h at flying height of up to 1.0 m, within a range of 300 km.
- Maximum take-off weight 7.2 t, including up to 20 passengers.
- The craft can take off and touch down safely in seastate 2–3.

Duralumin-type LY12 is used for the main hull structure, and CIBA honeycomb composite material for other parts, such as side buoys, main wing, tailplane and fin.

Fig. 2.35 Chinese passenger DACWIG type "SWAN"

Three aviation-type piston engines are installed, two HS6E-1 engines for lift driving bow-ducted four-blade air propellers and an HS6A engine for propulsion driving a two-blade controllable pitch-free propeller.

Model tests in MARIC's wind-tunnel laboratory and static hovering tests over a solid screen were carried out in MARIC from 1995. In order to save financial budget, MARIC were obliged to use relatively small experimental models with scale ratio $\lambda = 11.5–13$. More than 10 half models were tested in the wind-tunnel laboratory. Following the successful experiments on the half models, normal wind-tunnel tests with full models, free flying tests in wind-tunnel facility and static hovering tests for the whole model were carried out successively, prior to work starting on the full-scale craft (Fig. 6.9).

After the model tests had demonstrated satisfactory aerodynamic parameters for static lift/thrust ratio, aerodynamic properties, aerodynamic balance, stability, etc., a self-propulsion radio-controlled model test and towing tank test were carried out to validate its stable operation on practical water surface condition, and craft drag over water before and after take-off. Based on the results of these experiments, MARIC started re-design and construction in 1997. Operational trials were begun in 1998. Figure 2.36 shows the general arrangement of "SWAN" (after conversion as detailed below), with numbered keys as follows:

(1) Forward mounted ducted air propeller
(2) Guide vane
(3) Air propeller for propulsion
(4) Horizontal tail stabiliser and rudder
(5) Tail fin and rudder
(6) Composite wing
(7) Lift engine
(8) Propulsion engine
(9) Flap
(10) Forward and rear passenger cabin
(11) Navigation cabin
(12) Power transmission system for forward lift engine
(13) Main wing
(14) Side buoy (sidewall)
(15) Main hull

The main functions can be explained as follows:

- The forward-mounted ducted air propeller and lift engine (1,7) are used for blowing air into the air channel and create an air cushion for static hovering over ground, and take-off over water, in addition, providing thrust for the craft for take-off and cruising flight.
- The guide vanes (2) are used to adjust the direction of the ducted air propeller air jet to adjust the centre of lift as it moves forward at increasing speed.
- The propulsion air propeller (3) and propulsion engine are used for additional thrust for take-off and cruising flight.
- Tailplane and elevators (4) are used for maintaining stable dynamic flight trim.
- Fin and rudder (5) are used for course stability and manoeuvring.

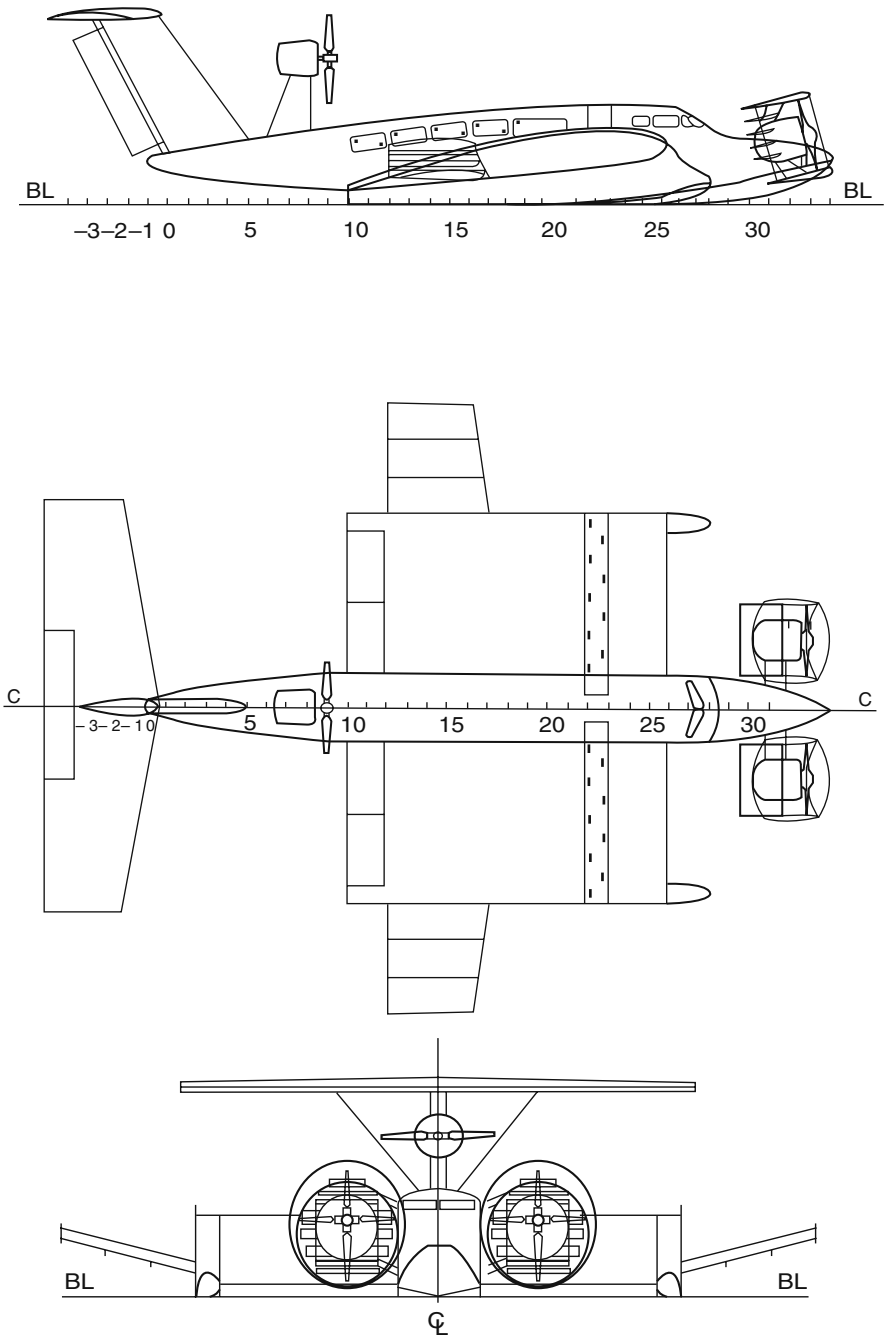

Fig. 2.36 Swan general arrangement

- Composite wing (6) is used for providing part of aerodynamic lift and, at the same time, for the adjustment to centre of lift for stable cruising flight.
- Flaps (9) are used as the sealing device for the air cushion and for the centre of lift adjustment, as well as adjusting the static trim of the craft in flight.
- In the forward and rear passenger cabins (10), there are 12 fixed and 6 additional seats for passengers.
- There are two seats for pilots and two additional seats in the navigation cabin (11).
- The power transmission system from the lift engine (12) to the ducted adjustable pitch air propeller comprises floating shafts and constant velocity joints.
- Main wing (13) provides the main aerodynamic lift;
- The side buoys (14) provide static buoyancy in hull-borne mode, air cushion sealing in cushion-borne mode, and act as aerodynamic endplates to the main wing in flying mode.
- Main hull (15) provides buoyancy when afloat and passenger accommodation. It also is the main structural element of the craft supporting the main wings and tailplane.
- A thin keel (16) at the stern is used to improve the course stability when hull and cushion borne at slow speed over water.

All the control surfaces, such as guide vanes, flaps and elevators, are driven by a hydraulic system, except the rudder.

The craft was designed by MARIC′ and constructed by Shanghai Qiu Xin Shipyard [17]. Construction of "SWAN" was completed in 1997, and initial testing carried out in the same year. The leading particulars are as follows:

Length, width, height overall	19.04, 13.4, 5.2 m
Weight overall	7,300–8,000 kg
Passengers	15–20
Engine model and number	HS6E × 1, HS6A × 2
Lift power	2 × 257 kW
Total power	724 kW
Speed	130+ km/h
Froude number at cruise speed	8.28

The craft carried out test and development trials between 1999 and 2002 in its original configuration. Operations of "SWAN" verified that the design objectives of the craft were achieved, such as good static hovering performance, overload ability of the craft during both static hovering and take-off, and fine speed performance. Tests of the craft have verified the following characteristics:

- High static lift thrust ratio and amphibious capability. The craft can be landed and launched as well as manoeuvred on a very small landing site along the Din Sah lake outside Shanghai.

- Low hump drag during take-off and maximum speed in excess of design specification.
- Satisfactory stability in the various operational modes.

The Conversion of "SWAN"

The initial trials programme showed that the long power transmission shaft to the bow engines was unreliable. In addition some of the engine auxiliary transmission components proved unreliable due to using radial-type aviation piston engines. The craft has therefore been converted from the long shaft transmission for the bow engines to a "composite air propeller-duct" system where the engine is put into the air duct and drives the air propeller directly, so as to eliminate the long transmission shaft. The engine-cooling conditions, vibration level and transmission reliability are all improved significantly.

However, since the width of the engines is large due to the radial arrangement of the cylinders, the blockage of airflow in the duct is serious and the aerodynamic force balance of the craft as well as longitudinal stability in flying mode of the craft became complicated.

After some redesign of the craft, using enlarged composite wings with significant dihedral angle and wing fences, as well as an enlarged tailplane, and redesign of both air duct and guide vanes at the bow-thruster duct-trailing edge, tests of the converted craft showed that static hovering characteristics, speed performance and stability were improved. Figure 2.37 shows the converted "SWAN" in flight.

Fig. 2.37 Swan mark 2

MARIC has planned to develop a fully commercial DACWIG based on the Swan, enlarged to 80–100 seats, with a service speed of 125 knots for application as a passenger ferry. Such a craft could be operated on Tai Wen Strait, Bo Hai Bay, Yellow sea and around the Hong Kong district. It is in the initial design stage. An outline is shown in Fig. 2.38.

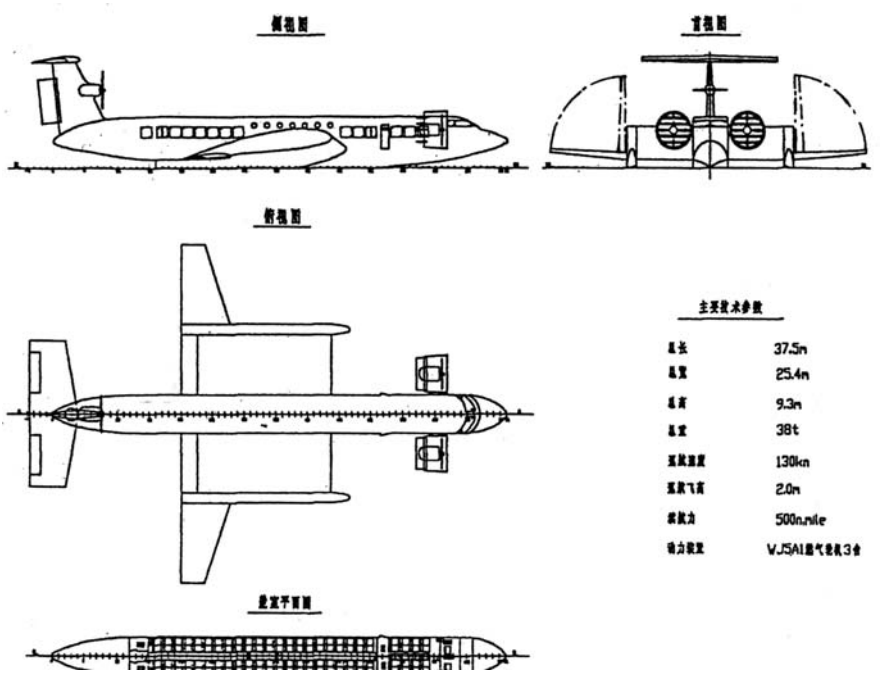

Fig. 2.38 Commercial development of Swan – 100-passenger craft

Leading particulars of the proposed craft are as follows:

Maximum length	34.00 m
Maximum width	23.50 m
Maximum height	9.30 m
Cruising speed	125 knots
Cruising flying height	2 m
Maximum flying height	2.5–3 m
Range	500 n.mile
Passengers	80–100
Total weight	35 t

Machinery:	Two gas turbines, model WJ5A1 rated at 1,750 kW, driving two ducted air propellers for lift and propulsion at bow and one WJ5A1 rated at 1,750 kW for cruise propulsion
Seakeeping:	The craft can take off and fly in seastate 4–5.
Manoeuvrability:	Can turn about its own CG and move in a zigzag in high speed flying mode.
Amphibious:	The craft can be landed and launched into water on cushion and operate over grass land, swamp and ground covered with snow.

WIG Developments in Germany

Tandem Airfoil Flairboats (TAF)

Dr. G.W. Jörg of Germany developed WIG designs based on his experience as a pilot of nearly 20 years during the 1970s and 1980s. Dr. Jörg's view is that if ground effect is to be used for a new transport system, especially to adapt better to shipping and harbour traffic, one should not base the system on the idea of an airplane flying in ground effect [18]. His concepts have been aimed at marine craft operating in the strong ground effect zone, with a small clearance relative to wing chord length.

The concepts developed by Dr. Jörg, began with a single negative delta wing form to encourage ram air cushion underneath the wing. Several models were built to investigate aerodynamic performance. The single ram-air wing in Jörg's early experiments was later replaced by two identical parallel wings in a tandem arrangement. The basis for this change was as follows:

- Higher efficiency of the wings was achieved.
- Stability improved, since both wings are moving in the same medium (strong ground effect).
- Tandem wings allowed an elongated hull configuration so total resistance was reduced.

The wings were linked by two endplates and these formed a kind of stream line channel for airflow. This resulted in better usage of ground effect and an increased static stability of the craft in motion over the sea (rough sea) and during landing in wave conditions.

The engine and air propeller was configured at the stern mounted on the fin with the following characteristics in mind:

- Better steering and resistance to side-winds by using a blown rudder
- Safety for motor and air propeller against wave impacts and in-harbour manoeuvring by placing them at the stern of the craft
- Higher efficiency forward thrust
- Usage of the "Coanda Effect" on the rear wing by induced velocity from the propeller
- Less water spray at take-off

For the Tandem front and rear wings, new computer-optimised ground effect profiles were developed. The improved stability by mutual positive influence was verified in wind-tunnel tests.

It is interesting that the initial problem experienced with the SM-1 in Russia was overcome by Jörg, principally by optimising the airfoil, designing for lower speed and connecting the two airfoils with a single side buoy! After several years

development of this type of craft, the German Ministry of Transport surveyed and approved the Tandem Airfoil Flair Boat as a boat or ship.

- IMO Annex 8 forms a basis in the International Standards Part 1, Definitions.
- IMO has classified the TAF equally in 1994 in "Group A", i.e. according to motorboat and motor ship regulations.

Figure 2.39 shows the main configuration of the TAF VIII-3 and Fig. 2.40 shows the TAF VIII-5 craft, both prototypes employed for testing, while Fig. 2.41 shows an impression of the TAFVIII-7, a proposed passenger ferry craft. Table 2.8 shows the leading particulars of TAF series.

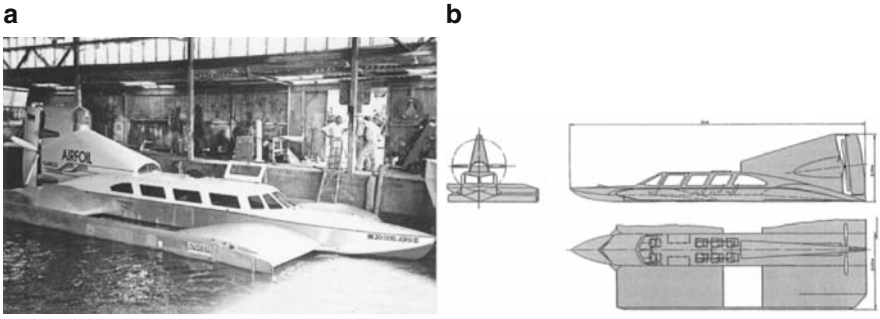

Fig. 2.39 TAF VIII-3 (**a**) photo; (**b**) diagram

Lippisch

At the beginning of the 1960s, Dr. Alexander Lippisch in Germany developed an alternative WIG configuration to the low aspect ratio rectangular wing configuration of Alexeyev in Russia. The configuration was characterised by the negative dihedral (anhedral) Delta Wing and three control surfaces (rudder, elevators and ailerons), similar to an aeroplane. The concept has no lift augmentation for take-off.

The X-113 single-seat test craft was designed by Lippisch and built under a contract with the German Ministry of defence by RFB, a company within the VFW/Fokker Aircraft group of Germany and Holland, in 1970. The craft configuration, Fig. 1.13, comprises a fuselage with stepped planing lower surfaces, main wings with significant anhedral and tapered chord so as to create a triangular dynamic air cushion space. Planing floats were mounted on the main wing tips and outer winglets with approximately 60° dihedral for roll stability. Propulsion was provided by a single two-cylinder Nelson engine of 48 bhp (38 kW) driving a two-blade open wood propeller mounted on a pylon above the main wing.

Table 2.8 Leading particulars of the TAF series WIG

Type of craft	TAF VIII-1	TAF VIII-2	TAF VIII-3	TAF VIII-4	TAF VIII-7
L B H (overall) (m)	8.30	11	14.0	18	45.6
	3.40	4.75	5.85	7.19	16.6
	2.00	2.35	3.30	4.05	9.00
Overall weight (t)	0.75	1.60	3.15	4.60	60
Maximum useful load (t)	0.20	0.40	0.80	1.20	14.0
Crew and passengers	1	1	1	1	2
	1	3	7	11	133
Engine power (HP)	100	238–300 Porsche M 44 3.0 L	550 Porsche 5.8 L	750 Marine Power 7.8 L	2 × 5,600
Cruising speed (km/h)	125–135	140–155	145–160	160–170	185–210
Cruising level (m)	0.25	0.30	0.42	0.53	1.25
Remark	Completed	Completed	Completed	Completed	Design

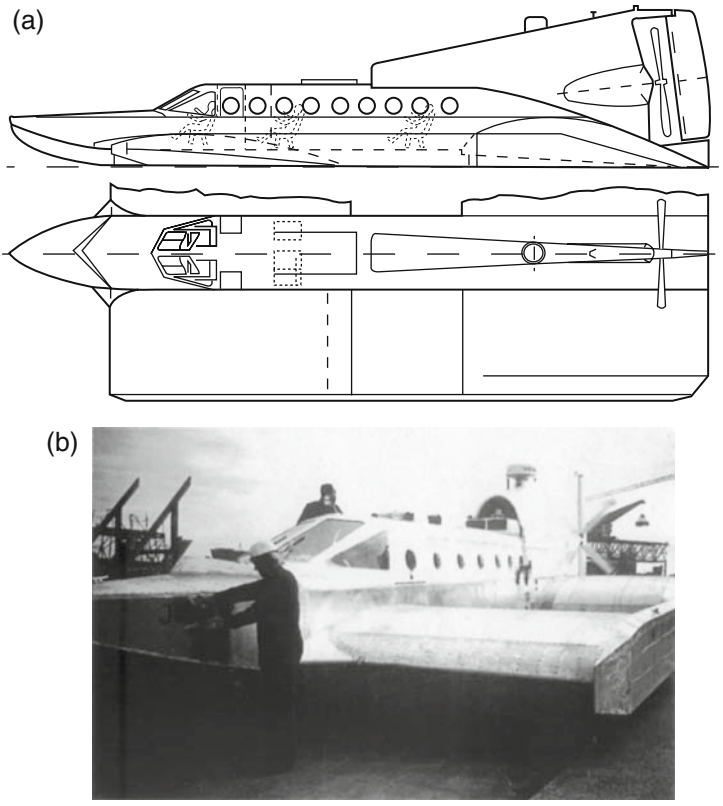

Fig. 2.40 TAF VIII-5 (**a**) external profile; (**b**) photo

Fig. 2.41 TAF commercial craft artists impression

The complete structure was built in composite materials, resulting in a very light weight for its dimensions, of 250 kg. It was able to fly in ground effect and also as a light aircraft up to 800 m (accompanied by a Bell Huey helicopter escort!) in trials during 1971 and 1972.

The success of X-113 led the German Ministry of Defence to support a follow-up development of a six-seat craft, the X-114 in 1977 (Fig. 2.42), as a prototype for coastal patrol duties. This craft, also built in composites, was powered by a 200 bhp. Lycoming light aircraft motor driving a 1.2-m diameter ducted fan mounted behind the passenger cabin above the wing. The X-114 retained the cranked single fin and high mounted tailplane and elevators of X-113. The wing tip side buoys were enlarged and extended further forward of the main-wing leading edge so as to provide the main buoyancy while afloat. The fuselage remained above water level while floating.

Fig. 2.42 X-114

X-114 had a retractable undercarriage so that it could drive up a launch ramp. During the development programme, the undercarriage was replaced by a set of retractable hydrofoils specially designed by Supramar of Switzerland. These were intended to shorten the take-off run for the craft by reducing drag, but created the opposite effect. The hydrofoils raised the side hulls clear of the water at lower speed, while at the same time lifting the main wing further away from the surface, reducing the ground effect. The craft then had to accelerate to a higher speed before take-off could occur. Up to 145 kph, the hydrofoils produced the lift without any other critical input. In an experiment, the pilot was requested to make water contact with foils lowered, at 150 kph. Unfortunately the foils touched the water at a negative pitch angle and subsequently pulled the craft into the water and destroyed it. The pilot was recovered safely.

Apart from the negative results with hydrofoils, the remainder of the X-114 trials were very successful, meeting all the Ministry of Defence objectives.

Following X-113 and X-114, RFB continued its developments with a number of different designs including the X-117 taxi and 15 seats, and 32 seat passenger ferry designs. In 1997 the Fokker aircraft group went into liquidation, and the complete design database together with the X-113 prototype was purchased by Flightship of Australia (leading particulars are given in Table 2.9).

Table 2.9 Leading Particulars X-113 and X-114

Geometry	X-113	X-114
Length (m)	8.43	12.83
Wingspan (m)	5.89	8.77
Height (m)	2.0	2.92
Weights		
Empty (kg)	250	1,040
Fuel (kg)	11	80
Payload (kg)	99	380
Maximum take-off weight (kg)	360	1,500
Payload fraction	0.275	0.253
Propulsion		
Engine	Nelson H63-CP	Lycoming IO-360
Type	Air-cooled 2 cylinder	Air-cooled 4 cylinder
Power (kW)	36	180
(bhp)	48	240
Propeller	Two-bladed wooden open propeller	Three-blade 1.2-m ducted variable pitch
Performance		
Take-off speed (kph)	40	100
Cruise speed (kph)	80	150

Hoverwing

Mr. Hanne Fischer was a technical director of RFB through the period of the X-113 and X-114 WIG developments and played an important part in its success. After retiring from RFB, Mr. Fischer founded the company Fischer-Flugmekanik (FF) together with his partner, Klaus Matjasic, their target being to develop ground effect technology towards commercial application [19]. Two prototypes, the AF1 and AF2, were built and tested and a production design developed, the AF-3, as a two-seat recreational craft. Production rights to the design were sold to RFB who subsequently built the production prototype designated AF3-A in 1990. The three craft are shown in Fig. 2.43a, b, c.

AF3 is an IMO type B WIG (capable of hops only, rather than free flight), a little larger than X-113, powered by a BMW 90-hp motorcycle engine driving a six-bladed 1.1-m ducted fan. While designed with folding outer wings, it is still too large to be towed on a trailer like a small boat and would require a permanent operational base and so was not able to be successfully marketed for recreational use in Europe. The craft was included in the package purchased by Flightship. Key data are shown in Table 2.10 .

FF turned their attention to the development of passenger ferry type WIG under the name Hoverwing. Their initial work was government sponsored by the German Ministry BMB+F. FF considered that a high-speed SES, utilising an air cushion between its catamaran floats and flexible sealing at the bow and stern

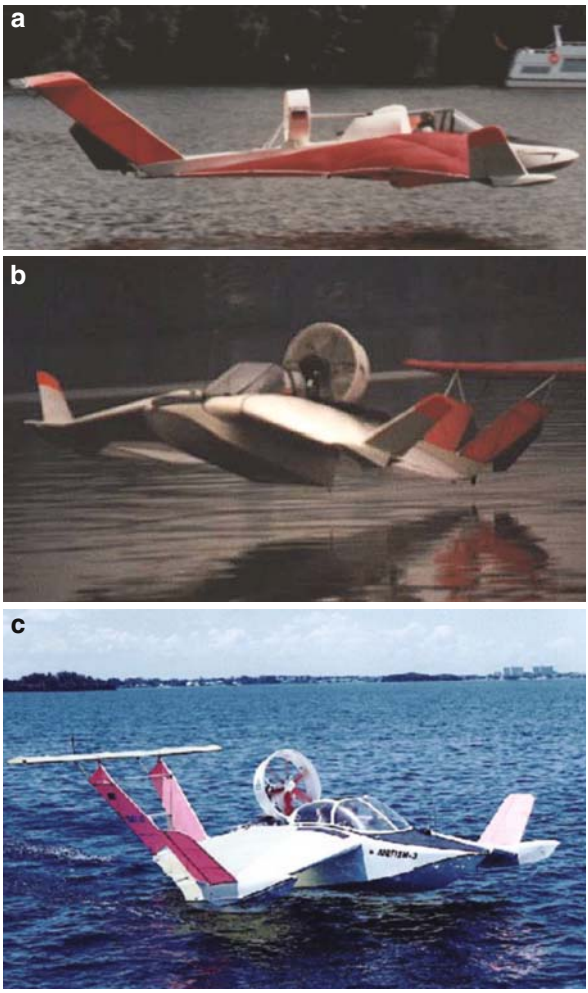

Fig. 2.43 Airfish: (**a**) AF-1, (**b**) AF-2 and (**c**) AF-3

of the vessel, was already technically advancing into the area of WIG take-off speeds. In order to utilise this advantage for the take-off phase of a WIG, FF developed a concept in which the catamaran float design is comparable with the SES, but in which the supply of the air cushion is achieved by using a small part of the propeller slipstream. Figure 2.44 explains the working principle of the Hoverwing.

FF has prepared a design, the "Hoverwing 80", with the target to transport 80 passengers at 100 knots. A prototype scale test craft at 1:3.35 scale designated the Hoverwing 2 VT has been completed. Figure 2.45 shows the craft operating on the Baltic Sea.

The leading particulars of Hoverwing 2 VT are as follows:

Table 2.10 Leading particulars Airfish 3-A

Geometry	AF3-A
Length (m)	9.9
Wingspan (m)	8.6
Height (m)	2.6
Weights	
Empty (kg)	540
Fuel (kg)	32
Payload (kg)	128
Maximum take-off weight 0.3-m waves, light wind (kg)	700
Payload fraction	0.182
Propulsion	
Engine	BMW 1200
Type	Air-cooled 2 cylinder, 4 str
Power (kW)	67 @ 7,500 rpm
(bhp)	90
Propeller	Six-blade, 1.1-m ducted fan
Performance	
Take-off speed (kph)	40
Cruise speed (kph)	120

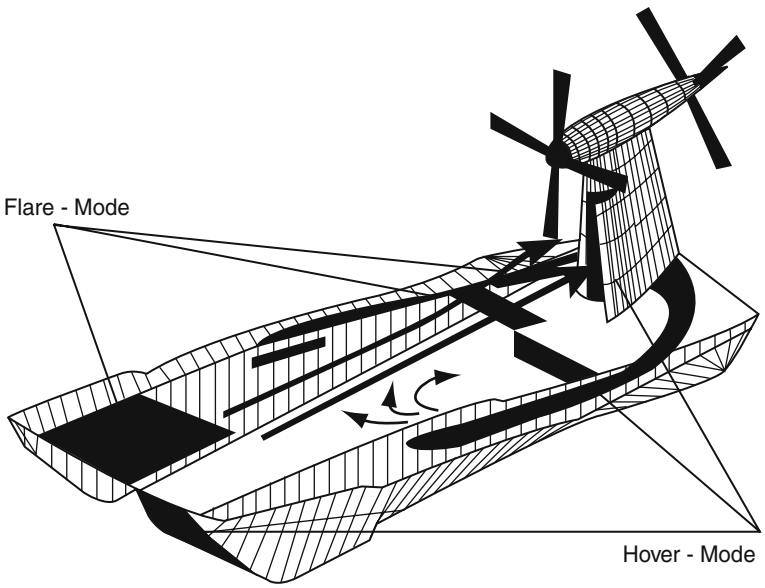

Fig. 2.44 Hoverwing design principle showing low and high speed configurations

Fig. 2.45 Hoverwing 80 flying in the Baltic Sea

Length overall	9.87 m
Width overall	7.73 m
Height overall	2.93 m
Weight	812 kg
Speed	120 km/h
Cruising flying height	20–40 cm

WIG in the United States

During the 1960s and 1970s, the model tests of a number of configurations of ground effect machines were carried out under defence development programmes to look at fast marine vehicles. While theoretical papers and some artist impressions of futuristic craft were published, for example Fig. 2.46, the development focus remained with high-speed SES until the mid-1970s and subsequently with hovercraft for amphibious assault. The US Navy did sponsor a number of research programmes into ram air winged craft, including analytical and model testing, for example the programme outlined by Gallington in Chapter 5 [3].

This work was mainly carried out in parallel to the research on ACVs, as part of the search towards the "100 knot Navy". In the early 1970s, the choice was made to develop large high-speed SES rather than other concepts. Subsequently this programme was cut short by the mid-east fuel crisis and the US Navy attention switched to other programmes such as the nuclear-powered submarine.

More recently, in the mid-1990s, a company named Wingships Inc. has performed conceptual studies for a hybrid Ekranoplan concept for the commercial market. The design, known as the Hoverplane, is a combination of existing WIG and conventional hovercraft technologies, see [20].

The main body of the vessel is designed as a shallow catamaran or tunnel hull, which is then sealed with semi-rigid skirts forward and aft. By pumping air into

Fig. 2.46 Artists impression of futuristic US flying machine

the resulting chamber, the vessel is able to manoeuvre on the water as a surface effect ship. As the forward motion of the craft increases, the pressure in front of the forward skirt overcomes the internal pressure behind it and the incoming air provides the support lift under the tunnel hull of the craft. The craft then operates for a short transitional period in this mode allowing all the engine power to be applied to forward thrust, further accelerating the craft to its take-off velocity.

Under current US regulations, WIG craft would be classified as boats requiring USCG certification, and not required to pass Federal Aviation Authority certification. The leading particulars of some Wingship Hoverplane design proposals are listed in Table 2.11 .

Table 2.11 Leading particulars of some Hoverplanes proposed by Wingships Inc. of the United States

Type of craft	HP-7	HP-16	HP-20	HP-60
Length overall (ft)	35	60	75	120
Wingspan overall (ft)	25	40	50	80
Seats	7	16	20	60
Flight elevation (ft)	3–5	5–8	6–10	10–16
Weight (lbs)				
-Empty	2,180	5,460	7,500	20,700
-Payload	1,500	3,640	5,000	13,800
-Gross	3,680	9,100	12,500	3,45,000
Power (hp)	300	2,250	2,300	2,600
Range (miles)	400	500	600	700
Fuel capacity (US gals)	50	100	200	300
Performance (mph)				
-Take-off speed	50	55	60	65
-Cruise speed	90	100	110	130
-Maximum speed	120	150	160	170

Separately to the large commercial venture proposals, in the United States during the last decade, a number of enthusiasts have begun to construct WIG craft for their own use. The first successful design has been that of Bob Windt, a pioneer also in ACV design. The Universal Hovercraft WIG is a modified UH-18P hovercraft design with a pair of simple fabric wings and an extended tail including a tailplane and elevator, Fig. 2.47. The craft flies in a steady manner in calm and near calm conditions. Take-off is at about 60 kph and the craft cruises at 90–100 kph. The cushion system is integrated with the propeller drive and so runs permanently. Since the wings are assembled on site, the craft can be trailed in the normal way, as a hovercraft. The craft has no main wing flaps, so flight altitude is controlled simply by engine power and elevator position.

Fig. 2.47 Universal Hovercraft UH-18P-WIG

The Weber brothers have also designed their own WIG employing a tandem wing configuration, Fig. 2.48, and a number of other enthusiasts are designing and building craft after being encouraged by the success of the UH18-P WIG.

WIG in Australia

Sea Wing

Hobart-based Sea Wing International has prepared design proposals for a WIG series named Sea Wing [21]. The design is based on the reverse delta main wing configuration and ram-air lift. Ducted propulsors are mounted above the wing. A retractable undercarriage with brakes and steering is incorporated for independent taxi, slipping and beaching which, allows for a reduced ground handling and maintenance infrastructure.

The Sea Wing range is proposed to be powered by twin diesel engines ranging in size from 80 to 350 kW each. These drive two overhead ducted fans giving a take-off run, again depending on the vessel size, of between 80 and 100 m on water, with

Fig. 2.48 Weber WIG craft

separation taking place at about 35–45 knots. Landing is achieved by decelerating over water, giving a run-out of 40–70 m. The larger craft proposed also include a water jet propulsion system to aid acceleration through to take-off.

Altitude is controlled exclusively by forward speed; automatic pitch stability prevents undue alteration to the angle of attack of the wing at any time. This aims to ensure a stall proof aerodynamic attitude on all points of the craft's performance envelope. The Sea Wing 02 vessels are proposed to operate in up to Force 6 (25 knots) wind speed, which equates to safe, high-speed travel over 2.5 m waves with take-off and landing in waves of up to 1.5 m (on page 90). The leading particulars of Sea Wing WIG are listed in Table 2.12 .

Table 2.12 Leading particulars of Sea Wing WIG craft designs

Craft type	Sea Wing 02	Sea Wing 05	Sea Wing 12
Length overall (m)	11	16.7	25.3
Width overall (m)	10.0	16.4	24.0
Height overall (m)	3.0	4.6	6.0
Draught-loaded (m)	0.4	0.6	0.9
Weights (kg), empty	1,400	3,000	6,500
payload	480	1,600	4,500
Maximum take-off	2,000	5,000	12,000
Normal fuel	120	400	500
Long range fuel	300	1,000	1,000
Engines	Detroit Diesel or similar, 80 kW	Detroit Diesel or similar, 240 kW + water jet	2 Detroit Diesel or similar, 350 kW + water jet
Fans	2 1.2 m warp drive	2 1.8 m Avia Hamilton V510 Variable pitch and reverse thrust	2 1.8 m Avia Hamilton V510 Variable pitch and reverse thrust
Construction	Carbon fibre, welded aluminium alloy	Welded aluminium alloy	Welded aluminium alloy

Table 2.12 (continued)

Craft type	Sea Wing 02	Sea Wing 05	Sea Wing 12
Take-off speed (knots)	35	40	45
Take-off distance (m)	80–100	100	100
Landing speed (knots)	35	40	45
Landing distance (m)	40–50	50–60	60–70
Operation speed (knots)	40–120	45–160	50–160
Operation altitude (m)	0.3–5.0	0.3–8.0	0.5–12.0
Operating range (n.miles)			
At full payload	630 2 crew + 2 passengers	520 3 crew + 18 passengers	1,800 3 crew + 42 passengers
Long range (crew only)	1,500	1,800	2,600

Radacraft

Rada Corporation of Australia has proposed another design aimed at the Australian tourist industry and perishable goods transport. The craft has a short-span lifting surface with planing outriggers and winglets. The raised tail provides attitude control. Ducted propellers mounted well forward give thrust and also improve lift at low speed by forcing air between wing and ground, see Figs. 2.49 and 2.50 , which show the Radacraft G35 test prototype.

From the figures, it can be seen that it has similarities to the Russian Volga 2. The main particulars of the proposed Radacraft C-850 commercial design are as follows:

Length	10.10 m
Width	8.50 m
Weight	950 kg (empty)
Payload	1,000 kg
Crew	1
Power	2 Rover V8 engines, with 150 hp each
Propulsion	Two-ducted, Multiwing 5Z, six-blade fans
Speed, maximum	130 knots
Cruise	100 knots
Altitude	0.5–1.0 m

Flightship

Flightship bought the technology database, trial craft X-113 (Fig. 1.13) and production prototype FS3-A (Fig. 2.43c) from Rhein Flugseugbau GmbH (RFB) in

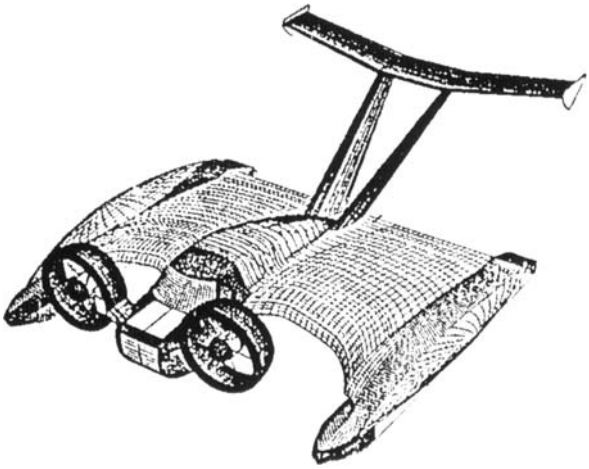

Fig. 2.49 High tail, twin-ducted fan and single hull layout are design features of RADACRAFT WIG

Fig. 2.50 Radacraft G35

1997 at a cost of DM 12 million when its parent company VFW/Fokker went into liquidation.

The original X-113 test craft has been located at Flightship's facility in Cairns, Queensland, and remains in flying condition, though it is not operated. The AF3-A has been developed somewhat and has been used as a flying test bed and pilot trainer while Flightship worked on development of its production designs, the FS8 and FS40.

In 1997, Flightship contracted Fischer Flugmechanik to scale the AF3 design into an eight seater using performance and outfit specifications provided by Flightship. FF completed the design and construction of the prototype FS8 in February 2001. The craft has subsequently completed type certification under the IMO high-speed craft rules by Germanischer Lloyd and Queensland Transport during 70 h of trials.

The FS8 is an all GRP/composite structure following the Lippisch/FF configuration, Fig. 2.51a, b. Power is from a single GM V8 petrol engine mounted behind the passenger cabin at the rear of the fuselage, this drives two 1.7 m open propellers

mounted on canted pylons above the rear of the main wing. The high mounted tailplane is supported by twin fins and rudders. The fuselage floats in the water and provides main buoyancy support for the craft. The wing tip side buoys provide for stability while afloat.

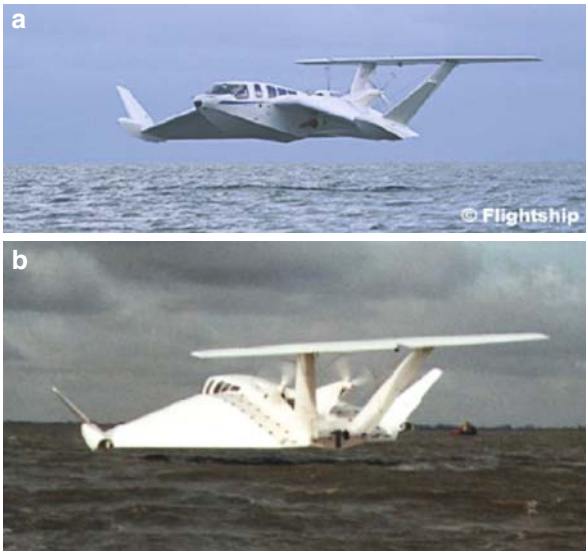

Fig. 2.51 (**a** and **b**) Flightship Dragon Commuter

The Dragon Commuter operates at a flying height up to half the wing span of 15.6 m and so has a considerable operating envelope of up to 2-m seastate for cruising at 158 kph (86 knots). Take-off is possible in up to 0.5 m seas. Lift-off is at 100 kph (55 knots). By selecting large diameter propellers with a low power loading, Flightship has been able to keep noise levels relatively low, at 75 dBA measured at 100 m distance.

The craft has a three-point retractable undercarriage for driving ashore up a ramp, and electric powered water jet propulsors in the side buoys that can propel the craft up to 6 knots. Placed at the wing tips, the water thrusters are clearly useful for harbour manoeuvring.

Flightship craft built in Australia were classified by Lloyds Register. The company developed a scheme for pilot and operating crew training and insisted that clients can only operate with such personnel. This enabled operator insurance and permitting, which otherwise would be difficult since WIG commercial operations are still very new.

The FS40 Dragon Clipper is Flightship's ferry or logistical craft design (Fig. 2.52). It is aimed at 1.2 m seas at take-off and 4 m at cruise speed of 220 kph (120 knots). The design, summarised in Table 2.13 , is configured so that it can take aviation freight containers, passengers, or a mix. Due to the power requirement for this larger craft, two Pratt & Whitney turboprop installations are planned. The larger

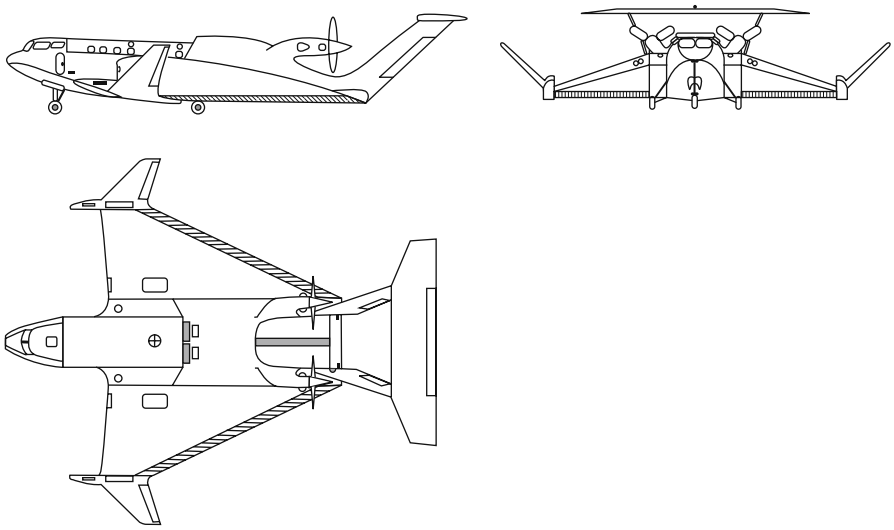

Fig. 2.52 FS-8 Three view

Table 2.13 Leading particulars Flightship Commuter and Clipper

Geometry	FS8 Dragon Commuter	FS40 Dragon Clipper
Length (m)	17.45	30
Wing span (m)	15.6	25
Height (m)	4.1	4.7
Weights		
Empty (kg)	3,740	13,400
Fuel (kg)	180	2,500
Payload (kg)	650	5,000
Maximum take-off weight (kg)	4,750	20,900
Payload fraction	0.137	0.24
Propulsion		
Engine	1 × GM V8	2 × P&W gas turbine
Type	Water-cooled petrol engine	Aviation turboprop motor
Power (kW)	338	1,000 (×2)
(bhp)	450	1,350 (×2)
Propeller	2 off 4 blade 1.7 m variable pitch propellers	2 off 3 blade variable pitch open propellers matched to turbine
Performance		
Take-off speed (kph)	101 at max 0.5 m seas	110
Cruise speed (kph)	158 at max 2.0 m seas	220
Landing speed (kph)	92	Less than 110
Water drives (kph)	11	Tba
Range (km)	550	2,780
Cruise clearance (m)	3	Tba

structural dimensions have meant that Flightship selected aluminium construction for the Clipper rather than GRP

Flightship experienced financial difficulties in 2002/2003 due to the heavy investment programme required for prototype certification prior to sales being possible. The company has since been purchased by entrepreneurs in Singapore with the intent to complete development to commercial viability.

Concluding Observations

We have surveyed the historical development of WIG design up to date in this chapter. The technology has developed a great deal over the last 30 years. At present, the focus is on much smaller craft than Alexeyev and his colleagues designed and operated in the Caspian Sea. Their technical achievement was so enormous that it will be a considerable time before commercial WIG craft of that size and speed are in operation. The outer limits have nevertheless been tested.

Today's challenge lies in developing craft suitable for commercial or logistical service. Work continues in Russia, China, Australia, Singapore, Germany and South Korea to meet this challenge. Differing design concepts have evolved depending on the target cruise speed or craft mission chosen by the particular organisation. A number of common threads are nevertheless evolving:

- Small craft for commuter, ferry and logistics are reaching the marketing stage.
- GRP suits craft for commuter size, while aluminium structure is likely to be more efficient for larger craft.
- Air cushion or lift augmentation is a powerful tool and most helpful in optimising larger/faster craft. It also introduces complexities to control during mode transition.
- Take-off environmental conditions are the most sensitive parameter for a WIG. Improved take-off envelope is therefore a valuable asset to a new design.
- Take-off and landing transition are the most difficult part of WIG design and also their flying technique.
- Different configurations are optimum for recreational and small craft, logistics craft and potential large trans-oceanic craft.

The summary in this chapter has not been exhaustive. There are many individuals and smaller organisations that have designed, built and operated prototypes, with varying amounts of success. Readers will find reference to the "WIG Page" on the Internet web useful for more detailed investigation of different designs.

In the further chapters of this book, we will discuss the theories related to the lifting wing, air cushion and ram lift augmentation, and performance assessment. The aim is to cover the range of parameters such that a designer may work out a design for any of the craft sizes or types mentioned above. The theories and data available are limited in this field, so readers are encouraged to carry out their own research to supplement the material presented here before attempting a build programme!

Chapter 3
Longitudinal Force Balance and Trim

Introduction

WIG trim is controlled by the dynamic balance of environmental loads against restoring forces from the flying surfaces – the main lifting wing and tailplane. Mean running trim when flying is generally adjusted by moving the neutral position of the control surfaces and so altering the centre of lift relative to centre of gravity.

Below take-off, the speed craft trim is controlled by hydrodynamic forces. These act on both the hull and wing tip side buoy planing surfaces. At speeds close to take-off, the main lifting wing provides most lift as a dynamic air cushion, with a different balance centre to that when flying in ground effect – further back from the wing leading edge. As the WIG takes off the balance centre moves forward, so that tailplane lift must be increased to keep the craft level. Maintaining stability during the transition through take off from hydrodynamic stability to aerodynamic stability is therefore a critical element of WIG design.

In this chapter, we will introduce trim and longitudinal force balance in the following sequence:

1. Explanation of operational modes and running trim
2. A simple method for determining longitudinal centre of effort of various forces
3. Solutions to problems concerned with the longitudinal balance of forces
4. Influence of various control mechanisms on the longitudinal aerodynamic centre of effort
5. Safe handling methods during WIG take-off

A WIG can start from rest via several means – by launching from ground into water down a slipway and by starting from static floating mode on water (hull borne) or from static or slow-speed hovering over water (cushion borne) if the WIG has air cushion assistance. Once a WIG has taken off into a flying mode over the water surface, steady-state cruising flight will ensue. We consider first these different operating modes for a WIG from rest to cruising, and the differing forces acting on the craft at each stage.

L. Yun et al., *WIG Craft and Ekranoplan*, DOI 10.1007/978-1-4419-0042-5_3,

Operational Modes

The modes of operation to consider, over different surfaces and at different speeds, are as follows:

1. Moving on the water at low speed, floating on the hull. This mode is used for manoeuvring craft after launching or approaching its terminal, or in restricted waterways.
2. Moving over the ground at very low speed while supported by an air cushion (DACC and DACWIG), launching from land to the water, and/or landing from the water to the land.
3. Moving on the water surface at a medium speed, i.e. in air cushion-borne operation mode for DACC and DACWIG, or jointly air cushion and planing mode for PARWIG. This mode is also used for manoeuvring craft on narrow waterways and is experienced when accelerating through take-off. In this operating mode, there are two speeds linked with resistance peaks that strongly influence the overall performance:

   - Hump speed, at which the hydrodynamic resistance reaches a peak, and with heavy spray acting on the craft so as to influence the main engine, bow thrusters, and the pilot's field of view from the cockpit. The main engine power setting will be high, while for reciprocating engines cooling airflow is low due to the low speed. The low cooling can sometimes make main engine cylinders and lubrication oil overheat if operation is prolonged at this speed, so pilots make an effort to pass through hump speed as quickly as possible.
   - Take-off speed. At this speed, the craft will lift off from the water surface to reach true flying mode in ground effect. After take-off, a daylight clearance will exist under the hull bottom, and the resistance will suddenly drop, allowing swift acceleration to cruising speed.

   The relation between hump and take-off speeds (i.e. the Froude numbers with respect to volume displacement of the craft F_{nd} or with respect to chord length F_{nc}) gives an indication of the proportion of craft weight supported by aerostatic lift at low speeds and is referred to as the take-off and landing aerodynamic arrangement (TLA) in this book. For example, take-off for PARWIG is with aid of both air cushion and planing hydrodynamic lift, but for DACC and DACWIG almost completely static air cushion lift, resulting in a much lower hump speed and peak drag force.
4. Moving at high speed over the ground and water (flying mode). Behaviour over ground or water at high speed is very similar.

Operational mode 3 is most affected by alternative WIG craft configurations. The air cushion created under the main lifting wing of a PARWIG or DACWIG provides aerostatic support that reduces the drag peaks experienced as the craft accelerates to take-off speed. The drag peaks (hump drag) are greatly reduced by reducing

the cushion pressure. The wing dimensions suitable for optimum air cushion performance generally lead to low take-off speeds (50–100 kph) and cruise speeds in the 150- to250-kph speed range. Increased wing loading, suitable for higher cruise speeds, leads back to the PARWIG configuration with a greater proportion of craft weight supported on the hull and side buoys directly. Clearly there is an optimisation spiral to be investigated, to select the best combination of hydrodynamic and aerostatic support for the WIG design in the pre-take-off mode of operation.

Beginning with the case where WIG start from rest floating on water, the operational modes are characterised as follows:

Hull-borne operation: The total weight of the craft is supported by the main hull buoyancy and side buoys at very slow speed. The balance of forces and craft trim are controlled by weight and centre of gravity, balanced by buoyancy, centre of buoyancy and position of the metacentre.

First transitional regime: Here the craft is supported by buoyancy and hydrodynamic lift (acting on hull and side buoys) and air cushion lift (acting on main lifting wing). The cushion lift is a larger portion of total lift force for DACC and DACWIG than PARWIG due to the aerodynamic configuration for forming the air cushion on these craft. As the craft accelerates, it will transit through two drag peaks: first, as the cushion passes through hump speed and later as the hull moves from displacement into planing mode. In this mode, the hydrodynamic and air cushion lift forces, acting through their respective centres of effort, will alter the trim unless balanced by adjustments to flying control surfaces, for example the tail stabiliser (elevators).

Cushion-lifting and/or planing mode: The total craft weight is supported by air cushion lift (on the wings) and hydrodynamic lift (on main hull and side buoys). Most of the supporting lift for DACC and DACWIG is supplied by static air cushion lift, a much higher proportion than in the case of PARWIG. Depending on the design of the air cushion system, the air cushion drag hump speed may be experienced in this mode (PARWIG) or in the first transitional mode (DACWIG, DACC). As the craft accelerates further, lift on the wings gradually increases, offloading the hull planes until the craft is supported on the wing lift and dynamic air cushion under the wings. It may be noted that for DACC and DACWIG, it is important that neutral trim is achievable while hovering, so the cushion centre of area needs to be under the centre of gravity of the craft in plane.

Once a DACC or DACWIG has accelerated above the hump speed, the drag reduces and acceleration can continue while cushion feed from thrusters is reduced until the lifting wing supports the craft on the dynamic air feed at the second transition.

A PARWIG has to transit the drag hump of its planing hull, which is a sharper peak than an air cushion. The second transition is generally closely linked to hull lift-off for a PARWIG. The position of the bow jet nozzles or bow-thruster ducts and so the proportion of lift provided by forced air feed

under the main wings is significant in determining the stability of the craft through the transition from main hull lift-off to steady cruise.

Second transitional regime: At take-off speed, the total WIG weight is supported by the dynamic air cushion lift and aerodynamic lift. As the craft continues to accelerate, an excess of lift is generated allowing the craft to rise to cruise elevation, and the main lifting wing flaps to be adjusted to level the craft out. In this mode, it is important that lift from the main wing acts slightly forward of the centre of gravity of the craft, to give tail down tendency when landing or ditching.

Flying in the ground effect zone (GEZ): The WIG's total weight will be supported by the aerodynamic lift acting on wings, hull and side buoys after take-off. In this flying mode, the flap at the trailing edge of the main wing will be adjusted so as to balance out the dynamic air cushion (not static air cushion at this speed) or wing-in-ground effect lift at the desired flight elevation. In addition, the guide vanes or air-jet deflectors aft of the bow thrusters will be rotated upwards to obtain higher propulsion recovery coefficient on DACC or DACWIG. PARWIG designed to cruise at significantly higher speed will reduce the power on the bow thrusters, allowing the main lifting wing to operate purely as a wing-in-ground effect. The centre of effort for lift forces should remain just forward of the centre of gravity.

Flying beyond the GEZ as an airplane: In this mode, a WIG designed to fly above the GEZ will lift the wing rear flap completely to reduce drag and allow acceleration to a maximum speed, which may be "jump mode" if the craft is designed to be able to dash for short periods.

Figure 1.15 (see Chapter 1) shows the various operation modes of a WIG and illustrates the inclination angle of bow-thruster shaft or guide vanes being rotated from positive to negative (positive = shaft down) during transition from low to higher speed.

Running Trim

Let us now review the forces and their variation through the different modes and their effect on trim. Figure 3.1 shows the variation of running trim of a DACWIG, in which I represents hull-borne operation, III represents the cushion-borne mode (including hydrodynamic lift), V represents the flying mode, and II and IV represent the first and second transition zones, respectively. The figure also shows the various forces, i.e. weight, buoyancy, cushion lift, hydrodynamic lift and aerodynamic lift, as well as the balance of these forces.

The Froude number at drag hump speed in the first transition regime is $F_{\mathrm{nd}} = v/(g \cdot V^{1/3})^{1/2}$, where v is the craft speed (m/s), and V is the volumetric displacement of craft (m^3), which is between 1.8 and 2.5, and between 4 and 9 for take-off at the end of second transition regime [1]. The more effective the TLA (air cushion lift

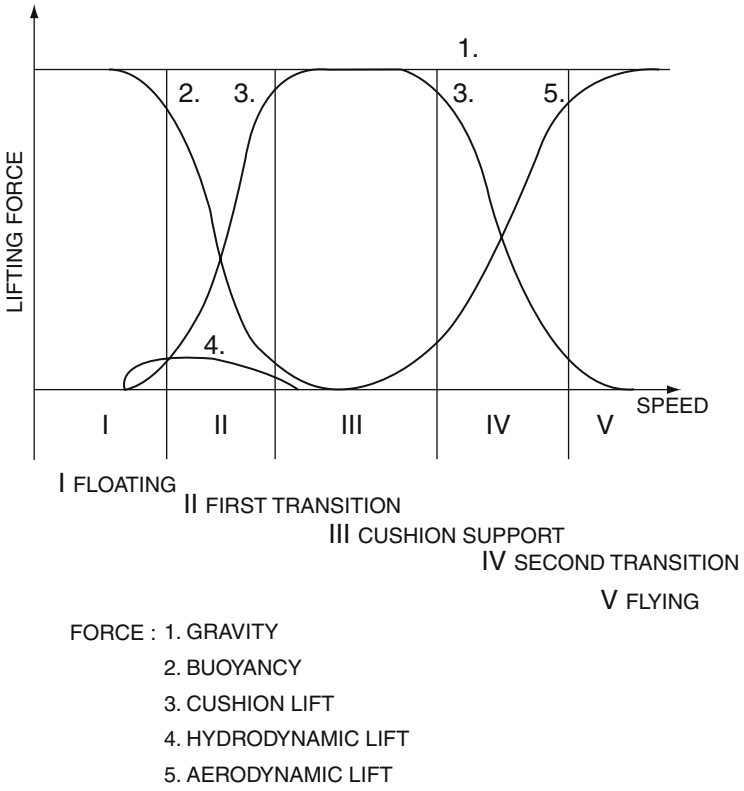

Fig. 3.1 Variation of DACWIG lifting force components with speed

fraction of total craft weight at zero speed), the lower F_{nd} becomes for hump and take-off speeds.

The hump drag and take-off speeds of DACC and DACWIG is much lower than PARWIG due to the higher air cushion lift that reduces the main hull planing surface loading. However, there is a penalty of lower aerodynamic performance of the craft at flying speed due to the lower wing aspect ratio needed for an efficient air cushion. This has led to development of WIG designs at the end of the 1990s with inner wings proportioned for air cushion efficiency and outer wings beyond the side buoys with dihedral and higher aspect ratio for efficiency in flying mode [2].

WIG craft of different types are illustrated in these operational modes in the following figures:

Figures 3.2, 3.3 and 3.4 show a self-propelled model of a DACWIG, in floating mode, cushion-borne operation and flying at high speed after take-off, in strong GEZ ($\bar{h} < 0.1$).

Figure 3.5a and b shows the Chinese PARWIG types “XTW-1” and “XTW-2” flying in strong GEZ.

Fig. 3.2 Radio-controlled model operating hull borne on the lake

Fig. 3.3 Radio-controlled self-propelled model cushion borne on the lake

Fig. 3.4 Radio-controlled self-propelled model flying on the lake

Figure 3.6 shows the Russian PARWIG type “Strizh” in flying operation beyond strong GEZ.

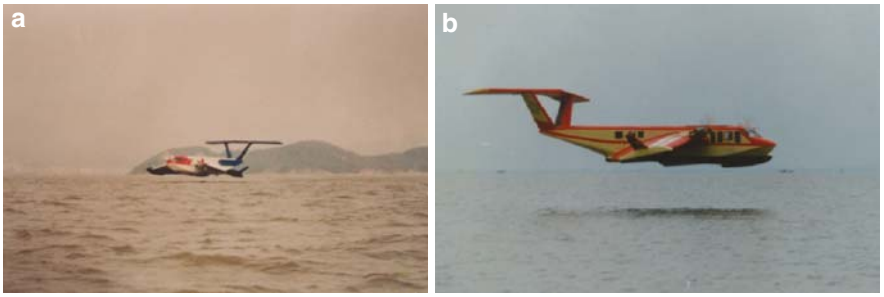

Fig. 3.5 (**a**) Chinese PARWIG "XTW-I" and (**b**) "XTW-II" in flying in ground effect

Fig. 3.6 Russian PARWIG "Strizh" in flight beyond the SEZ

Figure 3.7 shows the high-speed flying mode of a manned test Chinese DACWIG type "750" in strong GEZ. A daylight clearance can be seen under the base of the craft. The flying height at that moment was about 0.5 m. The craft had taken off from the water surface perfectly and ran very stably at this elevation. The take-off performance of MARIC's craft type 750 is listed in Table 3.1.

Fig. 3.7 Chinese test DACWIG "750"

Table 3.1 Take-off power settings of the MARIC "750"

Operation mode	Time (s)	Engine operation		Angle of elevator	Speed (km/h)	Distance (m)
		Forward	Rear			
Floating	/	/	/	0	0	0
Static hover	0	Rated power	/	Max	0	0
Hump speed	8	Rated power	Rated power	Max	30	30
Take-off	30	Rated power	Rated power	1/2 max	70	300
Cruising	120	0.5 rated power	0.85 rated power	0	150	4,300

Centres of Effort and Their Estimation

Introduction

A prerequisite for stable running attitude is a balance of the forces acting around the centre of gravity, i.e. the sum of moments due to the various forces about the centre of gravity of the craft is equal to zero. The forces acting on a WIG craft are static buoyancy, static air cushion pressure, craft weight, air propeller or jet propulsion forces, hydrodynamic lift and drag, and aerodynamic lift and drag [3].

Equilibrium for the different modes is as follows:

1. *Hull-borne operation*: The centre of buoyancy of the hull and side buoys (CB) has to provide a righting moment to the centre of gravity of the craft in longitudinal and transverse direction as the craft pitches or rolls – the floating craft must have a positive metacentric height, GM, so that it will return to a stable floating position if disturbed by waves or wind.
2. *Slow speed over ground or other rigid surface (DACWIG or DACC)*: The centre of gravity of the craft has to coincide with the centre of static air cushion pressure (CP) in longitudinal and transverse directions under the main wing. The CP must move so as to provide a positive air cushion metacentric height as the craft pitches and rolls.
3. *Cushion-borne operation (or the mode before take-off on water)*: The craft CG has to be matched with the resultant of lifting forces from the air cushion at the centre of air cushion pressure (CP), hydrodynamic lift centre (CH) of the hull and side buoys, and of aerodynamic force at the centre of lift of the main wing and tailplane. In addition, the trimming moments due to aerodynamic and hydrodynamic drag forces should balance, so that aerodynamic control surfaces can stay at neutral angle.
4. *Flying over water/ground in GEZ*: The craft CG has to be coincident with the aerodynamic centre of lift of main wings, tailplane and hull as well as side buoys.

The aerodynamic pitching moment due to drag should be minimised as far as possible.

5. *Flying over water/ground beyond GEZ*: The craft CG has to be matched with aerodynamic centre of lift of the craft. The aerodynamic moment in pitch should be minimised as far as possible.

The various force centres are not easy to bring into coincidence with the craft CG at the same time, and the position of some of them changes at different speeds so as to complicate the equilibrium condition of the craft. Dynamic trimming is therefore an important attribute for WIG. This has to be supplied via flaps and tailplane elevators. A high tailplane assists in providing a steady balance to the aerodynamic forces.

We will consider now how to establish the various centres of effort.

Longitudinal Centres of Forces Acting on WIG Craft

Centre of Buoyancy (CB)

The centre of buoyancy of the craft can be found by plotting the Bonjean curve accounting for both hull and side buoys, using traditional naval architecture calculations as, for example, in [4].

Centre of Hydrodynamic Force Acting on Hull and Side Buoys

The centre of hydrodynamic forces acting on the hull and side buoys is dependent on the lines, length to beam ratio, planing surface geometry including step positions and the operating trim of the craft. The analysis is similar to that for fast planing multihull craft, complicated a little by the stepped form of the hull and possibly also stepped side buoys to allow clean take-off. Analytical treatment is still the subject of much research, so practical designs tend to rely on hydrodynamic model testing in a towing tank and adjustment of geometry based on parametric variation of geometrical form. In the later stages of design, radio-controlled free-flight models are valuable design tools.

This operation mode is a transitional one for WIG, so the assessment of these forces can be focused on two cases of entry into the planing mode, and just less than take-off speed, during concept design of PARWIG or classic WIG. The magnitude of direct hydrodynamic forces in the cushion-borne mode of DACC and DACWIG should be small in proportion, due to the high length/beam ratio and small wetted area of the hull and side buoys together with the air lubrication from the cushion efflux, so these components can be built into design factors at the initial design stage.

Centre of Static Air Cushion Pressure (CP)

PARWIG do not create a static air cushion at boating speeds. The bow thrusters assist to create a dynamic air cushion under the main wing to reduce hydrodynamic drag and improve acceleration through to take-off at a minimum possible speed. The dynamic air cushion centre of area is determined either by computer calculation of the pressure field under the wing due to the partially forced air feed or alternatively by model tests in a wind tunnel, at the range of speeds up to take-off.

In case of DACC and DACWIG, the main wing, side buoys and flaps configuration is arranged so as to restrict outflow of captured air and create an air cushion supporting the whole craft weight at zero speed.

The cushion air feed is provided by bow thrusters with steerable exhausts or guide vanes. Based on ACV and SES experience, it is found that CP = 0.45–0.5 of the wing chord length *C* measured from the leading edge of the main wing, in the case where there are no guide vanes in the ducts. If horizontal guide vanes are installed at the efflux of the bow thrusters, their orientation will strongly affect the pressure field in the cushion and the position of the CP, so this needs to be investigated for a given craft design to optimise the wing, flap and thruster configurations. The simplest approach for this is to carry out model tests. At zero air speed, a tethered model on a test table is effective for initial design.

Centre of Aerodynamic Lift of a Single Wing Beyond the GEZ

The centre of lift of most wings beyond the ground effect is located about one quarter of the wing chord from the leading edge of the wing. Aerodynamic characteristics of some NACA wing profiles at low air speed can be found in Table 3.2 (see [5] for additional data):

From Table 3.2, one can see that the centre of lift of most wing profiles is located at close to 25% of the chord from the leading edge of the wing. The reason for this is that the majority of the lift is generated by the suction pressure profile over the upper surface. This peaks in the leading part of the wing chord. It should be noted that a wing profile is a combination of a chord line (which may be cambered, flat or even S-shaped) together with the section profile that varies in thickness and geometric form.

Centre of Lift of WIG Main Wing with Bow Thrusters in Ground Effect Zone

WIG bow thrusters are located directly in front of the main wing in order to improve the static hovering characteristics and take-off capability. The aerodynamic centre of effort of the main wing including main hull will move forward significantly due to the dynamic pressure of incoming free flow and mixing with the air jet blown by the bow thruster. Figure 3.8 shows such streamlines around the main wing and bow thrusters.

Table 3.2 Aerodynamic characteristics of some NACA wing profiles at low air speed

Wing profile	Re/10^6	C_y max	C_y^{α} (1/deg)	X/C
0006	9	0.92	0.103	0.25
0009	9	1.31	0.11	0.25
0010-34	6	0.80	0.098	0.245
0012	9	1.59	0.106	0.25
0015	8.61	1.66	0.097	0.2238
1408	9	1.34	0.11	0.25
23012	9	1.79	0.107	0.247
23012-64	8.4	1.71	0.095	0.240
23112	8.2	1.73	0.100	0.235
2408	9	1.50	0.104	0.247
2412	8.9	1.68	0.104	0.247
34012	8.34	1.8	0.1	0.244
4406	8.18	1.32	0.100	0.246
44012	8.50	1.82	0.098	0.245
4412	9	1.68	0.109	0.247
64-006	9	0.80	0.11	0.256
64-108	9	1.10	0.11	0.255
641-412	9	1.68	0.112	0.267
653-018	9	1.38	0.105	0.267

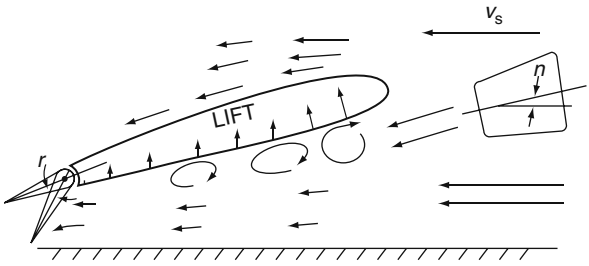

Fig. 3.8 Airflow lines around a main wing of WIG

In order to easily convert experimental data from model to full-scale craft, model tests should be carried out including the main wing with main hull and side buoys (except tail and outer composite wing) for model tests in a wind tunnel laboratory. The tail and outer composite wing are assumed to perform as in free airflow and so characteristics can be calculated from aerodynamics references such as [5].

The centre of lift is also changed with flight height h. At lower h values, the centre of lift moves backward due to the blockage of incoming airflow in the air channel under the main wing that increases the air pressure at the rear part of the main wing. However, in case of higher flight up to the height limit of GEZ, the centre of lift will be approximately unchanged, as Fig. 3.9 shows.

Figure 3.9 shows a typical curve for the main-wing centre of aerodynamic lift X_{dc}, including the effect of main hull and side buoys, versus relative flight height $\bar{h} = h/c$ of a DACWIG with and without bow thrusters. Here, $\bar{h}$ represents the

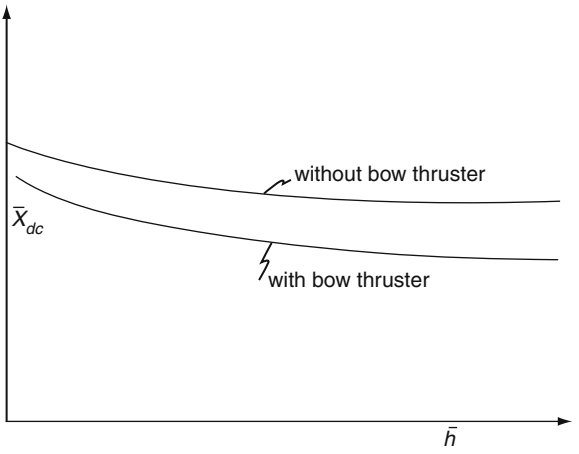

Fig. 3.9 Centre of aerodynamic lift $\overline{X_{dc}}$ of main wings with side buoys and hull, with and without thrusters

net clearance under the hull and side buoys, and C the wing chord length. $\overline{X_{dc}} = X_{dc}/C$, where X_{dc} represents the distance between the centre of lift and wing leading edge.

From this figure, one can see that both the bow thrusters and flight height influence the X_{dc} value. The value of X_{dc} is very difficult to calculate by theoretical methods. The simplest currently available method to determine this data is by means of model experiments.

Centre of Lift of a Whole WIG Craft Operating in GEZ

Completing the whole WIG, other than main wing as discussed above, there are the tailplane and elevators located at the stern for longitudinal force balance and craft stability, and outer "composite" wings for both longitudinal force balance and improving the aerodynamic efficiency of the craft when flying. The centre of lift for a WIG has therefore to be verified by means of wind tunnel tests of a complete model.

Influence of Control Mechanisms on Craft Aerodynamic Centres

The craft CG is unchanged through the operational modes, apart from changes due to fuel consumption, while the aerodynamic and hydrodynamic forces do change a great deal. The moments about the craft CG caused by the various forces has to be equal to zero if trim is to remain level. This means the centre of resultant acting forces has to be located around the CG of the craft. To achieve this, adjustments to

the stabilisers, flaps and air cushion feed need to be made to maintain equilibrium. To minimise the adjustments required, the following issues need to be considered:

- *Hull-borne operation mode*: It is best that the side buoy buoyancy centre coincides with horizontal CG of the craft at a small positive trim angle (bow up), and enough reserve buoyancy is provided particularly at the bow for safe landing and ditching from flying mode. If the horizontal CG is ahead of CB, the craft will be unstable and unsafe to operate, while if the horizontal CG is too far behind the CB the craft will float with significant bow-up trim and be difficult to accelerate into planing mode.
- *Static hovering over ground or landing/launching of a DACC or DACWIG*: The centre of air pressure (CP) has to coincide with CG, otherwise the craft will be very difficult to move due to contact of the hull/side buoys with the ground, causing high drag.
- *Cushion-borne operation*: The CP (for DACC and DACWIG) or the resultant centre of action of both cushion force and hydrodynamic lift has to coincide with CG, otherwise it will lead to a high trim angle and difficult take-off due to much higher hump drag.
- *Flying in GEZ*: The whole WIG centre of lift in flight has to coincide with the craft CG. The centre of lift at neutral stabiliser angle should be forward rather than aft of the centre of gravity at all operational conditions for the craft. Fuel usage may move CG forward, so this needs to be taken into account.
- *Flying beyond the GEZ*: The centre of lift of the craft free flying beyond the GEZ has to coincide with CG for the same reason mentioned above.

The centres of various acting forces are often not located at the CG. In addition, their location changes. For instance, the centre of lift changes with flying height; CP also changes with flying height and speed; and centre of hydrodynamic force changes with Fn. How to solve this problem? Using the aerodynamic control surfaces to adjust the centre of forces is the simplest method available. The influence of such mechanisms is introduced briefly as follows:

1. *Influence of flap angle on CP*. The greater the flap angle, where γ represents the angle between the centre line of main wing and flaps, the larger the flow blockage in the air channel under the main lifting wing. This causes an increase of air pressure on rear part of the main wing, and CP moves backward. The sensitivity of WIG stability to such CP movements is very high.
   Flaps can be opened to an optimal position when operating at higher speeds on cushion, in hydrodynamic planing mode, or prior to the transition of modes so as to move CP forward and optimise the trim angle during the transition. It is not recommended to adjust flap position when transiting between modes, as the transitions are not steady-state conditions.
   It is suggested that in general the flaps be designed to be operated fully open for flying at high speed, and use the elevator neutral position only for further adjustment once the cruise height is set. When launching the craft or hovering

during slow-speed manoeuvring, the flaps should be designed to be fully lowered so as to maintain the maximum cushion air pressure. A position between 40% and 60% open for planing mode and take-off or landing may be considered practical. WIG main-wing flaps should be considered in a similar manner as flaps on an airliner that are also deployed to preset positions.

2. *Influence of elevators on the craft centre of lift (CA)*. Since the elevators are located at the rear of the craft far from the CG and, in addition, their aspect ratio is high, the influence of elevator on the CA is great. Change of elevator position will mainly affect the aerodynamic moment, and the total lift of the craft much less so. Adjustment of elevator neutral position is the best way to regulate the craft-running trim when flying at cruising speed.
3. *Influence of bow-thruster jet direction*. Adjustment of the rotating jet nozzle or bow-thruster drive shaft angle for PARWIG, and horizontal guide vane angle aft of the air propeller blades for DACC or DACWIG, strongly influences the CP when static hovering and CA when flying.

   Rotating the jet nozzle, thruster shaft or guide vane more downward at slow speeds moves the CP of both static and dynamic air cushions forward rather sensitively, so fine adjustments to trim can be made. When the craft is flying, the opposite happens, so designers must take great care when planning the programme for bow thrusters in different modes.

Figure 3.10 shows the flow patterns of a DACWIG model in different operation modes.

Figure 3.10(a) shows the craft in static hovering mode. One can see that the air jet will be blown into the air tunnel under the main wing in case of guide vanes moving down. Then the air cushion can be made in the air tunnel sealed by side buoys, main hull and flaps. The guide vane angle should be set at an optimum during static hovering.

Figure 3.10(b) shows the flow pattern of DACWIG during take-off. The guide vane is kept down to keep the CP in a steady position and minimise the drag hump. The main-wing aerodynamic lift increases as speed increases, CP moves forward, and the bow-up trim will increase.

Figure 3.10(c) shows the flow pattern of DACWIG during flying. The guide vanes are up, to make most of the air jet blown across the back surface of the main wing, consequently the CP moves forward ahead of the CG and the elevator will be adjusted to maintain a steady trim.

Figure 3.11 shows the influence of guide vane angle θ on the lift–thrust ratio η_{ls} and X_{dc}. It may be noted that the higher the angle of guide vanes downward, the more CP moves forward (X_{dc} reduces). It is found that an optimum angle exists, where both high lift–thrust ratio and forward CP can be obtained to meet the requirement of the force balance of the craft moving over ground.

Bow-thruster guide vanes are a powerful control mechanism for DACC, and DACWIG to regulate the centres of aerodynamic and air cushion lift, to ensure effective amphibious operation of the craft.

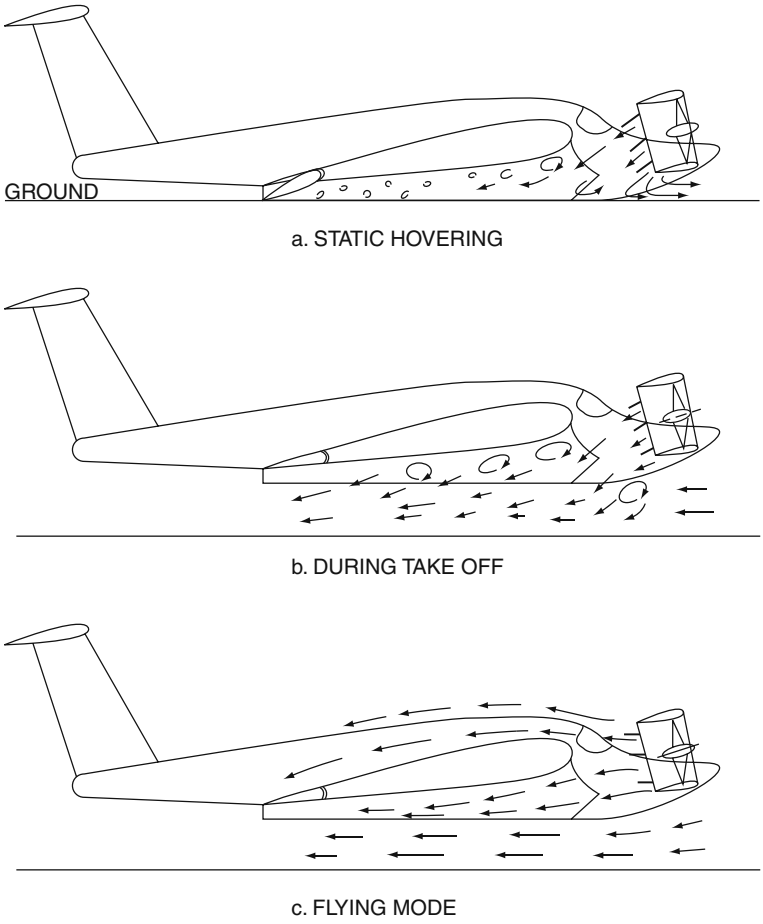

Fig. 3.10 (**a**) Static hovering airflow, flaps down; (**b**) at take-off; (**c**) flying

Longitudinal Force Balance

Condition for Normal Operation of a WIG in Various Operation Modes

For stable operation of a WIG, the following equations have to be satisfied in any operation mode, these are

$$W = L_{\mathrm{mw}} + L_{\mathrm{tw}} + T_{\mathrm{dc}} \sin\theta \tag{3.1}$$

where $T_{\mathrm{dc}} = \eta_{\mathrm{td}}\, T_{\mathrm{d0}}$ and

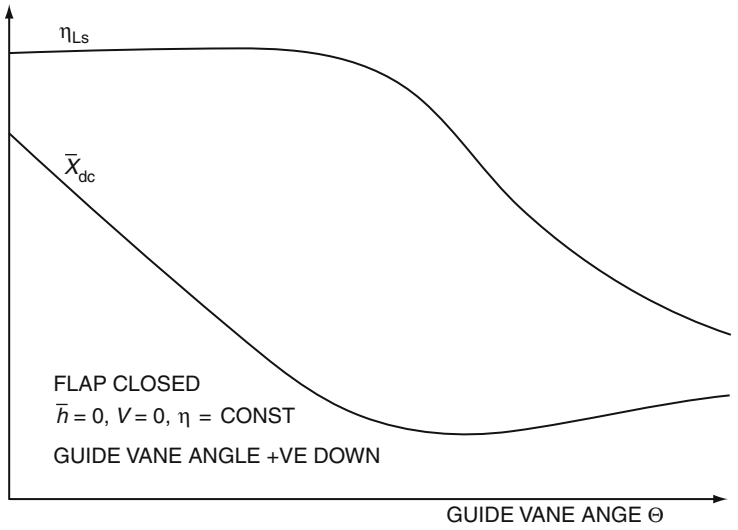

Fig. 3.11 Influence of guide vane angle θ on X_{dc} and η_{ls}

$$0 = L_{mw} \cdot l_{mw} + L_{at} \cdot l_{at} + L_{tw} \cdot l_{tw} + T_a.l_{pa} + T_{dc} \sin\theta \cdot l_{pf} + R \cdot l_r \qquad (3.2)$$

where

W	Craft weight
R	Craft total drag
L_{mw}	Lift of main wing, including the lift due to the craft hull
L_{at}	Lift due to the air tunnels
L_{tw}	Lift due to the tailplane (horizontal stabiliser and rudder)
T_{dc}	Bow thrusters' dynamic thrust at speed
η_{td}	Thrust deduction coefficient
T_{d0}	Thrust performance in wind tunnel
θ	Angle of bow thrusters' flow. Thruster angle, plus vane angle if fixed ducted thruster
η_P	Efficiency of thruster conversion to dynamic air cushion lift at speed considered
T_a	Thrust of rear thrusters
l_{mw}	Horizontal distance between main-wing aerodynamic centre and craft CG
l_{at}	Horizontal distance between the air cushion centre of the air tunnel (before take-off), or aerodynamic centre (after take-off) and the CG of the craft
l_{tw}	Horizontal distance between the aerodynamic centre of tail wing and the craft CG
l_{pf}	Perpendicular distance of the bow-thruster centre line about the CG
l_{pa}	Perpendicular distance of the rear thruster centre line about the CG
l_r	Perpendicular distance between the craft total drag acting line and the CG

Figure 3.12 shows the general arrangement of MARIC test DACWIG type 750. We will use the force balance of this craft as an example.

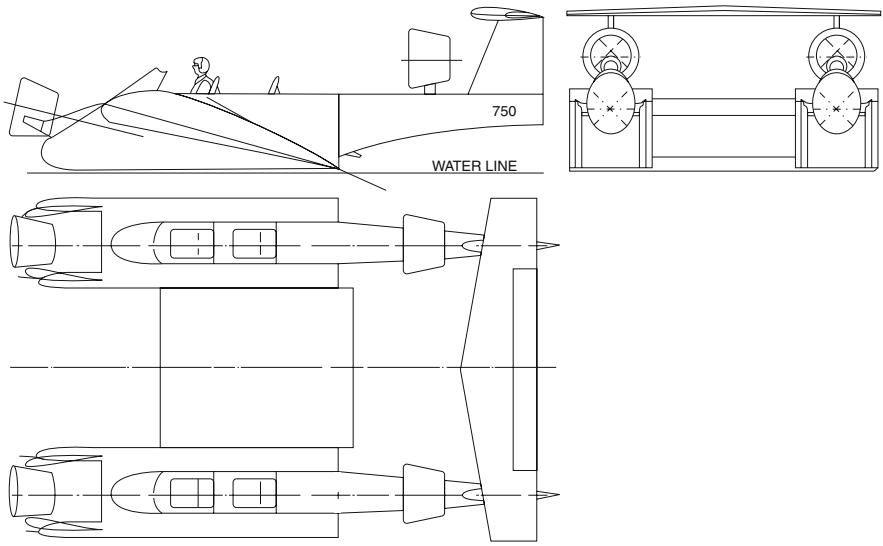

Fig. 3.12 Three view of DACWIG 750

The algorithm in Equation (3.2) should be interpreted to mean that a positive moment causes a bow-up trim while a negative moment causes bow-down trim.

It is difficult to satisfy equilibrium, Equation (3.2), for all the different operation modes in case of a fixed craft CG and fixed position of control surfaces, because of the variation in location of the air cushion and aerodynamic centres of the main wing. Two design approaches to satisfy the design requirements are offered here: the inherent force-balance method and the controllable equilibrium method.

Inherent Force-Balance Method

The aerodynamic centre of lift will move forward with an increase in speed and flying height, so in order to create equilibrium, the following steps have to be taken at the initial design stage:

1. The static air cushion centre of the air tunnel has to be placed close to the craft CG, in order to satisfy equilibrium while in static hovering operation mode.
2. The area and location of the main wing, and tail stabiliser have to be designed to balance the bow-up moment due to lift at the aerodynamic centre of the air tunnel of the craft moving forward at high speed, as ground effect takes over from ram aircushion lift.

Equilibrium is then satisfied for all craft operation modes. Figure 3.13 shows an artist's impression of a small DACWIG (or so-called flying motor car). One can see that the main wing is located behind the air tunnel to balance the aerodynamic centre of air tunnel moving forward during high-speed operation. Unfortunately, the structural configuration of this type of craft is complicated. The configuration of main wing and air tunnels makes the hull weight and construction cost high. In addition, the equilibrium problem may still occur at differing disposable loads and external circumstances.

Fig. 3.13 Artist impression of a DACWIG "Flying Jeep"

The so-called controllable equilibrium method might be used as an alternative, as described in the following.

Controllable Equilibrium Method

Figures 2.27 and 1.20 show the "Volga-2", a DACC design from Russia, and Fig. 2.37 shows the "SWAN", a DACWIG designed and built by MARIC in China. Both use the controllable equilibrium method for stability design, as follows:

There are three control mechanisms that may be employed for changing the pitching moment acting on the craft:

1. Guide vanes in the exhaust of the bow thrusters
2. Flaps on the main wings
3. Elevators on the tail horizontal surfaces

Each of these can create a pitching moment on the craft; however, some considerations regarding handling methods need to be explained:

- Bow-thruster guide vanes or jet nozzles (Fig. 3.14) are rather powerful for changing the craft running trim, particularly in the static hovering mode and high-speed flying mode for DACC and DACWIG. Rotating guide vanes down will cause the

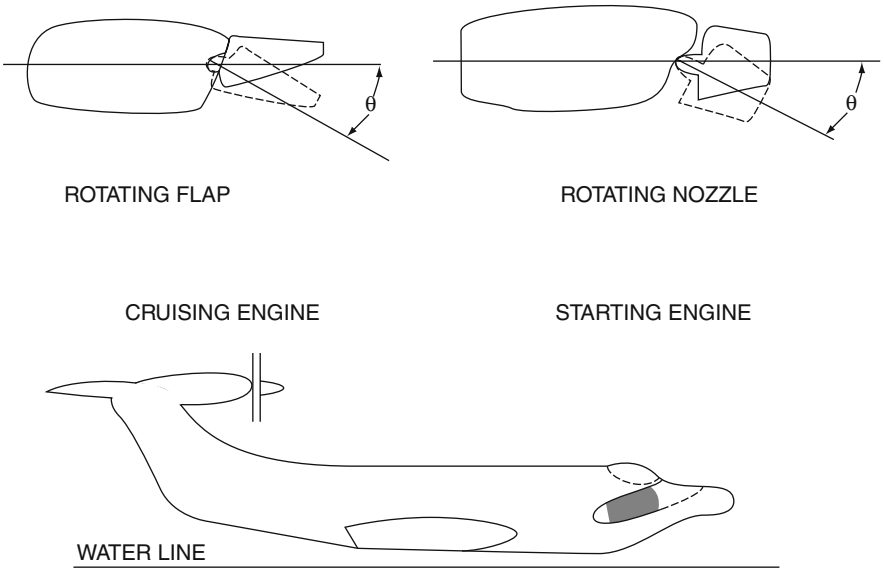

Fig. 3.14 Nozzle rotation on Orlynok

cushion centre CP to move forward, and guide vanes up cause the centre of lift to move backward.

When static hovering or during landing or launching operations, it is normal for pilots to close the main-wing flap to form the static air cushion and place guide vanes down so as to move the air cushion centre of lift forward from the cushion geometric centre of area during hovering. This is due to the CG normally being located above the centre of lift from the main wings for high-speed flight, which is about 25% of chord forward of the static air cushion centre of area.

- While on cushion or during hydrodynamic planing, the flap should be opened in planed stages in order to reduce the hydrodynamic drag acting on the flaps, and transition to the dynamic (ram air rather than power assisted) air cushion. Meanwhile, the jet nozzle or guide vanes should be rotated upward to move the CA due to the cushion component of lift backward, so as to maintain the craft-level trim. This is due to the CA moving forward as the craft accelerates and a greater proportion of the lift being developed from the main wing in ground effect mode (CA 25% of wing chord from leading edge).
- In flying mode, the flaps will be opened fully to maximise the aerodynamic efficiency of the main wing, and the guide vane or jet nozzles rotated fully upward to continue to maintain level trim as well as to increase the bow-thruster thrust-recovery coefficient. In this operation mode, the elevator is used to adjust craft trim to deal with the different external circumstances and changes of the centre of gravity due to fuel consumption.

The latter design approach for trim and stability control is more convenient for application, but more complicated for craft operation. In larger craft, the control systems can be synchronised through computer automation.

Handling of WIG During Take-Off

Figure 3.15 shows several handling methods of WIG, where θ represents the bow-thrust angle, t the time history, ψ the craft course angle and h the flying height. The figure shows the parameters θ, ψ and h versus time t.

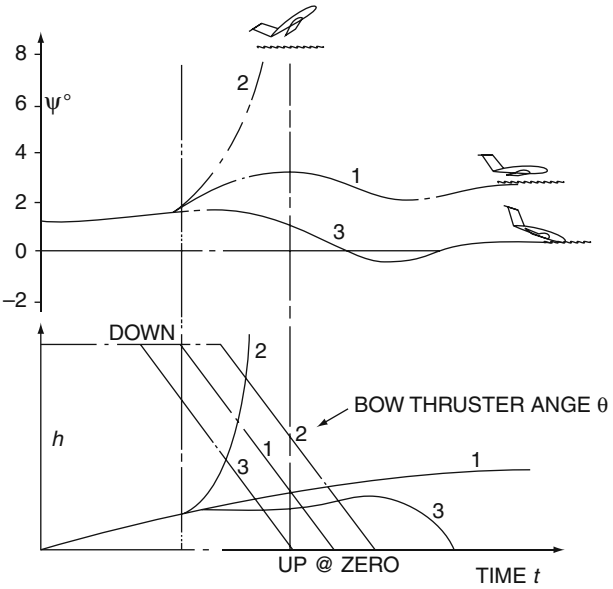

Fig. 3.15 Selecting the correct handling method for WIG for safety

Before and during take-off, pilots use positive bow thruster or guide vane angles (i.e. a down angle to guide the propeller airflow into the air channel), giving a bow-up pitching moment. After take-off, the bow-thruster nozzles or guide vanes are rotated horizontally. In this condition, the craft should also have a bow-up neutral trim, and the craft running trim is adjusted to an optimum angle by use of the tail stabiliser. Flying height is adjusted by small movements of the main-wing flap.

In the figure, it can be seen in line 1 that the trim is corrected by operating the bow-thruster angle on time. In this case, the craft operates with a proper trim angle and flying height. Line 2 shows where the pilot operates the bow-thruster angle upward too late, so that the craft bow is pitching up too much and might cause a craft to further pitch up and "stall". Line 3 shows where the pilot moves the bow-thruster angle upward too early so as to lead to failure to take-off or even craft

plough-in due to the decrease of cushion pressure at bow of the craft, and increase of drag because of negative trim angle of the craft.

Such phenomena are accentuated in case of the craft running in wind and waves, so pilots have to operate carefully in waves and windy climates. The second transitional phase for WIG is an operation requiring considerable skill for smooth operation. The DACC or DACWIG has lower drag peaks to negotiate than a PARWIG, so that the sensitivity to bow-thruster jet or vane changes is much lower, nevertheless the maintenance of WIG stability through this phase requires a combination of correct adjustment of power settings, bow thrust and flight controls, and the correct timing of the adjustments as take-off is transitioned.

A WIG craft that does not have bow thrusters will also experience the CA moving forward as the speed is increased. In the case of non-power-assisted craft, the trim is adjusted by application of the tail elevator and the main-wing flaps. During take-off, elevator down is required, to keep the tail up, and this can be reduced as take-off is achieved. For landing, elevator up is required so as to hold the bow up once CA starts to move back as the air cushion is established under the main wing.

Chapter 4
Hovering and Slow-Speed Performance

Introduction

The four main types of WIG design each use a different approach to aerodynamic support at zero and slow speeds. This is partly due to the primary design target – the cruise performance of each craft type.

The classic WIG employs geometry for the main lifting wing with a large inlet and tapered plan form that captures the incoming air as efficiently as possible and converts as much as possible the kinetic energy into static pressure. To create the lift it has to travel forward. The static pressure build-up is partial and most effective when the ground clearance is very small. The approach to design these craft is to optimise the geometry of the lifting wing to achieve lowest practical take-off speed consistent with the desired cruise speed.

The PARWIG employs bow thrusters, either propellers for smaller craft or gas turbines for larger craft, which blow over the main wing and provide lift from the velocity of the thruster jet. The lifting force is a complex combination of normal aerodynamic lift from the wing's upper and lower surfaces, lift from increased static pressure under the main wing and, possibly, a Coanda effect due to circulation around the airfoil. An ACV-type air cushion as such is not formed under the wing, rather, there is an additional lift from static pressure build-up due to airflow deceleration as it passes under the wing.

PARWIG using jet thrusters also derive some lift from deflection of the jet flow itself when the jet is deflected downward, directly impinging on the ground, and then on the underside of the lifting wing. There will be two components to this force, first the vertical component of the jet thrust itself, second the reaction from the ground deflection (flow reversal, with loss of velocity and generation of a static pressure) and, third, the same reaction as the jet contacts the under surface of the wing and is deflected back downwards. The first component is important to consider due to its location in the craft bow, while the second and third components will be much weaker, but still need careful assessment.

PARWIG performance targets are normally for a high cruise speed, requiring a rather streamlined design. This configuration is in conflict with a low take-off speed, and hence the approach for bow thrusters that enhance the main-wing performance, rather than creating a full air cushion.

L. Yun et al., *WIG Craft and Ekranoplan*, DOI 10.1007/978-1-4419-0042-5_4,

The DACWIG extends the approach of the PARWIG by forming the main wing and side buoys to form a cavity that can more effectively trap the incoming air and form a cushion even at zero speed. The thrusters will still create additional forces when the air jet is deflected downward, similar to a PARWIG. The cushion formed still has a large air leakage forward under the wing leading edge. This reduces as craft speed increases towards take-off. Once the arrangements necessary for an effective air cushion have been adopted, it is clear that the design for extreme speed is not appropriate and so DACWIG performance targets fall in the mid range of cruise speed.

The DACC takes cushion formation one stage further by including skirt-type seals. A DACC is normally designed to stay in strong ground effect so that the cushion seals can remain effective at all operation speeds, and craft support remains a combination of aerodynamic lift and cushion lift at cruise speed.

In this chapter, we will focus on the static pressure generated under the main wing at zero and slow speeds by bow thrusters, and in particular its application for DACWIG and DACC. Both of these craft have a configuration including a main lifting wing, side buoys and trailing edge flaps arranged so that the bow thrusters can create an air cushion to lift the craft off the ground even at zero-forward speed. The air cushion then allows take-off into the strong ground effect region at relatively slow speed, and reduces the drag peaks in the transitional phases.

Hovering Performance Requirements

Manoeuvring and Landing

Amphibious capability (slow-speed manoeuvring, take-off and landing over land or water) is enabled for DACC and DACWIG through having a clear air gap between the base plane of the main hull and side buoys with the ground or water when hovering statically. If no flexible skirt is installed under the side buoys, the clear air gap (daylight clearance) when hovering statically is particularly important to protect the hull and side buoy structures against ground impact. Improved obstacle clearance can therefore be achieved by installing inflatable skirts similar to those for a hovercraft, if the WIG hull geometry is suitable. The main hull and side buoys will need landing pads installed if no rolling wheels are fitted for overland manoeuvring off cushion.

Low-Speed Operations

Craft sometimes need to manoeuvre at low speed in narrow waterways, rivers or other areas close to harbours and terminals or military bases. PARWIG craft have high resistance and required power rating to operate in the hull-borne mode for

low-speed manoeuvring and so are only suited to open-water operation. DACC and DACWIG can use hovering mode for manoeuvring in confined conditions with minimum resistance, zero draft and relatively powerful response to controls. Over water, it is not necessary to have a clear air gap, as this creates a great deal of spray at low speed. Similar to an ACV, so long as the air cushion pressure is sufficient to support the weight and depress the internal water surface, controllability should be fine.

Hump Speed Transit and Take-Off into GEZ

The resistance curve of both PARWIG and DACWIG has significant peaks at hump and take-off speeds [1]. At hump speed, the resistance is two or three times that at cruising speed, while just after take-off the drag reduces to a minimum. Since the drag at hump speed is even larger than at design speed, the ability for passing through hump speed is the primary powering criteria for WIG.

Figure 1.13 shows a drag curve of a PARWIG model both on calm water and in a seaway, with and without air injection, i.e. with and without bow thrusters providing pressurised air into the air channel under the main lifting wing. It can be seen that the drag with air injection is significantly lower than that without the air injection both on calm water and in waves.

Figure 1.14 shows the aerodynamic and hydrodynamic lift force on a craft during take-off without and with air injection. Air injection under the wings of an Ekranoplan substantially decreases the hydrodynamic drag during take-off and, in addition, weakens the hydrodynamic impact force and vertical acceleration in waves. In the figure, L is the aerodynamic lift force and W is the weight of the craft. In the take-off run of a seaplane, hydrodynamic forces prevail – the forces acting on the floats and hull. A PARWIG has much lower hydrodynamic loads than a seaplane due to the dynamic air cushion support and damping. This has been verified by model experiments.

Air injection therefore improves the lift force and also reduces drag particularly through hump speed.

Seakeeping

There are three criteria to judge the seakeeping qualities of a WIG:

- Impact loads from waves acting on the hull before and during take-off
- Vertical acceleration of craft operating over waves
- Ability to accelerate through hump speed and take-off over waves

PARWIG Theory from the 1970s

Hovering performance has an important influence on the hump drag and so the ability to accelerate through hump speed and take-off. In addition, the seakeeping at speeds up to take-off are much improved with effective low-speed air cushion support. Due to lower hump drag, a craft with an effective air cushion can be designed with lower power, since the overall powering for WIG is controlled by hump drag and take-off, rather than cruise speed.

In the early 1960s, a joint Navy/Army programme investigating the feasibility of employing ground effect for high-speed marine craft was set up in the USA. Reference [2], and reference 10 from Chapter 1 both proposed that power-assisted ram air lift might reduce take-off speed and impact loads acting on the hull during operation in waves. The concept proposed included propulsors in front of the wing so the efflux from the propulsors was blown into the channel made by the wing, flap and endplates. It was proposed that static lift of over six times the thrust of the thruster could be produced by a PARWIG configuration while recovering 80% of the installed thrust for forward acceleration.

The potential flow theories and turbulent jet theory are described as follows:

The flow momentum model for a PARWIG is illustrated in Fig. 4.1. The nomenclature is as follows:

M_0	Jet momentum of thruster
M_1	Horizontal momentum of thruster flow entering cavity
M_2	Horizontal momentum of airflow leaving cavity under flap
M_3	Momentum of jet flow deflected over main wing
M_4	Momentum from reverse airflow from air curtain
V_0	Thruster jet airflow velocity
V_s	Average velocity of jet inside air cushion
V_1	Velocity of jet entering air cushion
V_2	Velocity of jet leaving air cushion
t_0	Thruster jet thickness
t_1	Jet thickness at ground contact
t_2	Gap between the lower tip of flap and ground
h	Flying height of PARWIG (measured to trailing edge of main wing)
θ	Thruster jet inclination angle
β_3	Angle of jet deflected over wing, assumed at V_0
C	Chord length of wing
ρ_a	Air density
Re	Reynold's number, $\mathrm{Re} = Vc/\nu_a$, where c is the relevant length dimension
ν_a	Dynamic viscosity coefficient of air

According to the conservation of horizontal momentum,

$$M_1 = M_0 \cos\theta + M_4 \tag{4.1}$$

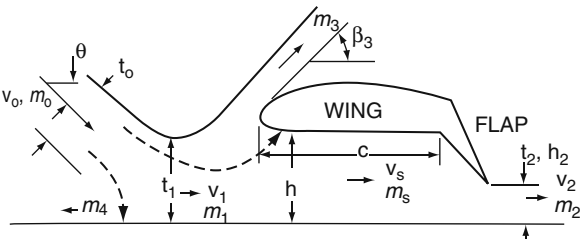

Fig. 4.1 Airflow momentum of a WIG model

If we neglect the momentum loss in the jet flow due to its jet inclination, then

$$M_4 = M_0 - M_1$$

so

$$M_1 M_0 = (1 + \cos\theta)/2 \tag{4.2}$$

We assume that the pressure and velocity under the wing are uniform, so that

$$P_c \cdot h + (P_3 - P_a)\, h = M_1 - M_3 \cos\beta_3 - \rho_a V_s^2\, h \tag{4.3}$$

where P_c is the static pressure and P_3 is the dynamic pressure under the wing. If we assume that V_s is uniform, the equilibrium equation of horizontal momentum at the trailing edge flap and under the wing can be written as:

$$P_c \cdot h = \rho_a V_2^2 t_2 - \rho_a V_s^2\, h + D_r \tag{4.4}$$

where D_r is the drag due to the flap, i.e. $D_r = \int_{t_2}^{h} (P - P_a)\mathrm{d}y$
Further, if we assume that the flow under the wing is one dimensional, then

$$P_c \cdot h = 0.5\rho_a V_2^2 \left[1 - (V_s/V_2)^2\right] \tag{4.5}$$

According to the law of continuity of flow, then

$$V_s/V_2 = t_2/h \,\text{and}\, M_2 = \rho_a V_2^2 t_2$$

so Equation (4.5) becomes

$$P_c \cdot h = 0.5 M_2 \left[h/t_2 - t_2/h\right] \tag{4.6}$$

From Equation (4.4), we have

$$D_r = 0.5 M_2 \left[h/t_2 - t_2/h - 2\right] \tag{4.7}$$

The wing lift per unit width can be written as $L = P_c \cdot C$, and using Equations (4.6) and (4.7), we have

$$L \cdot h/(M_1 \cdot C) = 0.5M_2/M_1 \left[h/t_2 - t_2/h\right] \tag{4.8}$$

$$D_r = 0.5M_2 \cdot \left[h/t_2 + t_2/h - 2\right] \tag{4.9}$$

The turbulent mixing injection effect can be described as a two-dimensional turbulent flow with a decaying velocity distribution from the origin to the wing tip. Using (') to represent coordinates measured from the centreline and perpendicular to it, the velocity distribution across the span is

$$v' = \left[3t_2 v_0^2 \frac{\sigma}{4x'}\right]^{1/2} \left[1 - \tan\,h^2 \eta_v\right] \tag{4.10}$$

where

$$\eta_v = \sigma y'/x' \text{ is the velocity decay function along with span} \tag{4.11}$$

and

$$\sigma = 7.67 \text{ is an experimental constant}$$

Using Equation (4.10),

$$\frac{M_1}{M_0} = \frac{1}{M_0} \int_{h_s}^{\infty} \rho v' dy' = \frac{3}{4}\left[\frac{2}{3} - \tan\,h\eta_v + \frac{1}{3}\tan\,h^3 \eta_v\right] \tag{4.12}$$

If we substitute Equation (4.12) into Equation (4.2), then we have

$$3\tanh \eta_s - \tan\,h^3 \eta_s + 2\cos\theta = 0 \tag{4.13}$$

The flow rate to the wing can be written as

$$\frac{Q_1}{Q_0} = \left(\frac{1}{Q_0}\right) \int_{h_s}^{\infty} \rho v^2 dy' = \left(\frac{3x'}{4t_0\sigma}\right)^{1/2} (1 - \tan\,h\eta_v) \tag{4.14}$$

$$\frac{Q}{Q_0} = \left[\frac{3x'}{t_0\sigma}\right]^{1/2} = 0.6254 \left(\frac{x'}{t_0}\right)^{1/2}$$

The two-dimensional turbulent jet velocity distribution can be written after some manipulation as

$$V/V_{\max} = 1 - \tan\,\mathrm{h}^2\eta_{\mathrm{v}} = \sec\,\mathrm{h}\eta_{\mathrm{v}}$$

$$M_1 = \rho v_{\max}^2 \frac{\bar{t}}{3}\left[\tan\,\mathrm{h}\eta_{\mathrm{v}} - \frac{1}{3}\tan\,\mathrm{h}^3\eta_{\mathrm{v}}\right]_0^{\infty} = \rho v_{\max}^2 \frac{\bar{t}}{3}\left[\tan\,\mathrm{h}\eta - \frac{1}{3}\tan\,\mathrm{h}\eta\right]_{\mathrm{n_s}}^{\infty}$$

where $\bar{t}$ represents equivalent flow thickness, and $\bar{t} = (1 + \cos\theta)\, t_1$

$$M_2 = \rho v_{\max}^2 \frac{\overline{t_1}}{3}\left[\tan\,h\left(\frac{3t_2}{\overline{t_1}}\right) - \frac{1}{3}\tan\,\mathrm{h}^3\left(\frac{3t_2}{\overline{t_1}}\right)\right]$$

Substitute this into Equation (4.8), and finally we have

$$\frac{Lh}{M_1 C} = \left[\tan\,\mathrm{h}\left(\frac{4}{3} - \frac{t_2}{h} - \sigma\right) - \frac{1}{3}\tan\,\mathrm{h}^3\left(\frac{4}{3}\frac{t_2}{h} - a\right)\left(\frac{1 - \left(\frac{t_2}{h}\right)^2}{\frac{4t_2}{3h}}\right)\right] \tag{4.15}$$

$$D/M_1 = 0.045 + \frac{1}{2}\left(\frac{Lh}{M_1 C}\right)\frac{\left(1 - \frac{t_2}{h}\right)}{\left(1 + \frac{t_2}{h}\right)} \tag{4.16}$$

where

$$\text{if } t > (9/4)\, t_0, \text{then } a = \left(\tfrac{9}{4}\right) h/\,(1 + \cos\theta)\,\bar{t}_0$$
$$t < (9/4)\, t_0, \text{then } a = h/\,(1 + \cos\theta)\,\bar{t}_0$$

In summary, the wing lift per unit span L is a function of

M_1	The flow momentum at the position before the air channel
h	Flying height of the main wing measured between the lower surface of main wing and ground
C	Chord length of main wing
t_2	Distance between the lower tip of flap and ground
t_0	Efflux thickness at the origin
θ	The inclination angle of the thruster jet

Lift and drag predictions derived from testing results are given in references [2] and Chapter 1 [10]. The model under test is shown in Fig. 4.2.

In order to simplify the calculation above, if we take $M_1 = M_0$ and $M_1 = t(1+\cos\theta)/2$, and $t = \pi d^2/4b_{\mathrm{c}}$, then the wing total lift can be calculated simply. However, there are some interesting problems with this formula, e.g.:

1. A specific air gap at the stern flap is assumed, however, actually the air gap when hovering statically is close to zero. In such a case, Equations (4.8) and (4.9) will be indeterminate. The physical phenomenon will be very similar to an air cushion vehicle. The equation can alternately be written as

$$M_1 \cos\theta - M_3 \cos\beta_3 + M_4 = P_{\mathrm{c}} \cdot \mathrm{h}$$

This formula may be more suitable for a PARWIG that is unable to operate over ground without landing gear. For a craft without amphibious ability, the function of static air cushion lift is then to lighten the pressure on the landing gear, and improve take-off performance. In this case, the flaps will be opened with a definite gap t_2, so as to reduce the drag from the flaps.

2. It is found that lift increases with efflux momentum M and wing chord C, and increases inversely with flying height h, and has no relation with the cushion beam. The hypothesis that the cushion pressure is only dependent upon the specific momentum of the thruster, i.e. the momentum per unit beam of cushion, is based upon the idea that the wider the cushion, the larger the cushion area and lower the specific momentum required.
   This may cause a misleading result, because the mixed efflux momentum M_1 is rather different from M_0 due to the air injection, and the wide cushion beam will cause a more effective mixture of the air injection than that where the cushion is narrow. It can be shown that sometimes the wider the air tunnel, the higher the lift acting on the wing.
   Therefore, these expressions may be most suited to craft with a narrow air tunnel compared with the width of jet flow, or for a multiple row of bow thrusters, as shown in Fig. 4.2. This figure shows a US Navy PARWIG model testing in towing tank. The model had a row of bow propulsors, and its corresponding turbulent mixing injection model is shown in Fig. 4.3. In this case, the expressions above may be suitable.

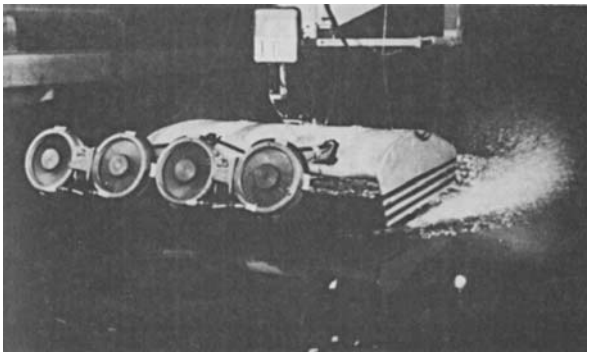

Fig. 4.2 US Navy PARWIG model in towing tank – may need to delete or substitute

3. In order to obtain a more effective turbulent mixing injection, the key parameters to relate position for bow thruster and wing will be X_j, and $h+\Delta h$, as shown in Fig. 4.4, together with the main wing chord C, and the bow thruster jet angle θ
4. The Coanda effect is not taken into consideration in the formula so that model test results will show higher lift than the calculations.
5. On real craft and models, normally there are side buoys at the tip of the main wings and a hull located at the centre of the craft, each with finite width. In the formula above, the lift provided by such hull and side buoys are not taken into

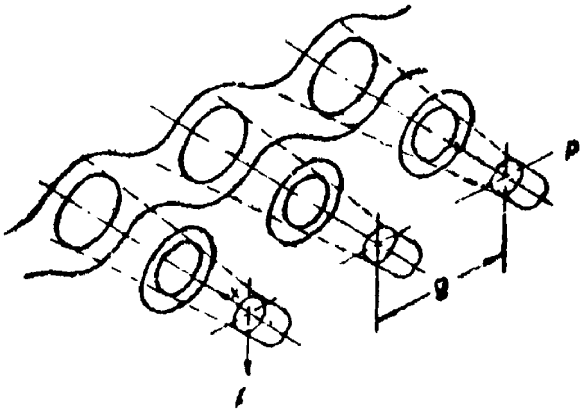

Fig. 4.3 Turbulent mixing air injection with multiple rows of bow thrusters on PARWIG model

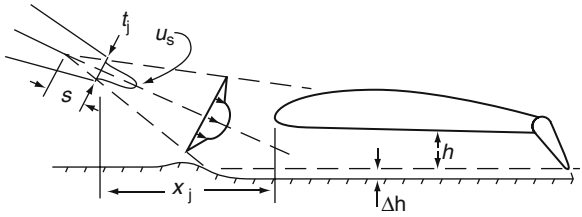

Fig. 4.4 Key parameters of related positions of bow thruster and main wing

account, so as to give conservative results compared to expectations from model tests.

Static Hovering Performance of DACWIG and DACC

Introduction

The PARWIG "Orlyonok" as shown in Fig. 2.17 is a very high-speed craft, and has good aerodynamic efficiency at higher flying height. The craft is characterised by a large aspect ratio, wide span main wing, thin side buoys and short flaps. This configuration makes it very difficult to form a steady air cushion and create sufficient static air cushion lift to support the total weight of craft at slow or zero speed. The bow thrusters of this type of craft aims instead to improve the take-off performance, seakeeping quality and payload capacity, by increasing the airspeed past the main wing compared to craft forward speed over both lower and upper surfaces.

Landing and launching of craft of this type are carried out using wheeled landing gear to roll onto the launch ramp, and both bow thrusters and cruising engines for propulsion as shown in the general arrangement of Orlyonok (Fig. 2.15).

DACC and DACWIG are characterised by their hovering capability without the need for landing wheels. This is their main advantage. For this reason, the craft has the following prerequisites, similar to an ACV:

Bow thrusters as fans to provide enough air pressure and flow rate to feed into the air channel during the static hovering
Configuration of the main wings and side buoys to form a suitable static air cushion
Some means to adjust the bow-thruster efflux from the pressure air provider to a propulsor with acceptable propulsion efficiency at the target cruise speed

Configuration of a DACC or DACWIG

Figure 4.5 below shows a typical DACC, the "Volga 2", and Fig. 4.6 shows a typical sketch of a DACC or DACWIG. From the figures, the prerequisite for making a steady and powerful air cushion will be satisfied by arranging the following elements in the correct configuration:

- Main wing: main lift-supporting surface.
- Main hull: main accommodation cabin of passengers or other disposable load, and also as an additional lifting surface.
- Side buoys: (1) With main hull, they should provide enough buoyancy to support the craft weight during hull-borne operation and avoid too deep static draught such that the bow thrusters submerge into water. Ideally the bow thrusters should have a static clearance from the water surface at least 100% of the design take-off wave height.
  (2) Seal the air cushion during static hovering;
  (3) Providing an additional surface area for the air cushion.
- Main-wing flaps: (1) Sealing the air cushion during static hovering;
  (2) Enhance the aerodynamic lift of main wing during flying operation mode through partial or full raising from the lowered-down position for hovering.
- Thruster guide vanes: To change the airflow direction to suit the need of various operation modes.
- c/b_{at} or b_{at}/c: Cushion length/beam ratio (where c is wing chord length and b_{at} is width of air channel) or aspect ratio of main wing from the point of view of static hovering, similar to an ACV, the larger the cushion length/beam ratio the more effective is static hovering performance. However, high c/b_{at}, meaning lower main-wing aspect ratio decreases the aerodynamic efficiency of the wing in flying mode so we have a trade-off problem.
- Wing aspect ratio: The aspect ratio of the whole wing is $(A.R)_w = b_w/c$, where $b_w = 2 \cdot b_{at} + b_h + 2 \cdot b_{sb}$. The main element of this aspect ratio is still b_{at}, the breadth of the main wing, and so the

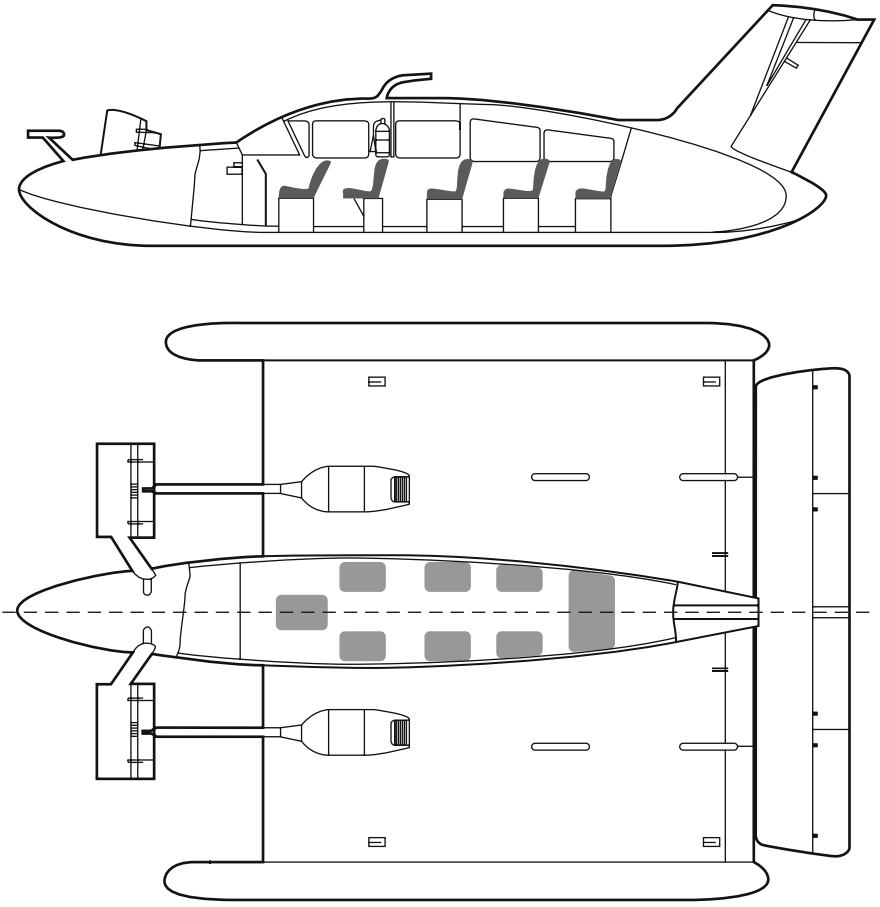

Fig. 4.5 Typical DACC – the Russian Volga 2

trade-off problem is not significantly changed when considering the craft rather than the main-wing air channel on its own.

Static Hovering Performance of DACC and DACWIG

Simplified Physical Model

Figure 4.7 shows a typical physical model of the airflow around a DACC or DACWIG, similar to Fig. 4.1 that shows a PARWIG. The difference of the flow characteristics between PARWIG and DACC is that the flaps of the latter are fully lowered during static hovering. To simplify, the physical model can be taken as that of an ACV so long as a suitable air curtain can be generated by the bow-thruster air jet. Figure 4.8 shows a typical transverse section of an ACV.

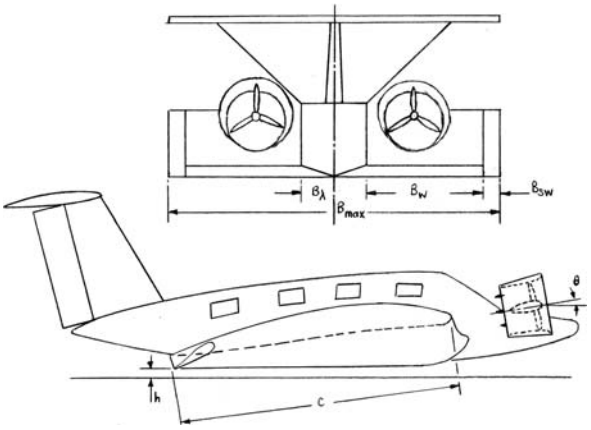

Fig. 4.6 DACWIG outline

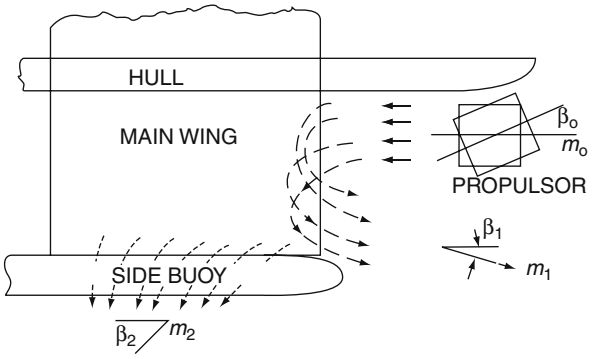

Fig. 4.7 Physical model of the airflow around a WIG in plan view

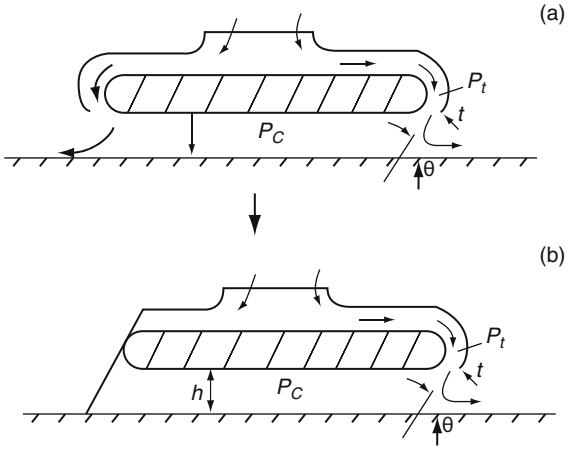

Fig. 4.8 (**a**) A transverse section of ACV and (**b**) adjustment to simulate WIG flow

In the case of DACC, the model can be changed from Fig. 4.8a to b, and also taking a look at Fig. 4.7, the average pressure in the air channel P_c can be obtained as follows, using the flow momentum theory based upon the unit length of transverse section of the wing. That is:

$$P_c (H + h) = \rho_a V_j^2 t (1 + \cos\theta) = \rho_a V_j^2 X \tag{4.17}$$

where

P_c Cushion pressure (N/m)
ρ_a Air density (N)
t Nozzle thickness (m)
H Cushion height (see Fig. 4.8) (m)
h Hovering height (m)
V_j The average velocity of airflow from bow thruster (m/s)
θ The angle between the centreline of nozzle and the craft base plan (°)

$$X = t/h (1 + \cos\theta)$$

Then the total pressure at the nozzle can be expressed as

$$P_t = 0.5\rho_a V_j^2 + fP_0 \tag{4.18}$$

where

P_t Total pressure at the exit of nozzle (N/m)
fP_0 Static pressure at the exit of nozzle (N/m) (=P_c)
Coefficient, according to the relative flying height h/t

Then the fan flow rate can be estimated as:

$$Q = V_j \cdot t \cdot l \tag{4.19}$$

where

Q Airflow from nozzle (m^3/s)
l Peripheral length of jet nozzle (m)

The lift power of an ACV can be estimated as:

$$N_L = QP_t / (75 \cdot \eta_s \cdot \eta) \tag{4.20}$$

where

η Efficiency of fan and air duct
η_s drive system efficiency
N_L Lift power (ps)

Assuming the cushion pressure is uniformly distributed, the liftable weight will be

$$W = P_c \cdot S_c$$

where

W liftable weight (N)
S_c Cushion area (m^2)

This is the basic formula for estimating the cushion pressure, flow rate and lift power of a DACC as an ACV. However, this expression cannot be used for DACWIG, for the following reasons:

- The jet nozzle is not uniformly distributed along the transverse direction of main wing, i.e. the jet nozzle cannot be used instead of the bow thrusters.
- The thickness is not thin enough so as to assume that the flow velocity along the exit is uniform.
- The turbulent mixing airflow has to be taken into consideration.
- There are air stream flows around the back surface of the wing and so the Coanda effect also has to be taken into consideration.

Practical Estimation of Static Hovering Performance of DACC and DACWIG

Theoretical calculation for estimating the static lift of a DACWIG or DACC is too complicated to rely on alone and so model experiments are normally used as the main study method and regression plots assessed from the test results to predict the static hovering performance. Both half and whole models can be used for such investigations. The half model shown in Fig. 4.9 includes the main hull and a side buoy as the endplate, and a bow blower, but without the tailplane and fin. The approach is to have a simple model and so more models for investigation at low cost. The figure shows a half model tested in a wind tunnel. Figures 4.10 and 4.11 show a DACWIG model hovering static on a rigid screen.

The static hovering performance of DACC or DACWIG is then tested for a number of variable parameters, i.e. the relative position of the bow thruster with the main wing and main hull as well as side buoy. The key geometric parameters, as shown in Fig. 4.8a, are as follows:

l_{btw} The distance between the leading edge of main wing and vertical plane of blades of bow thruster
b Distance between the craft centreline and bow thruster centreline
b_w Wing span
h Flying height, the distance between base plane of hull and ground
H Vertical distance between main-wing leading edge and the ground

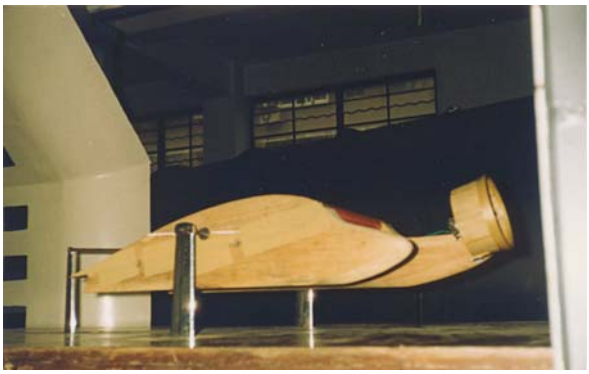

Fig. 4.9 Half model of DACWIG tested in wind tunnel

Fig. 4.10 Static hovering experiment of a WIG model on a rigid screen (front view)

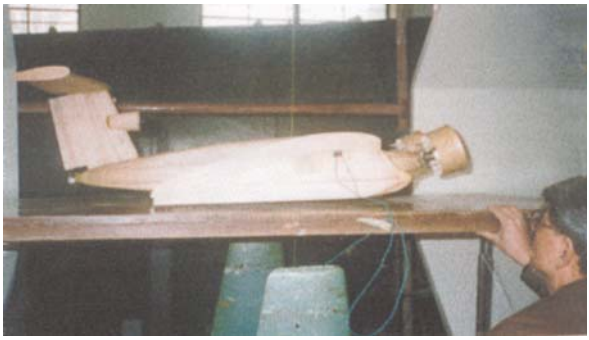

Fig. 4.11 Static hovering experiment of a WIG model on a rigid screen (side view)

h'	Height from the ground of centreline of bow thruster in the plane of the blade centreline
θ	Inclination angle of bow thrusters airflow
α_0	Main-wing angle relative to keel line of craft (wing assembly angle)

For estimation of static hovering performance of the craft, some basic assumptions have to be made as follows:

- The flaps are always lowered during static hovering.
- The flow pattern can be assumed as shown in Fig. 4.8b.
- The static cushion pressure P_c in the air tunnel can be assumed uniformly distributed, similar to an ACV or SES. This has been validated by the test results of the MARIC craft-type "750" and Swan.
- The air curtain will be formed under the main-wing leading edge. This air curtain is formed directly behind the bow thruster, generating reverse flow momentum M_4, and the other part of the air curtain is generated from transverse flow outward from the area covered by the thruster jet. The physical phenomena can be clearly observed both in model experiments and full-scale tests.

The jet flow from the bow thruster has to be concentrated and blown into the air tunnel at an optimum distance forward from it, and with effective barriers to contain the air cushion transversely, and at the wing trailing edge. The pressure distribution longitudinally and transversely across the main lifting wing under surface should then be similar to Fig. 4.12a,b , which show data from model tests of the "Swan" DACWIG.

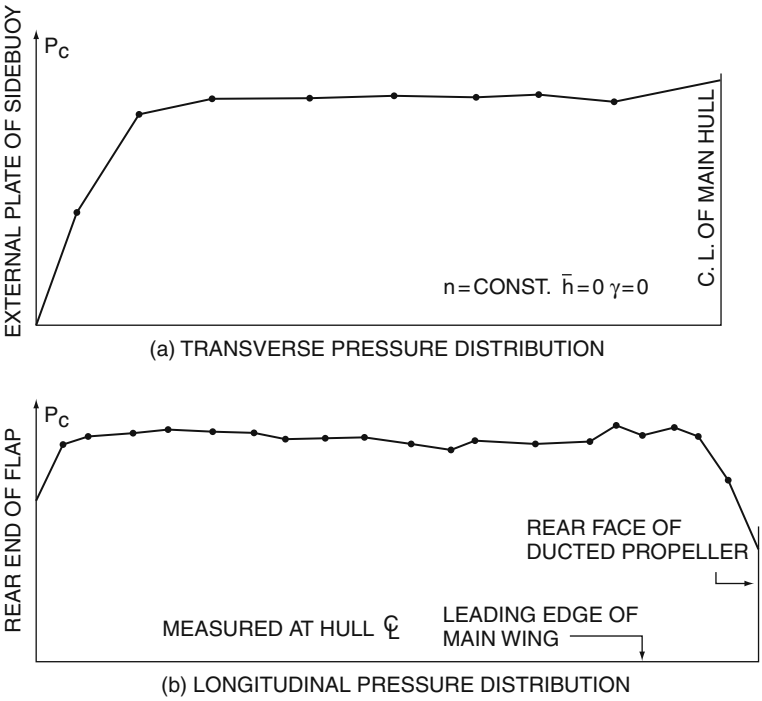

Fig. 4.12 (**a**) Transverse and (**b**) longitudinal pressure distributions under main wing of the Swan WIG

Then the flow momentum equation can be expressed as:

$$M_0 \cos\theta_0 - M_3 \cos\beta_3 - M_2 \cos\theta_2 + M_1 \cos\theta_1 + M_4 = Pc\,(H + h) \tag{4.21}$$

Since the H is rather large compared with h, the h may be neglected. In addition, since θ_2 has a large value (near perpendicular to the sidewall), M_2 also can be neglected. The M_3 (Coanda effect) also can be estimated by putting a coefficient on the lift caused by air cushion, then for analysis, the M_3 item can also be neglected. Then, Equation (4.21) can be written as follows:

$$M_0 \cos\theta_0 + M_1 \cos\theta_1 + M_4 = Pc \cdot H$$

Then

$$P_c = \frac{M_0 \cos\,\theta_0 + M_1 \cos\,\theta_1 + M_4}{H} \tag{4.22}$$

From the equations, there are some possibilities for increasing the cushion pressure and so the liftable weight may be proposed as follows:

- The lower H is, the higher the cushion pressure generated.
- It is most important to generate the air curtain to seal the air leakage from the air cushion at the cushion intake. From this point of view, a narrower wingspan makes it easier to maintain the air curtain in transverse direction along the wing. However, a wider span will create a larger cushion area, so this is a very interesting design challenge to optimise. Work is ongoing to develop more data for such optimisation.
- Making an inclined angle between the centreline of bow thruster and the craft (see Fig. 4.8a) will increase the cushion pressure.
- Lowering H gives higher cushion pressure. However, this drops down the position of the bow thruster, and thus potentially immersing the propeller into the water during hull-borne operation and take-off of craft in waves. In addition, a lower thruster position will be less efficient for thrust during ground effect flight.
- The calculation above does not consider the turbulent mixing effect of the efflux momentum from the bow thruster, for which the theoretical calculation is very complicated, so the expressions should be considered a means for discussion only.

Since there is no bow skirt or other sealing means at the bow, the most important measure for increasing the static lift is to take steps to seal the air leakage from cushion.

The air-jet momentum from the bow thruster can be expressed as:

$$M_0 = \rho_a Q V_j = \rho_a V_j^2 A_p = 2 q_j A_p \tag{4.23}$$

where

Q	Airflow rate from bow thruster (m^3/s)
A_p	Area of propeller disc (m^2)
q_j	Dynamic pressure of air jet (N/m^2)

Then from Equation (4.22), the non-dimensional average cushion pressure can be expressed as:

$$\bar{P}_c = P_c/q_j = f\,(h/C,H,b,l,\theta,\beta_3,\gamma) \tag{4.24}$$

where

l, H, b and θ	The parameters representing the geometric position of the bow thruster on the craft model, which can be found in Fig. 4.8a
γ	The inclination of flap, equal to zero in this case due to the static hovering situation of craft

In case of a fixed craft geometry and related position of bow thruster, then Equation (4.24) can be expressed simply as

$$\bar{P}_c = P_c/q_j = f\,(h/C) \tag{4.25}$$

where

$$q_j = 0.5\rho_a V_j^2$$

V_j is the average jet velocity of the bow thrusters

Figure 4.13 shows a typical relative cushion pressure $\overline{P_c}$ versus relative hovering height $\bar{h}$. It has been found the cushion pressure drops rapidly with increasing $\bar{h}$.

The optimum for relative position of a bow thruster and craft lines can be found by model experimental investigations. A ducted propeller (or turbofan) is often used as a bow thruster due to easy deflection of the jet fed into the air channel. In this case, the propeller thrust can be expressed as follows (Fig. 4.14)

In front of propeller disc,

$$P_{c0} = P_a - q_j \tag{4.26}$$

where

P_a	Relative atmosphere pressure, $= 0$
P_{c0}	air static pressure

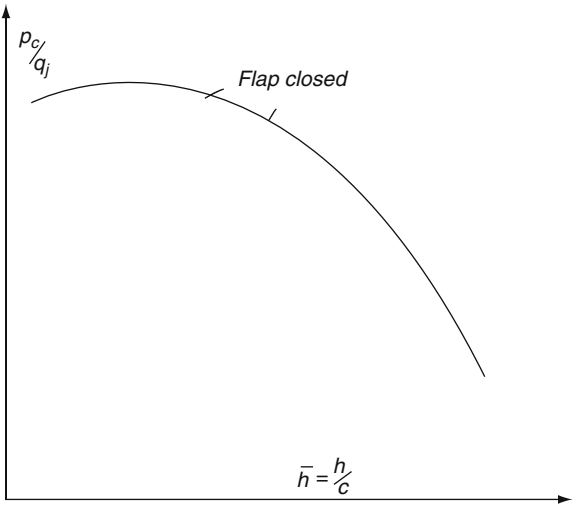

Fig. 4.13 P_c versus h of DACWIG model while flap closed

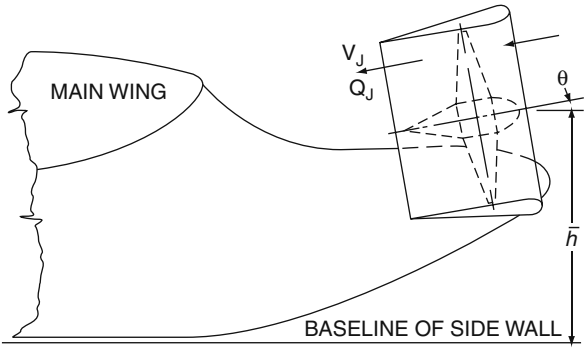

Fig. 4.14 Bow-ducted propeller sketches

Behind the propeller disc,

$$P_t = P_{c0} + q_j$$

$$T_p = (P_{c1} - P_{c0})\, A_p \cong P_t \cdot A_p \tag{4.27}$$

where

P_t Total pressure of propeller (N/m^2)
P_{c1} Static air pressure behind the propeller disc (N/m^2)

The total pressure of propeller or fan, P_t, can be expressed as: $P_t = k_q q_j$, where in general $k_q = 1.05 - 1.1$.

Then the propeller thrust can be expressed by

$$T_{\mathrm{p}} = A_{\mathrm{p}} k_{\mathrm{q}} q_{\mathrm{j}} \tag{4.28}$$

From the Equations (4.25) and (4.28), it is found that the propeller jet dynamic pressure and propeller thrust have the same influence on the cushion pressure of a DACWIG or DACC. From this point of view, the propeller thrust is simpler to use for estimating the lift of the craft due to its simplicity for direct measurement.

The total static lift can be expressed as

$$L = W = L_1 + L_2 + L_3 \tag{4.29}$$

where

L_1 Lift provided by air cushion pressure, $L_1 = P_{\mathrm{c}} \cdot S_{\mathrm{c}}$
L_2 Lift provided by Coanda effect, $L_2 = L_1 \cdot K_{\mathrm{c}}$
L_3 Lift provided by the vertical component of the thruster of bow thrusters, $L_3 = T \sin\theta$
W Craft weight
S_{c} Total cushion area, $S_{\mathrm{c}} = C\,(b_{\mathrm{h}} + 2b_{\mathrm{w}} + b_{\mathrm{sb}})$

It is important to note that the longitudinal centres of the three lifting force components are quite different. Craft static trim will be sensitive to the moments applied around the CG.

Since the pressure acting on the outside half-width of the base of each side buoy is close to atmospheric pressure, the supported area of the side buoy should be assumed half of the bottom area of the side buoys.

The flow rate and the power of the bow thruster (or lift fan) and lift engine can be calculated as:

$$Q = A_{\mathrm{p}} \cdot V_{\mathrm{j}} \tag{4.30}$$

$$N = Q \cdot H / \left[102 \cdot \eta_{\mathrm{p}} \cdot \eta_{\mathrm{t}}\right] \tag{4.31}$$

where

Q Flow rate of lift fan (m^3/s)
η_{p} Propeller/thruster efficiency
η_{t} Transmission efficiency
N Power of lift engine (kW)

Meanwhile, in order to simplify the calculation and treat the bow thruster as a ducted propeller, some useful parameters are also recommended as follows:

$$\eta_{\mathrm{Ls}} = L / T_{\mathrm{so}} \tag{4.32}$$

$$\eta_{\mathrm{Ts}} = T_{\mathrm{sc}}/T_{\mathrm{so}} \tag{4.33}$$

where

T_{so}	Static thrust of single ducted thruster (N)
η_{Ls}	Total static lift coefficient of air channel
L	Total lift provided by an air channel (N)
T_{sc}	Static thrust of a single-ducted thruster in air channel (N)
η_{Ts}	Static thrust-recovery coefficient of the ducted thruster in channel

The coefficients η_{Ls} and η_{Ts} are the main criteria characterising DACC's and DACWIG's static hovering performance. These coefficients are normally obtained from prototype or model tests. The power of the lift engine can be estimated as follows:

$$T_{\mathrm{so}} = K_{\mathrm{t}}\rho_{\mathrm{a}}n^2D^4, \text{ in case of } \lambda_{\mathrm{p}} = 0 \tag{4.34}$$

$$P = K_{\mathrm{p}}\rho_{\mathrm{a}}n^3D^5, \text{ in case of } \lambda_{\mathrm{p}} = 0 \tag{4.35}$$

$$K_{\mathrm{ts}} = T_{\mathrm{so}}/N, \text{ in case of } \lambda_{\mathrm{p}} = 0 \tag{4.36}$$

where

λ_{p}	Propeller advance ratio, $\lambda_{\mathrm{p}} = V/nD$
D	Diameter of the propeller (m)
n	Propeller speed (1/s)
K_{t}	Thruster coefficient
K_{p}	Power coefficient
K_{ts}	Specific static thrust of propeller (N/kw)

The coefficients can be derived from model testing or full-scale prototype testing, and then the lift power of the craft can be obtained.

Using K_{ts} for estimating the design lift power and hovering performance may be the simplest method during preliminary design. However, it should be noted that the expressions above do not include the effect of the propeller ducts, which are present in the data both from prototype and/or test results of model.

Figure 4.15 shows a typical static lift coefficient and thrust-recovery coefficient of a DACC or DACWIG versus relative hovering height in case of flaps fully lowered. It is found that η_{Ts} drops rapidly as $\overline{h_{\mathrm{c}}}$ increases. Sometimes, there is a turning point of the curve slope, the area inside of which may be taken as the strong surface effect zone during static hovering. In general $\overline{h_{\mathrm{c}}} = 0.05 - 0.1$ for DACC.

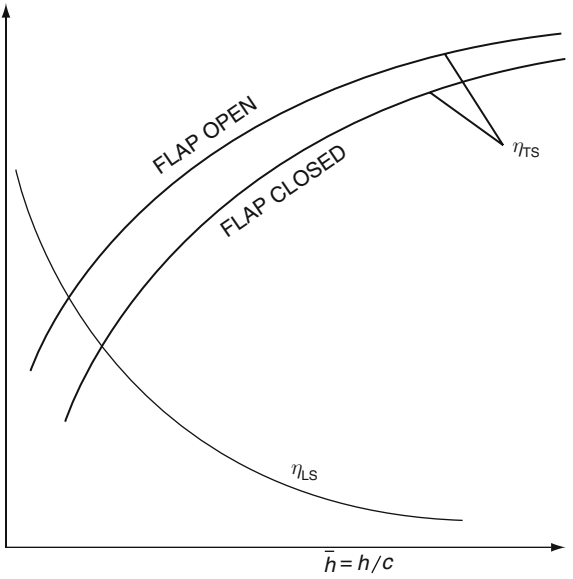

Fig. 4.15 η_{Ls} and η_{Ts} vs. h for DACC and DACWIG models with flap fully closed and open

Measures for Improving Slow-Speed Performance

Introducing static hovering capability on a WIG was similar to ACV first-generation development. Early ACVs had no skirt, and only a very small daylight gap under bottom of the hull. The specific lift power of both early ACV and DACC (or DACWIG) are close. For example, the specific lift power was 128 hp/t for the SR.N1 hovercraft in 1959, 111 hp/t for the prototype "Volga-2" (DACC) in 1986, 80 hp/t for "750" (DACWIG) in 1986 and 87 hp/t for Swan in 1996.

Both DACC and DACWIG possess very good amphibious qualities due to their efficient static hovering performance. The following figures illustrate this. Figure 4.16 shows the "750" launching from ground into the water. Figure 4.17 shows the "SWAN" taking off from its landing ramp on air cushion. Fig. 4.18 shows a static hovering test of a radio-controlled model of "SWAN" over ground, one can see an apparent daylight gap under the bottom of the craft, and Figs. 4.19 and 4.20 show the landing of "SWAN" with the aid of static air cushion and the craft static on the pad.

Figure 4.21 shows the static hovering test of "SWAN" on the landing site at Din Sa Lake close to Shanghai, which has limited space for manoeuvring; however, the craft can be turned around with the aid of manpower only, just as an ACV. However, since the daylight gap under the bottom of both main hull and side buoys is so small, the design still needs to be improved so as to negotiate rough or undulating ground for commercial application. The necessary measures are as follows.

Fig. 4.16 MARIC test craft 750 launching

Fig. 4.17 Radio-controlled model DACWIG hovering over land

Fig. 4.18 MARIC Swan taking off from the launch ramp on hover

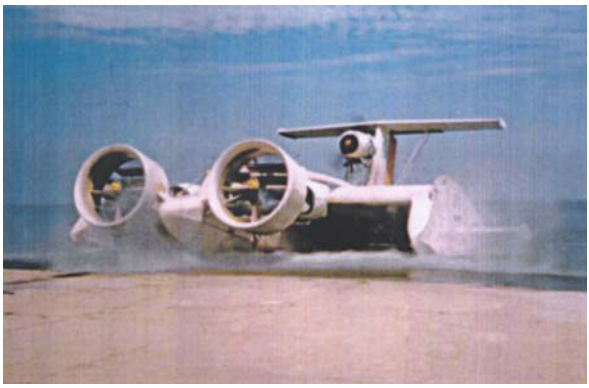

Fig. 4.19 MARIC Swan coming ashore

Fig. 4.20 MARIC Swan static on ramp

Fig. 4.21 Static hovering test of Swan with people turning it

Inflatable Air Bag

The most effective means to protect the hull and side buoys' bottom surface from damage during landing and launching is to mount a flexible inflatable air bag both under the hull and side buoys. Figure 1.20 shows the red air bags of the "Volga-2". In addition, the bags can absorb wave impact loads so as to improve comfort on the craft while taking off or landing in waves.

The pressure and the sizes of the air bags under the main hull and side buoys can be adjusted to make a uniform air gap under both parts. The bag may be replaced regularly just as the skirt on ACV/SES, depending on the severity of the service. Figure 4.22 shows a sketch of an air-bag transverse section under DACC bottom, and Fig. 4.23 also shows a sketch of a valve structure for adjusting pressure in the air bag. Main engines blow pressured air into the air bag continuously to maintain pressure.

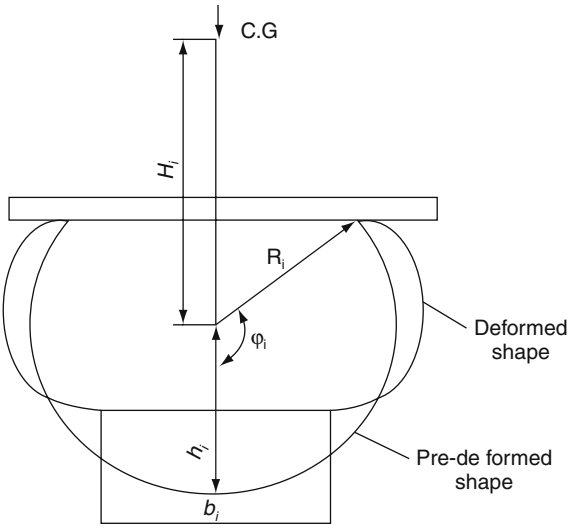

Fig. 4.22 Skirt bag shape and deformation

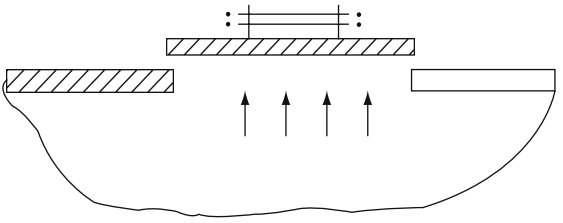

Fig. 4.23 Valve structure for pressure release

Skirt

If a bow skirt is fitted to a WIG, the leakage height (H, same as wing height) of cushion flow at bow will decrease significantly, thus decreasing the lift power or increasing the hovering height.

Figure 4.24 [3] shows the arrangement for a proposed large air cushion-assisted wing-in-ground effect vehicle. The air channel and main wing are separately arranged. The air channel is arranged for producing a static air cushion with the aid of skirts, air ducts and bow thrusters, while the latter is used for making an effective aerodynamic wing with a large aspect ratio of the craft when flying.

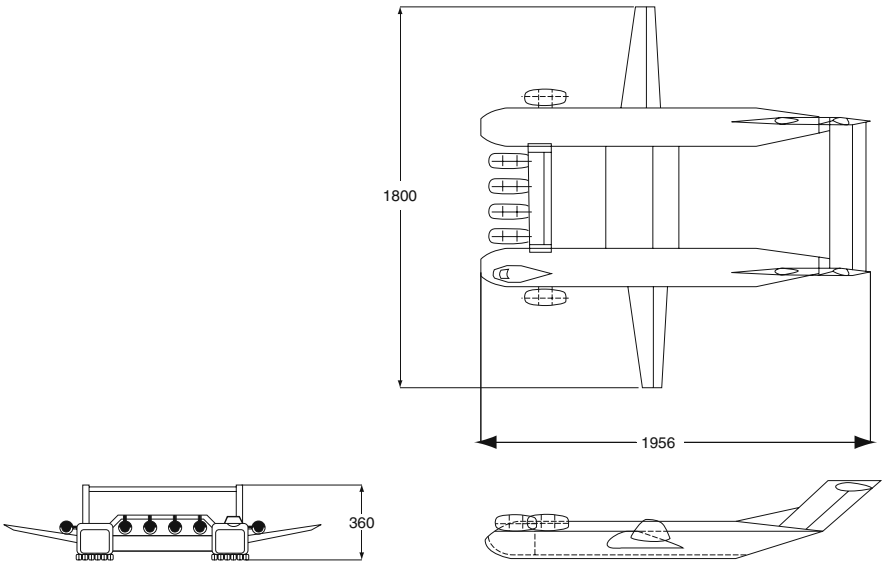

Fig. 4.24 Air cushion-assisted powered wing-in-ground-effect craft

Figure 4.25a, b shows the aerodynamic principle of the "Hoverwing" in hovering mode and flying (called flare mode by its designers). During hovering, both the bow-finger skirt and stern-bag-type skirts are closed to form the air cushion under the main hull, and the pressurised air is fed by air propeller via the air ducts into the air channel of the craft. When in "flare" mode, the bow and stern skirts are opened to allow a dynamic air cushion to form in the air channel.

Laminar Flow Coating on the Bottoms of Hull and Side Buoys

This is used for protecting against corrosion of the bottom plates of hull and side buoys, and also to create a smooth wetted surface for planing. The adhesion of laminar coatings to the bottom plates is insufficient to withstand the erosion from

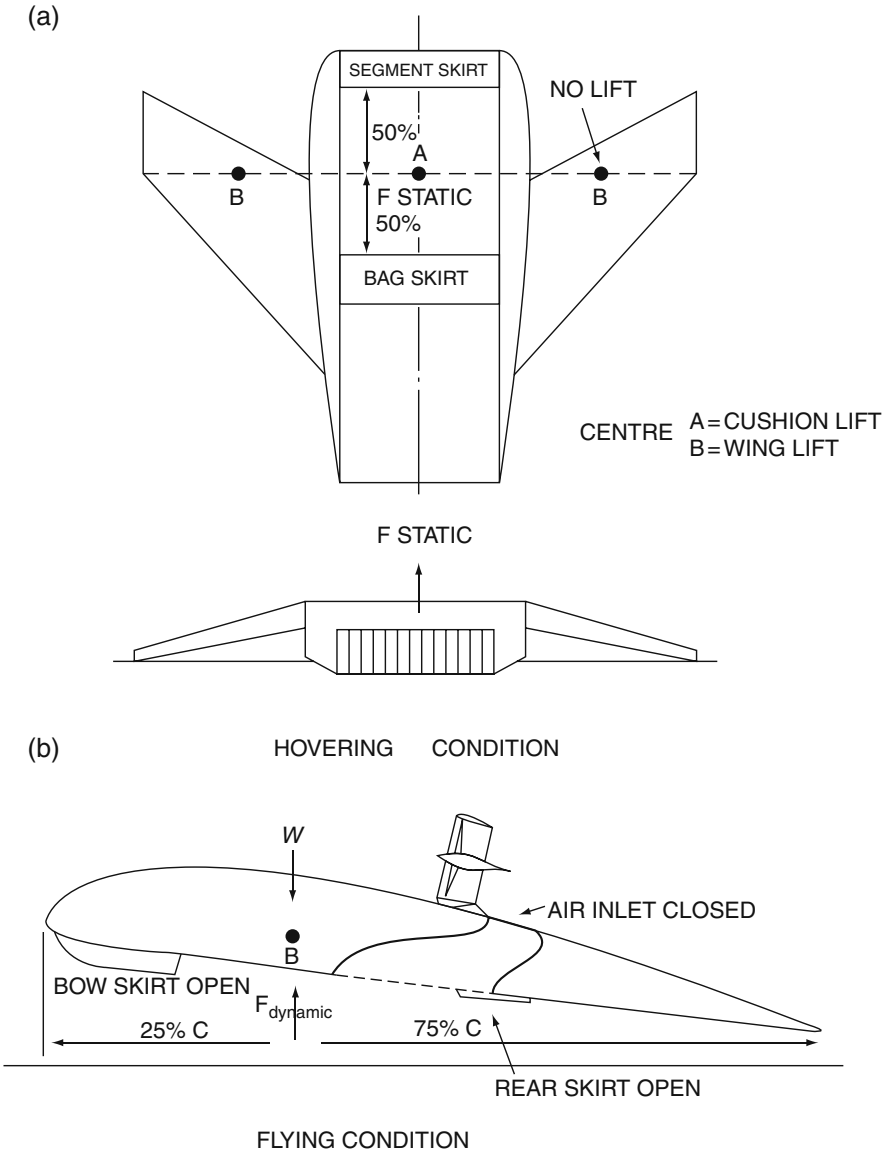

Fig. 4.25 Hoverwing airflow at high speed

turbulent hydrodynamic flow when landing for long and so is still a teething problem. At present, it seems advisable to use a coating encouraging a thin laminar flow layer and a steady turbulent layer.

Hard Landing Pads

Hard landing pads or strakes can also be arranged to protect the main hull and side buoys when alighting on the ground at a terminal, as an alternative to a wheeled undercarriage. In general, the hard landing pad may be mounted under the bottom of both main hull and side buoys. The function of the hard landing-pad system of amphibious WIG is the same as soft air bag and can be described as the following:

- Protecting the main hull and the side buoys from the foreign objects on the ground (cobblestones, etc.) during the craft moving slowly over the ground
- Protecting the hull and buoys against the corrosion by sand, mud, etc. during the landing and launching of the crafts
- Reducing the impact load acting on the hull and side buoys in case of the craft operating in waves
- The air gap between the bottoms of hull/buoys and ground can be adjusted by the landing pads so as to eliminate the difference caused by the deformation of main wings

The design principle for a hard landing pad should comply with the following (see Fig. 4.26):

- To seal air cushion against the air leakage from air cushion during static hovering operation mode, and forming an effective air cushion under the main wing
- To form a uniform air leakage under both side buoys, as well as adjust the air gap under the side buoys and main hull so as to eliminate the deformation effect during the static hovering operation
- To form a smooth wetted surface and effective planing surface during the first transit operation mode (i.e. planing and cushion mode), so as to reduce the hump and take-off drag
- Easy to manufacture and maintain as well as replace, and with long as possible service life

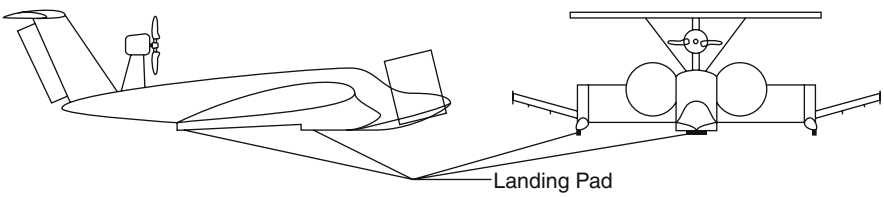

Fig. 4.26 DACWIG landing pads

The development situation of amphibious WIG right now is similar to the initial development stage of ACV/SES at the end of 1960s, before efficient skirt systems. Design and manufacture of both soft and hard landing-pad systems will be one of

most important components influencing the development of low-cost amphibious WIG, particularly in commercial applications.

PARWIG landing depends on having rolling landing gear, the design for which is similar to large seaplanes. The Orlyonok used a set of landing wheels under the centre fuselage similar to the main landing gear on modern airliners.

Chapter 5
Aerodynamics in steady Flight

Introduction

Aerodynamic characteristics of a WIG flying after take-off are similar over a water surface or solid ground. The main differences relate to dynamic response to waves over water or surface undulations when flying over ground, since ground is not deformed by passage of the WIG. The behaviour of WIG over water before and during take-off and their response to waves will be introduced in later chapters.

In this chapter, airfoil aerodynamic characteristics are introduced, including the basic aerodynamics of airfoils close to a rigid boundary. Some model-scale investigations of DACWIG in the wind-tunnel laboratory of MARIC are presented. The influence of various WIG design parameters on their aerodynamics is also discussed.

Aerodynamic characteristics for a wing-in-ground effect with thicker wing profiles, various camber lines, low aspect ratio and side plates are presented in this chapter. The influence of bow thrusters, various types of side plates on the buoys and composite wing geometry on the aerodynamic characteristics are also outlined.

Early WIG craft used classic wing sections such as the NACA series, see Chapter 1 [5], and Chapter 3 [5]. These are designed for operation in open air rather than close to a ground plane. The Russian Ekranoplan programme included many tests of airfoils that had been adjusted to improve the performance close to the ground plane – to reduce the movement of lift centre for example.

A group of WIG specialists in Japan extended the work in Russia by studying a thin wing profile with a reflex-curved camber line aimed at preventing airflow separation on the back surface trailing edge of the wing and so improve the aerodynamic characteristics for use as the main wing profile for WIG. This was thought to be the optimum design approach for high-speed WIG craft at the time of their studies.

For application to DACWIG vehicles at medium flight speeds in the range 150–250 kph, MARIC development engineers focused on the "winged hull" design idea using a thicker wing profile. This profile gives a stiffer wing structure, which was found to be important for designs where the main power plants are mounted on (or inside) the wings, to stabilise the power-transmission system to forward-mounted ducted bow thrusters.

L. Yun et al., *WIG Craft and Ekranoplan*, DOI 10.1007/978-1-4419-0042-5_5,

Craft using gas turbines mounted on or in the forward hull structure (Orlyonok for example) can take advantage of thinner airfoil sections. This design approach is consistent with the needs for craft with higher cruise speeds in the range of 250–450 kph.

In order to use the bow thruster as a take-off aid, and based on the one-degree-of-freedom theory for channel flow developed by Dr. R. W. Gallington in [1], a wing profile with a flat-base plane, side plates and a suitable angle of attack for both side plates and main wing is preferred. This creates a channel flow area that decreases gradually from bow to stern, consequently optimal longitudinal stability, and minimum momentum drag may be obtained. This configuration has been found favourable as geometry for a dynamic air cushion, validated by wind-tunnel tests described in [4].

The earlier work on WIG airfoils has all been through wind-tunnel tests and analytical interpretation based mainly on characteristics of two-dimensional foils in airflow. The craft designs resulting from this work also tend to be based on simple wing geometries. In more recent years, fluid finite element modelling tools have become available to model complex wing shapes and to simulate the turbulent flows and vortices generated at the wing tips and around wing side buoys; for example, the tools described in [3]. These tools can now greatly improve the analysis of WIG aerodynamics, reducing the amount of model testing required to verify the WIG performance.

Application of computer software to aerodynamic analysis (as against the development of software) is a task that should be tackled with care by a designer, first modelling simple geometries and building on initial experience in a stepwise fashion, similar to the approach to model testing discussed in Chapter 9.

Before working with such tools, it is useful to review the fundamentals and so, in this chapter, we focus on the aerodynamics of basic foils and leave readers to pursue software themselves to ease the design process.

Airfoil Fundamentals

When an aerofoil operates close to a rigid surface such as over ground or water, the incoming flow is restricted under the lower surface, increasing the pressure and thus producing additional lift compared with the free air stream. In addition, the reduction of down-wash angle due to the restriction from the proximity of the ground also results in a decrease of induced drag.

Borst studied a wing operating close to the ground, see Chapter 1 [5], and assumed that the effects of the ground can be simulated by the addition of a mirror image wing as shown in Fig. 1.8. Using lifting line theory, he calculated a correction factor σ that may be used to modify the classical induced drag and angle of attack equations as follows:

$$\sigma = \mathrm{e}^{x} \tag{5.1}$$

where

x $= -2.48\,(h/b)^{0.768}$
b Span of the airfoil
h Flying height

This correction factor can be used to calculate the angle of attack and induced drag coefficient for a wing without endplates (side buoys), with an elliptical aerodynamic loading:

$$C_{\mathrm{di}} = [C_y^2/\pi\lambda] \cdot (1 - \sigma) \tag{5.2}$$

$$\alpha_{\mathrm{i}} = [18.24 C_y/\lambda] \cdot (1 - \sigma) \tag{5.3}$$

where

C_y Lift coefficient
C_{di} Induced drag coefficient
α_{i} Induced angle of attack
λ Aspect ratio

Borst in Chapter 1 [5] also introduced the effect of endplates on wings operating in ground effect. The effect of endplates of different heights can be calculated as shown in Fig. 5.1 Figures 5.2 and 5.3 show the pressure distribution along a wing operating at various relative flying heights. It is found that when the craft flies closer to the ground, the pressure increases and so also does the pressure coefficient C_{p}

$$C_{\mathrm{p}} = P_{\mathrm{c}} / \left[0.5 \rho_{\mathrm{a}} V^2\right]$$

where

P_{c} Static pressure acting on the wing surface
V Speed of incoming airflow

This is why a WIG has higher aerodynamic efficiency and inherent heave stability compared with a free flying airplane.

Figure 5.4 shows a typical lift coefficient C_y against the relative flying height $\bar{h}$ and the angle of attack α, with a certain aspect ratio. The curve is nonlinear, and the lower the relative flying height the higher the lift coefficient becomes. This gives a WIG inherent heaving stability, although the ride flying close to the surface is harder. The choice of flying height is therefore dependent onf requirements for seaworthiness. If a WIG is to fly in open-ocean conditions, it will be necessary to fly higher than in river or coastal areas. Since the practical flying height for a WIG is a proportion of the main-wing chord, this also means that larger craft are required for open-ocean operation.

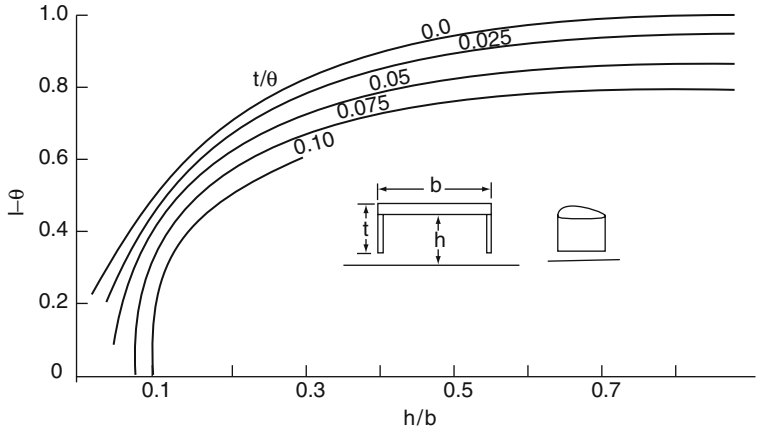

Fig. 5.1 Correction for ground effect wings with endplates

Fig. 5.2 Pressure distribution along a wing operating in/out of ground effect zone

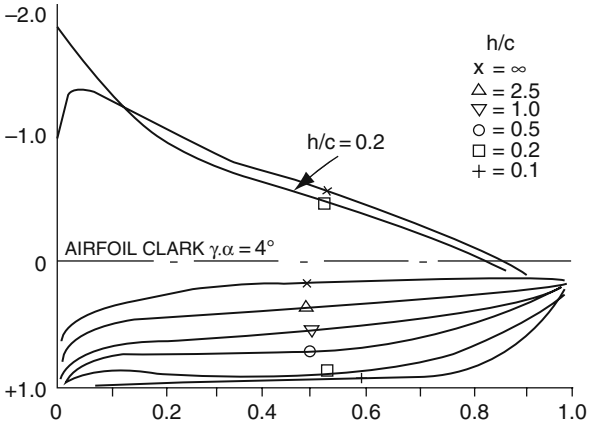

Figure 5.5 shows the decrease of induced velocity of a wing operating close to the ground caused by the mirror image tip vortex of the wing.

Figure 5.6 shows a sketch of a typical WIG transverse section. The three-dimensional aerodynamic properties of WIG relate to h_{sb}, where $h_{sb} = H - H_{sb}$. H_{sb} and also H depend upon the required buoyancy in hull-borne operation.

The induced drag of the wing in the ground effect zone can be written as [4]:

$$C_{xi} = C_y^2/[\pi\lambda \cdot \mu(\bar{h},\lambda)] \tag{5.4}$$

Then the aerodynamic efficiency of the wing, K, can be expressed as:

$$K = C_y/C_x = C_y/\,(C_{x0} + C_{xi}) \tag{5.5}$$

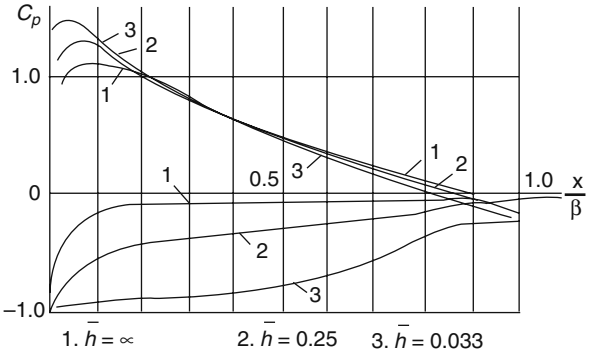

Fig. 5.3 Pressure distribution along the wing in/out of ground effect zone

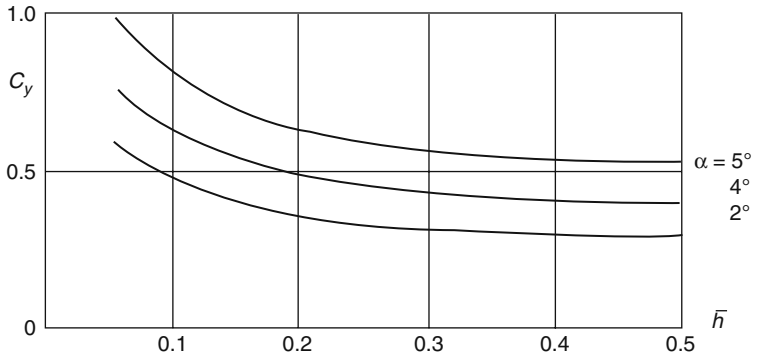

Fig. 5.4 Typical C_y versus h curves

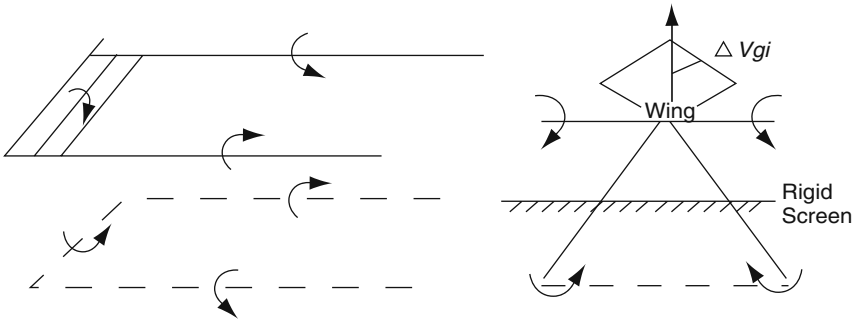

Fig. 5.5 Image vortex causes a decrease of induced velocity

where C_{x0} is the viscous drag coefficient, which is independent of lift coefficient C_y and the angle of attack α. From Equation (5.5), optimum C_y can be deduced as:

$$C_{y\text{opt}} = \left[\pi\lambda \cdot \mu\left(\bar{h},\lambda\right) \cdot C_{x0}\right]^{0.5} \tag{5.6}$$

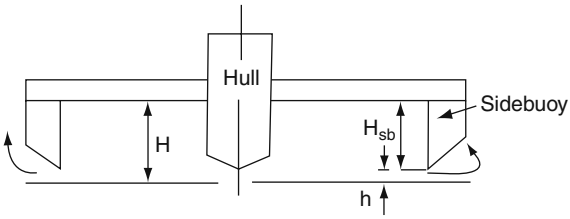

Fig. 5.6 A typical WIG transverse section

The maximum aerodynamic efficiency $K_{\max}$ is

$$K_{\max} = 0.5\left[\pi\lambda \cdot \mu\left(\bar{h},\lambda\right)/C_{x0}\right]^{0.5} \tag{5.7}$$

The function $\boldsymbol{\mu}$ can also be written as:

$$\mu\left(\bar{h},\lambda\right) = \lambda/\left[3\pi\bar{h}\right] \tag{5.8}$$

Then

$$C_{y\text{opt}} \cong \lambda\left[C_{x0}/3\bar{h}\right]^{0.5}$$

and

$$K_{\max} = \lambda/\left\{2 \cdot \left[C_{x0} \cdot 3\bar{h}\right]^{0.5}\right\} \tag{5.9}$$

where λ represents the aspect ratio of the wing.

From Equation (5.9), it is found that the $C_{y\text{opt}}$ and $K_{\max}$ increase inversely with $\bar{h}^{0.5}$.

The calculations to determine wing aerodynamic properties while operating in the ground effect zone are very approximate. A number of additional parameters that are not considered in the calculations presented here also affect these properties:

- Ground clearance gap at the bow and stern edge of the main wing, particularly the influence of flap position
- Geometry of side buoys
- Influence of bow thruster efflux
- Depression of the water surface due to the dynamic cushion pressure
- Influence of the inclination angle of the bow-thruster shaft line
- Influence of structural deflection of the main wing, hull and side buoys that affect the wing aerodynamics due to changing the air gap h in quite a sensitive

way. WIG aerodynamic performance can be significantly affected by structural deflection, unlike airplanes in free air flight

There are no satisfactory closed-form analytical solutions available to date for the WIG's three-dimensional wing aerodynamics. Once estimates have been made on the wing-section performance in two dimensions from wing-section data, the best way to study the airfoil performance is by model experimental investigation at a large-enough scale and sea trials of prototype craft. An example is presented in the next section for guidance.

An Experimental Investigation of Airfoil Aerodynamics

The work presented here was performed in MARIC as part of their WIG development programme, see [1, 4]. We begin with a summary of the nomenclature used.

Nomenclature

V	Wind speed
α	Angle between the base line of side plate and incoming flow
α_1	Angle between the base line of side plate and chord line of main wing
α	Angle between the chord line of main wing and incoming flow ($= \alpha + \alpha_1$)
h	Distance between the lower edge of side plate and screen plate (ground)
C	Chord length of the wing
$\bar{h}$	Relative flying height $\bar{h} = h/C$
b	Wing span
S	Wing area, $S = b \times C$
Λ	Aspect ratio, $\Lambda = b/C$
X	Drag
Y	Lift
M_z	Pitching moment
C_x	Drag coefficient, $C_x = X/\left(0.5\rho V^2 S\right)$
C_y	Lift coefficient, $C_y = Y/\left(0.5\rho V^2 S\right)$
C_m	Pitching moment coefficient, $C_\mathrm{m} = M_z/\left(0.5\rho V^2 S\, C\right)$
K	Lift–drag ratio, $K = C_y/C_x$;$K_1 = l_1/R_1$;$K_2 = l_2/R_2$;$K_3 = l_3/R_3$
$\bar{x}_\mathrm{c}$	Relative distance of aerodynamic centre from leading edge of main wing $\bar{x}_\mathrm{c} = X_\mathrm{c}/C$
$C_\mathrm{y}^{\bar{h}}$	Derivative of lift coefficient with respective to the relative flying height at constant angle of attack α
C_y^{α}	Slope of lift coefficient curve at constant relative flying height
$m_\mathrm{z}^{\bar{h}}$	Derivative of pitching moment coefficient versus relative flying height at constant α

m_z^{α} Derivative of pitching moment coefficient versus angle of attack at constant relative flying height $\bar{h}$
T_{so} Static thrust of single-ducted thruster
T_{do} Dynamic thrust of single-ducted thruster
T_{sc} Static thrust of ducted thruster in air channel, $T_{sc} = -R_1$
T_{dc} Dynamic thrust of ducted thruster in channel, $T_{dc} = R_3 - R_2$
R_1 Resistance of model with bow thruster at revolution of n in case of zero air speed, $R_1 = f(n)$
R_2 Resistance of bare model without bow thrusters in case of air speed of v, $R_2 = f(v)$
R_3 Resistance of model with bow thrusters at revolution of n and in case of v air speed, $R_3 = f(n,v)$
L_d Dynamic lift
L Lift of model without bow thruster
L_s Static lift of model with bow thruster
η_{ls} Total static lift coefficient of air channel, $\eta_{ls} = L_s/T_{so}$
η_{ld} Total dynamic lift coefficient of air channel, $\eta_{ld} = L_d/T_{do}$
η_{ts} Static thrust recovery coefficient of air channel, $\eta_{ts} = T_{sc}/T_{so}$
η_{td} Dynamic thrust recovery coefficient of air channel, $\eta_{td} = T_{dc}/T_{do}$

Basic Model

The basic wing profile for the model test is a re-formed Glenn Martin 21 form with six aspect ratios ($\lambda = 0.4, 0.6, 0.8, 1.0, 1.5$ and 2.0) and five relative flying heights $\bar{h}$. The model tests were carried out in MARIC's wind tunnel in Shanghai. At the same time, model tests of a wing with the same aspect ratio ($\lambda = 0.8$) and with three different profiles (NACA16-415, NACA0015 with flat base line, and NACA6415 with flat base line), as well as five relative flying heights, were also tested to measure the aerodynamic characteristics.

The section-profile dimensions are shown in Table 5.1 non-dimensional offsets of B-type section are shown in Table 5.2 and offsets of four model types, designated A, B, C and D, are listed in Table 5.3.

The models were made of wood with painted surfaces. The side plates were made of 3-mm thickness plywood. The installed angle of the wing relative to craft baseline was set at 9° (Fig. 5.7)

The side plates were fixed at the sides of the wing, with their baseline parallel to the ground for $\alpha = 0$ (thus $\bar{h}$ is defined for the wing at this angle of attack). The side plates are rotated with the wing profile when altering the angle of attack, α, so at lower values of h, the trailing edge of the side plate touched the ground plane and reduced the upper value of angle of attack able to be tested. This approach to the tests simulated the real case, since side buoys or plates would be fixed to the wing of the full-scale WIG. The complication introduced is that as the angle of attack increases,

Table 5.1 Dimensions of section profile of wings

Wing profile	NACA 16-415	Glenn Martin 21						NACA 0015 flat bottom	NACA 6415 flat bottom
Number	A	B	B	B	B	B	B	C	D
Chord length (mm)	420	420	420	420	420	420	420	420	420
Span (mm)	336	168	232	336	420	630	840	336	336
Aspect ratio	0.8	0.4	0.6	0.8	1.0	1.5	2.0	0.8	0.8

Table 5.2 Non-dimensional offsets of B-type section

Location at chord (%)	Offset of profile (% of chord length)		Location at chord (%)	Offset of profile (% of chord length)	
	Back surface	Lower surface		Back surface	Lower surface
0	8.86	8.86	40	21.13	0
1.25	12.21	6.03	50	19.20	0
2.5	13.81	4.79	60	16.64	0
5	15.98	3.33	70	13.55	0
7.5	17.65	2.35	80	9.45	0
10	18.92	1.72	90	5.00	0
15	20.72	0.75	95	2.57	0
20	21.68	0.28	100	0	0
30	22.13	0			

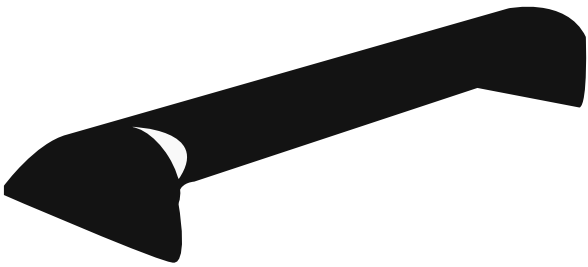

Fig. 5.7 Wing model (with side plates)

the gap under the side plate becomes a wedge rather than a constant height, and flow will be more three dimensional close to the wing tips.

Table 5.3 Offset of four types of models

Number			A		B		C		D	
Type of wing profile			NACA16-415		Glenn Martin 21		NACA0015 flat bottom		NACA6415 flat bottom	
Relative thickness			0.15		0.22		0.15		0.15	
Section number	Location at chord (mm)	Location at chord (%)	Back surface	Lower surface	Back surface	Lower surface	Back surface	Lower surface	Back surface	Lower surface
1	0	0	0	0	37.2	37.2	15.0	15.2	0	0
2	5.3	1.25	7.7	−5.9	51.3	25.3	28.0	4.0	14.5	−6.5
3	10.5	2.5	11.1	−7.9	58.0	20.1	33.0	0.8	19.6	−9.0
4	21.0	5	15.8	−10.5	67.1	14.0	40.2	0	27.1	−11.6
5	42.0	10	22.3	−13.8	79.5	7.2	49.2	0	37.3	−13.1
6	84	20	31.2	−17.8	91.1	1.2	60.2	0	49.6	−11.8
7	126.0	30	36.6	−20.3	92.9	0	63.0	0	55.3	−10.0
8	168.0	40	39.7	−21.7	88.7	0	60.9	0	55.7	−8.8
9	210.0	50	40.8	−22.2	80.6	0	55.6	0	52.4	−7.3
10	252.0	60	39.6	−21.6	69.9	0	47.9	0	46.6	−5.8
11	294.0	70	35.8	−19.5	56.9	0	38.5	0	38.5	−4.5
12	336.0	80	28.7	−15.4	39.7	0	27.5	0	28.2	−2.8
13	378.0	90	17.6	−8.9	21.0	0	15.2	0	15.6	−1.5
14	420	100	0.6	−0.6	0	0	0	0	0	0

Model Tests

The model tests were carried out in the wind-tunnel laboratory of MARIC, that has a test section with a diameter of 1.5 m, a wind speed of 20 m/s and $\mathrm{Re} = 5.8 \times 10^5$.

A fixed rigid screen (ground plate) was used to simulate the ground and water surfaces. Data processing did not consider the influence of the surface boundary layer. Test data were obtained using a three-component mechanical dynamometer via an electronic data-acquisition system. The dynamometer was located under the rigid screen. The influence of various parameters on the model aerodynamics was then determined by the analysis of the test programme results.

Change of flying height was obtained through a mechanical system with four screws. The range of flying height was changed in steps of 0.05, viz. $\bar{h} =$ 0.05, 0.10, 0.15, 0.20, 0.30, etc. The angle attack of the wing model was varied at $\alpha = -3°$ 0°, +3°, +6°, +9° and +12°s at each flying height. It should be noted that this model was not built including bow thrusters, so the influence of bow thrusters on the model aerodynamics was not considered here.

The non-dimensional lift coefficient C_y, drag coefficient C_x and moment coefficient C_m with respect to the angle of attack and relative flying height $\bar{h}$ obtained from testing at MARIC are shown in Figs. 5.8, 5.9, 5.10, 5.11, 5.12, 5.13, 5.14, 5.15, 5.16, 5.17, 5.18, 5.19, 5.20, 5.21, 5.22, 5.23, 5.24, 5.25, 5.26 and 5.27, shown on pages 158–177 below.

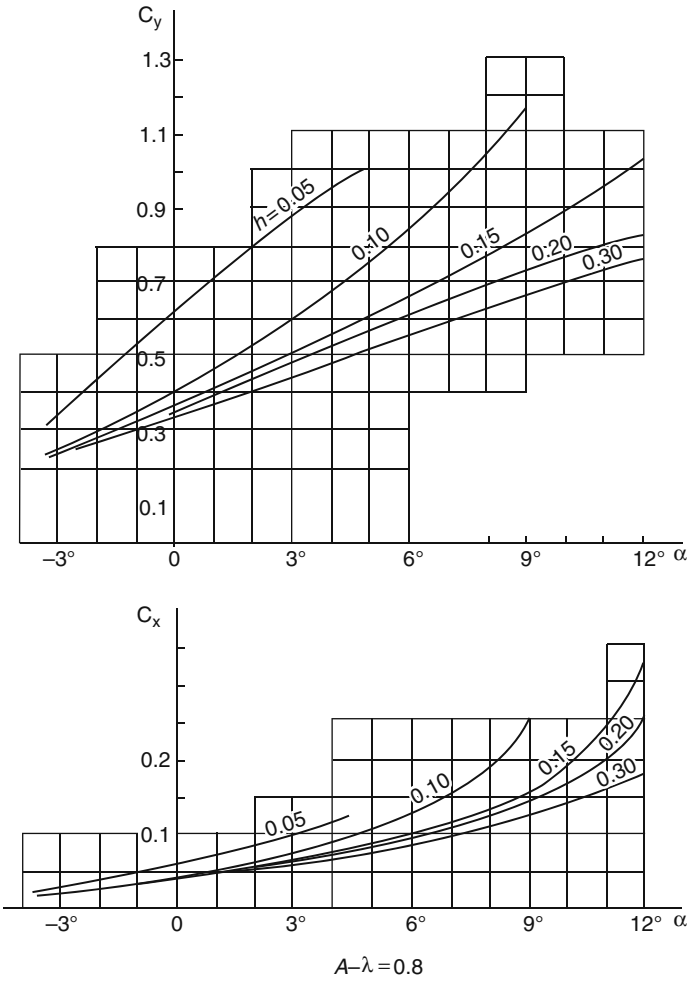

Fig. 5.8 C_y, C_x versus $\alpha, h\,\bar{h}, A - \lambda = 0.8$

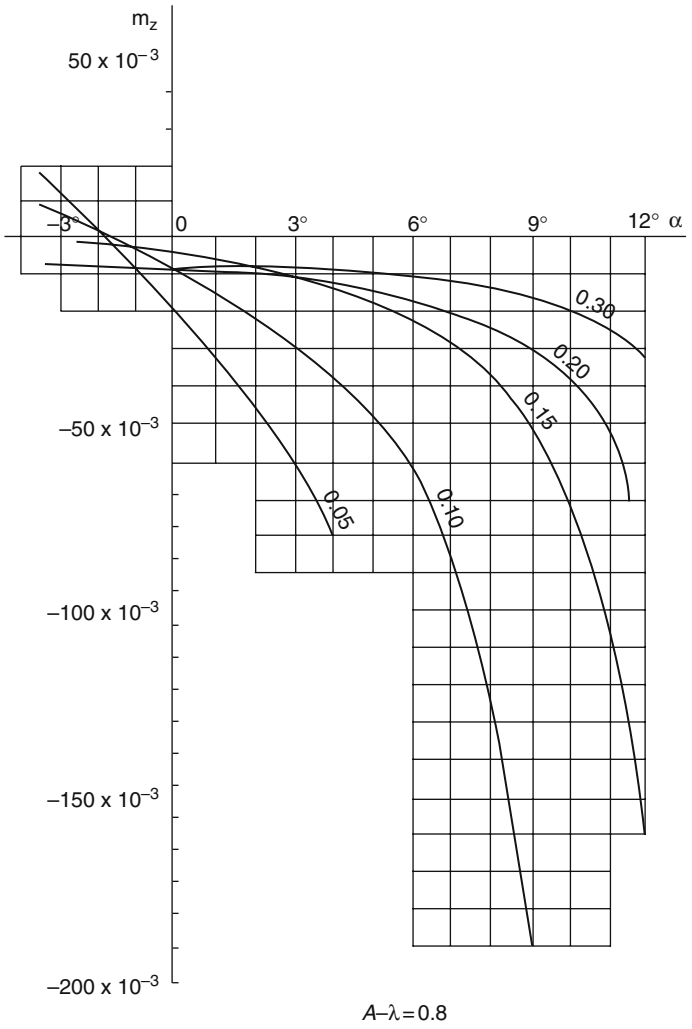

Fig. 5.9 m_z versus $\alpha, h\,\bar{h}, A - \lambda = 0.8$

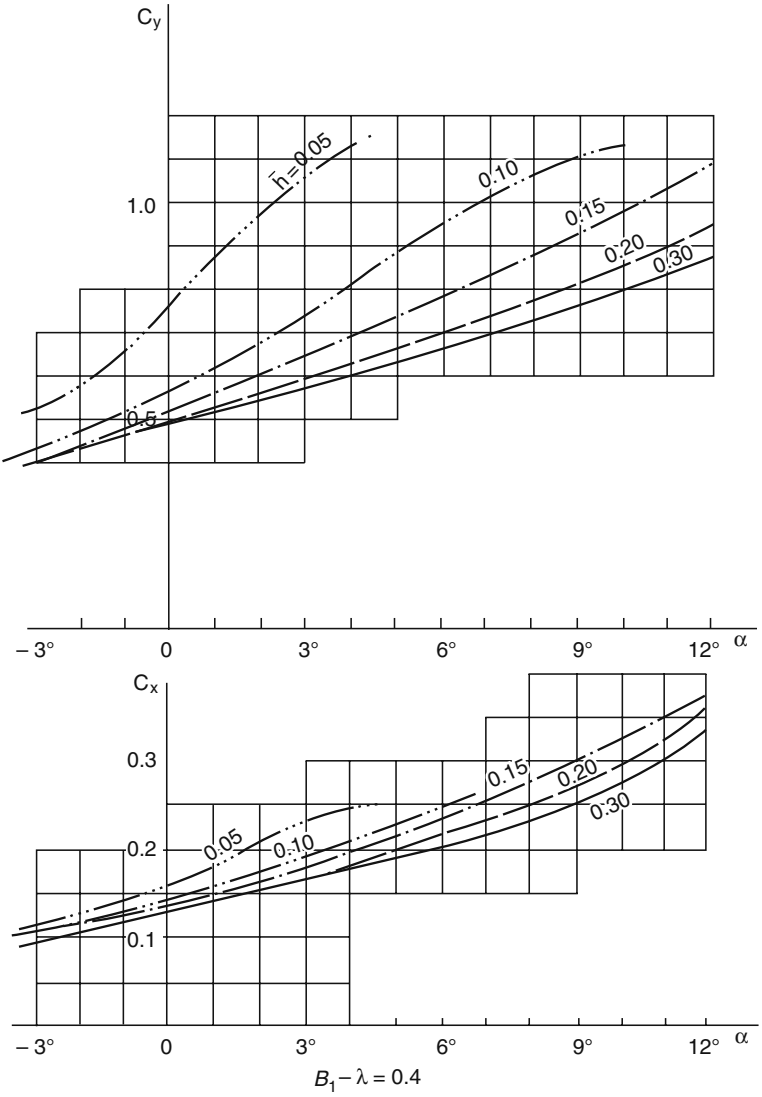

Fig. 5.10 C_y, C_x versus $\alpha, h\,\bar{h}, B - \lambda = 0.4$

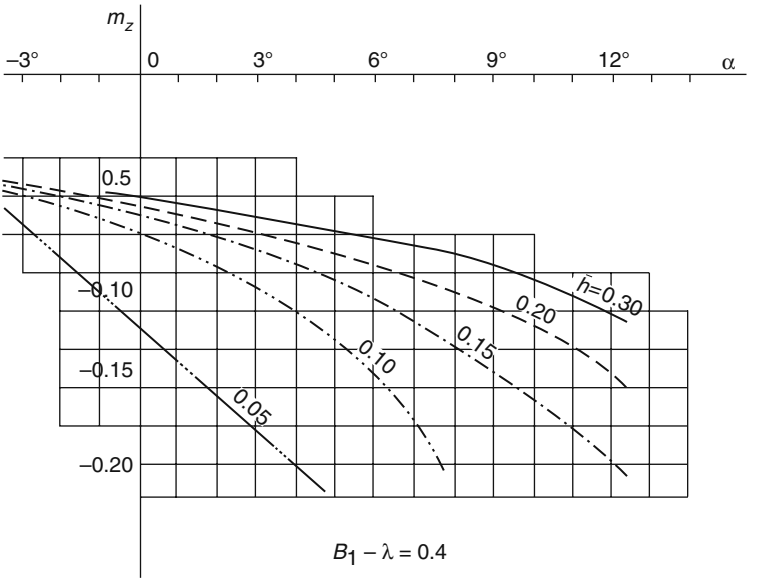

Fig. 5.11 m_z versus $\alpha, h\,\bar{h}, B - \lambda = 0.4$

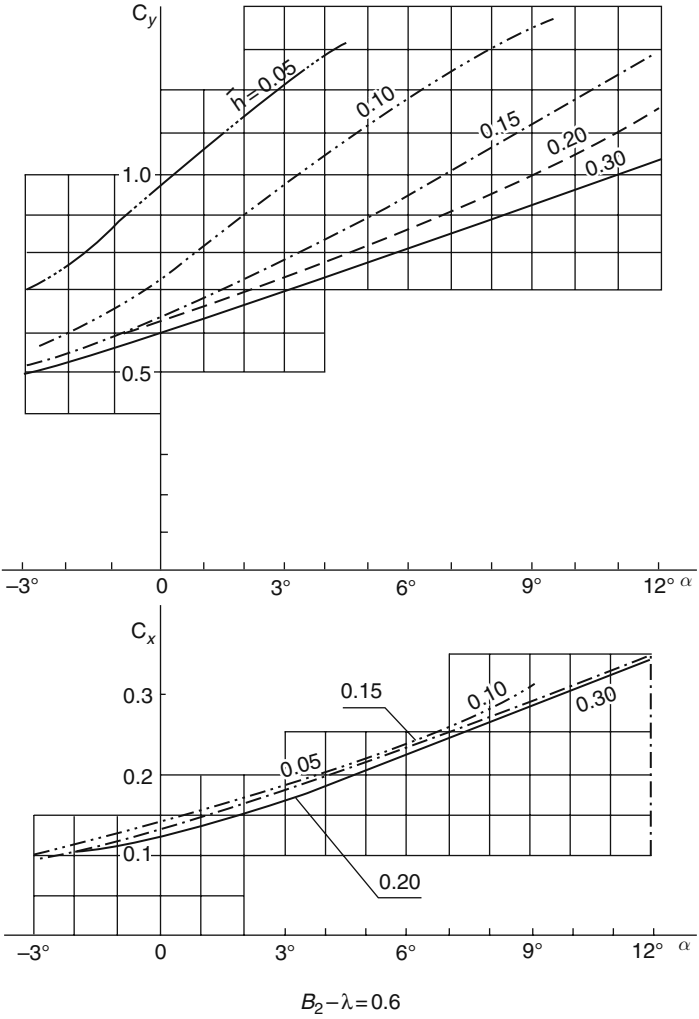

Fig. 5.12 C_y, C_x versus $\alpha, h\,\bar{h}, B-\lambda=0.6$

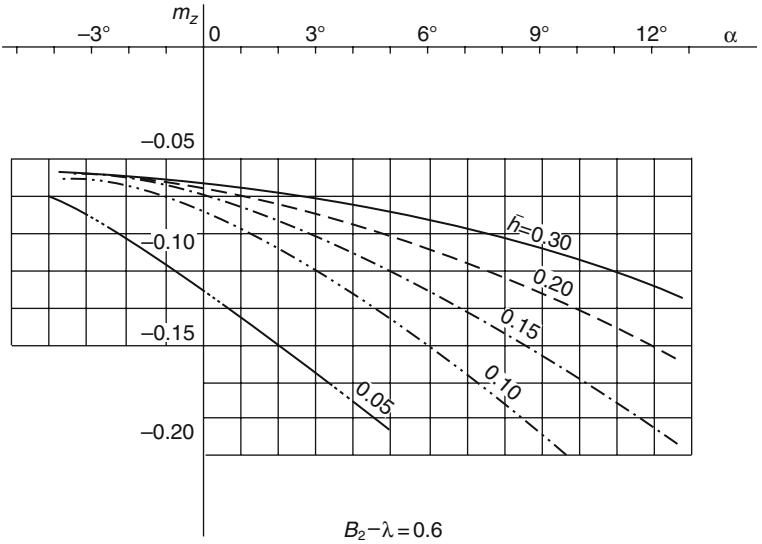

Fig. 5.13 m_z versus $\alpha, h\,\bar{h}, B - \lambda = 0.6$

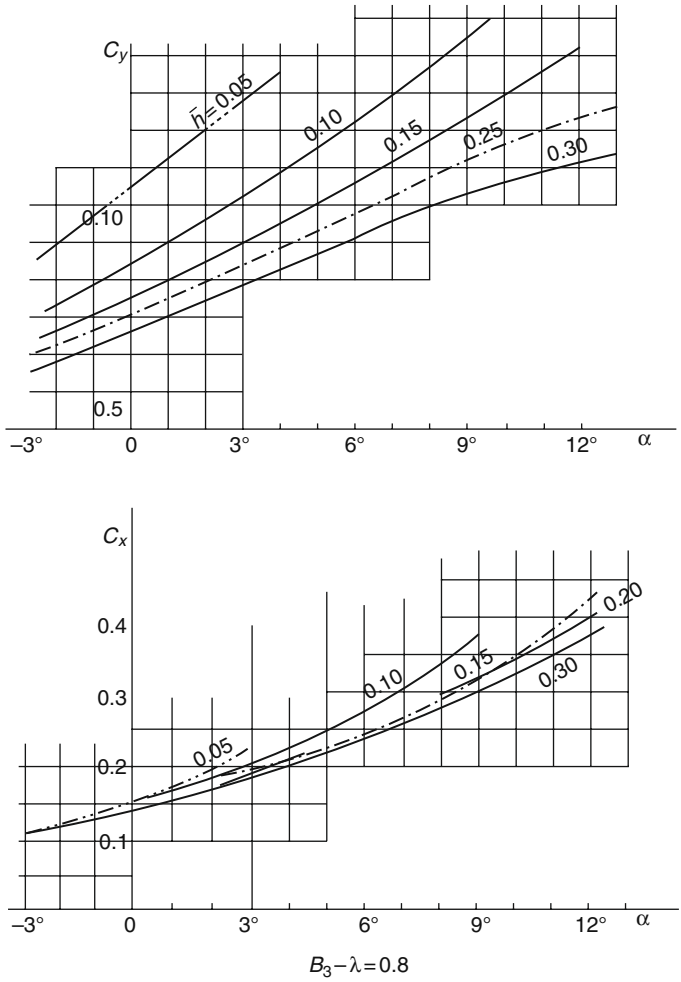

Fig. 5.14 C_y, C_x versus α,$h\,\bar{h}$,$B-\lambda=0.8$

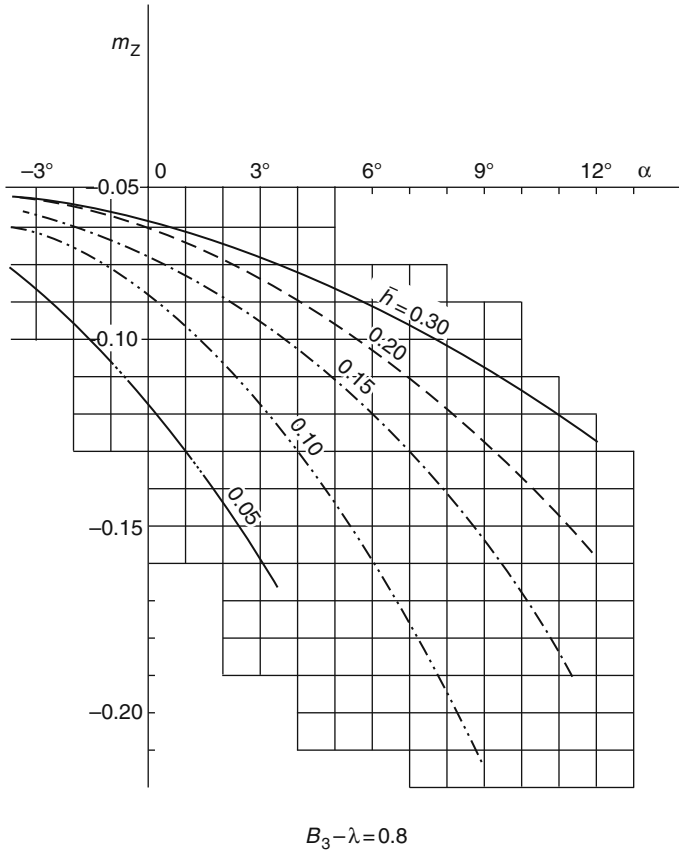

Fig. 5.15 m_z versus $\alpha, \bar{h}, B - \lambda = 0.8$

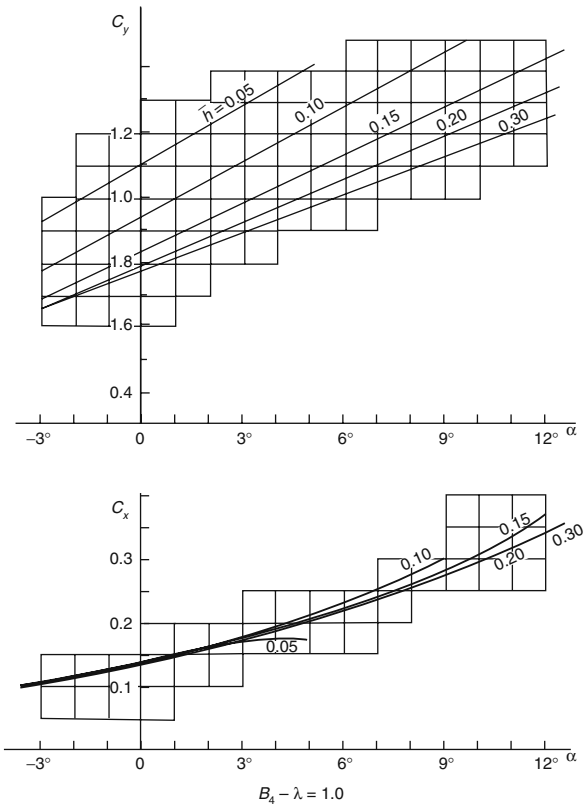

Fig. 5.16 C_y, C_x versus $\alpha, \bar{h}, B - \lambda = 0.8$

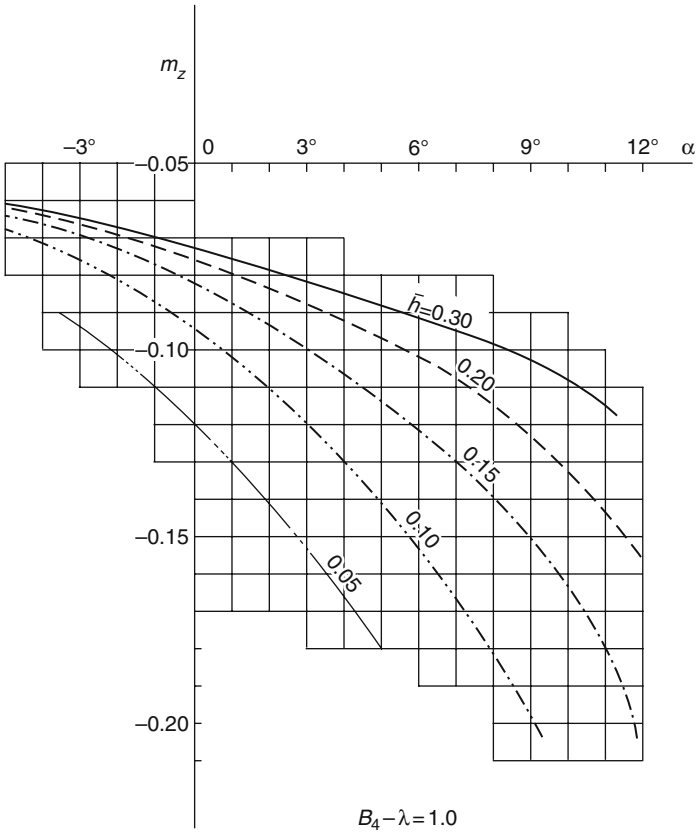

Fig. 5.17 m_z versus $\alpha, \bar{h}, B - \lambda = 0.8$

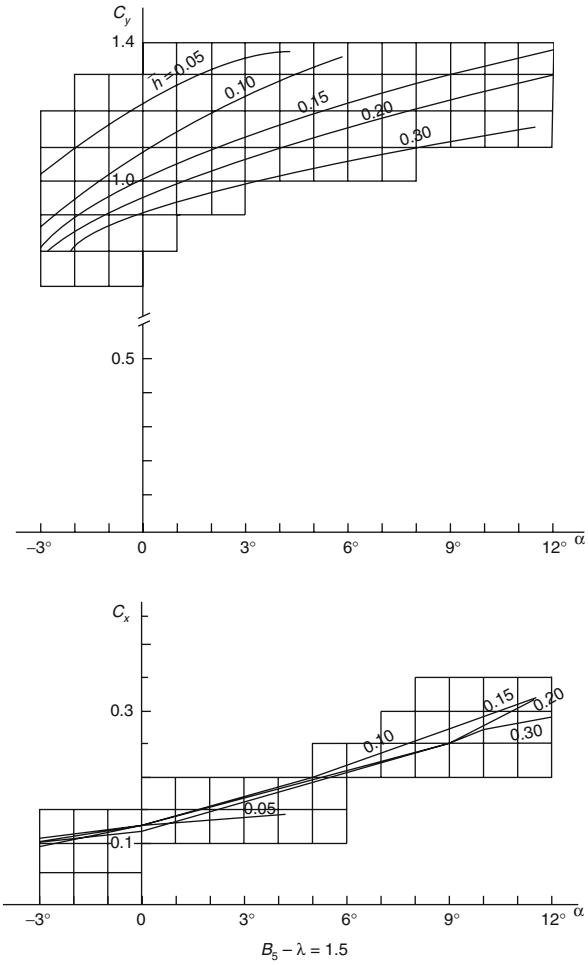

Fig. 5.18 C_y, C_x versus $\alpha, \bar{h}, B - \lambda = 1.5$

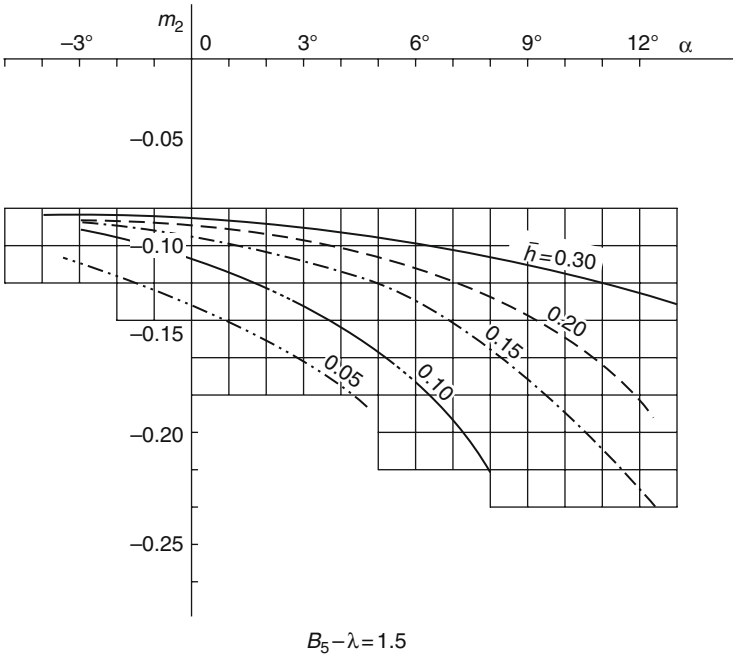

Fig. 5.19 m_z versus $\alpha, \bar{h}, B - \lambda = 1.5$

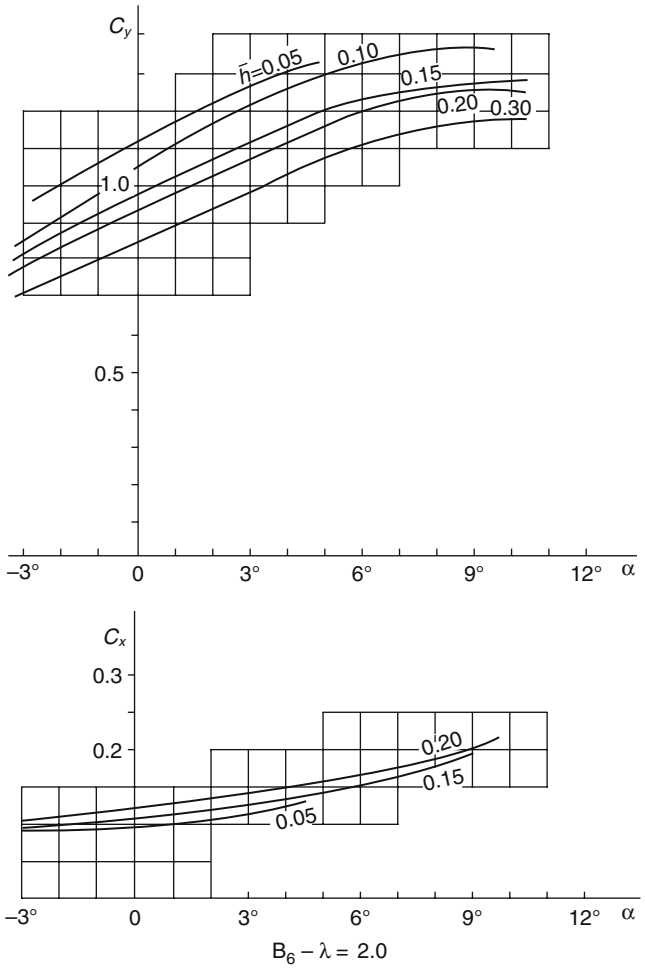

Fig. 5.20 C_y, C_x versus $\alpha, \bar{h}, B - \lambda = 2.0$

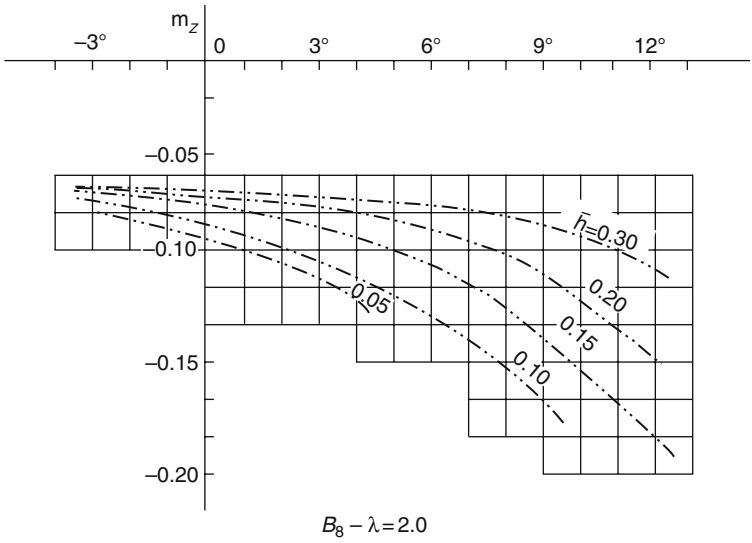

Fig. 5.21 m_z versus $\alpha, \bar{h}, B - \lambda = 2.0$

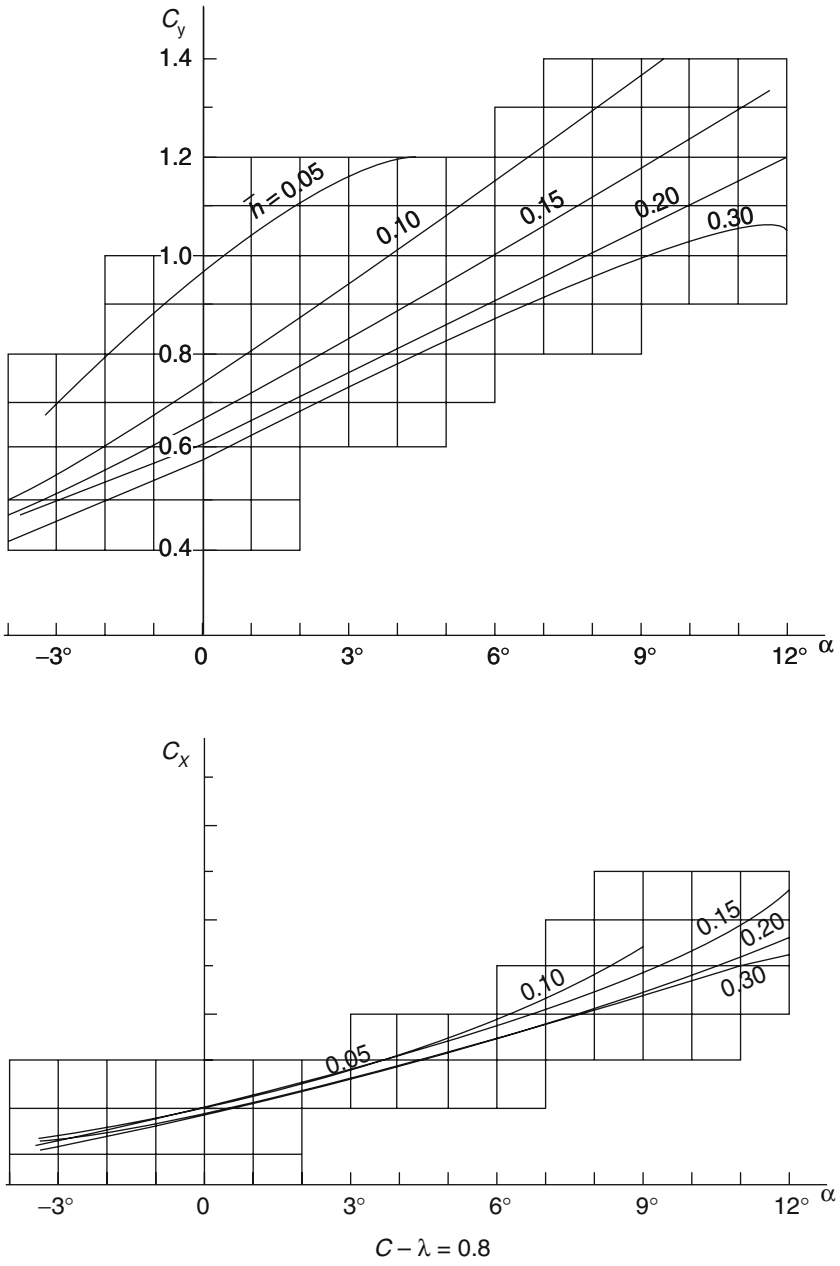

Fig. 5.22 C_y, C_x versus $\alpha, \bar{h}, C - \lambda = 0.8$

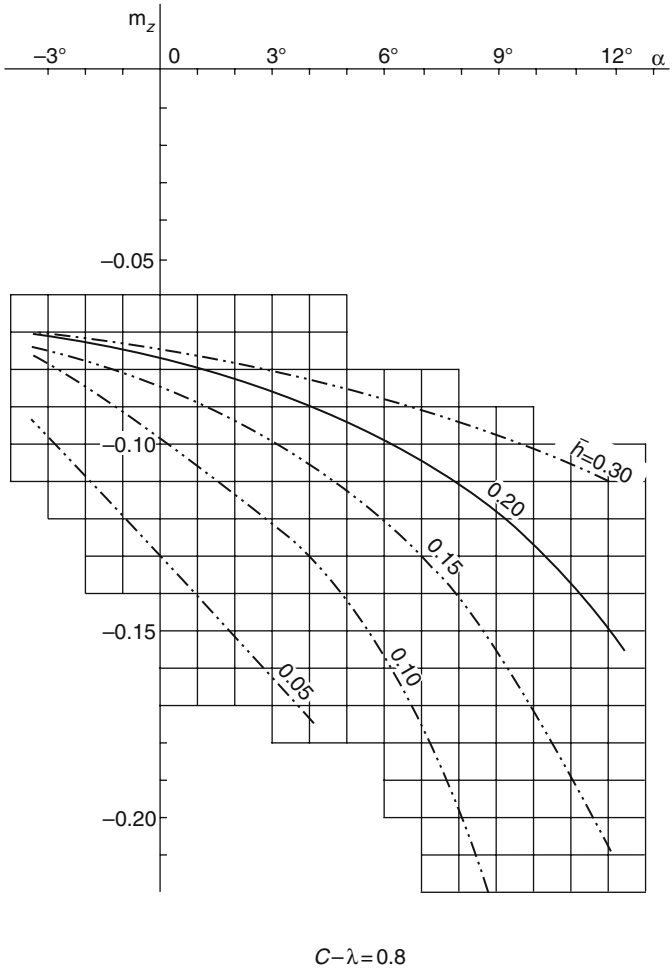

Fig. 5.23 m_z versus $\alpha, \bar{h}, C - \lambda = 0.8$

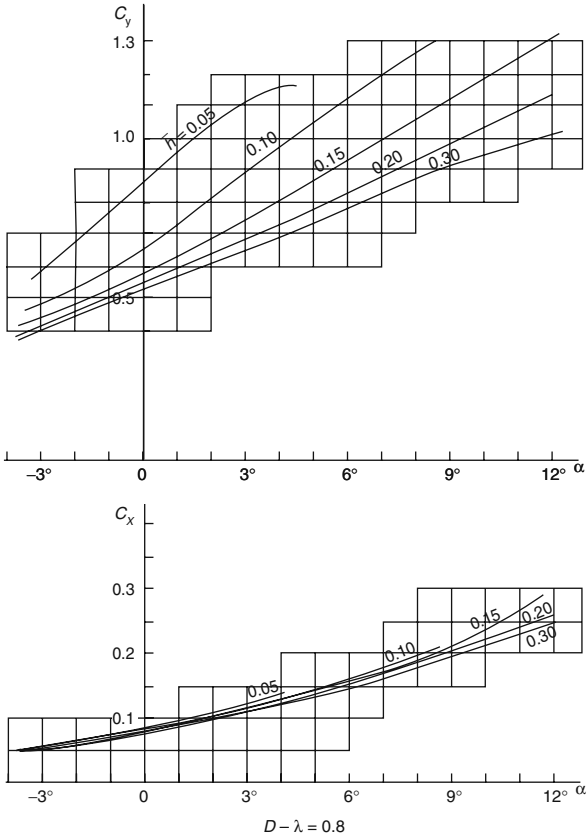

Fig. 5.24 C_y, C_x versus $\alpha, \bar{h}, D - \lambda = 0.8$

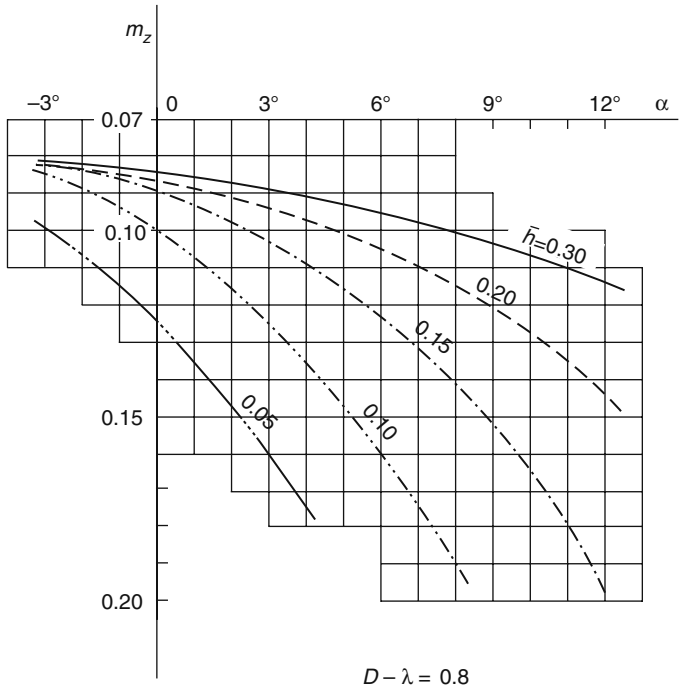

Fig. 5.25 m_z versus $\alpha, \bar{h}, D-\lambda=0.8$

Discussion

Lift

Comparison of the four different profile sections shows the lift coefficient of airfoil type B is the highest and the angle of zero lift is the smallest at same angle of attack. The influence of ground effect on the lift is that the slope of the lift coefficient curve increases inversely with flying height, but there is no obvious influence of flying height on the zero-lift angle.

The model-test results show that the lift force increases inversely with flying height for the angle of attack $\alpha = -3°$ to 12° approximately. According to the tests, the distribution of pressure on the wing and the influence of flying height on the pressure of wing back surface are not large, but the pressure on the front surface of the wing increases in inverse proportion with flying height. This verifies that an effective dynamic air cushion can be made in the air channel composed by the lower surface of wing and the side plates. The lift will be proportional to the flying height in case of $\alpha < -7$ due to the increase of pressure on the wing's upper surface (wing begins to be pressed downward).

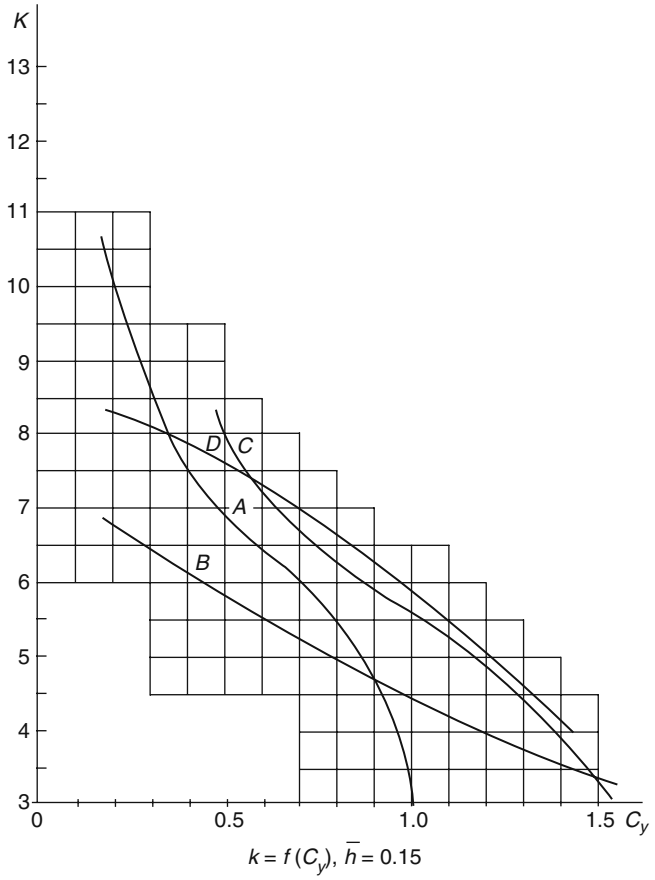

Fig. 5.26 Aerodynamic property K versus C_y of various wing profiles

The stable flying region can be expressed as follows:
In case of

$$\alpha < -2\text{:flying is unstable, because of } C_y^{\bar{h}} > 0;$$

$$\alpha > -2\text{:flying is stable, because of } C_y^{\bar{h}} < 0.$$

Motion stability is strongly affected by design flying height, as lift coeffient $C_y^{\bar{h}}$ is strongly affected by distance from the ground. The C_y values of various wing profiles for $\bar{h} = 0.15$, $\alpha = 0$, are listed in Table 5.4:

The tests demonstrate that when $\bar{h} > 0.4$, the influence of ground effect will be very weak. This means the wing is out of the strong ground effect region. In the strong ground effect region, e.g. $\bar{h} < 0.15$, both the lift and the slope of the lift curve increase directly with aspect ratio.

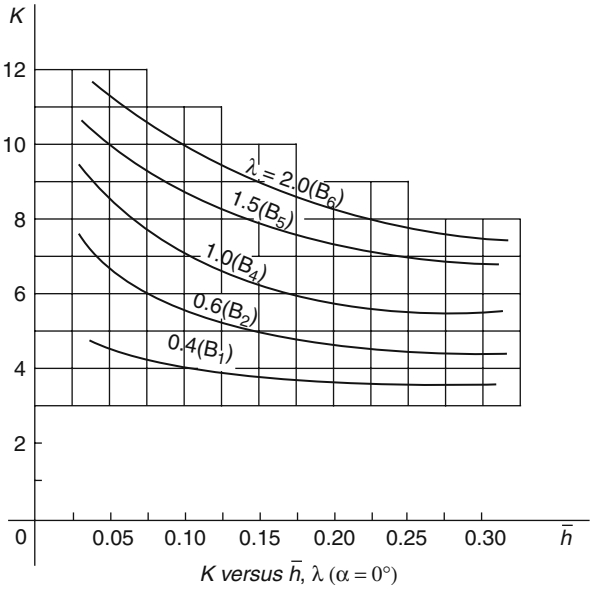

Fig. 5.27 Aerodynamic property K versus $\bar{h}$

Table 5.4 C_y values of various wing profiles

Wing profile	A	B	C	D	NACA 16-409	NACA 66-409	NACA 5409	CLARK YM-11
Aspect ratio	0.8	0.8	0.8	0.8	0.8	0.65	0.65	0.65
C_y	0.26	1.08	0.96	0.86	0.45	0.46	0.50	0.13

Drag

Where $\lambda > 1.0$, the drag decreases in proportion inversely to the flying height due to the decrease of induced drag. Where $\lambda = 1.0$, the drag is independent of flying height, and in the case where $\lambda < 1.0$, drag will increase proportional inversely to the flying height.

Lift–Drag Ratio

The relation between the lift–drag ratio and lift coefficient of the four types of wing profile, A, B, C and D at $\bar{h} = 0.15$ can be found in Fig. 5.26. When $C_y < 0.35$, the lift–drag ratio of A is the highest. When $C_y = 0.35$–1.5, the lift–drag ratios of C and D are rather higher, while in case of $C_y > 1.5$, the lift–drag ratio of B is the highest. The lift–drag ratios of several wing profiles are listed in Table 5.5

The relation of lift–drag ratio to flying height and aspect ratio is shown in Fig. 5.27. It is found that the lift–drag ratio is proportional to the aspect ratio.

Table 5.5 Lift–drag ratios of various wing sections in ground effect, with endplates

Wing profile		A	B	C	D	NACA 16-409	NACA 66-409	NACA 5409	CLARK Y M-11
Aspect ratio		0.8	0.8	0.8	0.8	0.8	0.8	0.8	0.65
C_y/C_x	$\bar{h} = 0.15$ $C_y = 0.5$	6.85	5.80	8.10	7.50	7.46	7.40	7.70	_
C_y/C_x	$\bar{h} = 0.15$ $C_y = 0.03$	7.74	5.06	7.20	7.29	8.13	8.90	7.80	4.4
C_y/C_x	$\bar{h} = 0.15$ $C_y = 1.5$	15	17	16	14	_	_	_	_

Maximum lift–drag ratio is located at $\alpha = 3$ ($\alpha* = 6$) while $\bar{h} = 0.05$; however, the angle of attack at the maximum lift–drag ratio will be $\alpha < -3$ in case of flying height $\bar{h} = 0.1 - 0.3$. This suggests that the installed angle of attack of the model wing at $\alpha = 9$ ($\alpha* = 12$) is excessively large from the point of view of optimum lift–drag ratio.

Profile drag can be decreased by reducing the wing-profile relative thickness. If relative thickness decreases from 15 to 9%, i.e. change the wing profile from NACA16-415 to NACA16-409, the lift–drag ratio will increase by 9% at $\bar{h} = 0.15$, and $C_y = 0.5$, see Chapter 3 [5].

Pitching Moment

A thick wing section in ground effect with side plates possesses positive longitudinal stability at a range of flying height, i.e. $m_z^\alpha < 0$. The stability is also improved by decreasing the flying height. The absolute value of m_z^α increases with the angle of attack.

The distance from the relative aerodynamic centre to the leading edge $\bar{x} = x/c = 0.35$ for wing profile B when $\bar{h} = 0.15$ and $\alpha = 0$, so it is difficult for this profile to be stable on a WIG without tail wing.

Figure 5.28 shows the relation between the aerodynamic centre and aspect ratio at $\alpha = 0$, $\bar{h} = 0.15$. The aerodynamic centre will move rearward if aspect ratio is reduced at the same flying height and angle of attack.

Conclusion

This experiment measured the longitudinal aerodynamic characteristics of several wing profiles in ground effect with relatively large chord thickness and side plates. The test data can be used as a reference for designing DACWIG craft. When designing a DACWIG, the aerodynamic characteristic should be considered preferably in combination with realistic structure. The strength of hull structure, and also the rigidity of main wing have to be considered carefully in case of using far forward

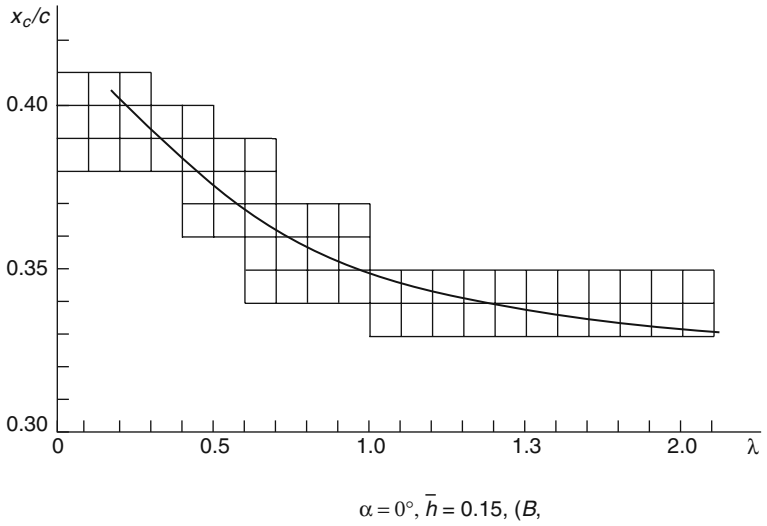

Fig. 5.28 Centre of aerodynamic force X_C/C versus aspect ratio λ

engine-thruster units with a long power transmission system in a DACWIG. From the point of view of designing a DACWIG operating at high lift coefficient, it may be considered favourable to use a thicker wing as the wing profile, such as C type, i.e. NACA0015.

WIG Aerodynamic Characteristics

Figures 5.8, 5.9, 5.10, 5.11, 5.12, 5.13, 5.14, 5.15, 5.16, 5.17, 5.18, 5.19, 5.20, 5.21, 5.22, 5.23, 5.24 and 5.25 on pages 158 to 175 show the aerodynamic characteristics of various wing profiles from the wind-tunnel tests, and Figs. 5.9, 5.11, 5.13, 5.15, 5.17, 5.19, 5.21, 5.23 and 5.25 show the longitudinal stability characteristics of a single wing (single air tunnel), i.e. the non-dimensional longitudinal aerodynamic moment $\overline{m_z}$ versus the angle of attack α. It can be seen that the curve has a down-slope tendency, i.e. a bow-down moment of the wing with various types of profiles increases with bow-up pitching angle so as to lead to a wing with positive longitudinal stability. In case of the single air-tunnel WIG with bow thruster, the pitching-moment versus pitching-angle curve may be rather different from the curves mentioned above, as the AR is related to the total wingspan rather than the half wingspan.

Figure 5.29 shows the longitudinal pitching moment versus pitching angle of a single air-channel model of a typical DACWIG craft. The model is also without high tail wing, the main-wing flap open or the bow thruster in operation. The figure shows the pitching moment coefficient $\overline{m_z}$ versus the angle of attack of the craft α at various relative flying height $\bar{h}$. The value h_4 represents the greatest flying height.

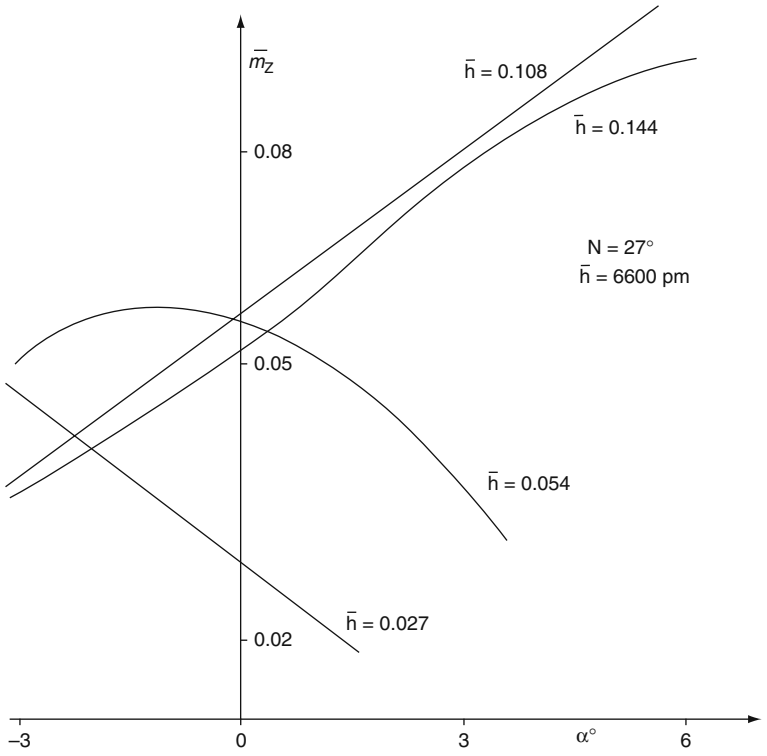

Fig. 5.29 M_z versus α at various $\bar{h}$

From this figure, one can see that the wing only possesses positive longitudinal stability in the very strong surface effect region, i.e. at lower flying height h_1, h_2. The stability will deteriorate in case of larger flying height, h_3 and h_4. The longitudinal stability of the wing in such cases is negative.

The rationale of this phenomenon can be described as follows: Fig. 5.30 shows the flow lines around the main wing and air channel of a typical DACC or DACWIG with the bow thruster in operation. The black line shows the incoming airflow line. The red line shows the air-jet aft of the bow thruster, and the mixture of air jet and incoming flow. It was found from the test that air pressure under the wing at the leading part of the wing is increased due to the impact of the air-jet incoming flow. This causes the aerodynamic centre of the wing to be moved forward and also the pitching centre of the wing to be moved ahead so as to reduce the longitudinal stability moment, particularly, in case of the WIG flying high. A single air-channel WIG with bow thruster therefore does not possess positive longitudinal stability and so a high tailplane is necessary to maintain stability at speed.

The aim of aerodynamic single-wing model testing is to understand the influence of various airfoil profiles on the aerodynamic characteristics of the wings so as to select the optimum wing profile for the WIG under design.

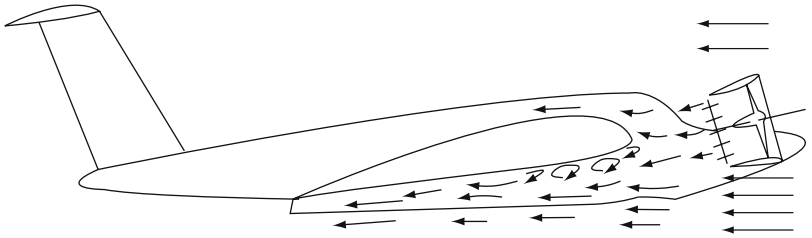

Fig. 5.30 Airflow lines around WIG main wing with bow thruster in operation

Once the base aerofoil characteristics are understood, it is necessary to investigate the aerodynamic characteristics of a whole WIG model. A complete aerodynamic model of a WIG will include the main wing, bow thrusters, guide vanes (if applicable), tail wing, main hull, side buoys, etc. Such a model provides all elements for the overall aerodynamic configuration of the craft. The following characteristic parameters should be included into selection of the aerodynamic configuration:

- Geometry parameters, i.e. the lines of the craft
- Rotation speed of the bow thrusters, n
- Inclination angle of the bow thrusters β_1
- Angle of the guide vane or jet nozzle β_2
- Angle of main-wing flaps γ
- Angle of tailplane φ

Figures 5.31 and 5.32 are typical test results of WIG in a wind-tunnel test facility. They show the C_y, C_x and $\overline{m_z}$, versus $\bar{h}$ and α, at constants n, β_1, β_2, γ and φ.

Figure 5.33 shows the aerodynamic characteristics of a typical DACWIG model, η_{ls}, η_{ld}, η_{ts}, η_{td} and $\overline{X_{dc}} = f(\bar{h})$, at constant bow-thruster speed n and air speed v. It is found that the bow thruster and main-wing flap strongly influence the WIG aerodynamic centre. X_{dc} moves ahead with the increase of bow thruster speed, but when flaps are rotated up away from the ground, the effect is to move X_{dc} backward.

Both the static and dynamic lift coefficient η_{ls} and η_{ld} increase inversely with relative flying height $\bar{h}$, but both static and dynamic thruster-recovery coefficients η_{ts} and η_{td} increase with $\bar{h}$.

Key criteria for selection of WIG aerodynamic characteristics can therefore be listed as follows:

1. $C_y = f(\bar{h},\lambda)$
   Since $L = 0.5\rho_a V^2 C_y S$, then $L = f(v,\bar{h})$, as shown in Fig. 5.34 can be obtained. The relation of flying height h with craft speed v can also be obtained from model tests, as shown in Fig. 5.35.
2. Aerodynamic efficiency:

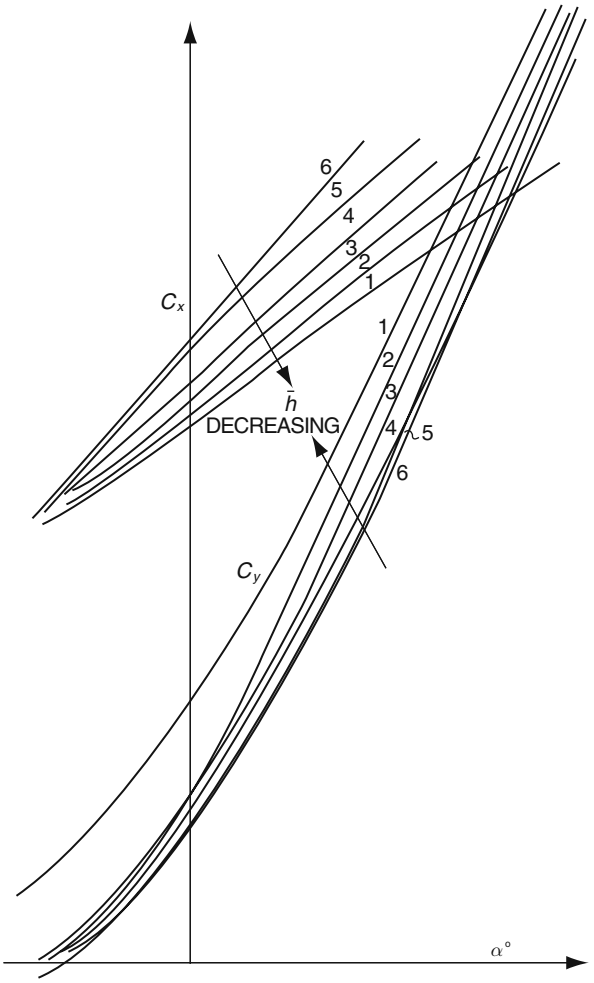

Fig. 5.31 Typical aerodynamic test result of WIG model at constants $\theta,\beta,\varphi_0,\gamma,n$ and different $\bar{h}$

K_3:$K_3 = L_3/R_3$, aerodynamic efficiency of craft with bow thruster in operation, the R_3 shows the necessary thrust of tail propellers, if available;
K_2:$K_2 = L_2/R_2$, aerodynamic efficiency of bare craft (without bow thrusters);
K_1:$K_1 = L_1/R_1$, aerodynamic efficiency of static hovering craft, R_1 represents the craft drag or thrust in static hovering mode.

3. $m_z\,(C_\mathrm{m}) = f\left(C_y,\bar{h}\right)$, from which the longitudinal position of pitching focus can be calculated. This is a very important longitudinal stability criteria for WIG (see next chapter).
4. $\eta_\mathrm{ls} = L_\mathrm{s}/T_\mathrm{so}$, the static hovering capability.

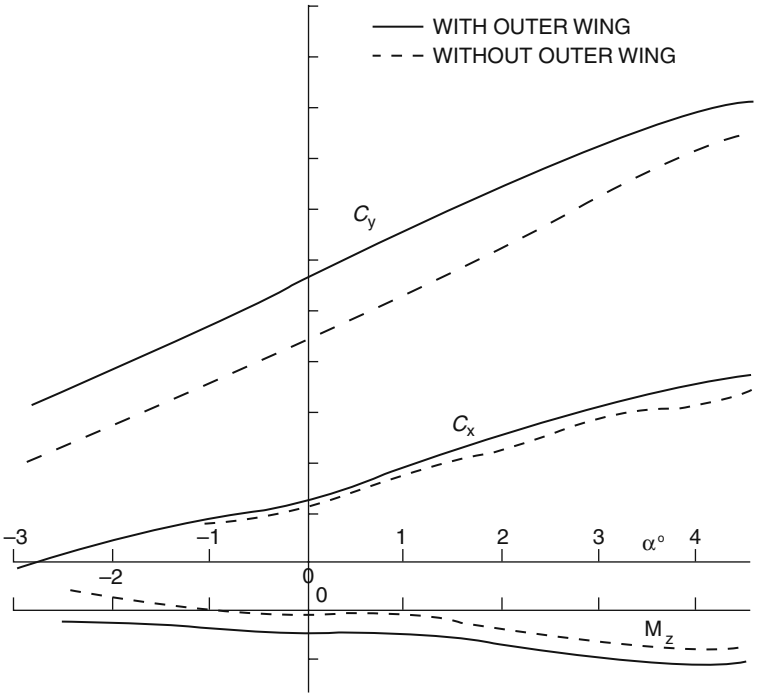

Fig. 5.32 Lift, Drag and moment coefficients C_y, C_x, and M_z variation with α

5. $\eta_{ld} = L_d/T_{so}$, the dynamic hovering capability, i.e. lift as a function of relative flying height $\bar{h}$ with constant bow-thruster speed n, which represents the flying height of the WIG at constant craft weight W (and so constant lift, L).
6. $\eta_{ts} = T_{sc}/T_{so}$, static thrust recovery coefficient of the air channel, which influences craft manoeuvrability over ground.
7. $\eta_{td} = T_{dc}/T_{do}$, dynamic thrust-recovery coefficient of the air channel, which influences the speed performance of WIG.
8. $\overline{X}_{dc} = X_{dc}/C$, dynamic aerodynamic centre of the craft, which influences the craft longitudinal force balance.

Factors Influencing WIG Aerodynamic Characteristics

Bow Thruster with Guide Vanes or Jet Nozzle

Bow thrusters with guide vanes or moveable jet nozzles are important for improving the static hovering performance (for DACC and DACWIG), take-off, longitudinal force-balance problems and seakeeping performance of WIGs, as described in

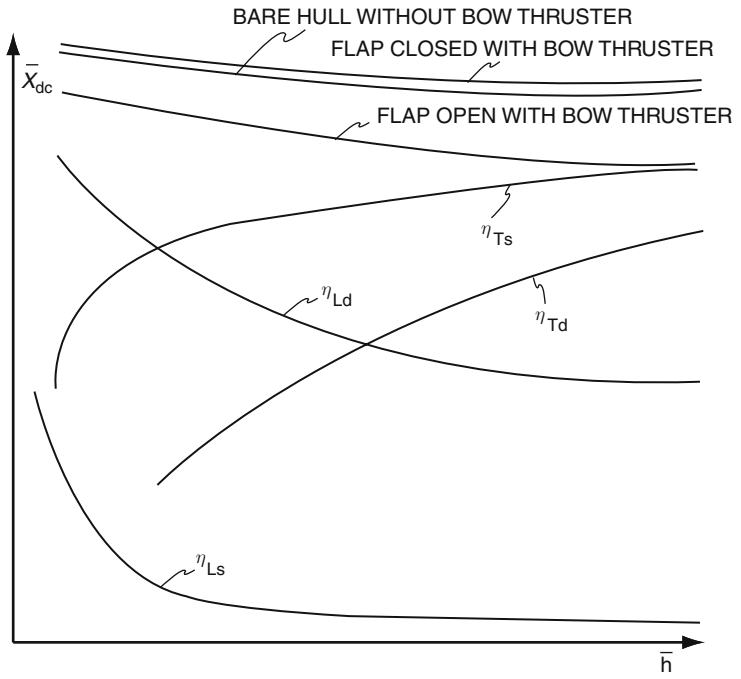

Fig. 5.33 Variation of lifting centre, and recovery coefficients with relative flying height

previous chapters. However, the jet flow from the bow thrust into the air channel will negatively affect the longitudinal stability. Consequently, an enlarged tail wing and stabiliser is required to counter the effect both statically and dynamically, and improve the craft stability.

The bow-thruster power may be a large proportion of total power of craft on DACC or DACWIG, so a lower λ will reduce the high-speed performance of the craft. Reduction of dynamic thrust recovery η_{td} is generally due to poor flow field behind the propeller. Model experimental investigations with different guide vane angles and installation position of the thruster in relation to the main wing, as well as the interference between the propeller and vanes, will need to be carried out to optimise the bow-thruster system.

Special Main-Wing Profile

In order to decrease the area of tail wing and so minimise the craft drag thus improving the aerodynamic efficiency of the craft with a satisfactory longitudinal stability, the special so-called *S*-type wing profiles have been suggested. A wing profile of this kind may possess fine inherent longitudinal stability; however, it is still in the stage of investigation and model testing.

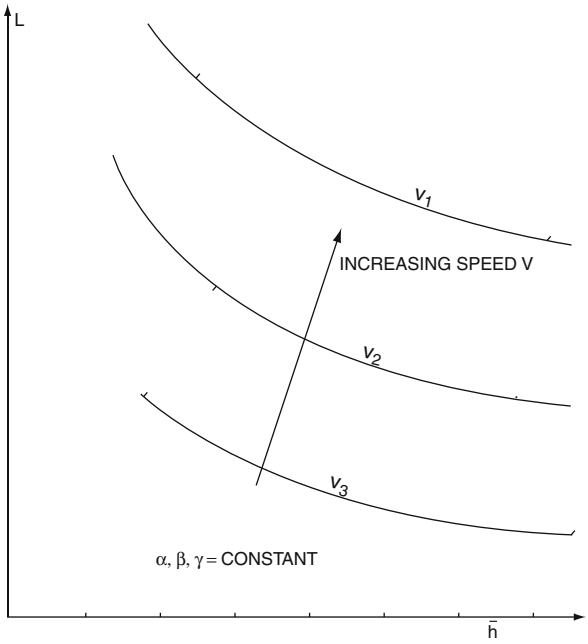

Fig. 5.34 Aerodynamic characteristics of a WIG model

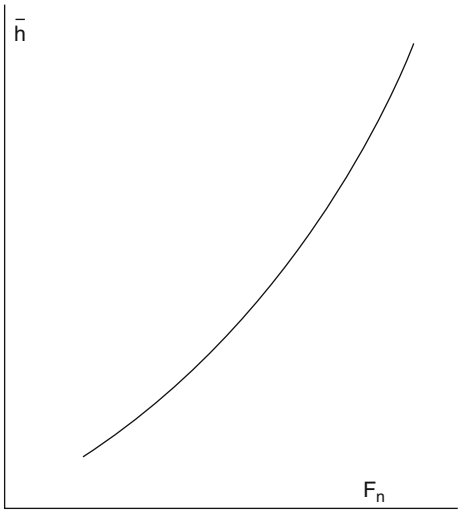

Fig. 5.35 Flying height versus craft speed *v*

Particularly in case of DACC and DACWIG, the influence of flow jet from bow thruster is so strong that any influence of special wing profile on the stability of craft might be negated. Further investigations are clearly required for this craft type. The

S-type camber line airfoil is better suited to craft with higher cruise speed and so with a smaller ratio of thruster to total power or to small WIG craft.

Aspect Ratio

From Figs. 1.10 and 2.21, it can be seen that the aerodynamic efficiency K increases with aspect ratio. However, it is difficult to increase the main-wing aspect ratio due to requirements for making an effective dynamic air cushion under the main wing to obtain the required amphibious qualities for DACC and DACWIG, and take-off for all WIG.

The most realistic solution is to introduce a composite wing configuration as shown in Fig. 1.16. In this case, a low aspect ratio is chosen for the main wing to create an effective air cushion or enhanced lift at low ground clearance, and a higher aspect ratio outer wing (referred to as a composite wing) to enhance the aerodynamic efficiency of the whole craft [5].

Figure 2.25 shows the effect of the tip vortex action of the main wing on the composite wing. The tip vortex of the main wing induces a vertical flow velocity, thus the total velocity of the incoming flow becomes the vector sum of $V_t = V_o + V_i$. The resultant force acting on the composite wing will be R, as shown in the figure; this not only increases the vertical component force, i.e. lift, but also creates added positive horizontal component force, i.e. propulsion force, consequently, reduces the effective drag of the craft.

The use of a composite wing can give a twofold improvement to craft overall aerodynamic efficiency K as follows:

- Enhancing K due to using the main wing tip vortex energy
- Enhancing K due to using a high composite wing aspect ratio

Such advantages have been validated both in general aviation (use of winglets on large jet airliners for example) and current generation WIG. However, a composite wing will create some aerodynamic problems as follows:

- Transverse flow under the composite wing: in general, the composite wing is to be mounted at the stern part of the main wing/side buoy to improve the aerodynamic force balance by inducing a bow-down trimming moment to compensate the main-wing aerodynamic centre moving ahead in flying mode with increasing speed and longitudinal stability. Transverse flow is generated particularly in case of large trim angle with lower altitude, which blows out from the air channel and interferes with the incoming airflow under the composite wing.
- The transverse flow will also cause the decrease of C_y, as well as increase of C_x, thus reducing the efficiency of the composite wing.
- The transverse flow also causes earlier separated flow around the back surface of the composite wing.

These problems can be solved as follows:

- Raising up the installation position of the composite wing on the side buoy
- Giving the composite wing a positive dihedral angle
- Putting the wing fences on the lower surface of the composite wing

Where a WIG craft with extended composite outer wing also has a large span, this outer part might be manufactured as foldable for easily manoeuvring and handling the craft during landing, and moving on the ground.

Since the main wing lift can be expressed as $L = 0.5\rho_a V^2 C_y S$, it may be seen that the value of S for constant lift force will decrease as craft design speed is increased. Using a high lift coefficient C_y (increasing the angle of attack or thickening the wing camber) also causes a decrease of wing area saving the weight and cost; however, it also reduces the longitudinal stability.

The determination of aspect ratio λ and design lift coefficient C_y at the design stage is very complicated and will involve some trade-off between performance and stability. Figure 13.13 shows the general tendency of C_y, and λ with Froude number of WIGs (without composite wing), which might be used as a reference.

Other Measures

The external surface of a WIG is not so smooth or "clean" as an airplane, due to inclusion of such elements as:

- Two or more large side buoys
- Thrusters with guide vanes at the bow. Particularly in case of DACC and DACWIG, the large ducts associated with their propulsors will cause a higher frontal area and thus drag, especially at high speed
- Bow engine and power-transmission equipment on DACC and DACWIG
- Specific take-off and landing arrangements (TLA), i.e. Hydro-ski and landing gear for PARWIG, skirt or air bag as well as some soft or hard landing pads for DACC and DACWIG operating on ground

Even though from a theoretical basis, a wing operating in ground effect zone possesses a very high aerodynamic efficiency K, as shown in Fig. 2.21, i.e. $K =$ 25–30 in case of $\bar{h} = 0.1 - 0.2$, in practice the aerodynamic properties of WIGs constructed to date are far lower than this value and may drop down to $K < 13$–16 or even less due to the reasons mentioned above. Perhaps this is why WIG craft have not achieved commerciality in general application compared with the conventional airplane so far!

To improve this state of affairs, during the design and construction of a WIG, serious considerations for smoothing and cleaning the external surface of craft should to be taken as follows:

- During construction of WIG, the external surfaces of wings, hull and side buoys have to be manufactured as smooth as possible, particularly in case of construction of DACC and DACWIG in shipyards, thus construction according to the "rule and regulation" issued by ship classification societies will not be sufficient. Aeronautical practice should be followed wherever practical and economical.
- Protrusions should be reduced or smoothed with stream line covers as far as possible in the craft design, such as skirt, air bag, landing pads, engine mountings, pipe lines for lubrication oil and fuel, as well as hydraulic working oil for DACC or DACWIG. Since such craft are generally taken as a ship but not an airplane, the problems mentioned above are often neglected during design and construction.
- Side plates can decrease or eliminate the vortex occurring on the tips of the wing due to the difference of pressure between upper and lower surfaces of the wing, so side plates are suggested to be mounted on main wing (side buoys), composite wing (fences, etc.), horizontal stabilizer (tip fences), etc.
- The size of side buoys is suggested to be as small as possible to minimise the weight, drag and cost of the craft.
- The clearance between the hull and side buoy base plane with the trailing edge of the DACC and DACWIG main wing should be reduced as small as possible to increase the ground effect on the craft.
- The flying height h (clearance to lowest structure) of a DACC is relatively small. The main-wing flying height $H = h + H_{sb}$, as shown in Fig. 5.6, where H_{sb} will be a large proportion of H to accommodate the bow-mounted thruster arrangement safely. The arrangement of bow thruster and installation angle of main wing will need to be considered carefully as a design trade-off, since the higher the wing mounting the larger the cushion cavity and front entry area. Above a certain proportion of wing chord, cushion generation efficiency will drop off. The optimum is specific to overall craft configuration and so has to be determined for the individual design by parametric studies and/or testing. Guidance is given in Chapter 4.

Chapter 6
Longitudinal and Transverse Stability

Introduction

In this chapter we will introduce the forces and moments influencing dynamic equilibrium of a WIG in flight, and the cases that need to be analysed to complete the design of a stable vehicle. We will then look at some topics that are special to WIG behaviour:

- Longitudinal stability flying in and beyond the surface/ground effect zone (GEZ)
- Static longitudinal stability over calm water and acceptance criteria
- Dynamic longitudinal stability
- Transverse stability
- Transient stability during transition phases

Aircraft longitudinal stability can be assured when the pitching centre of gravity is located behind the aerodynamic pitching centre of the aircraft. Stability is essentially constant over the operational flying envelope of speed and attitude.

WIG longitudinal stability [1] has additional constraints to an aircraft in that its aerodynamic characteristics in the GEZ are strongly affected by the presence of the ground plane and bow-thruster jet stream. The pitching centre moves significantly forward and aft in the different flying modes, so stability can also change a great deal. Let us first look at the forces and moments, and the pitching centres (pitching centre or trimming angle centre) for a WIG so as to gain an impression of the key factors.

Forces and Moments

The main aerodynamic forces are the lift and drag on the main wing, fin, tailplane or stabiliser, and fuselage. Main wing and tailplane forces dominate the equilibrium. We start by determining moments about the centre of gravity of the craft, using that as the origin for determining the balance of forces and moments. It is normal to

L. Yun et al., *WIG Craft and Ekranoplan*, DOI 10.1007/978-1-4419-0042-5_6,

make the values non-dimensional by dividing by $0.5\rho_a V^2 S$, giving us the lift, drag and pitching moment coefficients C_L, C_d and C_m.

Two additional variables important to WIG craft are flying height H and pitch angle ϑ. Height is made non-dimensional by dividing by the main-wing chord C, so that $\bar{h} = H/C$. The pitch angle is relative to the ground plane. It should be noted that the main-wing angle of attack α_0 will be designed to be optimum for flight at cruise speed and level trim – pitch angle zero of the WIG fuselage.

Craft stability is determined based on the rate of change, i.e. the derivative of these coefficients relative to $\bar{h}$ and ϑ. These may be defined as:

$$\begin{aligned} C_{y\vartheta} &= \mathrm{d}C_y/\mathrm{d}\vartheta \\ C_{M\vartheta} &= \mathrm{d}C_M/\mathrm{d}\vartheta \\ C_{yh} &= \mathrm{d}C_y/\mathrm{d}h \\ C_{Mh} &= \mathrm{d}C_M/\mathrm{d}h \end{aligned} \tag{6.1}$$

Once the coefficients above are determined for a range of ϑ and $\bar{h}$, and plotted, the WIG craft stability can be assessed against changes in air speed.

Longitudinal stability is evaluated here against three parameters, heaving and pitching velocity, as above, and additionally heave displacement from its neutral value.

Pitching Centres

The pitching pitching centre for an aircraft is defined as the point about which the pitching moment remains constant with changing the pitching angle ϑ. A WIG also has a second centre defined as the point about which the pitching moment remains constant with varying flying height $\bar{h}$. These two centres (i.e. the distance between the two centres and X_g) can be written as:

$$X_\vartheta = C_{M\vartheta}/C_{y\vartheta} \text{ and } X_h = C_{Mh}/C_{yh} \tag{6.2}$$

Since the coefficients and derivatives are non-dimensional based on main-wing chord, so are X_ϑ and X_h. We will refer to these two centres as the pitching and height centres respectively in what follows.

The physical explanation of the WIG-pitching centres is that in the case of changing pitch angle or steady trim angle of the WIG, the centre of action of the lift increment is called the pitching centre (or sometimes referred to as the focus point). Similarly in case of height change, the centre of action of the lift increment is called the height centre or focus.

Pitch Stability Design Criteria

A WIG is at a stable trim angle when the sum of aerodynamic forces about the CG is zero, and disturbances in pitch result in moments that return the trim angle to the initial condition. This condition is generally termed static stability.

Static stability is achieved when $C_{M\vartheta} < 0$ indicating that when the craft pitches up (positive pitch), a negative pitching moment occurs. The stiffness of response is determined by the (negative) value of $C_{M\vartheta}$.

It is possible that the stabilising forces and moments could have too steep an increment so that the pitch acceleration over compensates and the craft oscillates about the static trim. The craft is then termed statically stable, but dynamically unstable. This is not generally experienced with WIG except when they are at very small ground clearances during take-off and landing.

Height Stability Design Criteria

A WIG also needs to have stability in the vertical dimension so as to be able to fly steadily without constant active correction to the ground clearance. Height stability is achieved if the derivative of the lift coefficient with increasing height is negative. In addition, the moment coefficient should remain constant, otherwise the craft will change trim. This leads to an expression determined by Staufenbiel, viz:

$$C_{yh} - C_{y\vartheta}.C_{Mh}/C_{M\vartheta} < 0$$

This expression can be shown to be the same as the simpler relation

$$X_{\vartheta} - X_{h} > 0$$

derived by Iridov, where X is measured positive in the downstream direction from the leading edge. The actual value of $X_{\vartheta} - X_{h}$ is generally referred to as the stability margin. Essentially, the pitch centre for height should be ahead of the centre for change of pitch angle.

The Ekranoplan development work in Russia concluded that a stability margin of about 0.1 (the ratio of $[X_{\vartheta} - X_{h}]/C$) at cruise speed was necessary for a stable flight. Larger values than this tend to make a craft oscillate dynamically. This is accentuated by surface undulations or ocean swell. A stability margin closer to zero will make a craft marginally stable in pitch and difficult to maintain the steady ground clearance.

A simple aerofoil will not have an inherent stability margin for flight at constant close-ground clearance on its own. The Russian Ekranoplan development experimented with different sizes and relative position of tail stabiliser, and adjustments to the main-wing camber geometry. Meanwhile, Lippisch in Germany experimented quite successfully with strongly tapered wing plan forms and showed that smaller tail stabilisers could be used with such a configuration.

Main-Wing Airfoil and Geometry

The Russian Ekranoplan series (up to the third generation when outer winglets were added) utilised essentially rectangular main-wing plan forms. These craft depended on the action performed by large tailplanes eventually set high out of the main-wing slipstream to provide the pitch and height stability margin. The tails for these craft create significant drag, increasing powering requirements for acceleration through take-off.

Such craft geometries are efficient for very high speeds targeted in this programme (250 kph plus), but are inefficient for lower cruising speeds typical of smaller WIG craft.

Lippisch has performed significant research into alternative main-wing plan forms. His development focuses on a swept forward wing with a strong taper and negative dihedral. This form has high inherent stability so a smaller tail can be used. The form is most efficient for slower cruise speeds in the range of 150–250 kph typical of smaller craft. Lippisch's development is an extension of forward-sweep wing forms developed for tailless aircraft with washout from the fuselage to wing tip.

Wing forms on WIG have rather low aspect ratio, leading to a strong three-dimensional flow. The performance data for standard wing sections (usually for infinite aspect ratio) have to be adjusted for WIG applications. Lift coefficient slope reduces by reducing the aspect ratio and so the sensitivity to changing the angle of attack also reduces, see [2]. Aerofoil data are not normally available for the ground effect conditions that have a significant effect on lift coefficient. Some material is available for the DHMTU family though, see [3–5].

Improved longitudinal stability of an aerofoil can be achieved for WIG by loading the forward part of the foil so that the centre of lift moves less. This can be achieved by using higher camber in the front part, and flatter or even negative camber towards the trailing edge, similar to sections used on tailless aircraft. The problem with the more extreme forms is reduced C_{Lmax}. Since the improved lift due to ground effect is the main advantage of WIG craft, there is somewhat a contradiction in using low C_y airfoils. A better approach is to regard the complete WIG as the unit to optimise and so consider the aerodynamic stability of the wing and tail combination as the optimisation target.

Influence of Flaps

Flaps in the trailing edge of the main wing strongly affect the aerodynamic characteristics C_y and C_{M}, and thus the pitching centres. They can be used to alter camber and so adjust longitudinal stability. They are generally used as static trim devices though, set down during take-off and landing, and raised to a set position for cruising at a given altitude.

The main-wing flaps are larger on DACC and DACWIG craft than on PARWIG, to create a static air cushion at speeds below take-off by closing off the main-wing trailing edge against the ground plane.

Tailplane and Elevators

The effect of a tailplane is to move X_ϑ rearwards to a position behind X_h, thus creating a height stable configuration. The tailplane size required depends on the moment arm to the pitching centre and so the force needed to balance the shift in centre of lift at the main wing as its angle of attack changes. The elevators need to be sized to provide adequate change in tailplane lift forces without sending the craft into unstable oscillation as they are manoeuvred by the pilot.

Centre of Gravity

In theory, the position of X_h is not affected by CG position, while the position of X_ϑ is. In a free flying aircraft, the pitching centre is independent of CG and so the aerodynamic configuration can be designed, and stability checked against CG. The two parameters can then be adjusted independently to achieve a stable, controllable aircraft. WIG design needs to start by assessing the CG and using this as the origin for the aerodynamic analysis. Stable WIG aerodynamic configurations are obtained with CG located further back than for free flying aircraft, between 30 and 45% of mean chord, compared to 25–30% for aircraft. This rearward CG location generally requires the tailplane to have positive lift at cruising speed and trim.

If we start with Iridov's criterion for height stability, $X_\vartheta - X_\mathrm{h} > 0$ measured from wing leading edge, i.e. X_h is in front of X_ϑ, and also account for the fact that CG must be ahead of X_ϑ for pitch stability, then CG must be placed somewhere between X_ϑ and X_h. If CG is at the same location as X_h, then the pitch attitude will not change with alterations of speed and flight height. As it is moved rearwards towards X_ϑ, the tendency to change the pitch will increase with speed and height changes, and the tendency to change the altitude will diminish. The problem is that actually the pitching and height centres do also change with height and pitch. It is preferable for CG to be closer to X_h so that the tendency for pitch attitude to be changed by disturbances is minimised. The Russian Ekranoplan programme selected a position about 10% back from X_h in cruise conditions, i.e.

$$\left(X_\mathrm{g} - X_\mathrm{h}\right) / \left(X_\vartheta - X_\mathrm{h}\right) \cong 0.1 \text{ (measured from the wing leading edge)}$$

Influence of Ground Effect on Equilibrium

The lift coefficient of an aircraft is independent of the flying height due to operation in the free air stream. Aircraft are designed with the wings providing support for the aircraft weight, and tail surfaces that provide trimming or turning forces in yaw (fin and rudder) and pitch (tailplane and elevators).

A wind gust acting on a WIG flying in the GEZ (Fig. 6.1) will cause the flying height h_0 to increase to h_1. The centre of action of the added lift, i.e. the height centre, does not generally coincide with the pitch centre so the angle of attack of the WIG wing will also change from α_0 to α_1. In addition, the angle of attack will be changed further due to the heaving velocity of the craft. The increment of angle of attack, which can be expressed as $\Delta\alpha = \dot{h}/V = \Delta\alpha_h$ is shown in Fig. 6.1. The WIG tailplane surface needs to be designed to provide sufficient righting moment to return the main-wing angle of attack to its neutral position under the influence of wind-speed changes, while the elevators need to provide sufficient moment to change the angle of attack to allow the craft to adjust the flying height [6, 7].

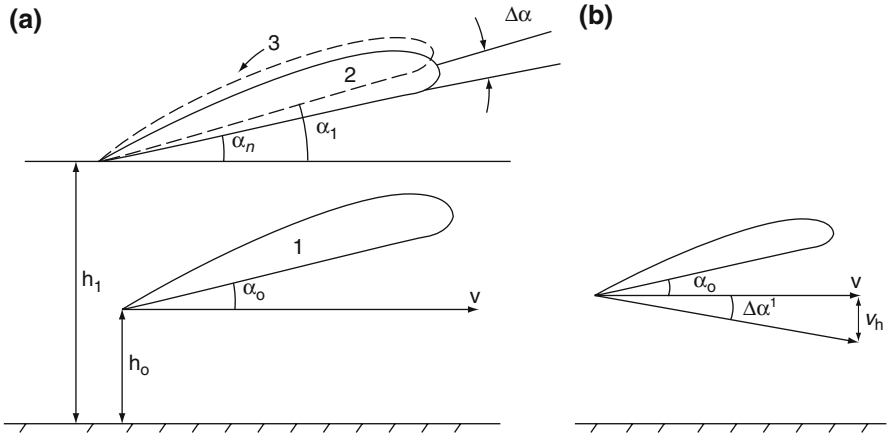

Fig. 6.1 (**a**) Change of flying height and angle of attack due to a gust. Change of flying height: 1, original position; 2, change of height; 3, angle of attack increases due to gust; (**b**) change of angle of attack due to heaving velocity

Influence of Bow Thrusters with Jet Nozzle or Guide Vanes

A bow thruster and guide vanes strongly affect the main-wing aerodynamic characteristics, so the position of the pitching and height centres X_ϑ and X_h will vary during craft operation, and will move with the adjustment of guide vane angle and bow-thruster power rating. This complicates the WIG aerodynamic design, and even more so a DACWIG that uses the bow thruster influences more strongly, to create a static air cushion sufficient to support the weight of the WIG at zero forward speed.

Automatic Control Systems

The variation of pitching centre with the change in flying height can cause problems to a pilot to manually maintain steady flight. DACC and DACWIG are somewhat self-correcting when in strong air cushion mode, but become more difficult to handle at higher flying heights. In such cases, an automatic control system is suited to solving the complicated operational handling problems [8]; however, the flying height for the WIG is so small in comparison with a conventional aircraft that the instruments for flying height, heaving velocity, pitching angle, etc. have to respond quickly and accurately, and be highly damped. Such instruments are very specialised indeed and increase the complexity and cost for WIG craft and so naturally statically stable configurations are preferred where possible.

Fortunately, DACC and DACWIG most often operate close to the surface at their cruising speed, so as to assure safe operation, even in the case of unsteady handling (incorrect operation of the guide vanes or/and flaps). However, a PARWIG operating beyond the GEZ for collision avoidance purposes needs the pilot to pay more attention to craft handling within the envelope of positive stability (particularly when adjusting the bow jet nozzles or guide vanes). Some accidents with model and full-scale WIG have demonstrated the small margin of stability available relative to the disturbing moment that thrusters can apply when incorrectly operated, and the critical need for pilots to be familiar with the safe envelope of operation of their controls.

Stability Analysis

We have so far reviewed the main forces and moments, and considered the influence of some special factors for WIG on stability in flight. The main disturbance from steady flight will come from wind gusts or unsteady conditions caused by the presence of waves and consequent turbulence in the surface effect zone. The aim of our craft design is to provide restoring moments from suitable fixed and moving control surfaces such that the craft will maintain a stable flight. The fixed tailplane should provide these righting forces as the craft pitches up or down. The elevators should in addition provide sufficient moment to control the craft attitude while the bow-thruster power is changed. Both righting forces should be sufficient to provide a stability margin without being too powerful and cause instability. To determine the requirements for the tail design, the characteristics of the main wing have to be investigated. This is outlined below as examples.

Figures 6.2 and 6.3 show the Russian training PARWIG, “Strizh”, operating at a low and medium flying height, while Fig. 6.6 shows it flying beyond the surface effect zone. In this condition, the stability characteristics are similar to a normal aircraft, so the main aerodynamic surfaces need to meet the criteria for safe free flight [9].

Figure 2.27 shows a Russian DACC type “Volga-2” operating at a small flying height in the strong surface effect zone, sometimes touching the water surface. In this case, the stability of the craft relates more closely to an ACV or planing hull.

Fig. 6.2 Russian two seat WIG "Strizh" in flight in strong SEZ

Fig. 6.3 Russian Training PARWIG Strizh flying in medium SEZ

Figures 6.4 and 6.5 show MARIC's DACWIG self-propelled radio-controlled model operating both at a small flying height (Fig. 6.4) and higher flying height (Fig. 6.5). This craft was designed to provide stability of operation in three different modes – hovering, in the strong GEZ and in the weaker GEZ.

Fig. 6.4 Chinese DACWIG model in flight with small $\bar{h}$

Fig. 6.5 Same model with higher $\bar{h}$

Static Longitudinal Stability in and Beyond the GEZ

Nomenclature (also see Figs. 6.8 and 6.9):

ϑ_0	Trim angle for craft in aerodynamic balance
α_0	Angle of attack for wing in aerodynamic balance
ϑ	Craft Trim/pitch angle
α	Angle of attack of wing
β_1	Angle between the shaft of bow thruster and base plane
γ'	Flap angle
β_2	Angle of guide vane in the bow ducted air propeller
ϕ	Angle of tailplane elevators
C	Main-wing chord
S	Total area of support surface
C_x	Aerodynamic coefficient of craft drag (or wing)
C_y	Aerodynamic coefficient of craft lift (or wing)
L	Lift from wing
L_H	Lift from tailplane
l_H	Lever arm from aerodynamic centre, of lift from tailplane
m_z	Aerodynamic coefficient of pitching moment
T	Air propeller thrust
X_a	aerodynamic centre
$\bar{X} = X_\mathrm{g}/C$	Relative position of CG
$\bar{X}_{\mathrm{F}\vartheta} = X_{\mathrm{F}\vartheta}/C$	Relative position of pitching centre
$\bar{X}_\mathrm{Fh} = X_\mathrm{Fh}/C$	Relative position of flying height centre

Static Longitudinal Stability of an Aircraft and a WIG Operating Beyond the GEZ

A craft has positive static stability if when it is disturbed from equilibrium it will tend to return to its state of equilibrium. Longitudinal stability flying beyond the surface effect zone can be analysed in the same way as that of an aircraft, i.e. not considering the surface effect on the WIG longitudinal static stability. Figure 6.6 shows the forces acting on an aircraft:

$$M_z = m_z qSC$$

represents the pitching moment of main wing the hull of aircraft about CG,
Where

$$q = 0.5\rho_a V^{2.}$$

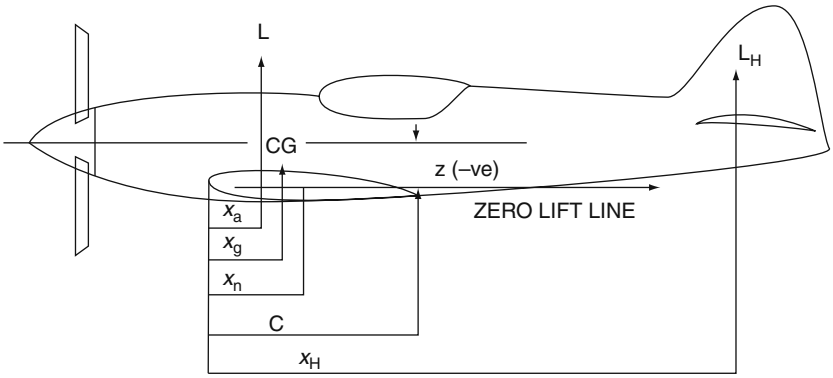

Fig. 6.6 Vertical force acting on an airplane

For balance:

$$\begin{aligned} L \cdot \left(X_g - X_a\right) - (L_H . l_H) = 0 \\ L \cdot \left(X_g - X_a\right) - (L_H \cdot l_H) \end{aligned} \tag{6.3}$$

Where

subscript H	Horizontal tailplane
L, L_H	Lift of main and tail wings, respectively
X_g	Position of CG of craft from the leading edge of main wing
X_a	Position of pitching centre of the wing (and hull as well as side buoys) from the leading edge of main wing, Fig. 6.7
l_H	Distance from tailplane lift centre to WIG pitch centre

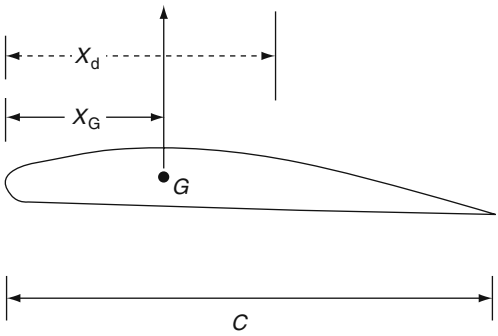

Fig. 6.7 Centre of lift of a wing

X_n Position of a neutral point representing the pitching centre of the wing plus tailplane configuration

In non-dimensional form, balance is defined by

$$C_y\left(\bar{X}_g - \bar{X}_a\right) = C_{yH}\,(S_H/S)\,(l_H/C) \tag{6.4}$$

Where
S_H Area of tailplane
S Area of main wing

$$\begin{aligned} \bar{X}_g &= X_g/C, \\ \bar{X}_a &= X_a/C \\ (S_H/S)\,(l_H/C) &= \bar{V}_H \text{Tailplane"volume"} \end{aligned}$$

Basic Stability Equation

An aircraft is stable, provided that

$$(\mathrm{d}L_H/\mathrm{d}\alpha)\,|l_H/C| > (\mathrm{d}L/\mathrm{d}\alpha)\,(\Delta X/C) \tag{6.5}$$

In case of nose up, the craft attitude $\alpha > 0$ and the restoring moment due to the tailplane should be greater than the disturbing moment on the main wing so as to keep the trim angle constant.

Now $\Delta X/C = \bar{X}_g - \bar{X}_a$, so by replacing the lift by its coefficient C_{yH}, and L_H by $C_{yH}\,qS_H$, then the positive longitudinal stability can be represented by the following expression:

$$\left(dC_{yH}/d\alpha\right)\bar{V}_H > \left(dC_y/d\alpha\right)(\Delta X/C) \tag{6.6}$$

On the basis of these equations, any combination of two "wings" might be made "stable", including tandem and canard configurations. The reasons for preferring one particular configuration, for example, a larger main wing plus comparatively small horizontal tailplane aft for aircraft are as follows:

- Concentration of lift in one large span wing is most efficient
- A "small" horizontal tail surface reduces drag
- Location at the tail offers longitudinal control up to and beyond $C_{l\alpha}$
- Location within the propeller slipstream provides improved control at low speed, such as on the ground

Equation (6.6) also suggests that for longitudinal stability, the difference of the two sides, equal to the derivatives of the complete system (for example, with fixed tailplane) must be negative, thus

$$\left(dm_Z/dC_y\right) = \left(dm_z/d\alpha\right)\left(d\alpha/dC_y\right) < 0 \tag{6.7}$$

Wing Pitching Centre

The definition of the pitching centre of a wing is "In case of changing the pitch angle of a wing, the acting point of the lift increment is at the pitching centre" [10, 11]. From Fig. 6.6 we have:

$$M_{z0} = M_z^0 + M_z^\alpha \cdot \alpha \tag{6.8}$$

Where M_z^0 is the pitching moment of the wing in case of $\alpha = 0$, then

$$m_z = \frac{L\left(X_\mathrm{G} - X_d\right)}{0.5\rho v^2 SC} = \frac{M_z}{0.5\rho v^2 SC}$$

$$m_z = C_y\left(\bar{X_\mathrm{G}} - \bar{X_d}\right)$$

where

$$\bar{X}_\mathrm{G} = X_\mathrm{G}/C, \bar{X}_d = X_d/C$$

X_d Aerodynamic centre (centre of pressure on the wing)

Thus

$$M_z^\alpha \alpha = L^\alpha \alpha\left(\bar{X_\mathrm{G}} - \bar{X_{\mathrm{F}\alpha}}\right) \text{ and}$$

$$m_z^{\alpha}\alpha = C_y^{\alpha}\alpha\left(\bar{X}_{\mathrm{G}} - \bar{X}_{\mathrm{F}\alpha}\right)$$

The position of pitching centre of a wing can then be expressed as:

$$\bar{X}_{\mathrm{F}\alpha} = \bar{X}_{\mathrm{G}} - \frac{m_z^{\alpha}}{C_y^{\alpha}} \tag{6.9}$$

Pitching Pitching Centre

The pitching centre of an aircraft or WIG can be expressed as follows (Fig. 6.8):

$$\bar{X_{\mathrm{F}\alpha}} = X_{\mathrm{G}} - m_z^{\alpha} / \left. C_y^{\alpha} \right|_{h=\mathrm{const}} \tag{6.10}$$

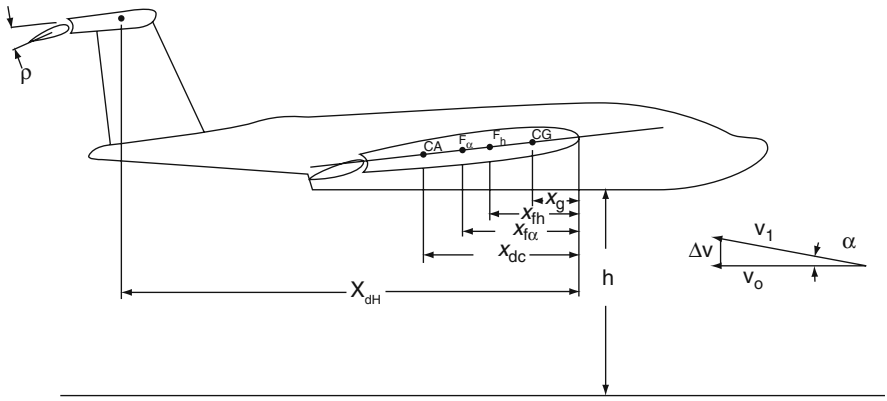

Fig. 6.8 Aerodynamic force acting on a WIG

In the case of an aeroplane in free air, the moments and lift coefficient are constant with changing height. The lift coefficient for a WIG changes with height and so we have to define the pitch centre for each flight height. Compare Equation (6.10) with Equation (6.9).

In case of changing the pitching angle of a WIG, the lift increment acts at the pitching centre. Based on the definition above, we have

$$(S_{\mathrm{W}} + S_{\mathrm{H}}) \cdot (X_{\mathrm{F}\alpha} - X_{\mathrm{G}})\, C_y^{\alpha} = C_{yw}^{\alpha}\,(X_{\mathrm{Fw}\alpha} - X_{\mathrm{G}})\, S_{\mathrm{w}} + C_{y\mathrm{H}}^{\alpha}\, k_{\mathrm{q}}\, S_{\mathrm{H}}\,(X_{\mathrm{FH}\alpha} - X_{\mathrm{G}}) \tag{6.11}$$

Where

S_{W}	Area of main wing, including the effective area of hull and sidewall
S_{H},	Area of the horizontal tailplane

$X_{F\alpha}$	WIG-pitching centre, the longitudinal location measured from the main-wing leading edge
C_y^α	The derivative of lift coefficient of whole plane with respect to the trimming angle α
C_y^αw	The derivative of lift coefficient of main wing (including main hull and composite wing) with respect to the trim angle α
$X_{FW\alpha}$	Position of pitching centre of the main wing, the longitudinal of which is measured from the leading edge of the main wing
C_y^αH	The derivative of lift coefficient of the horizontal tailplane with respect to the trimming angle
k_q	The effective coefficient of main wing down-wash flow with respect to the horizontal tailplane, thus $k_q = V_H^2/V^2$, where
V_H	The incoming flow velocity to the tailplane
V	The incoming flow velocity of main wing
$X_{FH\alpha}$	Position of pitching centre of the tailplane, calculating from the leading edge of main wing

If we assume that

$$X_{FW\alpha} = X_{dW} \text{ and } X_{FH\alpha} = X_{dH}$$

Where

X_{dW}	The longitudinal position of pitching centre of the main wing
X_{dH}	The longitudinal position of pitching centre of the horizontal tailplane

$$\text{Then } X_{F\alpha} = \frac{1}{C_y^\alpha}\left[C_{yw}^\alpha \cdot \frac{(X_{dw} - X_G)\, S_w}{S_w + S_H} + C_{yH}^\alpha\, k_q \frac{S_H}{S_w + S_H}\,(X_{dH} - X_G)\right] + X_G \tag{6.12}$$

$$\text{If } (S_W/\,(S_W + S_H)) \cong 1,$$

$$\text{then } X_{F\alpha} = \frac{1}{C_y^\alpha}\left[C_{yw}^\alpha .\,(X_{dw} - X_G) + C_{yH}^\alpha\, k_q\, X_{dH} \frac{S_H}{S_w}\right] + X_G \tag{6.13}$$

The tailplane is often located at a high position on WIG craft so that the influence of down-wash flow will be lessened, so we assume $k_q = 1$. The values for C_{yw}^α, X_{dw} can be obtained by means of wind tunnel tests, and X_{dH}, C_{yH}^α can be obtained from a standard aerodynamics reference text, provided that the section profile of the tailplane has been selected.

The methods for determining the static longitudinal stability of an aircraft and a WIG are similar. However, since the latter are operated in the ground effect zone,

the aerodynamic derivatives have to be found by means of model tests in wind-tunnel test facilities, rather than from published references that are suitable for wing sections in a free air stream, as used for aircraft, for example Chapter 3 [5].

Flying Height Pitching Centre

The pitching centre or focus with respect to the flying height (see Figs. 6.8 and 6.9) can be defined as:

$$\bar{X}_{\mathrm{G}} - \bar{X}_{\mathrm{Fh}} = \left. \frac{m_z^h}{C_y^h} \right|_{\alpha=\mathrm{const}} \tag{6.14}$$

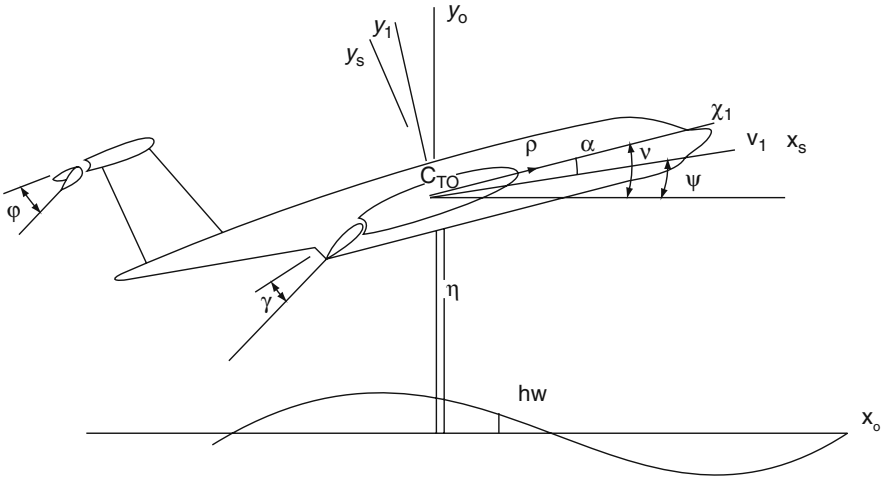

Fig. 6.9 Coordinate systems

Where

$\bar{X}_{\mathrm{Fh}}$ Flying height pitching centre
m_z^h, C_y^h Aerodynamic derivatives of the wing with respect to the flying height

The aerodynamic derivatives with respect to flying height of an aircraft will be zero. However, in the case of WIG, this is not the case. Using a similar method as for the pitch centre, the height centre of a WIG can be expressed as follows:

$$(X_{\mathrm{Fh}} - X_{\mathrm{G}})\, S_{\mathrm{w}} C_{\mathrm{h}} = C_y^h\, (x_{\mathrm{Fhw}} - X_{\mathrm{G}})\, S_{\mathrm{w}} + C_{y\mathrm{H}}^h\, k_{\mathrm{q}}\, S_{\mathrm{H}}\, X_{\mathrm{FhH}} \tag{6.15}$$

Where

X_{Fh}	Pitching centre of flying height
X_{Fhw}	Pitching centre of flying height of main wing (and hull)
X_{FhH}	Pitching centre of flying height of tailplane

If we assume that as the tailplane is mounted high at the stern

$$C_y^h H \cong 0, C_y^h = C_y^h \mathrm{w} \text{ and } k_{\mathrm{q}} = 1$$

Then

$$X_{\mathrm{Fh}} = 1/C_y^h \left[C_y^h \mathrm{W} \cdot X_{\mathrm{FhW}} \right] = X_{\mathrm{FhW}}$$

And

$$X_{\mathrm{G}} - \bar{X}_{\mathrm{Fh}} = m_z^h \mathrm{w}/C_y^h \mathrm{w} \tag{6.16}$$

The tailplane is always located high at the stern, preferably out of GEZ, so that the ground effect will not influence its aerodynamic performance. However, ground effect does also influence the tail, exhibited via altered down-wash flow from the main wing affecting the tail aerodynamics. The down-wash angle of the flow incoming to the tailplane ε_{m} is a function of craft-trimming angle, flying height and of installed tailplane height. Figure 6.10 shows test results of the average down-wash angle of the incoming flow to the tailplane [12]. It was found that lower flying height reduces down-wash angle due to the influence of the ground.

Average down-wash angle ε_{m} at the main wing increases with increasing flying altitude, i.e. ε_{m} will decrease with flying altitude due to the influence of ground effect and the airflow leaking from the air channel:

- ε_{m} decreases inversely with horizontal tailplane height due to lessening influence of the main wing
- ε_{m} increases with trim angle due to the stronger influence of the main wing

Due to the influence of ground effect, the tailplane will therefore need to be larger than that of an airplane, and the lower the flying height, the larger it needs to be due to higher pitching moments exerted by the main wing and thus more stable WIG.

Estimation of Balance Centres

The aerodynamic derivatives $C_{y\alpha}$, $C_{\mathrm{m}\alpha}$, C_{yh} and C_{mh} can be obtained from wind-tunnel model-test results. The WIG aerodynamic characteristics $C_y, m_z = f\,(h, \vartheta)$,

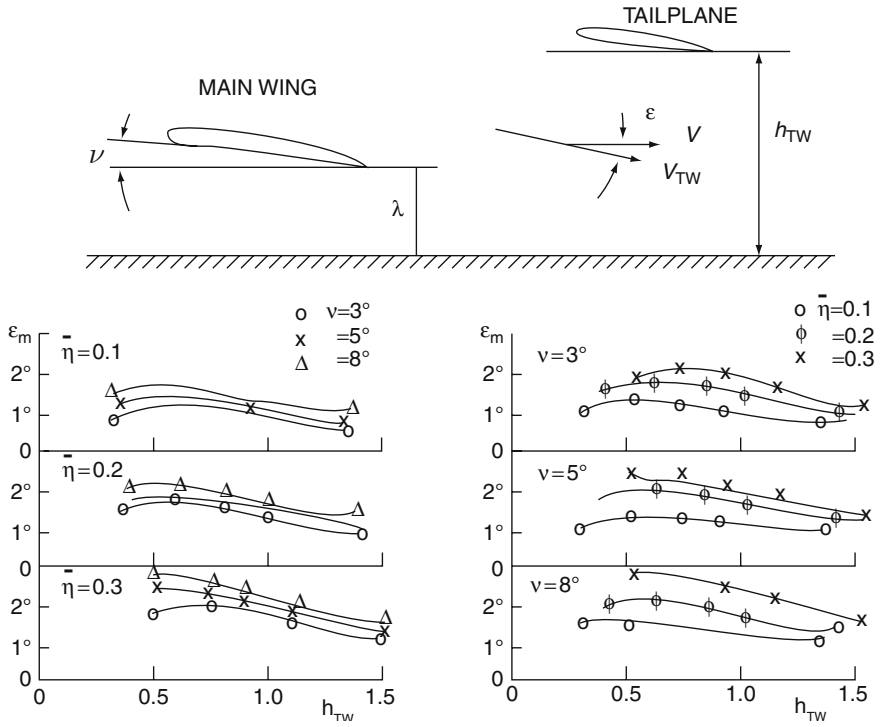

Fig. 6.10 A typical pitching centre curve $X_{F\alpha}$ of a DACWIG model tests results

can also be obtained from model tests in a wind tunnel and plotted, and the partial derivatives $\partial M_z/\partial C_y$, etc., can then be obtained from such plots.

Figure 6.11a, b, c, d shows the pitching and flying height centres of a DACWIG, derived from model aerodynamic characteristic curves with fixed bow-thruster speed, fully opened flaps and various guide vane angles. From the graphs, it can be seen that the centres $X_{F\alpha}$ and X_{Fh} are not constant but they vary with the relative flying height $\bar{h}$, wing angle of attack α, angle of guide vane β_2, etc. In fact the balance centres also vary with bow-thruster speed n and the flap opening γ', which are not shown in these plots.

The test results show that the variation of the centres of balance, particularly for pitching centre of flying height are very complicated and difficult to derive by theoretical methods. The only method currently available for accurately estimating the location of centres of balance is wind-tunnel model experiments at a satisfactory scale to minimise the scale effect, which will be discussed in a later chapter.

A brief calculation is presented below for determining the centres of balance, so as to be able to investigate the influence of the main wing with the hull and tailplane on the centres of balance, and determine the parameters of both wings to satisfy the requirements for stability.

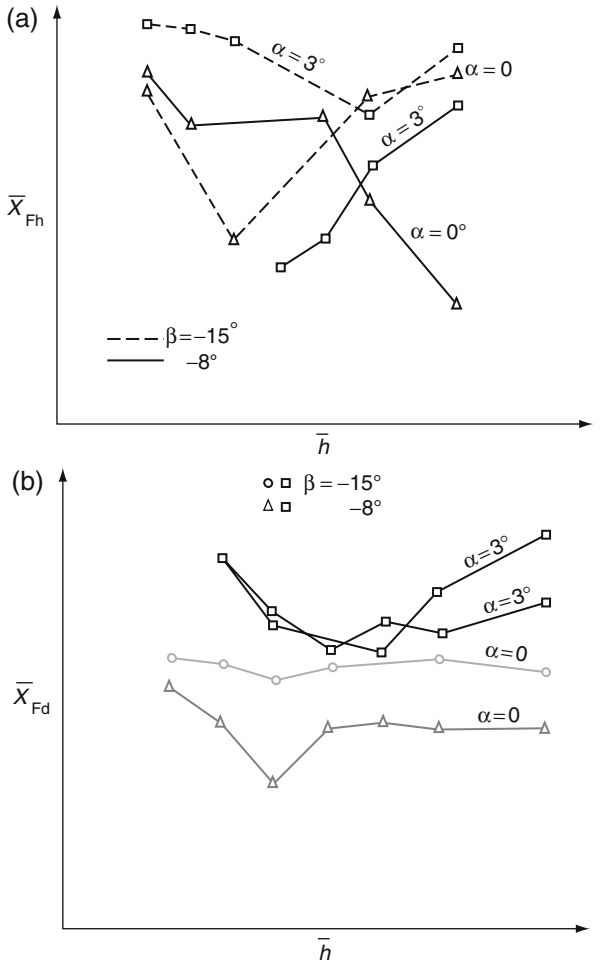

Fig. 6.11 A typical heaving centre curve X_{Fh} of a DACWIG model test results

Static Longitudinal Stability Criteria

Aircraft operate beyond the surface effect zone and so static positive longitudinal stability can be assured so long as the pitching centre of the craft $C_{F\vartheta}$ is located behind the centre of gravity of the craft, i.e. where $(X_{F\vartheta} - X_G) > 0$. In the case of WIG, the situation is rather different. Since the WIG and DACWIG are operated in the surface effect zone, there are three centre points influencing the craft longitudinal stability, i.e.

$\bar{X}_{F\vartheta}$ Relative position of pitching centre
$\bar{X}_{Fh}$ Relative position of flying height centre
$\bar{X}_{F\dot{h}}$. Relative position of heaving velocity centre

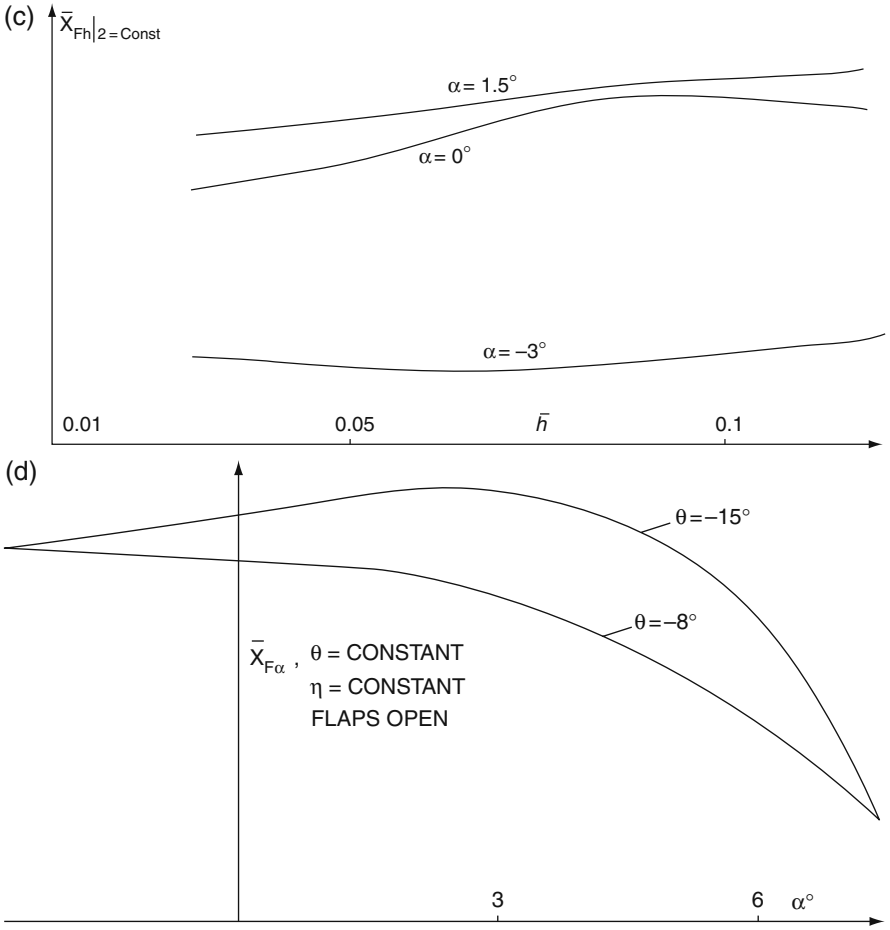

Fig. 6.11 (continued)

Since the flying heights of DACWIG and DACC are often small, say $\bar{h} < 0.2$, then $\bar{X}_{Fh\dot{}}$., the relative position of pitching centre due to heaving velocity may be neglected without significant error when initially estimating the static longitudinal stability. Meanwhile, the pitch centre, height centre and the relation between them are the most important criteria for predicting static DACWIG longitudinal stability.

Requirements for Positive Static Longitudinal Stability

Figure 6.8 shows the positions of various points of pitching centre, such as centre of pressure, CP, of main wing and horizontal tailplane, pitching centre $\bar{X}_{F\vartheta}$, vertical height pitching centre $\bar{X}_{Fh}$ and centre of gravity of the craft CG.

Since a WIG flies in GEZ, the craft will essentially be limited to 2 degrees of freedom, i.e. vertical motion (*XY* plane) and rotation about the *Z*-axis. The flying altitude h and trim angle ϑ will change in response to a perturbation. The new running attitude can be derived so long as meeting the following conditions. That is,

$$\begin{aligned} dC_y &= C_y^{\vartheta} d\vartheta + C_y^{\bar{h}} d\bar{h} = 0 \\ dm_z &= m_z^{\vartheta} d\vartheta + m_z^{\bar{h}} d\bar{h} = 0 \end{aligned} \tag{6.17}$$

From Equation (6.17), we can write:

$$\begin{aligned} &\frac{dC_y}{d\bar{h}} = C_y^{\vartheta} \frac{d\vartheta}{d\bar{h}} + c_y^{\bar{h}} \\ &\frac{d\vartheta}{d\bar{h}} = -\frac{m_z^{\bar{h}}}{m_z^{\alpha}} \\ &\textit{and use} \\ &\bar{X}_{F\vartheta} = \bar{X}_G - \frac{m_x^{\vartheta}}{C_y^{\vartheta}}, \\ &\bar{X}_{F\bar{h}} = \bar{X}_G - \frac{m_z^{\bar{h}}}{C_y^{\bar{h}}} \end{aligned} \tag{6.18}$$

Then the full derivative of lift coefficient C_y with respect to the flying altitude $\bar{h}$ can be written as:

$$\left(\frac{dC_y}{d\bar{h}}\right)_{m_z=0,\phi=\text{const}} = C_y^{\bar{h}} \frac{\bar{X}_{F\vartheta} - \bar{X}_{F\bar{h}}}{\bar{X}_{F\vartheta} - \bar{X}_G} \tag{6.19}$$

Where

$\mathrm{d}C_y$, $\mathrm{d}m_z$ The full differentials of lift coefficient and trimming moment, respectively

ϕ The tail elevator angle

The craft trim will change according to the expression (6.18). Since the longitudinal static stability with flying altitude has to comply with

$$\left(\frac{dC_y}{d\bar{h}}\right)_{m_z=0,\phi=\text{const}} < 0 \tag{6.20}$$

In general, we have

$$\begin{aligned} &\bar{X}_{F\vartheta} > \bar{X}_G \left(\because m_z^{\vartheta} < 0\right) \\ &C_y^{\vartheta} > 0 \\ &C_y^{\bar{h}} < 0 \end{aligned} \tag{6.21}$$

Then we have

$$\bar{X}_{F\vartheta} > \bar{X}_{F\bar{h}} \tag{6.22}$$

So the criteria for the static longitudinal stability can defined as follows.

Requirement for pitching pitching centre

$$\bar{X}_{F\vartheta} - \bar{X}_G = \left(\frac{\partial m_z}{\partial y}\right)_{\bar{h}=\text{const}} = C1 > 0 \tag{6.23}$$

C1 is called the static longitudinal stability margin, which can be determined from model test data or a similar full-scale craft. It should be satisfied at any operation condition of craft and guarantees sufficient restoring moment in case of changing the pitching angle.

Requirement for the difference of pitching and height centres of balance

Consider a WIG operating in stable condition, at constant velocity v, trim/pitch angle ϑ and constant elevator angle ϕ. A gust or other external disturbing force acts on the craft. The craft will change its flying height due to the disturbance. However, since the added lift acts at the flying height centre, which does not coincide with the CG, the craft will change its angle of attack as well as flying height so as to arrive at a new balanced attitude. The new trim equilibrium not only depends upon the $\bar{X}_{F\vartheta}$ but also upon the $\bar{X}_{Fh}$.

The derivative of the equation of motion for static longitudinal stability of the craft with constant elevator angle and velocity can be written as [3, 8]:

$$\left(\frac{dC_y}{d\bar{h}}\right)_{m_z=0,\phi=\text{const}} = C_y^{\bar{h}} k_\vartheta \tag{6.24}$$

Where

$$C_y^{\bar{h}} = \frac{\partial C_y}{\partial \bar{h}}$$

the partial derivative of lift coefficient with respect to flying height
And

$$C_y^{\bar{h}} = \frac{\partial C_y}{\partial \vartheta} \cdot \frac{\partial \vartheta}{\partial \bar{h}}$$

and k_∇ a coefficient taking into account the rebalancing in pitching angle
Where

$$k_\vartheta = \frac{\bar{X}_{F\vartheta} - \bar{X}_{F\bar{h}}}{\bar{X}_{F\vartheta} - \bar{X}_G} \tag{6.25}$$

There are a number of criteria concerning the relative locations of the pitching centre and height pitching centre, as follows:

(1) In case of $\bar{X}_{\mathrm{G}} = \bar{X}_{\mathrm{F}\bar{h}}$ then $k_{\vartheta} = 1$, so that $\left(\frac{dC_y}{d\bar{h}}\right)_{m_z=0,\phi=\text{const}} = \frac{\partial C_y}{\partial \bar{h}}$, so that the trim angle will stay constant while experiencing a gust force acting on the craft, and cause a positive flying height increase due to the added lift force acting at the height pitching centre, thus on CG.
This is the ideal condition for the pilot, as the craft will move smoothly in the vertical direction without the change of angle of attack.

(2) In the case that $\bar{X}_{\mathrm{F}\vartheta} - \bar{X}_{\mathrm{F}\bar{h}} < \left(\bar{X}_{\mathrm{F}\vartheta} - \bar{X}_{\mathrm{G}}\right)$, the height pitching centre is located between the pitch pitching centre $\bar{X}_{\mathrm{F}\vartheta}$ and the centre of gravity CG.
In this case $k_{\mathrm{q}} < 1$, $\left(\frac{dC_y}{d\bar{h}}\right)_{m_z,\phi=\text{const}} < C_y^{\bar{h}}$, and since $C_y^{\bar{h}} > 0, \frac{dC_y}{d\bar{h}} > 0$ from Equation (6.24), then $\frac{\partial C_y}{\partial \vartheta} \cdot \frac{\partial \vartheta}{\partial \bar{h}} > 0$; therefore, $\frac{\partial \vartheta}{\partial \bar{h}} > 0, \because \frac{\partial C_y}{\partial \vartheta} > 0$.
The rebalanced running attitude will be a changed height together with increased craft trim, which can often be seen in the tests of WIG. This situation leads to stable operation so long as the tail stabiliser can provide balancing moments to re-trim the craft.

(3) In case of $\left(\bar{X}_{\mathrm{F}\vartheta} - \bar{X}_{\mathrm{F}\bar{h}}\right) > \left(\bar{X}_{\mathrm{F}\vartheta} - \bar{X}_{\mathrm{G}}\right)$, the height pitching centre is located ahead of the pitch pitching centre and CG, which causes $k_{\vartheta} > 1$, then $\left(\frac{dC_y}{d\bar{h}}\right)_{m_z,\phi=\text{const}} > \frac{\partial C_y}{\partial \bar{h}} \cdot \frac{\partial \vartheta}{\partial \bar{h}} > 0$ and the rebalanced running attitude of the craft will be changed height together with an decreased trim and main-wing angle of attack. If the height centre and CG are close together, the tail stabiliser can be used to provide balancing moments to rebalance trim.
In the case where $\left(\bar{X}_{\mathrm{F}\vartheta} - \bar{X}_{\mathrm{F}\bar{h}}\right) >> \left(\bar{X}_{\mathrm{F}\vartheta} - \bar{X}_{\mathrm{G}}\right)$, i.e. large distance between pitch and height centres, and CG close to pitch centre, the wing angle of attack could become negative, so as to cause a plough in. This is a most dangerous condition and should be avoided.

In summary, it is suggested to locate the height centre close to the CG for smooth craft motion in windy weather conditions. Whether the height centre is located just in front or behind the CG will be influenced by the overall craft aerodynamic configuration. The designer will need to experiment somewhat with his design to determine the best arrangement over the range of flying heights intended.

It should also be remembered that the centre of lift of the main wing is strongly influenced by bow-thruster jet flow, as noted above, so the WIG stability needs to be carefully checked for the envelope of flight speeds and bow-thruster settings to ensure that the relative positions of CG, $\bar{X}_{\mathrm{F}\vartheta}$ and $\bar{X}_{\mathrm{F}\bar{h}}$remain in a safe relationship.

Static Transverse Stability of DACWIG in Steady Flight

Since DACWIG operate in the strong surface effect zone, and in general, $h < 0.1$–0.2, the craft has an inherent positive transverse stability, similar to a hydrofoil under the water surface. When the craft heels (rolls) (Fig. 6.12) to a small angle θ_1, i.e., the water surface is closer under the downward side buoy, the lift acting on the

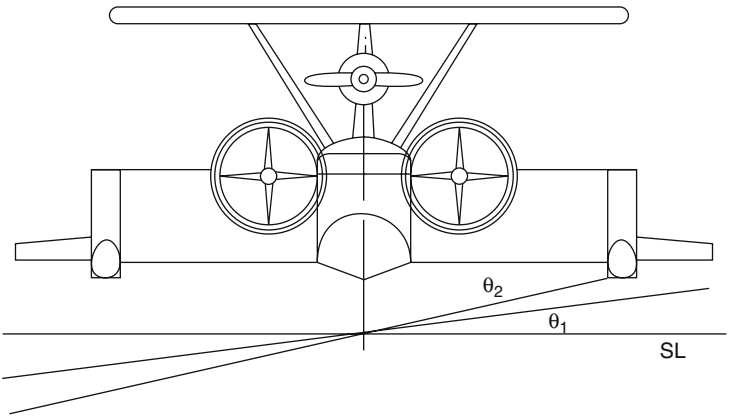

Fig. 6.12 DACC and DACWIG heeling motion

main and composite wing as well as the side buoy at the downward side will be greater than that on the other side, due to the increased surface effect. At larger heeling angles, the water surface will immerse the heeling down side buoy, and hydrodynamic forces on the side buoy will give a large restoring moment on the craft.

A brief estimation method for the restoring moment can be derived as follows:

The DACWIG model (Fig. 6.12) is simplified with AB representing the tips of the main wing, and

(1) The craft main wing has a rectangular plan, with a wing chord length C, and span 2b.
(2) Since the rolling angle is small, then the wing tip will not touch the water, and the lift acting on the unit longitudinal slice of wing can be considered as a function of flying height.

Then the lift acting on a unit longitudinal slice of wing before rolling can be taken as:

$$Y_b = (W/S_c) \cdot C = (Y/S_c) \cdot C = Y/2b_c$$

Where craft weight W, is equal to the lift of the craft Y, and b_c is the width of each main wing. It may be noted that in this analysis, we consider the whole wingspan since behaviour in roll involves the whole wing rather than one side as has been appropriate for the other analyses.

The incremental lift acting on the unit longitudinal slice of wing after rolling can be written as:

$$dY_b = Y_b^{\bar{h}} \Delta h dz = Y_b^{\bar{h}} z \gamma dz = Y_b^{\bar{h}} \gamma b_c^2 \bar{z} d\bar{z} \tag{6.26}$$

Where

$Y_b^{\bar{h}}$	The partial derivative of unit lift with respective to the relative flying height $\bar{h}$
$\bar{z} = z/b$,$\bar{z}$,	is the non-dimensional transverse coordinate along the wing
γ	The heeling angle and it will be positive in case of right side of wing down

Then the restoring moment contributed by this increment of lift acting on the unit longitudinal slice of the wing should be

$$dM_x = dY_b.z = b_c\bar{z}dY_b = Y_b^{\bar{h}}b_c^3\gamma\bar{z^2}dz$$

Then the total static transverse restoring moment can be written as

$$M_x = \int dM_z = \int_{-1}^{0} \gamma_b^{\bar{h}}b_c^3\gamma\bar{z^2}dz = \frac{1}{12}Y^{\bar{h}}\gamma\lambda\,(2b_c) \tag{6.27}$$

Where the aspect ratio considered in this section for the whole wing is $\lambda = 2\,b_{c/C}$
Then the coefficient of static restoring moment can be expressed as

$$m_x = \frac{M_x}{Sq2b_c} = \frac{1}{12}C_y^{\bar{h}}\gamma\lambda k_\gamma \tag{6.28}$$

Where K_γ is an aggregate coefficient, which can be obtained by experimental results, and is a function of wing profile and the sealing effect of the main wing.

The partial derivative of static transverse restoring coefficient with respect to the heeling angle can be expressed as

$$m_x^\gamma = \frac{1}{12}k_\gamma C_y^{\bar{h}}\lambda \tag{6.29}$$

It can be seen that this increases linearly with both the partial derivative of the wing aerodynamic lift coefficient with respect to the relative flying height $C_y^{\bar{h}}$ and aspect ratio of the wing λ .

A craft operating in the strong GEZ with high $C_y^{\bar{h}}$ will have strong static transverse stability; however, for craft with low aspect ratio main wings such as DACC

and DACWIG, for example, "Volga-2", "Amphistar" and "SWAN", the transverse stability will deteriorate when rising into flight in the weak GEZ.

WIG Operating in Weak GEZ

In order to increase the restoring moment of a WIG operating in the weak GEZ, the frontal surface of the main wing can be designed as a negative dihedral surface. Figure 2.42 shows a craft with typical negative dihedral frontal surface.

When the craft is rolling to right side down, then the pressure on the right side of the craft will be increased and the lift on left side lowered. The additional restoring moment can be written as:

$$M_x = L_\mathrm{r} Y_\mathrm{g}$$

Where

L_r Lift acting on the right side of the wing frontal surface and perpendicular to the surface

Y_g Distance between the original point of base plane and centre of gravity of the craft

In this case, the horizontal component force of the lift at the right side of the wing will cause a sway motion. In order to compensate such force, an outer wing with positive dihedral angle is recommended as shown in Fig. 2.42.

The additional restoring moment $\Delta M'_x$ then created is

$$\Delta M'_x - L_\mathrm{e} D_\mathrm{e}$$

Where

L_e Force acting perpendicularly on the side wing due to the sway of the craft

D_e The perpendicular distance of the force L_e acting on the side wing about the centre of gravity of the craft

Such configurations can be found on various WIG that are able to operate in/out of weak GEZ, such as the X series of Germany, XTW series of China and E-Volga of Russia.

In order to improve the static transverse stability, one option is to take steps for extending the aspect ratio, enhancing the aggregate coefficient $K\gamma$ and possibly using ailerons on outer composite wings.

Figure 6.13a shows a typical plot of lift force coefficient C_y versus $\bar{h}$ [11]. It can be seen that C_y increases significantly in the strong surface effect zone. Small h and large λ lead to higher C_y. The ground effect further increases for PAR or DACC. The DACC (Volga-2), DACWIG (SWAN) and Amphistar with small λ can appear unstable in roll, as the rapid change in lift force coefficient tends to cause a fluttering

motion in roll, particularly at small flying height. Higher up in the GEZ, this effect dies away and the flight is smooth.

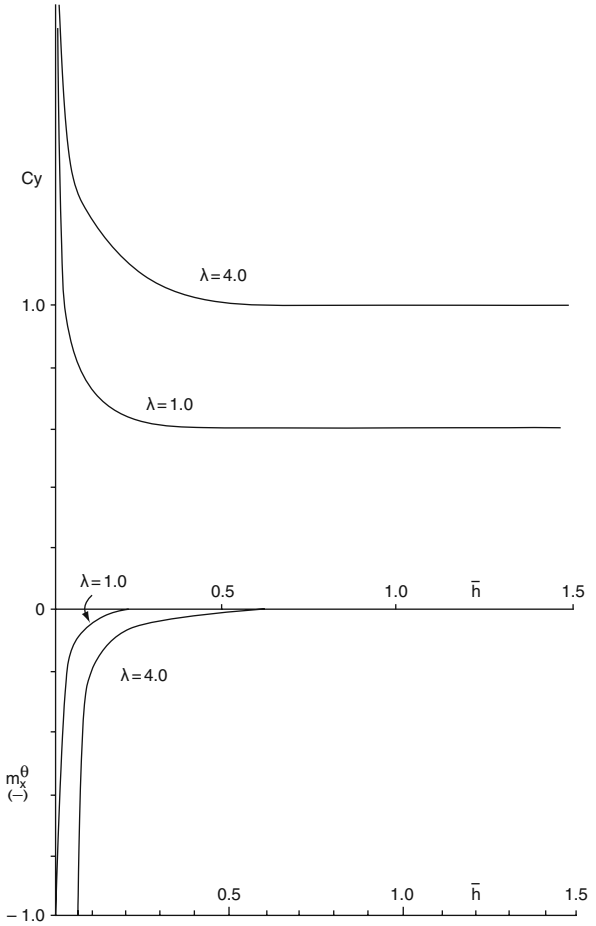

Fig. 6.13 C_y/M_{x0} versus $\bar{h}$

Figure 6.13b shows the transverse heeling moment with respect to the main wing λ and M_x^θ with respect to relative flying height $\bar{h}$. Reference [11] offers an expression for the coefficient, as a criterion of self-stabilisation of roll as follows:

$$M_x^\theta = A \,.\, \lambda \, C_y^{\bar{h}} < 0 \tag{6.30}$$

Where A is a constant depending on λ, the wing plan-form, and pressure distribution over the wing bottom surface. From the figure, one can see that M_x increases with higher λ and decreases with lower flying height h.

Low DACC and DACWIG transverse stability at larger flying height (for example, Volga and SWAN) is due to the low main-wing aspect ratio and consequently lower M_x. Craft with a strong dynamic air cushion effect operating in the strong surface effect zone have a high C_y, so, in case of flying higher, the C_y will decrease. In addition the since the main wingspan is shorter, it provides a low restoring moment in heel. Consequently, roll stability is rather low until the side buoy touches the water surface and hydrodynamic forces come into play.

To improve the heeling stability so as to avoid the side buoy skidding on the water surface once the craft has taken off into surface effect flight, composite wings outside the side buoys can be installed with higher λ, and ailerons for roll control, so as to have sufficient rolling stability at high speeds.

Transverse Stability Criteria

The static stability transverse curve of WIG operating on the flying mode in GEZ can be obtained by test results of models in a wind tunnel. WIG craft stability has been studied by an IMO committee, Reference [12], and may be considered to be sufficient based on the weather criterion K in the case that the dynamically applied heeling moment M_{v} due to the wind pressure (under the extreme design conditions from the worst loading combination in respect to stability) is equal to or less than the capsizing moment M_{c}, and the following conditions are satisfied:

$$M_{\mathrm{v}}\, M_{\mathrm{c}} \text{ or } K = M_{\mathrm{c}}/M_{\mathrm{v}} > 1.0 \tag{6.31}$$

Where

$$M_{\mathrm{v}} = 0.001\, P_{\mathrm{v}} A_{\mathrm{v}} Z f \tag{6.32}$$

and

- P_{v} Wind pressure, see also Table 6.1
- A_{v} Wind area (the projected lateral area of the portion of the craft above the acting waterline)
- Z The wind area lever, which is equal to the vertical distance to the centre of wind area from the centre of the projected lateral area of the portion of the craft below the plane of the acting waterline
- F streamline factor, $f = 1$ by default, f is determined by wind-tunnel testing and is usually >1, so the default assumption is conservative for design

Table 6.1 Wind pressure P_v, in pascals

Beaufort scale	Wind force (m/s)	Vertical distance between the projected lateral area (of portion) of WIG and sea surface (m)						
		1	2	3	4	5	6	7 and more
2	5	1.5	2.0	2.5	2.5	3.0	3.0	3.0
3	7	5.0	6.0	6.5	7.0	7.5	8.0	8.5
4	9	9.5	12.0	13.5	14.5	15.0	16.0	16.5
5	12	15.5	19.5	22.0	23.5	25.0	26.5	27.5
6	15	24.0	30.0	33.5	36.0	38.5	40.0	41.5
7	19	43.5	54.5	60.5	65.5	70.0	73.0	75.0
8	23	70.5	87.5	97.0	105.0	111.5	117.0	123.0

Transverse Stability at Slow Speed

Calculation of static transverse stability for PARWIG, DACC and DACWIG while hull borne, and in air cushion mode are similar to that for conventional SES, ACV and fast catamarans [1]. The intact static transverse stability curve can be obtained without difficulty by use of hydrostatic and hydrodynamic calculations. The calculation for checking the static transverse stability has to be carried out for various operational modes, i.e. hull borne, cushion borne or planing, and flying mode.

The determination of DACC and DACWIG in floating mode M_c is the same as that for SES and catamaran; however, the M_c for PARWIG has to be based on considerations as follows [13]:

- The floating angle due to accidental flooding of a buoyancy compartment in displacement mode should be less than the angle of heel corresponding to submergence up to a waterline that is situated 0.3 m lower than the lowest edge of the coaming of the watertight outside the entry door or other points of flooding of the main cabin, whichever is the less.
- In the surface effect mode, the maximum angle of heel should correspond to just less than the angle of side buoy entering the water.
- In the skimming mode, the angle of heel should correspond to half of the angle causing entrance of the main-wing tip or side buoy into the water.

Transverse Stability During Turning

During DACWIG high-speed turning, the force on the tail fin acts at its CP located above the craft CG, while the centrifugal force of the craft mass performing the turn acts at the craft CG. The resulting moment heels the craft outward. However, the lift force acting on main wings, composite wings and sidewalls located at outward side will be larger than those on the inward side, tending to roll the craft back upright, into

the turn. By careful design of main-wing flaps and composite wings with ailerons to give correcting forces, a WIG can perform flat and inward-banked turns.

A DACWIG operating in the strong surface effect zone can possess positive transverse stability both running on straight and curved courses. However, in case of operating at greater flying height, the transverse stability will be lower, as described above. For stable flight and manoeuvring, the use of composite outer wings becomes an essential part of the design.

PARWIG Transverse Stability

PARWIG operating in the weak GEZ and beyond the GEZ may not have inherent static transverse stability, so ailerons and automatic control equipment have to be mounted on such craft, just as on conventional aircraft.

Dynamic Longitudinal Stability over Calm Water

A vehicle with positive dynamic stability implies that following a disturbance, the vehicle will oscillate about the state of equilibrium and the oscillation will decay over a few cycles returning the vehicle to its steady state of equilibrium.

In the previous section, we discussed the problems related to static longitudinal stability. Here, we will address the dynamic longitudinal stability. Dynamic longitudinal stability means that in case a WIG experiences small perturbations from its original attitude, after a definite period of time, the perturbed WIG will restore itself to the original running attitude.

A craft with positive static longitudinal stability means that the craft can be restored to the original running attitude smoothly after the external perturbation (the quasi-static response). Dynamic longitudinal stability of a WIG means that the accelerations and perturbation velocities can be reduced back to zero by restraining forces that increase as the craft displaces from the neutral position (a damped response to the dynamic excitation).

Static longitudinal stability is related to steady motion and is dependent upon the static aerodynamic characteristics, i.e. the trimming angle and height centre of the WIG. At the same time, the WIG motion can be considered as a motion with 2 degrees of freedom, i.e. trimming angle and flying altitude of the craft. The trim angle will be changed from the original condition to another after the sudden external perturbation (such as a wind gust).

Since the aerodynamic force (moment) coefficients of the craft are nonlinear in relation to a the trim angle, theoretical investigation of the perturbation motion of WIG is ideally carried out by numerical integration methods using the non-dimensional differential equations of the WIG craft motion. However, for simplifying reasons and in addition to facilitate parametric analysis of the influence of

various parameters on dynamic longitudinal stability, the analysis of linear differential equations is recommended and so the analysis should be based on small external perturbations. Analysis of dynamic longitudinal stability can then be carried out using the linear differential equations of motion, as follows.

Basic Assumptions

1. The motions can be considered due to a small external perturbation.
2. Propeller thrust can be considered to act through the craft centre of gravity and parallel to the base plane of craft.

Basic Motion Equations

Coordinate System

X_o, G_o, Y_o Fixed coordinates
X, G_o, Y Coordinates on board
X_s, G_o, Y_s Coordinates with respect to the incoming flow

A WIG moving over calm water can be represented as (Fig. 6.9):

$$\vartheta = \alpha + \psi$$

Where

ψ Angle between the course of craft and sea level (craft climbing or descending)
α Angle of attack, i.e. the angle between the course and wing baseline of the craft
ϑ Trim angle, i.e. the angle between the base plane of craft and sea level

In general for level flight and a model tested in the wind tunnel, if we are using linear theory in the frequency domain $\psi = 0$, in which case,

$$\vartheta = \alpha$$

then the basic motion equations can be expressed as follows:

$$\begin{aligned} m\dot{v}_x &= P\cos\vartheta - x_a\cos\vartheta - y_a\sin\vartheta \\ m\ddot{h} &= P\sin\vartheta + y_a\cos\vartheta - x_a\sin\vartheta - w \\ J_z\ddot{\vartheta} &= M_z \end{aligned} \tag{6.33}$$

Where:

v	Craft speed
m	Craft mass
P	Propeller thrust acting along the X-axis
X_a, Y_a	Aerodynamic force acting on the craft along $X_sG_oY_s$ coordinates
W	Craft weight
Y_p	The vertical distance from the CG to the propeller axis
M_z	Aerodynamic moment acting on the craft about Z-axis
J_z	Moment of inertia of the craft through CG about Z-axis

We can also write the X_a, Y_a, M_z as:

$$\begin{aligned} X_a &= X_a\left(v,h,\dot{h},\vartheta\right) \\ Y_a &= Y_a\left(v,h,\dot{h},\vartheta,\dot{\vartheta}\right) \\ M_z &= M_z\left(v,h,\dot{h},\ddot{h},\vartheta,\dot{\vartheta}\right) \end{aligned} \tag{6.34}$$

Where V_x is the component of v on the X_g axis; $\vartheta = \frac{\dot{h}}{v_x}$.

We start with the original running attitude of the craft being steady horizontal flying, and the course and pitching angle θ is a small value and ψ can be considered as zero (assumed level flight on average), so we assume:

$$\sin\vartheta = \vartheta, \sin\theta = \theta, \cos\vartheta = 1 \text{ and } Y_p \cong 0$$

Then the Equations (6.33) can be rewritten as

$$\begin{aligned} m\dot{v}_x &= P - x_a - y_a\theta \\ m\ddot{h} &= P\vartheta + y_a - x_a\theta - w \\ J_z\ddot{\vartheta} &= Mz \end{aligned} \tag{6.35}$$

Then the coupled linear differential equations of motion of the craft can be expressed as

$$\begin{aligned} &m\Delta\dot{v} + \left(x_a^v - P^v\right)\Delta v + x_a^{\dot{h}}\Delta\dot{h} + x_a^h\Delta h + x_a^{\vartheta}\Delta\vartheta + y_{ao}\Delta\theta = 0 \\ &-y_a^v\Delta v + m\Delta\ddot{h} - y_a^{\dot{h}}\Delta\dot{h} - y_a^h\Delta h - y_a^{\dot{\vartheta}}\Delta\dot{\vartheta} - (y_a + Po)\Delta\vartheta + x_{a\Delta}\Delta\theta = 0 \\ &-M_z^v\Delta v - M_z^{\ddot{h}}\ddot{h} - M_z^{\dot{h}}\Delta\dot{h} - M_z^h\Delta h + Jz\Delta\ddot{\vartheta} - M_z^{\ddot{\vartheta}}\Delta\dot{\vartheta} - M_z^{\vartheta}\Delta\vartheta = 0 \end{aligned} \tag{6.36}$$

In Equations (6.36), $\Delta\dot{v}$,$\Delta\dot{h}$ represent the derivatives d/dt of the variable, where t is dimensional time value. Y_{a0}, X_{a0} and P_o are the lift, drag and thrust of the craft flying steady and horizontal on average.

In order to analyse the dynamic stability, the following relative values can be taken as:

$\bar{V} = v/v_0$	Relative speed
$\tau = t/t_0$	Relative (non-dimensional) time
$\tau_{\mathrm{m}} = 2m/\rho S v_0$	Time constant
$\mu = 2m/pSC$	Relative density of the craft
$i_z = J_z/mC^2$	Non-dimensional moment of inertia of the craft
C	Wing chord
S	Wing area
ρ	Air density
$\Delta\vartheta = \Delta\dot{h}/v_0$	

Then Equation (6.36) can be rewritten in non-dimensional form as:

$$\begin{aligned}
&\Delta\bar{v}' + \left(2C_{x0} - C_p^v\right)\Delta\bar{v} + \tfrac{1}{\mu}C_x^{\bar{\dot{h}}}\Delta\bar{\dot{h}} + C_x^{\bar{h}}\Delta\bar{h} + C_x^{\vartheta}\Delta\vartheta = 0\\
&-2\mu C_{y0}\Delta\bar{v} + \Delta\bar{h}'' - C_y^{\bar{\dot{h}}} - \mu C_y^{\bar{h}} - C_y^{\dot{\vartheta}}\Delta\vartheta' - \mu C_y^{\vartheta}\Delta\vartheta = 0\\
&-\tfrac{1}{\mu i_z}m_z^{\bar{\dot{h}}}\Delta\bar{h}'' - \tfrac{1}{i_z}M_z^{\bar{\dot{h}}}\Delta\bar{h}' - \tfrac{\mu}{i_z}m_z^{\bar{h}}\Delta\bar{h} + \Delta\vartheta'' - \tfrac{1}{i_z}m_z^{\dot{\vartheta}}\Delta\vartheta' - \tfrac{\mu}{i_z}m_z^{\vartheta}\Delta\vartheta = 0
\end{aligned} \tag{6.37}$$

Where

$\Delta\bar{v}', \Delta\vartheta'$	Partial derivatives with respect to the non-dimensional time
$C_p^{\bar{v}} = \frac{2P^v}{S\rho v}$	Partial derivative of thrust coefficient with respect to relative speed

In Equation (6.37), $C_x^{\bar{\dot{h}}}, C_y^{\bar{\dot{h}}}$ are the aerodynamic coefficients with respect to the ground coordinate system while $C_{xa}^{\bar{\dot{h}}}, C_y^{\bar{\dot{h}}}$ are the aerodynamic coefficients with respect to the incoming flow, so the relation between them can be expressed as:

$$\begin{aligned}
C_x^{\bar{\dot{h}}} &= C_{xa}^{\bar{\dot{h}}} + C_{y0},\\
C_y^{\bar{\dot{h}}} &= C_{ya}^{\bar{\dot{h}}} - C_{x0}
\end{aligned}$$

In order to analyse the dynamic longitudinal stability, the characteristic equation of the linear differential equation of motion, Equation (6.37) has the following determinant:

$$F(\lambda) = \begin{vmatrix}
\lambda + (2C_{x0} - C_{\mathrm{p}}^{\bar{v}}) & 1/\mu C_x^{\bar{h}'}\lambda + C_x^{\bar{h}} & C_x^{\theta}\\
-2\mu C_{y0} & \lambda^2 - C_y^{\bar{h}'}\lambda - \mu C_y^{\bar{h}} & -C_y^{\bar{\theta}'}\lambda - \mu C_y^{\theta}\\
0 & 1/\mu i_z m_z^{\bar{h}''}\lambda^2 - 1/i_z m_z^{h'}\lambda - \mu/i_z m_z^{\bar{h}} & \lambda^2 - 1/i_z m_z^{\bar{\theta}'}\lambda - \mu/i_z m_z^{\theta}
\end{vmatrix} \tag{6.38}$$

(blue marking indicates need for bar above the symbol)

Expanding the determinant and setting up a fifth-order polynomial as the characteristic equation, we obtain

$$F(\lambda) = \lambda^5 + A_1\lambda^4 + A_2\lambda^3 + A_3\lambda^2 + A_4\lambda + A_5 \tag{6.39}$$

The coefficients in the polynomial are

$$\begin{aligned}
A_1 &= \tfrac{1}{i_z} m_z^{\bar{\vartheta}} - C_y^{\bar{h}} - \tfrac{1}{\mu i_z} C_y^{\bar{\vartheta}} + 2C_{x0} - C_P^{\bar{v}} \\
A_2 &= \tfrac{1}{i_z}\left(\mu m_z^{\vartheta} - C_y^{\bar{h}} m_z^{\bar{\vartheta}} + C_y^{\vartheta} m_z^{\bar{h}} + C_y^{\bar{\vartheta}} m_z^{\bar{h}}\right) - \mu C_y^{\bar{h}} \\
&\quad + 2C_{y0} C_x^{\bar{h}} - \left(2C_{x0} - C_p^{\bar{v}}\right)\left(i_z m_z^{\bar{\vartheta}} + C_y^{\bar{h}} + \tfrac{1}{\mu i_z} C_y^{\bar{\vartheta}} m_z^{\bar{h}}\right) \\
A_3 &= -\tfrac{\mu}{i_z}\left[C_y^{\bar{h}} C_y^{\vartheta}\left(\bar{X}_{F\vartheta} - \bar{X}_{F\bar{h}}\right) - C_y^{\bar{h}} m_z^{\bar{\vartheta}} + C_y^{\bar{\vartheta}} m_z^{\bar{h}}\right] + 2C_{y0}\left(\tfrac{1}{i_z} C_x^{\vartheta} m_z^{\bar{h}} - \tfrac{1}{i_z} C_x^{\bar{h}} m_z^{\bar{\vartheta}} + \mu C_x^{\bar{h}}\right) \\
&\quad + \left(2C_{x0} - C_p^{\bar{v}}\right)\left[-\tfrac{\mu}{i_z} m_z^{\vartheta} + \tfrac{1}{i_z} C_y^{\bar{h}} m_z^{\bar{\vartheta}} - \mu C_y^{\bar{h}} - \tfrac{1}{i_z} C_y^{\bar{\vartheta}} m_z^{\bar{h}} - \tfrac{1}{i_z} C_y^{\vartheta} m_z^{\bar{h}}\right]; \\
A_4 &= \tfrac{\mu}{i_z}\Big\{ - \mu C_y^{\bar{h}} C_y^{\vartheta}\left(\bar{X}_{F\vartheta} - \bar{X}_{Fh}\right) \\
&\quad + 2C_{y0}\left(C_x^{\vartheta} m_z^{\bar{h}} - C_x^{\bar{h}} m_z^{\vartheta} - C_x^{\bar{h}} m_z^{\bar{\vartheta}}\right) \\
&\quad + 2\left(C_{x0} - C_p^{\bar{v}}\right)\left[-C_y^{\bar{h}} C_y^{\vartheta}\left(\bar{X}_{F\vartheta} - \bar{X}_{F\bar{h}}\right) - C_y^{\bar{h}} m_z^{\bar{\vartheta}} - C_y^{\bar{\vartheta}} m_z^{\bar{h}}\right]\Big\}; \\
A_5 &= \tfrac{\mu^2}{i_z} C_y^{\bar{h}} C_y^{\vartheta}\left\{\left(2C_{x0} - 2C_{y0}\tfrac{C_x^{\vartheta}}{C_y^{\vartheta}} - C_p^{v}\right)\left(\bar{X}_{F\vartheta} - \bar{X}_{Fh}\right) + \left(\tfrac{C_x^{\vartheta}}{C_y^{\vartheta}} - \tfrac{C_x^{\bar{h}}}{C_y^{\bar{h}}}\right)\left(-2C_{y0} m_{z\vartheta}^{C_y}\right)\right\};
\end{aligned}$$

The Requirements for Dynamic Longitudinal Stability of WIG

The necessary requirements for dynamic longitudinal stability of WIG craft are that the real parts of the roots of the characteristic equation must be negative values. In addition, the following should be true :

$$A_i > 0 \,(\text{where } i = 1,2,3,4,5)$$

$$A_1 A_2 - A_3 > 0$$

$$(A_1 A_2 - A_3)(A_3 A_4 - A_2 A_5) - (A_1 A_4 - A_5)^2 > 0 \tag{6.40}$$

From the characteristic equation and its coefficient expressions, we derive the following observations:

(1) In the coefficient expressions, the pitching centre difference $\Delta\bar{X}_{F\vartheta h} = \bar{X}_{F\vartheta} - \bar{X}_{F\bar{h}}$ and the lift-coefficient partial derivatives with respect to relative flying height $C_y{}^h$ are the most important parameters influencing both static and dynamic stability, as well as the trim angle.
(2) The steady aerodynamic derivatives in the expressions can be taken from wind tunnel model test results; however, the dynamic derivatives in the equations

should be taken from model tests with special equipment and facilities, such as parallel motion mechanisms in a wind-tunnel laboratory. Obtaining reliable data for these derivatives is still a difficult challenge facing researchers and designers.

A typical time history of running attitude of WIG subjected to a wind gust is shown in Fig. 6.14

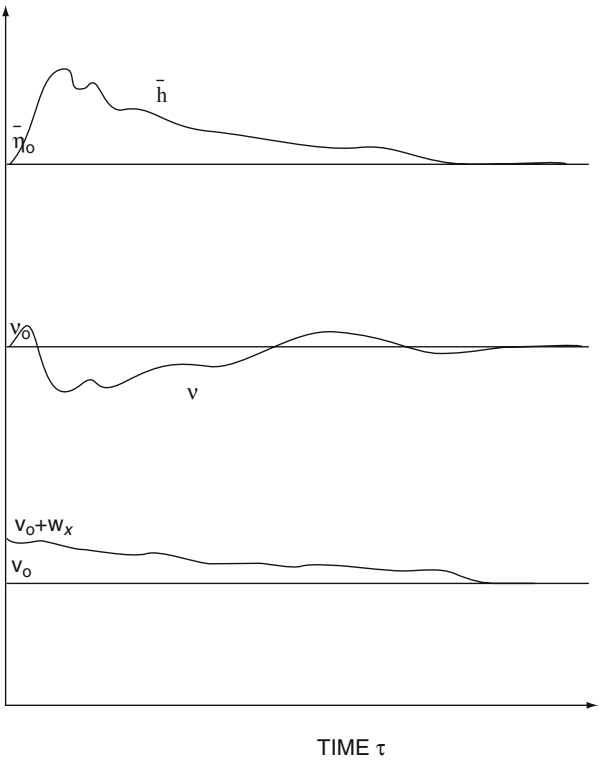

Fig. 6.14 Time history of WIG trim and flying height through a gust

Transient Stability During Transition Phases

The main transient phases to be considered are take-off and touch down. During either phase, controls on the craft will be altered so as to safely enter the subsequent operation mode. When taking off, the bow thrusters or thruster guide vanes have to be rotated to horizontal, and the main-wing flaps raised as speed increases, to maintain steady flying height. If the bow thrusters are rotated too slowly, there will

be a tendency for the craft to gain height and to accelerate more slowly. If the flaps are opened too quickly, the craft may loose height until speed is gained.

It is important therefore to have a reliable data set for performance of the specific craft with varying thruster settings and wing flap settings, so that the pilot can operate the controls in the correct relationship to each other and to the craft speed. Additionally, an assessment of how control operation at any given speed will adversely affect craft trim and stability is important. Carefully planned WIG trials programmes are therefore critical to operations safety in service.

When landing, the flaps have to be set down in advance of the bow-thruster efflux being rotated down. Lowering flaps will cause deceleration, as the drag is increased. Bow-thruster power and vane angles need to be increased so as to fully support the craft on its air cushion, as the flight height reduces to zero. The elevator will require careful operation to maintain nose-up trim as hydrodynamic resistance rapidly increases on the side buoys and hull planing surface.

The partial derivative of C_y with respect to flying height controls the dynamic behaviour of a WIG as it changes flying height climbing to cruise height after take-off or when slowing and descending into a landing. The change in longitudinal position of the centre of lift as C_y changes is the key controlling factor to smooth take-off and landing. The latter is affected by the operation of the bow thrusters – as they are rotated upward the centre of lift moves forward. Since CG is kept behind centre of lift by design, as thrusters are rotated up, so the tail elevators must be moved down, to lift the tail. The opposite must be carried out as thrusters are rotated down for landing. In short, a WIG pilot has to carry out a coordinated operation of the thrusters, wing flaps and tail elevators. The exact relationship is particular to the individual craft.

Chapter 7
Calm Water Drag and Power

Introduction

Analysis of WIG drag forces uses a combination of techniques adapted from other high-speed marine vehicles, such as seaplanes, catamarans, SES and ACV. There are more operating modes to contend with for WIG, however, as they can operate hull borne and air cushion borne as well as flying in ground effect.

WIG craft have two transition modes that have some similarities to seaplanes during take-off and so the analytical approach for these transitions is derived from this methodology rather than from high-speed boats.

The *first feature* of WIG drag forces is that drag is very low once the craft has taken off from the water surface into ground effect, enabling much higher cruise speed than other marine vehicles, and also a smaller speed loss during operation over waves. This is a significant advantage for the WIG compared to other fast marine craft. Both ACV and SES drags are small when the craft run at high speed in calm water; however, the air gap between the water surface and the lower tip of the skirt is so small that the skirt is always touching the water surface even in small waves. Skirt wetting in waves causes additional drag in comparison with the drag in calm water, leading to significant speed loss. This aspect of performance is still a challenge for both ACV and SES, even though the craft achieve high calm-water speed, as coastal operations require service speed to be specified typically in sea state 2–4.

The *second feature* of WIG drag is a larger primary hump compared with other high-speed craft due to the high hydrodynamic drag of its planing hull during take-off, which is similar to a hydroplane. The relative hump drag R_h/W (where R_h is the hump drag and W is the craft weight) of DACWIG can be from 1/7 up to 1/3 compared to a ratio of between 1/25 and 1/15 for the hump drag of modern SES and ACV. Design measures have to be taken to minimise WIG hump drag, and sufficient power installed to provide an acceleration margin over hump and through safe take-off.

The *third feature* of PARWIG, DACWIG and DACC drags is how to distribute the thrust of the WIG main propulsors between propulsion and dynamic air cushion feed to minimise the craft drag. On SES and ACV, the lift fan is

L. Yun et al., *WIG Craft and Ekranoplan*, DOI 10.1007/978-1-4419-0042-5_7,

dedicated as a lift device and feeds a cushion that is completely contained by a flexible skirt.

Normally, very little thrust is provided by air cushion efflux under the stern skirts, and the drag due to the lift air momentum can be calculated separately at the design stage. On hydrofoil craft, the hydrofoil drag can be obtained by model tests in a towing tank. However, on WIG, and particularly on DACC and DACWIG, the main propulsors are used both as lift devices and thrusters. The bow-thruster cushion-feed component causes a drag force that partially counters the thrust and is very difficult to extract as an individual element from the test results. Drag is also induced by the lift provided by the bow thrusters, acting on the main wing underside at its angle of attack. In addition, the thrust-recovery coefficient η_{Td} varies with the position of the aerodynamic control surfaces, such as flaps and bow-thruster guide vanes, and also depends on the running trim of the WIG.

$$\eta_{\mathrm{Td}} = T_{\mathrm{dc}}/T_{\mathrm{do}}$$

Here T_{dc} represents the dynamic thrust of the bow thruster mounted on the craft, and T_{do} represents the dynamic thrust of the ducted propeller or fan on its own.

For this reason, the resistance of a DACC or DACWIG is difficult to break down into individual elements, providing a continuing challenge for research in this field.

Before discussing the analysis of calm-water drag and powering, it is useful to review some examples of craft operating in various regimes. The following figures illustrate the three operation modes for DACWIG, i.e. hull borne, cushion borne and flying operation.

Figure 7.1 shows a DACWIG model in flying mode in a wind-tunnel test facility.

Fig. 7.1 DACWIG model test in a wind tunnel

Figure 7.2 shows a radio-controlled model flying over rough water after take-off.

Fig. 7.2 Radio-controlled model operated on the lake, after take-off

Figure 7.3 shows the radio-controlled model over calm water during take-off, illustrating cushion-borne operation mode of DACWIG.

Fig. 7.3 Same model operated in calm water during take-off

Figure 7.4 shows a model test in towing tank. Here the model is suspended on the rig before testing.
Figure 7.5 shows the model running over calm water in a towing tank.
Figure 7.6 shows the model test in regular waves in the towing tank.
Figure 7.7 shows a DACWIG craft on the landing ramp.
Figure 7.8 shows the 400-t Russian Guided Missile PARWIG type "Lun" floating, with the crew out on the port wing! Lun was designed by Alexeyev Hydrofoil Craft Design Bureau and completed in 1989. It accommodates six SS-N-22 guide missiles, in the range of 3,000 n.mile and speed up to 300 knots.

Fig. 7.4 DACWIG model test in towing tank (model suspended before test)

Fig. 7.5 DACWIG model test in towing tank (cushion borne running in calm water)

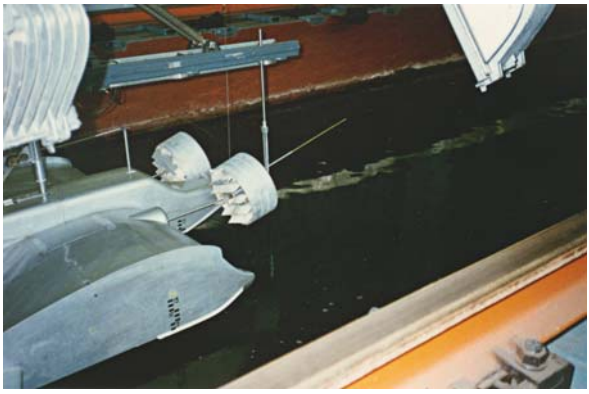

Fig. 7.6 Model test in waves in towing tank

Fig. 7.7 DACWIG craft on landing ramp

Fig. 7.8 Russian guide missile WIG craft "Lun" floating

Figure 7.9 shows the Russian PARWIG type "KM" (Caspian Sea Monster), also floating. The craft weighs 544 t, with a cruising speed of 250 knots, designed by Alexeev Hydrofoil Craft Design Bureau and completed in 1966.

Fig. 7.9 The KM PARWIG floating

A great deal of theoretical research was carried out in the 1960s and 1970s on air cushion pressure distributions to understand hovercraft drag and powering over water. WIG drag and power at speeds below take-off are more complex and have not yet been researched to the same depth. Some understanding has been developed for DACWIG by extension of ACV research, as discussed in Chapter 4. This work has been primarily based on a combination of model testing in wind tunnels, towing basins and open-water testing.

The main body of understanding developed in Russia from the Ekranoplan PARWIG programme has also been from the interpretation of model test data and, in this case, correlation with a whole series of full-scale test craft (the SM series described in Chapter 2).

There is a long way to go yet before analytical techniques might be used on their own for preliminary design. In the meantime, the material presented here is mainly derived from hydrodynamic and aerodynamic model testing, the techniques are discussed in Chapter 9.

The following topics will be introduced as we progress through this chapter:

- WIG drag before take-off and some measures for improving take-off performance
- WIG drag after take-off
- Powering estimates
- Influence of various factors on the drag and powering performance of WIG

WIG aerodynamic drag has been introduced in Chapter 5 as an integral part of obtaining the aerodynamic properties of the WIG wing and body form. This chapter builds on this data to apply it to prediction of the craft total drag for powering and performance estimation purposes. Two invaluable sources of data for drag and lift component estimation are given by S.F. Hoerner in [1] and Chapter 6 [10], who assembled data from a wealth of model testing and analysis.

WIG Drag Components

Taking a DACWIG as an example, the total craft drag before take-off can be expressed as follows:

$$R = R_{\mathrm{hw}} + R_{\mathrm{hf}} + R_{\mathrm{sww}} + R_{\mathrm{swf}} + R_{\mathrm{aw}} + R_{\mathrm{a}} + R_{\mathrm{fl}} \tag{7.1}$$

where

R	Total craft drag
R_{hw}	Wave-making drag of the hull, including the spray drag
R_{hf}	Water-friction resistance acting on the hull
R_{sww}	Wave-making drag caused by side buoys (or sidewall), also including their spray drag
R_{swf}	Water-friction resistance acting on the side buoys

R_{aw} Wave-making resistance caused by air cushion pressure under the main wing
R_a Air profile resistance of the whole craft
R_{fl} Fouling drag caused by marine growth on the hull and side buoys under the loaded water line on both hull and side buoys

Air cushion momentum drag is not considered in Equation (7.1). This drag element will be covered by the so-called thrust-recovery coefficient of the bow thrusters, which will be discussed later in this chapter.

After craft take-off, the total drag can expressed as follows:

$$R = R_{aw} + R_a \tag{7.2}$$

The total drag and each separate drag component are discussed in the following.

The determination of craft drag is divided into four steps linked to the operating modes, i.e. boating; hovering or planing before take-off; at take-off while still on water surface; and in flying mode. The most important task for pre-take-off mode is how to estimate and reduce the main drag hump, as this may be two or three times the drag at cruising speed after take-off; see, for example, Figs. 7.13 and 7.14.

WIG Drag Before Take-Off

Hump Drag and Its Minimisation

There are four main approaches to design the hull and dynamic support system for minimising the resistance and drag hump below take-off speed [2].

- Planing hull with steps (Fig. 7.10)
- Power augmented lift, i.e. PARWIG, see Fig. 7.8 and other Russian PARWIG types

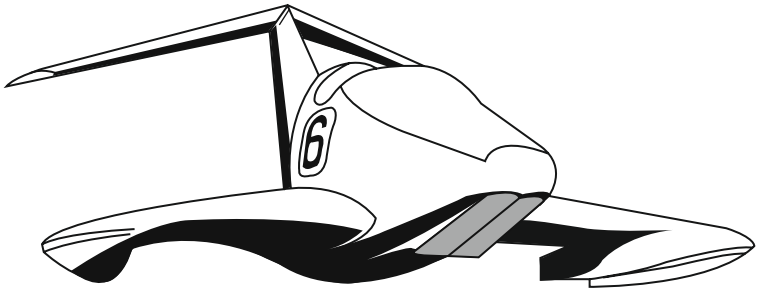

Fig. 7.10 TLA in the form of planing hull with steps, Scooter SM-0.4

- Dynamic air cushion, for example DACC type "Volga-2" (Fig. 1.20), DACWIG type "Swan" (Fig. 2.35)
- Specially designed hydrofoil arrangements, see Fig. 7.11a for a design proposal from Russia and Fig. 7.11b for the Lippisch X-114

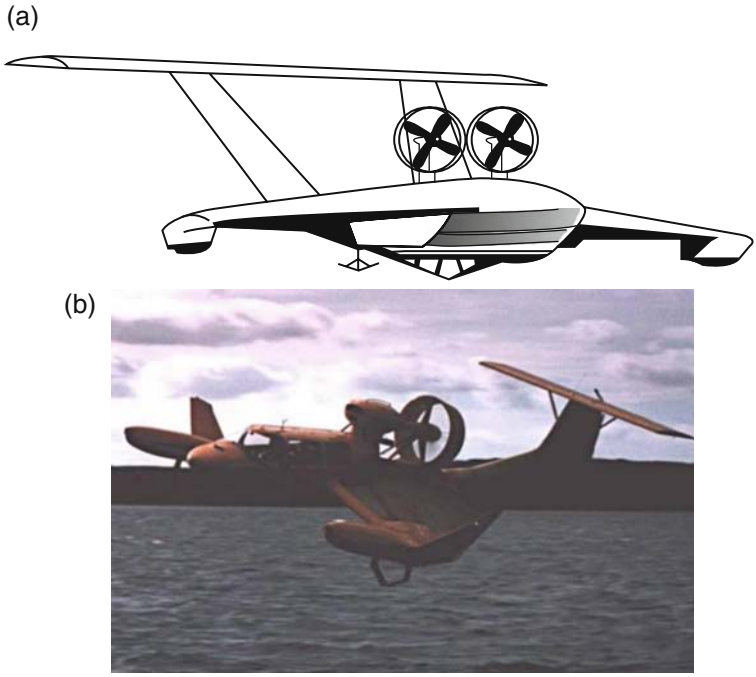

Fig. 7.11 (**a**) Hydrofoil TLA proposed test craft design and (**b**) X114H

Full-scale experiments with hydrofoils on the X-114 demonstrated that this arrangement was, in practice, a dangerous arrangement at high speed (see also Chapter 2). The hydrofoils can pull the craft into the water when landing, due to negative angle of attack, the opposite of the design intention.

Figure 7.12 shows the lift–drag ratio at drag hump speed (or maximum speed if drag is higher at this point) of various types of WIG from published data. The drag hump is highest for the planing type hull (similar to a hydroplane), where the $K_{\min} = L/R$ is as low as 2; then conventional WIG ($K_{\min}$= 4), then PARWIG ($K_{\min}$= 5.2). The $K_{\min}$ is the highest for Hoverwing. There are no published $K_{\min}$ for DACC and DACWIG; however, it is proposed that the $K_{\min}$ will be equal or higher than 6 due to the static air cushion developed on these craft.

Figure 7.13 shows a comparison of drag curves for WIG compared to SES. The drag hump of SES is lower that WIG or PARWIG due to its static air cushion and high cushion length/beam ratio. Once dynamic lift is built up under the wings of a WIG, drag is reduced allowing take-off, so that the upper end of the drag curve for WIG is the aerodynamic drag.

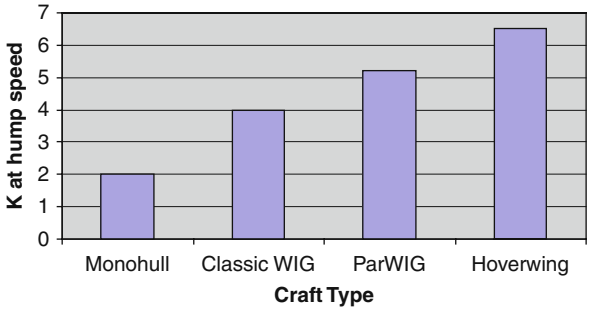

Fig. 7.12 Weight to thrust ratio

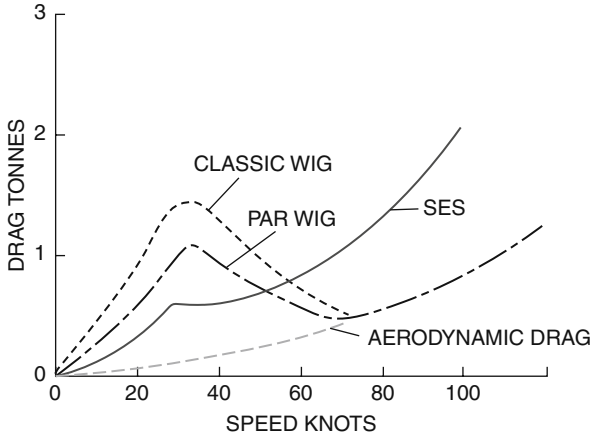

Fig. 7.13 Hump drag comparison for various high-speed craft

Figure 7.14 also shows a comparison of drags for various WIG configurations. A similar hump drag tendency can be found for several of them. The test results for hydrofoil support show this method can also lead to low hump drag; however, the cavitation barrier and complicated retraction mechanisms as well as its dangerous characteristics at high speed prevent its practical application.

This figure also shows a range of configurations for creating an air cushion under an aerofoil. The authors of [2] did not distinguish DACC from PARWIG, so it is believed that the range of drag before take-off covers the drag for both of them. It can be seen, however, that the more effective an air cushion is the lower is hump drag. The lift–drag ratio at hump speed can be as high as 7–10.

The most effective technique to minimise the hydrodynamic resistance and drag hump characteristics of the WIG appears therefore to be by blowing air under the lifting aerofoil [3, 4]. Nevertheless, how to judge which of the configurations really is most effective?

The following parameter for judging static performance of a WIG may be proposed (see also Chapter 13 for application in design):

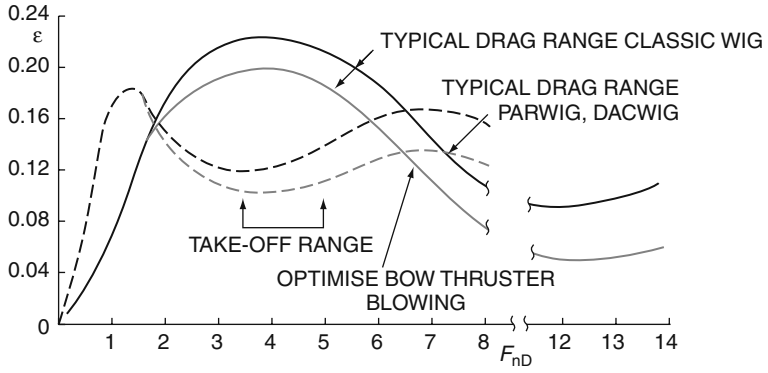

Fig. 7.14 Typical curves of relative resistance ε for WIG with different TLA versus Fn

$$\eta_{t3} = L_0/T_{so}$$

This is the lift–thrust ratio while hovering static with a gap approximately equal to zero. The lift–thrust ratio is a function of the wing geometry, relative location of bow thruster, angle of guide vanes and flaps, etc., and $\bar{h}$, the relative flying height of WIG at the rated bow-thruster speed.

In a similar way to ACV and SES, the lift–thrust ratio represents the minimum thrust for the propeller to generate the necessary cushion pressure so as to lift the craft into static hovering. The static hovering height $\bar{h}$ is the air gap under the craft base plane, and the flow rate Q leaked from the air cushion is proportional to $\bar{h}$. These are the most important criteria measuring the hovering efficiency for a DACWIG. Just as for ACV and SES, the craft will take off smoothly if the DACC or DACWIG can hover statically clear from the ground. Ability to hover in a stable manner, together with high η_{t3}, may therefore be used as a method for judging DACWIG's take-off performance.

Estimation of the Craft Drag Before Take-Off

Craft drag before take-off can be determined from Equation (7.1), where the separate elements of drag can be estimated as outlined below.

Wave-Making Resistance Due to the Air Cushion Pressure Under the Main Wings, R_{aw}

The wave-making resistance due to air cushion pressure under the main wings can be predicted based on Newman and Poole's formula as follows:

$$\begin{aligned} R_{aw} &= C_w B_c P_c^2/\rho_w g \text{ (N)} \\ C_w &= f(F_{rc}, C/B_c) \\ F_{rc} &= v/\sqrt{gC} \end{aligned} \tag{7.3}$$

Where

C_w	wave-making coefficient, a function of Froude number F_{rc} and cushion beam ratio, see Chapter 2 [1]
C	main-wing chord length
B_c	Cushion width of air channel (m), sometimes the hull and part of side buoys may be included into this corresponding width
P_c	Cushion pressure in the air channel

For approximate calculation, this can be written as:

$$P_c = kW/\left(B_c C n_{ac}\right)\ (\mathrm{N/m}) \tag{7.4}$$

Where

k	Coefficient for estimating the proportion of the weight lifted by craft air cushion on water surface, in case of DACC and DAWIG, may be k= 0.7–1.0, depending on the flaps' position
W	Total weight of the craft (N)
C	Chord length of main wing (m)
n_{ac}	Number of air channels on the craft

Friction Due to the Wetted Surface on Hull and Side Buoys, R_{hf}, R_{swf}

These two elements can be estimated as follows:

$$R_{hf} = \left(C_f + \Delta C_f\right) S_{hf} q\ (\mathrm{N})$$

$$R_{swf} = \left(C_f + \Delta C_f\right) S_{swf} q,\ (\mathrm{N}) \tag{7.5}$$

Where

R_{hf} and R_{swf}	Water friction of hull and sidewalls, respectively
C_f	Coefficient of water friction on a smooth plate, which can expressed by the Schoehai formula as follows:

$$C_f = 0.455/\left(\log \mathrm{Re}\right)^{2.58} \tag{7.6}$$

$$\mathrm{Re} = l_s V_s/\gamma_w \tag{7.7}$$

Where

L	Wetted length of hull or side buoys (m)
V_s	Craft speed (m/s)
γ_w	Kinetic viscosity coefficient
L	Specific length, here we take the chord length of wing (m)
ΔC_f	Additional friction coefficient for roughness of the plate

S_{hf} and S_{swf} are the wetted surface areas of the hull and sidewall, respectively, the value of which can be obtained by tests, either from a towing tank (Figs. 7.5 and 7.6), from a radio remote-control self-propulsion model test (Figs. 7.2 and 7.3) or from sea trial of prototypes. Similar to the tests of SES, ACV, catamaran or hydroplane models, the area of wetted surface can be calculated with aid of pictures describing the running attitude of the models and craft.

Air Profile Drag, R_a

Air profile drag can be predicted based on model experiments in wind tunnel.

$$R_a = 1/2\varrho_a V_s^2 C_x S_a$$

Where

ρ_a	Air density (Ns/m)
V_s	Craft speed (m/s)
S_a	Reference area for calculating the air profile drag and lift. In the case of DACC and DACWIG, with two air tunnels, then

$$S_a = (2b_{at} + b_{sb} + b_h) \cdot C$$

b_{at}	Air-tunnel beam
b_h	Hull width
b_{sb}	Side buoys width
C_x	Air profile drag coefficient of the craft model, which can be obtained from wind-tunnel test results, just as the expression in Chapter 6

Figure 5.31 shows a typical lift and drag coefficient from model testing in a wind tunnel with respect to the trim angle ? and the relative flying height $\bar{h}$.

In general, the air drag and lift coefficients can be expressed as:

$$C_x = C_{xo} + K(h)C_L^2/\pi A \tag{7.8}$$

$$C_L = W/(1/2\varrho_a V_s^2 S_a)$$

where C_{xo} is the sum of the viscous drag and other components measured when the wing is on cushion lift. The second term is the induced drag, a function of aspect ratio A and $K(h)$, called the vortex drag factor, which decreases below 0.5 when a WIG operates at $\bar{h}= 0.1 - 0.15$ relative flying height.

Figure 7.15 shows the lift and drag variation with height above the surface. Notice that as the height above the surface is decreased, the drag is essentially unchanged, while the lift increases significantly. In this condition, the induced drag factor (K/A) is decreasing while the lift increases and so the total induced drag term $(K(h)\pi/A)C_L^2$ remains the same. Figure 7.16 shows a plot of C_x versus $C_L{}^2$ at different K values, which shows that when in ground effect, the drag coefficient also increases more slowly as higher C_L wing forms are used, again due to the reduced effect of induced drag.

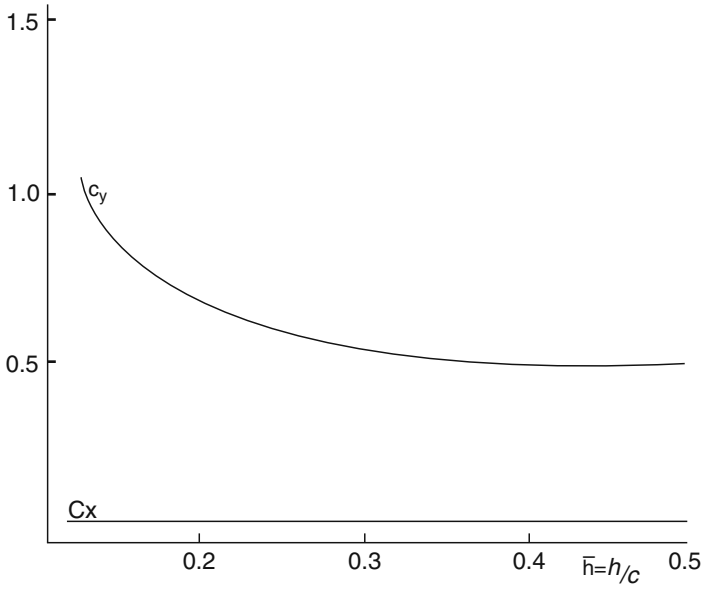

Fig. 7.15 C_L, C_x versus h/c

Fouling Drag, R_{fl}

Since the total drag of DACWIG is rather small compared with conventional ships, the drag caused by the fouling is more significant, particularly during take-off, as it effects the drag and also the lift acting on both hull and sidewall/side buoys. If left to grow on the hull, it will cause a larger hump drag, eventually preventing craft take-off. However, in case of newly built craft or models, this drag component can be neglected. A factor does need to be added for performance reduction in service; however, as the hull surfaces will never be perfectly clean, a suggested factor is to increase the skin friction drag by 10%.

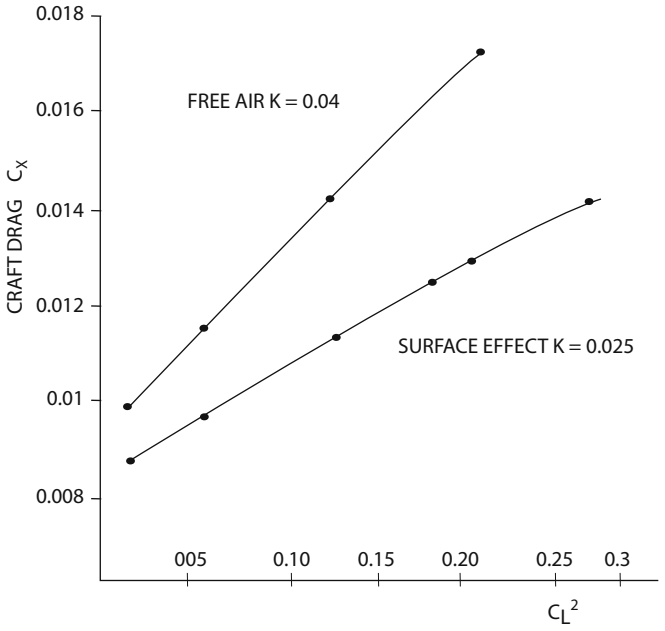

Fig. 7.16 C_L versus C_x at various K values

Wave-making Drag of Hull and Side Buoys, R_{hw}, R_{sww}

Wave-making drag is caused by the pressure field from the static displacement of the hull, and dynamic planing forces of the hull and side buoys; similar to SES, catamarans, planing hulls and hydroplanes. Two methods are suggested as follows.

1. *Calculation method.* The wetted length and trim angle can be obtained from the analysis of photos of a test tank model directly, or estimates made based on similar craft designs and the hull and side buoy wave-making drag can be calculated as for other high-speed marine craft, outlined in [5] and Chapter 2 [1].
2. *Prediction with aid of model test results* The wave-making drag of hull and side buoys can be considered as a residual drag R_r. Thus,

$$\begin{aligned} R_r &= R_{hw} + R_{sww} \\ &= R - (R_a + R_{hf} + R_{swf} + R_{aw}) \end{aligned} \tag{7.9}$$

$$\left.\begin{aligned} R_{rm} &= R_m - (R_{am} + R_{hfm} + R_{swfm} + R_{awm}) \\ R_{rs} &= R_s - (R_{as} + R_{hfs} + R_{swfs} + R_{aws}) \end{aligned}\right\} \tag{7.10}$$

where the Subscript m and s represents model and real craft, respectively, and

$$R_{rs} = R_{rm}.\lambda^3 \tag{7.11}$$

where λ is the linear scale ratio of the model to full size craft. The total resistance of the craft can be obtained from model test results, and the residual resistance obtained by reduction.

WIG Drag After Take-Off

Drag of WIG After Take-Off

Craft total drag after take-off R_t can be obtained by wind-tunnel tests as shown in Fig. 5.31. From the figure, it is seen that the air profile drag coefficient C_x is a function of trim angle $\propto$ and the relative flying height $\bar{h}$. It should be noted that C_x in this figure is C_{x3}, i.e. the drag of craft with bow thrusters in operation.

The figure can also be redrawn to show C_x of a typical DACWIG model versus $\bar{h}$ with constant trim angle and different position of guide vanes as shown in Fig. 7.17. This shows that the drag coefficient C_x is inversely proportional to the relative flying height, which contradicts the common sense that the air drag might be decreased with flying height, due to the reduction of wing tip vortex-induced drag when the craft is operated close to the ground.

This contradiction can be explained, as actually R_3 is the total drag of the craft minus the effective thrust of the bow thrusters. When at high speed and at flying height, the thrust recovery coefficient will be higher than that at lower flying height and C_{x3} is reduced. In model tests, the boundary layer on the non-moving wind-tunnel ground plate causes an increase in the measured air drag. This may be corrected by tests of models in wind-tunnel facility with moving ground belt or alternative arrangements, see Chapter 9.

Another important physical phenomenon to be tackled is how to deal with the bow thruster in model experiments. There are three kinds of air drag coefficients that can be used in drag calculation, as follows:

$$\begin{aligned} R_{a1} &= 1/2v^2 S_a C_{x1} \\ R_{a2} &= 1/2v^2 S_a C_{x2} \\ R_{a3} &= 1/2v^2 S_a C_{x3} \end{aligned} \tag{7.12}$$

Here R_{a1}, R_{a2} and R_{a3} represent the air drag of the model with non-rotating bow thruster, without bow thruster and with rotating bow thruster, respectively.

R_{a2} will be used as the bare craft drag (without any appendages) for predicting the powering performance. Figure 7.18 shows the drag coefficient of the bare model (without bow thruster) C_{x2} versus $\bar{h}$ with constant trimming angle. The model is with fully lowered flaps to create a high-speed dynamic air cushion.

In the figure, it is found that the C_x is nearly independent of the flying height, from which it is evident that the decreased drag in case of lower $\bar{h}$ is compensated by the boundary layer effect and increase of C_y, since $C_x = C_{xo} + K(h)C_y^2/A\pi$, when $\bar{h}$ decreases the $K(h)$ decreases because of surface effect; however, C_y increases, and eventually, the C_x will stay constant just as shown in Fig. 7.15.

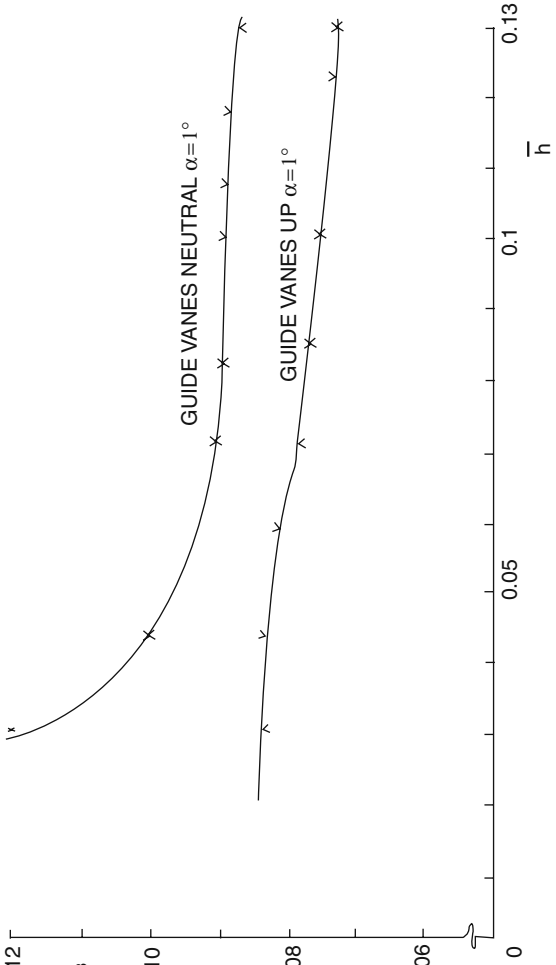

Fig. 7.17 C_{x3} (aerodynamic drag coefficient of model with bow-thruster operation) versus $\bar{h}$ at different guide vane angles

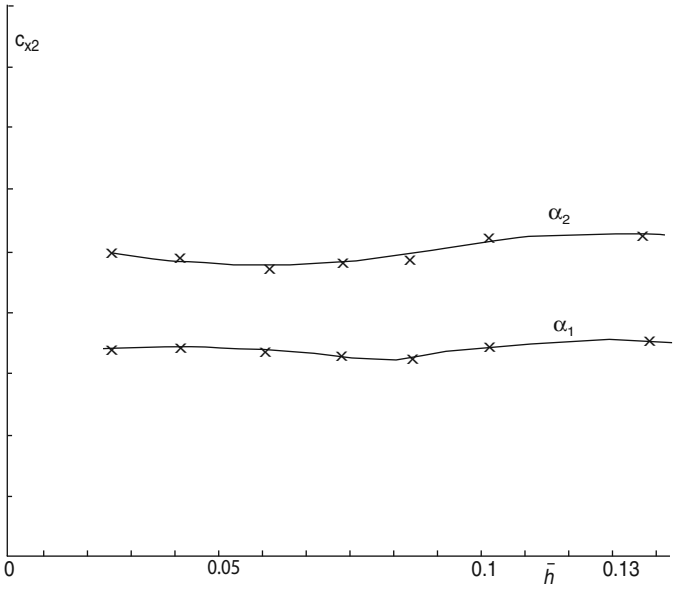

Fig. 7.18 C_{x2} (Aerodynamic drag coefficient of model without bow thrusters) versus h at different guide vane angles

R_{a3} is most suitable for predicting the craft air drag, subject to the model bow thruster dynamically simulating that of the real craft correctly.

R_{a1} is used for estimating the air drag in case of the bow thruster being out of order or not in operation (in hull borne operation). This operation mode is less important in the initial design phase.

Considering a complete WIG with n_t thrusters:

$$\begin{aligned}(R_{a3}-R_{a2}) &= n_t.T_{dc}\\ (R_{a3}-R_{a2}) &= n_t \cdot T_{do} \cdot \eta_{Td}\end{aligned} \tag{7.13}$$

The dynamic thrust-recovery coefficient ($\eta_{Td} = T_{dc}/T_{do}$, where T_{dc} represents the dynamic thrust of bow thrusters installed on the craft, and T_{do} represents the dynamic thrust of the thruster alone) is the function of various parameters and can be written as follows:

$$\eta_{Td} = (V_{jo}/V_s, V_r/V_{jo}\vartheta, \beta, \gamma, \bar{h}) \tag{7.14}$$

Where

V_{jo}	Speed of air jet efflux from air propeller
V_s	Craft speed
V_r	low speed at the stern exit under the main wing

γ, β Angle of flap and thruster jet inclination, respectively
ϑ Trim angle of craft
$\bar{h}$ Relative flying height

It is very difficult to calculate this coefficient due to its various interactive parameters. However, it nay be noted that the more unobstructed the airflow after the air propeller and air channel is, the larger the thruster coefficient.

Figure 7.19 shows the flow lines around the model with bow thrusters in operation, where (a) shows the craft operating before take-off with guide vanes downward and (b) after take-off with guide vanes upward. Taking $AA'BB'$ as a free body to approximately calculate R_3 for the craft, then

$$R_3 = \rho_a V_{si} Q_{AA'} - \rho_a V_r Q_r - \rho_a V_s' Q_{BB''} \tag{7.15}$$

In case of guide vanes downward as Fig. 7.19a, interference of flow might be caused at the bow of craft to generate the vortex as shown in the figure. This will

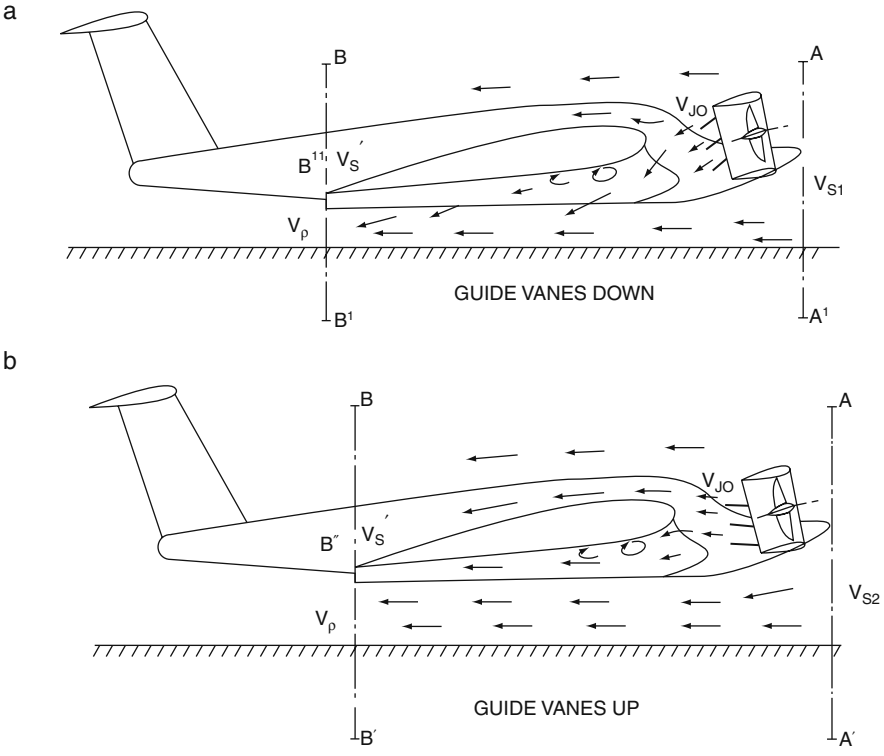

Fig. 7.19 Flow lines around a DACWIG with bow thrusters in operation

cause a decrease of air momentum at the stern so as to increase the residual resistance R_3. In contrast, in case of guide vanes upward, see Fig. 7.19b, the flow channel will be smoothed due to no blockage of inflow air. The air momentum at the craft stern will be increased so as to reduce the residual resistance R_3.

The dynamic thrust-recovery coefficient may be enhanced by the following measures:

- Rotating the guide vane or jet nozzles upward
- Reducing the air blockage after the bow propellers, such as power transmissions, engine mounting equipment, engine external piping and stern flaps opening
- High craft speed together with high flying height will give higher thrust recovery
- Reduction of craft trim angle ϑ

Sometimes, in order to increase the thrust-recovery coefficient, particularly in case of craft without stern propulsion engines (in this case the coefficient η_{Td} is most important at high speed), designers may raise the location of bow thrusters to decrease the blockage and increase the thrust recovery. This will decrease effectiveness of the thrusters at low speed, so the static lift–thrust ratio will reduce and take-off may become more difficult due to higher resistance hump. Optimising for the high-speed flying condition is not necessarily favourable for the pre-take-off condition, so a trade-off has to be made.

The thrust-recovery coefficient may fluctuate to a great extent, from nearly equal to 1 to close to zero, and sometimes even a negative value. When static hovering with fully closed flaps, the craft may go backward if the tail propeller is not running, on DACC and DACWIG models.

Figure 5.35 shows the static and dynamic thrust-recovery coefficients of a typical DACWIG craft model. The shape of the curves agrees with the above analysis.

Figure 7.20 shows C_{y3} and C_{x3} versus the thrusters jet angle β, and relative flying height $\bar{h}$ with constant trim angle and flaps fully lowered. It is found that the drag $R_{\mathrm{a}3}$ increases rapidly with thrusters guide vanes downward, particularly, in case of lower flying height.

Powering Estimation for WIG

To estimate power requirement for WIG up to take-off, or at cruise or maximum speed conditions, we first need to determine the total drag versus speed characteristic, and then plot this against the propulsion air propeller or gas turbine thrust characteristic at different power settings, to identify the cruise or maximum speed in still air. At take-off, the propulsion from bow thrusters as well as the stern propulsors should provide at least a 10 to 20% margin over the craft total drag, for acceleration purposes.

We have the drag characteristic from Section 7.3 for speeds up to take-off and from Section 7.4 for post-take-off speeds, so the next task is determining the power required to achieve take-off and our desired cruise/maximum speed.

It is assumed here that the thruster power estimation, consequent sizing and thrust characteristics in still air will have been determined in preliminary configuration

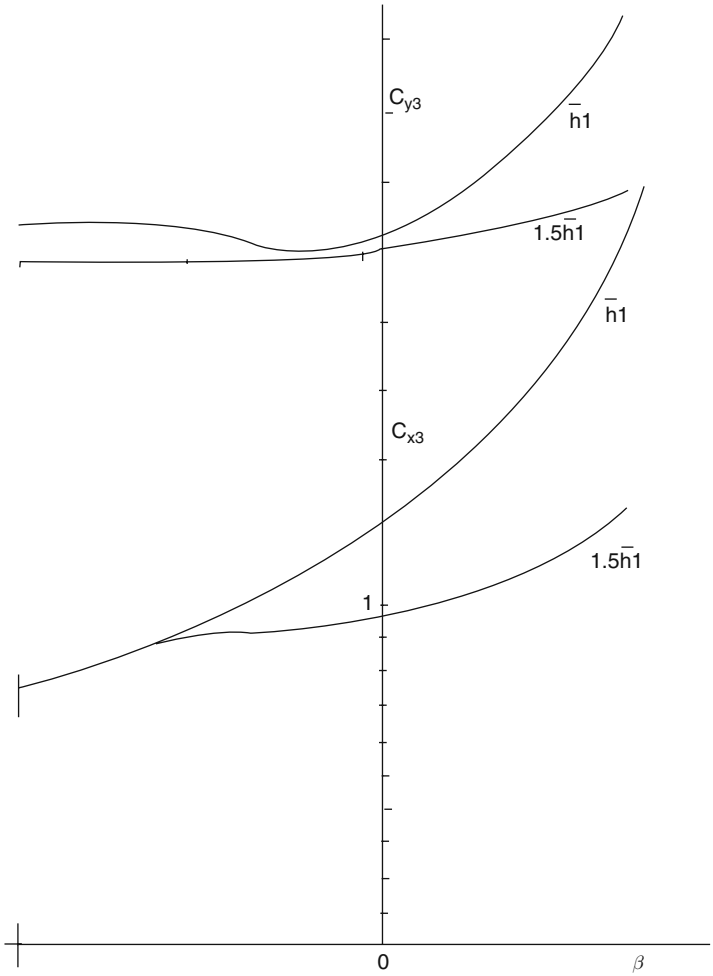

Fig. 7.20 Typical influence of guide vane angle on C_{y3}, C_{x3} from WIG model tests

selection, as outlined in Chapter 12, so that a total thrust characteristic with craft forward speed will be available for a range of different bow-thruster guide vane positions.

Performance Based on Wind-Tunnel Test Results of Model with Bow Thrusters in Operation

R_3 can be obtained from wind-tunnel test results. The thrust provided by the stern propellers needs to be at least equal to this at the craft cruising speed, so once

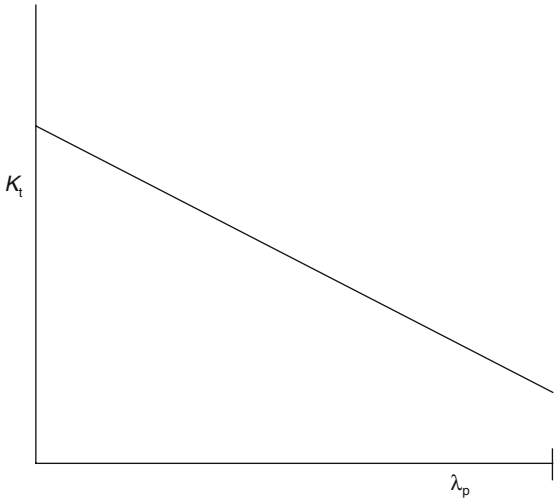

Fig. 7.21 Thrust coefficient K_t of a typical propeller versus advance ratio

the non-dimensional characteristics of the stern propeller are obtained, the WIG cruising and maximum speed can be estimated.

Figure 7.21 shows a typical non-dimensional characteristic of a stern air propeller, the thrust coefficient K_t versus advance ratio λ_p of the propeller:

$$\begin{aligned} K_t &= T/\left(\rho_a n^2 D^4\right) \\ \lambda_p &= V_s/(n \cdot D) \end{aligned} \tag{7.16}$$

Where

T	thrust (kg)
D	Diameter of the propeller (m)
n	propeller speed (1/s)
V_s	Craft speed (m/s)

Then the thrust related to craft speed and propeller rotation speed can be estimated as shown in Fig. 7.22, where T_{ps} represents the thrust of stern propellers at both maximum rated and cruising speed.

Estimation of WIG Total Drag

Once the dynamic thrust-recovery coefficient of bow thrusters has been obtained, the test results of drag of bare model R_2 will be very useful for estimating the WIG speed.

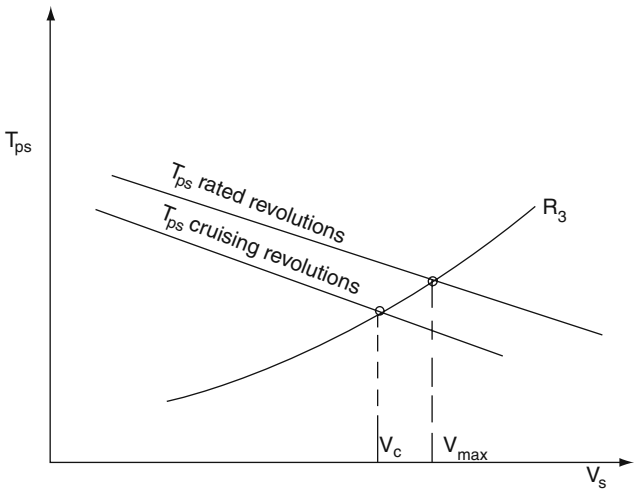

Fig. 7.22 Estimation of $V_{\max}$ and V_c

Figure 7.23 shows a typical bare WIG total drag R_2, and total thrust of the craft ΣT versus the speed V_s, where R_2 can be estimated by means of the methods above, and the total craft thrust can be expressed as:

$$\Sigma T = n_1 T_{ps} + n_2 T_{pb} \tag{7.17}$$

The figure shows the thrust for both fixed and variable pitch air propellers, where n_1 and n_2 are the number of bow and stern propellers, respectively.

This method appears straightforward for estimating craft drag and powering performance, just as the previous expressions for predicting craft drag. The precise prediction of ΣT is rather complicated however, due to the multiple parameters affecting thrust recovery. A parametric analysis is really required to identify the controlling design case.

Drag Prediction by Correlation with Hydrodynamic Model Test Results

The whole drag curve versus different Fn_d can be obtained by scaling from towing tank model tests for pre-take-off condition and from wind-tunnel test results of model flying after take-off. This is the simplest method for estimating the WIG craft drag through the whole speed range.

There are two approaches for towing tank tests at speeds below take-off, up to just above take-off speed, as follows:

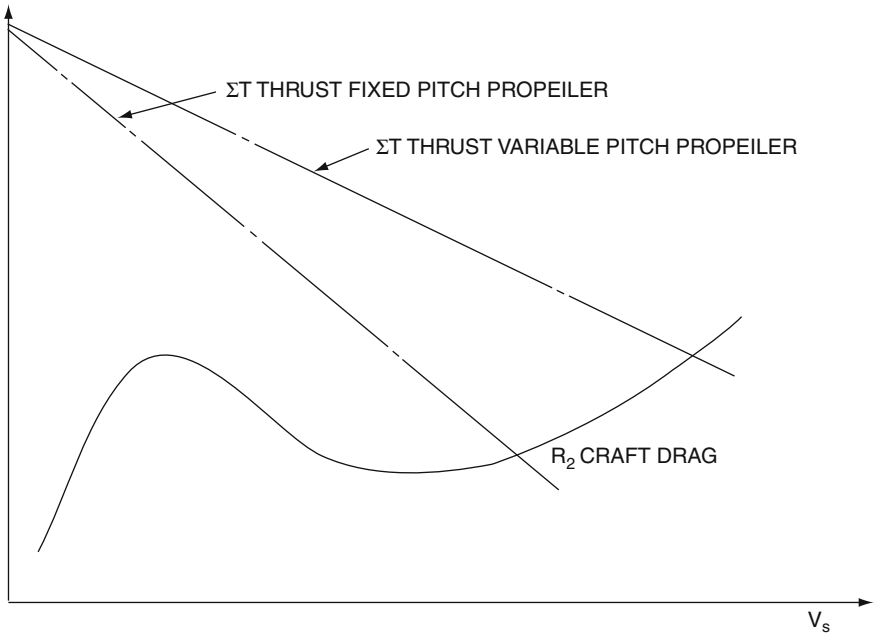

Fig. 7.23 Total drag of bare wing R and total thrust T of a typical WIG versus craft speed V_s

(1) Tests of a model with bow thruster and guide vane (or jet nozzle) in operation could be carried out in a towing tank. The static and dynamic thrust of the bow thruster can be measured either in towing tank or in wind tunnel. Then assume that the thrust-recovery coefficient of the propeller mounted on the model is 1, and add to the drag of test results, R_3, the dynamic thrust of the bow thrusters T_{do}, i.e.:

$$\Sigma R = R_3 + T_{do} \cdot n_t \tag{7.18}$$

Where

ΣR	Total drag of the model
R_3	Test data from dynamometer of towing facility
T_{do}	Test data of single bow thrusters from wind tunnel
n_t	Number of bow thrusters

This test approach is simple; nevertheless the test results are not accurate due to assuming the thrust-recovery coefficient to be the same in various operational modes and handling conditions. Typically, the test results over-predict the real drag, and the model data have to be corrected. The actual thrust-recovery coefficient can be obtained using Equation (7.13) to enable this correction.

(2) The other method is to install a dynamometer on the bow-thruster mounting so as to measure the actual thrust of the bow thruster. Then the thrust-recovery coefficient can be calculated as follows:

$$\eta_{\mathrm{Td}} = T_{\mathrm{ds}}/T_{\mathrm{do}}\Sigma R = R_3 + T_{\mathrm{ds}} \cdot n_t$$

Where

T_{ds} the dynamic thrust of bow thrusters installed on the model in running condition

The data from this test are precise; however, the cost will be higher due to the complication of installing a dynamometer on the bow-thruster mounting, and interpretation of results due to the vibration caused by both internal and external conditions.

Figure 7.24 shows a typical towing tank model test result. This figure shows the total drag–lift ratio ($\varepsilon = R/W$), the solid line represents the test results of method 1 and the dotted line method 2. Together with the test results from a wind-tunnel model, one can calculate the design drag of the craft, subject to the test model simulating the real craft geometry accurately, together with scaled dynamic characteristics.

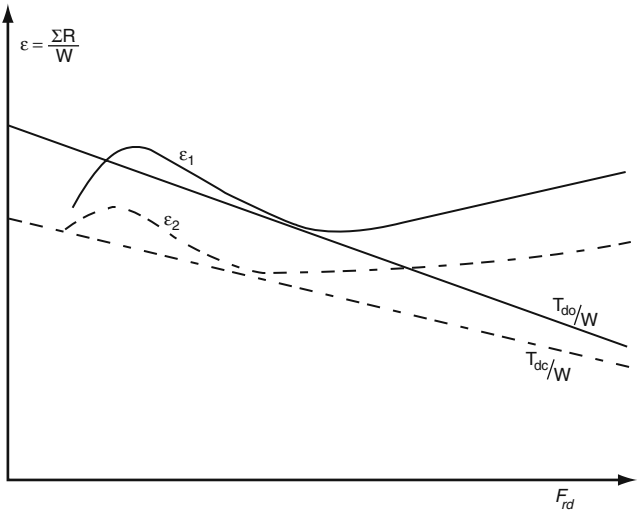

Fig. 7.24 A typical model test result of WIG in towing tank showing ε versus V

The drag hump speeds for DACC and DACWIG are approximately located at $\mathrm{Fn_d} = 1.8$–2.5 and take-off speed at $\mathrm{Fn_d} = 4.0$–5.0 [6, 7]. The hump speed for PARWIG is located at $\mathrm{Fn_d} = 2.5$–5.5 and take-off at $\mathrm{Fn_d} = 5.5$–9.0, see Chapter 6 [3, 4].

Influences on Drag and Powering Over Calm Water

The main wing of a WIG operating in the GEZ gives a high lift–drag ratio. However, as a WIG has various appendages and superstructure, the aerodynamic efficiency will decrease significantly from the basic performance of the wing form [8]. Figure 7.25 shows the aerodynamic parameter K of a typical WIG with different configurations versus relative flying height. One can see in this figure that the K of WIG with hull, buoys, pylon, etc. is reduced, so the effect of appendages and the overall configuration are important to WIG design. We discuss some of these issues below.

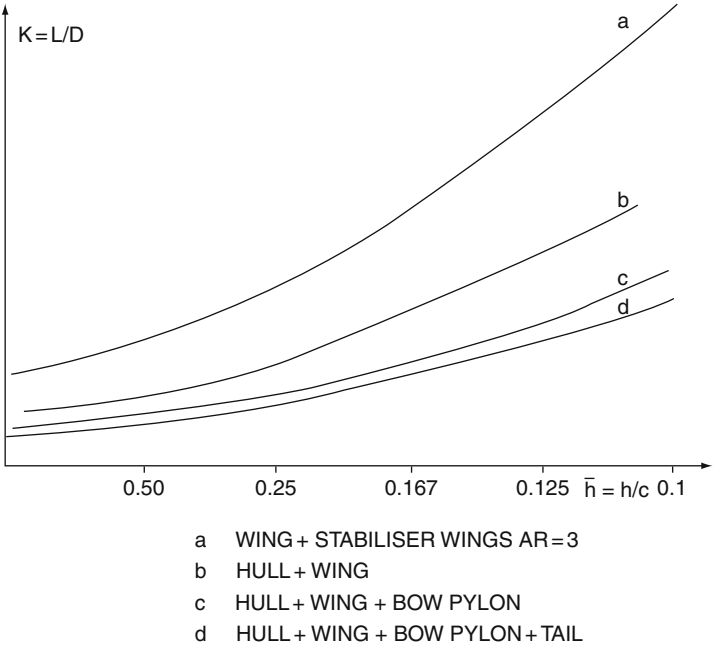

Fig. 7.25 K versus h/c for various craft configurations

Since water drag is much greater than air drag, the most sensitive problem on a WIG before take-off is contact of the craft with water surface. In addition, on conventional fast craft, the factors influencing trim are less powerful than those on a WIG. For instance, CG is the key factor influencing the trim angle of planing hull craft and SES, whereas for WIG there are several factors having a strong influence, i.e. CG, flap angle, guide vane angle (jet nozzle), elevator angle, bow-thruster power level, etc. WIG craft drag before and during take-off is therefore more complicated to assess than that on other high-speed marine vehicles.

Briefly speaking, WIG designers have to select control mechanisms (chosen combinations of settings for the control surfaces such as elevators and guide vanes) for controlling or changing the running trim, and then the operators have to use

and master such controls correctly to optimise the craft performance in the different modes from boating to full flying speed. We will discuss the influence of various factors on drag individually and some handling methods resulting from this are as follows.

Hull-Borne Mode

From model experiments, it is found the drag of WIG with the bow thrusters out of action is extremely large due to the hull immersion in the water. The craft drag is similar to a fast planing boat or hydroplane.

Transit Through Main Hump Speed (Fn = 2–4)

The craft have to have a small bow-up trim condition to provide a suitable lift (both for air cushion lift on wings and hydrodynamic planing lift of hull and side buoys) and to decrease the hump drag. The most important element is adjusting CG location and guide vane or jet nozzle angle.

Since the selection of CG is mainly based on the requirements of longitudinal stability in flying mode, the proper angle of guide vanes is critical. In addition, the CG position has to be considered and sometimes moved a little to obtain a suitable trimming angle during hump speed transit.

During Take-Off (Fn = 4.0–8.0)

Here the craft has transited the hump speed, but the stern part of both hull and side buoys still sticking the water surface due to the bow trimming-up angle unless controls on the WIG are altered to flatten trim. The elevators need to be fixed at such position so as to bring the bow down towards flying trim.

The CG and guide vane angle has to be regulated so as to make a small trimming-up angle to negotiate through hump speed, and a flatter trimming angle for take-off. X_g,γ and β are the most sensitive parameters of WIG for take-off. A great difference of take-off drag is obtained on the same model with different positions of the CG and these control surfaces.

In addition, some other factors also influence take-off as follows:

- *Wind direction during Take-off*

In general, WIG are easy to take-off in the case of head wind due to the greater air lift and so lower water drag at take-off airspeed. Therefore, WIG pilots are used to take off in head wind just as for an airplane

- *Wave force and wave direction*

This will be discussed in the next chapter

• *Bottom roughness of the of hull and side buoys*
On WIG, the roughness of the hull and side buoys not only influences the drag but also the lift. Increased roughness effectively increases the wetted surface drag so as to lead a cycle of deterioration; consequently the craft may fail to take-off. The surface smoothness of the hull and side buoys is very important to be maintained.
• *Spray formation*
Weber number on the scale model and full-scale craft are rather different, so the spray formation for the model and craft are also different, which can be seen from Figs. 7.2 and 7.5 (for model scale) and Figs. 2.7 and 2.12 (for full-scale craft). The spray on the craft is larger than that on the model and is characterised by a large volume of fine beads of spray. The spray not only reduces the sight of navigators, but also increases the craft drag. It also deteriorates the working condition of the engines located at the bow. In some cases, it may cause engine shutdown, so that the craft fails to take-off. Therefore, designers have to pay careful attention to such problems, and the larger the craft, the more serious the problem.
• *Shallow water*
Wave-making resistance will be increased significantly for WIG operating in a shallow water area especially during the take-off, similar to conventional fast craft. The additional wave-making drag will increase the difficulties of the take-off. In addition, the probability of such conditions will be enhanced on DACWIG due to the large span of the air cushion–hull-sidewalls complex body.
• *The lines of both hull and side buoys*
The lines of hull and side buoys have to be designed similar to a hydroplane hull or flying boat. Key characteristics for these craft are transverse steps (Fig. 7.10) and a stern step (Fig. 7.26) to eliminate the bottom suction at speeds close to take-off and allow a clean lift-off.

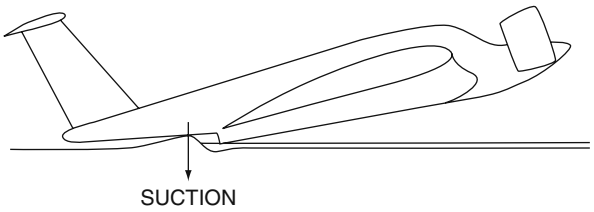

Fig. 7.26 Stern step for eliminating the suction on the bottom of main hull

Flying Mode

The influence of the flap angle, guide vane angle, craft trim and the main wing tip plates or side buoys, as well as an outer composite wing, on the craft drag in flying mode is as follows.

• *Influence of guide vane angle*
The influence of the guide vane angle is critical due to the change of thrust-recovery coefficient. The more level the vanes the greater the thrust is higher and lift is reduced when guide vanes are more horizontal, so pilots often move the vane upward after the take-off as the craft speed increases. Figure 7.20 shows the influence of the vanes on both lift and drag of a model tested in a wind tunnel with trim angle equal to 1° and a fully lowered flap.

In the figure, the drag coefficient drops down a large extent as the guide vane angle is changed from positive (down) to negative (up). However, the lift coefficient almost does not change due to the rather small influence of the bow thruster on the lift force when operating at high speed and at flying height.

• *Influence of trim angle*
Figure 5.31 shows the influence of angle of attack (trim angle) of a model tested in a wind tunnel. It is found that the drag will drop down about 60% by decreasing the trim angle from 3 to 0.5°. Of course there are some measures to drop down the trim angle, such as move X_g forward, and alter flap, elevators and guide vanes position; however, the last will be the best method due to both the increase of thrust and decrease of drag.

• *Influence of composite wing*
The rationale of the composite wing has been introduced in Chapter 2. Sketches of designs with composite wings are shown in Figs. 2.22 and 2.23. The brief rationale is that the tip vortex caused by the pressure difference between the upper and lower surface of the main wing induces an additional force acting on the composite wing not only in vertical direction so as to give additional lift force, but also horizontally to give additional propulsion force.

Model experiments demonstrate that the lift coefficient is increased, and drag coefficient decreased with the aid of composite wing; consequently, the lift–drag ratio is improved significantly, which validates the rationale for the composite wing. In addition, the composite wing can also move the aerodynamic centre of the wing complex rearward if it is located at the stern part of the main wing. This will improve the force balance and decrease the area requirement of the fixed part of the horizontal tailplane.

• *Influence of flap angle*
Closed flaps (flaps down towards ground) will pitch the craft bow down, at the same time increasing the lift and the drag. Figure 7.27 shows the influence of flap angle γ on C_x and C_y, of a typical bare model without bow thrusters, which represents the aerodynamic properties of the bare model tested in wind tunnel, and no interference by the bow thrusters at increasing flight height h/c. The lift–drag ratio K_{a2} deteriorates due to non-fair streamlines around the wing's lower surface in the case of the flap lowered or half lowered, so in general the flaps are suggested to be fully open by the time the craft has reached the take-off speed or is landing. The flaps are to be lowered only in the case of craft static hovering on the ground, or once landing speed has been reduced to boating, and hovering operation is required for negotiating the terminal ramp.

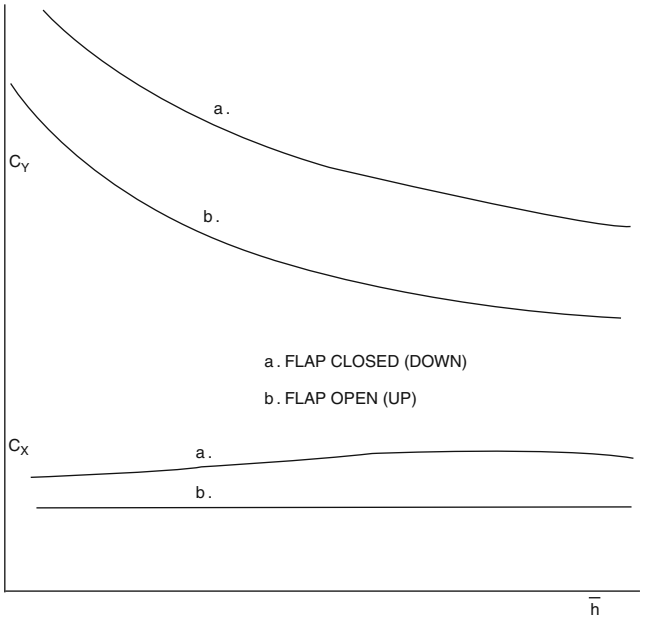

Fig. 7.27 Influence of guide vane angle on lift and drag coefficients

• *Influence of wing tip plates*

Since wing tip plates decrease the wing tip vortex, the drag will be decreased and lift increased; consequently the aerodynamic efficiency of the wing will be improved, this is illustrated in Fig. 7.28. Tip plates are suggested to be installed on all the wing elements, no matter they are main wings, composite wings or tailplane; see Fig. 7.29. In addition, fences have also been found helpful on underside of composite wings to improve the performance. see Table 7.1

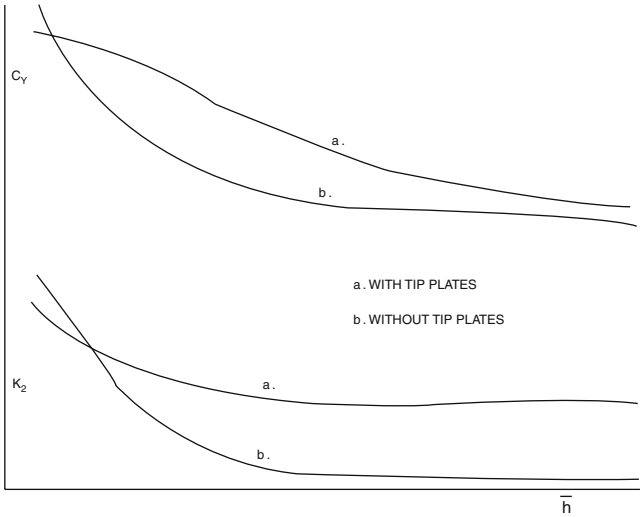

Fig. 7.28 Influence of flap angle on aerodynamic property of a typical bare WIG at various h

Fig. 7.29 Picture of Swan Mk 2 showing composite wing fences

Chapter 8
Seakeeping and Manoeuvrability

Introduction

WIG seakeeping and manoeuvrability includes the following topics:

- Longitudinal and transverse motions travelling over waves, including heaving, rolling, and pitching displacement and accelerations.
- Wave loading from impact on the bottom of both main hull and side buoys, and its influence on hull and side buoy strength requirements for extreme dynamic loads and for fatigue resistance. In addition, wave-impact loads on the main-wing flaps during take-off and touch down need to be considered.
- Crew and passenger comfort.
- Manoeuvrability in a seaway.
- Spray formation and its influence on pilot vision, main engine performance and air propeller erosion.
- Speed loss operating over waves compared to calm-water operation.
- Take-off capability in waves compared to calm water.

Seakeeping and manoeuvrability is presented here for the three different operating modes and two transitions characteristic of WIG, as in earlier chapters, viz. hull borne, hump speed transition, cushion borne or planing, take-off transition and flying at service speed.

A WIG operates in several different modes, and the influence of waves on the craft motion is significant, so the aerodynamics and hydrodynamics when operating in waves is somewhat complicated to analyse. Theoretical analysis of WIG seakeeping and manoeuvrability is still at the experimental stage, particularly for craft operating in the strong surface effect zone.

The interference of waves on WIG performance is significant, and with lower flying height the influence increases, so designers and operators generally select a high flying height for the craft operating in waves. However, at greater flying height, both longitudinal and transverse stability is reduced, and a trade-off has to be made.

There is seldom a case to mount an automatic control system for handling on smaller-sized WIG due to the difficulties to precisely measure the running trim and

L. Yun et al., *WIG Craft and Ekranoplan*, DOI 10.1007/978-1-4419-0042-5_8,

so safe flight is a matter for active piloting. The low longitudinal and transverse stability of WIG has so far been the main source of accidents, with pilot inability to maintain safe course being the triggering factor.

There are some handling devices on WIG that are useful, practical, sensible and having great influence on the motion of the craft. However, they increase the handling complexity and may lead to an accident in case of incorrect handling. Automatic control is more suitable for large craft, even with increased costs.

Since a WIG craft structure is light, the deflection of components such as wings, rudders, flaps, and even hull and side buoys are non-negligible, particularly in the case of craft running in waves. This affects the aerodynamics and hydrodynamics of the craft and consequently the seakeeping and manoeuvrability. The influence of hull, wing and side buoys deflection on the its performance are greater than that of an airplane, so research into aero-hydro-elastic problems on an Ekranoplan is more complicated and important than that on the airplane and other high-speed marine vehicles.

Finally, the relative static hovering height of DACC and DACWIG is also a critical parameter affecting the amphibious performance and take-off capability both on calm water and rough seas.

Differential Equation of WIG Motion in Waves

Since WIG generally fly in the stronger ground effect region, with inherent transverse stability, the analysis of craft motion in waves can be concentrated on solution of the longitudinal differential equations of motion. Following a similar approach taken for dynamic stability in Chapter 6, the differential equation of motion for a WIG in waves can be developed as follows.

Coordinate Systems

The coordinate system adopted here is as follows:

$X_oG_oY_o$ Global fixed coordinates
$X_1G_oY_1$ On board coordinates
$X_sG_oY_s$ Coordinates with respect to the incoming flow

Basic Longitudinal Differential Equations of DACWIG Motion in Waves

The basic assumptions for establishing these equations is that the craft is in high-speed flying mode, with no deformation occurring to the wave surface (no

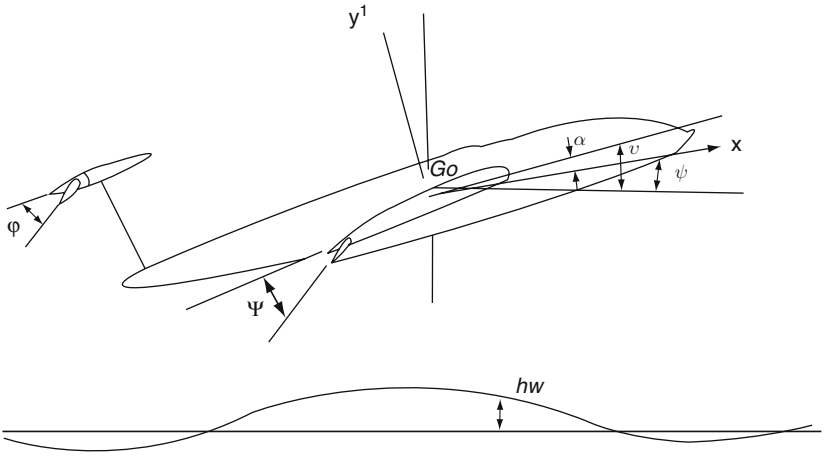

Fig. 8.1 Coordinate system of WIG in waves

hydrodynamic interference), then the coordinate system for a WIG moving over waves is as illustrated in Fig. 8.1.

In this figure, the following nomenclature applies:

- ψ Course angle, i.e. the angle in the vertical plane between the course of the craft and sea level, climbing positive and descending negative
- α Angle of attack, i.e. the angle between the course and base plane of the craft
- ϑ Trim angle of the craft, i.e. the angle between the base plane of craft and sea level

It may be noted that craft trim angle ϑ for steady flight will normally be designed to be zero, while the main-wing angle of attack α for zero trim will be designed to be optimal for the base camber line, depending on the wing thickness form adopted; see reference Chapter 3 [5]. When analysing the craft motion we will use craft trim angle rather than wing angle of attack as the reference variable.

Then the basic motion equation of the craft in waves can be expressed as follows:

$$\begin{aligned} m\frac{\mathrm{d}v}{\mathrm{d}t} &= P\cos\,\alpha - X - W\sin\,\psi + F_{\mathrm{xw}} \\ mv\frac{\mathrm{d}\vartheta}{\mathrm{d}t} &= P\sin\,\alpha + Y - W\cos\,\psi + F_{\mathrm{yw}} \\ J_{\mathrm{z}}\ddot{\vartheta} &= M_{\mathrm{z}} - PY_{\mathrm{p}} + M_{\mathrm{zw}} \end{aligned} \tag{8.1}$$

Where

- v Craft speed
- m Craft mass

P	Propellers thrust acting along X-axis
$X,\ Y$	Aerodynamic force acting on the craft along the $X_sG_oY_s$ coordinates
F_{xw}, F_{yw}, M_{zw}	Force and moment perturbations caused by waves
W	Craft weight
Y_p	The vertical distance from the CG to the propellers
M_z	Aerodynamic moment acting on the craft about Z-axis
J_z	Moment of inertia of the craft through CG about Z-axis

Since the perturbations are small values, then we can use the approximations as follows:

$$\sin\vartheta \cong \vartheta, \quad \sin\psi \cong \psi, \quad \cos\vartheta \cong 1, \quad \cos\psi \cong 1 \quad \text{and } Y_p \cong 0$$

Then Equation (8.1) can be written as

$$\begin{aligned}
\dot{v} &= \tfrac{1}{m} Cx\left(\alpha_0,\bar{h}\right) \tfrac{\rho v_0^2}{2} S - \tfrac{1}{m}\tfrac{\rho}{2} S v^2 Cx\left(\alpha,\bar{h}\right) \\
&\quad + \tfrac{1}{m}\tfrac{\partial T/\partial v}{T(v_0)}\left[2T_1\left(v_0\right) + Cx\left(\alpha_0,\overline{h_0}\right)\tfrac{\rho}{2} v_0^2 S\right]\left(v - v_0\right) - g\psi + \tfrac{1}{m} F_{\mathrm{xw}} \\
\dot{\vartheta} &= \tfrac{1}{mv}\tfrac{\rho_a}{2} S v^2\left[Cy\left(\alpha,\bar{h}\right) + C_y^{\varphi}\Delta\varphi\right] - \tfrac{1}{m} Cy\left(\alpha_{0,} h_0\right)\tfrac{\rho_a}{2v} S + \tfrac{F_{yw}}{mv} \qquad (8.2) \\
\dot{\omega}_z &= \tfrac{1}{J_z}\tfrac{\rho_a}{2} S C v^2\left[m_z\left(\alpha,\bar{h}\right) + m_z^{\varphi}\Delta\varphi\right] \\
&\quad - \tfrac{1}{J_z} m_z\left(\alpha_{0,} h_0\right)\tfrac{\rho_a}{2} v^2 SC + \tfrac{1}{J_z} m_z^{\overline{\omega_z}}\tfrac{\rho_a}{2} v S C^2\dot{\vartheta} + \tfrac{1}{J_z} M_{zw}
\end{aligned}$$

Above equation of motion is Equation (8.2)
Where

v_0	Initial speed of craft
$T1(v_0)$	Propeller thrust at $v = v_0$
$\underline{T}(v_0)$	Total thrust of propellers
N	Number of propellers
φ_0	Balance angle of the elevator
m_z	Rotational aerodynamic derivative with respect to non-dimensional angular velocity

$$\overline{\omega}_z = \frac{\dot{\vartheta} C}{v}$$

$m_z\left(\alpha,\bar{h}\right)$ $C_x\left(\alpha,\bar{h}\right)$ and $C_y\left(\alpha,\bar{h}\right)$ are the aerodynamic coefficients of the craft with respect to

$$\dot{\vartheta} = \omega_z$$

$$\alpha = \vartheta - \psi$$
$$\Delta\varphi - \varphi_0$$

The longitudinal and vertical perturbation forces and pitching perturbation moment caused by waves can be expressed as follows:

$$\begin{aligned} F_{xw} &= X_w = X_{HH} + 2X_{HS} + X_{fH} + 2X_{fs} \\ F_{yw} &= Y_w = Y_{HH} + 2Y_{HS} + Y_{awl} + Y_{aw2} \\ M_{zw} &= M_{zHH} + 2M_{zHS} + M_{zaw2} \end{aligned} \tag{8.3}$$

Where

X_{HH}, Y_{HH}, M_{zHH}	Longitudinal and vertical hydrodynamic force, and pitching moment of waves acting on the hull, respectively
X_{HS}, Y_{HS}, M_{zHS}	Longitudinal and vertical hydrodynamic force, and pitching moment of waves acting on the sidewalls, respectively
X_{fH}, X_{fS}	Longitudinal friction force of waves acting on the hull and sidewalls, respectively
Y_{aw1}, Y_{aw2}	Aerodynamic perturbation lift force caused by waves and wind, respectively
M_{zaw1}, M_{zaw2}	Aerodynamic perturbation pitching moment caused by waves and wind, respectively

The nonlinear differential equation above can be solved by computed time-domain simulations; however, the coefficients in the equation have to be obtained by model experiments first.

Seakeeping Model Tests

Model experimental investigation of seakeeping performance is most conveniently carried out in three steps, see references Chapter 2 [26, 27] and Chapter 3 [6]. The *first step* is working with radio control model experiments as shown in Figs. 3.2, 3.3 and 3.4. This model was made from aviation-type plywood and with an electric motor as the main engine to drive both bow and stern air propellers. The model operates on a lake under radio remote control. Such models can allow experimentation with model parameters in the various operation modes, i.e. hull borne, cushion borne and free flying. The model can also be operated in various directions relative to wind and waves and in different environmental conditions. The conditions themselves cannot be modified and so it is important to have accurate instrumentation to log the environment while the tests are on, to ensure that any changes can be correlated with the model behaviour.

Since a free flying test model is rather small and cost-effective, it can be used for qualitative estimation of the craft performance including the influence of the various handling mechanisms, and profile of hull, side buoys, composite wings, as

well as preliminary aerodynamic configuration on the seakeeping qualities of the craft. Figure 3.2 shows a radio-controlled model of a DACWIG running in small waves while boating, while Fig. 3.3 shows the model running in small waves just after take-off.

A model like this is too small to take precise performance data from, so model tests in towing tanks are still the main source of quantitative data for WIG design. The first step with free flying models is a qualitative experiment, to demonstrate if the WIG can be operated in waves with satisfactory stability and motions for the specified aerodynamic configuration.

The *second step* is model testing in a towing tank. This is a quantitative experiment and aims at the development of design parameters from the test data. Figure 7.6 shows a model under test in waves in a towing tank. The model is mounted on the moving carriage of the tank and towed at constant speed in regular waves. The speed, resistance, heave displacement and acceleration, pitching displacement and impact load of waves on the hull and side buoys can be taken from the tests. The motion responses of the craft model can also be obtained from the towing test, reduced to response amplitude operators (RAOs) on the basis of assumed linear response to differing wave height, so that the spectral analysis can be used to predict motions of the craft operated in irregular wave sea states.

The *third step* is a manned model test in waves. The size of such a model will be significantly larger than a towing tank model and installed with various instruments to record the motion displacement and loads acting on the craft. The manned model is operated by a pilot, enabling direct observation of its performance in waves. This is very useful for both designers and test pilots of full-scale craft for seeking an improved aerodynamic design and handling methods for the new craft. Figure 3.7 shows the Chinese manned DACWIG 750 operating in waves on a lake. Leading particulars of the craft have been given in Chapter 2. The craft as shown is at a take-off weight of 745 kg and a payload of 172 kg (one pilot and one technician). Its overall length is 8.47 m, with a wing span of 4.8 m.

The craft was equipped with four Cayuna 2 stroke petrol engines with rated power of 30 bhp at 6,000 rpm. Two motor-powered ducted bow thrusters located in front of the leading edge of the main wing, and the others are used as propulsion engines driving two ducted air propellers.

The craft has been tested in waves at Din Sah lake west of Shanghai, and the results showed that the craft could take-off in 0.5–0.7 m wave height with Beaufort 4–5 wind scale and 6 wind scale gust force in the lake. The craft can be turned at flying speed, and fly into different wind and wave directions holding the level to within 0.3° average pitching angle and 0.52° of average roll angle. Figure 3.7 shows the craft in flying mode so as to see clearly the air gap under the bottom of the craft, even in waves.

Figure 3.5 shows another Chinese PARWIG prototype “XTW-II” with principal dimensions of length 12.6 m, span 8.20 m, maximum height 3.35 m, cruising speed 100–130 km/h, flying height 0.6–1.0 m, maximum take-off weight 950 kg, carrying 3 crew and passengers. The craft was equipped with two Rotax 2 stroke engines

rated at 40 bhp each for propulsion. Figure 3.5 shows the seakeeping test of the craft in Tia Lake, at 6–7 Beaufort wind scale (gust).

Test results obtained by MARIC and other WIG development groups with prototype craft may be discussed as follows:

1. From the figures, it is found that both DACWIG and PARWIG run smoothly with small motions (vertical, longitudinal and transverse) and small loads acting on the craft in flying mode. This is due to the craft operating clear of the water surface, and at supercritical operation, i.e. the encounter frequency is far greater than the natural frequency of the craft. In this case, the craft will be almost in platforming operation, which seldom occurs in other fast marine vehicles, even though it is the ideal operational condition.
   As an example, consider a small WIG with 10 m overall length running at 110 km/h speed, in sea state 2 into head waves with 12 m wave length, then the encounter frequency will be

$$\omega_e = \frac{v + 1.25\lambda^{0.5}}{\lambda} = 2.35 \tag{8.4}$$

   This may be 2–4 times the longitudinal (pitch) and vertical (heave) natural frequency of the WIG, causing rather small longitudinal and vertical motions of the craft and excellent seakeeping quality. The seakeeping quality of WIG running in flying mode in rough seas is generally excellent, until wave heights are so large that they impact on the hull and/or side buoys.
   Based on statistics for their occurrence, the wave height with 50% likelihood in an inland sea might be 2–3 m, and 5–6 m in open sea. To avoid the wave impact, a WIG needs to be designed to operate to clear these waves and have the ability to adjust the mean flying height up to around twice this height, so as to just clear extreme wave heights. It may be noted that the WIG flying height $\bar{h}$ is effectively measured from the mean water level (MWL or MSL), so we are concerned here with the wave height above this level. Typically where seas are not fetch limited, the visible height or mean height of the highest one third of waves is about 1.7 times as high as the mean height, and that of the highest one tenth approximately 2 times as high, reaching to about 6 m above MSL in open ocean for the average sea state considered here.
   For a WIG operating in the GEZ at $\bar{h} = 0.1 - 0.2$, then the wing chord of the craft C will need to be at least 20–50 m for safe cruising in open seas. This gives us a simple method for first estimation of the principal dimensions for a WIG.
   Since on the DACWIG or PARWIG there are bow thrusters mounted at the leading edge of the wing, the strong air jet blown on the wave surface will influence the wave peak or weaken the force from waves acting on the craft. In addition, there are slender leading edges of the hull and side buoys, but without blunt skirts on the bow as mounted on ACV/SES, so the requirements for

operating the flying height of WIG even can, in certain conditions, be decreased to 60–70% while keeping satisfactory seaworthiness.
From Fig. 5.34, it is found that the neutral relative flying height $\bar{h}$ is approximately proportional to speed squared, so WIG can maintain high speed in waves so long as they can maintain high clearance.

2. The speed loss of WIG after take-off is very small compared with other fast marine craft such as ACV and SES, so it is most important to take every step to enable the craft's take-off at low speed when operating in waves. The most effective method is an air jet blown by bow thrusters into the air channel. The better the craft amphibious performance the better will also be its take-off capability in waves.
3. In Fig. 7.14, there are two drag humps on the curve. However, from the point of view of the principal author, this is not a rule for the drag curve for WIG in all operational conditions, particularly for DACWIG with a strong air jet caused by bow thrusters. Clearly, the first hump is the wave-making resistance caused by hull and side buoys immersed into the water surface at $Fn_d = 1–2$; however, the second drag hump, located at $Fn_d = 6–7$ on the curves, is caused by spray drag acting on the hull and side buoys. Although spray might not be great after the first hump speed, the higher speed in such case can cause significant spray drag, particularly at bad running attitudes, where hull or side buoys just touches the surface. For this reason, the second hump might not exist on the drag curve of WIG at a good running attitude; however, it will exist on the drag curve of WIG operating in waves, due to the influence of spray caused by waves.
This condition will be improved when using correct handling to improve the running attitude, particularly in case of craft running on calm water. During take-off, it is most important to use the control surfaces to reduce contact with the water both at bow and stern of the craft so as to reduce spray making and surface contact drag.
Figure 8.2 shows the drag curve (R–T) of the model of DACWIG type "SWAN". From the curves one can see the following:

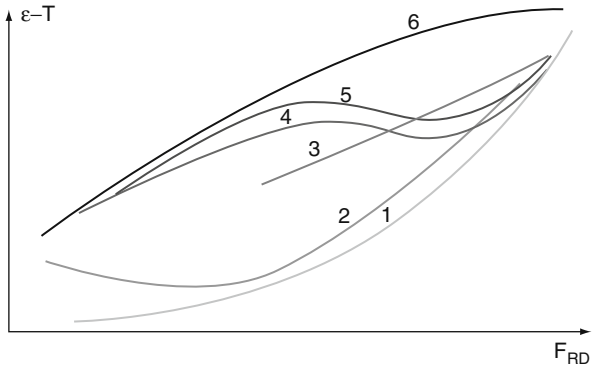

Fig. 8.2 Drag curves of DACWIG model type "SWAN" in waves

- The first drag hump of the craft in waves is close to that on calm water either in head or following seas, due to the existence of the air cushion.
- The second drag hump (i.e. the drag caused by spray at take-off speed) is greater in waves than in calm water, particularly in following waves with a long wavelength. However, in case of shorter waves, the second drag hump may be decreased significantly. The wave and chord length ratio in the figure is rather great, i.e. $\lambda/C = 3.5$, so the probability of encountering this situation for the small craft-like "SWAN" operating along the coast line is rather small, so it seems the seakeeping quality should be satisfactory.

4. Seakeeping tests of models in towing tanks are carried out in zero wind speed. In the full-scale world, the craft will normally take-off into head winds. In this case, the take-off capability for craft will be improved greatly due to the higher relative air speed and lift on the main wing, particularly at the second hump speed. Tests of "SWAN" and "750" in Lake Din-Sah supported this, a phenomenon that does not exist for conventional fast marine craft.
5. Take-off speed (for model tests) is higher because of the zero wind in a tow tank. The model can take-off only at a higher speed. The relative net drag of the model both on calm water and in waves are almost the same, no matter it is in head or following waves.
6. A power margin is necessary for the craft operating over waves. In case of craft with high cruising speed, the problems mentioned above will be solved easily due to high propulsion power. Slower cruising speed craft may have to be designed for lower take-off environments so as to match the powering at take-off and cruising.
7. Model drag in head seas with different wavelength show little difference, so the influence of wave length on the drag appears to be small. However, in the case of following seas, the influence of wave length cannot be neglected. Longer waves cause higher drag due to the decrease of encounter wave frequency during take-off, making it more difficult to take-off and causing more spray acting on the craft. In general, the drag of models in following seas before take-off is greater than that in head seas.
8. With respect to the dynamic trim in waves, Fig. 8.3 shows the relative draught or flying height of SWAN model in both calm water and waves in head and following seas against forward speed $\mathrm{Fn_d}$. From the figure, one can see the relative flying height of model both in following and head waves is close to that on calm water.

   Figure 8.4 shows the relative heave displacement $\Delta h/h_\mathrm{w}$ and relative pitch angle ϑ/ξ (double amplitude in the figure) versus the relative encounter frequency of the model of SWAN in waves.

   Where

   $\omega_\mathrm{e}\sqrt{\frac{C}{g}}$ Relative wave encounter frequency
   C Wing chord length
   ω_e Wave encounter frequency

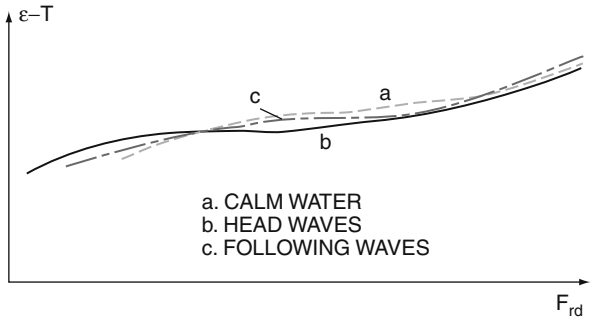

Fig. 8.3 Heaving and pitching response of a WIG model type SWAN in waves versus encounter frequency

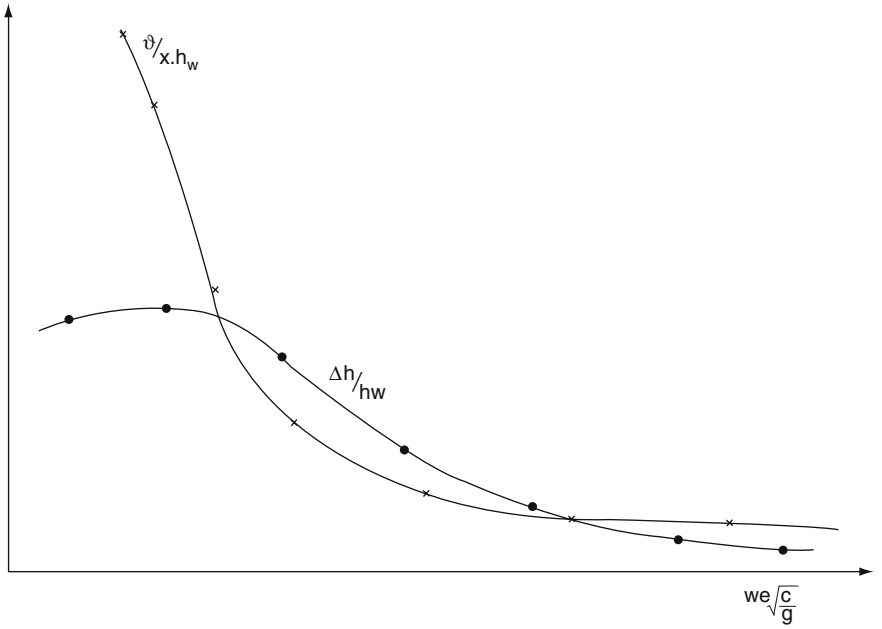

Fig. 8.4 Relative draught or flying height and pitching angle ψ of the model of a DACWIG craft type SWAN in calm water and waves

ω_e	$= (V \pm 1.25\lambda^{0.5})/\lambda$+represents head waves, − represents following waves
ϑ	Pitching angle (°)
ξ	$= h_w/\lambda$Wave steepness
λ	Wave length
Δh	Heaving displacement
h_w	Wave height

It is found that the trim angle and the tendency of the trim angle change for the model at different speeds both on calm water and in head waves are similar; however, it is rather different for the model in following seas. The model trim angle in a following sea may decrease, sometimes as far as negative trim angle. This is a rather dangerous situation for the craft, which may lead to plough in. Such physical phenomena may occur for medium-size models in following waves, where the wave and wing chord length ratio may be at $2(\lambda/C = 2$, where λ is wave length) as on ACV/SES. This may be interpreted as the main wing is located with bow part over wave trough and stern over wave peak, which causes a bow trim-down moment.

The drag of models running in following seas is greater than that in head seas due to the decrease of trim angle for the former case, even if the average draft for both cases is the same. For this reason, pilots always take-off into head seas and head wind.

Tests can be carried out in a towing tank with regular waves at various wave lengths and a representative wave height in head and following seas. The dimensional and linearised non-dimensional heaving/pitching wave response function can then be determined.

Some physical phenomena related to WIG performance in waves can be described as follows:

- The motions of model, both for heave and pitch amplitude, will decrease significantly with increased wave encounter frequency. Once craft take-off in waves, the motion of the craft will be very small, once the craft is in so-called super critical operation, up to almost platforming operation. The maximum model pitching amplitude is rather small compared with other high-speed vessels.
- If we assume the model motion running in waves complies with linear theory, the motions of a model in irregular waves can be calculated from the linear transfer functions of the craft model obtained from model test data mentioned above.
- Assuming the craft will be operated in sea with limited fetch (rather than the open ocean), we can use the Jonswap wave spectrum for motion analysis, and according to ITTC reference material, the energy density spectrum of two-dimensional waves can be expressed in terms of wave frequency as follows. It should be noted here that the encounter frequency of WIG with the waves will change in relation with the craft speed.

$$S_j(\omega) = 0.658S(\omega)\gamma^{\exp}C \tag{8.5}$$

Where

$\omega = f/2\pi$ (rads/s), where f is expressed in cycles/s
$\gamma = 3.3$
$C = [-(0.206\omega_{T_1} - 1)/2\sigma^2]$

Where

$\sigma = 0.07$ while $\omega \leq 4.85/T_1$, and

$\sigma = 0.09$ while $\omega > 4.85/T_1$

$S(\omega) = (A\omega^{-5})\exp(-B\omega^{-4})$, where

$A = 174(H_{w1/3})^2$

$B = 691 \cdot T_1^{-4}$

In which the significant wave height and average wave period for various sea states can be listed as follows:

Sea state	Significant wave height $H_{w1/3}$ (m)	Average wave period T_1 (s)
2	0.8	1.0
3	1.0	2.2

For simplification, the motion characteristics of craft running in irregular waves can be estimated to be the same value as model motion running in regular waves with 1.5–1.7 times the value of the irregular wave significant height.

9. Wave impact loading on a WIG hull, an important criterion of seaworthiness, both acting on the CG and bow part of the model running in head and following waves has to be determined from towing tank and full-scale testing.
Since craft speed is high, the wave impact load is a critical criterion for a WIG, just as for hydroplanes. High loading will cause damage to WIG hull, side buoys and especially wing flaps, and discomfort to crew and passengers. Some measures for decreasing these loads can be discussed as follows, see [1, 2].
The bow jet nozzles and Hydro-ski on PARWIG "Orlyonok" as shown in Figs. 2.14 and 2.15 can help to decrease the wave impact load. The hydro-ski can also be used as a TLA, as hydraulic dampers are connected between the hydro-ski and hull structure.
The adjustment of craft damping with different draft and trim is very important for reducing the wave impact loads during take-off and touch down both on calm water and in waves. It is found that almost one-half of the impact load can be reduced by means of using correct handling methods, compared with the incorrect handling methods. It should be noted that the hydro-ski must be retracted to be clear of the water surface during flying operation to avoid damage.

DACWIG and DACC operating in waves respond as follows:

- The flap should be lifted fully to avoid the impacting waves after take-off. In addition, the relative wavelength of 2 is unfavourable for craft motions (similar to ACV plough-in) and so should be avoided in operation during hovering and take-off.
- Shorter waves give smaller impact load on the hull both for head and following seas.
- Impact loads at both bow and CG for following waves are lower than that for the heading waves, similar to other fast marine vehicles.

- Impact loads on bow are greater than that on CG of craft in waves both in heading and following seas.
- In most cases, the impact loads will decrease after take-off and, at high speed, are lower still due to increased flying height.
- Impact loads on the hull of DACWIG are the lowest compared to other high-speed marine vehicles due to the strong air jet fed into the air channel, and large flying height, as well as thinner hull and side buoys.
- In order to reduce impact loads and as a landing pad, inflatable bag skirts can be mounted under the main hull and side buoys [3], as shown on the Russian DACC type "Volga-2" in Fig. 2.27.

10. Immersion of bow thrusters in waves would be a serious problem on DACWIG operating in a seaway. Bow thrusters are often located relatively low in order to feed the pressured air into the air channel; in addition, the pitching down angle might be increased when running in following seas. The probability of immersion of the bow thrusters will be increased in such a case. Immersion would be serious, causing damage to the air propeller and its power transmission system, so designers have to take measures to prevent the immersion of bow thrusters. The main measure is to design the main hull or fuselage bow shape to provide sufficient buoyancy or planing lift to prevent the lower edge of the bow-thruster ducts contacting the wave surface.

Manoeuvrability and Controllability

Aerodynamic characteristics of WIG operating in GEZ are strongly nonlinear, so the analysis of manoeuvrability and controllability of WIG is complex. In order to analyse the manoeuvrability of the craft in more simple terms, linear analysis methods are recommended in this section.

The controls and control surfaces available for adjustment of longitudinal running attitude of WIG are engine speed (engine throttles), flaps, guide vanes and elevators. However, the guide vanes are usually applied to adjust the running attitude before take-off and during operation over ground. The controls used during flight are usually engine throttles, flaps and tail elevators.

Pilots usually use these controls to change the running attitude from one condition to another, i.e. from initial flying altitude $\bar{h}_0$, trim angle ϑ_0 and speed V_0, to $\bar{h}_1$, ϑ_1 and V_1, respectively, whilst maintaining longitudinal static stability. Therefore, in this section, we will discuss the proper handling method to change the running attitude with safe static longitudinal stability. Since the analysis is based upon small perturbations of motion, linear analysis is reliable and reasonable. In addition, the external disturbing forces such as wind gusting has to be considered in the analysis.

The manoeuvrability of WIG when hull borne, and on air cushion, as well as planing modes are similar to ACV, SES and planing hulls, so in this section the analysis of manoeuvrability of WIG focuses on that in the flying mode.

WIG Control in Flight

Consider a WIG at sea in flying mode. The pilot wishes to increase the craft speed by raising the engine throttle. If this is done, the flying height will increase accompanied with an altered trim angle, as the trimming centre and height centre both change, and static longitudinal stability reserve of the craft will alter, as discussed in previous chapters.

Generally, pilots aim to increase the speed and flying height while keeping constant trim angle for safety and comfort reasons. Therefore they have to use the elevator or adjust the main wing flaps, together with engine throttle adjustment. We call this the complex handling method.

If the pilot keeps the main wing flap angle constant, and uses the engine throttle and tail elevator to increase speed, and flying height, with unchanged trimming angle, then the derivative of flying height with respect to craft speed can be obtained as follows. First, we assume that the propeller thrust operates through the centre of gravity, so that it does not create any additional trimming moment. In addition, we assume that the pilot keeps the flap and guide vane angles unchanged, and only push the engine throttle and elevator forward, so as to increase speed and keep the trim angle unchanged.

Since

$$Y = 1/2\rho v^2 C_y S = Y(v,C_y) \tag{8.6}$$

$$M_z = 1/2\rho v^2 CSm_2 = M_z(v,m_z) \tag{8.7}$$

Then

$$\frac{\mathrm{d}Y}{Y} = 2\frac{\mathrm{d}v}{v} + \frac{\mathrm{d}C_\mathrm{y}}{C_\mathrm{y}} = 0 \tag{8.8}$$

$$\frac{\mathrm{d}M}{M} = 2\frac{\mathrm{d}v}{v} + \frac{\mathrm{d}m_\mathrm{z}}{m_\mathrm{z}} = 0 \tag{8.9}$$

Also $C_y = C_y(\bar{h},\varphi)$, and $M_z = m_z(\bar{h},\varphi)$

Then

$$\mathrm{d}C_\mathrm{y} = C_\mathrm{y}^{\bar{h}}\mathrm{d}\bar{h} + C_\mathrm{y}^{\varphi}\mathrm{d}\varphi \tag{8.10}$$

$$\mathrm{d}m_\mathrm{z} = m_\mathrm{z}^{\bar{h}}\mathrm{d}\bar{h} + m_\mathrm{z}^{\varphi}\mathrm{d}\varphi \tag{8.11}$$

If we insert Equations (8.10) and (8.11) into Equations (8.8) and (8.9), then we have

$$2C_\mathrm{y} + vC_\mathrm{y}^{\bar{h}}\frac{\mathrm{d}\bar{h}}{\mathrm{d}v} + vC_\mathrm{y}^{\varphi}\frac{\mathrm{d}\varphi}{\mathrm{d}v} = 0 \tag{8.12}$$

$$2m_z + vm_z^{\bar{h}}\frac{d\bar{h}}{dv} + vm_z^{\varphi}\frac{d\varphi}{dv} = 0 \tag{8.13}$$

From Equation (8.12), we have

$$\frac{d\varphi}{dv} = -\frac{2C_y + vC_y^{\bar{h}}\frac{d\bar{h}}{dv}}{vC_y^{\varphi}} \tag{8.14}$$

Substitute Equation (8.14) into Equation (8.13), then

$$\left(\frac{d\bar{h}}{dv}\right)_{\vartheta,v=\text{const}} = \frac{2C_y m_z^{\varphi} - 2m_z C_y^{\varphi}}{v\left(m_z^{\bar{h}}C_y^{\varphi} - m_z^{\varphi}C_y^{h}\right)} = \frac{2}{v} \bullet \frac{C_{y0}}{C_y^{\bar{h}}} \bullet \frac{m_{z\varphi}^{C_y}}{\Delta\overline{X}_{F\varphi\bar{h}}} \tag{8.15}$$

because $m_{z0} = 0$ and $m_{z\varphi}^{C_y} = m_z^{\varphi}/C_y^{\varphi}$

Where

ϑ	Trim angle
γ	Flap angle
φ	Elevator angle
$\left(\frac{d\bar{h}}{dv}\right)$	Derivative of flying height with respect to speed, the gradient of flying height to speed
$\overline{X}_{F\varphi}$	Aerodynamic centre for changing elevator angle
$\Delta\overline{X}_{F\varphi\bar{h}}$	Difference between elevator angle and flying altitude:

$$\Delta\overline{X}_{F\varphi\bar{h}} = \overline{X}_{F\varphi} - \overline{X}_{F\bar{h}}$$

C_{y0} Initial aerodynamic lift coefficient

From Equation (8.15), it is found that $\left(\frac{d\bar{h}}{dv}\right)_{\vartheta,v=\text{const}}$ increases in direct ratio with initial lift coefficient C_{y0} and the pitching centre on elevator angle, $\overline{X}_{F\varphi}$, and in reverse ratio with the derivative of lift coefficient with respect to flying altitude $C_y^{\bar{h}}$ and centre difference between elevator angle and flying height $\Delta\overline{X}_{F\varphi\bar{h}}$.

Particularly for a craft at high flying altitude, $C_y^{\bar{h}}$ is small, and in this case the pilot should be careful in his handling, otherwise the craft will fly out of GEZ when pushing the engine throttle too high so as to greatly increase the speed.

For the same reason,

$$\left(\frac{d\bar{h}}{dv}\right)_{\vartheta,\varphi=\text{const}} = \frac{2}{v_0} \bullet \frac{C_{y0}}{C_y^{\bar{h}}} \bullet \frac{m_{zv}^{C_y}}{\Delta\overline{X}_{Fv\bar{h}}} \tag{8.16}$$

The variables $\overline{X}_{\mathrm{F}\nu}, \Delta\overline{X}_{\mathrm{F}\nu\bar{h}}$ represent the aerodynamic centre related to flap angle, and the centre difference between the flap angle and flying height centres.

Using the same method, we can derive the gradient of trimming angle with respect to the speed, i.e.

$$\left(\frac{\mathrm{d}\vartheta}{\mathrm{d}v}\right)_{\bar{h},v=\mathrm{const}} = \frac{2}{v_0} \bullet \frac{C_{\mathrm{y}0}}{C_{\mathrm{y}}^{\vartheta}} \bullet \frac{m_{\mathrm{z}\varphi}^{C_{\mathrm{y}}}}{\Delta\overline{X}_{\mathrm{F}\varphi\vartheta}} \tag{8.17}$$

The gradient of trim angle to the speed is given by Equation (8.17). The physical relationship is that a pilot wants to push the engine throttle to increase the speed and also change the elevator angle to keep the trim angle unchanged.

The Influence of a Wind Gust on the Running Trim of WIG in Steady Flight

In general, pilots handle WIG operating in flying mode at a steady cruising speed with the so-called loose bar handling. This means the controls will be kept steady, and the craft static stability allowed to keep it in steady flight. This is a fine handling method for WIG with good dynamic stability, with low physical demand on pilots.

What happens if a wind gust is encountered? In such a case, the influence of the gust on flying altitude and trimming angle of craft can be expressed as follows, similar to Equations (8.15) and (8.17).

$$\left(\frac{\mathrm{d}\bar{h}}{\mathrm{d}w_x}\right)_{\varphi\gamma=\mathrm{const}} = \frac{2}{v} \bullet \frac{C_{\mathrm{y}0}}{C_{\mathrm{y}}^{\bar{h}}} \bullet \frac{m_{\mathrm{z}0}^{C_{\mathrm{y}}}}{\left(\overline{X}_{\mathrm{F}\vartheta} - \overline{X}_{\mathrm{F}\bar{h}}\right)} \tag{8.18}$$

$$\left(\frac{\mathrm{d}\vartheta}{\mathrm{d}w_x}\right)_{\varphi,\gamma=\mathrm{const}} = \frac{2}{v} \bullet \frac{C_{\mathrm{y}0}}{C_{\mathrm{y}}^{\vartheta}} \bullet \frac{m_{\mathrm{z}\bar{h}}^{C_{\mathrm{y}}}}{\left(\overline{X}_{\mathrm{F}\vartheta} - \overline{X}_{\mathrm{F}\bar{h}}\right)} \tag{8.19}$$

Where W_x represents the speed of the gust and

$$m_{\mathrm{z}\bar{h}}^{C} = \overline{X}_{\mathrm{G}} - \overline{X}_{\mathrm{F}\bar{h}} = \frac{\dfrac{\partial m_{\mathrm{z}}}{\partial\bar{h}}}{\dfrac{\partial C_{\mathrm{y}}}{\partial\bar{h}}}$$

also

$$m_{\mathrm{z}\bar{h}}^{C} = \overline{X}_{\mathrm{G}} - \overline{X}_{\mathrm{F}\bar{h}} = \frac{\frac{\partial m_z}{\partial\bar{h}}}{\frac{\partial C_y}{\partial\bar{h}}}$$

The effect of a wind gust on the craft air speed, trimming angle and flying altitude can be seen in Fig. 8.5.

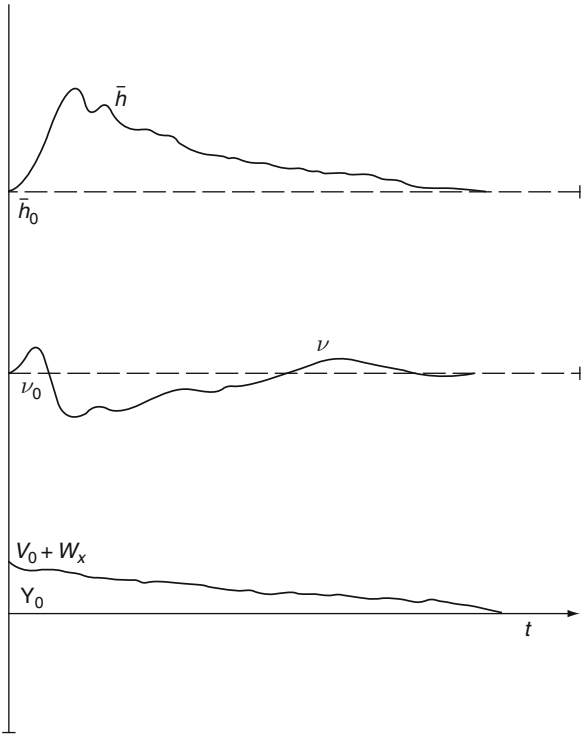

Fig. 8.5 Transitory time history for flying height, trimming angle, and speed of WIG in wind gust

Nonlinear Analysis of WIG Motion

The linear analysis described above can only be used for craft motion based on small perturbations. In practice, WIG motion can be large in high sea states, so requiring use of nonlinear analysis.

In this case, the logic diagram for the variables of speed, trimming angle, flying height, drag and thrust has to be drawn up first as shown in Fig. 8.6. Each point on the curves in this figure represents a steady craft trim condition in flying mode. The curve can be drawn in the following steps.

- Suppose we have the static aerodynamic coefficients of the model, i.e. C_y, C_x and m_z, for various angles of attack (i.e. trimming angle ϑ), at a definite flying height h_i of the WIG craft and constant speed. Since the weight is W_0 and the centre of gravity X_{dc0} of the craft is constant at the various trim values, the C_y can be calculated at various craft speeds.
- Then the curves C_y, C_x, R (drag of the craft model) and X_{dc} of the craft at constant speed can be obtained as shown in Fig. 8.7. Then the trim angle ϑ can be determined at the fixed C_y obtained above. However, X_{dc} of the craft at such trim

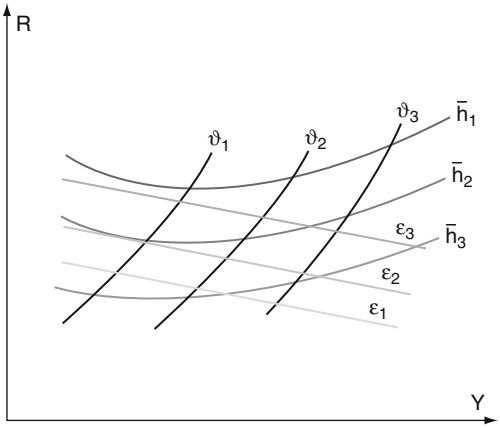

Fig. 8.6 Logic diagram for nonlinear motion analysis

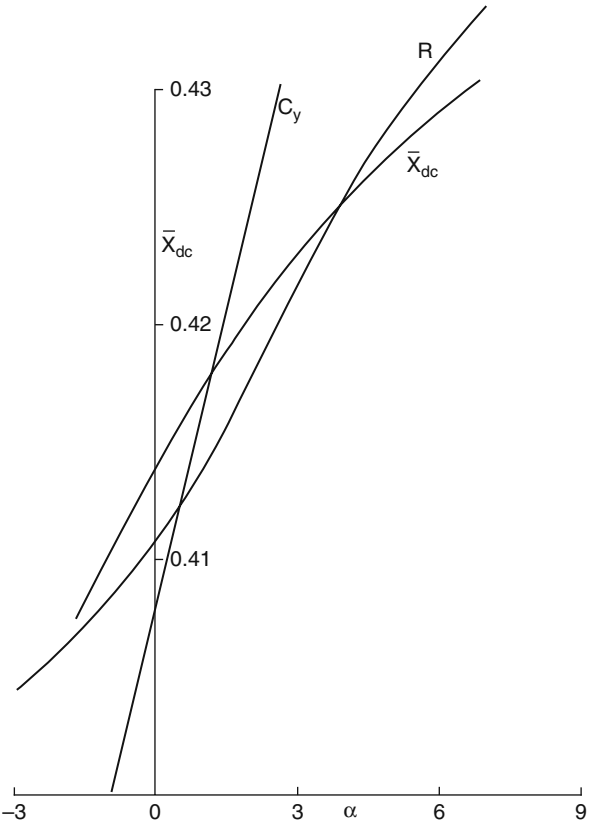

Fig. 8.7 Determination of equilibrium at various flying flights and speeds

angle might not be equal to X_{dc0}, just close to X_{dc0}. Then the trimming angle will change a little together with a small change in flying height.

- Finally, the equilibrium point can be obtained when $C_{yi} - C_{y0}$ and $X_{dci} = X_{dc0}$.

The determination of every equilibrium point at various flying heights and speeds, as well as constants φ, γ and ϑ is rather complicated; however, it can be obtained as shown in Fig. 8.8. In this figure, ϵ, $\bar{h}$ and ϑ represent constant throttle position of engine, flying height and trimming angle of the craft with constant φ, γ and ϑ, respectively, at various speeds.

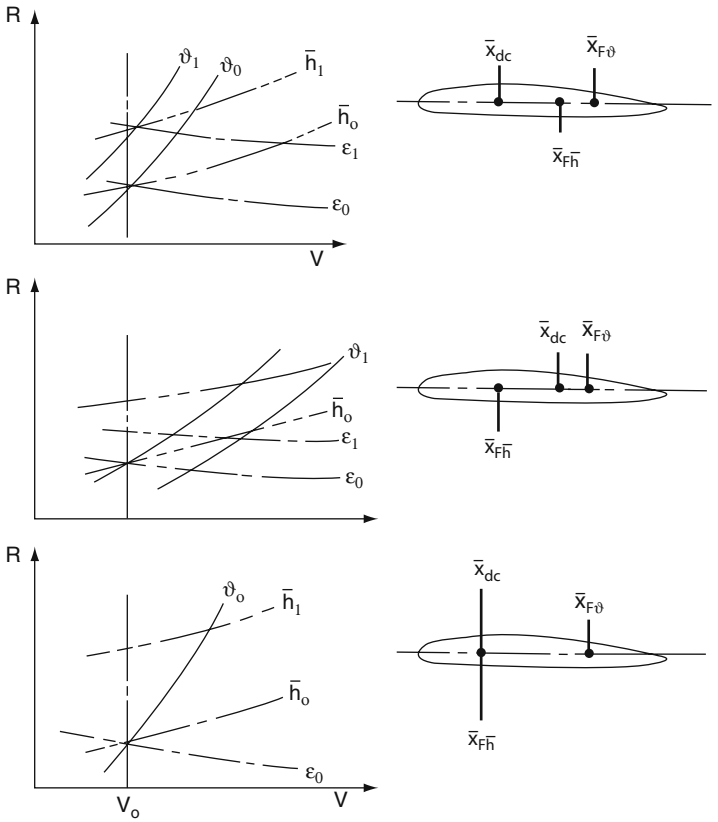

Fig. 8.8 C_x, C_y, R and X_{dc} at constant speed

Special Cases of Craft Motion

There are three typical running height levels when operating in different aerodynamic configurations, i.e. three circumstances of longitudinal stability with constant elevator, flap and guide vane angles, each of which has a different response to change of engine power [3].

(1) Trim and flying height centre coincident

$$\overline{X}_{\mathrm{F}\bar{h}} = \overline{X}_{\mathrm{F}\vartheta}, \quad \text{i.e.} \quad \Delta\overline{X}_{\mathrm{F}\vartheta\bar{h}} = 0 \tag{8.20}$$

In this case, where the trim angle centre is equal to the flying height centre, when the pilot pushes the engine throttle bar to increase thrust and speed, and if the flying height centre is ahead of the centre of gravity, the trim angle will be increased together with increasing flying height. Elevator down will be needed to level the trim and stabilise the height, increasing drag and reducing speed. Eventually, the craft speed might be nearly constant, as shown in Fig. 8.5.

(2) Flying trim centre at craft CG

$$m_{\mathrm{z}\vartheta}^{C_{\mathrm{y}}} = 0, \quad \text{i.e.} \quad \overline{X}_{\mathrm{dc}} = \overline{X}_{\mathrm{F}\vartheta} \tag{8.21}$$

In this case, the static longitudinal stability of the craft is nearly equal to zero. From Equation (8.18), it is found that the flying height will stay constant due to $m_{\mathrm{z}\vartheta}^{C_{\mathrm{y}}} = 0$, in the case of increasing thrust, and speed.
The craft behaviour can be described as follows. If the pilot increases the thrust and speed, the flying height will be increased. Since in general the difference between the trimming angle centre and flying height centre is larger than 0, so the flying height centre must be ahead of the CG and the trimming centre. In this case, the trim angle would decrease as the height is gained; consequently, the flying height will be kept nearly constant as shown in the mid part of Fig. 8.5.

(3) Flying height centre is at the craft CG

$$m_{\mathrm{z}\bar{h}}^{C_{\mathrm{y}}} = 0, \quad \text{i.e.} \quad \overline{X}_{\mathrm{dc}} = \overline{X}_{\mathrm{F}\bar{h}} \tag{8.22}$$

Since the flying height centre is at the same point as the craft centre of gravity, the changed lift will be located at the CG of the craft when pushing throttle bar ahead, so as to keep the trim angle constant. In this case, flight will be most safe and comfortable, and found acceptable by both pilots and passengers

(4) Flying height centre aft of the flying trim centre

$$\overline{X}_{\mathrm{F}\bar{h}} > \overline{X}_{\mathrm{F}\vartheta}, \quad \text{i.e.} \quad \Delta\overline{X}_{\mathrm{F}\vartheta\bar{h}} < 0 \tag{8.23}$$

In this case, since $m_{\mathrm{z}\bar{h}}^{C_{\mathrm{y}}} < 0$ so $\mathrm{d}\theta/\mathrm{d}w_x > 0$, according to Equation (8.19), so that in a head wind, the craft will climb together with increasing trim angle. This is not desirable and can lead to dangerous situations. Some craft, as TY-1 and SWAN in China, have $\Delta_{\mathrm{F}\vartheta h} < 0$ when operating at positive steady trimming angles, so the operation parameters (v, h, ϑ) have to be limited for safety.

In fact, as discussed within Chapter 6, to achieve static stability, the height centre should be ahead of the CG, the pitch centre a little behind, and the difference between the centres being less than 10% wing chord. In this case, the craft will

have a small bow-up tendency when throttle is increased together with a small but controllable tendency to reducing pitch as the height is gained, and up as height is lost.

Manoeuvring in Hull-Borne Mode

There are two design issues for a WIG in hull-borne operation as follows:

(1) Course keeping ability of the craft: Since the lateral profile centre of area may be located towards the rear of the craft but not far from the CG due to the arrangement of bow thrusters at craft bow, course keeping ability may be low when floating. To correct for this, a skeg can be mounted at the rear part of the main hull to improve course keeping when afloat. In addition, a skeg will be helpful for improving the main hull global strength where the planing steps are located.
(2) Manoeuvring of floating WIG in winds: pilots generally find difficulty to manoeuvre a floating WIG in beam winds. In order to improve this situation, the use of a combination of different right and left flap angles can be very useful. In addition, installation of small water thrusters in the stern of the side buoys can be very helpful for slow-speed manoeuvring.

Take-Off Handling in Waves

Take-off is always a sensitive operation for WIG, because the engine power required for take-off will be 2–3 times that at cruising speed, particularly in waves. For this reason, some measures have to be taken during design and operation as follows:

(1) Using correct handling method and design method as described in previous chapters.
(2) Selecting correct head wind direction for take-off. Figure 8.9 shows a transitional time history for flying height, trim angle, and speed in head and following wind speed of 5 m/s of an example WIG craft. The figure was plotted by calculation. Though the method is not precise enough for prediction of the running trim, it can be used for comparison of craft performance in various wind directions.

From the figure, it is found that this craft running down wind is rather difficult to take-off in the case of 5 m/s wind speed, but not when facing head winds.

Figure 8.10 shows the same comparison but with a wind speed of 7 m/s; in this case, this particular craft fails to take-off down wind, while it successfully takes off in head winds. This illustrates why pilots generally operate craft into head wind during take-off, similar to the procedure for seaplane take-off.

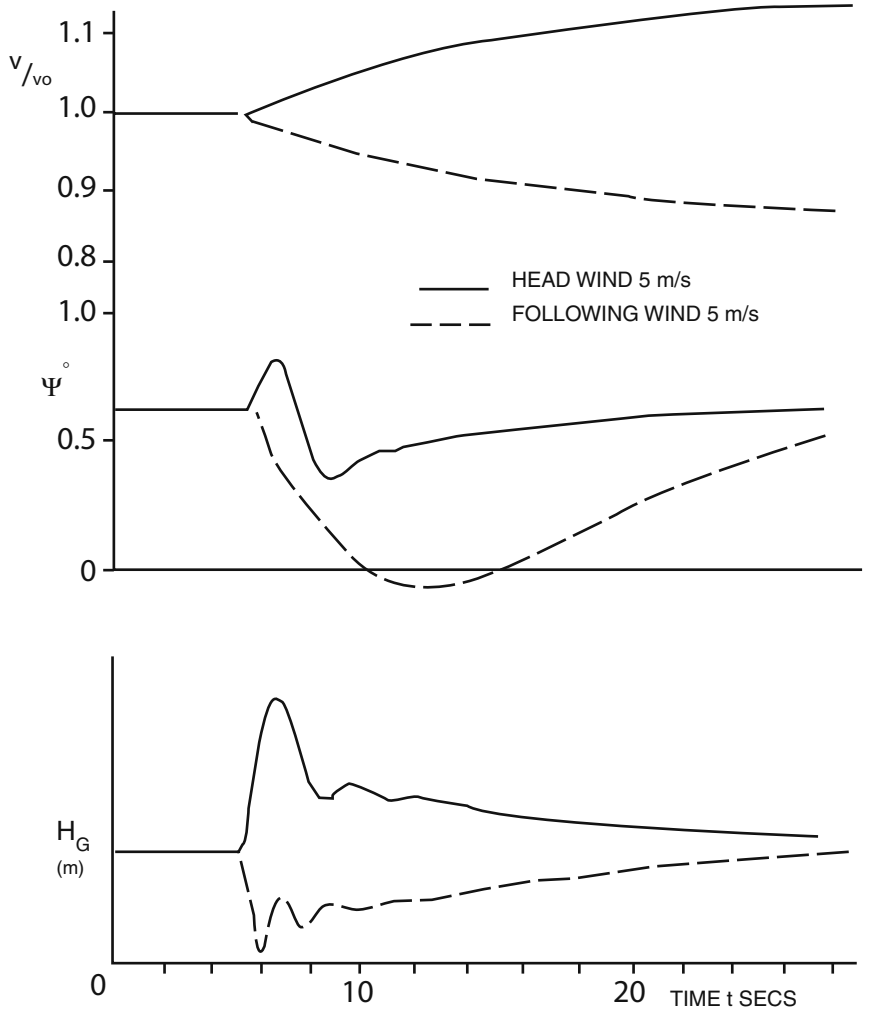

Fig. 8.9 Transitory time history of WIG in wind speed of 5 m/s

During the craft taking off into head wind, greater lift acts on the wings due to the higher relative speed of the wing, so as to reduce the water drag. Up to take-off speed, the water drag is always far greater than air profile drag.

Turning Performance

Turning while hull borne and cushion borne are similar to conventional high-speed craft, such as ACV and SES; however, in case of WIG operating in flying mode. the turning operation is different from conventional fast marine craft due

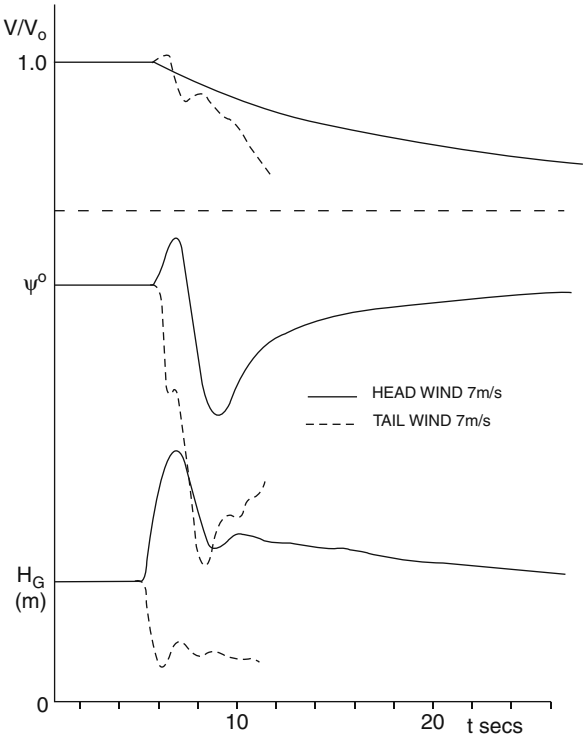

Fig. 8.10 Transitory time history of WIG in wind speed of 7 m/s

to the much higher speed and also different from an airplane due to lower flying altitude.

The centripetal force during a turn is very important for high-speed vehicles in the case of turning operation for balancing the centrifugal force acting on the centre of gravity of the craft. Otherwise the craft might overturn during rapid turning manoeuvres. An inward bank angle (both for ground and water vehicles) is necessary to create the centripetal force on a craft during the turn.

From this point of view, it is clear that the turning radius of amphibious WIG will be large due to the lower flying height and lower bank angle during turning compared to free flying aircraft. The pilots of DACWIG often manoeuvre rapidly on air cushion using different revolutions of starboard and port propellers, just as hovercraft do. The effect of bank angle on the turning radius and rate of turn of the craft can be seen in Fig. 8.11. It is found that higher bank angle reduces the turn radius and gives a higher rate of turn.

The turning radius of an aircraft is smaller than a WIG as it can bank steeply into a turn. Meanwhile, a hovercraft has no ability to bank and so has a larger turning radius than even a WIG. This is why pilots raise up a WIG flying height prior to turning so as to enable a banked turn, for example the Strizh in Fig. 3.6. So the

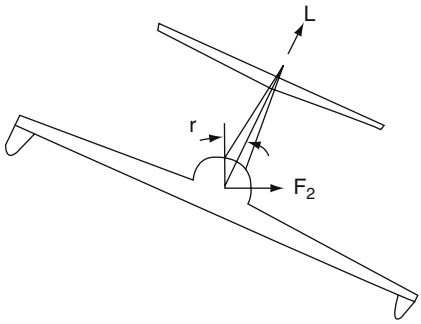

Fig. 8.11 Bank turn geometry diagram

ability to alter flying height is important, not only for seaworthiness, but also for manoeuvrability.

The bank angle is dependent upon altitude to avoid contacting the water surface by the tip plates or side buoys. Similar to an airplane, the turning radius during a steady turn can be expressed as follows, where the centrifugal force will be balanced by the lateral force, i.e.

$$V^2 \cdot W/R = F_z \tag{8.24}$$

Where

W	Craft weight
R	Turning radius
F_z	Lateral force

The simplest method to cause a lateral force is to bank turn, therefore the turn bank angle can be determined as follows, see Fig. 8.11

$$\sin \gamma = F_z/W \tag{8.25}$$

Where

F_z	$= L \sin \gamma$
L	$= W$, i.e. craft lift
γ	Heeling angle

The lateral force or heeling moment during turning can be generated by the following methods:

(1) Using ailerons to actively create a heeling moment,
(2) Using a swept wing (Fig. 8.12), to generate a centripetal force as craft is turned and banked [4, 5].

In Fig. 8.12, one can see that the air velocity normal to the wing is rather different at both sides of the craft wing during slip of the craft, i.e.

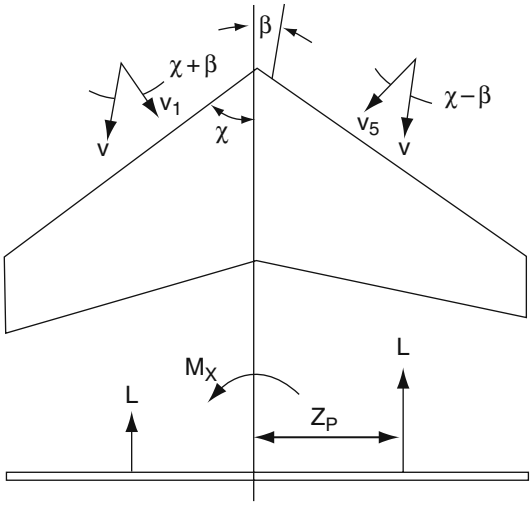

Fig. 8.12 Wing with a sweep angle in a turn

$$V_r = V\cos(\chi - \beta)$$

$$V_1 = V\cos(\chi - \beta)$$

Where β is the slip angle and χ the sweep angle.

Then the heeling moment can be generated due to the different airflow velocity on both sides. It is found the heeling moment increases with sweep angle.

(3) Positive wing dihedral angle.

From Fig. 8.13, one can see the effective angle of attack for both right and left wings are rather different during craft slip, so the heeling moment should be generated due to the Δy, while Δy is directed up at the right wing and down on left wing [6].

In addition, from the lower part of the figure, one can see the effective angle of attack at the right wing will be larger than that on left wing, so as to generate the additional heeling moment during slipping or turning of the craft.

The maximum banked turn angle can be determined according to the altitude and can be expressed by

$$\gamma_{max} = \tan^{-1} h/(0.5B_{max}) \tag{8.26}$$

Where

h	Flying altitude
B_{max}	Maximum wing span

The higher the WIG is flying the higher the pilot can bank.

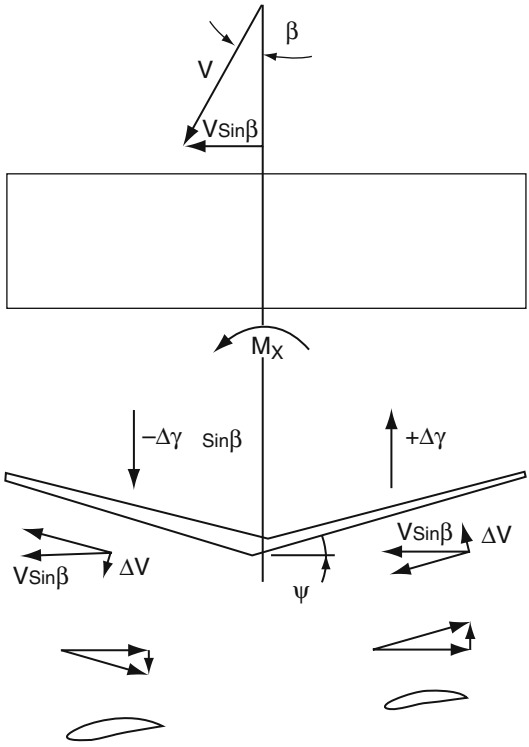

Fig. 8.13 Wing with dihedral in a turn

Operation of WIG Craft in Higher GEZ

Operation of WIG in higher GEZ ($\bar{h} = 0.15 - 0.5$), i.e. the so-called transit flying zone may be more sensitive due to lower transverse and longitudinal stability and strong coupling effect of transverse and lateral motion of the craft. This can be explained as follows:

(1) In case of the WIG operating in strong GEZ ($\bar{h} < 0.15$), both transverse and longitudinal stability of the craft are satisfied due to the strong surface effect.
(2) In case of the craft operating beyond the GEZ ($\bar{h} > 0.5$), actually the craft has no inherent transverse and heaving stability, and no coupled relation between the transverse and longitudinal motion, just as an airplane. In this case, the WIG has to be provided with control surfaces such as ailerons to give satisfactory control and dynamic stability, particularly transverse stability.
(3) In case of the WIG operating in weak GEZ, i.e. $\bar{h} = 0.15 < 0.3 < 0.5$, and also not having the necessary equipment for operating beyond GEZ (i.e. aileron, automatic control systems, etc.), the following will happen in a gust. In case of a gust acting head on the WIG, the craft will rise up, even beyond the GEZ

due to the small C_y^h, then the craft will be difficult to handle, and even in great danger, due to following reasons:

The transverse stability is poor, m_x^γ is small.

- The static longitudinal stability is reduced due to large down-wash angle on main wing and consequent reduced effectiveness of tailplane.
- The coupled relation between the slip and rolling motion is strong, which means the slip (or turn) motion will cause high rolling angle due to weakened transverse stability. In such case, the following relation has to be satisfied:

$$|m_x^\beta| > |m_{xL}^\beta| \tag{8.27}$$

Where

m_x^β The partial derivative of heeling moment with respect to the slip angle of craft

m_{xL}^β The practical limit of m_x^β If the limit is exceeded, the craft may be in danger of excessive rolling motion.

Therefore in case the WIG is operating in higher altitude (weak GEZ), the pilots have to pay a great attention for not making fast large manoeuvres and pushing throttle too fast, otherwise the craft might begin significant rolling motion, even overturning, as well as flying beyond the GEZ.

Figure 8.14 shows the relation between m_x^β and m_{xL}^β of Russian WIG "Orlyonok" derived by calculation.

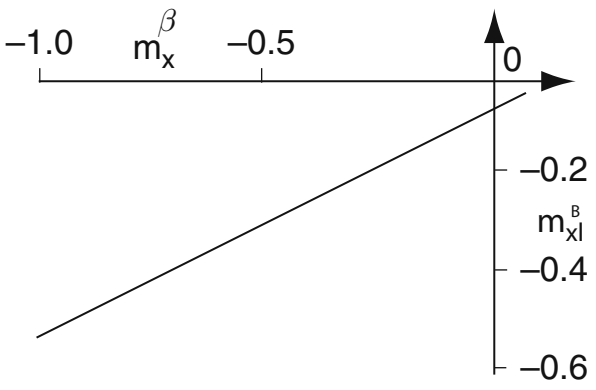

Fig. 8.14 Relation between m_x^β and m_{xL}^β of Russian WIG "Orlyonok"

Chapter 9
Model Tests and Aero-hydrodynamic Simulation

Introduction

Model testing is normally used to obtain performance characteristics for detailed design once a basic configuration has been selected, due to the complex geometry of a WIG craft and consequent three-dimensional airflow. Several model test series are carried out to analyse the different performance parameters, and provide the force coefficients or motion response operators that can then be used by scaling up to full size and inserting in the equations of motion for the WIG design. A static hovering platform, wind tunnel, ship towing tank and free running models in open water are all useful tools to gather data on the different aerodynamic and hydrodynamic characteristics.

Model test data for the whole craft can then be broken down into components by subtraction of elements that are predictable by analysis, such as lift and drag forces on the fin and tailplane, or from separate model tests of the main elements such as the wing. The remaining elements can then be related to the specific configuration and used directly in performance evaluation after scaling up to the prototype craft dimensions. Verification of the scaling relationship assumed initially, by comparison with full-scale trials of a prototype, is an important final step in the design process.

Scaling parameters for hydrodynamic model testing are similar to other high-speed marine vehicles and seaplanes, including Froude, Euler and Weber numbers. Aerodynamic data have to be obtained separately to hydrodynamic data due to the conflict between Reynolds and Froude numbers. It is not possible to model both at the same time, due to air being 800 times less dense than water.

In this chapter, we will summarise the scaling parameters, the tests that they can be applied to, and discuss results that have been obtained through WIG research at MARIC, including full-scale craft trials.

A separate issue to be addressed for WIG is how to deal with problems concerning the effect of structural elasticity on hydrodynamic and aerodynamic tests. Aerodynamic performance including the effect of structural elasticity is particularly important in WIG performance analysis due to the light-weight structure and significant hull and wing deformation – and the sensitivity of the aerodynamic characteristics to such flexure in the proximity to the ground. Structural stiffness can

L. Yun et al., *WIG Craft and Ekranoplan*, DOI 10.1007/978-1-4419-0042-5_9,

also affect hydrodynamic performance, though only to a minor extent, so that it can usually be ignored, and stiff models used. Modelling of cushion system characteristics, where flexible members are used, as in DACC, need to be addressed in the same way as other ACV modelling. The reader is referred to reference Chapter 2 [1] for guidelines on this aspect.

Procedures for testing WIG, as well as the relations between the various model experiments and theoretical analysis are also introduced in this chapter. Some problems that have occurred in MARIC model and theoretical investigations will be given as examples, and some remedial measures offered in this chapter for reference. We conclude with a short discussion of WIG concept design based on test data.

Experimental Methodology

There are four experimental methods used for WIG hydrodynamic and aerodynamic studies (particularly for DACC and DACWIG) as follows.

Static Hovering Experiments on a Rigid Ground Plane

Figure 4.11 shows static experiments on a rigid ground plane, and Fig. 4.21 shows the same tests for a full-scale craft over ground. In these tests, the static hovering characteristics such as clearance height and static stability can be investigated for DACC and DACWIG, and so evaluate the potential manoeuvrability over ground and during take-off. Such tests can also be used to study static characteristics of craft with separate lift fans if these are used for air cushion feed for DACC type craft, and their interaction with the propulsion and lift augmentation systems.

Model Tests in a Towing Tank

These tests can obtain the resistance, running attitude (dynamic trim) and wave impact loads on a WIG model at low speeds at various positions of control surfaces (flaps, elevator, thruster guide vanes), CG and bow thruster speed, both on calm water and in waves.

Towing tank testing is the basic tool for estimating the craft performance before, during and after (but not far away from) take-off over calm water and in waves. In these tests, the aerodynamic forces are not measured. The model may be self-supporting on an air cushion (DACC or DACWIG), or suspended in the case of a WIG or PARWIG. In both cases, the model will be attached to the normal towing assembly installed on the towing carriage so as to measure the hydrodynamic forces and moments at various speeds and in different wave heights. The results will be a set of data to enable loads and moments within an envelope of sea states to be estimated for the full-scale craft, scaled using Froude's law.

Model Experiments in a Wind Tunnel

In these tests, the aerodynamic properties, such as lift, drag, moment coefficients and derivatives of complete or half WIG models at various positions of flaps, rudders and elevators, guide vanes aft of bow propellers, trim angle, flying height, and drift angle of the model, can be investigated for the craft when flying in ground effect.

In addition, the dynamic properties of bow-thruster systems can be obtained for varying deflection of the jet into the main-wing cavity. Figure 4.10 shows a half model of a typical DACWIG in the wind-tunnel laboratory at MARIC.

Wind-tunnel tests are also used to determine the longitudinal and transverse stability parameters, and by subsequent analysis the manoeuvrability parameters (rate of turn for example), in a similar way to determination of aircraft manoeuvring performance [1].

Wind-tunnel models of the main lifting wing or the tail can also be tested to determine lift and drag coefficients for these components on their own, and with parametric variations to the geometry, test out such changes and identify the direction to optimise performance. The interaction of wings with the craft hull can also be investigated by comparison with data obtained from whole or half models of the craft.

In these tests, the air velocity used should be such as to keep the Reynolds number above 10^{-5} so as to ensure an appropriate degree of turbulent flow against the laminar flow over the model surfaces compared with the full-scale craft. Laminar flow would give very different data since the boundary layer is much thinner and the energy losses are so much lower. Small models may also give unrepresentative results if the breakaway for the turbulent boundary layer is too far back from the leading edge. Reference to aerodynamic texts such as Hoerner Fluid Dynamic DRag, and Lift, references Chapter 6 [10] and Chapter 7 [1], very helpful to give advice on these phenomena so as to assist modelling.

Radio-controlled Model Tests on Open Water and Catapult Model Testing Over Ground

Figure 7.3 shows a radio-controlled model test on a lake. Although less experimental instruments and sensors can be mounted on these models due to their small size, such tests are very useful for qualitative analysis of WIG performance, particularly for testing the dynamic stability in flight. Since the model is small, the construction and operational cost of this test is low. Radio-controlled model tests are very useful in WIG research at the preliminary and concept design stage for this reason.

Care should be taken to interpret the results from such tests though, as Froude number will be high and Reynolds number may be low compared to the full-scale craft.

Catapult model tests have also been used for the qualitative study of longitudinal and transverse stability, as well as aerodynamic characteristics of WIG models. Such

tests are most suitable for investigating the aerodynamic configuration of novel WIG types during preliminary research. Models are made of GRP with a light hull and no engines, launched from the catapult, and flying in GEZ. Although the flight can only last for a few seconds, the running attitude can be observed briefly so as to judge the model stability. The test cost is very low, so a large number of aerodynamic configurations can be tested for parametric analysis [2].

Based on these tests, creative ideas for WIG design can be developed inexpensively, and the reliability and practicality tested with low risk, due to the un-powered and cost-effective nature of the models.

WIG Model Scaling Rules

As with all marine vehicles, the model has to be an accurate geometric simulation of hull and wings, as well as key appendages on the craft, such as rudder, flaps and guide vanes. Based on the model geometric scale, the equivalent physical values for the full-size craft and model can be determined as in Table 9.1:

Table 9.1 The equivalent size ratio of various physical value for the full size craft and model based on the geometric simulation

Physical value	Symbol	Scale ratio
Length	L (wing chord length, etc.)	λ
Area	S (air cushion area, wing area, etc.)	λ^2
Weight and force	F(N)	λ^3
Gravity acceleration	g	Constant
Air and water density	ρ	Constant
Air cushion pressure	P_c (N/ m^2)	λ
Speed	V (craft speed, airflow speed, etc.)	$\lambda^{0.5}$
Airflow	Q	$\lambda^{2.5}$
Power	N (engine power, propeller power, etc.)	$\lambda^{3.5}$
Frequency	f(vibration, wave encounter frequency)	$\lambda^{-0.5}$

where λ is the linear scale ratio

Scaling Parameters for WIG

Reynold's Number

Reynold's number (Re) is the most important non-dimensional parameter for WIG performance prediction. In contrast to conventional high-speed marine craft, Re not only influences the drag forces on hull, wings, fin and tailplane, but also influences the lift forces on these same components. For this reason, Re affects the speed performance and also stability, manoeuvrability and operational safety. The influence of Re on performance of different components of a WIG is as follows.

Reynold's Number of Bow-Thruster Jet Flow

$$\mathrm{Re}_1 = V_\mathrm{j} t/\nu,$$

where

V_j	Jet velocity
t	Average thickness of the jet nozzle
ν	Kinetic coefficient of viscosity

This Reynold's number relates to scaling of the mixture of jet flow and its surrounding air from the jet nozzle to the entrance of the air channel. The greater the Re, the larger is the external volume flow mixed into the jet and the higher the air cushion pressure generated.

According to Krause and Gallington, Chapter 1 [10], the effective static cushion pressure generated can be expressed as:

$$P_c/q_\mathrm{j} = f\left(\overline{h}, \mathrm{Re}_1\right) \tag{9.1}$$

where

P_c	Effective static air cushion pressure under main wing

$q_\mathrm{j} = 1/2\rho_\mathrm{a} V_\mathrm{j}^2$ pressure due to jet flow

Reynold's Number of Bow-Ducted Air Propeller Blades (Re_2) and Duct (Re_3)

$$\mathrm{Re}_2 = V_\mathrm{p} B/\nu_\mathrm{a}$$

$$\mathrm{Re}_3 = V_\mathrm{o} L/\nu_\mathrm{a} \tag{9.2}$$

where

V_p	Resultant velocity of flow on the propeller blade
B	Blade width
V_o	Axial velocity of flow in propeller disc
L	Length of duct
ν_a	Relative viscosity of air

The Reynold's number at the blade/duct of model and full-scale craft are different, and sometimes there may be a larger difference between different scale models than model to full scale. Table 9.2 shows Re_2 of two models and a full-scale craft.

Table 9.2 Re_2 of the models and a full-scale craft

	Model No. 1	Model No. 2	Full-scale craft
Re_2	5.2E5	1E6	2.5E6
Scale ratio (λ)	1/13	1/6.5	1

The models simulate the full-scale craft geometry, for hull, wings and appendages. In addition, the thrust of the models is also simulated. However, sometimes it is found that the maximum lift–thrust ratio (i.e. the ratio of maximum lift and rated thrust of bow thrusters when the model has just taken off from ground) for the models and full-scale craft are rather different. Errors can therefore occur during the design of the WIG if the lift–thrust ratio is used as an aerodynamic scaling criterion, as Dr. Kraus and Dr. Gallington suggested.

Sometimes, it is found that the lift–thrust ratio for models, particularly for small-size models, is too high to achieve on full-scale craft. This is due to the different Re of the models and full-scale craft.

Figure 9.1 shows the maximum lift of a rectangular airfoil as a function of Re, where the thickness to chord ratio is 12%. The figure shows the general tendency of lift coefficient with respect to Re.

Figure 9.2 shows the lift comparison at low Re, it is found the influence of Re on the lift coefficient is very large, particularly at lower Re.

Figure 9.3 shows the lift–drag characteristic of thin section airfoils at low turbulence and Re; it can be seen that the aerodynamic performance of the airfoils with larger Re is much better than that with lower Re.

Figure 9.4 shows the lift coefficient of an N-60 two-dimensional airfoil versus various Re and changing trim angles [1]. The author was trying to understand why

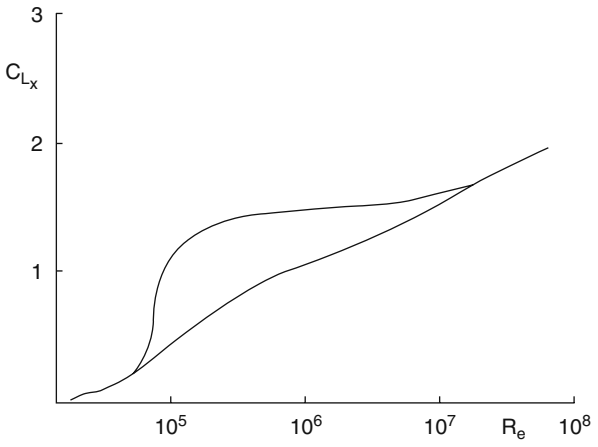

Fig. 9.1 Maximum lift of a rectangular airfoil as a function of Re

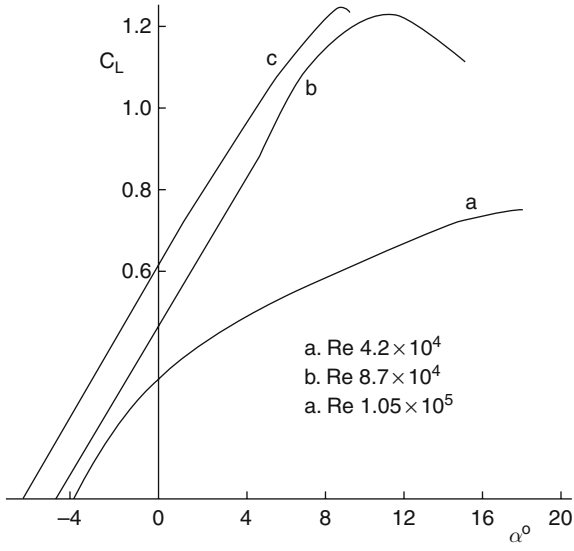

Fig. 9.2 Lift comparison at low Re

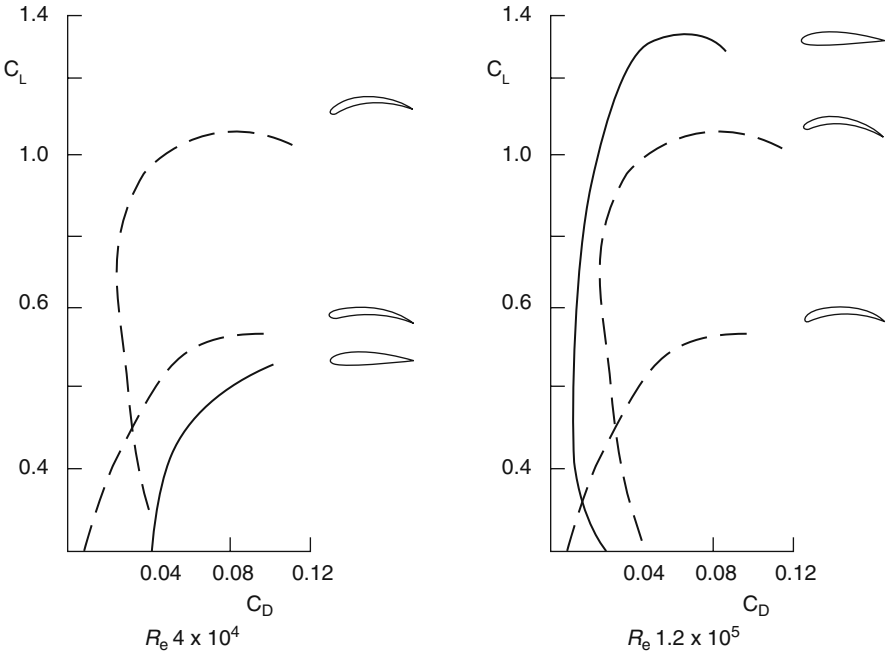

Fig. 9.3 Lift–drag characteristics of thin section airfoil at low turbulence and Re

the lift coefficient, aerodynamic properties and longitudinal stability of a model airplane are poor compared to the full-scale aircraft, particularly at small scale. From the figure, it can be seen that the lift coefficients drop rapidly with a decrease in Re, particularly in case of Re lower than 1×10^5 (1E5). The curves from 1 to 6 in Fig. 9.4 below show Re$1.47 \times 10^5, 1.05 \times 10^5, 8.4 \times 10^4 6.3 \times 10^4, 4.2 \times 10^4$ and 2.1×10^4, respectively.

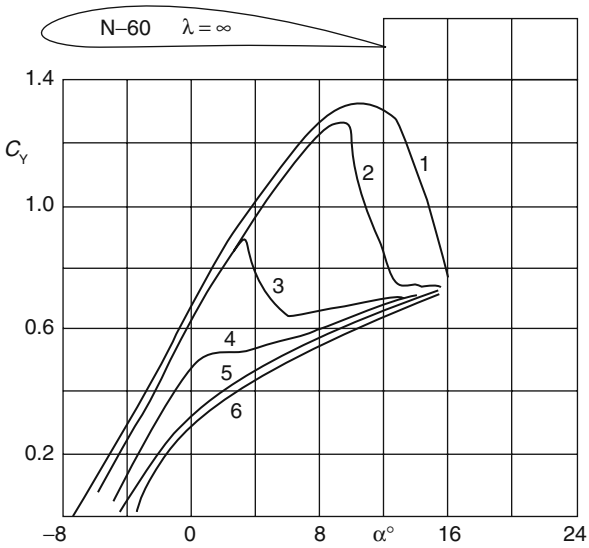

Fig. 9.4 C_{Lmax} versus Re for N-60 aerofoil

Figures 9.5 and 9.6 show both drag and lift coefficients of four airfoil profiles (NACA 6412, 2412, 4412 and 0012) with respect to Re. It is found that both drag and lift coefficients decrease with Re; however, the lift coefficient drops more rapidly than the drag coefficient. This may be why the aerodynamic properties of airplane and WIG models are worse than those of full-scale craft.

If the model Re is closer to the real craft value, the lift–thrust ratio and model aerodynamic properties more closely resemble the full-scale craft. For this reason, it is suggested that WIG models have to be large enough to obtain Re larger than $1 \times$ E6, otherwise great care is needed when using the lift–thrust ratio as a scaling criterion for estimating the lift power of real craft due to the distortion of model lift coefficient.

A designer can also use the parameter P_c/q_j (where P_c is the cushion pressure and $q_j = 1/2\rho_a V_j^2$) as a scaling criterion for predicting the lift power and functional requirements of bow thrusters, such as the overall pressure head and lift propeller flow rate in static hovering mode, particularly in case of small model with lower Re (Re_1 lower than critical Re). The cushion pressure is established from the total pressure head delivered by the lift air propeller, rather than the propeller thrust. The lift provided by the cushion under the wing is reduced compared to a fully contained air cushion by the decaying pressure pattern under the outer wing away from the

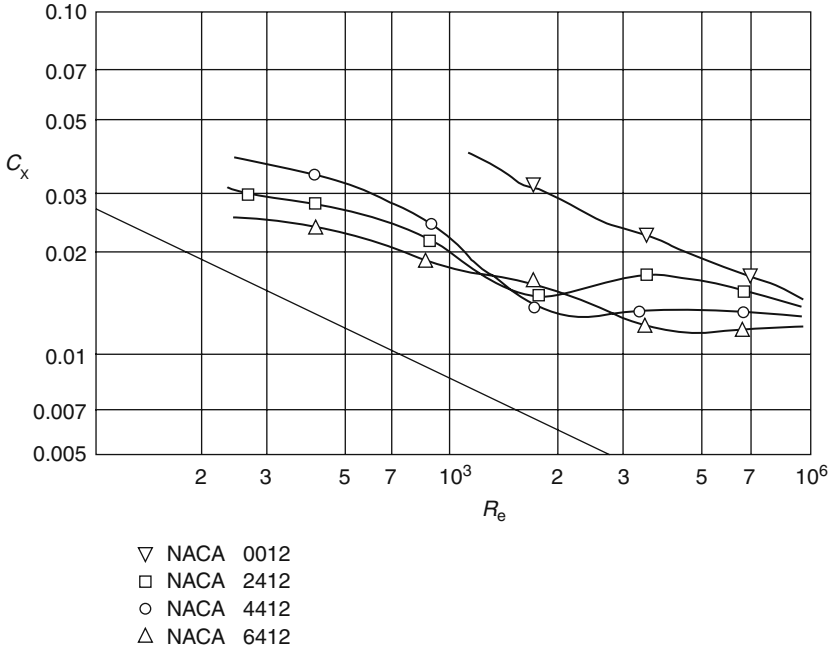

Fig. 9.5 C_y versus Re for different aerofoils NACA 00/24/44/64 – 12

thruster feed, where air leaks away into the free air stream. Increasing the forward speed reduces this decay, increasing the air gap under the cushion, until take-off occurs and ground effect can be utilised fully for support.

Reynold's Number of the Tailplane, Fin and Rudder (Re_4)

Reynold's number is particularly important for the tailplane and elevators, which strongly influence the longitudinal stability.

$$\mathrm{Re}_4 = V_s L_r / \nu_a \tag{9.3}$$

where

V_s Craft speed
L_r Chord length of tailplane or fin/rudder

The tailplane is the key component for maintaining positive longitudinal stability and vertical force balance about the WIG CG in flying mode. Determination of the correct angle of attack for installation of the tailplane is therefore essential. Figure 9.7 shows the relative aerodynamic centre X_{dc} versus tailplane installation angle of attack Π of a typical DACWIG model. It can be seen that the larger the

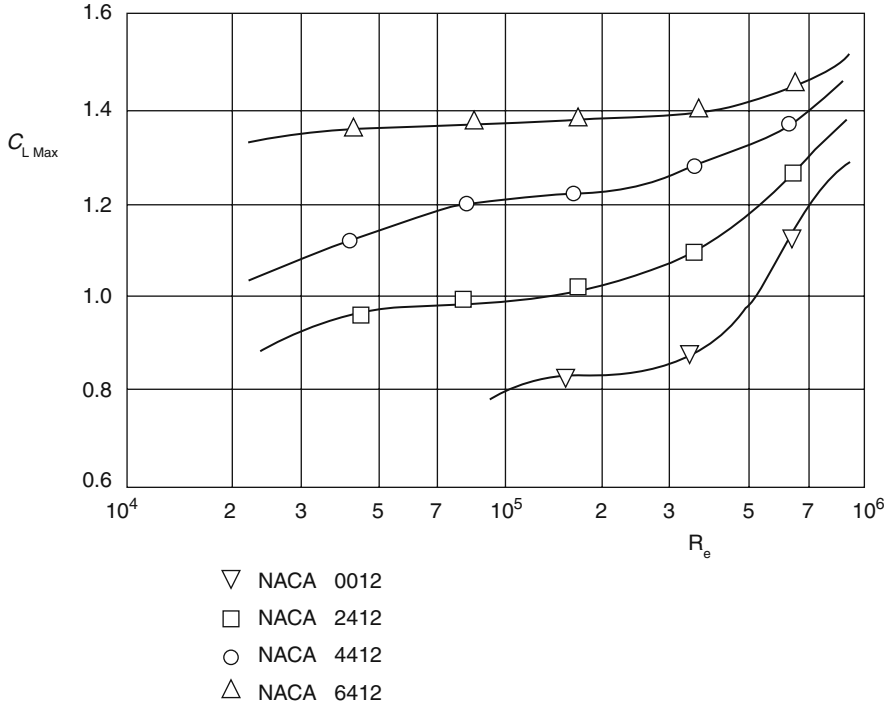

Fig. 9.6 C_x versus Re for different aerofoils NACA 00/24/44/64 – 12

horizontal angle downward, the more the equilibrium CG of the craft model moves rearward, as the lift force on the tailplane increases.

Figure 9.8 shows the relative pitching moment versus the aerodynamic lift coefficient C_y of a DACWIG from a wind-tunnel model test with two different tailplane

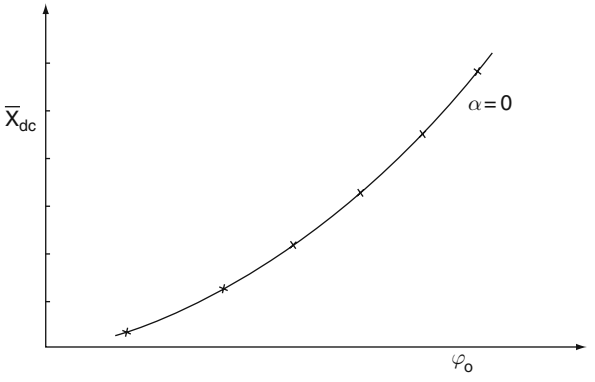

Fig. 9.7 Relative aerodynamic centre X_{dc} versus installed angle of horizontal stabilizer of a typical DACWIG model

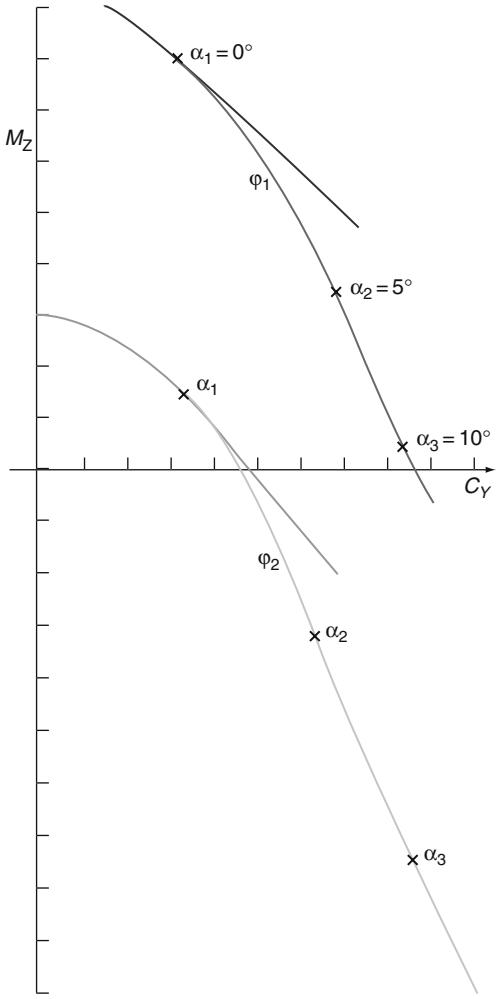

Fig. 9.8 M_Z versus C_y of a typical DACWIG model

installation angles, $\prod_1$ and $\prod_2$. During this model test, the relative flying height $\overline{h}$ is in strong GEZ, flap opened fully, and guide vanes turned horizontal, which is a typical position of controls for a DACWIG flying after take-off.

The slope of these curves represents the longitudinal position of the aerodynamic pitching centre (or aerodynamic centre of lift increment) with respect to the trim angle, $\overline{X}_{F9}$. From Figs. 9.7 and 9.8, it can be seen that the tailplane angle of attack strongly affects $\overline{X}_{F9}$ and also the aerodynamic centre of lift increment due to pitch for the model.

One question is whether the model test results will be representative at full scale. Table 9.3 shows an example of Re_4 for models and a full-scale craft.

Table 9.3 Re_4 for different models and full-scale craft

	Model No. 1	Model No. 2	Full-scale craft
Scale ratio	13	6.5	1
Re_4	5E4	1.4E5	1.95E6

The value of model No. 1 Re_4 is too small to correctly model tailplane stabilizer and rudder lift coefficient. It is found that the difference between experimental and two-dimensional data (infinite AR) from tests at high Re of standard airfoil forms is significant. Sometimes the 2D value is as large as twice that of test results for WIG. This is mainly due to the difference in Re. Remedial measures for improving the design data for stability and longitudinal force balance are

- Use a larger model with Re_4 larger than critical Re (approx. 1E5)
- Adjust the installed angle of full-scale craft tailplane to compensate the difference of lift coefficient between model and full-scale craft

Euler Number (H_q) and Relation to Cushion Pressure Ratio

In order to simulate the external aerodynamics of a WIG craft in a wind tunnel, the cushion pressure ratio has to comply with

$$\mathrm{H_q} = P_c / \left(1/2\rho_\mathrm{a} V_\mathrm{a}^2\right) \tag{9.4}$$

where

$P_\mathbf{c}$ Cushion pressure in the air channel (N/m^2)
$V_\mathbf{a}$ Air velocity (m/s)

According to Table 9.1, $V_\mathrm{a} \propto \lambda^{0.5}$, so the air speed in the tunnel is similar to the craft speed in the towing tank and $\mathbf{H_q}$ is similar to Fn.

Wind-Tunnel Testing

During model testing of WIG in a wind tunnel, after ensuring that Re is modelled correctly, the tunnel surface under the WIG model should ideally be a moving belt of some kind running at the same speed as the airflow or craft speed. This then avoids unwanted boundary layer effects from a static tunnel surface that will cause unrealistic flow in the area under the main lifting wing and make it difficult to analyse the internal and external aerodynamic characteristics.

A rolling ground is not a standard feature in wind tunnels, so alternative methods may have to be used if one cannot be fitted. Three possible approaches are considered first. Figure 9.9 shows the airflow velocity distribution under the wings for WIG tests in a wind tunnel with three types of supported rigid ground [2]. If the wing speed is V_c (i.e. airflow speed in the wind tunnel), then the velocity distribution of the right side of Fig. 9.9 is with respect to the fixed earth coordinate system and the left part with respect to the coordinate system fixed on the wing. Figure 9.9a shows the velocity distribution for the real moving wing of WIG model or craft, and Fig. 9.9b the velocity distribution for a wing in a wind tunnel with fixed boundary surfaces. Since the ground surface is static, the boundary layer influences the velocity distribution of both wing and ground. Figure 9.9c shows the velocity distribution of wing and ground when using the method of wing image, i.e. putting an identical model opposite to the original wing model to eliminate the rigid ground and the boundary layer influence.

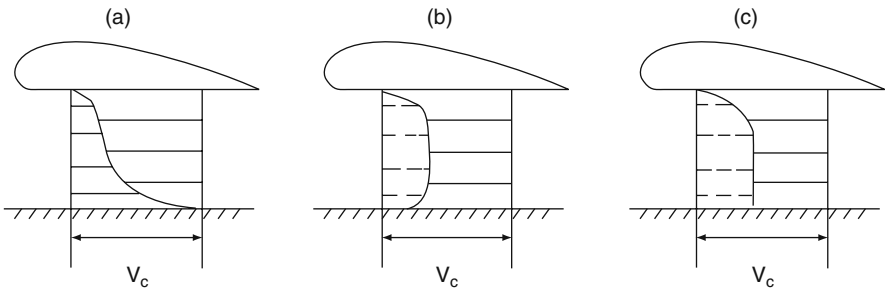

Fig. 9.9 The velocity distribution of airflow under the wings for WIG test in wind tunnel with three types of supported rigid screen

Figure 9.9a shows the real moving wing velocity distribution, i.e. the velocity at the ground is equal to zero and V_c on the wing. The difference between wing and ground is equal to V_c. However, in Fig. 9.9b, the speed difference is zero, and in Fig. 9.9c between 0 and V_c.

Methods (b) and (c) do not correctly simulate the ground boundary velocity. As a result, significant errors in prediction of the wing lift coefficient C_y will occur; too small for (b) and too large for (c). For this reason the Krylov Ship Research Institute (KSRI) in Russia has established a large wind tunnel with a moving ground as shown in Fig. 9.10, to eliminate the test errors mentioned above and obtain more precise test results for WIG [3]. Figure 9.10a shows the overall arrangement, including the moving ground plate arrangement with circulating belt and static leading edge. The ground plate is supported on hydraulic jacks for adjusting the ground level and angle, see Fig. 9.10b.

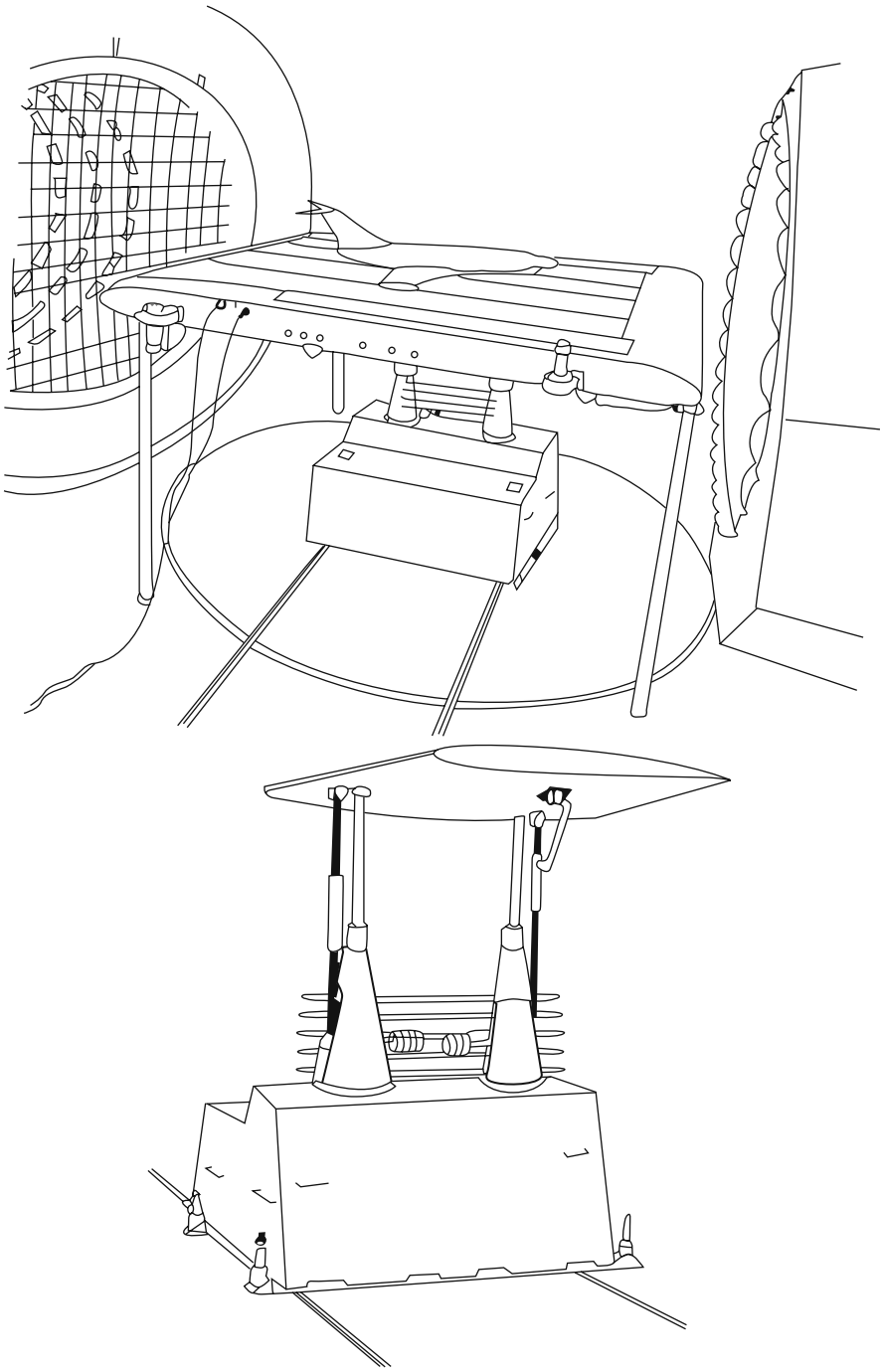

Fig. 9.10 "Moving screen" equipment in wind-tunnel laboratory of KSRI of Russia

The leading particulars of the KSRI wind-tunnel laboratory are as follows:

Dimensions of working section of the wind tunnel	$4 \times 4 \times 2.3$	m
Maximum wind speed	100	m/s
Velocity field non-uniformity	<1%	
Maximum down wash and lateral wash angle	$\pm 0.3, \pm 0.5$	degrees
Maximum Re (for full craft model)	2 E7	
Linear velocity of moving ground	30	m/s

An alternative method, a fourth approach, aimed at decreasing the boundary layer influence on a static ground plate is to make two slots in the ground plate connected to small suction fans and also mount two disturbance plates under the slots so as to make a turbulent flow and a suction field under the slots. The boundary layer thickness can then be reduced effectively. Figure 9.11 shows a general arrangement of the slots and disturbance strakes in a wind tunnel, the dimensions of which are: test section length 1.95 m and test section diameter 1.5 m. Two slots are located at 800 mm and 1,200 mm from the leading edge of the ground plate, respectively, with a width of 30 mm. The inclination angle of the disturbance strakes is 60°.

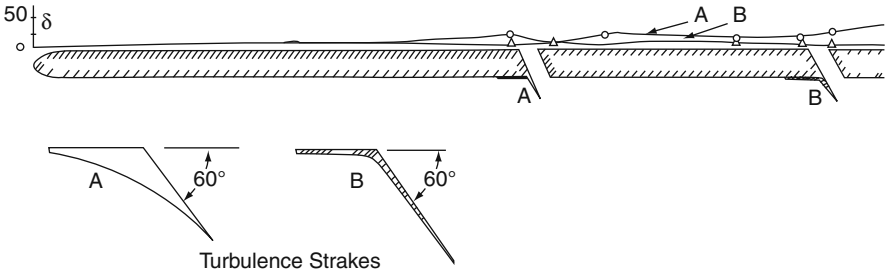

Fig. 9.11 The distribution of boundary layer thickness on the rigid screen of the wind-tunnel facility

The turbulence generator strakes have to be made with knuckles to give more effective turbulent flow under the slots as shown in Fig. 9.11. Boundary layer thickness at the rear part of the plate can be reduced to as low as 10 mm for the knuckle-type turbulence strake, but 55 mm for the smooth-type turbulence strake. The calculated boundary layer thickness without the turbulence equipment is about 30 mm so the equipment is useful for reducing the boundary layer influence in the wind-tunnel laboratory.

Bow Thruster or Lift Fan Non-dimensional Characteristics of DACC and DACWIG

The bow thruster non-dimensional characteristic is most important for correctly simulating static hovering performance, speed performance, longitudinal stability,

take-off, wave impact loads on the hull, etc. Since the bow thruster can be either a ducted air propeller or an axial fan, two types of scaling criteria can be used as follows.

Air Propeller Type

$$K_t = f\left(\lambda_{\mathrm{p}}, \mathrm{Re}\right) \tag{9.5}$$

where

$$K_{\mathrm{t}} = T/\rho_{\mathrm{a}} n^2 \mathrm{D}^4$$

$$\lambda_{\mathrm{p}} = V_s/Dn,$$

the influence of Re has been discussed in the previous section.

- T Thrust of the air propeller (N)
- ρ_{a} Air density (N s/m)
- n Propeller speed (r/s)
- D Diameter of propeller (m)
- K_{t} Thrust coefficient of propeller
- λ_{p} Advance ratio of propeller

In this case, if the non-dimensional thrust characteristic is correctly modelled, the lift–thrust ratio can be used as a design criterion for predicting the static hovering performance of the WIG.

Ducted Fan Type

$$\overline{H}_{\mathrm{j}} = H_{\mathrm{j}}/\left[\rho_{\mathrm{a}} n^2 D^2\right] \tag{9.6}$$

$$\overline{Q} = Q/\left[nD^3\right] \tag{9.7}$$

where

- $\overline{H}_{\mathrm{j}}$ Non-dimensional pressure coefficient of ducted fan
- $\overline{Q}$ Non-dimensional flow coefficient of ducted fan
- H_{j} Overall pressure of fan (N/m)
- Q Flow rate of fan (m/s)
- N Fan speed (r/s)
- D Diameter of fan impeller (m)

The fan-specific speed can be written as follows for selecting the type of fan in preliminary design.

$$\mathrm{Ns} = \left(\overline{Q}\right) / \left(\overline{H_{\mathrm{j}}}\right)^{0.75} \tag{9.8}$$

In model experiments, it is difficult to satisfy this criterion due to the higher speed of model electric motors. In this case, one can take lift–thrust ratio as the design scaling criterion in the case of Re larger than critical Re, otherwise take Euler number H_q as the design scaling criterion.

Froude Number, Fn

From Chapter 7, WIG total drag before and around the take-off speed is expressed as:

$$R = R_{\mathrm{hw}} + R_{\mathrm{sww}} + R_{\mathrm{aw}} + R_{\mathrm{hf}} + R_{\mathrm{swf}} + R_{\mathrm{a}} + R_{\mathrm{fl}} \tag{9.9}$$

The main drag force in this mode is wave-making drag caused by hull, sidewall and air cushion. In addition, the friction drag of hull and side buoys depends on the craft's running trim. In short, WIG drag before take-off is similar to that of an SES or hydroplane. This drag force characteristic can be obtained by model experiments in a towing tank. Scaling of the forces will then be carried out using the Froude number Fn as the criterion.

$$\text{Where } \mathrm{Fn_c} = V_s/\sqrt{gC} \text{ or } \mathrm{Fn_d} = V_s/\sqrt{gw^{\frac{1}{3}}} \tag{9.10}$$

V_s Craft speed (m/s)
C Wing chord (m)
W Craft displacement (m^3)

Weber Number, We

During the investigation of WIG spray formation, the relation between inertia force and surface tension of water has to be taken into consideration. The size and direction of the spray droplets are a function of We, where

$$\mathrm{We} = \left(\rho_w V^2 L\right) / \sigma_s \tag{9.11}$$

where

ρ_w Density of water ($N\ s^2/m^4$)

V Speed of water flow (m/s)
σ_s Surface tension of water (N/m)

Since σ_s and ρ_w for both model and full-scale craft are constant, then $We \propto \lambda^2$, $We_s \gg We_m$. This means that spray from full-size craft will be significantly greater than at model scale, and the spray droplets on the full-scale craft will be much finer than that of a model.

This phenomenon has been observed during testing of model and full-scale craft, which affect the spray drag and pilot vision as well as the water spray ingestion into the bow engines.

On the Orlyonok WIG, there are turbojet engines mounted in the fuselage nose as bow thrusters. The higher the speed of the exhaust gases from the engine's nozzle, the more intense is this cloud of spray. Jet engines produce the largest spray cloud while the air propeller engine produces smaller such clouds. The process of water spray generation due to "under wing gas-air jets" on some WIG craft, like the Orlyonok, cannot be simulated in model experiments, so the analysis of full-scale trails data is important for such designs. So far there is no published data available.

Other Scaling Terms for Towing Tank Test Models

From Chapter 7 , we have the total resistance of WIG; R is equal to the measured drag plus the effective thrust of bow propellers as follows:

$$R = R_t + T_d.\eta_{Td} \tag{9.12}$$

$$\eta_{Td} = (R_{a3} - R_{a2}) / T_d \tag{9.13}$$

$$\eta_{Td} = f\left[V_{jo}/V_s, V_r/V_{jo}, \gamma, \beta, \vartheta, \bar{h}\right] \tag{9.14}$$

The critical data to obtain from wind-tunnel tests is the thrust recovery coefficient. In Equation (9.13), R_{a2} and R_{a3} represent the air drag of the model without bow thruster and with rotating bow thrusters, respectively. However, both R_{a2} and R_{a3} are large values with similar accuracy (or inaccuracy ...). According to the theory of probability, the result of subtraction of two large test values is a value with a large error. For this reason, it is difficult to obtain a precise thrust-recovery coefficient from wind-tunnel testing.

Equation (9.14) proposes that η_{Td} is a function of various parameters, such as

V_{jo} Speed of jet flow after the bow propeller
V_s Craft speed
V_r Airflow speed at the trailing edge exit under the main wing
γ, β Angle of flap and thruster guide vanes, respectively
ϑ Craft trim angle
$\bar{h}$ Relative flying height

It is also very difficult to determine the thrust-recovery coefficient by calculation. Perhaps the best way to obtain η_{Td} is to put a strain gauge probe on the bow thruster to test the thrust directly.

$$\text{Then } R = R_t + \mathrm{T_d} \tag{9.15}$$

where

R Total resistance of the model
R_{t} Measured resistance of the model
T_{d} Dynamic thrust of the bow propellers

Structural Simulation

It is not possible to scale the structural rigidity of the model from the real craft. In general, the structural rigidity of a model is much greater. The structural deformation at full scale will be significantly greater than that of the model due to the scale effect. In addition, since the static hovering height (i.e. the gap between the ground and base plane of both main hull and side buoys during craft static hovering) is rather small, the structural deformation will significantly influence the craft aerodynamic properties, particularly in case of static hovering. The aero-elasticity effect will thus influence the model aerodynamics particularly in tests of amphibious characteristics.

Figure 9.12 shows the hull and sidewall structural deformation of a typical DACC or DACWIG, exaggerated. It is assumed that the aerodynamic lift is acting on the main wing uniformly, and most of the craft weight is concentrated in the main hull. During static hovering, the main wing is deformed upward and main hull downward, consequently significant cushion flow leaks outward under the side buoys and outer wing section trailing edge, while the hull still touches the ground. Higher cushion airflow is required to give a particular hovering height for the full-scale craft than predicted by model tests, as the model will be stiffer than the full-scale WIG. This needs to be corrected by analysis of the full-scale craft wing deflection when hovering, and additional airflow provided to account for this.

The deformation of the structure will be higher on a riveted hull structure compared to a welded aluminium hull due to the small movements of rivets in their joint holes on the plates of the craft and so this influences the aero-elastic properties of the craft. Since riveted structure would normally be selected so as to design for strength rather than stiffness, it would be natural for greater flexibility to be present. This may influence the designers' choice of structural design for the hull and main-wing section for a WIG, so as to obtain the stiffest possible structural configuration.

Scaling Criteria

Some of the scaling criteria and terms discussed above, which have to be complied with in the model experiments, are listed in Table 9.5, where λ represents the linear scale ratio.

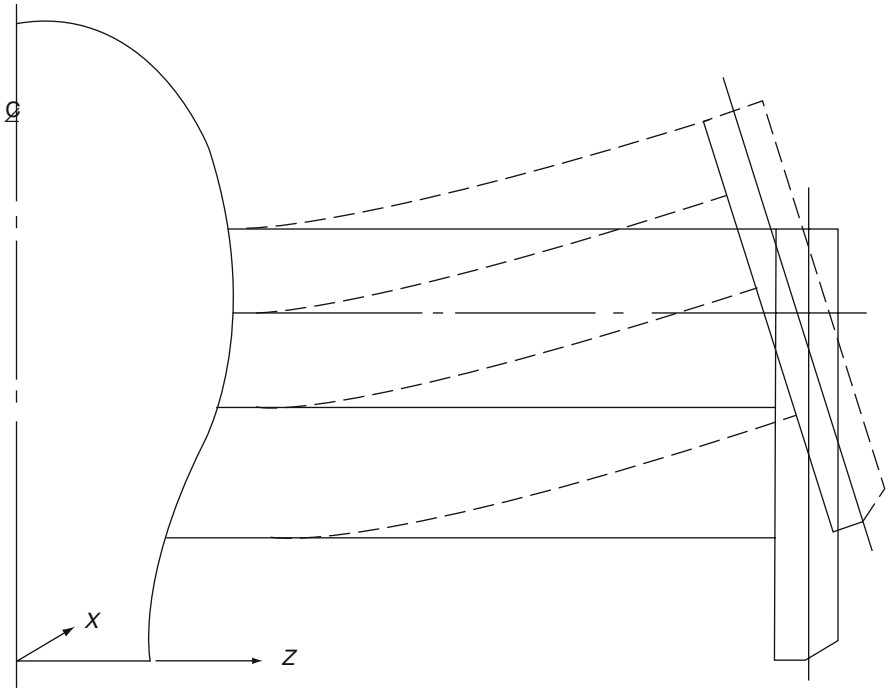

Fig. 9.12 Deformation of the structures of typical DACC and DACWIG in static hovering

Model Test Procedures

A flow chart showing typical model experimental investigations of the aerodynamics and hydrodynamics of WIG and how they fit into the design sequence is shown in Fig. 9.13

There are three main tests to be carried out as follows:

- Static hovering test of the models over ground (including a few tests of model clearing obstacles on ground)
- Wind-tunnel aerodynamic tests on rigid ground plate, either moving or with boundary layer control slots
- Hydrodynamic test in a towing tank and radio remote control self-propelled model tests in open water, as well as manned craft tests

The relation between the three test series and between these experimental investigations compared to theoretical calculation is illustrated in Fig. 9.13.

Table 9.5 Scaling criteria and terms to be complied with in WIG model experimental testing

Item	Simulation criteria	Used in what kind of tests	Practical possibility	Degree of influence	Remarks
1	Re_1 (Re with respect to jet flow after bow thrusters)	(1) Static hovering on ground (2) Wind-tunnel test (3) Radio remote control model free flying (4) Towing tank tests	1. Impossible 2. $Re_1 > Re_c$	On the mixture of airflow Medium	
2	Re_2, Re_3 (Re with respect to bow ducted air propeller blades and duct)	(1),(2),(3),(4)	1. Impossible due to high speed of electric motor 2. $Re > Re_c$	1. Very high influence on (1) 2. High influence on others	1. Enlarged model for $Re > Re_c$
3	Re_4 (Re with respect to stabilizers and rudders)	(2),(3),(4)	1. Very difficult 2. $Re > Re_c$	1. Strong affect to stability of running model 2. Lead to misunderstanding the stability of design craft	1. Enlarged model for $Re > Re_c$, 2. Otherwise, carefully designing the stabilizers and rudders of real craft
4	Non-dimensional characteristics of bow air propeller K_t	(1),(2),(3),(4)	1. Possible, if $Re_2 > Re_{c2}$ 2. Otherwise, no use	Great influence on all tests, particularly (1)	Enlarged model for $Re > Re_c$
5	Non-dimensional characteristics of bow lift fan $\overline{H}_j$,$\overline{Q}7$	(1),(2),(3),(4)	1. Possible if $Re_2 > Re_{c2}$ 2. Otherwise, no use	Great influence on all tests, particularly (1)	Enlarged model for $Re > Re_c$
6	Euler number H_q	(1),(2),(3),(4)	Possible	Great	
7	Lift–thrust ratio $= W/T_o$	(1),(2),(3),(4)	1. Possible if $Re_2 > Re_c$ 2. Otherwise, take H_q as the design criterion	Great influence, particularly on static hovering performance	Enlarged model for $Re_2 > Re_c$

Table 9.5 (continued)

Item	Simulation criteria	Used in what kind of tests	Practical possibility	Degree of influence	Remarks
8	$V_g = V_s$, where V_g is the linear moving speed of rigid ground in wind tunnel	(2)	Possible, but too expensive	Medium	If no moving ground, take slot equipment on ground
9	Fn	(3),(4)	Possible	Great	
Item	**Simulation criteria and terms in tests**	**Used in what kind of tests**	**Practical possibility**	**Influence degree**	**Remarks**
10	We	(3),(4)	Impossible	Influences spray forming	
11	Thrust-recovery coefficient, $(R_{a3} - R_{a2}) / T_d$,where T_d is the dynamic thrust on a single thruster separated from the craft, R_{a3} is the drag of model with rotating bow thrusters and R_{a2} drag of bare model	(2),(4)	1. In wind-tunnel test, it can be taken, but not precise 2. In towing tank, strain gauge probes can be taken for measuring the dynamic thrust of bow thruster on model	Medium	(1) Is possible, but not precise (2) Rather difficult to mount
12	Aero-elastic simulation Structure problems	(1),(2),(3),(4)	Impossible	Great influence on (1)	If according to model test data, carefully predicting the static hovering height of real craft

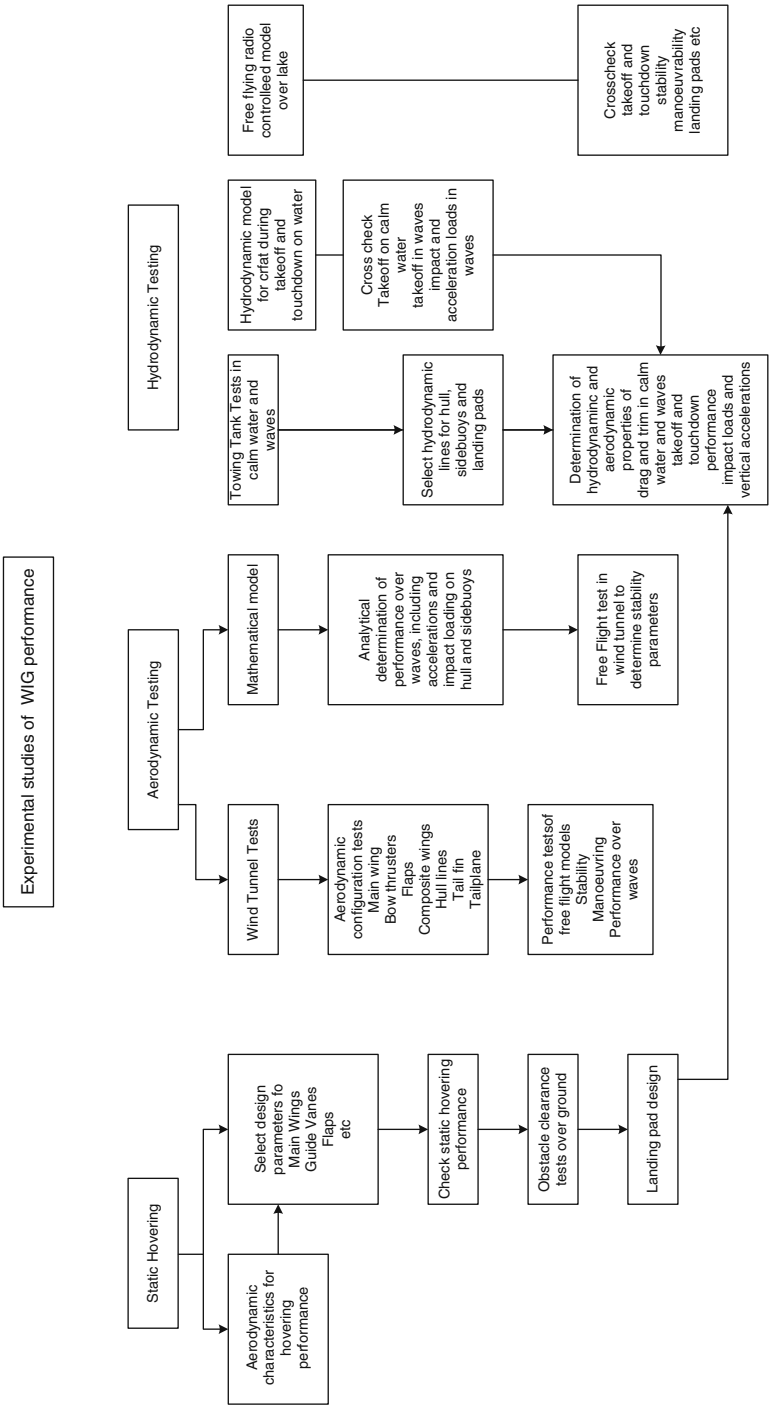

Fig. 9.13 Block diagram for model testing and its relationship with preliminary design of WIG

Chapter 10
Structural Design and Materials

Introduction

The structural configuration of a WIG comprises the same key elements as an aircraft – in particular a flying boat, see Fig. 10.1. The payload of freight or passengers is contained in a fuselage or hull. To each side are wing structures, and at the stern there will be either a single or a pair of vertical fins with rudders and a large horizontal stabiliser with elevator surfaces.

The wings on a WIG have much deeper chord than a typical aircraft's wings and support large floats or "side buoys" at their tips. Beyond the side buoys, there are normally further smaller wings that have significant dihedral and are fitted with ailerons. The main wings may be horizontal, or have negative dihedral, and may either be rectangular or tapered. The figures of various craft shown in chapter 2 give a feel for the diversity of WIG geometry.

In addition to the main structural elements, a WIG will normally have propulsion systems and in most cases also bow thrusters for low speed lift or air cushion assist power system installed over and in front of the main wing. The structures in this area have to be designed to transmit the thrust forces efficiently into the WIG airframe, with minimum possible stress concentrations.

The fin and tailplane for a WIG can be designed following aerospace practice, with the addition of using materials that will be resistant to corrosion in a salty environment. The main hull can be designed following flying boat practice, with global structural design for the normal set of flying load cases, and the lower surfaces designed for planing pressure loads and slamming loads in a seaway for the speeds below take-off.

The main wings will be configured in a similar way to aircraft wing structures, but the design cases will be more complex since the air cushion-assisted lift below take-off speed will induce different load distributions to the lower and upper surfaces. There will be significant bending moments applied to the main wings by the hydrodynamic loads under the side buoys at speeds up to take-off.

One aspect of aircraft design that does not have to be tackled by the WIG designer is cabin pressurisation. Since a WIG typically does not fly at any significant altitude, pressurisation is not necessary.

L. Yun et al., *WIG Craft and Ekranoplan*, DOI 10.1007/978-1-4419-0042-5_10,

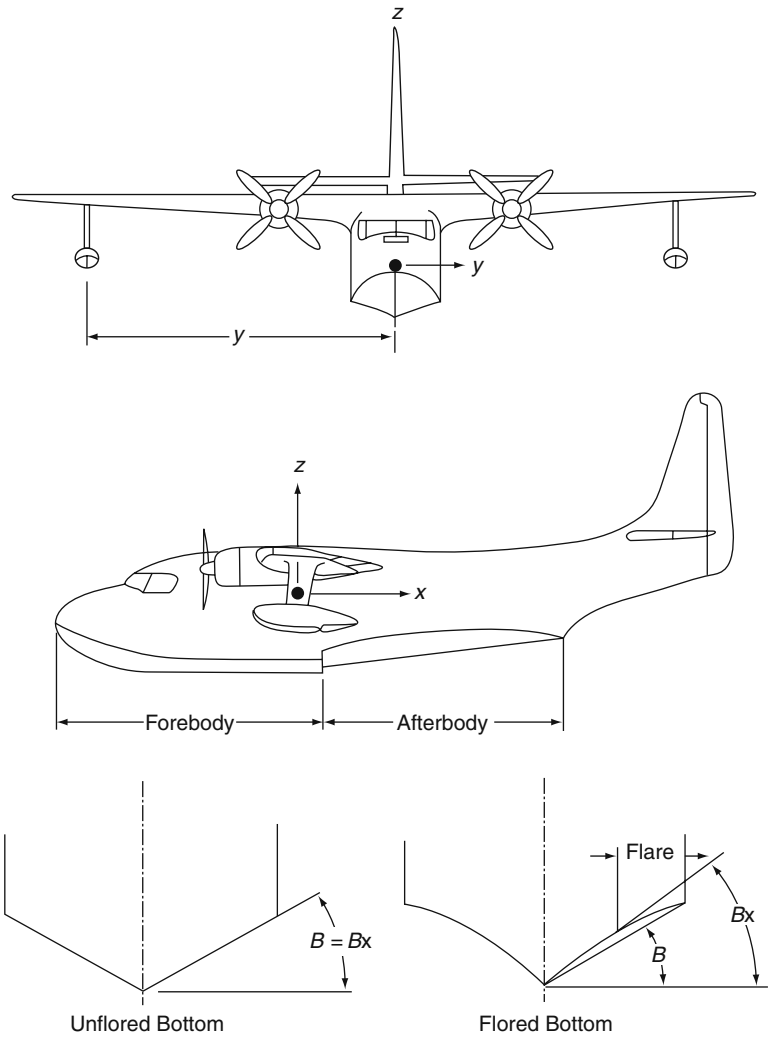

Fig. 10.1 Flying boat hull planing surface geometry

In this chapter, we will discuss the structural design approach for WIG-referencing standard aircraft and high-performance marine craft design practice where it is applicable. Once the principles have been established, readers will find texts such as [1–4] provide a basis for developing their WIG structure design as such. Since these texts provide the detailed background and tools needed for design, we concentrate here on the application to WIG craft and any key differences that need to be taken into account.

Structural design and construction of WIG vehicles requires a combination of aircraft and high-performance marine craft technology. Aircraft structures are generally expensive, since successful aircraft design requires a very light airframe

to maximise the payload ratio and minimise the required power at cruise speed. This leads to use of high strength materials and design against strength and fatigue criteria. Structural stiffness is not the controlling design parameter for the majority of an airframe.

In contrast, WIG design is controlled by stiffness for the majority of the structure. In addition, the lower part of the main hull and side buoys need to be designed to marine practice for a WIG. In addition, to be commercially successful, a WIG needs to have a lower cost than an aircraft. High-performance marine craft structural design is much more cost-effective than using aircraft materials and techniques but, in general, is still too heavy to provide the performance and operating efficiency needed for a successful WIG vehicle if the whole craft is built using marine practice.

The most promising approach is to combine and integrate the technology developed in these two industries and carefully apply the appropriate design and analysis methodologies, material database and manufacturing techniques. Due to their high strength, corrosion resistance, cost-effectiveness for medium-scale structural fabrication and low weight, modern composites are a very attractive material for WIG application, just as for fast marine craft. However, well-established aircraft metallic materials are not to be ignored as they have proven to be suitable for lightweight structures and their application is supported by a wealth of design and test data.

Modern high-performance commercial aircraft structures are generally speaking highly stressed. Transport class aircraft, especially lower airspeed turboprop utility aircraft, are more comparable to medium-size WIG with similar take-off weight due to similar design speed and loading density.

To define the structure of our WIG design, we need to gather information on composites for smaller/medium-size craft and more traditional metallic structural design for upper fuselage and wing/side buoy structures. Reference [5] gives a general introduction to the characteristics of metallic and composite structural materials. The lower part of the fuselage or hull will need to be constructed of either welded aluminium or composite material. Lastly the main hull needs to be compartmented to conform with the requirements of the IMO Code of Safety for WIG craft, see reference Chapter 13 [6]. DACWIG craft can also usefully make reference to the IMO High Speed Craft code, Reference [6], as the WIG is fundamentally a marine vehicle.

The geometric configuration, design speeds, weights and loading as well as operating conditions define the design loads required to begin a safe WIG structural design, so we will begin by examining the loads and develop the load cases needed to analyse the structure. Materials are the next item to be tackled, followed by some discussion of structural configuration.

Design Loads

WIG structural design is more challenging than that of any other type of fast marine craft, mainly due to its varied operating conditions from low-speed waterborne operation, transitions to planing and take-off, followed by ground effect operating mode and out-of-ground effect mode for some special craft. Speeds of up to 400 knots

at low operating altitude, wave impact, take-off and landing loads as well as bird strike all have to be taken into consideration in the design process. Take-off and landing operations in rough water at speeds from 50 kph up to 150 kph involve hydrodynamic forces much larger than experienced by all except the fastest marine craft.

Waterborne and Pre-take-off Loads

When a WIG is operating in waterborne mode, the structural loads are similar to that of a surface effect ship. The hull and wing loads are from the cushion pressure and the buoyancy and hydrodynamic planing forces on the hull and side buoys. References [2] and Chapter 7 [5] give some guidance on estimation of these loads and [7] some of the background theory, both related to seaplanes and flying boats. Reference Chapter 2 [1] gives the background on cushion loads for either SES or ACV configurations.

For WIG designed with a fuselage and wing configuration such as the Russian Orlyonok, the lift forces on the main wings are much lower until speeds close to take-off are reached. Flying boat design experience is directly applicable, see Fig. 10.2. For WIG with an air cushion under the main hull, SES experience can be the best source for deriving the hull design loads, for example the data shown in Fig. 10.3.

Wing loads can be varied depending on the WIG geometric configuration. For classic WIG designs, when the craft is at low speed, the wing is often very close to or contacting the water. The water impact load on the side buoys, and consequent bending moment, is then significant compared to the uniform loading on the wing itself. For PARWIG designs, the wing uniform loading is higher due to the air pressure generated by the jet engine, propeller or ducted fan, so the loads on the side buoys are lower. In both cases, the flap at the main-wing trailing edge is subject to significant water impact load during the take-off run.

Wing loads are derived from five main sources:

- Pressure load generated by the forward velocity induced ram air pressure
- Pressure loads generated by the power source – jet engine, propeller or fan
- Under-pressure on the wing top surface generated by the airfoil section
- Wave impact loads (localised loads on side buoys and trailing edge flap)
- Wing-mounted propulsion/lift system induced loads (if applicable)

The total fuselage design loads should include the bottom surface pressure and hydrodynamic planing loads together with the wing and tailplane aerodynamic loads when deriving the shear force and bending moment diagrams for design and stress analysis.

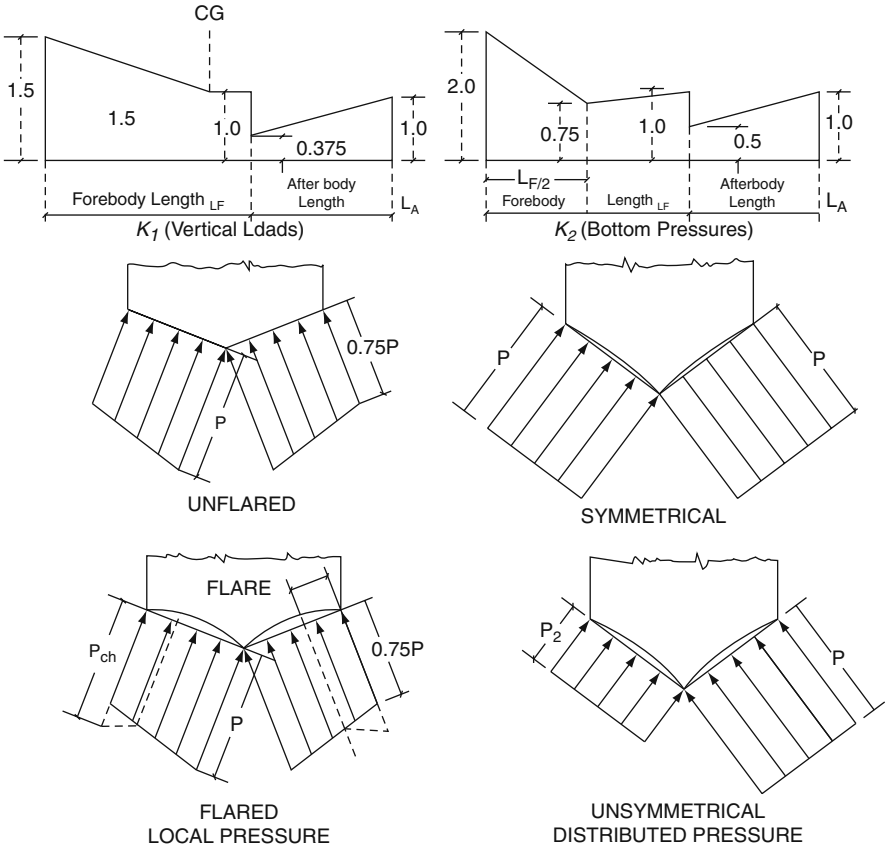

Fig. 10.2 Pressure distribution on flying boat planing surfaces

Take-Off and Landing Loads

For small to medium size WIG, the water surface take-off and landing loads can be derived from the basic criteria developed for seaplanes, as shown in Figs. 10.1 and 10.2. The US Federal Aviation Regulations (FAR) design documentation provides one suitable means to calculate take-off and landing design loads. References [2, 7] also give useful guidance.

For very large WIG, these loads require detailed computation through finite element analyses and experimental work for verification. Recent advances in computational fluid dynamic analysis (CFD) allow dynamic simulation of a variety of wave interactions with large WIG structures that can provide more precise design criteria and optimised loads.

The loads applied to the main wing from the flaps when they are lowered for hovering, take-off and landing need to be included in the structural analysis. Guidelines are shown in Fig. 10.4.

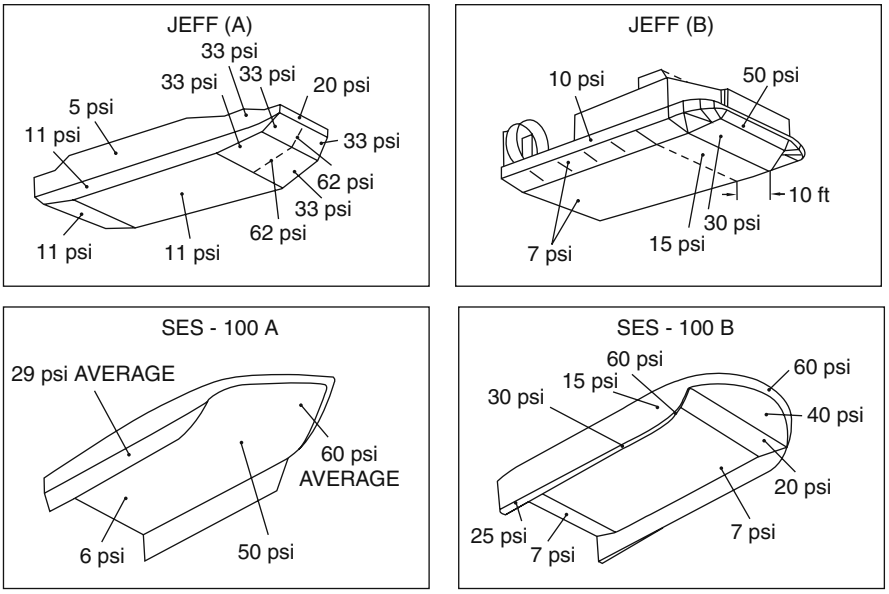

Fig. 10.3 Cushion craft hull design loads

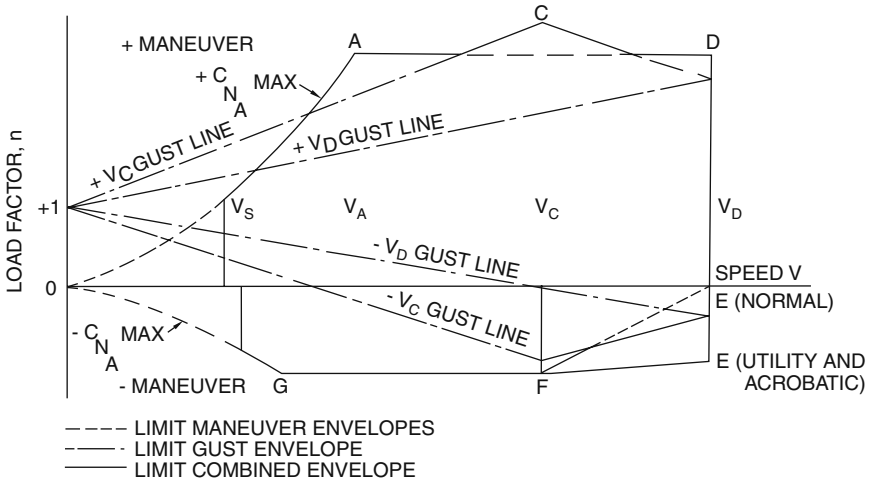

Fig. 10.4 Manoeuvring load factors, when flaps are lowered and retracted

Ground-Manoeuvring Loads

Most WIG equipped with landing gear are not designed to take-off or land on these devices but rather they are used as low-speed ground-manoeuvring devices. The design loads are much lower than aircraft landing gear allowing lighter systems and

also limiting the concentrated landing gear loads that have to be handled by the fuselage or the wing structures.

For WIG designed without landing gear, the keel structures will have to be designed to handle the ground impact load. Deleting landing gear is only practical for DACC and DACWIG that are able to support themselves on an air cushion at zero speed. The worst case loading for landing pads for such craft is 1 g and a suitable sharing of the craft weight between pads, bearing in mind the likelihood of settling on a minimum of one pad initially, and rotating onto the remainder.

Flight Loads

Steady Flight

During steady flight, a WIG is supported by lift forces on the main wings and the outer wings in the form of a pressure distribution. The tailplane will also provide a smaller lift force to maintain steady altitude.

Gust Loads

For small- to medium-size WIG, the discrete gust loading approach by applying the US FAR gust load factor equation, see Fig. 10.5 provides reasonable structural design criteria. For large WIG designs, the power spectral approach allows better

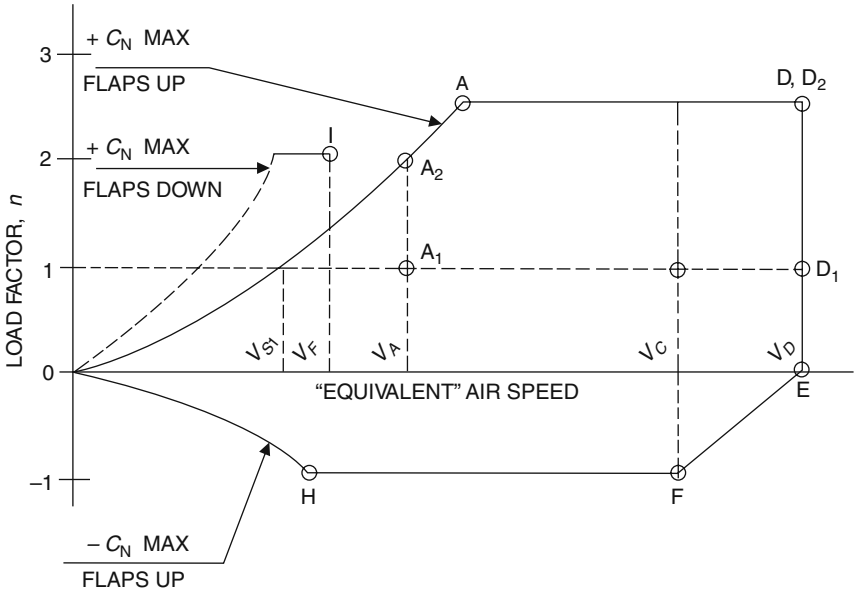

Fig. 10.5 Load factors for design in gusts and when manoeuvring

tuned design load factors that can provide the required structural integrity with loads better tailored to the design-operating envelope and mission.

Manoeuvring Loads Including System Malfunction

An aircraft structure has to be designed for an envelope of manoeuvres (climb, dive, turn, etc.) that apply acceleration forces to the structure. A WIG will also be subjected to considerable acceleration forces due to manoeuvring, though the manoeuvres will be more two-dimensional. The following conditions should be considered (Fig. 10.5):

- Elevator manoeuvres for height adjustment in unsteady winds
- Aileron and rudder manoeuvres for banked turns
- Rudder manoeuvres for level turns
- Adjustment of the main wing flaps for "steady" flight height adjustment
- Combinations of elevator, rudder, and aileron manoeuvres
- Engine failure

In each case, the flight control surface movement and also local loading that creates the manoeuvre have to be analysed, and the WIG global structure checked against the manoeuvres themselves.

Aero-Elasticity

Due to the low aspect ratio of the main wing, relatively thick airfoil and low sweep angle, wing deflection under load (aero-elasticity effects) can be ignored for practical design purposes for small- to medium-size WIG.

Most WIG have a medium aspect ratio tailplane and so deflection under dynamic loading should be considered in analysing these loads. Depending on the configuration, in many cases the aero-elasticity effect of the tailplane can reduce the effective manoeuvring forces and consequent loads applied to the surfaces. This will also reduce the manoeuvring envelope at higher speed. The first-order effect can be analysed by using a simplified structure "stick" model to represent the basic stiffness behaviour of the structure. The aero-elasticity effect can cause a significant problem to predict loads accurately and also the controllability of the more "flexible" structure on large WIG.

Impact and Handling Loads

Bird Strike

Since WIG are designed to operate at low altitude and in many cases at medium to high speed, the structures will have to be designed to handle bird impact loads. The windshield and/or cockpit canopy structures, the wing and the tailplane structures all need to be designed such that in case of bird strike, the damage will not cause

a catastrophic result. It is recommended that a 2-kg bird impact at maximum low-altitude cruise speed can be used as a design criterion.

Crash

It is very difficult to have a set of predetermined crash loads because they are unique to each craft design/configuration. However, it is common for aircraft to design to a set of simplified impact loads to enhance the safety of the passengers in case of a crash as shown in Table 10.1.

Table 10.1 Impact load factors

Condition	Load factors
Forward	9 g
Vertical	6 g
Lateral	1.5 g

In addition, the seat and environment design plays an important role in crash safety. The FAR/JAR 25 criteria typically result in 19 g vertical and 16 g forward impact load for occupant protection seat/environment requirements, which is also applicable to WIG design.

Docking, Towing, Hoisting, Jacking and Cargo Handling

A WIG is often designed to be able to operate in a "rough" environment and therefore have to take into account docking, towing and cargo handling loads. In many cases, human induced loads (handling, body weight and impact) are much higher than operational loads for some local structures and system installation design. For services, transportation and maintenance, hoisting and jacking loads should be accounted for in design, applied to the specific jacking or lifting points on the craft.

Design Approach

The WIG designer will define a set of load cases that test the complete operational envelope for the craft. Global analysis of the structure will be carried out for all the load cases with maximum design stresses and fatigue life determined. The controlling load case(s) for the main elements of the structure will be determined from this analysis and the structure dimensions adjusted so that the controlling stresses are within the appropriate criteria for durability. These criteria are normally a combination of limiting extreme stress in relation to the material's yield stress or equivalent (the limit beyond which the material starts to exhibit hysteresis) and limiting the fatigue degradation to an acceptable proportion of the cycles to failure based upon the cyclic loading from operating over waves. The relation of the acceptable design stress to the extreme stress is termed the factor of safety.

Recommended factors of safety (FS) on loadings for WIG structural design are listed in Table 10.2, taking into consideration accepted design practice for high-speed air cushion craft and aircraft. The final choices and the load cases they are applied to will need to be determined between the regulatory body and the craft builder based on the specific design and operating envelope. It should be noted that in addition to these factors of safety, the structural design should be based on safe material utilisation factors taking account of the material ductility and the loading mechanism (extreme loading or fatigue).

Table 10.2 Typical factors of safety

	Loading factors of safety	
Loading condition	Extreme limit state	Service limit state
Hull-borne, ground effect	1.0–1.5	1.5–2.0
Out-of-ground effect	1.0	1.5
Emergency	1.0	1.5
Crash	1.0	n/a
Towing, hoisting, jacking, cargo handling	n/a	2.0–3.0

Some guidance on the general performance of different materials is given in [6]. We will discuss characteristics of some metallic and non-metallic materials applicable to WIG in the next section.

Metallic Materials

Metallic structures, specifically high-performance riveted aluminium plate, sheet, and extruded sections, form the mainstay of aerospace structures. Some magnesium alloy is used and titanium for heavily loaded components. Seaplanes and flying boats use aluminium alloys that are more corrosion resistant. These alloys are lower strength materials than used on commercial aircraft. A large amount of material property data are readily available through industry sources and also from government databases in the United States and Europe. For the speed range of the modern day WIG, aluminium alloys remain the most suitable primary structure material for medium- and large-size craft.

Since WIG operate in waterways and open seas, corrosion resistance is critically important and this can be addressed starting from the material selection. Ease of construction is also an important factor.

WIG need to be less expensive than an aircraft, so the more exotic high strength alloys used in large commercial aircraft will not be the best choice. Two base families of aluminium alloy stand out as attractive for WIG application.

- The 20 series including 2024 and 2014 material are produced in large quantity, making them very cost-effective with the wealth of material test data available to support the design analysis.

- The 60-series aluminium alloy is another commonly available alloy that, although having lesser mechanical properties, is able to be welded, allowing components and structure assemblies to be constructed much more simply and cheaply than riveted assemblies. This is particularly useful for larger structures. The familiar 6061 aluminium alloy is a useful example. Also a newer family member 6063 demonstrates far better mechanical properties as well as stress corrosion properties than its predecessor, so it may be considered as one of the most usable aluminium alloys for welded structure design for the marine environment. The physical properties of 6013 alloy sheet are given in Table 10.3.

Table 10.3 6013 Aluminium alloy material properties

Specification	AMS 4216 and AMS 4347		
Form	Sheet		
Temper	T6		
Thickness, in.	0.010–0.062	0.063–0.125	0.126–0.249
Basis	S	S	S
Mechanical properties:			
F_{tu}, ksi:			
L	52	52	52
LT	52	52	52
F_{ty}, ksi:			
L	47	47	48
LT	46	46	46
F_{cy}, ksi:			
L	48	48	48
LT	48	48	49
F_{sm}, ksi:	32	32	32
F_{bru}[a], ksi:			
(e/D=1.5)	85	85	85
(e/D=2.0)	111	111	111
F_{bry}[a], ksi:			
(e/D=1.5)	66	69	71
(e/D=2.0)	76	80	82
e, percent:			
LT	8	8	8
$E.10^3$ ksi:		9.9	
$E_{e.10}{}^3$ ksi:		10.1	
$G.10^3$ ksi		3.8	
μ		0.33	
Physical properties:			
ω, lb/in.^{3}		0.098	
C, K, and α		...	

[a]Bearing values are "dry pin" values per Section 1.4.7.1.

Stainless steel is also very useful for WIG application due to its high ultimate to yield the strength ratio F_{tu}/F_{ty} in conjunction to the very best corrosion resistance. With their higher strength and stiffness than aluminium, stainless steel alloys are suitable for highly loaded structural elements such as engine mount attachments and wing joints. The 304 grade stainless steels are useful for limited exposure to salty environments, though if the structural component is likely to become heated, it will be wiser to utilise either 316 grade or 6Mo stainless alloys.

It is important to pay special attention to the finishing process of stainless steel as this can significantly affect corrosion resistance characteristics. A finely polished part will demonstrate significantly better corrosion resistance than a roughly machined or a welded stainless steel element without proper surface finishing or chemical cleaning.

There are many other metallic material families that are suitable for specific WIG structure applications. Careful evaluation is required of material strength, corrosion resistance properties, fatigue and crack growth characteristics, cost, suitable fabrication and process methods for durable, light-weight and cost-efficient structural design to be achieved. A summary of material properties for a selection of candidate materials is given in Table 10.4.

Composite Materials

Composite material has been widely used in marine design for many years. The same can be said for the kit-build aeroplane industry in the United States and Europe over the last 20 years. The business and commercial airplane industry took longer to build up a certifiable database and consistent process control suitable for large airplane structure assemblies and so has begun its application more recently.

Marine design applications, especially high-performance racing boat design has similarities to the design requirements for small WIG design application. For larger structures, the material and processes developed for the aerospace industry is better suited to WIG. The corrosion resistance and water tightness characteristics of a composite structure lend itself to WIG applications.

Composites have somewhat different characteristics to metallic structures, see Table 10.5. Composites are generally more brittle, see Fig. 10.6, showing the stress/strain curve of fibre/epoxy composite. Glass or aramid fibre composites with polyester, vinylester or epoxy have lower stiffness than an aluminium structure for the same function and a similar weight. Designers are able to compensate for the lower stiffness by using sandwich panels with foam of honeycomb materials.

For WIG applications, the temperature and long-term humidity exposure effect on composite material mechanical properties should be account for in design analysis, additional safety factors needs to be applied in most cases.

Table 10.4 Comparison of various metallic and composite materials

		Properties (room temp.)					Structural efficiency	
Material	Conditions	F_{nl} (ksi)	F_{rv} (ksi)	F_{ry} (ksi)	E (10^6 psi)	*Density* ρ (lb/in^3)	F_{tu}/ρ (10^3 in)	E/ρ 10^6 in)
Aluminum	2014-T6	68	56	48	10.7	.101	673	106
	2024-T4 extrusion	57	42	38	10.7	.100	570	107
	2024-T81	64	56	57	10.8	.101	634	107
	2024-T6	78	71	70	10.3	.101	772	102
	7075-T6 extrusion	78	70	70	10.4	.101	772	103
Titanium	6A1-4 V annealed	134	126	132	16.0	.160	838	100
	6A1-4 V heat-treated	157	143	152	16.0	.160	981	100
Steel	4340 180 Ksi H.T.	180	163	173	29.0	.283	636	102
	17-7PH TH1050	177	150	160	29.0	.276	641	105
	AMS6520 Maraging steel	252	242	255	26.5	.283	890	94
	H-11	280	240	240	30.0	.281	996	107
	300 M	280	230	247	29.0	.283	989	102
Nickel	Inconel X-750	155	100	100	31.0	.300	517	103
	A-286	130	85	85	29.1	.287	453	101
Beryllium	Be Cross-rolled, SR200D	65	43	43	42.5	.067	970	634
Magnesium	AZ31B-H24	40	30	25	6.5	.064	625	102
Fibler-glass	Glass/epoxy*	80	"	60	5	.065	1230	77
Kevlar	Kelvar/epoxy*	160		40	12	.05	3200	240
Graphite	Graphite/epoxy*	170		140	22	.056	3040	393

* Unidirectional with 60% of fiber contents.

Table 10.5 Composite vs. metal material properties

	Graphite (expoxy (unidirectional							
	High strength	High modulus	Kelvar/ expoxy (woven cloth)	Glass/ epoxy (woven cloth)	Boron/ epoxy	Aluminum	Beryllium	Titanium
Specific strength, 10^6 in	5.4	2.1	1	0.7	3.3	0.7	1.1	0.8
Specific stiffness, 10^a in	400	700	80	45	457	100	700	100
Density, lb/in^3	0.056	0.063	0.05	0.065	0.07	0.10	0.07	0.16

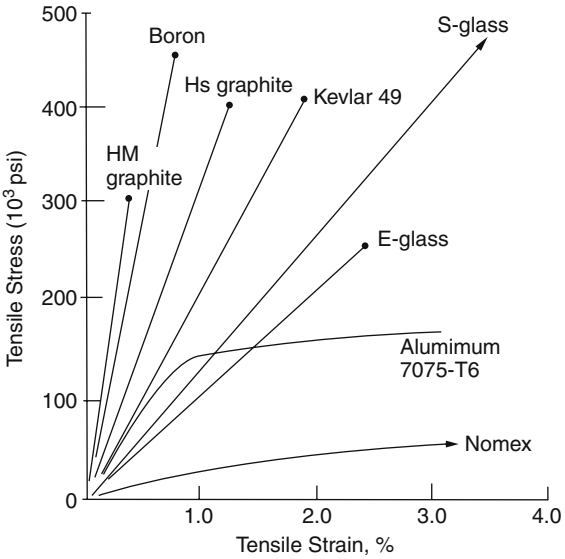

Fig. 10.6 Stress–strain curves for different materials

Sandwich Construction

Sandwich structures offer damage tolerant buoyancy for marine vehicles. For WIG application, the best approach is to combine the technology and experiences developed in the marine industry and in the aerospace industry together. A typical honeycomb core panel is shown in Fig. 10.7. The relative stiffness of sandwich materials against stiffened alloy panels is illustrated in Fig. 10.8

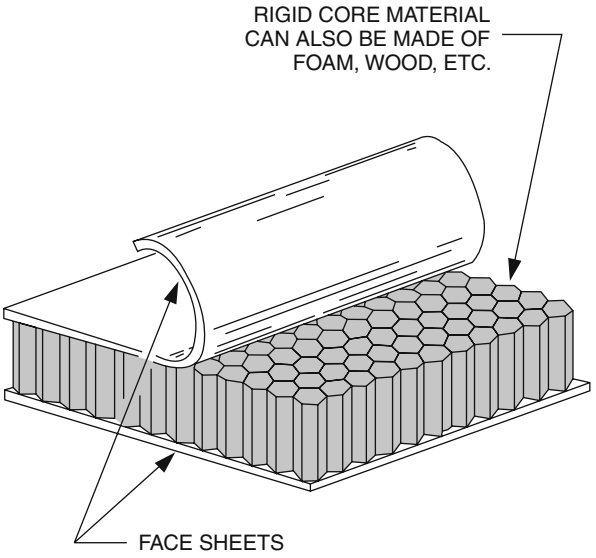

Fig. 10.7 Honeycomb core material

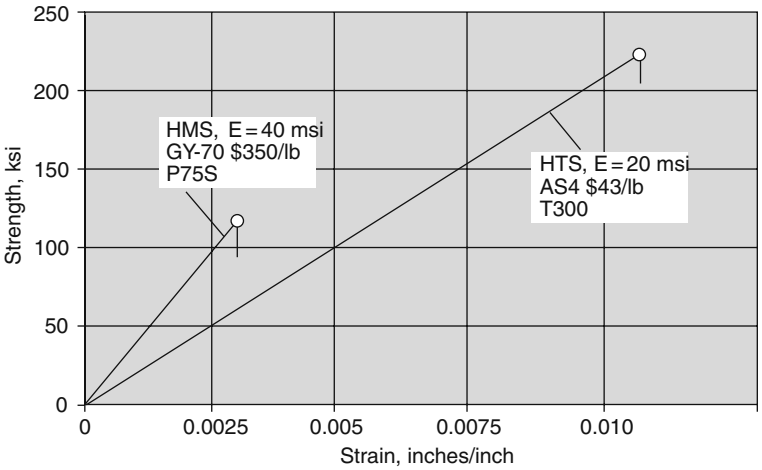

Fig. 10.8 Stress–strain for honeycomb core material versus ATS

The low cost moulding construction method used in the boating industry is important for WIG application, as cost-efficiency is one of the most important design criteria for even considering WIG in transportation role. Lightweight structure construction and fabrication methods including autoclave methods produce a lightweight structure desirable for successful transportation class WIG design. Autoclaves are generally not available for full craft structures, so the craft has to be

broken down into key elements and these autoclave cured units assembled together by a combination of bolting and gluing and over-taping seams for water-tightness. Resin transfer moulding process especially in conjunction with "out-of-autoclave" oven curing process is gaining wider acceptance in composite industry and can be an attractive method in cost-effective WIG composite structural fabrication method.

The current production cost of the high-performance aerospace fabrication technology for composites (using high performance materials such as carbon) is still high for WIG application at this time, but the cost trend downward as the technology matures, with a wider range applications developed every year. Further, NASA has recognised the variables that limit the use of composite materials for more budget-limited projects and has implemented an Advanced General Aviation Technology Experiment (AGATE) programme with one of the elements to develop cost-effective composite materials and production processes with standard material/structure database that can be applied for analysis, optimisation and certification aiming at significantly reducing the total cost of flight vehicle composite structure applications. The NCAMP (National Center for Advanced Material Performance) took the next step expanding the AGATE effort to the next level in conjunction with FAA, CMH-17 (Composite Material Handbook 17) leadership and the aerospace industry. This should be helpful for the incorporation of high-strength composite components in the near to medium term for WIG craft. Figure 10.9 shows a comparison of metallic and composite material working and maximum stress ratios.

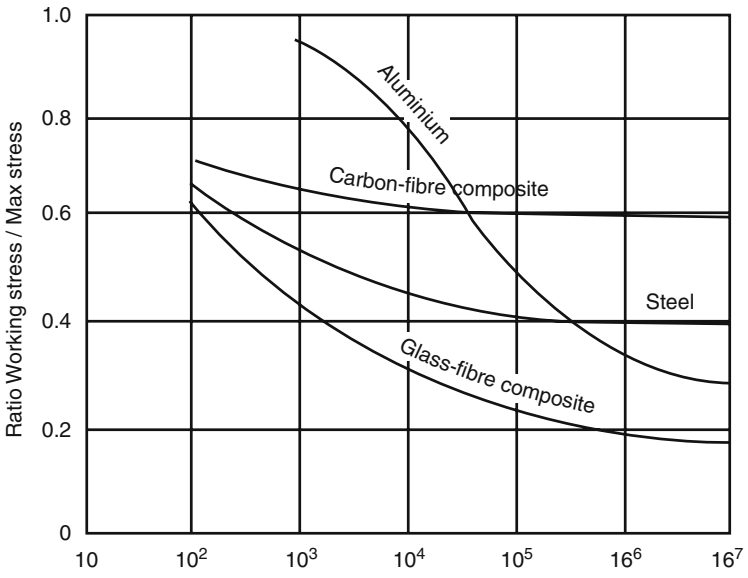

Fig. 10.9 Working stress–maximum stress versus cycles for different materials

One of the difficulties of large composite structure development is the size limitation of the fabrication process equipment. Mould, autoclave or automated fibre placement equipment size all limit the maximum size of each individual unit that can be fabricated. Composite structures are most efficient with one-piece construction as this removes joints and connections that add weight and create stress concentration. Autoclave dimensions will therefore most likely control a designers' concept for medium-sized WIG craft construction. The craft weight will depend on the efficiency with which he designs the connecting joints between the craft components.

Composite structure design will also focus more on larger simple panels, in contrast to an aluminium structure that will normally comprise a multitude of frames, stringers attached to central spars, and the whole skinned with a thin plate or sheeting of aluminium.

Fatigue, Damage Tolerance and Fail-Safe

A wing-in-ground effect vehicle operates close to sea level most of the time, imposing significant structure integrity requirements. Due to the low-level flight, turbulence levels are high, particularly when flying over rough water. Unlike long range transport aircraft that are exposed to high turbulence levels mostly during take-off, climb, descent and landing, and experience much less fluctuation loads during cruise at 7,000 m plus, WIG design requirements are rather more challenging.

Durability and damage tolerance of a WIG design needs to be the fundamental design requirement. For small-size WIG designed for low usage such as recreation or personal transportation, the design life can be limited, while for most WIG designed for commuter or transportation purposes and with many flights a day the structure will need to be highly resistant to fatigue loading.

The only aircraft type that has similar design requirements is the regional (commuter) aircraft that is designed to operate six to seven flights a day with a significant portion of the flight exposed to low altitude turbulence and multiple take-off/landing loads.

The basic design philosophy has to be established and consistently followed in order to have a weight-efficient design. A mixture of design approach in the same structure can result in weight and cost penalty, and difficulties in establishing an appropriate structural inspection programme for continuous safe operation of the vehicle.

The safe life concept and also the fail-safe concept have been applied successfully in flight vehicle design for many years. More recently, the damage tolerant approach, together with a scheduled structural inspection programme to detect crack development in order to prevent catastrophic failure, has been more widely applied in military and FAR/JAR 25 aircraft design.

Composite structures have generally been considered very good in fatigue characteristics so long as low dynamic load amplitude compared to proof stress is

adopted. However, this does not mean composite structures will out-last a well-designed metal structure. Impact damage is the major problem associated with composite structures due to the potential structural strength degradation together with the difficulties in damage detection and inspection.

In case of a foreign object impact on a composite primary structure element, the damage may be significant but not visible from the surface. Recent development in composite structure inspection methodology and equipment is promising in providing practical and cost-effective means for operational inspection, but are still in the R&D and early implementation stage at present, so the practical approach for a WIG designer is to adopt conservative operating stress levels and accept a heavier structure.

Design for fatigue and damage tolerance is relatively simple if the guidelines below are followed:

- Distributed loadings are more favourable to fatigue – avoid concentrated loadings where possible
- Identify local stress concentrations and reduce them as far as possible
- Maintain 3D (diameter of fastener) edge distance on structural joints with fasteners
- Assure good inspectability for major structures and structures with risk to experience FOD (foreign object damage) – i.e. forward and downward facing structures such as wing LE, duct LE, noses and flap
- Reduce design-operating stress level for structural elements that have low damage tolerance details due to other design constraints

The primary causes of structural fatigue and crack propagation are fluctuating loads during take-off, landing and turbulence in flight. The larger the fluctuations the more damaging it is, so methods to reduce the flight load fluctuations can significantly improve the structure service life and extend the required inspection intervals, and improve the operating economy without sacrificing safety.

One possibility for WIG is to incorporate a semi-passive system that opens venting louvers on the wing to reduce the pressure build-up due to either vertical or head on gust. The system cannot be totally passive as it requires different pressure relief settings for various flight modes and manoeuvres, but may be simple enough to install on a medium or large WIG. A load alleviation system might also significantly improve the ride quality of WIG at high speed and therefore reduce crew fatigue and increase passenger comfort.

WIG Structural Design Concepts and Considerations

Basic Design Considerations

Basic design considerations for a WIG structure are as follows.

Project Design Practices

Before setting out to design the WIG structure, the designer needs to establish the design targets and philosophy. These include the following:

- Establish project specific design practices, including design constraints related to available construction techniques, tooling, etc.
- Establish a construction strategy and procedures, including construction tolerances.
- Establish standard material selections based on cost criteria and supply availability.
- Establish fastener specification and usage for the project.
- Establish CAD modelling and drawing standards, together with structural modelling procedure.
- Develop cost and weight targets for the overall structure and main components, together with a monitoring system for both controls. Analyse the structure for both parameters through the design process and establish sensitivity of changes to components on both parameters.

The choice of a composite main structure or a metallic main structure will lead a designer in quite different directions for the craft overall design, so this initial choice will be a most important one. As a rule of thumb, craft with a payload of less than 2 to 3 tonnes may be designed fully in composites, above this payload, it may be possible to build the flying surfaces in composites, but the main hull will generally be more efficient in aluminium (combination welded lower and fastened high-proof strength upper). Like any rule, of course, there will be exceptions, but it is a place to start.

Overall Layout

The basic WIG in most cases is designed to carry people and/or cargo. The fuselage is commonly laid out to provide maximum usable volume. The lifting surfaces are required to be lightweight and sometimes also designed to have integrated fuel tanks built in. Most WIGS have stern mounted rudder and elevators and additional winglets outside the side buoys for additional lift and trim control. Figure 10.10 shows the wingship configuration layout and structure concept as an example; an artists' impression of the craft is shown in Fig. 12.23.

Basic WIG structural design layout is a similar process to designing an airplane. The basic crew and passenger accommodation or freight volume is first defined. That identifies the minimum fuselage size and configuration. The structure will then be designed to minimise structural volume and to minimise the aerodynamic drag.

The trade-off between the structure weight and the structure volume with opposite requirements is not unusual, but structure volume can be translated to drag and then equivalent thrust power required. By estimating the weight of the extra power to be produced by the type of power plant selected, the design decision can be made logically to achieve minimum equivalent total vehicle weight.

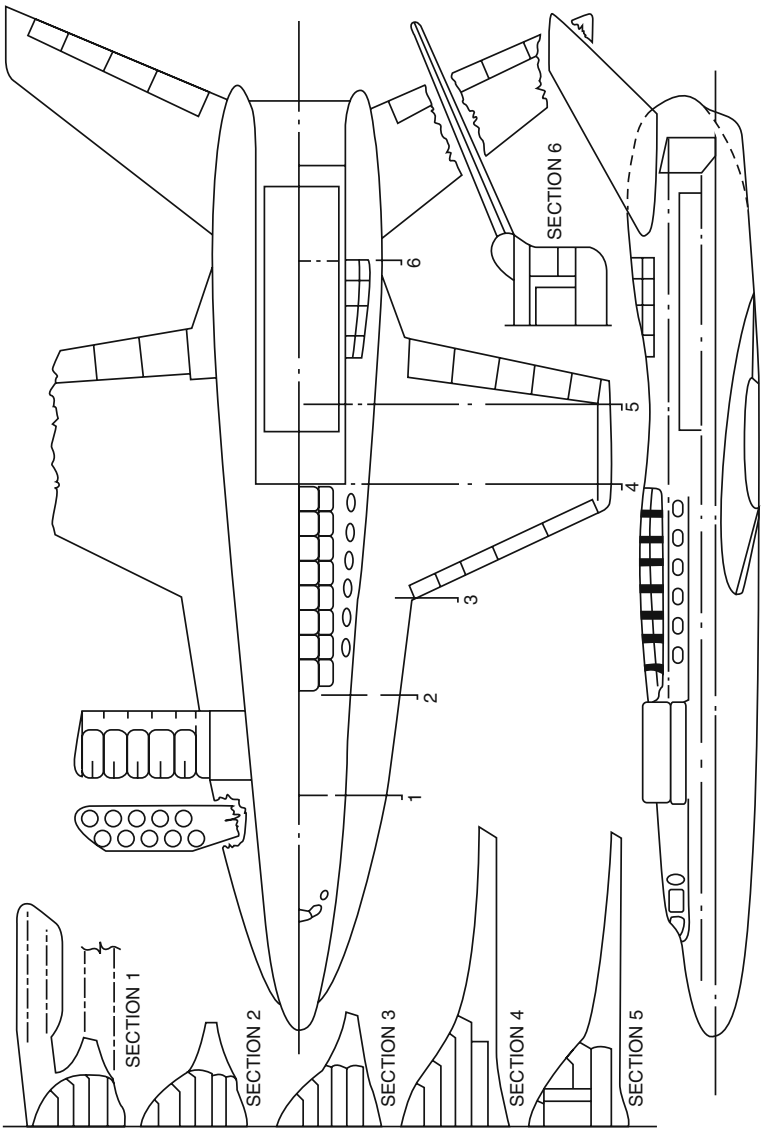

Fig. 10.10 Wingship configuration – a small composite WIG structure

Wing Design

The wing design is always a trade-off between cruise efficiency, pre-take-off lift-augmentation system performance, structure weight and cost, and construction complexity. A WIG has a medium to low aspect ratio main wing. Low aspect ratio wings have a thicker wing section for the same foil geometry and much reduced wing bending moment for the same wing area, resulting in lighter and more efficient wing structure. The extra depth in the primary wing structure also allows simpler systems installation, such as a high mechanical advantage flap drive system within the wing section envelope, resulting in weight savings compared to normal aircraft.

Basic Wing Structures

Among several wing structure types, modern aircraft tend to apply spar, stringer and rib combinations to maximise the contribution of each and every structural element in total load carrying capabilities. Some designs use multiple spars in lieu of stringers. Figure 10.11 shows an example modern Spar/stringer wing structural arrangement.

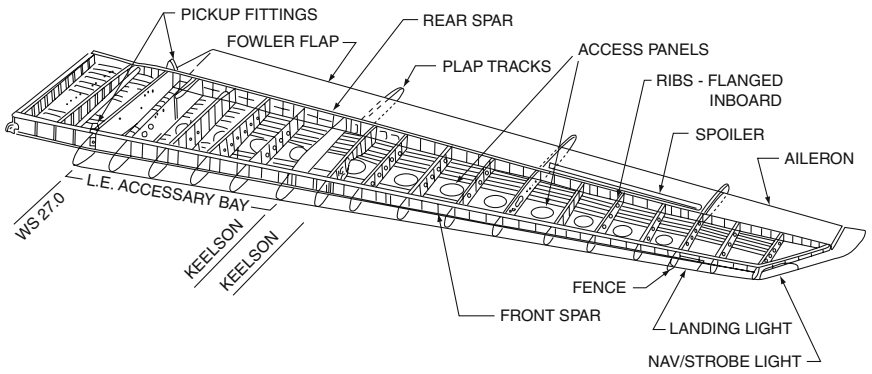

Fig. 10.11 Wing structure

The rib and stringer spacing, stringer cross-section, and skin gauge can all be optimised by dimensioning the components so that skin buckling and stringer crippling occur at roughly the same time. Modern machining capabilities and steadily reducing cost allow skins for medium-size wings to incorporate integrally machined stringers designed to eliminate a large amount of fastener and assembly time. For wing assemblies designed to be the fuel tank, the elimination of large amounts of fasteners can significantly reduce the fuel leakage in production and in service.

Aluminium honeycomb sandwich skin panels and composite sandwich panels with foam or honeycomb core provide excellent skin panel structural stability. This

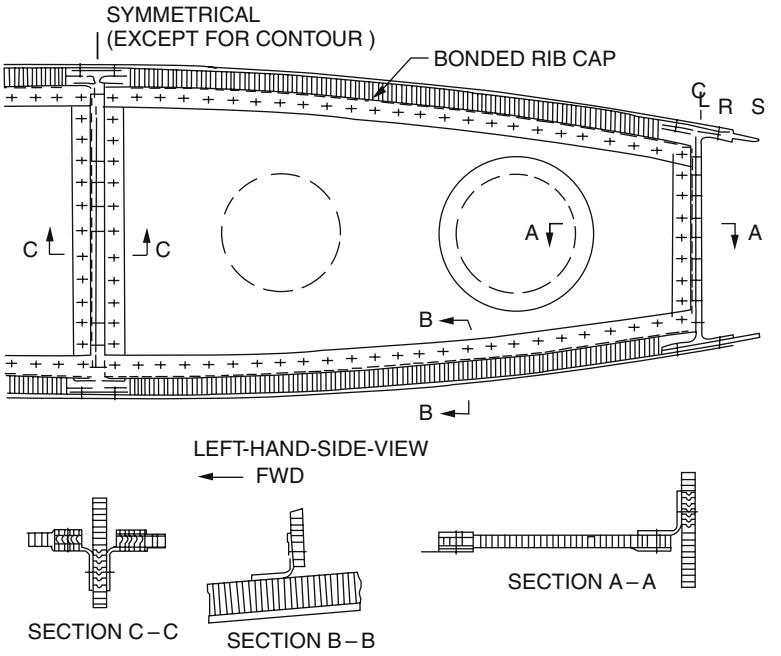

Fig. 10.12 Wing cross section

allows much larger unsupported panel bay area and thus reduces the number of stringers and ribs, number of fasteners and assembly cost. Figure 10.12 shows a Bonded Honeycomb Wing Box Design, while Fig. 10.13 shows a Honeycomb Composite Wing Spar Joint Design.

It is important to consider the structure inspection methods and accessibility for this type of design due to the hidden structure elements. For composite wing design, lightning protection provision is very important especially with integrated wing fuel tanks. Embedded metal wire mesh has been applied successfully for lightning protection.

Material selection is critical for an optimised wing structure that will meet the goal for light weight and durability. For the upper surface, skin compression loads are higher than tension loads. Fatigue and crack growth are a lesser issue. Designers may therefore choose materials with higher stiffness and compression strength for the upper surfaces, while high-strength ductile materials will be more suitable for the lower surfaces. The lower surface skin experiences much higher tension loads than the compression loads. The material selected will need to have very good fatigue characteristics like aluminium 2024-T3 or 2324-T3. The sizing of the lower skin/stringer and spar caps are likely to be driven by the fatigue and operating stress level required to achieve reasonable structure inspection intervals.

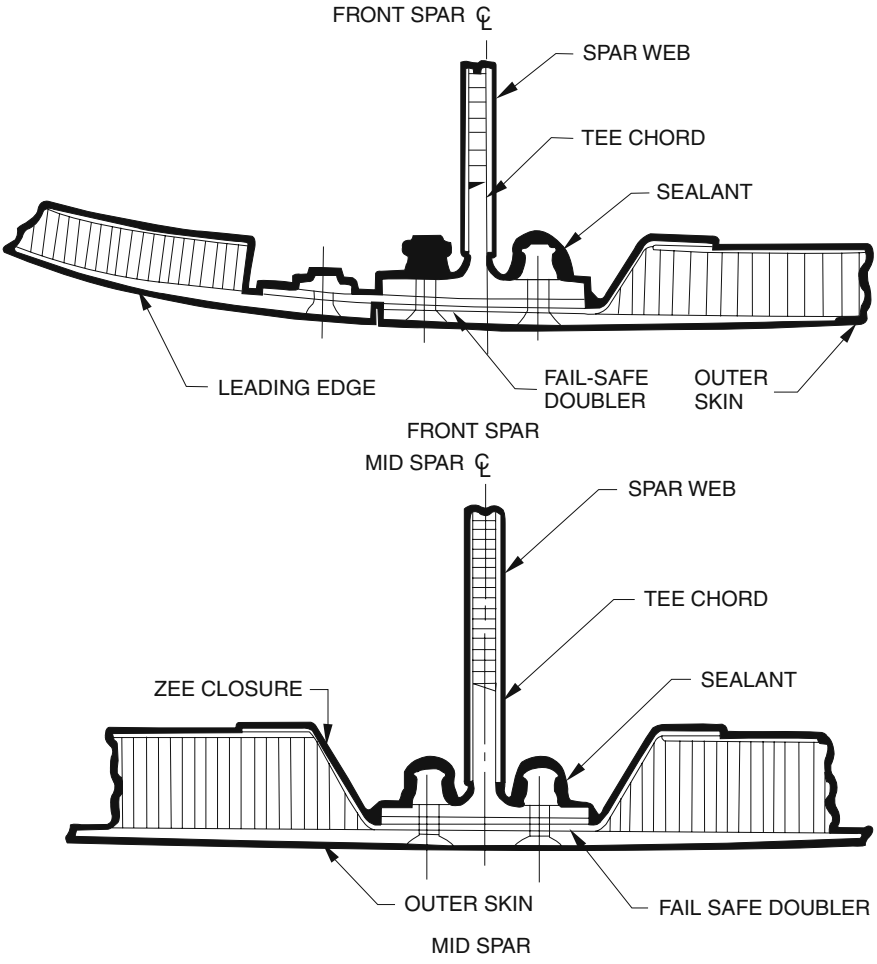

Fig. 10.13 Wing structural detail

High Lift Devices and Control Surfaces

The commonly incorporated high lift device on a WIG is the trailing edge flap. The flap not only functions as high lift device but also is the key feature that reduces the gap between the wing and the operating surface to provide amplified ground effect or a dynamic air cushion during take-off and landing. The device is normally very close to the operating surface therefore requires to be designed to be very rugged.

The flap hinge or track arrangements significantly affect the structure loads. With three or more hinges on a single flap, the wing bending will force the flap to bend and therefore induce significant loads into the flap structure and reacted by the wing

structures through the flap hinge/track attach points. The effective wing/flap structural stiffness and therefore the induced loads can be quite high when the flap is at 30–45° deployed position and its moment of inertia is high in the wing plan axis. WIG flaps are generally single hinge type. While this is less efficient when considered as a lift augmentation device, it is more effective as a means to contain a dynamic air cushion at low flying height. The flap also has to be designed to withstand the impact damage due to the water impact with forward velocity or debris generated by the high velocity nose-mounted engine jet blast during ground operation.

Other control surface designs such as the ailerons and elevators have similar structure functional requirements and associated design problems to flaps. Structural stiffness requirements often drive the design configurations and material selection for these devices. Metal and composite sandwich structures are good applications here as they provide high structural stiffness at low weight.

Aileron, rudder and elevator design has one additional requirement – the control surface requires a certain amount of mass balance to provide adequate flutter margin for the design-operating speed range. This requirement encourages the maximum effort in lightweight design as for every kilograms of weight reduction in the control surface itself there can be 2 to 3 kilo of weight saving in the balance weight.

Hull and Superstructures (Fuselage)

Hull and superstructure design for fast marine craft is somewhat different from aircraft. The hull may be equated to the fuselage while the deckhouse or superstructure has no equivalent. Modern fast catamarans have developed towards a monocoque construction, but the hulls do not have to accommodate the local loading from the root of the wings of an aeroplane.

WIG design has the greatest similarity to a flying boat. The global structural arrangement of the fuselage or hull is a stressed skin supported by ring frames and longitudinal stringers. The central section of the hull has heavier frames and stringers to distribute the loading from the payload contained in the hull, plus its own weight into the structure of the wings. The lower part of the hull has heavier skin plating and supporting frame and stringer dimensions to resist the hydrodynamic loads while planing at speeds up to take-off.

WIG designs incorporating a more effective air cushion such as the DACWIG experience much lower hydrodynamic loads on the hull underside, though wave impact loads are not avoided unless the central fuselage is raised to a much higher level and the side buoys enlarged to enable the craft to float on them alone.

The basic design approach to dimensioning the fuselage is therefore to consider the structure as a tubular beam supported by the wings, with the payload, fuel and secondary structures such as the fin and tailplane as mass loading. Design principles as outlined in [3] will apply.

In addition, once the main configuration been selected, for example a dynamic cushion supported WIG with low slung fuselage, the hydrodynamic loads can be estimated based on cushion performance in a seaway and the hydrodynamic loads

on the planing surfaces calculated. The plate and stiffener dimensions can then be selected and the fuselage global scantlings adjusted.

Since a WIG hull does not need to be pressurised for flight, the cross section does not need to be oval or circular. A more rectangular section is likely to improve manufacturing cost significantly, by simplifying tooling or moulds for composite structures. A structure blended with the main wings can further improve structural efficiency as well as manufacturing cost for a WIG due to reduced stress concentrations.

Cockpit and Windshield

The primary design goal for the cockpit configuration is to provide good visibility for both the pilot and the co-pilot. For better visibility, it is desirable to provide as large window area as possible. Unfortunately a glass or polycarbon windshield is heavy compared to the metal or composite structure of the hull if designed to handle bird strikes, so there will always be a trade-off for windshield size against weight.

Since WIG always operate at low altitude, bird strike protection is absolutely required. The modern windshield is made of several layers of laminated transparent materials, so there is no problem to design a windshield that will withstand a 2-kg bird impacted up to 300 knots without penetration. The designer needs to pay more attention at the windshield surrounding structure as they can collapse, even though the windshield may survive the impact.

Canard Wings and Tail Surfaces

Some WIG designs incorporate a forward lifting/control surface or canard. The canard has to be designed to handle not only the steady state lift and the gust loads, but also the potential water impact loads.

There are many different tail assemblies applied to WIG. The configuration largely depends on the stability and control requirements of the specific WIG configuration. Due to the significant shift of the aerodynamic centre when WIG take off into surface effect flight, and the need to finely control pitch attitude compared to an aircraft in free flight, the typical WIG has much larger tailplane than conventional aircraft.

For commercial WIG, the CG variation between fully loaded and empty payload requires a large longitudinal trim capability which either requires even larger tail surface area or to incorporate a trim-able elevator design. The structural configuration of a tailplane is similar to a wing, with ribs and stringers, and one or more main transverse spars. The higher the aspect ratio, the lower the trim drag but at the expense of heavier structure weight. Due to the difficulty of providing significant ballast for CG compensation for a WIG, it is important to determine the minimum payload/fuel load and unfavourable distribution to explore CG excursion envelope. This may well suggest an adjustment of craft hull geometry relative to the wings so as to improve the overall balance. Trial flights will most likely have to be carried out with cargo simulation ballast.

The tail fin provides directional stability and directional control to a WIG. The fin is normally not loaded and so is generally designed with a lower aspect ratio to provide a lighter structure weight without normal operating drag penalty.

Many WIG designs incorporate a T-tail arrangement to place the tailplane and elevator out of ground effect. T-tail design should carefully account for yawing or sideslip rolling moment from the horizontal tail superimposed on the side force on the vertical tail. For high aspect ratio, horizontal tails that are common on WIG, the tail aero-elasticity effect and flutter should be carefully considered to avoid control reversal and to ensure adequate flutter margin. Figure 10.14 shows a high aspect ratio fin structural configuration

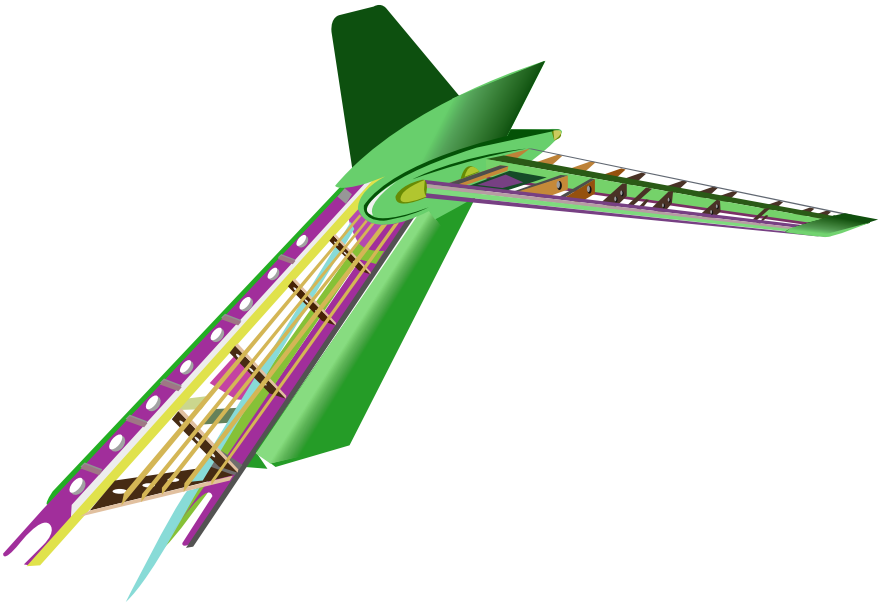

Fig. 10.14 Fin structure

If a propulsor is installed on top of the vertical tail-like Ekranoplan Orlyonok, the mass inertia and the propeller induced torque moment require special structural analysis. The propeller also produces a tangential force vector when encountering a gust, which has to be included in the tail structural design loads. Figure 10.15 shows a model of a WIG with a tail-mounted propulsion engine.

Pylons and Engine Mounts

There are as many different power plant installation configurations as there are WIG vehicles. Many designers choose to have main propulsion engines installed on a pylon with direct propeller drive or to have belt or geared shaft drive from a hull-mounted engine to pylon-mounted propellers above the main wings. Higher mass

Fig. 10.15 Antonov WIG model

internal combustion engines are better installed in the hull, while gas turbines are light enough to be mounted in line with a propeller on a pylon. All these alternatives involve heavy loadings being transmitted from the propeller thrust bearing via the pylon down into the hull structure. WIG-manoeuvring accelerations need to be carefully analysed for these structures.

PARWIG and DACWIG often have engines installed near the front end of the fuselage or in the front of the main wing. The structural design of engine supports for these configurations, especially for those mounting four to six engines per side in the configuration of the KM or Spasatel, requires considerable attention, as the inertial loads of such installations are significant. Figure 10.16 shows the construction of Spasatel.

The critical load cases to account for include gust loads, vertical and horizontal impact loads, as well as the thrust vectors at various operating conditions. The engine mounts should also be capable of sustaining limited operating loads in case of engine exposed to fire for a limited time prior to auto-extinguishing system taking effect and thus allow bringing the vehicle to the nearest base safely.

PARWIG and DACWIG configured with propeller ducts mounted forward of the main wings are generally mounted on to the craft forward fuselage and have similar loadings to the nose-mounted jet propulsors of the KM and SM-8. Figure 10.17 shows the construction of TY-1 with its nose-mounted propeller ducts, at the Hongtu aircraft factory in China.

Landing Gear and Cushion Systems

Many WIG are designed to operate from the water surface only, which somewhat limits the possible operating base. The power-augmented WIG system provides limited ground operation capabilities for the vehicle to operate without docking facilities.

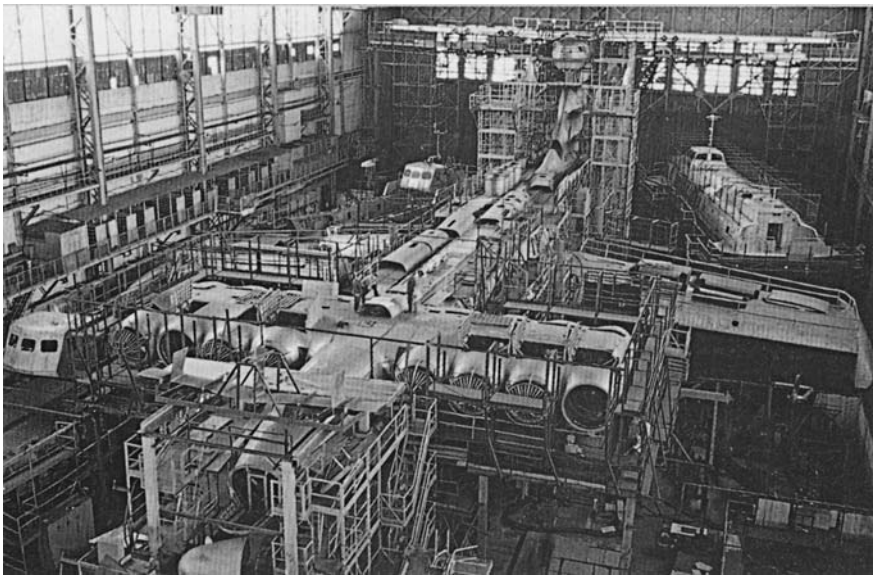

Fig. 10.16 Undercarriage

Fig. 10.17 Super WIG artists' impression

Some designs have landing gear or a cushion system to enhance the operating basis at the expense of weight and cost. These two provisions have significantly different impact on the structural design. The landing gear system requires the fuselage or wing structural design to be able to handle heavy concentrated loads from the landing gears and redistribute the loads through an appropriate load path into the main wing root structure, this being the heaviest structure of the craft. Figure 10.18 shows a trailing link retractable landing gear designed for a 60,000 lb flight vehicle

A cushion system is easier on the basic wing and fuselage structures due to the distributed loading from low pressure lifting force in the cushion. The only structural impact is the local skirt attachments that can be dealt with by local structure reinforcement.

Fig. 10.18 Wing/body airplane

Very Large WIG-Blended Hull Configurations

For very large WIG craft, the stress level required to support the heavy loading can be very high, so a more structural efficient hull configuration concept may be useful to reduce structural weight. Once again the fact that the hull does not need to be pressurised for altitude gives the opportunity to look at more radical shapes than traditional aircraft configurations. For large WIG vehicle design, flying wing concept becomes a possible configuration to take advantage of distributed loading and minimise structural weight along with possible low total vehicle drag benefits.

Stability and control as well as power plant arrangement are always difficult issues to deal with for the "flying wing" design, but the potential benefit is too attractive to ignore. The "blended wing" designed with partial span loading have been studied by NASA and Boeing recently. A potential problem with using this configuration in aircraft design is that it requires about 8 psi or more cabin pressurisation for altitude operation and it is difficult to design a weight efficient structure with flat surface pressure boundary compared to a circular fuselage for this requirement. However, this is not a problem for WIG design as minimum or no cabin

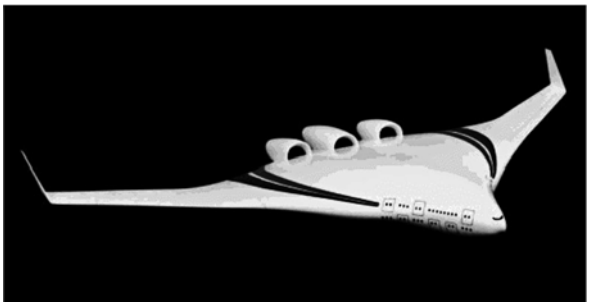

Fig. 10.19 Scale model of NASA/Boeing blended wing aeroplane concept

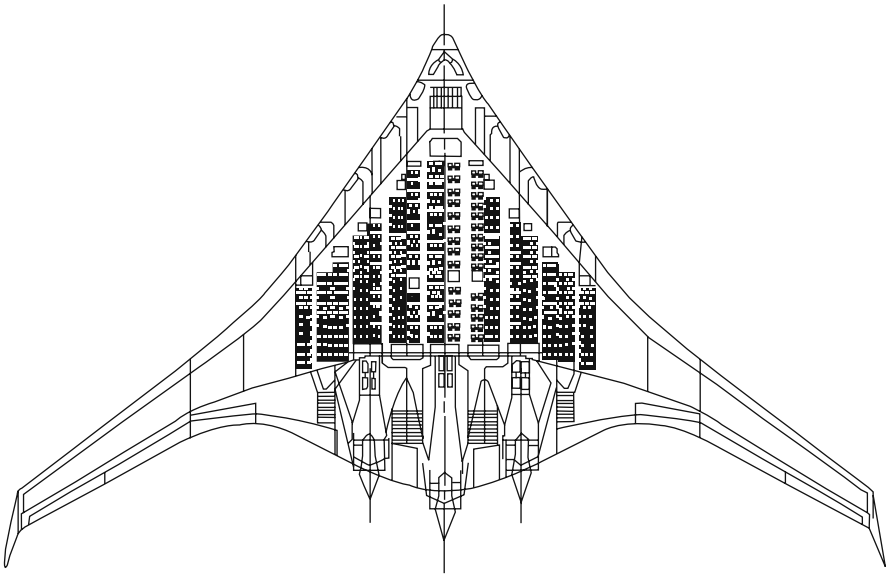

Fig. 10.20 General arrangement plan of blended wing aeroplane concept

pressurisation is required, so the distributed loading benefit can be realised without paying the weight penalty of the non-circular pressure vessel. Figures 10.19 and 10.20 show a NASA/Boeing blended wing design concept.

Chapter 11
Power plant and Transmission

Introduction

A WIG is a flying machine that takes off and lands on water, in a similar manner to a flying boat. The craft structure has to follow much of the experience and concepts developed in aviation in order to achieve successful flight performance. Power plants also need to comply with aviation criteria of acceptability – reliability, lightest possible weight and highest practical fuel economy.

An important additional criterion to take into consideration for power plant selection is the total weight combining the engine, transmission and propulsor system.

The WIG performance envelope will also have a strong influence on power plant selection. High-speed WIG, with cruise speed above 300 kph, demands jet engine propulsion, preferably high bypass turbofan(s).

Modern lightweight internal combustion engines are useful candidates for medium to small WIG application, so long as the electronic systems have been uprated for marine service. Automotive engine technology has significantly improved durability and power-to-weight ratio over the last two decades. A turbo charger can be effective in increasing the power output of an engine and achieve higher power-to-weight ratio design.

Although diesel engines have been successfully used in modern hovercraft, the highest power-to-weight ratio engines are only available at power ratings suitable for cars. Small WIG craft may be able to use these engines, but larger WIG have to base engine selection on aviation power plants, whether reciprocating, or gas turbines. A recent NASA supported development programme as well as other recently commercialised lightweight aviation diesel engines has nevertheless introduced a possible new engine source for small-size WIG once such power plants become available commercially.

Gas turbine engines in the past have been complex and expensive with relatively poor specific fuel consumption. New technology development in the last 15 years has revolutionised modern turbine engines. New generation engines have been developed with 40% better specific fuel consumption while some of the smaller turbine engines have 70% lower part count than before. Very high bypass turbofans and

L. Yun et al., *WIG Craft and Ekranoplan*, DOI 10.1007/978-1-4419-0042-5_11,

high efficiency turboshaft engines paired with ducted fans hold promise for various size WIG applications.

ACV and SES have utilised industrial power units successfully as an alternative to heavier marine engines with steel crankcase and cylinder heads, for example air-cooled diesel engines. ACV face the same challenge as WIG related to engine-cooling systems, in that direct one path through salt water cooling, as used on most high-speed marine craft, is not possible. Water-cooled engines therefore have to be designed with a closed-cooling system incorporating a heat exchanger (radiator). This system adds weight, which is not so critical for an ACV, but may become so for WIG craft. An air-cooled engine is attractive for the simplicity and light weight, but water-cooled system (with radiator and cooling fan) has its advantage in terms of better cooling and control especially at low operating speed.

Whether an automotive, marine or aerospace derivative power plant is selected, the WIG designer has to be aware that engines are available in specific power ranges. There are a limited number of products available, and powering of a WIG has to be based on selection of an existing power plant, as development of a new engine specifically for the WIG project would be prohibitive in both time and cost. The WIG craft sizing and mission potential will have to be adjusted so as to obtain the maximum from the available power plant!

In this chapter, we will discuss selection criteria for WIG and design issues for incorporation of power plant and their associated systems (control, cooling, fuel, etc.) into the overall craft design.

WIG Power Plant Type Selection

The basic requirements of WIG power plant are linked to the operating environment of the WIG, including similar conditions to fast marine craft for the take-off and landing runs, and aviation conditions of high-speed during cruising. Key elements for success are

- High power-to-weight ratio
- Ruggedness of engine *and* support systems for multi-environment operation
- Low acquisition cost
- Low operating and maintenance cost
- Adaptability to the proposed transmission and connected propulsion/lift system

Various engine types are suitable for WIG application, as discussed above, depending on the size of the vehicle, the operating envelope and the basic vehicle configuration, particularly the lift and propulsion system arrangements.

Selection of engine type has often been driven by the power requirement in the different operating modes. For a design that requires significantly more power for take-off than cruise mode, an automotive engine may be readily adaptable for the application, while turbine engines are often designed to operate continuously at

near maximum power so are more suitable for high-speed craft. A comparison of characteristics for different engine types in aviation use is shown in Fig. 11.1.

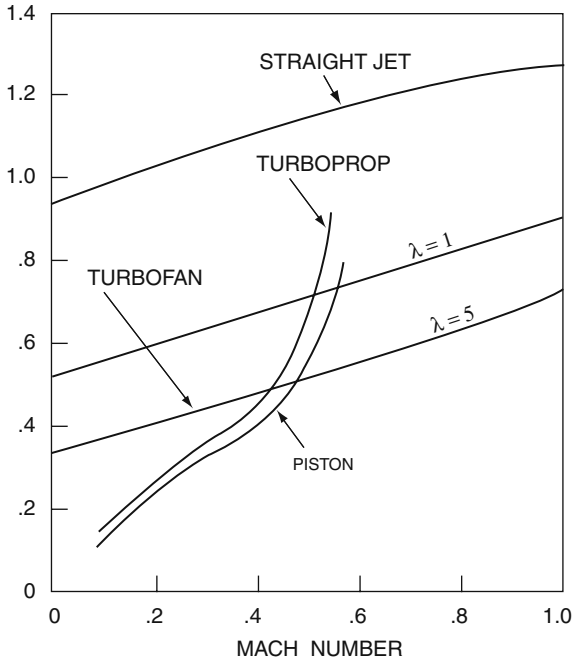

Fig. 11.1 Fuel consumption/drag versus mach number

Internal Combustion Engines

For small WIG vehicles, the internal combustion engine is a very good choice due to its low acquisition cost, minimum or no special maintenance equipment or training required, and reasonable power-to-weight ratio.

The advancement in two- and four-cycle gasoline engines today offers high fuel efficiency, low environmental emissions and low weight. Modern automotive engines use aluminium for both the crankcase block and the head. A good example is the lightweight Northstar all aluminum 300 hp 4.6 L V8 IC engine shown in Fig. 11.2, the same engine is now available in marinised form that can be directly adapted for small WIG craft application.

Generally the automotive power rating of an engine is not intended for continuous operation at the rated horsepower. The rating is for maximum power for a short period of continuous output mostly during acceleration, cars generally operate at speeds where an engine is at 50% maximum power or less. For automotive applications, a more important parameter than power is torque for acceleration but this is less critical for WIG applications especially with variable pitch propeller or fan system.

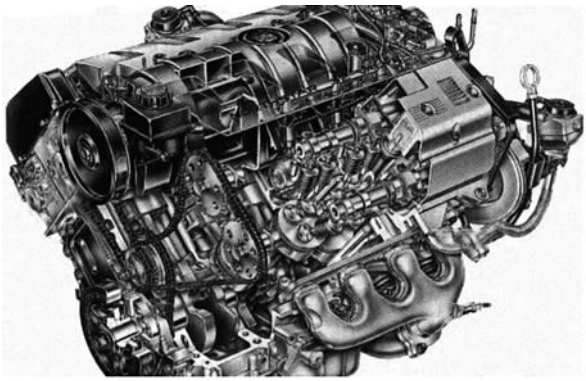

Fig. 11.2 Northstar all aluminum 300 hp 4.6 L V8 IC engine

Aircraft engines normally have a continuous rating between 70 and 85% of maximum power. The maximum rating is valid for transitions such as take-off and landing. Aircraft cruise speed is then set, so the engine is running below 85% power rating. The cooling system is arranged so that engine temperature can be maintained optimal at cruise speed, and maintain CHT within limits during take-off and climb flight segments especially for hot day operations.

A marine engine is rated with a maximum power suitable for short burst operations up of 10–15 min and a continuous rating at 80–85% of maximum power. Torque is only important at the matching speed of the propulsor it is connected to. If the propulsor is a variable pitch device, there will be two design conditions to consider, maximum thrust while in still water at zero speed and maximum thrust while passing through hump speed or take-off to planing, which ever is the most demanding.

For WIG applications, the requirements for power plant are quite similar to marine power plant, while needing a lower engine weight.

For small personal WIG craft or experimental trials craft, two-cycle petrol engines developed for snow-mobiles, jet-ski water craft and hovercraft applications offer high power-to-weight ratio. Although not the most fuel-efficient power plant for short-range small WIG craft that do not require years of daily operations, the light weight and low acquisition cost of two-cycle petrol engines can easily offset the shortcomings. Figure 11.3 shows a typical installation as installed in a small hovercraft. This type of engine was also used for the MARIC 750 manned test craft, two-ducted engine and fan units as bow thrusters, and a further two-ducted fan and engine units for propulsion, see Fig. 3.7. Modern developments of this type of engine have been adapted to the flight requirements of microlight aircraft with uprated ignition and fuel systems for reliability. These models are particularly suitable for smaller WIG craft.

The small two stroke motors have been developed for micro-light aircraft applications, including dual ignition systems. These reliability based upgrades are important for WIG craft. In the same way, larger automotive derivative engines need

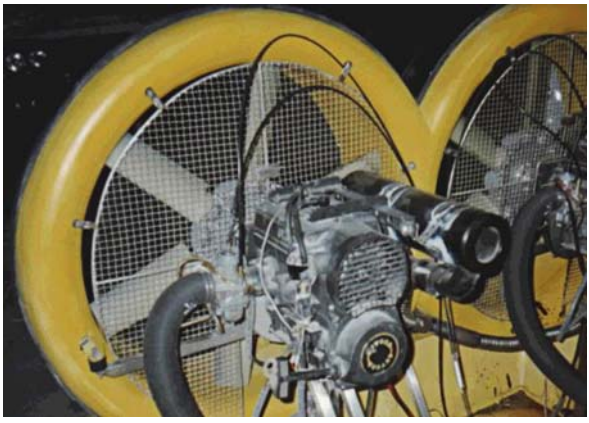

Fig. 11.3 ACV engine plus fan duct

to be modified both for marine use, and to incorporate the system redundancy of aircraft specifications. An appreciation of the systems specifications required can be gained from [1].

Turbofan/Turboshaft/Turboprop Engines

The aircraft turbine engine has long been the choice for high-performance vehicles that require high power output. The fuel efficiency of turbine engines has improved at least 30% over the last 10 years. Modern turbine engines offer the very high power-to-weight ratio and fuel efficiency needed for medium- to large-size WIG. The fuel efficiency improvement is vitally important for medium- to long-range WIG craft as it can reduce the fuel fraction of total vehicle weight, reducing the maximum take-off weight of the resulting design and improving the overall performance.

Of course, there is nothing in the world that is perfect. Turbine engines are still expensive – not only the acquisition cost but also maintenance. Also not every turbine engine type is available in a marinised version, which limits the choices.

Among turbine engines, turbofan, turboprop and turboshaft versions are all applicable for WIG craft. Figure 11.4 shows the Rolls Royce RB 580 turbofan engine as an example. The choice depends on the vehicle configuration and specifically whether a power augmented lift system is planned, whether engines are to be imbedded in fuselage and whether direct drive or shaft transmission is intended.

Interestingly, the small turbine engine development in the last 10 years has been even more dramatic than the big engines. The current generation small turbofan engine may be represented, for example, by the Williams International FJ44 engine family. Figure 11.5 shows the FJ44-3 3,000 lb Thrust Fanjet Engine. This offers

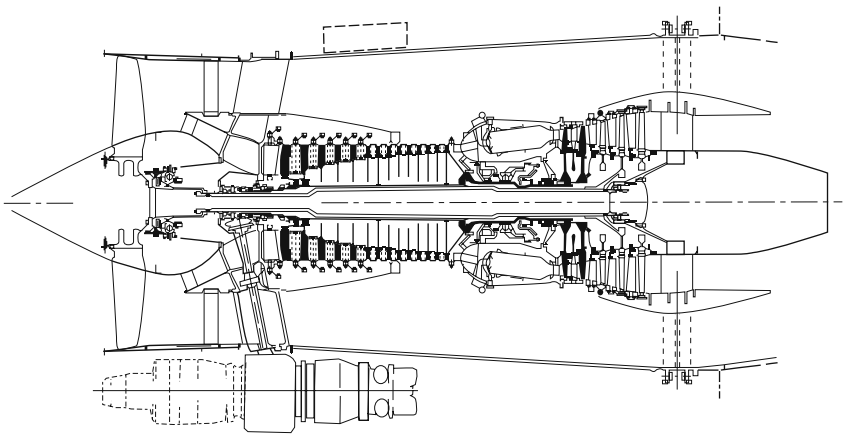

Fig. 11.4 Rolls Royce RB 580 turbofan engine

Fig. 11.5 FJ44-2C 2,300 lb thrust fanjet engine

the fuel efficiency of its much larger counter parts, light weight, simple installation and only one third of the component parts of older generation engines. This translates to lower manufacturing cost as well as simpler and lower maintenance requirements.

It should be noted that most aerospace turbofan engines are designed and optimised for high-speed and high-altitude operations. Marine versions will generally configure as a turboshaft unit, in a fairly large and heavy modular enclosure. The air intake for a marine turbine is separate to the engine itself and incorporates filter banks to remove water droplets. Unless a WIG gas turbine is located inside the hull with air intakes on the upper side, such as arranged for Orlyonok (see Fig. 11.6), air filters are difficult to configure. The banks of gas turbines at the bow of KM and Spasatel created a large amount of heavy salt spray during take-off and landing

(see Fig. 11.7) and so the engines required careful washing after each mission. The figure shows how powerful the action of the high-speed jet efflux is in creating spray at slow speeds over water. While the bow thrusters are out of the spray, the tail is completely enveloped, including the cruising engine.

Fig. 11.6 Orlynok showing bow intakes

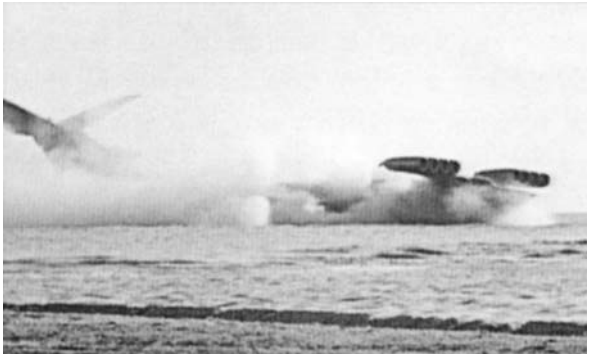

Fig. 11.7 KM launching

The Orlyonok thrusters do not create quite such a cloud of spray, as shown in Fig. 11.8, though the main wings are clearly enveloped, and rough water accentuates the problem. Placing the main propulsion engine at the top of the fin is at least a partial solution to the spray problem and is most convenient for close coupled turboprop installations. Figure 11.9 shows an allison turboprop engine installation with six-blade propeller on a regional airline aircraft, this engine and propeller system would suit a medium-sized WIG installation very well. An alternative arrangement for turbofan engines would be the over-wing location towards the back of a WIG main wing in an arrangement similar to Fig. 11.10. While being a little more sensitive to spray, this arrangement has a lower pitching moment than fin top installations.

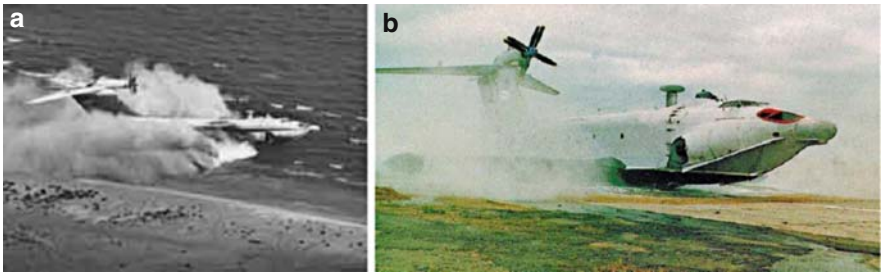

Fig. 11.8 Orlynok launching: (**a**) crossing beach edge and (**b**) accelerating over waves

Fig. 11.9 Allison turboprop engine installation with six-blade propeller

Fig. 11.10 A-40 flying boat with over-wing mounted turbofan propulsion

Such a position may also be better favoured for the classic WIG configuration since there will be less spray without a bow-thruster installation.

Classic WIG designs such as the Flightship series in Australia and the AFD Hoverwing series from Germany have adopted this configuration, see Fig. 2.51 for example. These craft are powered by engines installed in the rear cabin space.

WIG Application Special Requirements

Marinisation

WIG normally operate at or near the water surface, so it is important to ensure that the power plant selected can handle the water spray of the worst operating condition envisioned. The inlet location and its relationship to the bow are a very critical configuration design choice.

Operating in a high water content environment requires additional corrosion protection for the engines; this is particularly critical if the WIG is designed for salt-water operations. Aluminium engine components are vulnerable to salt-water corrosion and so special coating is required for proper protection. Watertight sealed wiring and connectors are a necessary practice for marinised engines.

All engine controls and linkages require stainless steel or non-metallic parts. For the turbine engines, the housing requires special treatment for protection, and the compressor and turbine blades may also require either coating or material changes. Figure 11.11 shows the allied signal TF40 marine gas-turbine engine that includes all these reliability upgrades for marine application. The TF40 is used in US Navy LCAC assault hovercraft and so has been designed with both heavy salt and sand particle ingestion in mind, and makes it a useful candidate for medium-size WIG.

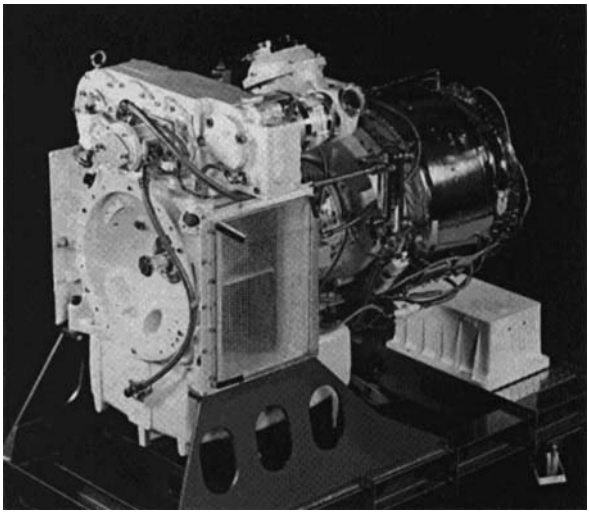

Fig. 11.11 Allied signal TF40 marine gas-turbine engine

Altitude Operations

Since WIG generally operate at low altitude compared to typical aircraft, the engine can be optimised for sea level operation. In the case of turbofan engines, a higher by pass ratio engine will be preferred since these have higher static and low-speed thrust and fuel efficiency.

Internal combustion engines can also be optimised for sea level operation, rather than aircraft engines that are set up for cruise altitude. The only challenge comes if a WIG is to operate on a high-altitude lake, where a different set up of turbo charging may be required and an intercooler might be needed. To maximise the power available for a specific engine under consideration, an intercooler installed between the turbocharger and engine induction air intake can be effective in cooling down induction air and thus improve engine power rating compared to turbo charging only.

Some turbo-charged/intercooled engine designs can provide sea level power up to 2500 m. If high elevation operation is an important design parameter, the WIG designer should also consider aircraft engines for this application. Some aircraft engines are already designed to have matched and tuned turbocharger and intercooler, but more helpfully there is test data available for high elevation operation allowing much easier and effective power plant/vehicle design matching and optimisation. Of course, aircraft engines come with a high price tag and still require proper marinisation to be done for WIG-operating environment. Figure 11.12 shows a Teledyne Continental Motors turbocharged combustion engine performance chart as an example.

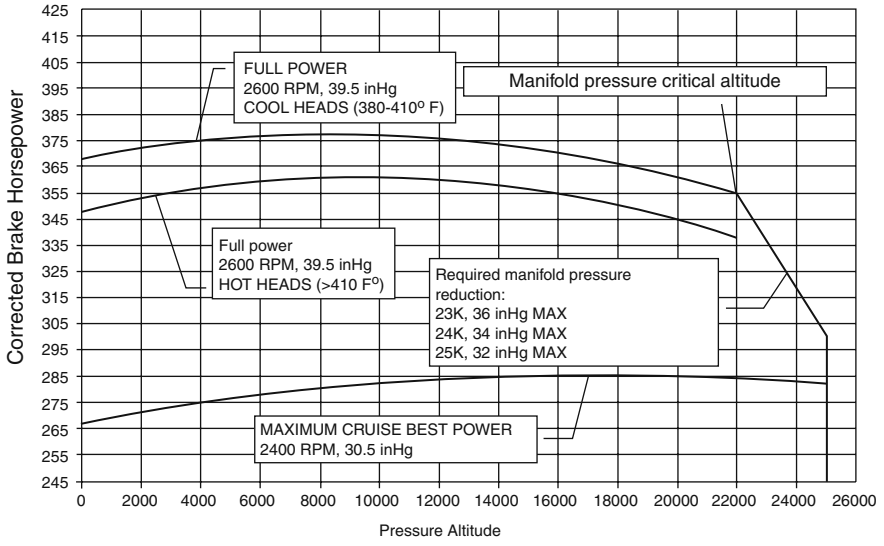

Fig. 11.12 AVCO Lycoming IC aircraft engine performance diagram

Power Plant Installation Design

Pylon/Nacelle Installation

For turbofan, turboprop and aircraft IC engines that are designed to provide direct mounted propulsor or lift system, the pylon/nacelle combination provides an efficient configuration. The suitability depends on the vehicle/power plant configuration. The pylon can be vertically or horizontally arranged with the engine axis parallel to the vehicle. Horizontal mounting would be designed similar to an aircraft aft fuselage turbofan engine installation. Vertical pylon mount for WIG application would be a mirror image of the under-wing engine installation for most large-passenger aircraft like the Boeing 737 airliner design.

Key design considerations include pylon structural stiffness, effective load path through into the fuselage or wing/tail main structures, pylon aerodynamics, firewall protection and engine yoke fireproofing. The engine controls and engine electronic data link will all have to go through the pylon, therefore adequate system penetrations should be provided in the design. Figure 11.13 shows a typical jet engine pod pylon structure and systems configuration.

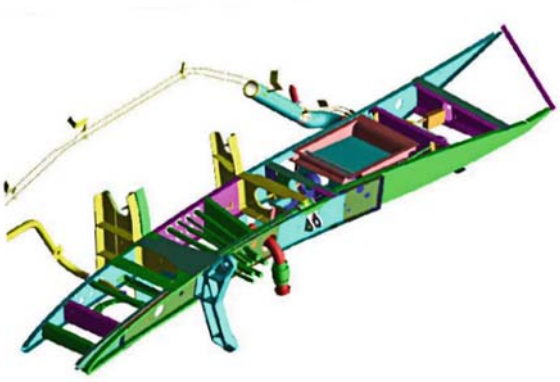

Fig. 11.13 Pylon structural and system configuration

The pylon-mounted turbofan and turboprop engine installation provides a simple configuration and easy maintenance accessibility by using large nacelle panels. A turboprop engine pylon mounting requires special attention to structural dynamics, to ensure avoidance of structural tuning to the engine natural vibration frequencies.

Turboprop installations require the engine to be cantilevered further away from fuselage or wing to clear the large diameter propeller. The propeller disk also acts as a lifting surface such that when a vertical gust is encountered in forward flight for instance, there is a tangential force vector generated on the propeller disk. The

gust load, engine mass under various g-loads and propeller thrust all act on the cantilevered pylon structure. These loads can be significant and will have to be properly analysed to verify adequate structural design.

Flexible shock mounting is used in many engine installations to reduce engine vibration transmission into the fuselage structure and cabin to improve structural fatigue and provide improved passenger comfort. Shock mounting adds additional springs into the structural system and this must be taken into account during the structural analysis of the propulsion system assembly.

A turbofan engine installation has similar design challenges, though with a smaller "disk" diameter, shorter distance from engine to the mounting fuselage or wing, the problem is somewhat less than the equivalent turboprop installation design. Figure 11.10 shows the A-40 flying boat with over-wing mounted turbofan engines. Figure 11.14 shows pylon-mounted turboprop propulsion engines for a proposed large twin fuselage WIG.

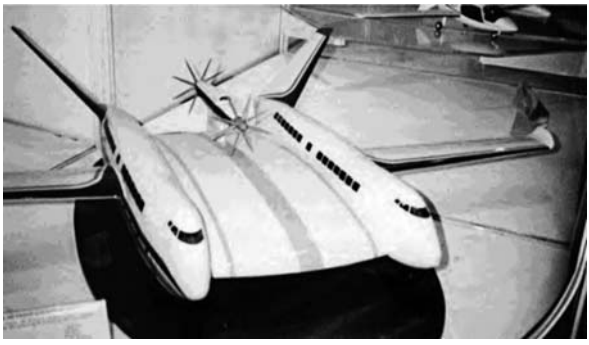

Fig. 11.14 Pylon-mounted turboprop propulsion engine arrangement for large WIG

Engine and System Cooling

Internal Systems Installation

For designs that install the basic power plant internally, there are some different design issues to deal with. The obvious one is that there are requirements for a transmission system that transfer the power from the internally mounted engine to the external lift or propulsion units.

The weight and cost of the additional transmission system should be taken into consideration when conducting the overall vehicle design optimisation. The internal engine installation does provide some benefits and one is the design and engine selection flexibility. The engine envelope, size and profile are less restricted compared to external mounted engines. The engine frontal area does not cause excessive

drag. The cooling system, especially with remote-located radiators, can be arranged to give a flexible hull internal layout.

Internally installed turbine engines do require provision for effective inlet and exhaust systems that can handle the large airflow required. The inlet can be a scoop or pitot type or it can be flush like the NACA inlet design.

The pitot-type inlet generally provides better inlet pressure recovery and thus offers better engine performance, but inlet de-icing is required. The NACA flush inlet does not offer as high-pressure recovery as the pitot-type inlet, but the vortex formation in the curved lip profile eliminates the ice protection requirement.

Fuselage-mounted side inlet designs are sensitive to vehicle sideslip angle, and similarly the top-mounted inlets are sensitive to the angle of attack. Care must be taken to design an inlet configuration that can handle various flight conditions within the design flight envelope.

In many cases, an inlet is designed offset from the fuselage therefore offering a boundary layer bypass effect to provide more uniform inlet flow velocity and recovery effectiveness. The benefit of top or near top-mounted engine inlet designs is to locate the inlet such that the water spray ingestion issues are minimised.

Water Spray

Water spray is always a major design consideration for engine location for a WIG vehicle. Most turbine engines are designed to be able to handle a moderate amount of water to be swallowed by the engine, but a WIG has to be designed to be able to operate on water at various wave conditions.

The locations of externally mounted engines are critically important in order to minimise the possible water spray ingestion. Designers normally mount the engine as high above the waterline as possible, but that also creates a problem as the high thrust line creates a significant pitching moment. Taking advantage of wing, canard or fuselage to shield the engine inlet from water spray is common design practice for WIG as it is also for seaplane design.

Engine and System Cooling

Turbine engines have airflow pass through the engine core continuously and require no additional engine-cooling provision in most designs. The cooling requirements are in the systems such as the generator and the ECU (engine control unit).

For internal combustion engines, the installation considerations are similar to turbine engines but the system functions and cooling design are different. Internal combustion engines require a separate cooling system. For designs that incorporate propulsor direct mounting to the engine output shaft flange, a nacelle that provides a streamlined engine housing and also incorporates an engine-cooling inlet and exhaust passage are required.

The aircraft-type air-cooled IC engines are normally designed to have cylinders with cooling fins arranged such that the cooling airflow either comes from the top then flows through cylinder fins downward or the other way around. It is important to divide the nacelle into two chambers, the upper (relative to inlet-connected chamber) chamber and the lower chamber should be separated by the engine cylinders.

The higher pressure of the upper chamber is to be generated by ram air through the inlet and pressure recovery generated by the diffuser (if any). The low pressure of the lower chamber can be just ambient pressure at the exit or further lowered by an aft-facing exit ramp that generates negative pressure.

The pressure differential between the two chambers forces the airflow through the engine-cooling fins that maintain CHT to be within design spec throughout the operating envelop. The cooling flow rate can be adjusted by opening up the exit ramp angle to generate more negative pressure as necessary. Propeller slip stream can be helpful in engine cooling especially at low forward speed operations (low dynamic pressure from free air stream generated by the vehicle speed)

Some designs provide a tighter seal around the upper chamber by adding a "dog house" on to the engine so that the inlet flows directly into the dog house to maximise cooling effectiveness. It is very important to understand that internal drag is as bad as external drag. A well-optimised cooling system for an IC installation can reduce the cooling drag from an average 12% down to 5% of total engine power compared to a brute force low-tech design.

Additional provisions for an oil cooler, air-conditioning condenser unit and intercooler system if applicable require special attention, as if any of these systems over-heat the result will be operating limitations for the vehicle. Figure 11.15 shows a Teledyne Continental Motor FADEC internal combustion engine installation in a light aircraft.

Fig. 11.15 Avco Lycoming light aircraft engine installation showing air-cooling arrangement

Automotive and marine engines are mostly designed to work with a radiator for engine cooling (water-cooled) as well as some aircraft engines. This arrangement

allows remote installation of the radiators that offers some flexibility in configuration design. The cooling air system for a radiator is no different than a direct air-cooled engine-cooling system design. The inlet, the diffuser, the exhaust duct, etc. all have to be designed to maximise the ram air dynamic pressure recovery, avoid any flow separation in the ducting and the diffuser, and that the exit chamber and exit flow dynamic pressure recovery are maximised for minimum cooling drag. Variable speed electrical cooling fan for the radiator can be a useful device for adjusting the amount of cooling provided to the engine under different operating speed and conditions.

Ice Protection

The WIG vehicle's low operating altitude exposes these vehicles to the worst possible icing envelope. All lifting surfaces and engine inlets are required to be anti-iced or with de-ice capabilities in order to operate safely in icing conditions.

Engine bleed air from the high- or low-pressure compressor stages of the turbine engines is commonly used to provide anti-ice heating for the engine inlet. This is to prevent large ice block build-up on the inlet and that would cause engine damage if sucked into the engine after breakage.

The inlet anti-icing can be accomplished by routing a fraction of the available engine bleed air through the ducted inlet lip. The high bleed air temperature will prevent ice from forming on the inlet. Additional bleed air can be routed to the wing and tail leading edge to provide ice protection. The power plant installation design should include all these system connections, routing and control unit installations.

Transmission Systems

Drive Shaft

For WIG designed with an engine installed separate from the fan or propeller for either a lift system or propulsion requires a gearbox and/or drive shaft as part of the transmission. One of the important parameters to take into consideration in drive system design is the system dynamics.

It is very important to design a drive system that will not create vibration at the structure natural frequencies. This can be accomplished by designing the fuselage and transmission support structures to have natural frequencies away from the drive system or adjusting the propulsion system to operate at rpm offset from the structural natural frequencies.

If the natural frequency of the drive shaft coincides with the first several harmonics of the basic vehicle structure or flight control system natural frequencies, sympathetic vibration can result and induce fatigue failure quickly. Depending on the drive shaft length and diameter ratio, a long slender drive shaft can have a low

natural frequency that is more likely to fall in the range of the structural natural frequencies. Modern graphite composite drive shafts can be designed to provide a lightweight, rigid drive system with high natural frequency thus avoiding many of the system dynamics problems. Figure 11.16 shows a WIG drive shaft arrangement. Figure 11.17 shows a composite drive shaft design.

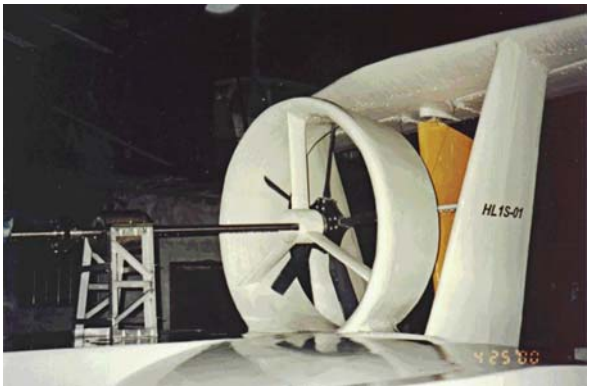

Fig. 11.16 WIG-ducted fan installation

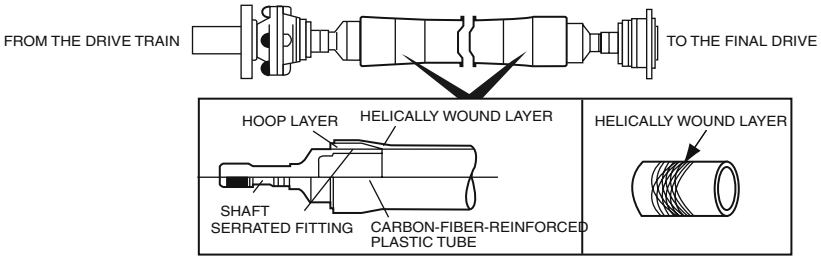

Fig. 11.17 Carbon fibre transmission shaft

Transmission

For some engines, the engine rpm can be significantly higher than the propulsor or lift fan requirement. To match the rpm and torque to the "driven device", a reduction drive is required. There are many possible designs including gearboxes, belt drive and a fluid drive system. The requirement for transmission can come from the need for the offset of drive shaft centreline to the engine output shaft. In many cases, the transmission design would provide the combined solution. Figure 11.18 shows a belt drive reduction system with centreline offset.

A planetary gear reduction system is sometimes installed on turbine engines where the core operates at 40,000 rpm or higher. Turboprop engines sometimes

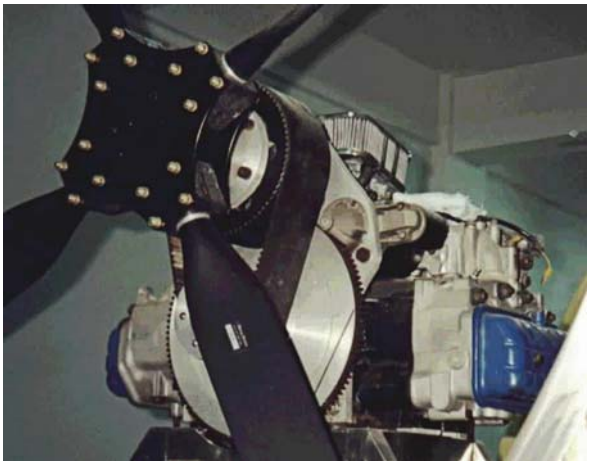

Fig. 11.18 Belt drive reduction to propeller transmission

incorporate an additional external-mounted gear reduction unit attached to the core engine to match with the required propeller speed. These engines are often designed as a package to interface with a propeller directly and are equipped with hydraulic lines through the shaft to provide hydraulic propeller pitch control. Figure 11.19 shows the Honeywell TPE 331 turboprop engine with direct mounted reduction gearbox

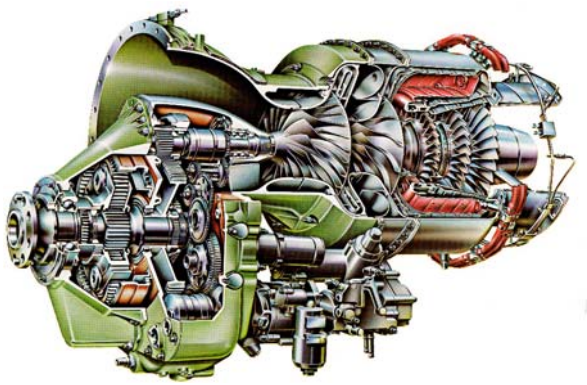

Fig. 11.19 Garrett TPE 331 turboprop engine with direct mounted reduction gearbox

For internal engine installation, a turboshaft engine would commonly incorporate an integrated gear reduction drive to reduce the output shaft to 3,000 rpm range. For turboshaft applications, an additional drive system to interface the engine output to the propulsor or lift system is required.

Chapter 12
Lift and Propulsion Systems

Introduction

The WIG designers' choice of lift and propulsion system configuration is strongly driven by the WIG overall configuration itself. The classic WIG has a main-wing configuration to create a dynamic cushion without assistance of bow thrusters and so the designer can concentrate on the main propulsor location(s) and the transmission from the engine(s).

The story gets a little more complex for the PARWIG and DACWIG as the bow thrusters need to be selected with the craft cruise speed in mind and considering their function – whether they are for pre-take-off and acceleration purposes or whether they are also to be used for cruise propulsion. If additional cruise propulsion is installed, the influence of bow-thrusters efflux on the propulsion system has to be investigated. A ducted fan, open propeller or very high bypass turbofan engine can all provide effective propulsion, as well as low-speed lift enhancement for a WIG, depending on the operating speed range of the craft. The key to a successful WIG design is to select the most efficient option for the craft-operating envelope.

A ducted fan can provide high-volume low-pressure flow for low to medium wing loading or a turbofan engine for WIG with medium to high wing loading. The wing loading has a direct relation to the target cruise speed, in a similar way to aircraft design.

Hybrid WIG that include a dedicated air cushion will also have either a lift fan to feed the cushion or an inlet behind the propulsion fan, and air distribution system to the cushion.

Recent developments in computational aerodynamics allow optimisation of propeller and ducted fan characteristics as well as the lifting wing geometry itself, before testing models in a wind tunnel. High bypass turbofan engines applied to WIG also share many common design features with aircraft applications, with the exception of the ground effect issues that are unique to WIG.

In this chapter, we will discuss the main criteria for the selection of propulsors and lift fan systems, to give the designer a starting point for his/her own work.

L. Yun et al., *WIG Craft and Ekranoplan*, DOI 10.1007/978-1-4419-0042-5_12,

Power-Augmented Lift

The commonly applied method of providing powered cushion flow (other than a skirted air cushion system) is to install an air power source near the nose of the craft and generate high-energy airflow directed towards the channel between the main wing and the water surface. The design can apply a turbofan engine, an open propeller (either a close coupled engine and propeller, or perhaps a low mounted engine and a transmission system through a pylon structure) or a ducted fan system either with integrated mounted engine or through drive shafts. Figure 12.1 illustrates the general concept for power-augmented lifting systems.

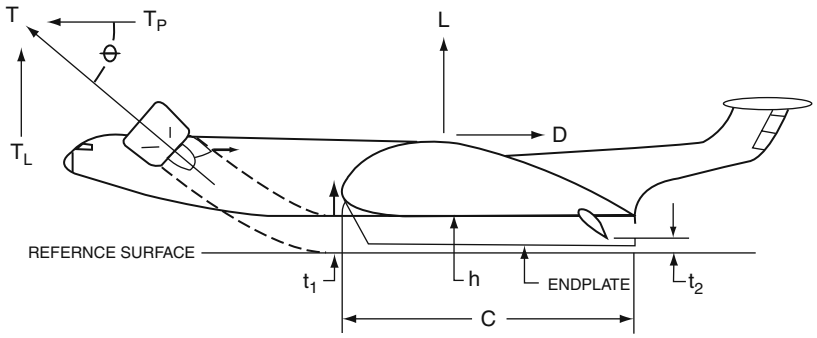

Fig. 12.1 WIG thruster diagram

The turbofan engine can be considered an "all in one" power package for lift augmentation with no external transmission system, so this installation design sometimes can be simpler for the designer to incorporate.

Turbofan engines generate much higher velocity airflow than a propeller or ducted fan and so are more suitable for higher wing loadings and craft speeds. The turbofan propulsor is a good match for craft designed to cruise at speeds above 150 knots (280 kph). An internally mounted fanjet engine can reduce engine nacelle/pylon/fuselage profile and interference drag but may give up some level of accessibility for maintenance. The best example of this type of design is the Russian Orlyonok with its inlets located on top of the craft nose and vectoring nozzles mounted on the side of the forward fuselage, as shown in Fig. 12.2.

The open propeller has also been adopted for PARWIG, see Fig. 2.31 and Fig. 2.32. Due to the large diameter required to obtain desired thrust and volume flow rate for the cushion flow, there are some configuration limitations in the design of craft with open propellers. For propellers installed with blade tips sweeping close to the water surface at low vehicle speed, water erosion can be a significant issue. Another design consideration with open propellers are that there is no easy way to deflect the propeller flow field to tailor how much flow to be directed under the wing for PAR effect and how much to be contributed for thrust at various mode and speed of the WIG operation. This has been overcome by adopting the approach of

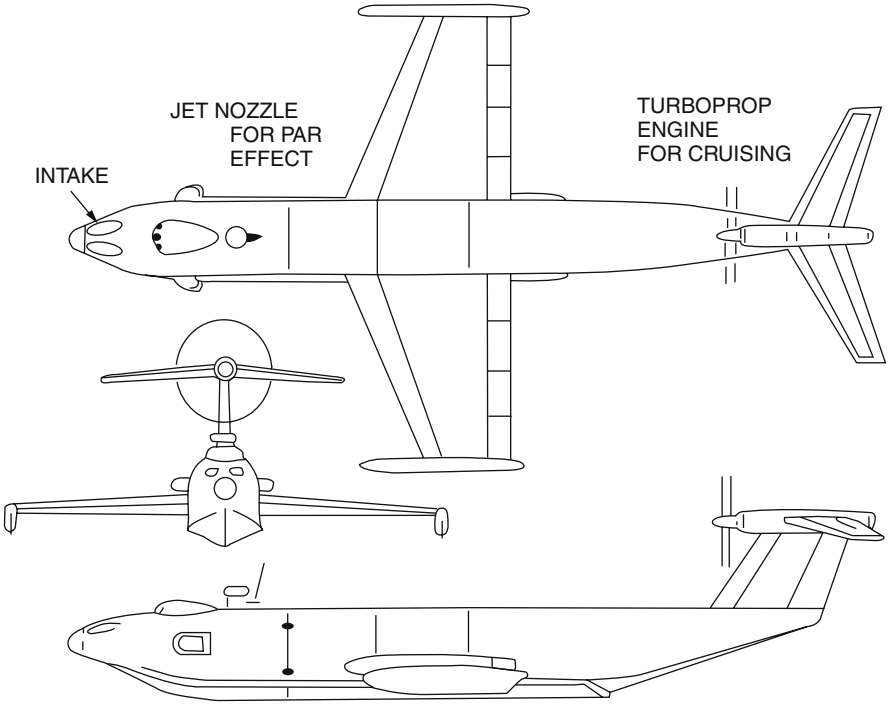

Fig. 12.2 Orlynok diagram

Fig. 12.3 Amphistar DACC

installing open propellers with a tilting mechanism to control the direction of the slipstream on the Amphistar 8 seat DACC shown in Fig. 12.3.

For craft designed to operate at medium speed and with medium to low wing loading, a ducted fan system can be most efficient. A ducted fan normally generates high volume flow at low air velocity very efficiently. This can be beneficial in

producing larger surface clearance for PARWIG or DACWIG craft. Mounted forward of the main wing, a ducted fan system is efficient for speeds up to 150 knots. An example is shown in Fig. 12.4. Above 150–180 knots (280–330 kph), duct drag starts to become an issue and the designer's choice of unit may graduate towards selecting a high bypass fanjet system.

Fig. 12.4 Swan

The duct inlet design can be tailored to maximise thrust at a particular speed. A duct with a bell mouth-type inlet is best to generate low-speed thrust, while duct profile drag becomes too high at speeds above 150 kph. More streamline-profiled duct inlets can be optimised for higher cruise speed but may suffer from inlet flow separation at low speed. A careful balance in duct profile design is essential for efficient power-augmented lifting as well as higher speed thrust generation. Variable geometry inlet and exit duct design can provide the best of both worlds but at the expense of mechanical complexity, cost and weight penalty. The penalties are so great that variable geometry has so far always been discarded.

Many power-augmented WIG designs incorporate "thrust vectoring". During ground operation, take-off and low-speed flight, the powered lift system airflow is directed downward aiming at the wing/surface channel for maximum lift augmentation. During high-speed cruise, the lift system airflow is re-directed to near horizontal direction to provide additional thrust, as the dynamic pressure generated by the craft's forward velocity is sufficient to provide the lift.

Thrust vectoring can be accomplished by either tilting the complete nacelle unit to change the direction of the exhaust flow or by keeping the nacelle stationary and deflect the exhaust flow. Deflecting the exhaust flow can be accomplished by deflecting "vanes" installed behind the ducted fan unit or by vectoring the exhaust nozzle on a turbofan engine. Figure 12.5 shows a vane exhaust flow vector control fitted to a ducted fan.

Rotating the complete propulsion unit imposes significant structural design challenges especially with multiple units installed side-by-side. The dynamic loads due to gust or water impact induced by the large mass of the propulsion units cantilevered outboard can be difficult to handle, especially when they are mounted on rotating mechanism. Noticeable weight penalty may also be expected. Exhaust vectoring is therefore a much easier design choice.

Fig. 12.5 TY-1 propulsor installation

For turbofan or turbojet engine installations, locating vanes in the high velocity exhaust flow has a detrimental effect on engine performance, in addition to the structural problem with long-term exposure in high-temperature engine core flow. The better solution is to tilt the tail pipe either with a two-dimensional vectoring nozzle or a three-dimensional vectoring nozzle, as many successful applications have been demonstrated in the aircraft industry already.

For ducted fan designs, the exhaust flow velocity is relatively low and lends itself better for outflow vane control design. Due to the large diameter of the ducted fan, the vertical and fore-and-aft location relative to the wing requires careful consideration especially when the duct flow is to be directed under the wing for power-augmented mode and directed aft over the wing for cruise mode.

Independent Lift Systems

Some WIG designs incorporate a dedicated lift fan system in a hovercraft like arrangement. This type of system is used in air cushion equipped WIG as shown in Fig. 12.6. The benefit of a dedicated lift system is that it only needs to operate within a narrow band of operating conditions and power settings, so it is simpler to optimise the lift system performance. The draw back is that the lift system has no significant effect in cruise flight (a large percentage of the WIG operation) even if it is left running, and the cost and weight of the system as well as the drag would cause performance penalties. The main benefit of a dedicated cushion system is that an undercarriage is not needed for coming ashore at a terminal or beach, see Fig. 12.7, and take-off hump drag is significantly reduced, similar to the DACWIG.

A stand-alone lift system is designed in the same way as the lift system for a hovercraft. The main hull or catamaran hulls plan geometry needs to provide an air cushion that gives the craft adequate pitch and roll stability at low speed. The

Fig. 12.6 Weber WIG on land

Fig. 12.7 UH-18P air cushion WIG coming ashore

skirt system needs to efficiently contain the air cushion and provide obstacle clearance sufficient for the ground terrain and waves that the craft will encounter while hovering.

The hybrid air cushion WIG has an advantage over a DACWIG for small-size craft in that bow thrusters are not required, and the main propulsion unit can be mounted towards the stern providing higher velocity airflow over the rudder and elevators for increased control moments.

Two craft speeds need to be carefully considered for the lift fan system design: static hovering and take-off speed. Static hovering is straightforward, the craft is simply a hovercraft. At take-off speed that may be from 50 kph up to above 100 kph for larger craft, the airflow into the lift fan will strongly affect the aerodynamics of the nose area of the main hull, and accelerating the airflow to craft forward speed will generate a significant air momentum drag.

Propulsion Systems

Propulsion system sizing and configuration are determined by the intended WIG-operating envelope. The key parameters are

- Design-operating speed range
- Total thrust required for take-off
- Total thrust required for design cruise speed
- Desired system configuration
- Installation design and integration – tail mount, wing mount, nose mount
- Support structures and structural dynamics
- Aerodynamic Interference
- Specific fuel consumption

High-speed craft with cruise speeds exceeding 250 knots are better suited to high bypass turbofan selection, see Fig. 12.8. The turbofan installation can be relatively simple as a complete propulsion unit since it does not require separate engine installation with transmission shafting and separate propulsion fans or propellers. Although the turbofan engine has historically been expensive, the trend over the last decade has been that the cost premium of the turbofan over other power units

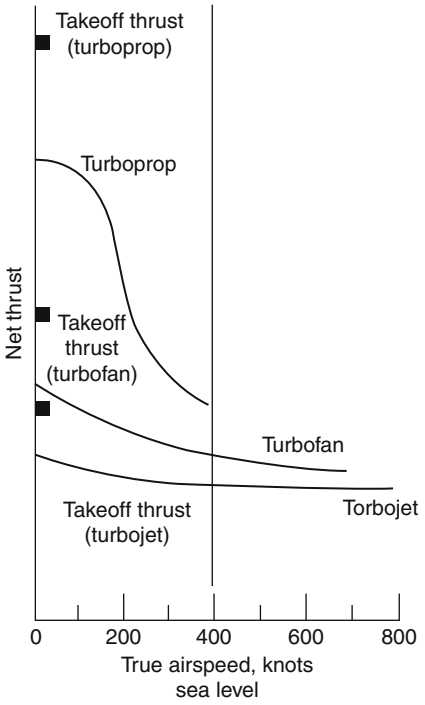

Fig. 12.8 Net thrust versus speed for propellers and fans

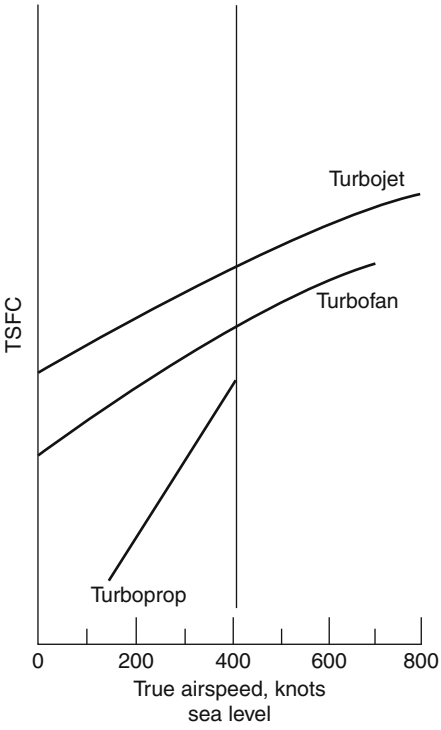

Fig. 12.9 TSFC versus speed for propellers and jets

is reducing. Further, the fuel efficiency of current-generation fan-jet engines has improved by more than 20% over the last 20 years, rendering the turbofan engine attractive for future WIG applications, see Fig. 12.9.

Medium- and low-speed craft can obtain higher static and low-speed thrust for the same horsepower and fuel consumption by using an open propeller or ducted fan. Ducted fan design can be further tailored for either medium-speed operation or maximise static thrust for acceleration performance. Figure 12.10 shows a PARWIG with a contra-rotating propeller propulsion system driven by a close-coupled gas turbine.

For the classic WIG design, there is no power-augmented lift and it is up to the propulsion system to provide enough thrust to accelerate the craft to reach a speed that can generate adequate wing-in-ground effect to lift the craft off the water/surface. Without the power-augmented lifting capabilities, the take-off thrust required is normally higher as it has to counter the waterborne drag during initial acceleration. Operating at cruise speed allows throttle back since operating in ground effect will require less power than take-off. The benefit of course is the simplicity in that only propulsion system is required at the expense that larger engine may be required. Figure 12.11 shows an open propeller classic WIG design.

Fig. 12.10 Orlynok in flight

Fig. 12.11 AF-3 classic WIG in flight

Propeller and Ducted Fan Characteristics

The propeller has been widely used in aircraft design mainly for the effectiveness in generating thrust at speeds in the range of 100–250 knots. Propeller design can be tailored to maximise static thrust if the critical operation mode is low-speed take-off acceleration or can be tailored to a higher speed that provides optimum cruise performance. Open propeller design has been shown to be most effective from zero forward velocity to 250 knots. The crossover region choice between a propeller and turbofan engine is between 200 and 300 knots. Propellers are considered very reliable and light weight for the thrust they can produce, but have several limitations as follows:

- Large diameter require high position to clear water level and avoid foreign object damage
- Trade-off between rotor diameter/tip speed and noise level
- Personnel and passenger protection
- Blade water and sand erosion protection

Figure 12.12 shows a typical plot of propeller thrust versus speed for different blade pitch.

The advancement of prop-fan technology (propellers with higher numbers of blades, rather like a fan without a duct) might provide an interesting propulsor

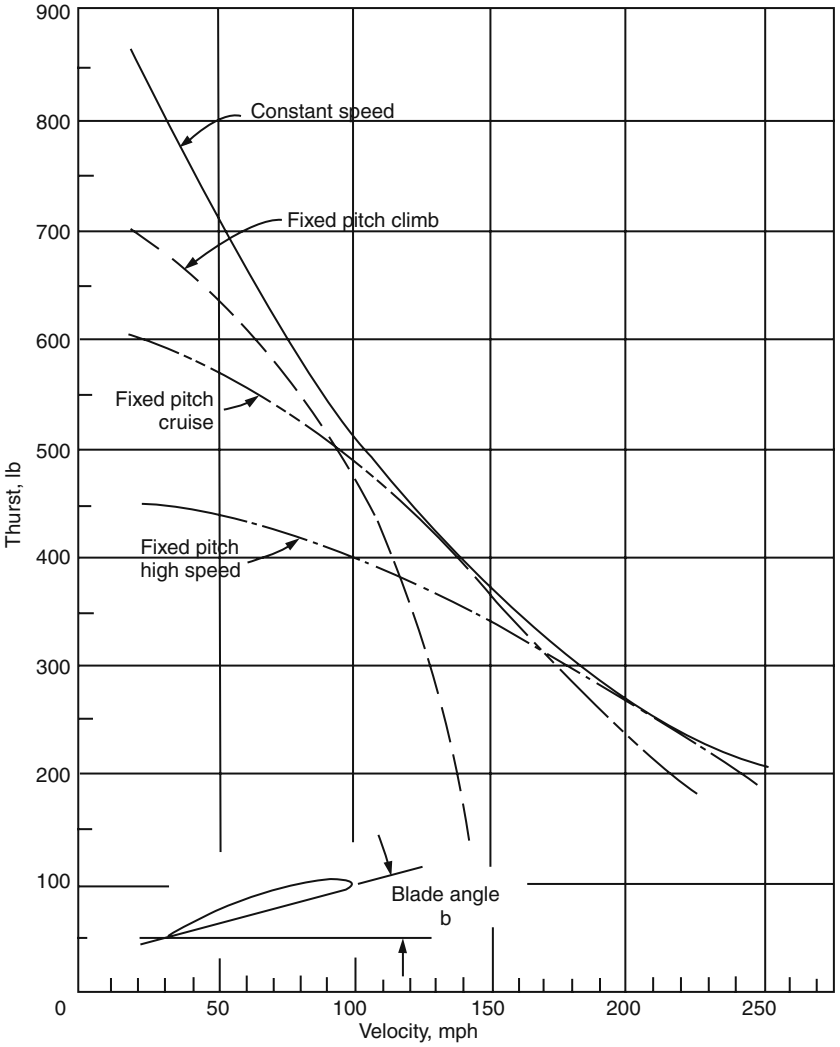

Fig. 12.12 Thrust versus speed for propeller pitch

package that allows smaller rotor for open propellers, see Fig. 12.13. The prop-fan concept was developed in the 1980s for fuel-efficient medium-size airliners and the technology might be applicable to WIG designs for cruise speed up to 350 knots. The prop-fan technology developed in the 1980s was focused on fuel efficiency at cruise up to Mach 0.80, but the resulting highly swept back blade design introduced significant structural challenge. For WIG application with lower cruise speed, slightly reduced blade sweep design can reduce the implementation problems. The

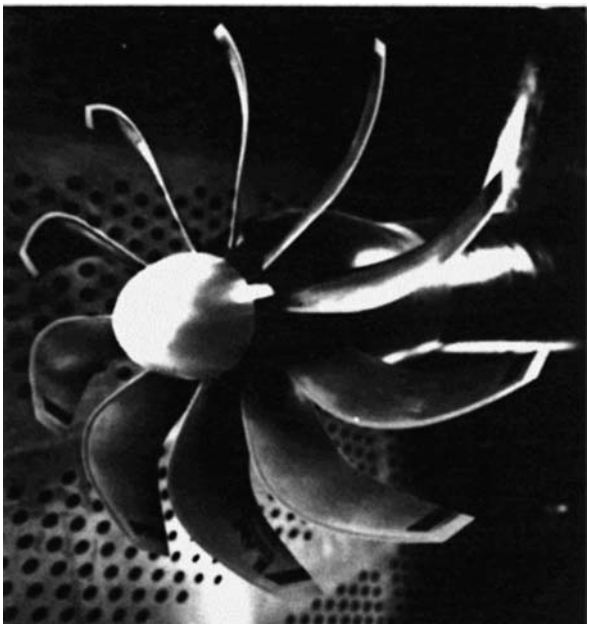

Fig. 12.13 Prop-fan system

main drawback for this propulsor is blade tip noise. This is lesser an issue in ducted fans and high bypass turbofans, together with the ability to select smaller diameter units.

The ducted fan is widely used in WIG applications for several good reasons:

- Smaller rotor diameter than propeller for same amount of thrust
- Lower tip noise
- Noise reduction duct acoustic treatment possible
- Rotor protection with shroud
- Easier to install exhaust vane for exhaust flow vector control
- Operating safety

A properly designed duct system can enhance the thrust with the same disc loading or achieve the same design thrust with higher disc loading, i.e. a smaller propulsion unit as shown in Fig. 12.14.

Research effort in the UK in the 1970s showed that a 4.5-ft diameter ducted fan design with 350 hp can produce the same amount of thrust at 150 knots cruise speed and yield 30% higher static thrust as shown in Fig. 12.15.

The ducted propulsor requires some different design consideration:

- Maintain small fan tip to duct clearance for required performance
- Engine vibration versus fan tip clearance for all-in-one power unit

Fig. 12.14 Ducted fan and side float for craft in Holland

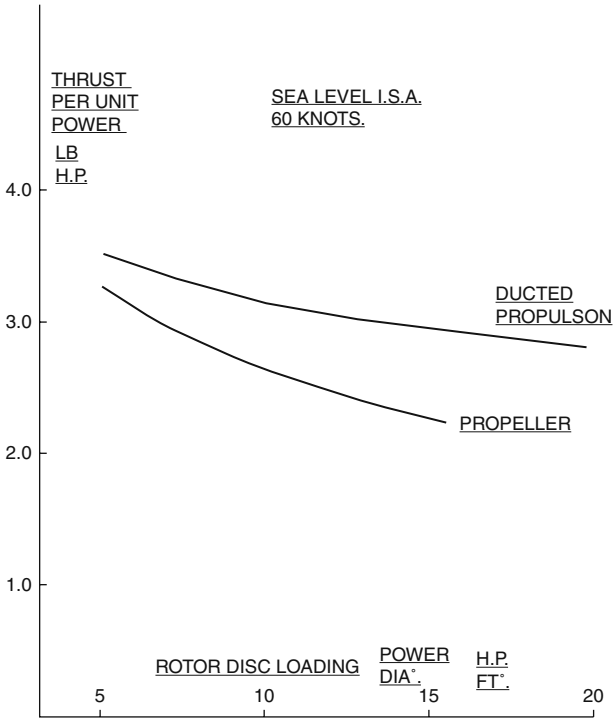

Fig. 12.15 T/power against rotor disc loading

- Duct rigidity under various loading conditions
- Multiple fan blade pitch control mechanism complexity

Even with some of the design challenges of the ducted propulsor, it is still a very attractive propulsion unit for WIG craft. Figure 12.16 shows a comparison between an open propeller of 2.1 m diameter, compared with a 1.4-m diameter ducted propeller. The thrust characteristic is almost the same, except that the ducted propulsor has higher static thrust.

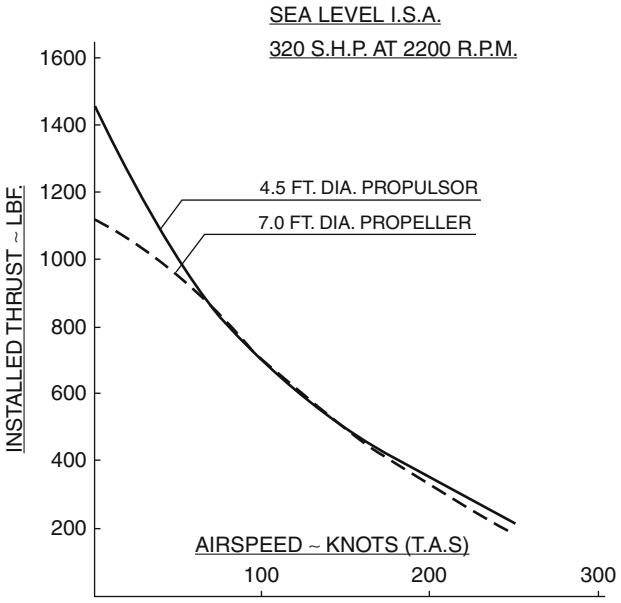

Fig. 12.16 Seven-feet open propeller versus 4.5-feet ducted propulsor diagram

Turbofan System

As mentioned in the introduction, modern turbofan engines provide a very attractive power system for high-speed WIG propulsion applications. There are several advantages in turbofan engines:

- Compact installed package (relative to the thrust delivered)
- Wide range of thrust available (320–46,000 kg thrust)
- Very good specific fuel consumption especially for cruise speed of 200 knots or higher
- Relatively simple support structures and installation
- Significant amount of aviation industry experiences available for design optimisation
- Well-established worldwide service and support network available

Figure 12.17 illustrates the thrust-specific fuel consumption versus bypass ratio for turbofan engines.

For WIG application, special attention is required in the selection of the engine location. Tail mount engines are likely to experience considerable water spray that can drastically reduce the time between overhaul, especially if operating in salt-water environment. Locating the engines high up can reduce the amount of exposure

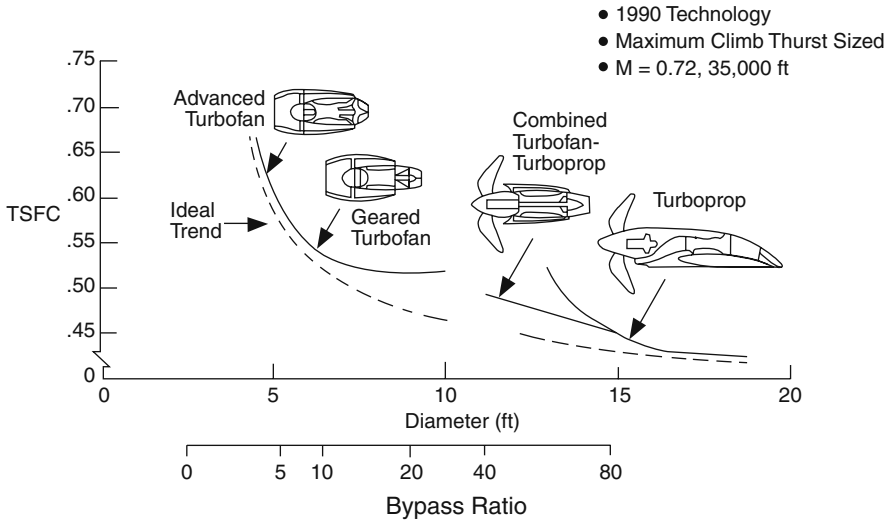

Fig. 12.17 TSFC versus bypass ratio for turbofans

but not eliminate it. One method to address the problem is to incorporate an "inertial separation system" at the engine air intake to force heavier water droplets to go around the engine while air will make more rapid turn and feed the engine properly. The main problem with an inertial separation system is that it can reduce inlet recovery and thus reduce installed thrust.

Figure 12.18a, b shows the KM Ekranoplan in flight and floating, showing its eight jet bow-mounted PAR system and two jet propulsion units in the tail.

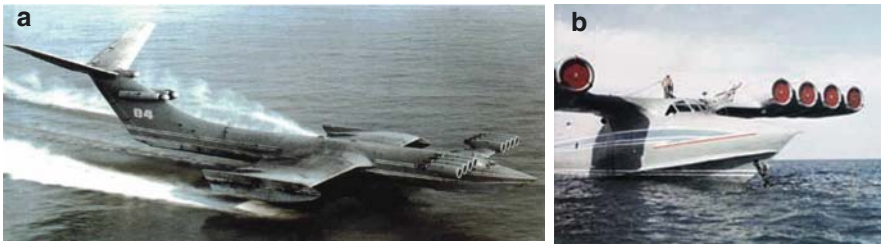

Fig. 12.18 (**a** and **b**) Views of KM bow-thruster installation

For most aircraft applications, turbofan engines are mounted either under the wing as shown in Fig. 12.19 or on the aft-fuselage with a side pylon. For WIG applications, neither location is a good idea due to the fact that for most WIG designs the wing is too close to the water surface and aft-fuselage installations are subject to too much water spray. For the higher tail mount design that is more suitable for

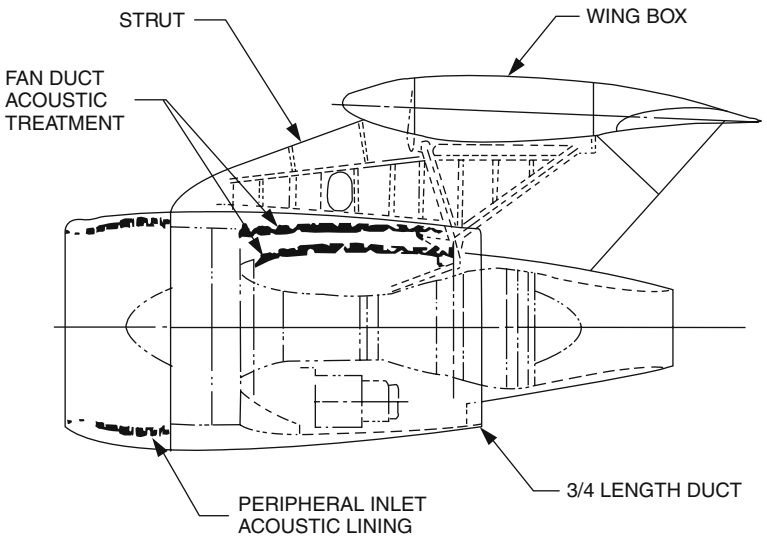

Fig. 12.19 Turbofan performance – under-wing location

WIG operations, installation can be structurally similar to aft-fuselage installation with side-pylon configuration.

The other possible propulsion unit location is above the fuselage or over the wing. For over-wing design, the engine-induced flow field effect on the wing pressure distribution must be considered. Some research indicates that over-wing installation can produce additional lift at little or no drag penalty as shown in Fig. 12.20.

Care must be taken to consider the span-wise location of the engine, as it can induce additional lift. Additionally if an engine stops it can induce sizeable rolling moment that must be controllable. An example of the over-wing jet velocity effect on wing pressure distribution is shown in Fig. 12.21. The fore-and-aft location of the engine is critical for the overall craft performance since the resulting pressure distribution can change significantly as shown in Fig. 12.22.

Integrated Lift/Propulsion System

For medium and small WIG craft, the possibility of using the same propulsor for augmented lift and propulsion provides the potential weight and cost savings that are always important design considerations.

A typical integrated lift/propulsion system may be arranged to have the propulsion unit located in front of the craft so that the airflow can be directed towards the wing/surface channel for take-off. There is still enough forward thrust in take-off mode even with flow directed more downward to provide take-off acceleration.

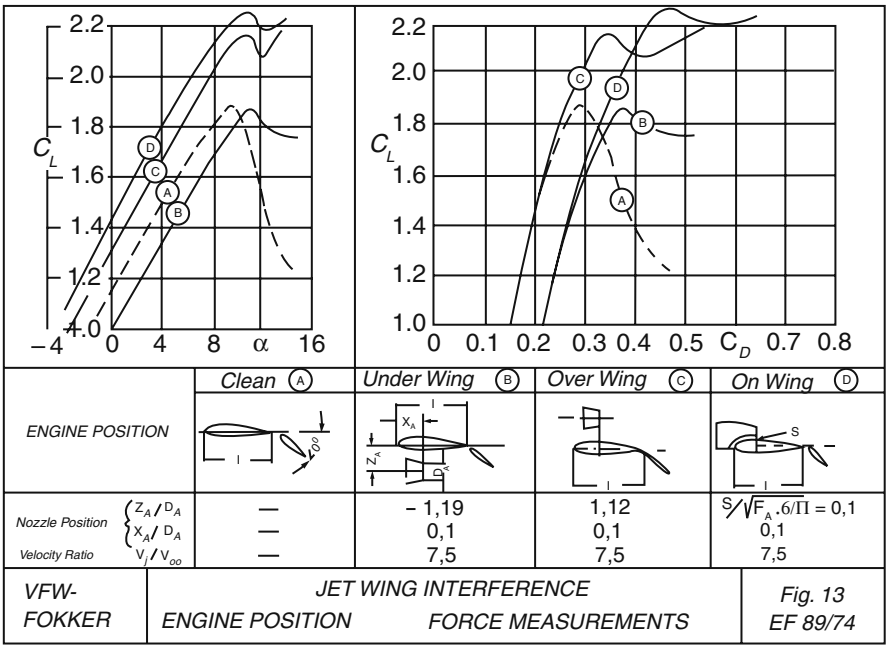

Fig. 12.20 Turbofan performance – over-wing location-1

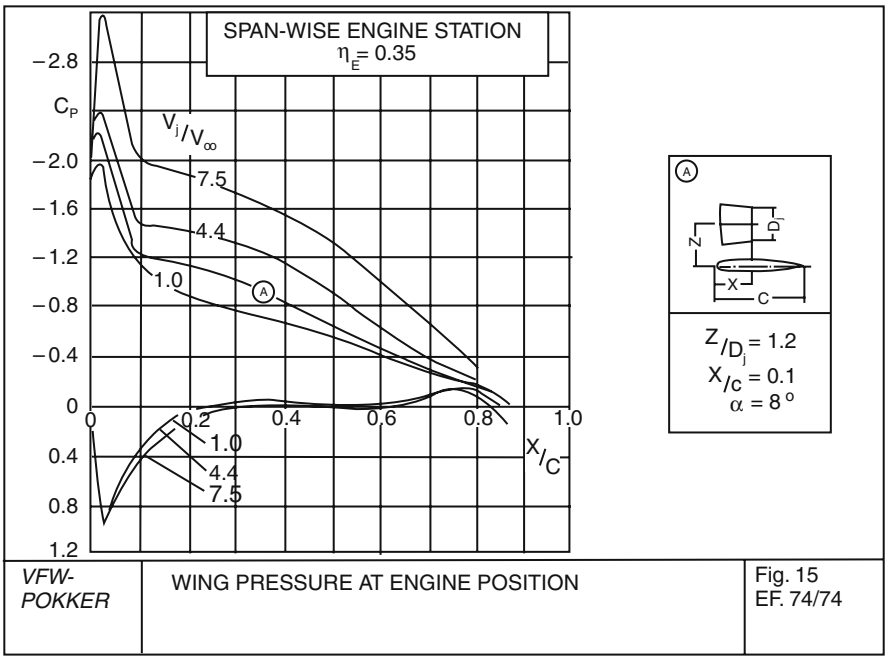

Fig. 12.21 Turbofan performance – over-wing location-2

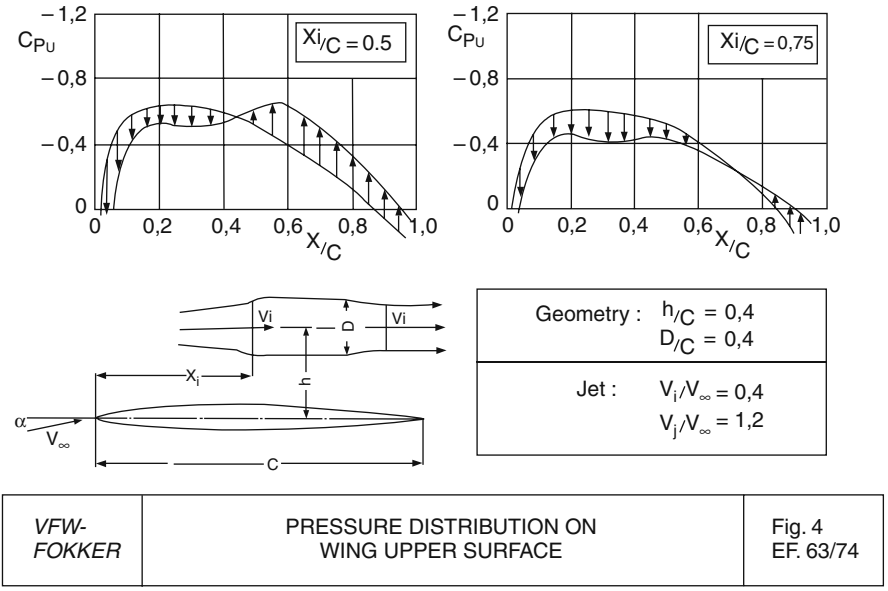

Fig. 12.22 Turbofan performance – over-wing location-3

Fig. 12.23 TY-1 WIG

Once in cruise mode, the airflow is directed afterward to increase propulsion effectiveness and possibility of throttling back to reduce fuel consumption and extend engine life. Figure 12.23 shows an integrated lift/propulsion system PARWIG.

Figure 12.24 shows an artist's impression of a futuristic PARWIG concept with an integrated turbofan lift and propulsion system mounted on horizontal pylons in the craft nose.

Fig. 12.24 Super jet WIG

Propulsor Selection and Design

Fans, propellers, turbofan engines and jet engines are all available as production units from manufacturers supplying for use in aircraft, hovercraft, microlight aircraft or in the case of axial fans – the heating and ventilating industry.

The WIG designer will normally have to select a candidate propulsor, obtain the performance characteristics from the manufacturer and analyse whether it can fulfil his needs. Propellers for use in light aircraft have been adapted in the recent past for application as ducted propulsors on a number of utility hovercraft and so provide a useful starting point for medium speed utility WIG.

The WIG designer may choose to design his/her own propeller and have it manufactured. This is practical if the propeller is to be a fixed pitch unit, while variable pitch units are best purchased from manufacturers who have certification for supply to the aviation industry.

Propulsor thrust performance will need to be determined and plotted through the range of the WIG craft speed, and compared with the total drag for the craft in the envelope of wind speed, and wave conditions projected for operation. It is advisable at the initial design stage to include a margin of 10–20% for uncertainty in propulsor performance until the effect of propulsor position relative to the hull and main wing can be properly assessed. It is always better to be able to optimise downwards later on, rather than having to increase propulsor specification and associated engine powering.

Chapter 13
Concept Design

Introduction

In this chapter, we will explore potential applications and then discuss preparation of concept designs.

To date, the use of WIG craft has been restricted to prototype trials and test operations, mainly for military and paramilitary purposes. In Russia in particular, as described in Chapter 2, the navy invested heavily during the 1960s and 1970s in a succession of craft. The initial series of pure trials craft lead to design of larger vehicles suitable for fast logistic service for the Russian Navy in the Caspian Sea. These developments and operations demonstrated the effectiveness of the technology and gained valuable practical experience.

The Russian programme has been followed by a more recent WIG development programme in China aimed at medium-sized craft effective for utility or ferry service. Many lessons have been learned already in this programme about improved efficiency. The deployment of coastal patrol WIG craft is the next technical objective and will also be attractive to many other coastal and island nations in the Far East for combating piracy and smuggling.

If this knowledge can be put to use in the development of medium and large craft aimed at commercial duties, there is also the potential to fill a gap in the transport spectrum between fast marine ferries and cargo aircraft in the near future.

At the smaller end of the scale, prototype WIG craft with a wide range of lifting surface geometries have been built in countries ranging from Australia and China to Germany and the United States. The technology is continually being advanced, mainly by private individuals and small private companies. There is a substantial potential market for such craft, once the hurdle of acceptance of a new technology has been overcome.

Since the late 1990s, the WIG concepts developed at RFB in Germany have been taken over by Flightship in Australia (later moved to Singapore ownership and location) and further evolved into craft that are economic for air taxi services. The craft have been certified under the IMO and Australian regulations for operation, so may be considered the first major breakthrough into commercial operations for WIG.

L. Yun et al., *WIG Craft and Ekranoplan*, DOI 10.1007/978-1-4419-0042-5_13,

So, what are the key WIG attributes? They may be characterised by

- High service speed: The craft take off from the water surface and are fully aerodynamically supported during normal service operations, so hydrodynamic drag is small compared with conventional high-speed ferries and military craft. WIG are able to operate economically at speeds from 100 up to about 500 kph, a region currently possible only with aircraft.
- Seakeeping quality: Since the craft fly above the sea surface, seakeeping quality is high compared with other marine craft, and there is only small speed loss in a seaway. The sea state for take-off is more restrictive and so relatively sheltered conditions are necessary, together with service routing across sea areas with limited extreme sea states, for example, coastal areas, inland seas and the equatorial oceans.
- High work capacity: There are no particular difficulties to develop very large WIG, for example, as large as 5,000 t displacement, 500–1,500 t payload, 400 km/h and 2–10 m flying height. Conventional aircraft are very costly to scale up this far due to the limitations of available airport runways. Medium-sized WIG have potential work capacity that is larger than conventional high-speed marine vessels, due to their higher service speed and lower speed loss in a seaway.
- Marine terminal/base facilities: WIG craft can take off from the water surface and so do not need a prepared runway or airport-type facilities. So long as the craft is designed for manoeuvring in the floating condition and there is a suitable take-off area close to the terminal where other marine traffic can be controlled, such craft can operate in a similar manner to high-speed ferries or seaplanes. Many of the world's larger cities are located in river estuaries or at a coastline, so development of useful "Blue Highways" may help to lighten the road and air commuter-based traffic in the future for medium distance operations and offer an intermediate-speed freight service on intercontinental routes.
- Safety: WIG craft operate close to the water surface and in the strong surface effect zone during take-off and touch down. The design of lifting surfaces for take-off and normal flight provides a stable response in ditching, so WIG craft can be designed for safe landing in case of engine failure, with a softer landing than normal aircraft in such conditions.
- Low fuel consumption: Since WIG are operated in the surface effect zone, aerodynamic efficiency is high, so reducing fuel consumption to less than half that of an equivalent aircraft.
- Construction: WIG craft are classified as a marine vehicle through IMO rules, so the requirements for qualification of craft construction and the equipment on board are different to that of an aircraft. Prototype development costs should be limited, following marine practice rather than that of the aeronautical industry. Construction cost will be in between the level for a fast ferry and a turbo-propeller aircraft.

From Fig. 13.1, it can be seen from the relation between speed and craft weight that the ideal application for WIG is located between the aircraft and conventional high-speed marine craft, such as ACV, SES and hydrofoils.

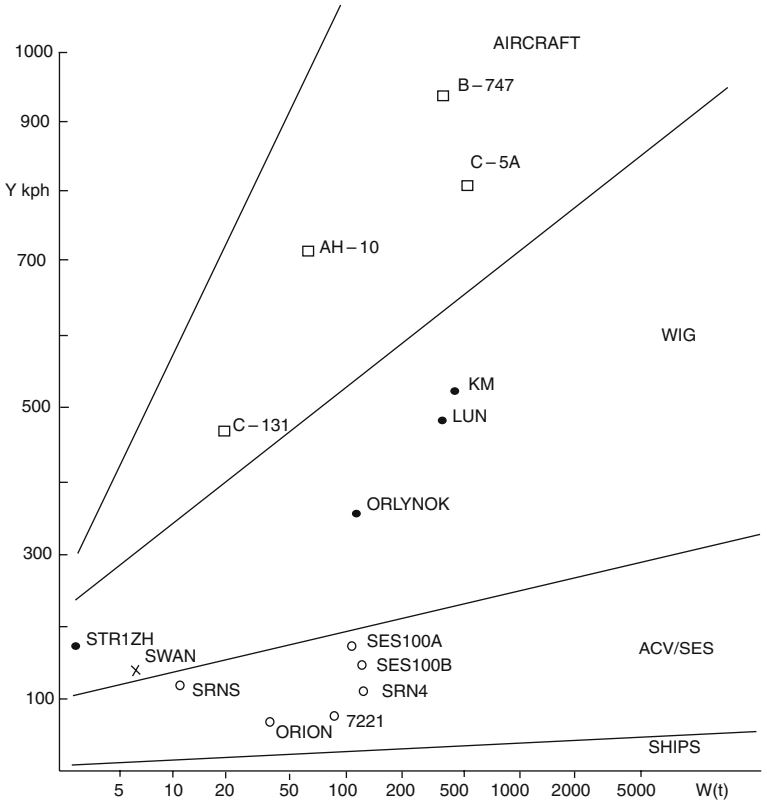

Fig. 13.1 Application zone for various craft max craft weight and speed

Figure 13.2 shows the relation between the speed and lift/drag ratio of various vehicles (figure appears wrong – need careful data check – e.g. helicopters – think labels are just mixed up).

Figure 13.3 shows the specific power, i.e. engine power over vehicle weight (horsepower/tonne) plotted against vehicle speed, for different lift–drag ratios. It can be seen that WIG are an efficient means of transport at speeds of 150–500 kph both at small and large sizes.

Figure 13.4 also shows the relation between the specific power and maximum cruising speed. The specific power of WIG in this figure is much higher than that in Fig. 13.3 due to the different source of data. There is a considerable variation in the absolute values of such parameters found by engineers working with different design styles for WIG.

Figure 13.5 shows the required power for different transport vehicle types. The co-ordinate P/W is normalised to the power of a standard automobile at a speed of 100 kph. This figure suggests that the optimum for WIG is 150–400 kph. In general, WIG are found to be most efficient at this service speed range, while the limitation for all up weight is determined by available propulsion power plant.

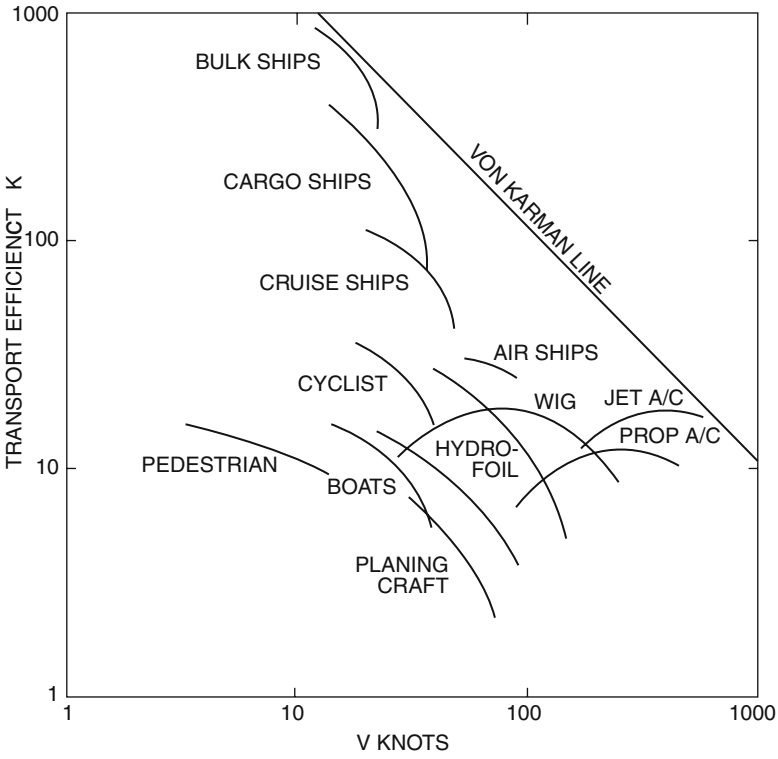

Fig. 13.2 Lift versus speed for various transport

General WIG Application Issues

There are no WIG commercial service routes operated so far, even though the WIG has been successfully operated and tested for more than 30 years. While technically successful, development of the support systems for WIG commercial operation will require significant investment in terminal facilities similar to large amphibious hovercraft terminals. References [1–3] provide background information on operational considerations and route selection based on current available craft.

Successful operation of small-scale operational trials are likely to be necessary, rather like the ACV passenger operations in the 1960s with SR.N6s that provided the encouragement for the cross-channel SR.N4 ACV ferries. The following main aspects need to be further improved compared to prototypes constructed to date:

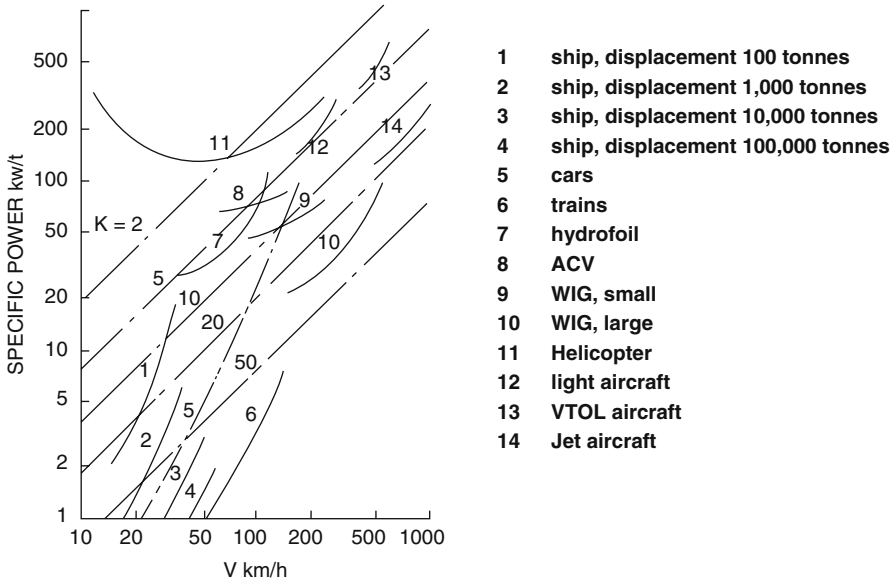

Fig. 13.3 Specific power versus speed for various transport

Technical Factors

- *Take-off*: The take-off speed of a WIG without lift enhancement is high due to its high hump speed. Reducing the hump drag and take-off speed so as to reduce take-off and overall installed power requires a PARWIG or DACWIG design. On PARWIG, the bow lift enhancing blowers may shut down after take-off, but become excess weight during cruise. Small WIG may be designed with lighter wing loading so as to reduce take-off speed, but this limits the cruise speed attainable. Air cushion systems can be very useful for lowering take-off speed, but require incorporation of flaps and perhaps other means to change the main-wing profile after take-off so as to enable high cruise speed. Active control surfaces have the penalty that they require constant adjustment in flight, placing a high demand on the pilot.
- *Stability*: Automated control systems for WIG will be more complicated than that on an airplane or hydrofoil craft, because the WIG has to assure its safe operation while at great speed very close to the surface. At present, there are no commercial systems available that are suitable for high-speed WIG autopilot service, and so all designers of WIG, small or large, have to aim at a craft that is statically stable and have a stable response to dynamic controls in flight, so that the pilot can fly the craft manually in a safe manner.

Aerodynamic efficiency: The aerodynamic efficiency K increases with aspect ratio; however, the main wing lift force during take-off increases inversely with

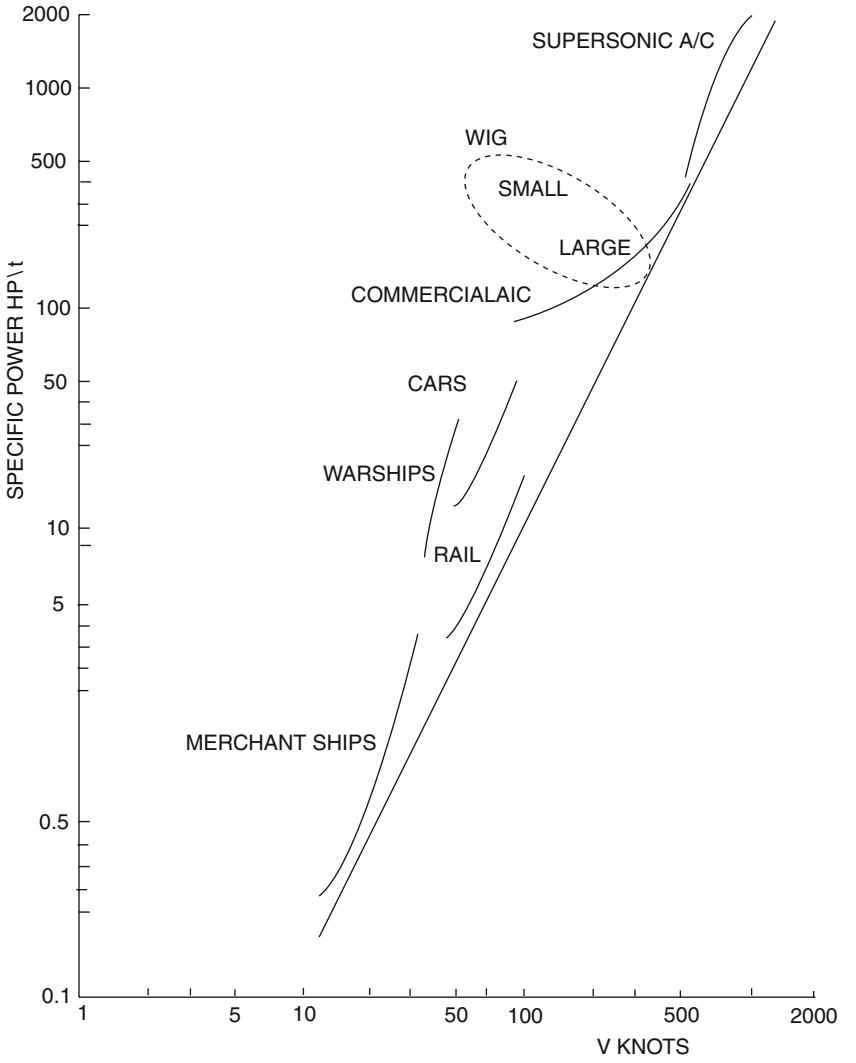

Fig. 13.4 Specific power versus maximum cruising speed as a function of installed power for propulsion and gross weight (displacement), compared with state of the art line defined by G. Gabrieli and T. Von Karman

aspect ratio. The best way to solve this problem is to use a composite wing with AR = 0.5–0.8 for main wing and AR = 3–4 for the extended wing. In addition, the main-wing plan form needs careful design. WIG targeted at cruise speed up to 300 kph can employ a strongly tapered wing with anhedral and washout to improve static stability through the speed range. High-speed craft require a more rectangular main wing with careful attention to flap design for low-speed operation.

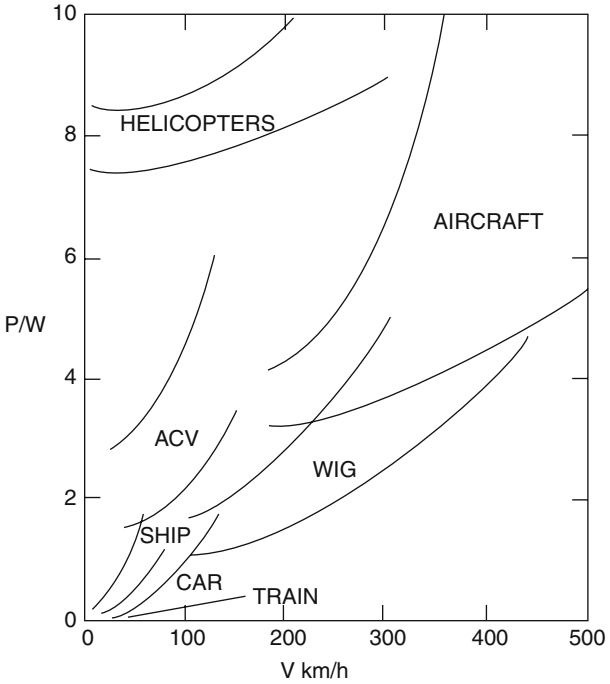

Fig. 13.5 Required power for different transport vehicles

Operational Factors

- *Terminals*: A WIG operation will need to be near coastal cities, similar to existing ports designed for ships and boats. WIG facilities needed are similar to a Hoverport for amphibious hovercraft with entry and leaving slipways and a large manoeuvring apron, see [4]. Deep water is not required, rather, and area outside normal navigation channels suitable for a water runway of 1,000–2,000 m in length and 500 m in width.
- *Manoeuvrability*: WIG are difficult to operate alongside other craft or a quayside due to their protruding main and tail wings, so terminal operations need an approach similar to amphibious hovercraft. Design of low power water thrusters for floating manoeuvring of WIG up to the slipway is an area requiring development so as to avoid excessive use of main engine power close to a terminal. The DACWIG and DACC are able to manoeuvre on their air cushion at slow speed, so do not have the same design constraints. During flight all WIG require more space to manoeuvre than an ACV simply due to their higher speed. While many WIG can bank into a turn, the reduction in manoeuvring space does not change the overall requirement. WIG navigation therefore needs to be separate from other marine craft. Due to its speed, a WIG has to be operated on the basis

that it is invisible to all other craft and ensure that it takes collision avoidance action, including maintaining a safe distance from other craft of (for example) between 1 and 5 km depending on speed.

- *Safety*: The collision risk for WIG is higher than that of conventional high-speed craft because of its very high speed and operation essentially at ground level, so the navigation equipment installed such as radar has to be responsive, precise, light and reliable. In addition, the requirements for the equipment used in navigation ground stations at terminals are also rather higher than normal for ferries or aircraft.
- *New technology*: The WIG is a new vehicle type operating at high speed essentially on the water surface, so both aircraft pilots and captains of high-speed marine craft have little applicable experience. For aircraft pilots, flying close to the ground, with manoeuvring available only in the horizontal plane and little possibility to bank, is a major challenge. Using the "Jump" technique for collision avoidance is also a very special driving method, requiring practice. For a marine captain, the extreme high speed requires a different approach to normal marine craft. Clearly therefore, setting up operations with a WIG service will require considerable vision on the part of the operator and careful training of personnel.
- *Noise*: For a current generation WIG, the noise pattern is similar to a turbo-propeller aircraft operating close to the water surface. Ducted propulsors are a help to reduce noise signature, similar to the ducted propulsors on modern ACVs. However, since the water surface absorbs some noise and as the WIG is always operating in GEZ influencing the noise dispersion, the actual noise pattern should be lower than aircraft with the same power. There are few investigations about this so far due to most WIG craft being built for military duties. It is likely that noise close to terminals, i.e. slow-speed manoeuvring noise, will be the controlling factor to acceptance, both by travellers and the communities around the terminals. Adoption of ducted propulsors, and high bypass turbofans on larger craft should allow design to acceptable criteria.
- *Economy*: Figure 13.6 shows the aerodynamic properties of WIG in both first and second generations, and airplane weighing 450 t [5], where 1 – first-generation WIG, 2 – second-generation WIG, 3 – airplane, K_{max} the maximum aerodynamic efficiency, h the flying height and C the wing chord. The figure shows the K_{max} of second-generation WIG can exceed airplane transport efficiency. Figure 13.7 shows the WIG weight composition compared with aircraft, where W_p and W_f represent the payload and fuel weight, respectively, and W craft take-off weight. WIG have a lower payload weight fraction due to their marine construction. Figure 13.8 shows the comparison of fuel consumption of WIG with an airplane, where R represents the range. From these figures, one can see that the second-generation WIG can begin to compete with large jet aircraft. It is proposed nevertheless that the WIG at present are more suitable for short-range routes of 100–400 nm length, on which aircraft are less efficient due to the many take-off and landing operations.

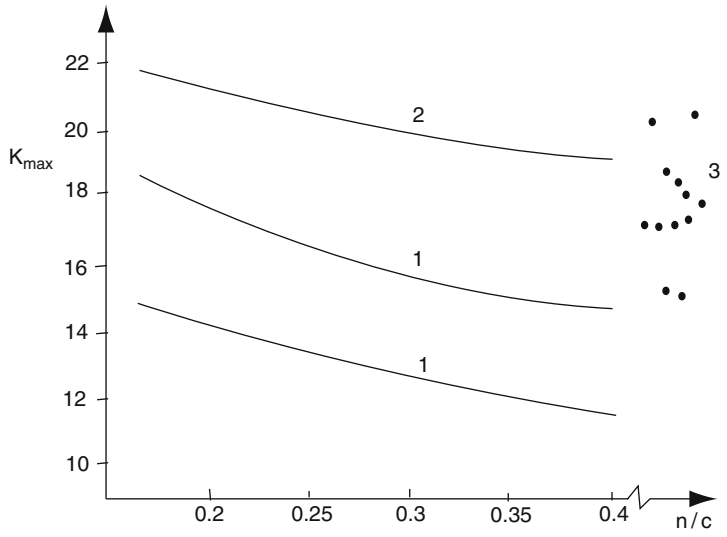

Fig. 13.6 Aerodynamic properties of first- and second-generation WIG

WIG Subtypes and Their Application

The WIG concept includes a range of subtypes as has been discussed through this book. Each has its own potential niche in the transport spectrum, as introduced in Chapter 1. General attributes affect the specification and design of all types of WIG and so should be considered first are as follows:

- As the craft will not be operated at high altitudes, the fuselage (or cabin) of the craft need not be constructed for pressurisation, as for commercial aircraft. On the other hand, since most operations will be over salt water, the structure must be watertight and resistant to salt water corrosion.
- The navigation of WIG is different from that of conventional marine craft. The WIG can be operated across shallows and does not need marked channels by water depth or pre-designated navigation routes. Tidal conditions are also no problem if a slipway and hard standing terminal apron is used.
- Terminal equipment has to be similar to that at airports for seaplanes, or a Hoverport, and provide for:
  - Embarkation and disembarkation safely of passengers from/to shore
  - Loading and unloading fuel, fresh water and provisions
  - Radio communication over the service routes
  - Provision of weather, and sea state and marine traffic data along the route
  - Equipment and systems maintenance and support for pre-flight preparations.

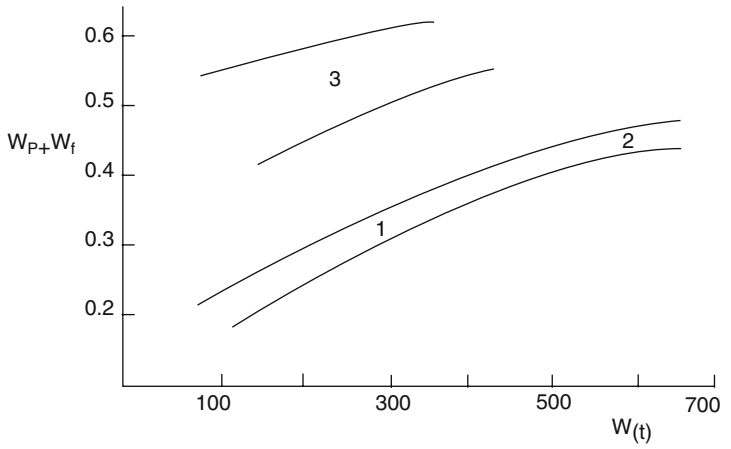

Fig. 13.7 Weight composition of WIG

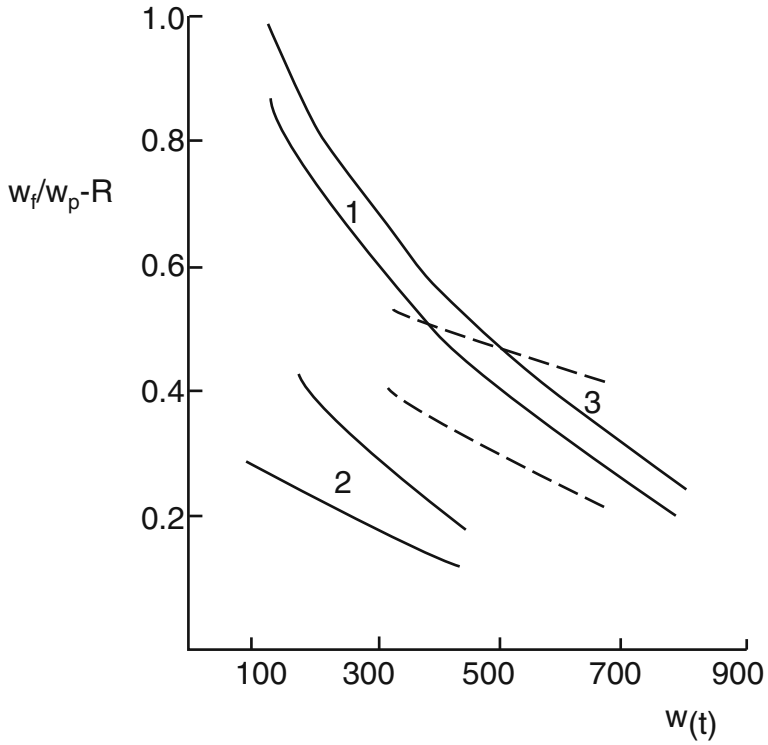

Fig. 13.8 Fuel consumption of WIG

In addition, the following has to be prepared for WIG passenger routes:

- WIG operational support including terminal and cabin staff, and handling of passengers and luggage
- Technical service and maintenance organisation, facilities for crews and passengers, take-off "runways", landing slipways and manoeuvring aprons
- Operational communication with the WIG vehicles in service and call up of equipment for service support
- Wind and wave data on the route, e.g. sea state and wind occurrence, direction and persistence

For successful and safe commercial operations, the route of an established service should be designated as a WIG route and documented on charts so that ships would be warned of the presence of these high-speed craft. There are rather different requirements for navigation between conventional ships, ACV, hydrofoils and WIG. These differences and the expected behaviour of other traffic when faced with WIG in the same area will need to be communicated to other marine traffic in the marine pilot handbooks for the locality.

WIG Preliminary Design

In the following sections, we will introduce a suggested procedure for WIG preliminary design, using comparison with other high-speed marine vehicles as a starting point. In general, the overall design of WIG is similar to conventional high-speed marine vehicles; however, there are some differences:

1. *Modes*: There are several operational modes to analyse, such as floating, air cushion borne and flying operation over ground, calm water and in waves. Both hydrodynamic and aerodynamic performance analysis has to be performed and balanced.
2. *Dynamic stability*: The PARWIG and DACWIG operate close to the water surface, in the strong surface effect zone without direct contact. Dynamic stability has to be provided from aerodynamic forces alone. This is different from conventional fast marine craft or so-called dynamic supported craft such as ACV/SES/hydrofoil/catamaran, which interact with the water surface itself.
3. *Water impact loading*: The craft will interact with waves in extreme sea states; hence wave impact loads on the hull and side buoy structure have to be taken into consideration. WIG craft speed is much higher than conventional high-speed craft, so the impact loads are increased.
4. *Low-speed manoeuvring*: It is difficult to employ flexible skirts as on amphibious hovercraft, or retractable landing gear as on aircraft, for a WIG without compromising the cruise speed or requiring complex retraction systems, so the design

of a cushion system and landing pads or wheels requires careful specification for manoeuvring and support at the operational base.

5. S*tructural design*: The hull and wing has to meet a compromise between conflicting requirements of low weight against a rather large specific area of shell plating and high structural loads on the underside of the hull and floats, similar to a flying boat. A DACWIG craft has multiple "hulls" to design and optimise. Figure 13.9 shows a transverse section of various high-speed marine vehicles. There are two sidewalls on a conventional monohull and hydrofoil, four sidewalls on catamaran and SES, six sidewalls on DACWIG type 1 (i.e. the craft with two air channels) and ten sidewalls on DACWIG type II (craft with two air channels and one mid airfoil). More hull weight is dedicated to the sidewalls as the configuration becomes more complex. A comparison of the specific area of various high-speed marine vehicles is shown in the following table:

	Monohull	Hydrofoil	SES	ACV	WIG
Specific area	10	10	13	21	28–35

Where Specific area $= S/\nabla^{2/3}$

S Area of shell plate and framework (m^2)
∇ Volume displacement of the craft (m^3)

6. *Machinery*: The air propellers and power plant are to be installed on the craft taking into consideration water spray (operating in waves during take-off), weight, potential corrosion and erosion by mud (if operating over ground), and potentially long power-transmission shafts.
7. *Construction*: WIG craft structural design includes elements of both marine craft and aircraft design, so where should it be constructed, in a shipyard or aircraft plant? This is still a strong debate in the WIG design community.
8. *Safety and certification*: Which organisation will be responsible for policing the IMO code of safety and operation [6] for WIG within nation states? This is still a problem that has not been finally clarified, though ship classification societies such a Germanischer Lloyd and Lloyd's Register have taken a lead so far.

Design Sequence

WIG design should follow the overall sequence below:

(i) The determination of specifications, design standards and criteria, safety code and some requirements for the overall design of WIG, such as:

- Specification of functional requirements (see 1. below)
- Inclusion of performance-related design requirements (see 2. below)

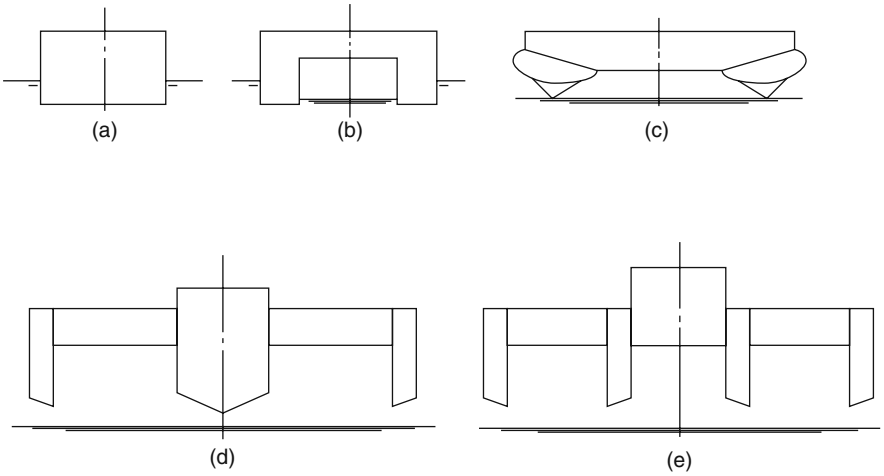

Fig. 13.9 Transverse section sketch for various high-speed marine vehicles

- Inclusion of relevant safety code requirements for the WIG (see 3. below)
- Inclusion of requirements for amphibious capability (see Chapter 5)
- Specification of main dimensions;

(ii) The determination of aerodynamic configuration and principal dimensions.
(iii) Model experimental investigation of the aerodynamic and hydrodynamic of WIG (see Chapter 9).
(iv) Initial design establishing structural configuration, main machinery selection, configuration of cargo spaces, control surfaces, fuel tankage, etc.
(v) Determination of craft cost, operational economics, construction planning, etc.
(vi) Detailed design.
(vii) Operations and maintenance guidelines and manuals.

Functional Specification for a WIG

First we set up a typical specification for a passenger WIG. References [1, 7, 8] provide additional material that may assist this process. The designer should identify his requirements for the parameters outlined below, taking guidance from the theory chapters of this book presented earlier and making reference initially to craft of similar specification that have already been built. The designer should expect to make two or three successive estimates for the different parameters, since initial choices may be incompatible. As experience is gained, a design selection will be closer to a practical data set in the first cycle!

1. *Specify the craft mission*: Function (passenger, freight and military duty), normal route or operational area and range, cruising operation speed and desired mode.
2. *Specify desired calm-water performance*as follows:

   - Maximum flying speed at normal displacement and flying height
   - Cruising speed and flying height
   - Desired range at cruising speed
   - Target take-off speed and time as well as distance
   - Target touch down-to-stop distance (inertia of the craft)
   - Minimum turning diameter with rolling angle when hull borne, cushion borne and in flying mode
   - Jump (permitted or not), jump altitude desired
   - Desired draft in hull-borne mode
   - Requirements for compartmentation and reserve buoyancy from IMO requirements, etc.

3. *Specify desired performance in waves* (seaworthiness) at normal displacement

   - Take-off and touch down at maximum significant wave height and wind force
   - Target cruising speed and maximum speed at maximum significant wave height and wind force
   - Flying height at above-mentioned speed
   - Minimum turning diameter in the various operation modes in waves
   - Jump possibility (normally same as over calm water)

4. *Specify desired amphibious capability*: With exception of DACC, which may be designed with mission requirements similar to an ACV, DACWIG use their cushion system primarily to improve take-off and landing and allow manoeuvring at a terminal [4]. The DACC may need to consider its mission terrain and design the skirt system accordingly, while the DACWIG needs only to consider the smoother terrain of a concrete apron and launch ramp curves.

   - Possibility of hovering up landing ramp from water surface
   - Landing ramp slope
   - Dimensions of landing area
   - Condition of landing area
   - Obstacle clearing ability of the craft, height and terms of obstacles
   - Ability for passing across ditches or other obstacles, its width and depth.
   - Performance over rough ground, estuaries, everglade areas, etc. (DACC)

5. *Specify passenger accommodation and freight payload*:

   - Seat number and requirements
   - Accommodation of passenger cabin

- Requirements for comfort, noise level, acceleration level and vibration in passenger cabin
- Safety equipment
- Luggage and equipment storage
- Freight volume and weight, loading container design

Carriage of freight aboard a WIG will be most conveniently loaded on standard air freight containers for medium-sized freight WIG. If operations are associated with a coastal airport, the freight service will be able to be linked in with its infrastructure for freight forwarding, so optimising container usage. Large WIG are more likely to base freight carriage on palletised units that can be transferred into standard rail or road containers, or Ro–Ro trailer units. Data for both these freight carriage forms are available from the air freight and sea freight industries.

6. *Make preliminary choice of WIG type*: The craft type and aerodynamic configuration can now be selected, such as

- aircraft type layout with trapezium-shape wing (Russian PARWIG type Orlyonok) or
- aircraft type layout with straight square-cut wing (Russian Ekranoplans) or
- aircraft type layout with rectangular wing (typical for dynamic air cushion craft type such as Volga-2) or
- aircraft-type layout with rectangular main wing and trapezium composite side wing, so-called DACWIG, etc. or
- forward swept and tapered wing such as flightship craft

7. *Select principal dimensions and estimate weight*:

- Payload: weight of cargo, passenger seats and their luggage
- Maximum take-off weight: use a rule-based multiple of the payload initially
- Length overall: select based on take-off weight and the mission parameters
- Width overall: main-wing span and chord based on chosen WIG type
- Maximum height: tail height based on fin area requirements and propulsion engine/propeller dimension

8. *Select main machinery*:

- Bow engine (lift engine, type, maximum take-off and rated power, revolution, specific fuel and oil consumption, etc.) and its driven air propeller, as well as power transmission
- Stern engine (propulsion engine, type, maximum take-off and rated power, revolution, fuel and oil consumption, etc.) and driven air propeller
- Pitch adjusting mechanism for both bow and stern propellers
- Air propeller ducts, if applicable

9. *Select auxiliary machinery*:
   - Hydraulic system for driving rudders, flaps and guide vane after bow propellers of bow thruster itself, etc.
   - Electrical power plant and equipment
10. *Select navigational, communication and automatic control systems*:
   - Navigational complex and separated navigational devices
   - Radio engineering collision warning and above-water surroundings display system
   - Centralised control system for communication complex
   - Inter-crew communication devices
   - Automatic pilot system
11. *Select hull, wings and stabilisers material and construction:*
   - Hull material and construction method
   - Material of main wing, composite wing and vertical as well as horizontal fixed stabiliser and their construction methods
   - Material for vertical and horizontal rudders and their construction methods
   - Material for side buoys and their construction method
12. *Specify other equipment*:
   - Material and construction method for landing pads or alternative landing undercarriage
   - Life-saving equipment
   - Fire detection and protection equipment

Preparation of this base data for the craft design then enables the designer to begin drafting out the craft geometry, and beginning the procedures outlined below to analyse the craft characteristics and performance, and adjust the parameters until they are in balance.

Design Requirements

Before proceeding into preliminary design for our WIG, we have to select some further design parameters that will set the requirements for overall geometry and compartmentation of the craft. Once these requirements are set, the influence of IMO and Classification Society criteria can be assessed, as outlined in Section 3 below.

1. *Requirements for intact stability*
   (1) Floating and cushion-borne stability can be calculated by the same method applied for conventional high-speed craft. The requirements for initial stability and stability at large heeling angle are the same.

(2) Longitudinal stability requirements in flying mode are see [8]:

$$\bar{X}_{F\vartheta >}\ \bar{X}_{F\bar{h}>}\ \bar{X}_G \text{ and } \bar{X}_{F\vartheta} - \bar{X}_{F\bar{h}} = 0.1\text{–}0.15 \tag{13.1}$$

$$\text{Or} \qquad \bar{X}_{F\vartheta >}\ \bar{X}_{F\bar{h}} = \bar{X}_G \tag{13.2}$$

$$\bar{X}_{F\vartheta} - \bar{X}_G > 0.03 - 0.08 \tag{13.3}$$

Where

$\bar{X}_{F\vartheta}$ Relative position of trimming centre
$\bar{X}_{F\bar{h}}$ Relative position of heaving centre
$\bar{X}_G$ Relative position of centre of gravity of craft (*X*/*C* from wing leading edge)

The physical explanation for these relations can be described as follows:

1. In case of head wind, the craft will rise up with a slight of decrease in the trim angle and also
2. In the case of the craft descending in altitude, lift will be increased and acting at heaving centre, behind the CG, causing trim angle to decrease; however, since the pitching centre is behind both the heaving centre and CG, and with a negative pitching moment acting, so the trim angle will increase a little and finally cause the craft to descend stably
3. For the same reason as in 1 and 2, the craft can also climb stably

On many WIG, $\bar{X}_{F\vartheta}$ decreases with increasing ϑ, but $\bar{X}_{F\bar{h}}$ increases with increasing ϑ, so in the case of trim angle greater than critical trim angle, the $\Delta\bar{X}_{F\vartheta\bar{h}}$ will be negative and may cause overturning backward (bow pitch up). This situation is most dangerous for WIG. In general, $\vartheta_{critical} = \sim 5 - 7^0$. Therefore, pilots should be careful to avoid running at trim angle close to $\vartheta_{\text{critical}}$ and designers should try their best to make critical trim angle as high as possible.

Relation (13.1) gives the criteria for positive longitudinal stability. Achieving (13.2) will ensure that small gust disturbance leading to a positive increase of flying height will not disturb the craft trim angle severely. Equation (13.3) defines minimum reserve values for the longitudinal stability.

It may be noted that these criteria are somewhat tighter than the recommended values from the original Russian trials programme and represent the needs for a craft that has to meet criteria suitable for hovering as well as flying. However, the difference between the trimming centre and heaving centre cannot be too great, as it will cause a decrease of pitching decay coefficient, so as to reduce the longitudinal dynamic stability. Perhaps this is why the aerodynamic configuration design for longitudinal stability of a WIG is so difficult.

2. *Requirements for damage stability*

The requirements for damage stability are similar to the requirements for conventional high-speed craft [6, 9, 10]. According to the safety code issued by IMO, if a craft is damaged, it should maintain

- Positive buoyancy and the minimum distance between the damaged condition water line and main deck (or holes on the side plate of hull) should be greater than 76 mm
- Positive static hydrodynamic stability
- The calculated flooding conditions are
- One cabin (or compartment) either in hull, side buoys or in main wing, flooded with a total length equal to the largest single compartment, or 20% of the hull, buoy or wing length for smaller craft, whichever is greater

Two adjacent compartments flooding with same condition as above, for larger craft.

3. *Restrictions on overall dimensions*

The principal dimensions may be constrained by the following functional requirements:

- Interface to terminal facilities for passengers or freight
- Landing area and slipway geometry
- Workshop or covered storage of the craft
- Bridges or other physical obstacles along the service route
- Width of rivers used for service route, etc.

Detachable structures and/or foldable composite geometry wings may be useful for accommodating restrictions at the terminal or maintenance base. Obstacles or restrictions on the service route itself have to be accommodated by the craft's overall design. Bridges and narrow parts of a route may be approached at lower speed and restricted flying height.

4. *Requirements for seakeeping safety*

*Steady operation over waves:*Analytical methods for predicting craft safety in a seaway are still difficult. However, some experimental investigations can be carried out during the design stage as follows:

- Radio-controlled self-propelled model tests over open water can be used for estimating qualitatively the safe operation of the craft at various wind/waves force and directions, including take-off and ditching
- Model tests in a seakeeping tank with various wave/wind directions and force for determining quantitatively the model stability, also including ditching

The tests mentioned above mainly check the stability of the craft and the possibility of immersion of bow thrusters into the water, which is a most dangerous occurrence.

Existing experience [11] suggests DACWIG craft can operate safely if the following equation can be satisfied:

$$H_{\min} = 0.5 + 0.2.H_{\mathrm{w}} \tag{13.4}$$

Where

H_w Design maximum wave height for operation (m)
H_{min} minimum safe height at which WIG can fly (m)

Or $H_m > (0.6-0.7)\,H_w$, where H_m is minimum safe flying height over a seaway

Take-off over waves: A very important criterion for craft safe operation in waves is the ability to take-off. Sufficient reserve power for both lift and propulsion engines have to be accounted for in design. Seakeeping tests of a model in a towing tank to predict the additional wave drag are very useful. The lower the cruising speed, the more important are tests, as the craft drag at take-off speed being the controlling factor for installed power rather than power needed to maintain cruising speed in such a case.

Slamming loads: Design of the under body shape of main hull and side buoys should follow marine and seaplane practice so far as possible, using inclined planing surfaces, curved rather than straight planes and preferably two or three steps in the main hull. This approach will help to minimise the drag hump and reduce slamming loads in the seaway during the take-off and landing runs.

5. *Requirements for habitability*: The ride for WIG in flying mode is smooth and so internal craft vibrations due to the main engine and transmission will be the main issue for passenger comfort. During take-off the ride will be somewhat bumpy, so that all personnel should be seated and strapped in, similar to aircraft take-off. Provisions, luggage and cargo should also be locked down or in lockable containers/compartments.

   The following points should be considered in addition to the general requirements for the habitability of conventional fast marine craft. Analysis should be carried out for two key conditions, waterborne just prior to take-off in the design limiting seastate and the ditching condition into the limiting seastate.

   - *Vertical acceleration* in passenger cabins running in waves has to satisfy ISO2631 for passenger comfort.
   - *Internal noise level* in passenger cabin: Passenger cabins are generally surrounded by both lift and propulsion engines, so internal noise level will be unacceptable unless care is taken to install sound isolation in the rear (and possibly front) bulkhead and also the main fuselage shell. The standard for the internal noise level has to satisfy the rules issued by the classification society or the requirements demanded by operators, typically below 80 dBA. Noise is much less of a problem once flying, nevertheless the direct impingement zone from propellers (in line with the blade disc and a cone from directly behind) needs to be protected. Ducted propulsors are useful as the duct itself can be used as a sound absorber.

- *External noise:* The external noise level of a WIG is less than an aircraft because it is localised by its proximity to the water surface as a sound-absorbing barrier. The criteria for acceptance of WIG operating close to cities will be rather more stringent than for aircraft. Typically, 95 dBA at 100 m distance should be a target for smaller craft and the same level at 300 m for larger craft.
- *Field of vision* for pilots, navigators and passengers: This is strongly affected by spray generation during take-off and operation in waves, and the navigation cabin arrangement, located between the wings, which is rather different from the arrangement on other high-speed craft. The poor field of vision for pilots and navigators increased the difficulty of handling of early WIG. Use of video cameras for side and rear views can improve this at low cost on modern craft. Passengers will be more comfortable and less susceptible to travel sickness if windows allow good vision outside so as to maintain a steady sight horizon. WIG unsteadiness in roll in the higher GEZ makes this an important area to achieve the correct balance of design for the craft layout.

6. *Terminal requirements:*In order to ease landing and manoeuvring at a terminal, it is suggested to design terminals as follows:

- *Slope of ramp for landing*: Depends on craft size. For small craft a slope of 5–15° is negotiable without trouble, while for larger craft a slope of 5° or less is preferred.
- *Number of ramps*: If one craft only is likely to be arriving or leaving at one time and the local wind conditions are consistent, then a single ramp may suffice. Where multiple craft will operate together and/or the wind conditions can change direction significantly, then a second ramp oriented 60–90° apart will assist operations considerably. The manoeuvring apron will also need to be rearranged to allow craft to access either ramp from its loading station or dock.
- *Manoeuvring apron*: This is also craft size dependent and relates to the number of craft expected to be resident at any one time. For a single craft operation, an apron of about three craft lengths square will be acceptable, including the loading station area or docking station. Care must be taken to orient the loading station so that craft can approach into wind.
- *Maintenance and storage*: Craft are likely to need a maintenance facility together with the terminal. This needs to be located outside the manoeuvring area and include a lightweight hangar since major maintenance operations will be associated with main engine and transmission overhaul, control systems and propellers.
- *Passenger and freight facilities***:** Passenger facilities for WIG terminals will be similar to air taxi terminals at an airport for taxi services, Fast Ferry or Hovercraft terminals for larger scale passenger operations and to air freight terminals for freight services.

Safety Codes for WIG Craft

Where WIG are used as passenger transport, the safety code introduced by the IMO forms the basis for our design criteria. Here we introduce briefly the safety code for WIG issued by IMO in 2000 and offer some additional suggestions. WIG for freight should also consider the IMO requirements as well as the normal International Regulations for maritime traffic. Small WIG will be exempted from a number of the requirements, partly due to size and partly due to their more limited range of operation.

Basic Concepts

1. *International regulations*
   The following aspects of operation are taken into account:

   - Start and landing of WIG is carried out on the water surface.
   - Operation is close to the surface of the water.
   - Possibility to jump up to overcome or over-fly obstacles is limited to a transitory mode. The height of such jump up is much smaller (a few metres only) and does not come within the altitude foreseen for the normal operation of aviation transportation covered by general aviation classification requirements.

   The IMO definition, agreed with the ICAO is as follows:
   "A WIG craft is a multimodal marine craft capable of operation in a mode where the craft is supported wholly in the air above water or some other surface, and not having constant contact with such surface, through the use of an aerodynamic lifting force known as ground effect. Ground Effect is generated during forward movement of the craft by interaction between the lower surfaces of the crafts wing (wings), hull, or their respective parts, and the water or other surface being traversed up to a maximum height above such surface equal to 100% of the overall width of the WIG craft" [IMO DE44/17 WIG correspondence Group].

   WIG is therefore related to marine transport and their safety must relate to maritime rules. IMO is mandated internationally to set up international rules and regulations for marine dynamic supported craft and high-speed craft, including WIG. These are then incorporated into regulations issued by national authorities from the countries that form the IMO and maritime classification societies design rules that are used to control design of ships and other marine vehicles.

   We can only design and construct a WIG according to the IMO "Safety Code for WIG Craft" at present as no other regulations have been issued on an international basis to date.

   If a WIG is designed to be capable of free flight above the GEZ, then the requirements of ICAO will have to be met, the craft then being designed as a (sea) plane.

2. *Classification of WIG*

WIG designed according to IMO requirements can be subdivided into three types as follows:

- "A" Craft not capable of operation without the ground effect.
- "B" Craft capable to increase its altitude limited in time and magnitude outside influence of the ground effect in order to over fly a ship, an obstacle or for other purpose. The maximal height of such an "over flight" should be less than the minimal safe altitude of an aircraft prescribed by ICAO.
- "C" Craft capable to take-off from the ground and cruise at an altitude that exceeds the minimal safety altitude of an aircraft prescribed by ICAO.

In general DACC and DACWIG belong to "A" type, classic WIG and PARWIG belong to "B" type, and seaplanes and flying boats belong to "C" type. The International Maritime Organization (IMO) and International Civil Aviation Organization (ICAO) will therefore be responsible for jointly setting up the safety code of such craft operating in various operation modes.

The fields of competency of IMO and ICAO are as follows:

	WIG craft types		
Operational modes	A	B	C
Competency			
1. Displacement	IMO	IMO	IMO
2. Transitional	IMO	IMO	IMO
3. Skimming	IMO	IMO	IMO
4. Take-off/landing	IMO	IMO	IMO
5. Surface effect-main operational mode	IMO	IMO	IMO
6. Fly over		IMO/ICAO	IMO/ICAO
7. Aircraft mode			ICAO

Supplementary Safety Criteria for DACWIG

Proposal has been put forward to IMO for some modifications to the regulations in [6] so as to satisfy additional characteristics of WIG types such as the DACWIG. The suggestions for brief supplementary rules are as follows [12, 13]:

The proposals here are derived mainly from experience with DACWIG, which is somewhat different from PARWIG (Ekranoplan) and DACC (dynamic air cushion craft) due to its relative flying height not being beyond the surface effect zone (as PARWIG), nor nearly sticking the water surface (as DACC), but $0 < \bar{h} < 0.3$.

(1) *Design cases*: Due to DACWIG and DACC amphibious capabilities that they can be operated on ground, sand, swamp, ice, snow and water surfaces, etc.

the performance analysis and subsequent operational permit envelopes should include all these different conditions.

(2) *Collision*: In case of potential collision with other objects occurring during its flight in the surface effect zone, the pilot generally performs an avoiding manoeuvre, either in flying mode or in air cushion mode, or makes an emergency stop to avoid the possible collision accident. DACWIG and DACC cannot make a "jump", as might be taken by pilots of PARWIG. Therefore, the regulation for avoiding collision, requirements for navigation and lighting of DACC and DACWIG should be similar to conventional high-speed vessels.

However, since the speed of DACWIG and DACC is far higher than the conventional high-speed craft, seat belts for passengers will be mounted on the craft similarly to commercial aircraft, with safety belts provided for all seats.

(3) *Static stability*: A DACWIG flying at cruise velocity should have inherent static and dynamic stability. The craft should be designed without automatic control systems to improve the stability of craft under action of foreign interference (wind, waves, gust, etc.). Instead, the main-wing and side buoy configuration should provide stability through the captured air bubble effect as flying height is reduced. DACC will have static stability provided by the cushion system.

(4) *Passenger restraint*: On small/medium-size DACWIG up to 30 passengers should not be free to move around in the craft during flight, as transverse stability is relatively sensitive to weight transfer.

(5) *Accommodation and escape*: Since DACWIG will be operated at high speed, collision avoidance in flying or cushion-borne mode is crucial. The collision load for craft structure and equipment will be considered as an accidental case bearing in mind the need for the WIG to remain floating and if possible operational. Passenger evacuation should be provided to life rafts. The evacuation time and route, exit and means of escape, etc. have to be considered in case of fire or other emergency conditions as described in the IOM guidelines. It is suggested that the fire hazard area should be enclosed by fire-resistant or heat-insulated material in compliance with the requirements of IMO and classification societies. The design should as far as practical comply with the rules and codes for conventional high-speed craft for these aspects.

(6) *Anchoring, towing and berthing*: In order to save weight, the conventional anchor equipment for mooring high-speed craft may be reconsidered for WIG. For safety in emergency stop conditions, WIG can float with aid of a cone anchor to maintain heading into sea. Towing and berthing equipment will have to be included in the outfitting.

(7) *Redundancy and sparing of equipment*: The issues concerning redundancy of systems or machinery on high-speed craft for improving reliability have to be considered carefully on WIG. The ability to continue operation on one engine, where more than one is installed should be considered a requirement at least to enable boating to a safe harbour.

Setting Up a Preliminary Configuration

The determination of principal dimensions and overall preliminary design of a DACWIG may be carried out as follows (see also Table 13.1)

Table 13.1 WIG preliminary design flow chart

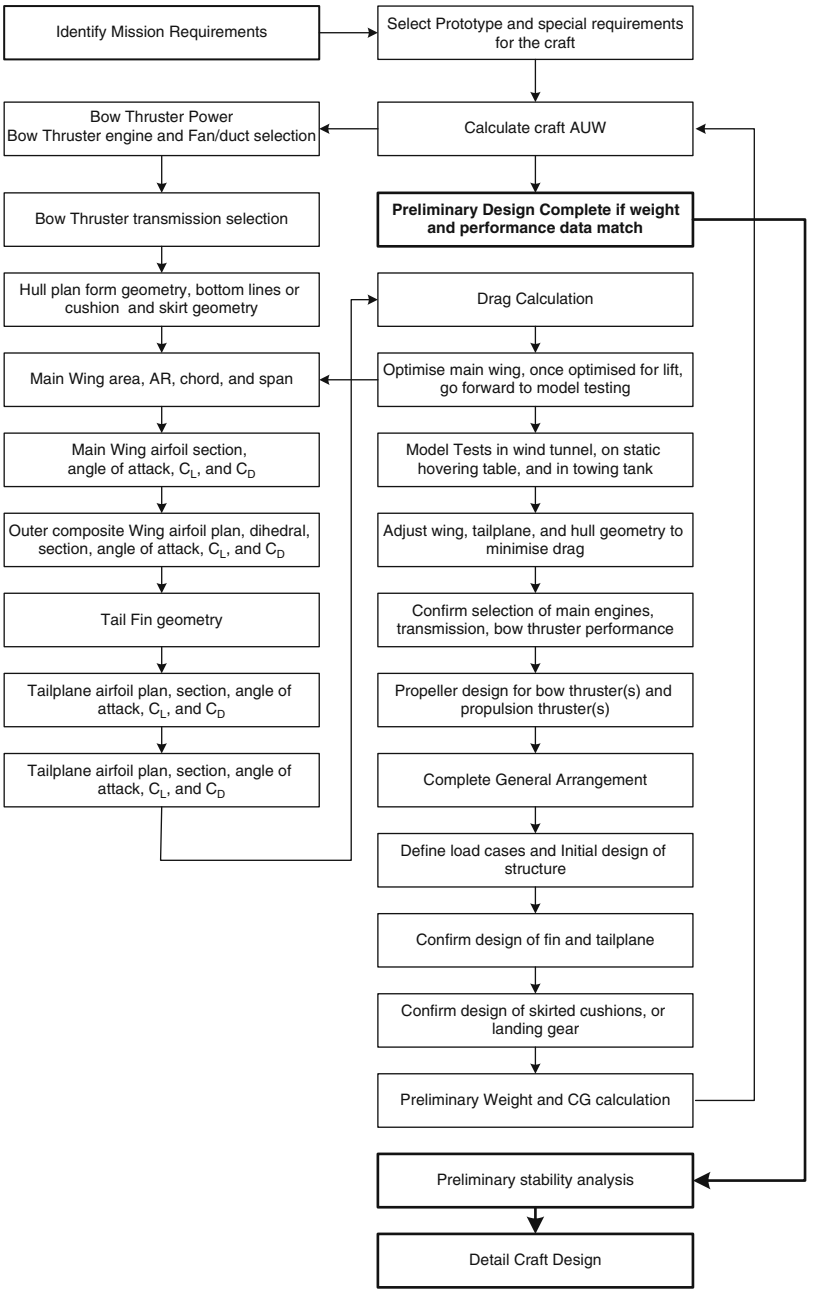

1. ***Determination of craft overall weight***

Based on the mission specification of the design, the payload can be obtained, then

$$W = W_{\mathrm{p}}/K_{\mathrm{p}} \tag{13.5}$$

Where

W Weight overall of the craft
W_{p} Payload weight
K_{p} Coefficient of payload, in general, take $K_{\mathrm{p}} = 0.2 - 0.3$

Typically a WIG should be able to achieve 20–30% of the overall take-off weight as a useable payload excluding fuel. The value will vary depending on the craft size, power plant chosen and structural material. It is suggested to try 25% as a first shot. Table 13.2 gives the percentage breakdown for Lun and Orlyonok, craft built with aluminium hulls and form the 1970/1980s design era to give some starting ideas.

Table 13.2 Weight breakdown (% W_{o}) of Russian WIG

Item	Weight	Lun	Orlyonok
1	Payload	20.6	12.2
2	Hull structure	44.0	54.5
2.1	hull	14.6	17.8
2.2	main wing	16.3	16.8
2.3	Tail in	2.3	2.9
2.4	Tailplane	3.6	3.9
2.5	Hydraulic ski	2.9	9.4
2.6	Other elements of hull structure	4.3	3.7
3	Power plant	11.8	13.4
3.1	Main engine	10.4	10.4
3.2	Equipments for main engine	1.4	3.0
4	Provisions, etc.	7.8	10.1
5	Fuel	15.8	9.8

2. ***Estimation of bow-thruster power and selecting the bow engines and type of bow thrusters***

(1) *Rated power of bow thrusters*

The rated power of bow thrusters can be defined based on the maximum static lift–thrust ratio of the prototype being used for comparison and specific thrust of the bow thrusters, as follows:

$$N_{\mathrm{t}} = \frac{W}{n_{\mathrm{t}}^{\eta_{\mathrm{Ls}} K_{\mathrm{t}}}} \tag{13.6}$$

where

N_t Rated power of each bow thruster
n_t Number of bow thrusters
η_{Ls} Maximum static lift thrust ratio, for DACWIG, $\eta_{Ls} = 4.5 - 7$for full-scale craft or 4.5–8 for models
K_t Specific thrust, where $K_t = f\left(C_p\right)$, C_p is the power coefficient of ducted propeller

$$C_p = N_t / \left(\rho_a n^3 D^5\right) \tag{13.7}$$

where

n propeller speed (rps)
D propeller diameter (m)

Figure 13.10 shows an example relation between specific thrust and power coefficient of ducted air propellers.

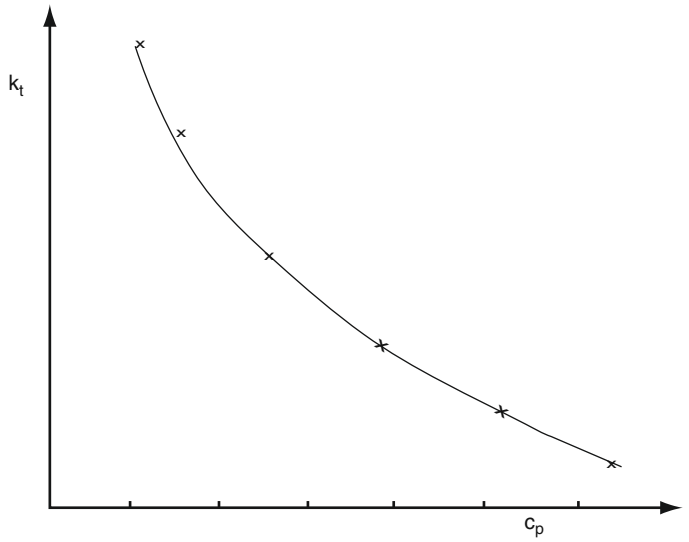

Fig. 13.10 K_t versus C_p from various ducted air propellers

(2) ***Selecting the type of bow engine and thrusters***

Based on the rated power, one can select an appropriate engine type and air propeller (see Chapters 11 and 12). References Chapter 6 [14] and Chapter 10 [7] introduce the theory and design of open and ducted

air propellers. When installing ducted propeller systems on WIG, the following issues have to be taken into consideration:

Air propeller diameter: In general, a ducted air propeller is preferred for bow thrusters due to its ability to create higher cushion pressure under the main lifting wing. However, what diameter has to be chosen? In previous chapters, we have considered maximum. Thrust to be the controlling factor for designing the air propeller.

In fact, there are two separate criteria that are not unlike the requirements for ACV ducted propulsors. At low speed, the total pressure of the air-jet efflux from the air propeller H_j, rather than the free air thrust from the propeller, is most important. This suggests use of a small diameter high-solidity propeller system (four blades or more). At hump speed while accelerating into ground effect, it is important that the propulsors do have high total thrust including both propeller and duct thrust. This suggests that the duct system should be optimised for forward speeds around primary hump, having a normal airfoil section rather than a bell-mouth type with high mean line camber as on slower speed ACVs. Some experimentation will be necessary depending on the propellers available to the designer.

There is a strong relation between propeller thrust and diameter, but still not perfect. Figure 13.11 shows a relation between propeller diameter D_p, total pressure H_j and thrust of air propeller T_p for an example. It is found that an optimum D_p can be selected with both reasonable high-speed thrust and total pressure at zero speed. Higher total pressure equals higher cushion pressure and lift.

It is suggested that following points be considered for the ducted propulsors during general craft design:

- Choose several D_p alternatives for the propeller so as to compare both H_j and T_p as well as total thrust of the ducted propeller.
- Use the ratio A_p/A_f as a factor for selecting the diameter of propeller, where A_p is the frontal area of propeller and A_f frontal area of cushion air tunnel. The design ratio can be taken from existing prototypes and model test results. A useful starting point may be a value of 0.5.
- Consider the dynamic thrust-recovery coefficient η_{TD}. This strongly influences high-speed performance. Sometimes, a propeller/duct system can be designed with high static thrust, while only achieving lower η_{TD}. The most important factors influencing this are flight height $\bar{h}$, the angle of guide vanes β and relative distance between the propeller and main wing. Figure 13.12 shows η_{TD} versus relative flying height $\bar{h}$ and guide vane angle β. It is found that at higher $\bar{h}$, the greater the negative angle β the higher η_{TD} becomes. In addition a higher propeller position raises η_{TD} due to less interference of main wing on the airflow downstream of the propeller.

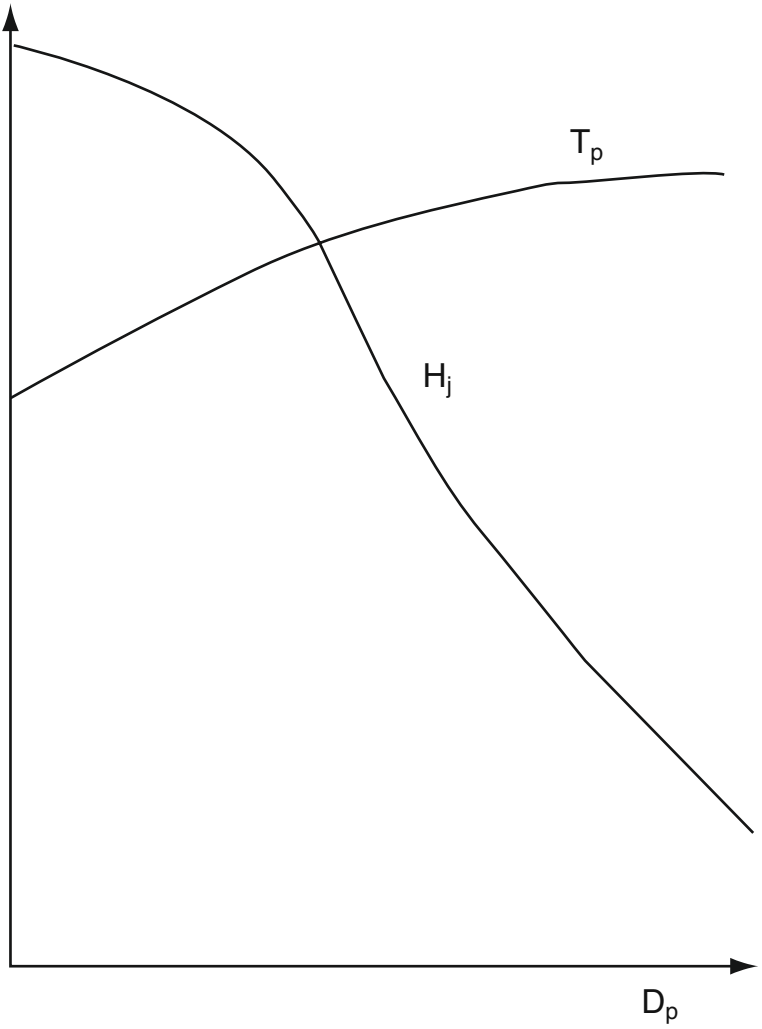

Fig. 13.11 Air propeller *T*, *D* and *H* relation

Selection of the ducted propulsor size, solidity, duct geometry, position relative to the main wing and guide vane system design is an extremely complicated task. One has to treat this as a trade-off problem, using the expertise introduced in previous chapters and considering both slow speed and high speed – particularly take-off performance of the craft.

3. *Overall powering assessment by comparison with existing craft*

WIG power estimation for preliminary design may be made by comparison with other fast marine craft together with study results from earlier WIG

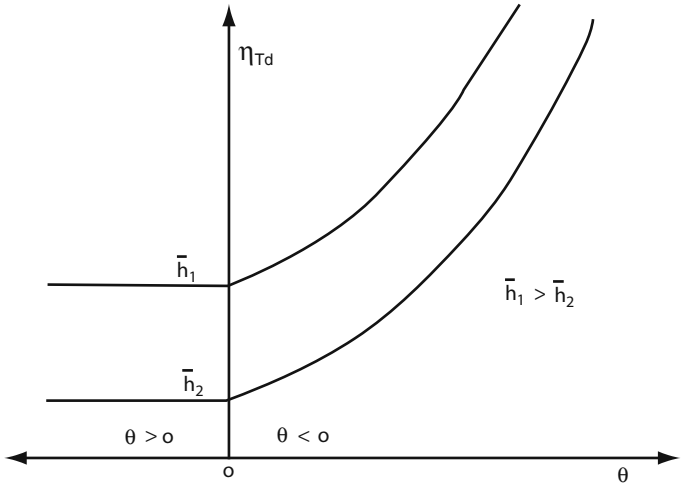

Fig. 13.12 η_{TD} versus relative flying height h and the angle of guide vane

designs. Sample data are included below. The reader is encouraged to assemble their own additional data into the same format so as to develop their own powering ground rules. Table 13.3 below presents the comparative transport efficiency of WIG with other high-speed craft, where

$\mathrm{Fn_d}$	Froude number, based on displacement, $= V_s/\left(g.W_o^{0.333}\right)^{0.5}$
W_e	Empty weight of craft (light weight)
W_o	All up weight
W_{us}	Useful load (payload together with fuel and consumables)
W_p	Payload
N	Full power of craft
N_p	Propulsive power at cruising speed, lift power can be shutdown (for PARWIG) or reduced (for DACC and DACWIG)
K_n	Propulsive efficiency coefficient based on total power, $= W_o V_s/N$
K_{np}	Propulsive efficiency coefficient based on propulsive power, $= W_o V_s/N_p$
T_e	Transport efficiency, $= W_p V_s/N = K_n W_p/W_o$
T_{eus}	Transport efficiency based on useful load, $= W_{us} V_s/N = K_n W_{us}/W_o$
T_{ep}	Transport efficiency based on propulsive power, $= W_p V_s/N_p = K_{np} W_p/W_o$
T_{epus}	Transport efficiency based on useful load and propulsive power, $= W_{us} V_s/N_p = K_{np} W_{us}/W_o$
	SFC Specific fuel consumption (kg/km × number passengers), $= Q_f N_p/V_s n_{pass}$
Q_f	Fuel consumption of engine (kg/kw h)
n_{pass}	Number of passengers

Table 13.3 Comparison of transport efficiency of WIG with other high-speed craft

	Semi-displacement ships	Catamaran	Hydrofoil	SES	ACV	WIG (PARWIG)	Airplane
Fn_d	1.5 – 2.5	2.0 – 2.8	2.5 – 3.5	2.5 – 4.0	3.5 – 5.0	10 – 15	20–35
W_e/W_o	0.60 – 0.70	0.65 – 0.80	0.70 – 0.80	0.55 – 0.65	0.55 – 0.70	0.55 – 0.72	0.55–0.65 (0.5 for $d > 5{,}000$ km)
W_{us}/W_o	0.30 – 0.40	0.20 – 0.35	0.20 – 0.30	0.35 – 0.45	0.30 – 0.45	0.28 – 0.45	0.35–0.45
W_p/W_o	0.25 – 0.35	0.15 – 0.30	0.15 – 0.25	0.33 – 0.40	0.28 – 0.40	0.20 – 0.35	0.15–0.30
K_n	5.0 – 9.0	4.5 – 8.0	5.0 – 6.0	5.5 – 7.5	2.5 – 4.5	5.5 – 10.5	5.0–9.0
K_{np}	5.5 – 10.0	5.0 – 9.0	5.5 – 6.7	6.0 – 8.5	2.8 – 5.0	8.0 – 15	6.0–10.0
T_e	1.6 – 2.6	1.0 – 1.8	1.0 – 1.5	1.6 – 3.2	0.6 – 1.5	1.5 – 2.0	1.0–2.0
T_{eus}	2.0 – 2.9	1.2 – 2.2	1.2 – 1.7	2.0 – 4.0	0.7 – 2.0	2.0 – 4.0	1.5–4.0 3.5 for $n_{pass} > 50$
T_{ep}	1.8 – 2.9	1.1 – 2.0	1.1 – 1.7	1.8 – 3.5	0.7 – 1.7	1.9 – 3.9	1.5–4.4
T_{epus}	2.2 – 3.2	1.3 – 2.4	1.3 – 1.9	2.2 – 4.4	0.8 – 2.2	2.9 – 5.8	2.2–5.0
SFC	0.022 – 0.036	0.033 – 0.060	0.040 – 0.065	0.023 – 0.045	0.030 – 0.10	0.022 – 0.049	0.020–0.050

From the table, it can be seen that

- The hydrodynamic efficiency can be written as $K_n = W_o \cdot V_s/N = K_{np} \cdot L/R$, where K_{np} is propulsion efficiency. The K_n for WIG is close to that of SES and catamarans, but at a higher Froude number Fn_d. In fact the hydrodynamic efficiency of WIG is similar to the aerodynamic efficiency of an airplane.
- The specific fuel consumption SFC is improved for WIG compared with other high-speed marine craft due to the ability to cruise at a much lower proportion of total installed power, the performance for larger WIG with modern engines (most WIG so far have been prototypes with engines that are low cost rather than high efficiency) should be higher than large transport aircraft of today.
- W_e/W_o of WIG is closer to that of an airplane than the other types of craft due to the lightweight aviation type of structure, equipment and engines used. Adopting heavier marine structure will have a direct impact on payload fraction and therefore transport efficiency. There is a trade-off for designers to analyse here, since structures are a significant portion of the construction cost.
- The economical efficiency of WIG can compete with an airplane. At short range, the lower fuel requirement for WIG can be translated into higher payload. At present, there is no precedent for long range WIG to compare with aircraft. Logically, the WIG higher payload capacity should further improve with increasing size, suitable for trans-oceanic routes, and the lower cruise power should maintain the advantage over aircraft, making them suitable for high-value freight delivery. This remains to be proven. Additionally, when the DACWIG configuration is utilised, an additional payload increment may be available, so further improving the efficiency, say by 10–15% at cruise speed into the range of 100–200 knots. Such speeds may be better suited to shorter routes up to 1,000 n.miles.

The construction cost of WIG will be higher than conventional high-speed craft and closer to aircraft due to higher powering and demand for lighter structure to improve payload fraction. The DACC/DACWIG cost price will be closer to marine practice as air cushion reduces take-off drag and powering.

WIG transport efficiency needs to improve further to give a clearer advantage compared with the alternative of using aircraft or fast marine ferries, to overcome the in-built market resistance to a new transport form. Recent research and prototype developments have pointed the way in this respect. Designers should therefore target improved aerodynamic efficiency compared to the existing data.

Figure 13.6 can be used for initial performance estimation. The aerodynamic efficiency of WIG first and second generations and an aircraft weighing 450 t is shown in this figure, where 1 – first-generation WIG, 2 – second-generation WIG, 3 – aircraft, K_{max} the maximum aerodynamic property, $\bar{h}$ the flying

height and C the wing chord. Figure 13.7 shows the WIG weight composition compared with aircraft, where W_p and W_f are the payload and fuel weight, respectively, and W_0 craft take-off weight. This data may also be used as a starting point, bearing in mind modern structural techniques should improve on this. Figure 13.8 shows a comparison of WIG fuel consumption with aircraft, where R represents craft range.

From these figures, second-generation WIG can be seen to compete with jumbo jet flying at 10,000 m altitude, where aerodynamic drag is lower. These data are useful as a starting point for designing larger WIG craft. Modern engines should be able to give an improved performance, either longer range or lower fuel fraction for a given range.

Once the designer has made an assessment of the target K_n and K_{np}, a first definition of installed power for cruising and takeoff can be made. This can be checked with the bow-thruster powering assessed earlier and the necessity for separate cruising propulsors evaluated.

4. ***Selecting type of power transmission, directly or via gearbox, flexible coupling and intermission shaft***

   At this point, the designer will wish to select the overall configuration for the power system, including the number of engines and propellers and their location.

   If the craft is a small one, say for taxi service, it is likely that a single engine would be selected and transmission shafts used to connect the engine, mounted in the central hull with the propellers. Such a system is realistic for a classic WIG configuration with propellers mounted above the trailing edge of the main wing. A DACWIG or DACC with propellers mounted in front of the main wings will require twin engines mounted on the wings to minimise the transmission length. The alternative is a single or multiple engines within the central hull and geared shaft or belt drive out to the propeller. This configuration adds some weight and complexity, but may give improved aerodynamics.

   Larger craft using gas turbine engines are easier to design into a system, since the engine will be mounted in a nacelle inside the propeller duct or on a pylon ahead of its propeller.

5. ***Determination of main-wing chord***

   We suggest that designers select a range of spans of the main lifting wing so as to check the effect of aspect ratio and compare the aerodynamic properties of the different wings.

   Where a classic WIG is being designed, the designer will want to investigate the effect of anhedral and swept/tapered geometries to provide optimum air bubble capture at speeds up to take-off, including the use of trailing edge flaps. The aim should be to develop an air cushion pressure supporting 50–70% of craft weight below 100 kph for larger craft and 50–70 kph for smaller craft. This will reduce hump drag and allow smoother take-off in the speed range of 120–140 kph for larger craft and 60–80 kph for smaller craft.

The main-wing chord has to be considered carefully so as to optimise air injection of the bow thruster and static lift–thrust ratio for bow-thrusters-assisted craft (PARWIG, DACWIG and DACC). It is suggested that the minimum beam of the wing air channel $d_P/B_a = 0.5\text{-}0.7$, where D_p is the diameter of propeller and B_a is the width of air tunnel (i.e. main wing). The maximum wing span will also be restricted by permissible maximum width of the craft.

Another criterion for selecting the width of the air tunnel is A_f/A_p, where A_f is the frontal projected area of air tunnel and A_p is the area of propeller disc. Then

$$A_f = B_a \cdot H_b$$

where H_b is the height between the craft base plane and main-wing leading edge (for a wing without anhedral). It may be seen that H_b is a function of the design angle of attack of the main wing.

$$A_p = (\pi D_p^2)/4$$

The ratio of A_f/A_p is an important parameter that affects the air-jet formation and cushion pressure. In general, it is recommended that

$$A_f/A_p = 1.5\text{-}2.5$$

6. *Determination of the surface area of the main wing*

The area providing the lift for the craft in air cushion mode (whether dynamic or thruster assisted) includes the surface area of the main support wing and also that under the main hull and side buoys. This area may also be referred to as the equivalent wing area.

The design hovering height, either static for thruster-assisted craft or at chosen design speed for classic WIG, and the wing area can be found from Chapter 4 and cushion static pressure can be found as

$$P_c = f(\bar{h}) \cdot q_j \tag{13.8}$$

where

$q_j = 0.5\rho_a V_j^2$ The velocity head of air jet (pascals) of incoming airflow

$P_c = kq_j$ $k = 1.05\text{-}1.15$ for a channel with $A_f/A_p = 2.5\text{-}1.5$ may be used as a start point for calculations

$$\text{Now} \quad q_j = T_p/A_p \tag{13.9}$$

where

A_p The area of propeller disc
T_p Static thrust of propeller

Coefficient k will vary greatly with geometry of the cushion cavity and main wing, together with the position of the bow thrusters if present. It is necessary to carry out experimental work to determine the value accurately.

For non-assisted WIG, V_j is simply the airspeed and resultant H is the dynamic head. The relevant capture area will be the presented area bounded by the ground plane, the wing leading edge and the hull and side buoys. At forward speeds, a DACWIG benefits from the captured air bubble as well as the thruster's injection, the forward speed gradually increasing the efficiency of the thruster generated air cushion.

$$\text{Now} \qquad S_c = (W/P_c) \cdot \xi_1 \cdot \xi_2 \tag{13.10}$$

ξ_1 The coefficient of pressure non-uniformity of air cushion, =0.95–1.0
ξ_2 Coefficient of Coanda effect, =1.05–1.15

It may be noted that the cushion area S_c will include the lift area under the hull and side buoys as well as the main lifting wing, therefore

$$S_c = S_{c1} + S_{c2} + S_{c3} \tag{13.11}$$

Where

S_{c1} Horizontal area under the wing surface
S_{c2} Horizontal area under the hull surface
S_{c3} Horizontal area under the side buoys

The craft width overall in the case of having two air tunnels is B_m
Where

$$B_m = 2B_c + b_h + 2(b_{sb}/2) \tag{13.12}$$

B_c Cushion beam or main-wing half span
b_h Hull beam
b_{sb} Sidewall or side buoy beam

In assessing area for the cushion, half of the width of each side buoy is used since the outer half has a sharply decaying pressure towards ambient if the side buoys are designed with a central keel and planing surfaces with deadrise, as is normal.

The craft beam can be assessed once the geometry for the main wings has been selected, whether rectangular or trapezoidal, and the average chord determined. Once this is known and the proposed hull and side buoy widths selected, the overall beam can be determined.

7. ***Length and width of main hull***

   The length L_h and the beam b_h as well as the height H_h can be obtained once a sketch of the craft general arrangement for passenger cabin, navigation cabin has been prepared.

   The minimum permissible distance between the bow air propeller disc lower tip and the static water surface at the bow so as to prevent possible water impact on the propeller blades in hull-borne operation can be determined based on the design take-off and landing sea state, and checked against the desired cruising height and sea state. It is recommended that the clearance of lower tip of a propeller or propeller duct should always be larger than 0.5 m for bow propellers.

   The sidewalls beam b_{sb} can be obtained by the calculation of craft static draft.

8. ***Chord length C and aspect ratio (AR) of the equivalent wing***

$$C = S_c/B_m \tag{13.13}$$

$$\mathrm{AR} = B_m/C \tag{13.14}$$

9. ***Wing profile***

   The main-wing profile can then be selected by reference to Chapter 5.

10. ***Aerodynamic lift coefficient $C_y$and aspect ratio of the main wing***

    The aerodynamic lift coefficient C_y has a great influence on the selection of optimum angle of attack of the wing for flying mode operation. Larger C_y can decrease the total area of wing (including the area of composite wing), but with a penalty of reducing the longitudinal stability. A useful starting point is to make reference to existing craft and select a suitable C_y. Examples of existing WIG C_y are listed in Table 13.4 .

    Figure 13.13 shows the relation between the C_y, AR and the Froude number $\mathrm{Fn_d}$; it is found that the average tendency of various parameters mentioned above is at higher $\mathrm{Fn_d}$, C_y becomes smaller, AR larger. This is reasonable in the view of aerodynamic characteristics and stability, so the figure can be referenced in the design of WIG to choose C_y and AR.

11. ***Determination of area and some design considerations for composite wing and tailplane***

    When using a composite wing outboard of the side buoys to give additional stability and controllability, the composite wing area S_{cw} can be estimated as follows:

$$W_0 = 0.5\rho_a v^2 C_y S_{eq} \tag{13.15}$$

Table 13.4 Aerodynamic lift coefficients of some existing WIG (estimated values)

Craft type	KM (WIG)	Spasatel (WIG)	Orlyonok (WIG)	SM-6 (WIG)	Strizh (WIG)	Amphistar (DACC)	Volga-2 (DACC)	Swan (DACWIG)
Country	Russia	Russia	Russia	Russia	Russia	Russia	Russia	China
Weight (t)	540	400	140	26	1.8	2.2	2.5	7.2
Cruising speed (km/h)	500	480	350	360	185	150	120	130
Cruising speed (m/s)	138.9	133.3	97.2	100	51.4	41.6	33.3	36.1
Wing area, S_c(m)	662.5	?	307	73.8	18.18	32	43.89	?
AR $= B_c/C$	2.0	?	3.07	2.86	2.47	1.10	1.36	?
Wing span, B_c (m)	37	44.0	31.5	14.8	6.7	5.92	7.73	?
Chord length, $C = S_c/B_c$ (m)	17.9	?	9.74	4.99	2.71	5.37	5.68	?
Fn	15.5	?	13.6	18.54	14.87	11.6	9.12	?
C_y*	0.676	?	0.778	0.56	0.6	0.636	0.82	?

$*C_y = \frac{W}{0.5\rho_a v^2 S_c}$

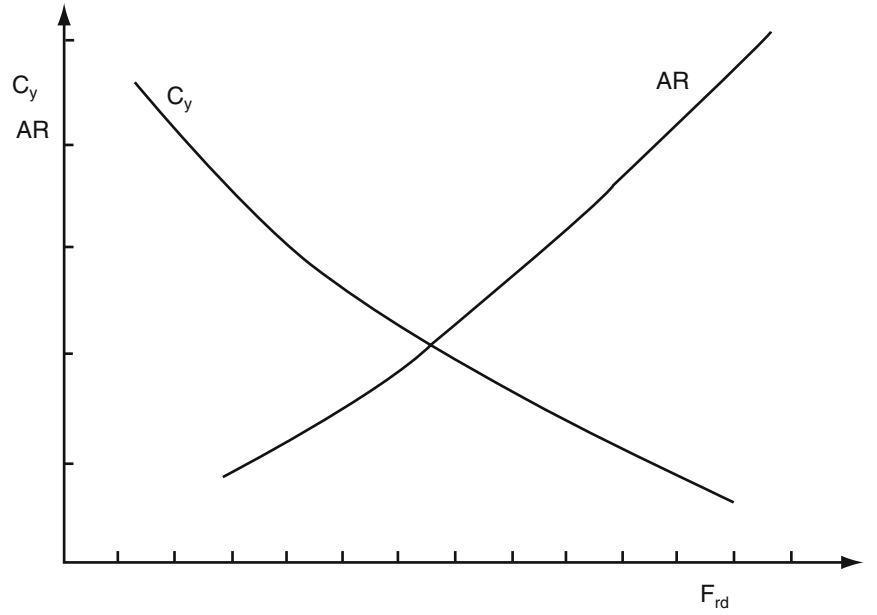

Fig. 13.13 C_y versus Fn_d, and AR versus Fn_d from various WIG craft

$$S_{eq} = S_c + S_{cw} + S_{tw} \tag{13.16}$$

where

W Craft weight
S_c Area of main wing, hull and side buoys
S_{cw} Area of composite wing

It is assumed here that normally the tailplane or horizontal tail wing is designed purely as a stability and control surface and will not contribute to lifting the craft. The term S_{tw} in Equation (13.16) can therefore normally be left out. The sizing of the tail wing (stabiliser and elevators) can be started as follows:

S_{tw} Area of horizontal tail wing

At first step of preliminary design, we can take

$S_{tw} = (S_c + S_{cw})/K_{tw}$ as the first approximation, where
$K_{tw} = 1.15\text{-}1.3$ is the coefficient taken from prototype.

This is a conservative estimate based on experience with DACWIG. The tailplane can be reduced by lengthening the hull so that it has a greater lever arm. It is best to make an assessment of the needed moment at take-off and cruise speeds, and then try a number of combinations of lever arm and sizing until a satisfactory combination is achieved.

Then we have to consider the design of the composite wing as follows:

Area and foldability: The aerodynamic efficiency of a composite wing is higher than that of the main wing due to its higher aspect ratio, so designers will make the area and span of composite wing as large as possible, so long as the main-wing area is large enough for static hovering. However, since a large span composite wing will negatively influence craft slow speed manoeuvrability, it is possible to make the composite wing foldable for smaller craft, similar to the Russian WIG I-Volga-2, Fig. 13.14. The composite wing can be folded when floating, and on cushion, particularly for operation over ground.

Fig. 13.14 IVolga

Longitudinal position: There are two design possibilities for the longitudinal position of the composite wing as follows:

- Composite wing located near the CG of the craft, as shown in Fig. 13.15. Since the aerodynamic efficiency of the composite wing is higher due to its high aspect ratio, location here will influence the overall craft aerodynamic properties less during large trimming angles.
- Located at the rear part of main wing (Fig. 2.36). This design is to improve longitudinal force balance and decrease the horizontal tail wing area.

Figure 13.15 shows three-view drawing of WIG with forward composite wing. Key to Figure 13.15 is as follows:

1. Main fuselage/hull
2. Main wing
3. Tailplane
4. Nose of fuselage
5. Bow thruster
6. Cruising engines
7. hull planing surface
8. Wing flaps
9. Outer stabiliser wing (composite wing)
10. Tail fin
11. Rudder
12. Elevator

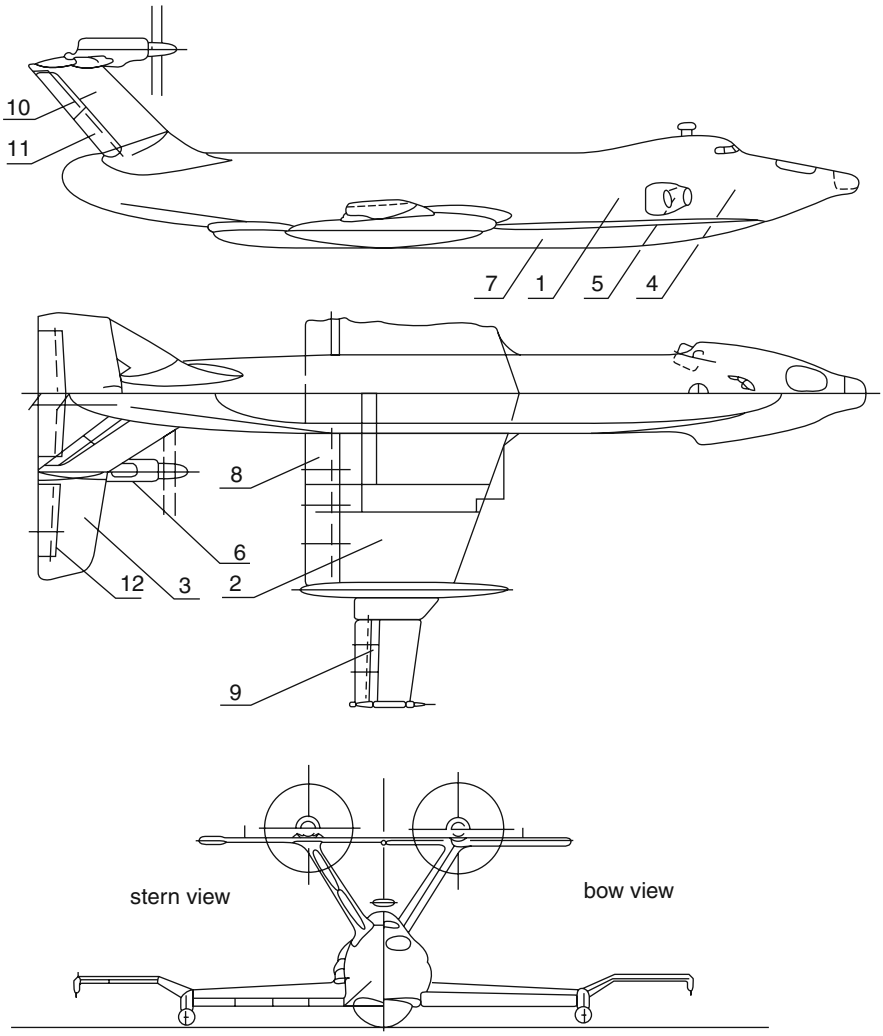

Fig. 13.15 Composite wing located near craft CG

Vertical position: The advantages of composite wings have been described in the previous chapters, including increasing lift, aerodynamic efficiency, and decreasing air drag. This is due to using fully the residual energy of the tip vortex around the side buoys. However, the interference of transverse airflow from the air channel will reduce the aerodynamic efficiency of the composite wing, particularly in case of location at rear of the side buoy and in lower position. In this case, the transverse and upward airflow from the air channel will be intensified, particularly in case of lower flying height and large trim angle. Such flow

will cause a decrease of lift–drag ratio, and sometimes lead to separation of the flow on the composite wing. This is a serious problem and may be improved with aid of following measures:

- Using wing fences located on the lower surface of the composite wing (Fig. 7.29), to prevent transverse flow
- Positive dihedral angle of the composite wing for reducing the influence of transverse airflow
- Decreasing the installed angle of attack of the composite wing so as to defer the separation angle of composite wing at large trimming angle

All such measures should be validated by wind-tunnel tests for the proposed design.

12. ***Determination of angle of attack of main wing and composite wing***

The influence of wing profile on the aerodynamic characteristics of WIG was described in Chapter 5, Designers can choose reasonable wing profiles with aid of this chapter together with the referenced standard texts for low-speed airfoils, for example references in Chapters 3 [8], 6 [5, 6, 14] and 10 [7].

The installed angle of attack of both main wing and composite wing can be specified based on the aerodynamic characteristics of the wing, using the selected C_y and wing profile to check the total lift.

13. ***Determination of the longitudinal location of composite wing, parameters and location of horizontal tail stabiliser***

With aid of Chapters 5 and 6, the location of the composite wing and geometrical parameters, as well as the tailplane location can be determined by the following equations.

Longitudinal force balance equation:

$$L_{\mathrm{mw}} \cdot l_{\mathrm{mw}} + L_{\mathrm{cw}} \cdot l_{\mathrm{cw}} + L_{\mathrm{tw}} \cdot l_{\mathrm{tw}} + T_{\mathrm{pb}} \cdot l_{\mathrm{pb}} + T_{\mathrm{pa}} \cdot l_{\mathrm{pa}} + R_{\mathrm{a}} \cdot l_{\mathrm{a}} = 0 \quad (13.17)$$

where

L_{mw}	Main wing lift including the lift due to the hull and sidewalls of craft, then $L_{\mathrm{mw}} = 1/2\rho_{\mathrm{a}} V^2 S_{\mathrm{c}} C_y$
l_{mw}	Horizontal distance between the aerodynamic centre of main wing (including the hull and sidewalls) and CG of the craft
L_{cw}	Composite wing lift
l_{cw}	Horizontal distance between the aerodynamic centre of composite wing and CG
L_{tw}	Horizontal tail stabiliser lift
l_{tw}	Horizontal distance between the aerodynamic centre of the horizontal tail and CG
T_{pb}	Bow propellers thrust
l_{pb}	Perpendicular distance between thrust of bow propellers and CG of craft
T_{pa}	Stern propellers thrust

L_{pa} Perpendicular distance between the thrust of stern propellers and CG of the craft
R_a Air profile drag of the craft
l_a Perpendicular distance of the centre of action of air drag, from the CG

At the first approximation, the influence of propeller thrust and air drag as well as airflow down-wash can be neglected, as these can be determined in the during design optimisation, then

$$T_{pb} \cdot l_{pb} + T_{pa} \cdot l_{pa} + R_a \cdot l_a = 0 \tag{13.18}$$

So that Equation (13.17) becomes

$$L_{mw} \cdot l_{mw} + L_{cw} \cdot l_{cw} + L_{tw} \cdot l_{tw} = 0 \tag{13.19}$$

The CG of the craft has to be located near the centre of action of static hovering lift to satisfy the longitudinal force balance when hovering static (during landing and launching of craft). A starting assessment will be

$$X_g = (0.40\text{-}0.48) \cdot C \tag{13.20}$$

X_g is the horizontal distance calculated from the leading edge of the main wing, varied according to the position of the flaps and guide vanes after the bow propeller. A preliminary weight distribution can be prepared to test the position of X_g for the chosen craft geometrical configuration.

Another equation that has to be complied with is the longitudinal stability equation, that is

$$\begin{aligned}(S_{mw} + S_{cw} + S_{tw})\,\bar{X}_{F\vartheta} C_y^{\vartheta} = {} & C_{ymw}^{\vartheta} X_{F\vartheta\,mw} S_{mw} + C_{ycw}^{\vartheta} X_{F\vartheta\,cw} S_{cw} \\ & + C_{ytw}^{\vartheta} X_{F\vartheta\,tw} S_{tw} \cdot k_q\end{aligned} \tag{13.21}$$

Where $C_{ymw}^{\alpha} = C_y^{\alpha} k_{\alpha}$

At first approximation, take $k_{\alpha} = 1$ and $k_q = 1$ and $\bar{X}_F\vartheta - \bar{X}_g = 0.03\text{-}0.08$

Since all of the values in Equations (13.18) and (13.21) are given except l_{cw} and l_{tw}, then the defined values l_{cw} and l_{tw} can be calculated. It should be noted that the influence of the air-jet blown from the bow thruster into the air channel on the centre of aerodynamic lift (CA) of main wing has to be considered. The CA cannot be taken from the aerodynamic characteristic table of the wing section, but it can be taken from a prototype, model test results or analysis.

Procedure for Overall Preliminary Design

Once the WIG preliminary configuration has been set up and perhaps a cycle or two carried out to test adjustments, the preliminary design itself may be started. At this point, general arrangements for the proposed craft should be prepared, preliminary structural design carried out and weight estimates prepared, so that more accurate analysis of craft lift, drag and powering can be completed.

The procedure for overall preliminary design is as follows:

1. Layout of lines for the hulls and side buoys
2. Layout of general arrangement
3. Select the stern power plant (cruise engine(s) for thrusters assisted or main engines for classic WIG)
4. Select bow thrusters power plant, location and transmission
5. Structure preliminary design
6. Calculation of weight of the craft
7. Drag calculations for the craft at various operation modes
8. Air propeller design
9. Appendage design (including horizontal and vertical rudders, as well as landing pads and air inflatable bag as side buoy)

This design work is based on the selection of dimensions and characteristics described in the section above "Setting up a preliminary Configuration" and follows a similar approach as used for propeller-driven aircraft and to some extent amphibious ACVs.

Once the preliminary design is available, the first pass at aerodynamic performance of the WIG can be carried out. It is likely that this work will require adjustments to the configuration and so the preliminary design may have to be revisited, or possibly a reconsideration of the functional requirements taken into account

The block diagram for the overall preliminary design is as shown in Table 13.1; this includes the design adjustment loops for optimisation.

Determination of WIG Aerodynamic and Hydrodynamic Characteristics

There is no self-contained analytical method available at present to determine the aerodynamic and hydrodynamic configuration of a WIG, due to the complicated airflow related to both the surface effect and air-jet effect on the craft main wings. Designers generally use both theoretical calculation and experimental investigation to find a reasonable compromise of aerodynamic and hydrodynamic configuration. Based on the preliminary design determined above, the aerodynamics and hydrodynamics of the design can be analysed by

(1) Select a suitable prototype and reference data, if available, to make a preliminary assessment of the new craft performance and adjust the configuration.
(2) Develop the aerodynamic configuration of the WIG, by carrying out model tests to determine the characteristic data specific to the new design.

A summary of possible experimental investigations into aerodynamics and hydrodynamics of WIG can be found in Table 10.5.

In general, we take six steps as follows:

- Model test on rigid table to study the static hovering performance of the craft (if necessary) to define the geometry and size of air tunnel, the arrangement of bow thrusters, etc.
- Catapult test of WIG to study the both longitudinal and transverse stability of an unpowered model craft
- Wind-tunnel test to study the aerodynamic properties
- Radio-controlled free flight model tests on open water area to study both aerodynamic and hydrodynamic properties and stability, as well as take-off ability of the craft model
- Towing tank test to study the craft performance both in calm water and waves
- Manned control test craft to study the craft performance at larger scale, if the design is for a very large craft

(3) Refinement of the principal dimensions followed by detailed design of the DACWIG.

WIG Detailed Design

WIG detailed design should follow a similar path to design of an aircraft. Once the initial performance has been established based on preliminary design and machinery selection has been confirmed, a detailed design of the main structure can be carried out.

Structural design for WIG will be based on two main analysis cases, take-off and cruise speed, and a series of appropriate load cases defining the operational envelope of craft operating weights and environmental loadings associated with these two analysis cases.

The aerodynamic component of structural design can be completed following the methods of references such as reference Chapter 10 [3], while the marine aspects should be carried out following normal practice in naval architecture, with reference to works such as references Chapters 3 [7], and 7 [6].

Design of machinery systems will largely follow aircraft practice, a useful text for which is Chapter 11 [1].

Following primary structural design, assessment of intact and damaged floating stability, and development of a detailed weight take-off, the data necessary to build wind tunnel and towing tank models will be available. The results of these tests will be able to confirm the earlier projected performance data.

Following confirmation of the overall craft design, outfitting design can begin, and as the equipment HVAC, lighting and other ancillary systems are added, their weight data can replace the nominal figures used as a basis for structural design.

Finally the construction methodology for the craft can be completed, including moulds for elements to be formed in fibre-reinforced plastics and tooling for aluminium structures.

In parallel with detailed design, the initial commercial proposal for the craft can be refined based on detailed costs estimates once construction methodology has been selected. The cost estimates should be refined based on assessment of the complete project delivery including prototype development, testing and certification, preparation of operating guidelines and manuals. Most importantly contingencies should be applied to both cost estimates and schedules. If the craft is a prototype, then particular care is needed to accommodate "unknowns" into the schedule and allow for schedule delays while bugs are sorted out. Since the time is cost, it is important to have a flexible commercial arrangement with the supporting engineering and construction organisations, so as not to incur excessive costs due to schedule delay as a craft is refined into a commercial proposition.

Postscript

We have introduced you to a transport technology that is halfway between the sea and the sky. A technology that can deliver different craft with operating speeds anywhere from 80 kph up to 600 kph and one where craft size can also be significantly larger than aircraft.

A series of opportunities for WIG has been described in this book, and in theory there should by now be a whole new industry developing in the high-speed craft family of the twenty-first century. After all, it is three decades after the launching of Russian 550 t, 300 knot "Caspian Sea Monster", Fig. 1, in 1968, the largest WIG and airplane in the world at that time?

Why has not it spawned a large industry already? Well, maybe at some time it might. Boeing in the United States has earlier in first decade of twenty-first century publicised one of its research projects that it hopes to develop in the near future, subject to government support – the Pelican project – see Fig. 2 and [1].

There have been other large-scale proposals before, such as the Superliner of Figs. 12.24 and 10.10. The US Navy had even begun the development of a multi-thousand ton WIG called the Columbia in the 1960s, though the project was shut

Fig. 1 Caspian sea monster (KM) afloat

L. Yun et al., *WIG Craft and Ekranoplan*, DOI 10.1007/978-1-4419-0042-5,

Fig. 2 Boeing pelican

down later before getting beyond the paper design stage, so a healthy dose of scepticism is appropriate. Such design proposals are useful nevertheless for testing industry, government and society's readiness to support a major step forward in transport concepts.

A large-scale WIG development would be very capital intensive and so require major government funding if it were to succeed, just as the Russian Ekranoplan development in the 1970s and 1980s. That programme died when the government funding was unable to be continued.

At a smaller scale, WIG developments appear to be alive and well right now, though probably not highly visible to the general public. Fischer Flugmechanik in Germany (Fig. 3) and Flightship in Singapore (Figs. 2.51) both have practical and robust designs, together with a carefully thought through approach to placing

Fig. 3 Fischer flugmechanik HW20

them in operation. Flightship set up their own flight training school and had stringent requirements for potential operators, so as to maintain their safety record. The craft are economic for their specified mission, so it just remains to develop the market. The WIG as a fast passenger transport is not (yet) a replacement for a fast ferry. Rather, it has a new over water commuter or local fast transfer market to develop. Building new markets in transportation is a slow job. This may actually be an advantage, so that experience is built in a measured manner.

One requirement WIG have taken some time to respond to is wave height capability. While cruising, wave height is not so much of a problem, but if you can only take off and land in rather small waves, how you can dare to plan long journeys where the seas will exceed the landing criteria – not really. Just like hovercraft, for big seas you need a big craft, so while the smaller WIG can be fine for coastal and estuary environments and calm sea areas, the open ocean is really only suited to large craft. Even then, an examination of an oceanographic atlas will indicate that tropical routings are the key to Transatlantic or trans-pacific operation.

We have spent a good deal of this book explaining the background and theory related to lift augmentation, by thruster efflux and by air cushion principles. These devices significantly improve the take-off performance of WIG craft, but do create their own technical challenges. Jet engine efflux is at such a high velocity that the spray generated is extremely heavy, significantly affecting drag. To reach very high cruise speeds, a jet engine is essential, so the take-off problem is the one that has to be solved and demands much more research! At smaller scale and somewhat slower, though still much faster than marine craft, the ducted propulsors of DACWIG provide an efficient and compact machine, but one that has a natural upper bound for cruise speed, due to the rapidly increasing drag of the duct at flying speeds (Fig. 4).

Fig. 4 Swan launching

The DACWIG concept should offer operating economics that are attractive for coastal patrol and similar utility duties, and the typical cruise speed in the range up to 250 kph would suit this role very well – fast enough to outrun any other vessel and slow enough to carry out observation runs.

This is all just future potential though, just now. The hard facts are that without a major military imperative, the development will just have to move forward in rather small steps until the transport industry accepts the technology as proven

and has a commercial need to fill. Market pull rather than sales push is a healthy way to do business, but it can only occur once acceptance of the technology is available.

Technology development and capability demonstration requires more trials craft to gain experience. Smaller scale privately owned craft and sponsored expeditions are a way to gather this operating experience, particularly if it is shared and built upon jointly. At present, there is a significant band of researchers working on the fundamentals, but not so many operators out there building up the miles. Hopefully, the next few years will see that change.

We offer some parting thoughts on WIG design for readers to consider:

1. Although theoretically the aerodynamic efficiency K of a wing operating in strong surface effect can be as high as 20, the aerodynamic efficiency of the whole WIG might be as low as half of this value due to the appendages and embryonic technology so far of the WIG. Creating a WIG configuration with overall high K is an important target demanding attention to hull, side buoys, tail, composite wings, etc. as a complete vehicle.
2. If the performance of a jumbo jet is used as a benchmark, in order to compete by improving the seaworthiness, aerodynamic efficiency and economy of the craft, it is necessary to develop ultra large WIG operating in strong GEZ. However, this will cause a series of problems such as air compression under the main wing in strong GEZ, aero-elasticity of the structure, structural vibration, etc., so a lot of technical problems still face designers of very large craft.
3. In order to overcome the hump drag for PARWIG during take-off, reserve power has to be installed, even though it will be shut down or reduced after take-off. Unless PARWIG have an operating cruise speed that is rather high, it will have excess power for cruise and be less efficient than a commercial airliner.
4. In order to get the WIG into commercial operation, a good deal of equipment, facilitiesand regulations will need to be designed and agreed as standards, such as special ground equipment, allocated air navigation zones close to terminals, agreed methods for collision avoidance with marine craft and new safety codes for operation. These represent a significant investment in time and money for pioneer WIG operations, so that the business case will have to be compelling for the service to get off the ground – literally. A good start has at least been made with the IMO regulations since this provides a supranational framework for individual countries to build on.
5. PARWIG will operate in the GEZ and occasionally just beyond the GEZ for collision avoidance, so stability is an important operational criteria. Designers have to consider the co-location of three centres of movement for longitudinal and transverse stability, i.e. the pitching centre, heaving centre and heaving velocity centre, particularly beyond the GEZ. Significantly different approaches to this aspect of WIG design have been adopted, with varying degrees of success. The basics are known, while development of optimised designs is as much an art as it is science at present. A potentially fertile area for postgraduate research!

6. The protection of forward-mounted air propellers and engines from spray, mud, sand, stones and birds is still a problem due to WIG operating close to the water and ground surfaces. There are many lessons to be learnt from ACV experience with their propulsion systems as WIG technology moves forward.
7. The take-off capability, impact loading and maintaining a level flying height above waves are still an important challenge for WIG. Similar to conventional high-speed craft, the WIG has to be above a certain size and AUW to be efficient and stable in a given seastate. Development of large craft requires use of smaller scale operational prototypes to verify performance in addition to model testing, an expensive problem for the manufacturer and one that has faced military and commercial high-speed marine craft builders for many decades – the demonstrator craft is a powerful tool to convince the potential operator, but is a costly commitment that finance houses are often not willing to fund.
8. Noise will be an issue, similarly to hovercraft, as commercialisation advances. Ducted propulsors are an important tool in noise control, though duct mass and aerodynamic design to enhance thrust will be important. The lessons from ACV development and also from airliner nacelle design are useful guidelines in this respect.
9. Since the WIG is a mixture of aviation, shipbuilding and air cushion industry technology, including both aerodynamics and hydrodynamics, some novel problems will continue to be encountered as craft designs evolve. Researchers need to be prepared for surprises!

All of these cause the researchers, engineers and particularly builders and operators to need bravery, tenacity, devotion, time and in most cases significant financial resources. This is not an easy combination and may be it is one of the reasons for WIG not developing rapidly in the world so far.

We do believe that certain key elements should be de developed in the next few years for successful advancement of the WIG as transportation is as follows:

- Use of the outer composite wing with larger AR (ideally around 5) with functional division of the wing area into the stabilizing lift surface and the surface that provides lift from “air blowing”.
- Composite outer wings that are foldable for terminal manoeuvring on cushion should enable compact terminal facilities to be provided, minimising terminal investment.
- Use of an S-shape airfoil undersurface can reduce the required area of the tailplane for stability and so reduce drag and powering somewhat, recent research has advanced understanding of this, see [2].
- Use of bag skirts under the side buoys and also under the main hull can provide a useful flexible lower surface that improves performance in waves prior to take-off. While less useable for very large craft, mid-size WIG can be improved by removing need for landing gear and in some cases also removing the need for large paved terminal manoeuvring aprons and launch ramps.

Given a positive world economy, the near-term potential for commercial and military WIG may be

- DACC, DACWIG will be developed from the smaller prototypes in operation today up to passenger craft of 50–150 seats cruising at 80–180 knots. They might operate on coastal routes, large inland rivers and river estuaries, to compete with feeder airliners and other high-speed marine craft.
- High-speed PARWIG with larger flight height and medium size will be suitable for military and utility applications such as Search and Rescue, and Coastal Patrol.
- Very large WIG may provide transoceanic cargo transport.

Finally, we leave you with a couple of illustrations of individuals' early interpretation of surface effect craft – the Dikinson Ram Wing (Fig. 5), built in the 1960s which skimmed the surface and the ultra light fabric construction of Rameses (Fig. 6), another early Ram Wing prototype that had quite a satisfactory flying height! There are still many enthusiastic individuals in the background of WIG research, from Russia to the United States, providing a touchstone for new ideas.

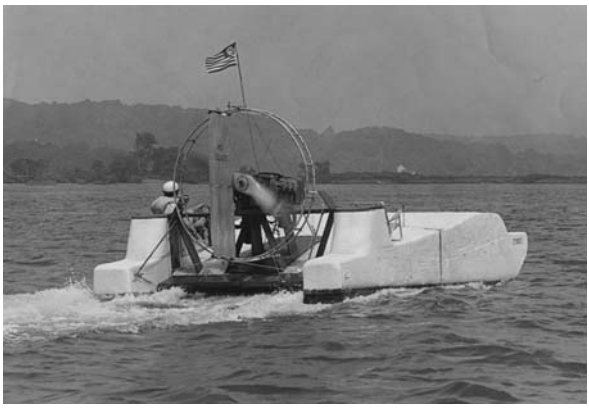

Fig. 5 Dickinson ram wing

Fig. 6 Rameses

Glossary

Note

Some letters are used to represent more than one global variable in different chapters of the book, for example, L is used to represent length and lift force. The letter is commonly associated with the different global variables, so rather than use letters that would be unfamiliar, the reader is requested to take care of the context with such variables.

ACV	Air cushion vehicle
AR	Aspect ratio
A_p	Area of propeller disc, m^2
A_v	Wind area (projected lateral area of the portion of the craft above the waterline),
B_c	Cushion width of air channel (m) sometimes the hull and part of side buoys may be included into this corresponding width
b	distance between the craft centreline and bow thruster centreline
b_{at}	Beam of air tunnel
B_w	wing span, main wing (Chapter 4)
b_h	Width of hull
b_{sb}	Sidewall or side buoy beam, Chapter 13
C, c	Wing chord
CA	Craft centre of lift (total), lift from wings, including any cushion effect at slow speed
CASTD	China Academy of Science & Technology Development
CB	centre of buoyancy
C_{di}	Induced drag coefficient
ΔC_f	Additional friction coefficient for roughness of the plate
CG	centre of gravity
CH	centre of hydrodynamic lift
C_L	Lift coefficient (of wing or whole craft)
C_{Lmax}	Maximum value of lift coefficient

C_M	Aerodynamic coefficient of pitching moment;
COANDA	the coanda effect is increased lift by blowing air at higher velocity than the free stream over the upper surface of the wing
Composite wing	wing outside side buoy usually with strong dihedral
CP	centre of pressure (of cushion)
$C_p = N_t/(\varrho_a n^3 D^5)$	Power coefficient of ducted propeller
CSSRC	China Shipbuilding Scientific Research Centre
C_w	wave-making coefficient, a function of F_{rc} and cushion beam ratio, see ref (2.31);
C_x	Aerodynamic coefficient of craft drag (or wing)
C_y	Aerodynamic coefficient of craft lift (or wing)
$C_y{}^h$	Derivative of lift coefficient with respective to the relative flying height at constant angle of attack α
$C_y{}^\alpha$	Slope of lift coefficient curve at constant relative flying height
$C_y{}^\alpha$	The derivative of lift coefficient of whole plane with respect to the trimming angle α
$C_y{}^\alpha{}_W$	The derivative of lift coefficient of main wing (including main hull and composite wing) with respect to the trim angle α
$C_y{}^\alpha{}_H$	The derivative of lift coefficient of the horizontal tailplane with respect to the trimming angle
D	Drag, total drag of craft
D	Diameter of the propeller, or fan impellor (m) (Chapters 4 and 9)
DACC	Dynamic air cushion craft
DACWIG	Dynamic air cushion wing-in-ground effect craft
D_e	The perpendicular distance of the force L_e acting on the side wing about the centre of gravity of the craft
D_r	drag due to the flap
Ekranolet	Russian name for a small WIG that can also fly in weak SEZ
Ekranoplan	Russian name for a WIG
F	Streamline factor, $f = 1$ by default, f is determined by wind-tunnel testing and is usually >1, so the default assumption is conservative for design
f	Coefficient, according to the relative flying height h/t,
Fn	Froude number
Fn_d	Froude number, based on displacement, $=V_s/(g\ .\ W_o{}^{0.333})^{0.5}$
Fn_c	Froude number with respect to wing chord length
F_{xw},F_{yw},M_{zw}	Force and moment perturbations caused by waves
g	Force due to gravity
GEM	Ground effect machine
GEZ	Ground effect zone
Ground effect	Increased lift experienced by a wing or flying body when within one chord length from the surface

h	Flying height measured to trailing edge of main wing or hull keel to ground (Chapter 4)
h	hovering height (m) (Chapter 4) Relative flying height, $= h/C$
H	Vertical distance between main wing leading edge and the ground (Chapter 4)
H	Cushion height (m) (see Fig. 4.9) (Chapter 4)
$\mathrm{H_q}$	Euler number (see Chapter 9)
H_h	Hull height
H_min	Minimum safe height at which WIG can fly (m)
H_w	Design maximum wave height for operation (m)
h'	Height from the ground of centreline of bow thruster in the plane of the blade centreline (Chapter 4)
H_j	Overall pressure of fan (N/m)
$\bar{H}_j$	Non-dimensional pressure coefficient of lift fan
$i_z = J_z/mC^2$	Non-dimensional moment of inertia of the craft
J_z	Moment of inertia of the craft through CG about Z-axis
K	Lift drag ratio, $K = C_y/C_x$; $K_1 = l_1/R_1$; $K_2 = l_2/R_2$; $K_3 = l_3/R_3$
k	Coefficient for estimating the proportion of the weight lifted by craft air cushion on water surface, in case of DACC and DAWIG, may be $k = 0.7$–1.0, depending on the position of flaps
K_n	Transport efficiency (Chapter 13 uses Te)
K_t	Thrust coefficient of propeller or ducted thruster
K_n	Propulsive efficiency coefficient based on total power $=W_\mathrm{o}V_\mathrm{s}/N$ (Chapter 13)
$K_{n\mathrm{p}}$	Propulsive efficiency coefficient based on propulsive power $=W_\mathrm{o}V_\mathrm{s}/N_\mathrm{p}$ (Chapter 13)
K_p	Coefficient of payload, in general, take $K_\mathrm{p} = 0.2$—0.3 (Chapter 13)
Kph	kilometres per hour
k_q	The effective coefficient of main wing down-wash flow with respect to the horizontal tailplane, $k_\mathrm{q} = {V_\mathrm{H}}^2/V^2$
K_t	Specific thrust, where $K_\mathrm{t} = \mathrm{f}(C_\mathrm{p})$, C_p is the power coefficient of ducted propeller (Chapter 13)
K_ts	Specific static thrust of propeller (N/kw)
L	Length
L	Lift
L	Wetted length of hull or side buoys (m)
L	Lift of model without bow thruster (Chapter 7)
l	Peripheral length of jet nozzle (m)
L_1	Lift provided by air cushion pressure, $L_1 = P_\mathrm{c} \,.\, S_\mathrm{c}$
L_2	Lift provided by Coanda effect, $L_2 = L_1 \,.\, K_\mathrm{c}$

L_3	Lift provided by the vertical component of the thruster of bow thrusters, $L_3 = T \sin \theta$
L_e	Force acting perpendicularly on the side wing due to the sway of the craft
L_r	Lift acting on the right side of the wing frontal surface and perpendicular to the surface
L_d	Dynamic lift
L_{cw}	Composite wing lift
L_{tw}	Horizontal tail stabilizer lift
l_a	Perpendicular distance of the centre of action of air drag, from the CG
l_{at}	Horizontal distance between the air cushion centre of the air tunnel (before take-off) or aerodynamic centre (after take-off) and the CG of the craft
l_{btw}	the distance between the leading edge of main wing and vertical plane of blades of bow thruster (Chapter 4)
l_{cw}	Horizontal distance between the aerodynamic centre of composite wing and CG
l_{mw}	Horizontal distance between main wing aerodynamic centre (including the Hull and sidewalls) and CG of the craft (Chapter 13)
l_{pa}	Perpendicular distance of the rear thruster centreline about the CG
l_{pa}	Perpendicular distance between the thrust of stern propellers and CG of the craft
l_{pb}	Perpendicular distance between thrust of bow propellers and CG of craft
l_{pf}	Perpendicular distance of the bow-thruster centreline about the CG
l_{tw}	Horizontal distance between the aerodynamic centre of the horizontal tail and CG
l_r	Perpendicular distance between the craft total drag acting line and the CG
M	The flow momentum at the position before the air channel
MARIC	Marine Design and Research Institute of China
M_o	Jet momentum of thruster
M_1	Horizontal momentum of thruster flow entering cavity
M_2	Horizontal momentum of airflow leaving cavity under flap
M_3	Momentum of jet flow deflected over main wing
M_4	Momentum from reverse airflow from air curtain
M_v	$= 0.001\, P_v A_v Z f$
M_z	Aerodynamic moment acting on the craft about Z-axis
M_{zaw1}, M_{zaw2}	Aerodynamic perturbation pitching moment caused by waves and wind

m	Craft mass
$m_z{}^h$	Derivative of pitching moment coefficient versus relative flying height $\bar{h}$ at constant angle of attack α
$m_z{}^\alpha$	Derivative of pitching moment coefficient versus angle of attack at constant relative flying height $\bar{h}$
N	Power output (kw)
N	Full power of craft (Chapter 13)
N_t	Rated power of each bow thruster (Chapter 13)
N_p	Propulsive power at cruising speed, lift power can be shutdown (for PARWIG) or reduced (for DACC and DACWIG) (Chapter 13)
N_L	Lift power
n	Propeller speed, fan speed (r/s)
n_ac	Number of air channels on the craft; (Chapter 7)
n_t	Number of bow thrusters (Chapters 7 and 13)
n_t	Number of propellers (Chapter 8)
n_pass	Number of passengers
P	Propeller thrust acting along the X-axis
PARWIG	power-augmented wing-in-ground effect craft
P_a	Relative atmosphere pressure, $=0$
P_c	Cushion pressure
P_c0	Air static pressure
P_c1	Static air pressure behind the propeller disc ($\mathrm{N/m^2}$)
P_t	Total pressure on the exit of nozzle, ($\mathrm{N/m^2}$)
P_t	Total pressure of propeller, ($\mathrm{N/m^2}$)
P_v	Wind pressure
Q	Airflow from nozzle/bow thrusters or lift fan ($\mathrm{m^3/s}$)
Q_f	Fuel consumption of engine (kg/kw h)
q	Dynamic pressure of airflow
q_j	Dynamic pressure of air jet ($\mathrm{N/m^2}$)
Q	Non-dimensional flow coefficient of lift fan
R	Total craft drag
R_a	Air profile resistance of the whole craft
R_aw	Wave-making resistance caused by air cushion pressure under the main wing
Re	Reynold's number, $\mathrm{Re} = vl/\upsilon_\mathrm{a}$
R_1	Resistance of model with bow thruster at revolution of n in case of zero air speed, $R_1 = f(n)$
R_2	Resistance of bare model without bow thrusters in case of air speed of v, $R_2 = f(v)$
R_3	Resistance of model with bow thrusters at revolution of n and in case of v air speed, $R_3 = f(n, v)$
R_3	Test data on dynamometer of towing facility (Chapter 7)
R_hw	Wave-making drag of the hull, including the spray drag

R_{hf}	Water-friction resistance acting on the hull
R_{sww}	Wave making drag caused by side buoys (or sidewall), also including their spray drag
R_{swf}	Water friction resistance acting on the side buoys
R_{fl}	Fouling drag caused by marine growth on the hull and side buoys under the loaded waterline on both hull and side buoys.
ΣR	Total drag of the model
S	Total area of supporting surface, $S = b \times C$
S_a	Reference area for calculating the air profile drag and lift, in case of DACC and DACWIG, with two air tunnels, then $S_a = (2b_{at} + b_{sb} + b_h)$. C
S_c	Cushion area, $S_c = C(B_h + 2B_w + B_{sb})$
S_{c1}	Horizontal area under the main wing surface
S_{c2}	Horizontal area under the hull surface
S_{c3}	Horizontal area under the side buoys
S_{cw}	Area of composite wing
S_{tw}	Area of horizontal tail wing
SES	Surface effect ship
SEZ	Surface effect zone
SFC	Specific fuel consumption (kg/km N_{pass}), $=Q_f N_p/V_s N_{pass}$
Static air cushion	An air cushion created under a craft by the action of air fans and contained by skirts or a combination of skirts and sidewalls
Side wings	Composite wings outside side buoys
Side buoys	Buoyant structures at the tip of main wing
T	Thrust of air propeller
T_a	Thrust of rear thrusters
T_{dc}	Dynamic thrust of ducted thruster in channel, $T_{dc} = R_3 - R_2$
T_{do}	Dynamic thrust of single ducted thruster
TLA	Relationship between drag hump speed and take-off speed
T_{so}	Static thrust of single ducted thruster
T_{sc}	Static thrust of a single ducted thruster in air channel (N)
T_e	Transport efficiency (Chapter 13), $=W_p V_s/N = K_n W_p/W_o$
T_{eus}	Transport efficiency based on useful load, $=W_{us} V_s/N = K_n W_{us}/W_o$
T_{ep}	Transport efficiency based on propulsive power, $=W_p V_s/N_p = K_{np} W_p/W_o$
T_{epus}	Transport efficiency based on use of load and thrust power, $= W_{us} V_s/N_p = K_{np} W_{us}/W_o$
T_{pb}	Bow propellers thrust
T_{pa}	Stern propellers thrust
t	Time history (Chapter 3),
t	Nozzle thickness (m) (Chapter 4)
$\bar{t}$	Equivalent flow thickness of thruster jet, $\bar{t} = (1+ \cos \theta)\, t_1$
$T1(V_o)$	Propeller thrust at $V = V_o$ (Chapter 8)

$T(V_o)$	Total thrust of propellers
t_0	Thruster jet thickness at efflux
t_1	Jet thickness at ground contact
t_2	Gap between the lower tip of flap and ground (Chapter 4)
v	Craft speed;
V	speed of incoming airflow to the WIG Craft
V	speed of water flow (Chapter 9)
V_a	Air velocity
V_H	The incoming flow velocity to the tail plane;
V_i	Upwards airflow induced by tip vortex
V_j	The average air low velocity from bow thruster (m/s)
V_{jo}	Speed of jet air after the air propeller
V_r	low speed at the stern exit under the main wing
V_o.	Incoming velocity (tip vortex)
V_o	Average airflow velocity (Chapter 4)
V_o	Initial craft speed (Chapter 8)
V_s	Craft speed (m/s)
V_{javg}	Average velocity of jet
$\bar{V} = v/v_0$	Relative speed;
W	Overall craft weight (kg)
W	Craft displacement (m^3) (Chapter 9)
W_e	Empty weight of craft (lightweight)
WIG	Wing-in-ground effect
W_p	Payload weight;
W_o	All up weight
W_{us}	Useful load (payload together with fuel and consumables)
X	Drag
X_a, Y_a	Aerodynamic force acting on the craft along $X_sG_oY_s$ coordinates (Chapter 9)
X_a	Position of pitching centre of the wing (and hull as well as side buoys) from the leading edge of main wing, Fig. 6.7
X_c	Relative distance of aerodynamic centre from leading edge of main wing
$\bar{X}_c = X_c/C$	X is positive back from LE
X_{dc}	Wing centre of lift distance from leading edge
$\bar{X}_{F9}$=$X_{F\alpha}/C$	Relative position of pitching centre
$\bar{X}_{Fh}$	Relative position of flying height pitching centre
$\bar{X}_{F\bar{h}} = X_{Fh}/C$	Relative position of heaving centre
$\bar{X}_{F\ddot{h}}$	Relative position of heaving velocity pitching centre
$\bar{X}_G = X_g/C$	Relative position of CG of craft from wing leading edge
X_n	Position of a neutral point representing the pitching centre of the wing plus tailplane configuration

$X_{\mathrm{FW}\vartheta}$	Position of pitching centre of the main wing, measured from the leading edge of the main wing
$X_{\mathrm{FH}\vartheta}$	Position of pitching centre of the tailplane, calculating from the leading edge of main wing
X_{dW}	The longitudinal position of pitching centre of the main wing
X_{dH}	The longitudinal position of pitching centre of the tailplane
X_{Fh}	Pitching centre of flying height
X_{FhW}	Pitching centre of flying height of main wing
X_{FhH}	Pitching centre of flying height of tailplane
X_{fH}, X_{fS}	Longitudinal friction force of waves acting on the hull and sidewalls
X_{HH}, Y_{HH}, $M_{z\mathrm{HH}}$	Longitudinal and vertical hydrodynamic force and pitching moment of waves acting on the hull
X_{HS}, Y_{HS}, $M_{z\mathrm{HS}}$	Longitudinal and vertical hydrodynamic force and pitching moment of waves acting on the sidewalls
X_{h}	Distance of wing height centre from leading edge of wing
X_{g}	Distance of WIG centre of gravity leading edge of wing
X_{ϑ}	Distance of wing pitching centre from leading edge of wing
Y	Lift
Y_{aw1}, Y_{aw2}	Aerodynamic perturbation lift force caused by waves and wind
$Y_{\mathrm{b}}{}^{h}$	The partial derivative of unit lift with respective to the relative flying height h
Y_{g}	Distance between the original point of base plane and craft centre of gravity
Y_{p}	The vertical distance from the CG to the propeller axis
Z	The wind area lever which is equal to the vertical distance to the centre of wind area from the centre of the projected lateral area of the portion of the craft below the plane of the acting waterline
$\bar{z}$	$=z/b$, $\bar{z}$ is the non-dimensional transverse coordinate along the wing
α	The angle between the course and base plane of the craft, craft angle of attack
α	Angle between the baseline of side plate and incoming flow
α_0	Main-wing angle of attack
α_{i}	Induced angle of attack
α_1	Angle between the baseline of side plate and chord line of main wing
$\alpha*$	Angle between the chord line of main wing and incoming flow $(=\alpha + \alpha_1)$
θ	Angle of bow-thrusters flow. Thruster angle, plus vane angle if fixed ducted thrusters, positive down
θ	Jet inclination angle

θ_2	The angle of negative dihedral surface
β_1	Angle between the shaft of bow thruster and base plane
β_2	Angle of guide vane behind bow thruster
β_3	Angle of jet deflected over wing, assumed at V_0
γ	Heeling angle, positive in case of right side of wing down
γ	Angle between wing chord line and flap angle
γ'	Angle of flap
γ_w	Dynamic/kinematic viscosity coefficient
η	Propulsion efficiency
η	Efficiency of fan and air duct (Chapter 4)
η_f	Lift fan efficiency
η_p	Thruster efficiency (including hull coefficient)
η_s	System efficiency
η_t	Transmission efficiency
η_{ls}	Lift–thrust ratio for a bow thruster
η_{Ts}	Static thrust-recovery coefficient of the ducted thruster in channel
η_{Td}	Dynamic thrust-recovery coefficient
η_{ls}	Total static lift coefficient of air channel, $\eta_{ls} = L_s/T_{so}$
η_{ld}	Total dynamic lift coefficient of air channel, $\eta_{ld} = L_d/T_{do}$
η_{sc}	Static thrust-recovery coefficient of air channel, $\eta_{sc} = T_{sc}/T_{so}$
η_{dc}	Dynamic thrust-recovery coefficient of air channel, $\eta_{dc} = T_{dc}/T_{do}$
η_v	Velocity decay function along wing span, $\eta_v = \sigma\, y'/x'$
λ	Aspect ratio (alternatively referred to as AR in text)
λ	Linear scale ratio (Chapter 9)
λ_p	Propeller advance ratio, $\lambda_p = V/nD$
μ	Relative density of the craft; $\mu = 2m/\rho SC$
ν_a	Dynamic viscosity coefficient of air
φ	Angle of elevators
φ_0	Balance angle of the elevator
ψ	Course angle, i.e. the angle in the vertical plane between the course of the craft and sea level, climbing positive and descending negative
ρ_a	Density of air (N s^2/m^4)
ρ_w	Density of water (N s^2/m^4)
ϑ	Trim or pitch angle of the craft, i.e. the angle between the base plane of craft and sea level
ϑ_0	Balanced trim or pitch angle
σ_s	Surface tension of water (N/m)
τ	Relative (non-dimensional) time, $= t/t_0$

τ_m	Time constant, $=2m/\rho S v_0$
ξ_1	The coefficient of pressure non-uniformity of air cushion, $=0.95-1.0$
ξ_2	Coefficient of Coanda effect, $=1.05-1.15$
ϵ_m	downwash angle of the flow incoming to the tailplane

References and Resources

References

Chapter 1

1. N.I. Gee: “The Practical Application of Hybrid Design Technique to Fast Ferries for the 1990’s”, 8th HSSC Conference, Jan 21–23, 1992, UK.
2. L. Yun: “The Comparison of Performance for Various High Speed Marine Vehicles”, published by MARIC, June, 1995, Shanghai, China.(in Chinese).
3. Wing in Ground Effect Craft (Part I,II,III), Ship & Boat International, May–July, 1995.
4. H. Fischer, K. Matjasic: “The Hoverwing Technology—Bridge Between WIG and ACV”, Proceedings of International Conference on WIGs, Dec. 4–5, 1997, London.
5. H. V. Borst: “Analysis of Vehicles with Wings Operating in Ground Effect”, AIAA Paper 79-2034.
6. USSR Research and Design Efforts in the Development of Marine *Ekranoplan*s and Their Transportation Capacity in Various Water Areas, HPMV’92, Arlington, USA.
7. D.N. Sinitsin: “Basic Summary of the Establishment of Domestic *Ekranoplan*s and some Reliability Problems Influencing the Establishment of Future Passenger/Cargo Transport Ekranoplan”, Proceedings of First International Conference on *Ekranoplan*, May 3–5, 1993, (in Russian).
8. R.W. Gallington: “Power Augmentation of Ram Wings”, The Royal Aeronautical Society, May19, 1987.
9. B.H. Carson: “Experimental Observations of the Two Dimensional Power-Augmented Ram Wing Operated Statically Over Water”, AIAA Paper 1978.
10. F.H. Krause, R.W. Gallington: “The Current Status of Power-Augmented Ram Wing Technology”, AIAA Paper 78-752.
11. F.H. Krause: “Power Augmented -Ram Landing craft-A New Concept in Marine Mobility”, HSSC Conference, June, 1980, UK.
12. A.Y. Maskalik: “Summary of the Aero-Hydrodynamics and Flying Dynamics of Ekranoplan – Basic Problems on the Establishment of Second Generation of Ekranoplan”, Proceedings of the First International Conference on WIG, May 3–5, 1993, Saint Petersburg, Russia, (in Russian).
13. A.V. Neburov: “The Measurement of Flying Parameters Close to Sea Surface” Saint Petersburg, 1994, (in Russian).
14. M.I. Malyshev: “Experience of Using Ekranoplan in Russian Navy” Workshop Proceedings of Ekranoplane & Very Fast Craft at The University of New South Wales, Sydney, Australia on Dec 5–6, 1996.

15. L. Yun, P. Gui-Hua: “Dynamic Air Cushion Wing in Ground Effect Craft (DACWIG) – The Prospect of High Speed Water Transportation Tool in the 21st Century”, Proceedings of 25th International Conference on Air Cushion Technology, June 16–20, 1998, Montreal, Canada.

Chapter 2

1. L. Yun, A. Bliault: “Air Cushion Craft”, Published by Arnold Publishers Ltd (Now Hodder Headline, Part of Elsevier Publishers), 2000, London, ISBN 0 34067650 7 (UK), ISBN 0 470 23621 3 (Wiley).
2. USSR Research and Design Effort in the Development of Marine Ekranoplane and Transportation Capability in Various Water Areas, HPMV’92, June, 1992, USA.
3. D.N.Sinitsin: “Basic Summary on the Establishments of Domestic Ekranoplane and Some Problems on the Establishments of Future Passenger/Cargo Transport Ekranoplane”, Proceedings of First International Conference on Ekranoplane, May 3–5, 1993, Russia, (in Russian).
4. J.B. Je: “Development and Application of WIG in Russia”, Ship & Boat, Published in MARIC, (in Chinese), No.1, 1995.
5. N.Y. Belavian: “Chief Designer R.Y. Alexeev’s Super Large Ekranoplane”, Shipbuilding, Saint Petersburg, Russia, Jan, 1993, (in Russian).
6. N.N. Birogov: “On Seagoing Passenger WIG”, Shipbuilding, Apr/May, 1994, Saint Petersburg, Russia, (in Russian).
7. D. Sinitsyn, et al.: “The Present Day State and Prospect for the Development of Commercial Ekranoplanes”, Workshop Proceedings of Ekranoplane and Very Fast Craft of UNSW, Australia, Dec 5–6, 1996.
8. D. Sinitsyn: “Summary of the Construction of the First Commercial Ekranoplane Amphistar”, Workshop Proceedings of Ekranoplane and Very Fast Craft of UNSW, Sydney, Australia, Dec 5–6, 1996.
9. S.S. Alexeyev: “Creation of High-Speed Amphibian Boat Using Ground Proximity Effect on the Example of Sever Boat”, Workshop Proceedings of Ekranoplane and Very Fast Craft of UNSW, Sydney, Australia, Dec 5–6, 1996.
10. U. Makalov: “E Volga-2” in Trial, Power & Sailing Boats, 2 (168), July–Aug, 1999 (in Russian).
11. L. Su-Ming, and L. Ke-Si: “Development of PARWIG Craft in China Shipbuilding Scientific Research Center (CSSRC) of China”, Proceedings of First International High Performance Marine Vehicles Conference of China, Nov 2–5, 1988, Shanghai, China.
12. L. Ke-Si, L. Su-Ming: “Development of PARWIG Craft in China Shipbuilding Scientific Research Center (CSSRC) of China”, Proceedings of Second International High Performance Marine Vehicles Conference of China, Nov 1992, Sheng-Zheng, China.
13. H. Anding: “Development of an Amphibious Wing in Ground Effect Craft”, Proceedings of First International High Performance Marine Vehicles Conference of China, Nov 2–5, 1988, Shanghai, China.
14. L. Qi-Kang, L. Yun, P. Gui-Hua: “Taking Steps to Promote the Fast Development of WIG in China”, Proceedings of 25th International Conference on Air Cushion Technology, June 16–20, 1998, Montreal, Canada.
15. L. Yun, P. Gui-Hua: “Dynamic Air Cushion Wing in Ground Effect Craft (DACWIG)—The Prospect of High Speed Water Transportation Tool in the 21st Century”, Proceedings of 25th International Conference on Air Cushion Technology, June 16–20, 1998, Montreal Canada.
16. L. Yun, P. Gui-Hua, W. Cheng-Ji: “Research and Development of Chinese Amphibious Wing in Ground Effect craft”, International Boat Show and Technical Conference, Shanghai, China, Mar 28–30, 1999.

17. L. Yun, et al.: “Research and Design of the Dynamic Air Cushion Wing in Ground Effect Craft (DACWIG) type ‘SWAN’”, HPMV’2000 China, Shanghai, China, Apr, 2000.
18. G.W. Jorg: “Tandem Airfoil Flairboats (TAF)”, Proceedings of International Conference on WIGs”, Dec 4–5, 1997, London.
19. H. Fischer, K. Matjasic: “The Hoverwing Technology—Bridge Between WIG and ACV”, Proceedings of International Conference on WIGs, Dec 4–5, 1997, London.
20. “WIGs – No longer a flight of fancy?”, Fast Ferry International, May 1996.
21. “An Australian Ekranoplane that Breaks the Mould”, Ship & Boat International, October, 1996.

Chapter 3

1. M. Basin, et al.: “WIG (Ekranoplane) as a Transport Vessel and Sport Craft”, Proceedings of the International Conference on Wing-In-Ground-Effect Craft (WIGs), Dec 4–5, 1997, London.
2. L. Yun, P. , Gui-Hua: “Dynamic Air Cushion Wing in Ground Effect Craft (DACWIG—The Prospect of High Speed Water Transportation Tool in the 21st Century”, 25th International Conference on Air Cushion Technology, June 16–19, 1998, Montreal, Canada.
3. L. Yun, C.-J. Wu, Y.-N. Xie: “Investigation on Aerodynamic Characteristic of DACWIG Craft Type ‘SWAN’”, Proceedings of HPMV’2000CHINA, Apr 19–23, 2000, Shanghai, China.
4. Principles of Naval Architecture, The Society of Naval Architects and Marine Engineers, New York, USA.
5. Theory of Wing Sections, Abbott and von Doenhoff, Dover Publications, 1959 (subsequently reprinted several times).

Chapter 4

1. USSR Research and Design Effects in the Development of Marine Ekranoplanes and Their Transportation Capability in Various Water Areas, HPMV ‘92, Arlington, VA, USA.
2. W.J.W. Smithey, B.S. Papadales: “Effect of Turbulent Jet Mixing on the Static Lift Performance of a Powering Augmented-Ram Wing”, AD-A049620.
3. J.T. Doo, V. Consentino: “Air-Cushion-Assisted Powered Wing-in-Ground –Effect Vehicle Concept”, International Vehicle Research, Inc., July 26,1994, USA.

Chapter 5

1. H. An-Ding, M. Ru-Ren: “On the Aerodynamic Characteristics of Thicker Wings in Ground Effect with End Plates”, Chinese Shipbuilding, Apr 1980.
2. R.W. Gallington: “The Ram Wing Surface Effect Vehicles: Comparison of one Dimensional Theory with Wind Tunnel and Free Flight Results”, Hovering Craft and Hydrofoil, Nov 1972.
3. N.V. Kornev, A.E. Taranov: “Application of the Vortex Method for Investigating the Behaviour and Potential Hazard of the WIG Training Vortices”, Proceedings of the Second International Conference on Vortex Methods, Istanbul, Turkey, 2001 pp. 219–227.
4. L.D. Volkov: “Principles of Aerodynamics for Dynamic Supported Craft”, National Saint Petersburg Ocean Technology University, Saint Petersburg, Russia, 1995 (in Russian).

5. L. Yun, et al.: “Investigation on Aerodynamic Characteristics of DACWIG Type ‘SWAN’”, Proceedings of HPMV’ 2000 CHINA Conference, Apr 19–23, Shanghai, China.
6. Volkov, L.D., Roussetsky, A.A.: “ Problems and Prospect of Ekranoplane”, Shipbuilding, Jan, 1995, Saint Petersburg, Russia (in Russian).

Chapter 6

1. “International Code of Safety for WIG Craft”, Report of the correspondence group, submitted by Russian Federation, International Maritime Organization (IMO), 1997.
2. “The Design of the Aeroplane”, Darrol Stinton, 1983, ISBN 0-632-01877-1, Published by Blackwell Science.
3. A.Y. Maskalik: “Summary on the Aerodynamics and Flying Dynamics of Ekranoplane, Basic Problems on the Establishments of Second Generation of Ekranoplane”, Proceedings of the First International Conference on Ekranoplane, May 3–5, 1993, Russia (in Russian).
4. V.I. Zhukov: “Dynamic Characteristics of Ekranoplane”, Proceedings of the First International Conference on Ekranoplane, Russia, (in Russian).
5. L.D. Volkov: “Calculating Investigation on the Aerodynamic Characteristics of Running WIG with various Wing Profiles”, Proceedings of the First International Conference on Ekranoplane, May 3–5, 1993, Russia, (in Russian).
6. V.I. Zhukov: “Peculiarities of Aerodynamics, Stability and Handling of Ekranoplanes”, Proceeding of International Conference on Wing-In-Ground-Effect Craft, Dec 4-5, 1997, Royal Institution of Naval Architects, London. ISBN 0 903055 34 1.
7. K.V. Rozhdestvensky: “Stability of a Simple Lifting Configuration in Extreme Ground Effect”, Proceedings of International Conference on Wing in Ground Effect Craft (WIGs), Dec 4-5, 1997, Royal Institution of Naval Architects, London, ISBN 0 903055 34 1.
8. V.B. Teomagov: “Automatic Control of WIG Motion”, Saint Petersburg, Russia, 1996 (in Russian).
9. “The Anatomy of the Aeroplane”, Darrol Stinton, Second Edition 1998, ISBN 0-632-04029-7, Published by Blackwell Science.
10. S.F. Hoerner: “Fluid Dynamic Lift”, Chapter XI, Longitudinal Stability Characteristics of Aircraft.
11. P.N. Hwang: “Aerodynamics and Flying Dynamics”, Nanking Aircraft and Aeronautics University, 1994. China (in Chinese).
12. L. Shu-Ming et al.: “Development of WIG craft at CSSRC”, Workshop Proceedings of Ekranoplane and Very Fast Craft at UNSW, Sydney, Australia, Dec 5–6, 1996.
13. A.S. Afremov et al.: “Hydrodynamics of Ekranoplanes”, Krylov Shipbuilding Research Institute, Russia, (in Russian).

Chapter 7

1. S.F. Hoerner, Fluid Dynamic Drag, 1965, Published by the Author.
2. M. Basin, et al.: “WIG (Ekranoplane) as a Transport Vessel and Sport Craft”, International Conference on Wing-In-Ground-Effect Craft, Dec 4-5, 1997, London.
3. V.N. Kirillovikh: “Russian Ekranoplane”, 21st Century Flying Ships at UNSW, Sydney, Australia, Nov 7, 1995.
4. S.F. Hooker: “Twenty First century Shipping at Aircraft Speed”, 21st Century Flying Ships at UNSW, Sydney, Australia, Nov 7, 1995.
5. R. Du Cane: High Speed Small Craft, Revised 3rd Edition, David and Charles, 1974, ISBN 0 7153 5926 6.

6. L. Shu Ming: “The 902 Single Seat Ram Wing Surface Effect Craft”, International High Performance Vehicle Conference, Shanghai, China, 1988.
7. L. Yun, et al.: “Design Considerations for Aero-Hydrodynamic Configuration of DACWIG Type SWAN”, Proceedings of International Boat Show and Conference, Apr, 2001, Shanghai, China.
8. L.L. Volkov: Principle of Aerodynamics for Dynamic Supported Craft, National Saint Petersburg Ocean Technology University, Saint Petersburg, Russia, 1995, (in Russian).

Chapter 8

1. L.D. Volkov, A.A. Rosinski: “Problems and Prospect of Ekranoplane”, Shipbuilding, Jan 1995, Saint Petersburg, Russia, (in Russian).
2. V.B. Sokolov: “Novel Generation of Wings Ships”, Shipbuilding, Russia, Jan, 1991, (in Russian).
3. V.Y. Zhukov: “Aerodynamic Performance, Stability, and Maneuverability of Ekranoplane”, Central Aerodynamic & Hydrodynamic Institute Named Prof. N.Y Zhukovski”, Moscow, 1997, (in Russian).
4. V.V. Strelkov: “Control Tasks and Manual Control System for the Wing–in-Ground Effect Vehicle”, Proceedings GEM2000, Saint Petersburg, Russia, June 21–23, 2000.
5. H. Fischer: “Airfoil Technique on X-113 & X-114”, Proceedings of 1st International Conference on High Performance Marine Vehicles, Shanghai, China, November, 1988.
6. P.N. Hwang: “Aerodynamic and Flying Dynamics”, Nanking Airplane and Aeronautics University, 1994, China (in Chinese).

Chapter 9

1. Z.J. Liu : “Wing Profile of Model Airplane”, 1956, (in Chinese).
2. Z. Go-Lin: “On the Aerodynamic Problems of Wind tunnel with Fixed Ground Plate”. 1977, Harbin (in Chinese).
3. M.H. Avakumov et al.: “Special Method on the Experimental and Theoretical Investigation for WIG Design, Krylov Ship Research Institute”, Saint Petersburg, Russia, (in Russian).

Chapter 10

1. J.P. Fielding: “Introduction to Aircraft design”, Cambridge University Press, Cambridge, 1999, ISBN 0-521-65722-9.
2. D. Stinton: “The Design of the Aeroplane”, Blackwell Science Ltd, Boston, MA, 1995, ISBN 0-632-01877-1.
3. T.H.G Megson: “Aircraft Structures for Engineering Students”, Edward Arnold, London, 1999, ISBN 0-340-70588-4.
4. L.R. Jenkinson, P. Simpkin, D. Rhodes: “Civil Jet Aircraft Design”, Edward Arnold, London, 1999, ISBN 0-34074152-X.
5. G. Weidmann, P. Lewis, N. Reid: “Structural Materials”, Butterworth Scientific Ltd, Guildford, 1990, ISBN 0-408-04658-9.
6. “International Code of Safety for High Speed Craft - HSC Code”, IMO-187E, International Maritime Organisation, London, 2000, ISBN 92-801-1326-7.

7. W.F. Durand (ed.): “Aerodynamic Theory”, Vol 6, Division S, Seaplanes, Dover Publications Inc, Mineola, NY, 1963 (reprinted from 1936), Library of Congress 63-19489.

Chapter 11

1. M.J. Kroes, T.W. Wild, “Aircraft Power Plants”, McGraw-Hill, New York, 7th Edition, 1995, ISBN 0-07-113429-8.

Chapter 12

(none)

Chapter 13

1. V. Liubimov et al.: “High Speed Passenger Craft—The Technical-Economical Prerequisite for Application in Inland Water Transport”, Inland River Transport, Saint Petersburg, Russia, May, 1994, (in Russian).
2. N.H. Cross: “The Third Level: Operational Considerations”, Proceedings of International Conference on Wing-In-Ground-Effect Craft, Dec 4 & 5, 1997, London.
3. R.Y. Armhanitski, et al.: “Selection of Navigation Route of the Transport and Passenger WIG” Shipbuilding May/June, 1994, (in Russian).
4. I. Cross, C. O’Flaherty: “Hovercraft and Hoverports”, Pitman Publishing, London, 1975, ISBN 0 273 00316 X.
5. A.I. Afromeev: “Prospect of WIG Manufacture”, Shipbuilding, Jan, 2000, (in Russian).
6. International Code of Safety For WIG Craft, Issued by IMO, 2000.
7. M. McDaniel, C. Snyder: “Airborne Amphibians are Here Again”, U.S. Navy Proceedings, October 1993.
8. A.V. Neburov: “The Measurement of Flying Parameters Close to Sea Surface”, Saint Petersburg National Academy, 1994.
9. A.Y. Bogdanov et al.: “New IMO High Speed Craft Code and the Problems of Ekranoplanes Certification”, FAST’93.
10. A.Y. Bogdanov et al.: “New IMO High Speed Craft Code and the Problems of Ekranoplanes in Russia”, FAST’93, Yokohama, Japan, Dec 1993.
11. L. Yun, et al.: “Design Features & Evolution of Dynamic Air Cushion Wing in Ground Effect craft in China”, International Conference on Ground Effect Machine GEM2000, Saint Petersburg, Russia, June 2000.
12. L. Yun, : “Proposals to the Draft of WIG Craft Safety Code in IMO (draft), MARIC, China, August, 1996.
13. “Information about the Preparation of Safety Code for WIG in IMO”, China Classification Society, Shanghai, China, 1997.

Chapter 14

1. Pelican – a Big Bird for the Long Haul – Phantom Works New Project Proposal – Article in Boeing House Magazine September 2002.
2. Aerodynamic Properties of Wings in Surface Effect with S-Shaped Profiles on the Upper and Lower Surface by CDF method, by H Akimoto, S Kubo and H Ikeda, Third International Conference for High Performance Marine Vehicles (HPMV) China, April 2000.

Additional Resources

1. Ekranoplans, Peculiarity of the theory and design, by Maskalik a., Synitsin D. et al. Published by Sudostroenie, St Petersberg, Russia 2000 ISBN 5-7355-0509-2.
2. Aerodynamics of a lifting system in extreme ground effect, by K Rozhdestvensky Published by Springer, Germany, 2000 ISBN 3-5406-6277-4

Additional Reference Material

1. A. Bogdanov, D. V. I. Zhukov: “The Setting of a Ground Effect Action in Relation to Altitude on the New International Code of WIG Craft Safety”, Workshop Proceedings of Ekranoplane and Very Fast Craft at UNSW, Sydney, Australia, Dec 5–6, 1996.
2. N.Y. Belavin: “Future Flying Boat”, Shipbuilding, May/June, 1993, Saint Petersburg, Russia, (in Russian).
3. N.Y. Belavian: “Chief Designer R.Y. Alexeev’s Super Large Ekranoplane”, Shipbuilding, Jan1993. (in Russian).
4. N.N. Birogov: “On Seagoing Passenger WIG”, Shipbuilding, April/May, 1994 (in Russian).
5. H. Fischer, K. Metjasic: “Some Thoughts About the Use of Lift-Off-Aids as One Condition for the Economical Operation of WIG Ships”, Workshop Proceedings of Ekranoplane & Very Fast Craft at UNSW, Sydney, Australia, Dec 5–6, 1996.
6. V.Y. Genisov: “Search-Salvage WIG”, Shipbuilding, Saint Petersburg, Russia, Jan 1995, (in Russian).
7. W.J. Greene: “Wing-In-Surface-Effect Ferries”, Proceedings of International Conference on Wing-In-Ground-Effect Craft, Dec 4 and 5, 1997, London.
8. S.F. Hooker, M.R. Terry: “Hydroaviation”, Proceedings of HPMV Conference, June, 1992, Arlington, VA, USA.
9. H. Anding, W. Gao-Zhong: “20 Passenger Power Augmented Ram Wing in Ground Effect Craft Type AF-1”, Second International High Performance Marine Vehicles Conference of China, Nov 1992, San Zheng, China. – Not Used.
10. Kubo, S: “Outline of Presentation on The 1st International Conference on WIG”, Proceedings of The 1st International Conference on WIG in Russia, May 3–5, 1993, Saint Petersburg, Russia, (in Russian).
11. T. Kuhmstedt: “Aerodynamic Design Procedure and Results of the Development of Commercial WIG Craft”, Workshop Proceedings of Ekranoplane & Very Fast Craft at The University of New South Wales, Sydney, Australia on Dec 5–6, 1996.
12. L. Qi-Kang, Y. Liang, P. Gui-Hua: “Strengthening the Cooperation Between China and Russia for Promoting the Fast Development of Wing in Ground Effect Craft in China”, Shanghai Shipbuilding, 1997, 5/6 (in Chinese).
13. S.-M. Li, et al.: “Development of WIGC at CSSRC”, Workshop Proceedings of Ekranoplane & Very Fast Craft at The University of New South Wales, Sydney, Australia on Dec 5–6, 1996.

14. M.I. Malyshev: “Experience of Using Ekranoplan in Russian Navy” Workshop Proceedings of Ekranoplane & Very Fast Craft at The University of New South Wales, Sydney, Australia on Dec 5–6, 1996.
15. U. Makarov: “E-Volga-2” on Trial, Power & Sailing Boats, 2 (168) 1999 (June–July).
16. K.V. Rozhdestvensky: “State -of-the – Art and Perspectives of Development of Ekranoplanes in Russia”, FAST’93, Yokohama, Japan.
17. K. V. Rozhdestvensky: “Aerodynamics Characteristics of WIG in the Strong Ground Effect Zone”, Shipbuilding Jan, 1995, Saint Petersburg, Russia (in Russian).
18. V.B. Sokolov: “Novel Generation of Wings Ship”, Shipbuilding, Saint Petersburg, Russia, Jan,1991, (in Russian).
19. D.N. Sinitsin, et al.: “Peculiarity of Theory and Design of WIG Crafts”.
20. D.N. Sinitsin: “Basic Summary on the Establishments of Domestic Ekranoplane and Some Problems on the Establishments of Future Passenger/Cargo Transport Ekranoplane”, Proceedings of First International Conference on Ekranoplane, May 3–5, 1993, Russia (in Russian).
21. L.D. Volkov, A.A. Roussetsky: “Problems and Prospect of Ekranoplane”, Shipbuilding, Saint Petersburg, Russia, Jan, 1995 (in Russian).
22. L.L Volkov : “Principles of Aerodynamics for Dynamic Supported Craft”, National Saint Petersburg Ocean Technology Institute, Saint Petersburg, Russia, (in Russian).
23. L. Yun, et al.: “Design Consideration of Aero-Hydrodynamic Configuration of DACWIG Type SWAN During Conversion”, Proceedings of International Boat Show and Conference, Apr, 2001, Shanghai, China.
24. “Wing in Ground Effect”, Ship and Boat International, May–July, 1995.
25. K.P. Wong, L. Yun: “Development of Russian WIG”, Hong Kong Flying Dragon Science & Technology Ltd, Proceedings of International HPMV Conference, 2002, Shanghai, China.
26. V.V. Kolganov, V.G. Sergeev : “Design features of WIG craft EL-7 Ivolga and test results”, Proceedings of International HPMV Conference, 2002, Shanghai, China.

Subject Index